UNIVERSITAT DE BARCELONA

Modulación Post-Transcripcional de Genes Expresados en Neuronas Serotoninérgicas de Ratón como Nuevas Dianas Terapéuticas en Depresión

Albert Ferrés i Coy

Modulación post-transcripcional de genes expresados en neuronas serotoninérgicas de ratón como nuevas dianas terapéuticas en depresión

Tesis doctoral presentada por

Albert Ferrés i Coy

Barcelona, Diciembre 2016

TRABAJO PRESENTADO PARA OPTAR AL GRADO DE DOCTOR POR LA UNIVERSIDAD DE BARCELONA EN EL PROGRAMA DE DOCTORADO DE BIOMEDICINA

DEPARTAMENTO DE NUROQUÍMICA Y NEUROFARMACOLOGÍA

INSTITUTO DE INVESTIGACIONES BIOMÉDICAS DE BARCELONA (IIBB)

CONSEJO SUPERIOR DE INVESTIGACIONES CIENTÍFICAS (CSIC)

DEPARTAMENT DE NEUROFARMACOLOGIA I NEUROPATOLOGIA EXPERIMENTAL

INSTITUT D'INVESTIGACIONS BIOMÈDIQUES AUGUST PI I SUNYER (IDIBAPS)

Director: **Francesc Artigas Pérez**

Co-director: **Analía Bortolozzi Biassoni**

Doctorando:

Albert Ferrés i Coy

El presente trabajo ha sido financiado por los siguientes proyectos:

1. “Novel Methods leading to New Medications in Depression and Schizophrenia”, con código 115008 y financiado por IMI JU (Comisión Europea y Federación Europea de Industrias Farmacéuticas).

2. “Papel de la corteza infralímbica en depresión: conectividad funcional y desarrollo de un modelo animal”, con código SAF2012-35183 y financiado por el Ministerio de Economía y Competitividad, cofinanciado FEDER.

3. “Modulación de los genes asociados al sistema serotoninérgico con moléculas RNA antisentido (siRNA) y su efecto en modelos de Depresión”, con nº de expediente IDIBAPS 10/166 y financiado por nLife Therapeutics, Programa de Consorcios Estratégicos Nacionales en Investigación (CENIT) y Ministerio de Ciencia e Innovación.

4. “Papel de los canales de K en el mecanismo de acción de los fármacos antidepresivos. Relevancia del canal TREK-1 y su relación con el receptor de serotonina 1A”, con código PI10/00290 y financiado por el Instituto de Salud Carlos III, Ministerio de Economía y Competitividad y cofinanciada por el FEDER.

5. “K_{2P} Potassium Channels: A New Therapeutic Target for Mood and Cognitive Disorders”, con código 20003 y financiado por Brain and Behavior Research Foundation (NARSAD).

6. “Grupo de investigación consolidado, Neuroquímica y Neurofarmacología”, con código 2014SGR798 y financiado por la Generalitat de Catalunya.

Y ha sido realizado con la ayuda de la siguiente beca predoctoral:

Ayuda para la formación de profesorado universitario (FPU), con código AP2012-1066 y financiada por el Ministerio de Educación, Cultura y Deporte.

“El azar afortunado suele ser casi siempre el premio del esfuerzo perseverante”

Santiago Ramón y Cajal

Dedicat a la meva dona i al meu fill,

qui més estimo en aquest món,

per sempre.

Agraïments

Aquesta tesis no hauria estat possible sense l'ajuda, el suport i l'esforç de moltíssima gent. A tots vosaltres: els que sortiu més avall, els que no, els companys de feina, els excompanys, la família, els amics y els demés que no encaixeu en aquestes categories, moltes i moltes gràcies.

Concretament agraeixo molt als meus directors, l'Analía i el Paco, l'haver confiat amb mi, permetre'm participar en els seus projectes i oferint-me sempre la possibilitat d'aprendre d'ells. Analía, me has enseñado a hacer experimentos, luego a diseñarlos, y finalmente a transmitirlos a los que vinieron luego. Gracias por ello y por la motivación y energía que desprendes, que me engancharon. Paco, t'agreixo molt el teu tracte tan proper. Es molt reconfortant saber que la teva porta es sempre oberta quan un en té necessitat. Gracies!

Esther (¿va aquí esa "h"?), considera esta tesis también tuya. Tú me has acompañado en este viaje desde la primera clase en la facultad, hasta hoy. ¿Menuda paciencia tengo eh? Un trayecto estupendo al cual no le imagino mejor compañía. ¡Gracias! Y quién sabe, quizás algún día volvamos a compartir trayecto.

Mireia, l'Esther la pot considerar seva, si, igual que tu. M'ha encantat compartir quatre anys d'experiments amb un àngel com tu. Espero que tu també amb un dimoni com jo. Gracies per la teva empatia i la paciència infinita.

Amagades, elles van fent i no diuen res. Dues formiguetes, la Vero i la Leti, que ni elles ni jo sabem les hores invertides en aquestes pàgines. Gràcies

Sabeu bé que m'agrada molt explicar i ensenyar. Neus, Rubén i Diana, gracies al tres per donar-me l'oportunitat de fer-ho. Molta sort amb les vostres tesis.

Noe, Anna, Maria, Júlia, Mau, Pau i excompanys Laura, Mer, Laia i Eva, ha estat un plaer compartir laboratori amb vosaltres, xerrant, pensant protocols, discutint resultats i viatjant a congressos. Gràcies a tots per ser-hi.

Gràcies també als que porteu tota la vida al meu costat patint les meves frikades i neures: Canyi, Clara, Claudia, Dantí, Maria i Meri, els amics que voldria pel meu fill.

Abraçades també a tots els demés col·legues que fent birres o un cafè m'heu escoltat heroicament explicar-vos un experiment.

Finalment, un agraïment molt especial al meu germà i als meus pares, que m'han educat en l'esforç i el valor de les coses. Us estimo molt!

Feu tots molta bondat!

El disseny i la fotografia de la coberta és obra de Vanessa Serra Bonet i Alejandro Cañizares Moreno.

Contenido

Abreviaciones

1A-siRNA: siRNA contra el receptor 5-HT_{1A}

3'UTR: *3' untranslated region* (región 3' no traducida)

5-HT: *5-hydroxy tryptamine* (5-hidroxi triptamina - serotonina)

5-HT_{1A}: *5-HT 1A receptor* (receptor de serotonina 1A)

5-HT_{1B}: *5-HT 1B receptor* (receptor de serotonina 1B)

5-HTTLPR: *serotonin-transporter-linked polymorphic region* (región polimórfica asociada al transportador de serotonina)

8-OH-DPAT: *7-(Dipropylamino)-5,6,7,8-tetrahydronaphthalen-1-ol* (7-(dipropilamino)-5,6,7,8-tetrahidronaftalen-1-ol)

AChE: *acetylcholinesterase* (acetilcolinesterasa)

aCSF: *artificial cerebrospinal fluid* (líquido cefalorraquídeo artificial)

ACTH: *adrenocorticotropic hormone* (hormona adrenocorticotropa)

AMG: *amygdala* (amígdala)

AP: anteroposterior

BDNF: *brain-derived neurotrophic factor* (factor neurotrófico derivado del cerebro)

BrdU: *bromodeoxyuridine* (bromodesoxiuridina)

C-1A-siRNA: siRNA contra el receptor 5-HT_{1A} conjugado con sertralina

C-SERT-siRNA: siRNA contra el SERT conjugado con sertralina

cAMP: *cyclic adenosine monophosphate* (adenosina monofosfato cíclico)

CNS: *central nervous system* (sistema nervioso central)

CREB*: cAMP response element-binding protein* (proteína de unión a elemento de respuesta al cAMP)

CRH: *corticotropin-releasing hormone* (hormona liberadora de hormona adrenocorticotropa)

D3V: *dorsal third ventricle* (tercer ventrículo dorsal)

DA: *dopamine* (dopamina)

DAB: *3,3'-diaminobenzidine* (3,3'-diaminobencidina)

DAG: *diacylglycerol* (diacilglicerol)

DBH: *dopamine beta-hydroxylase* (dopamina beta-hidroxilasa)

DBS: *deep brain stimulation* (estimulación cerebral profunda)

DG: *dentate gyrus* (giro dentado)

DLB: *dark-light box* (caja luz-oscuridad)

DR: *dorsal raphe nucleus* (núcleo del rafe dorsal)

dsRNA: *double-stranded RNA* (RNA de doble hebra)

DV: dorsoventral

ECT: *electroconvulsive therapy* (terapia electroconvulsiva)

EPM: *elevated plus maze* (laberinto en cruz elevado)

FST: *forced swim test* (test de natación forzada)

GIRK: *G protein-coupled inwardly-rectifying potassium channel* (canales de potasio rectificadores internos acoplados a proteína G)

HPA: *hypothalamic-pituitary-adrenal axis* (eje hipotalámico-hipofisario-adrenal)

HPC: *hippocampus* (hipocampo)

HPLC: *high-performance liquid chromatography* (cromatografía líquida de alta resolución)

Hyp: *hypothalamus* (hipotálamo)

i.p.: intraperitoneal

IF: *immunofluorescence* (inmunofluorescencia)

IFNγ: *interferon gamma* (interferón gamma)

IHC: *immunohistochemistry* (inmunohistoquímica)

IP_3: *inositol trisphosphate* (inositol trifosfato)

ISH: *in situ hybridization* (hibridación *in situ*)

K_{2P}: *two-pore domain potassium channel* (canal de potasio con dos dominios de poro)

KCa: *calcium-activated potassium channel* (canal de potasio activado por calcio)

Kir: *inwardly rectifying potassium channel* (canal de potasio rectificador interno)

Kv: *voltage-gated potassium channel* (canal de potasio activado por voltaje)

LC: *locus coeruleus* (locus cerúleo)

MAO: *monoamine oxidase* (monoamino oxidasa)

MAOI: *monoamine oxidase inhibitor* (inhibidor de la monoamino oxidasa)

MBT: *marble burying test* (test de enterramiento de cánicas)

mGlu7: *metabotropic glutamate receptor 7* (receptor metabotrópico de glutamato 7)

mGlu2/3: *metabotropic glutamate receptor 2/3* (receptor metabotrópico de glutamato 2/3)

miRNA: *micro* RNA (micro RNA)

ML: mediolateral

MR: *median raphe nucleus* (núcleo del rafe medial)

mRNA: *messenger RNA* (RNA mensajero)

mPFC: *medial prefrontal cortex* (corteza prefrontal medial)

NAc: *nucleus accumbens* (núcleo accumbens)

ncRNA: *non-coding RNA* (RNA pequeño no codificante)

NE: *norepinephrine* (noradrenalina)

NERI: *norepinephrine reuptake inhibitor* (inhibidor selectivo de la recaptación de noradrenalina)

NET: *norepinephrine transporter* (transportador de noradrenalina)

NMDA: *N-methyl-D-aspartate* (N-metilo-D-aspartato)

NSFT: *novelty suppressed feeding test* (test de supresión de la ingesta por novedad)

OF: *open field* (campo abierto)

PBS: *phosphate-buffered saline* (tampón fosfato salino)

PDE4: *phosphodiesterase 4* (fosfodiesterasa 4)

PFA: *paraformaldehyde* (paraformaldehido)

PFC: *prefrontal cortex* (corteza prefrontal)

PIP_2: *phosphatidylinositol 4,5-bisphosphate* (fosfatidilinositol 4,5-bifosfato)

PKA: *protein kinase A* (proteína quinasa A)

PKC: *protein kinase C* (proteína quinasa C)

PKR: *protein kinase R* (proteína quinasa R)

PLC: *fosfolipase C* (fosfolipasa C)

pre-miRNA: *precursor-miRNA* (precursor de miRNA)

pri-miRNA: *primary miRNA* (miRNA primario)

PSD95: *postsynaptic density protein 95* (proteína de densidad postsináptica 95)

PVN: *paraventricular nucleus* (núcleo paraventricular)

Reb-TASK3-siRNA: siRNA contra TASK3 conjugado con reboxetina

RISC: *RNA-induced silencing complex* (complejo silenciador inducido por RNA)

RNAi: *RNA interference* (RNA interferente)

ROD: *relative optical density* (densidad óptica relativa)

Ser-TASK3-siRNA: siRNA contra TASK3 conjugado con sertralina

SERT: *serotonin transporter* (transportador de serotonina)

SERT-siRNA: siRNA contra el SERT

shRNA: *short hairpin RNA* (RNA corto en horquilla)

siRNA: *small interfering RNA (*RNA pequeño de interferencia)

SNP: *single-nucleotide polymorphism* (polimorfismo de nucleótido único)

SNRI: *serotonin-norepinephrine reuptake inhibitor* (inhibidor dual de la recaptación de serotonina y noradrenalina)

SSRI: *selective serotonin reuptake inhibitor* (inhibidor selectivo de la recaptación de serotonina)

ssRNA: *single-stranded RNA* (RNA de cadena simple)

TALK: *TWIK-related alkaline-activated K^+ channel* (canal de potasio activado por alcalinidad semejante a TWIK)

TASK: *TWIK-related acid-sensing K^+ channel* (canal de potasio sensor de ácido semejante a TWIK)

TASK3-siRNA: siRNA contra el TASK3

TCA: *tricyclic antidepressant* (antidepresivo tricíclico)

TH: *tyrosine hydroxylase* (tirosina hidroxilasa)

THIK: *TWIK-related halothane-inhibited K^+ channel* (canal de potasio inhibido por halotano semejante a TWIK)

TLR: *toll-like receptor* (receptor similar a toll)

TNFα: *tumor necrosis factor alpha* (factor de necrosis tumoral alfa)

TPH: *tryptophan hydroxylase* (triptófano hidroxilasa)

TREK: *TWIK-related K^+ channel* (canal de potasio semejante a TWIK)

TRESK: *TWIK-related spinal cord K^+ channel* (canal de potasio de médula espinal semejante a TWIK)

TrkB*: tropomyosin receptor kinase B* (receptor tropomiosina quinasa B)

TST: *tail suspension test* (test de suspensión de la cola)

TWIK: *tandem pore domain weak inwardly rectifying K^+ channel* (canal de potasio rectificador interno débil con dominio de poro en tándem)

UCMS: *unpredictable chronic mild stress* (estrés leve crónico impredecible)

VMAT2: *vesicular monoamine transporter 2* (transportador vesicular de monoaminas 2)

β-Gal-128: siRNA contra la β-galactosidasa

1. Introducción

1.1. Depresión

La depresión mayor es una enfermedad devastadora con una prevalencia a lo largo de la vida que puede llegar hasta el 10% y 20% para hombres y mujeres, respectivamente (Berton and Nestler, 2006). Según la Organización Mundial de la Salud afecta directamente a 350 millones de personas en todo el mundo y su incidencia va en aumento (Smith, 2014). Asimismo, un estudio global indica un aumento del 37% de la incapacidad debida a depresión entre 1990 y 2010, siendo la 11ª causa de incapacidad a nivel mundial (Murray et al., 2012). No solo afecta al propio paciente, sino también a los familiares y personas más cercanas. La depresión es la patología psiquiátrica con mayor repercusión socioeconómica. En su último estudio publicado sobre el impacto de las enfermedades del cerebro, *el European Brain Council* estima que éstas cuestan a los europeos un total de 797.000 millones de €, de los que 113.000 millones corresponden a los trastornos depresivos (Gustavsson et al., 2011; Smith, 2011). Los elevados costos derivados de la depresión se deben a su alta incidencia, duración de los episodios depresivos, aparición en etapas productivas de la vida y a la baja eficacia de los fármacos antidepresivos (Wittchen et al., 2010).

La sintomatología clínica central se caracteriza por un bajo estado de ánimo, anhedonia y fatiga. Otros síntomas que suelen presentar los pacientes con depresión son alteraciones del sueño, alteraciones motoras, pesimismo, sentimiento de culpa, baja autoestima, dificultad para concentrarse y pensamientos recurrentes de muerte. Según la cuarta edición del manual diagnóstico y estadístico de los trastornos mentales (DSM-IV), el diagnóstico requiere la presencia de 5 de los síntomas mencionados durante 2 semanas, siendo al menos uno de ellos el bajo estado anímico o anhedonia (Wong and Licinio, 2004). En base a la sintomatología se definen varios subtipos de depresión: depresión melancólica, depresión reactiva, depresión psicótica, depresión atípica y distimia (Akiskal, 2000; Blazer, 2000; Nestler et al., 2002).

A pesar de la elevada prevalencia de la depresión, el conocimiento fisiopatológico así como las bases moleculares que subyacen a la patología continúan siendo en la actualidad poco conocidas (Krishnan and Nestler, 2008; Duman, 2014). No obstante, se han identificado diversos factores ambientales que aumentan la susceptibilidad de padecer depresión, incluyendo los traumas emocionales y el estrés, el funcionamiento inapropiado del sistema inmunitario innato, fluctuaciones en los niveles de estrógenos y progesterona y alteraciones de los sistemas gastrointestinal y cardiovascular (ver figura 1) (Kessler, 1997; Duman et al., 2016).

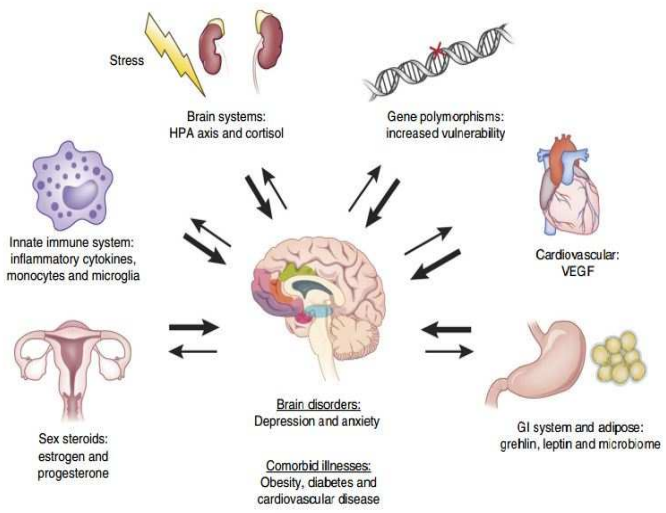

Figura 1. Factores de susceptibilidad que predisponen a la depresión. La heterogeneidad de la depresión resulta de uno o más determinantes patológicos (estrés, sistema inmunitario innato, fluctuaciones de los esteroides ováricos, el sistema gastrointestinal, el tejido adiposo, el sistema cardiovascular y polimorfismos génicos) que contribuyen en menor o mayor medida a incrementar la incidencia de la depresión así como las enfermedades asociadas o comorbidas. Adaptada de Duman et al., 2016.

Los estudios familiares y de gemelos han acumulado considerables evidencias de que mecanismos genéticos complejos están involucrados en la vulnerabilidad de los trastornos depresivos (Kendler, 1998; Malhi et al., 2000). El parentesco de primer grado con un individuo con depresión incrementa alrededor de tres veces el riesgo de desarrollar la enfermedad. En general, estudios de gemelos adultos depresivos sugieren que los genes y los factores ambientales específicos son fundamentales y que los factores ambientales compartidos, aunque relevantes en ciertos subtipos de depresión de menor gravedad, son posiblemente de menor importancia (Lyons et al., 1998; McGuffin et al., 1996; Kendler, 1999; Silberg et al., 1999). La heredabilidad de la depresión parece ser notable, con estimaciones de entre el 40% y el 70% (McGuffin et al., 2003; Lesch, 2004). De este modo, la carga genética contribuye a desencadenar adaptaciones moleculares y celulares que generaran vulnerabilidad o resiliencia frente a las perturbaciones ambientales (Russo et al., 2012; Schratt, 2014).

Se han identificado polimorfismos que incrementan el riesgo de padecer depresión en genes responsables del control de la fracción activa de serotonina (5-HT; *5-hydroxy tryptamine*). Por ejemplo, en el gen del transportador de serotonina (SERT; *serotonin transporter*) se ha identificado la región polimórfica asociada al transportador de serotonina (5-HTTLPR; *serotonin-transporter-linked polymorphic region*), que consiste en una inserción de 44 pares de bases (L) o su eliminación (S) (Caspi et al., 2003). Los alelos L y S del 5-HTTLPR tienen distintas eficiencias transcripcionales, produciendo el alelo L mayores niveles de proteína SERT que el S. Estudios de asociación han mostrado que la expresión y función reducidas del SERT, resultado del alelo S, están asociadas con ansiedad y depresión (Lesch et al., 1996; Karg et al., 2011; Haenisch et al., 2013). Además, se ha observado interacción del 5-HTTLPR con los tratamientos antidepresivos, vinculándose el alelo S con resistencias (Murphy et al., 2004; Serreti et al., 2007; Outhred et al., 2014) y el L con mejores respuestas (Yu et al., 2002; Serretti et al., 2007; Porcelli et al., 2012).

Otro polimorfismo de especial interés en esta Tesis es el polimorfismo de nucleótido único (SNP; *single-nucleotide polymorphism*) G(-1019)C del gen que codifica para el receptor de serotonina 1A (5-HT_{1A}; *5-HT 1A receptor*). La presencia del alelo G en lugar del C, produce la disrupción del sitio de unión del factor de transcripción NUDR de represión de la expresión del receptor 5-HT_{1A} (Lemonde et al., 2003; Le François et al., 2008; Fakra et al., 2009). Aunque observaciones iniciales han sugerido que este polimorfismo puede controlar la expresión y función del autoreceptor 5-HT_{1A} sin afectar los niveles de los receptores postsinápticos 5-HT_{1A} (Lemonde et al., 2003), estudios de neuroimagen mostraron que ambos receptores están afectados (Parsey et al., 2006). En cualquier caso, la presencia del alelo G se relaciona con un incremento de la frecuencia de sintomatología depresiva y menor respuesta a los tratamientos antidepresivos (Lemonde et al., 2003, 2004; Serreti et al 2004).

Otros polimorfismos que se han asociado con mayor incidencia de depresión son el haplotipo GAACC del SNP rs3770018 del gen de la fosfodiesterasa 11A (Wong et al., 2006), al menos 6 SNPs en el gen del factor neurotrófico derivado del cerebro (BDNF; *brain-derived neurotrophic factor*) (Lang et al., 2005; Schumacher et al., 2005; Chen

et al., 2006; Frodl et al., 2007; Ribeiro et al., 2007; Licinio et al., 2009; Verhagen et al., 2010), el SNP A(218)C en el gen de la triptófano hidroxilasa (TPH; tryptophan hydroxylase) (Tsai et al., 1999) o el SNP G(861)C del gen del receptor de serotonina 1B (5-HT_{1B}; *5-HT 1B receptor*) (Huang et al., 2003).

Por tanto, la depresión está asociada con: i) patologías relacionadas con estrés y sistema inmunitario, ii) polimorfismos en circuitos cerebrales que regulan la emoción y cognición y, iii) con alteraciones estructurales y de la plasticidad sináptica (Nestler et al., 2002, 2014; Russo and Nestler, 2013; Ota and Duman, 2013). La literatura referida a los estudios de imagen cerebral y asociación con depresión es extensa y ha sido revisada en detalle (Savitz and Drevets, 2009). Brevemente, los estudios de neuroimagen en pacientes con depresión revelaron reducciones regionales en el volumen de numerosas áreas del sistema nervioso central (CNS; *central nervous system*) así como reducciones de la señal BOLD (*blood oxigen level-dependent*) durante la ejecución de una tarea específica. Entre las áreas cerebrales se incluyen la corteza prefrontal medial (mPFC; *medial prefrontal cortex*), hipotálamo (Hyp; *hypothalamus*), hipocampo (HPC; *hippocampus*), estriado, núcleo accumbens (NAc; *nucleus accumbens*), amígdala (AMG; *amygdala*) y tálamo, áreas implicadas en el comportamiento emocional y cognitivo (Drevets, 2001; Liotti and Mayberg, 2001; Sacher et al., 2012). Además, en estudios utilizando cerebros de seres humanos post-mortem se han descrito: 1) alteraciones de la expresión de genes implicados en la función sináptica y la neuroplasticidad como BDNF y la proteína de unión a elemento de respuesta al cAMP (CREB; *cAMP response element-binding protein*), 2) reducción de la densidad sináptica, 3) reducción de la densidad glial y 4) disminución de la arborización dendrítica principalmente en las mismas áreas cerebrales mencionadas (Duman et al., 2000, 2016; Manji et al., 2001; Krishnan and Nestler, 2008). Todas estas áreas cerebrales están, en mayor o menor grado, altamente interconectadas, recibiendo todas ellas inervación de los sistemas monoaminérgicos (sitio principal de acción los fármacos antidepresivos) formando en conjunto una compleja circuitería involucrada en la fisiopatología y tratamiento de la depresión (Nestler et al., 2002).

Desde mediados del siglo pasado se han postulado diferentes hipótesis acerca de la depresión. Estas incluyen: 1) monoaminérgica, 2) neuroendocrina, 3) neurotrófica y 4) glutamatérgica. Cada una de ellas contempla ciertos aspectos de la fisiopatología de la depresión. Éstas no son excluyentes, por el contrario están relacionadas entre sí y ayudan a entender la vasta complejidad de esta enfermedad.

1.1.1. Hipótesis Monoaminérgica

Los dos primeros fármacos antidepresivos de la historia fueron la iproniazida (de la familia de los inhibidores de la monoamino oxidasa, MAOI; *monoamine oxidase inhibitor*) y la imipramina (perteneciente a los antidepresivos tricíclicos, TCA; *tricyclic antidepressant*), y ambos actúan como moduladores de los sistemas monoaminérgicos. Conjuntamente con el descubrimiento de la acción depresógena de la reserpina (Brodie et al., 1957), contribuyeron a postular la hipótesis catecolaminérgica de la depresión (Schildkraut, 1965), en la que se describe el déficit de dopamina (DA; *dopamine*) y noradrenalina (NE; *norepinephrine*) como causa subyacente de la depresión. Posteriormente en 1967, Coppen postuló un enfoque mucho más serotoninérgico (Coppen, 1967), basándose en que la administración del aminoácido triptófano (precursor de la síntesis de 5-HT) potenciaba los efectos terapéuticos de los MAOI (Coppen et al., 1963). La hipótesis serotoninérgica se ve reforzada con la aparición de los inhibidores selectivos de la recaptación de serotonina (SSRI; *selective serotonin reuptake inhibitor*) en los años 70. Finalmente en 1977, la hipótesis monoaminérgica de la depresión postula una hipofunción generalizada de los sistemas monoaminérgicos (5-HT, NE y DA) como base etiológica de la depresión (de Montigny, 1977).

1.1.2. Hipótesis Neuroendocrina

Uno de los principales factores que aumenta la vulnerabilidad a la depresión es la exposición crónica a situaciones de estrés o la incapacidad de afrontarlo adecuadamente (Kessler, 1997). El estrés es un mecanismo necesario para la supervivencia del individuo e implica la activación del sistema nervioso autónomo y del eje hipotalámico-hipofisario-adrenal (HPA; *hypothalamic-pituitary-adrenal axis*).

Durante el estrés se libera la hormona liberadora de hormona adrenocorticotropa (CRH; *corticotropin-releasing hormone*) desde el núcleo paraventricular (PVN; *paraventricular nucleus*) del Hyp, que a su vez estimula la producción y regula la liberación de hormona adrenocorticotropa (ACTH; *adrenocorticotropic hormone*) por parte de la glándula pituitaria (hipófisis) (Antoni, 1986). Finalmente, la ACTH estimula la síntesis de cortisol (glucocorticoide en seres humanos equivalente a la corticosterona en roedores) en la corteza adrenal. La actividad del eje HPA está controlada por la inhibición que el propio cortisol ejerce sobre la liberación de CRH (ver figura 2) (Herman and Cullinan, 1997). El cortisol interviene en diversos procesos fisiológicos como la modulación del metabolismo incrementando la disponibilidad de carbohidratos en sangre (activa las vías de gluconeogénesis y de glucogenólisis hepática) y la supresión de la acción del sistema inmunológico (acción antiinflamatoria) (Kino and Chrousos, 2005). Además, el cortisol también estimula la función hipocampal general facilitando las funciones cognitivas y el aprendizaje. No obstante, un incremento sostenido de cortisol puede producir atrofia hipocampal (Sapolsky, 2000).

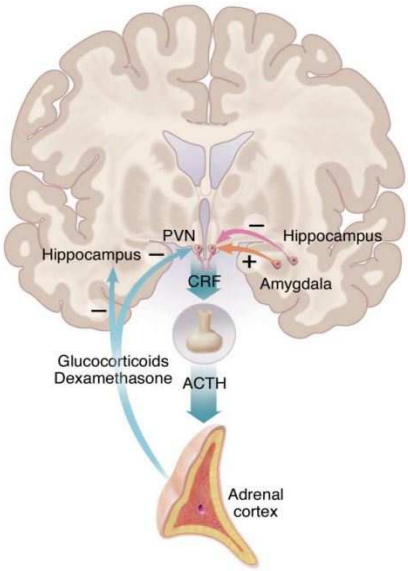

Figura 2. Regulación del eje HPA. El PVN integra las entradas excitatorias procedentes de la AMG e inhibitorias del HPC sobre las neuronas productoras de CRH. Otros inputs importantes que no se muestran en la figura son los procedentes de los sistemas monoaminérgicos. Obtenido de Nestler et al., 2002.

Alrededor del 40% - 60% de los pacientes con depresión no medicados presentan niveles elevados de cortisol y CRH en sangre (sobreactivación del eje HPA) (Gold and Chrousos, 1985; Murphy, 1991), variables que se normalizan después del tratamiento antidepresivo (Sachar and Baron, 1979; Arborelius et al., 1999; Holsboer, 2001; Parker et al., 2003; de Kloet et al., 2005; Vreeburg et al., 2009). El aumento sostenido de glucocorticoides en sangre se ha vinculado con la disminución de la proliferación celular (Gould et al., 1998), neurogénesis (Fuchs and Gould, 2000; Yu et al., 2010) y plasticidad sináptica (McEwen, 1999) en el HPC, conduciendo a una disminución del

volumen hipocampal y las alteraciones cognitivas asociadas a la depresión (Sheline et al., 2003). Es más, la atrofia hipocampal conlleva una reducción del control inhibitorio que esta área ejerce sobre el eje HPA, retroalimentando positivamente los niveles de cortisol en sangre (ver figura 2) (Nestler et al., 2002).

1.1.3. Hipótesis Neurotrófica

Esta hipótesis propone que la alteración de los mecanismos de neuroplasticidad subyace la fisiopatología de la depresión. La misma plantea que la vulnerabilidad al estrés y la acción terapéutica de los antidepresivos ocurren a través de mecanismos intracelulares que disminuyen o incrementan la expresión de factores tróficos, respectivamente (Duman et al., 1997; Jacobs et al., 2000; Duman, 2004).

Estudios preclínicos en roedores han demostrado que la exposición crónica al estrés disminuye la expresión de BDNF y del receptor tropomiosina quinasa B (TrkB; *tropomyosin receptor kinase B*) en áreas cerebrales relacionadas con la depresión tales como la corteza prefrontal (PFC; *prefrontal cortex*) y el HPC (Smith et al., 1995; Nibuya et al., 1995, 1999; Duman, 2004; Holtmaat and Svoboda, 2009). Esto podría deberse a que el estrés incrementa los niveles de glucocorticoides y de interleukina 1β, quienes regularían negativamente la

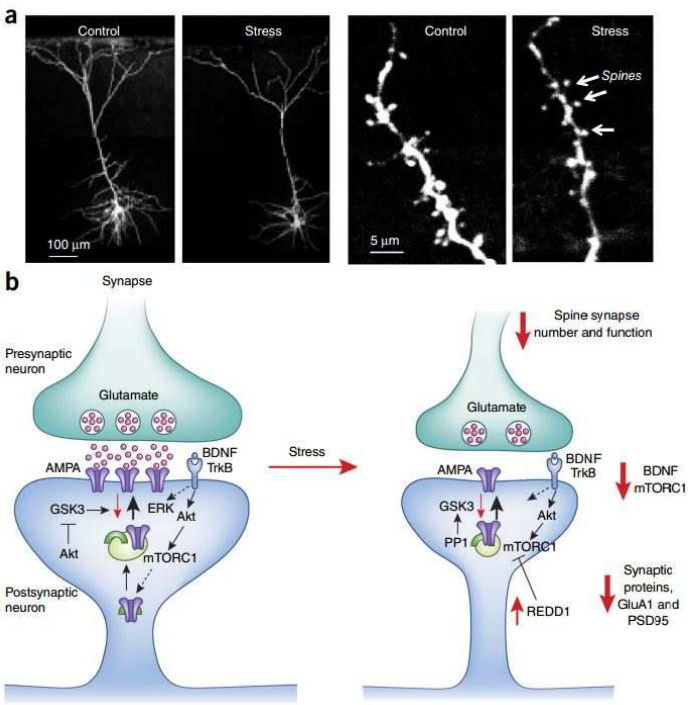

Figura 3. El estrés crónico causa atrofia neuronal y disminución del número de espinas sinápticas. (a) Efecto de la inmovilidad crónica repetida durante 7 días en la mPFC de ratón. El panel de la izquierda muestra reducción en longitud de las dendritas apicales (stress) y el panel de la derecha la disminución del número de espinas sinápticas (stress) en comparación con los controles. (b) En condiciones normales la neurotransmisión glutamatérgica activa vías de señalización intracelular (BDNF y mTORC1) esenciales para la maduración e incremento del número de sinapsis. El estrés crónico disminuye esta señalización inhibiéndose la síntesis de proteínas sinápticas, contribuyendo a la pérdida de espinas. Adaptado de Duman et al., 2016.

expresión de BDNF (Smith et al., 1995; Duman, 2004). En condiciones normales la neurotransmisión glutamatérgica es imprescindible para la formación y mantenimiento de las conexiones sinápticas, que a través de la señalización por BDNF activa mTORC1, quien a modo de sensor integra toda la actividad eléctrica promoviendo la síntesis de proteínas sinápticas como GluA1 y la proteína de densidad postsináptica 95 (PSD95; *postsynaptic density protein 95*). La función y el número de espinas sinápticas se ven reducidas durante situaciones de estrés y en la depresión (ver figura 3) (Pittenger and Duman, 2008; Duman and Aghajanian, 2012; Duman et al., 2016). No obstante, la acción del BDNF podría ser diferente e incluso opuesta en otras áreas cerebrales. El mejor ejemplo es el circuito dopaminérgico mesolímbico comprendido por el área tegmental ventral y el NAc, en el cual el estrés crónico incrementa la expresión de BDNF. Mientras que la infusión local de BDNF en este circuito tiene un efecto depresógeno, el bloqueo de la función del BDNF tiene efecto antidepresivo (Berton et al., 2006).

Además, se ha reportado que la neurogénesis hipocampal, definida como la progresión de células progenitores a neuronas granulares integradas en el giro dentado (DG; *dentate gyrus*), es clave en la fisiopatología de la depresión así como en los tratamientos antidepresivos (Zhao et al., 2008). Mientras que el ejercicio físico o el aprendizaje pueden estimular la generación de nuevas neuronas en el HPC adulto, el estrés agudo y crónico actuarían en sentido contrario (van Praag et al., 2000; Warner-Schmidt and Duman, 2006). En roedores, la exposición a diferentes tipos de estrés provoca la reducción de la expresión de BDNF impactando negativamente sobre la proliferación celular y neurogénesis (Gould et al., 1997; McEwen, 1999; Duman et al., 2001; Malberg and Duman, 2003; Dranovsky and Hen, 2006; Warner-Schmidt and Duman, 2006). Este efecto puede ser revertido por tratamientos antidepresivos incluyendo los SSRI, los inhibidores duales de la recaptación de serotonina y noradrenalina (SNRI; *serotonin-norepinephrine reuptake inhibitor*), los antagonistas no competitivos del receptor N-metilo-D-aspartato (NMDA; *N-methyl-D-aspartate*) como la ketamina, la estimulación cerebral profunda (DBS; *deep brain stimulation*), y la terapia electroconvulsiva (ECT; *electroconvulsive therapy*), entre otros. Estos tratamientos incrementan no solo el número de células progenitores en

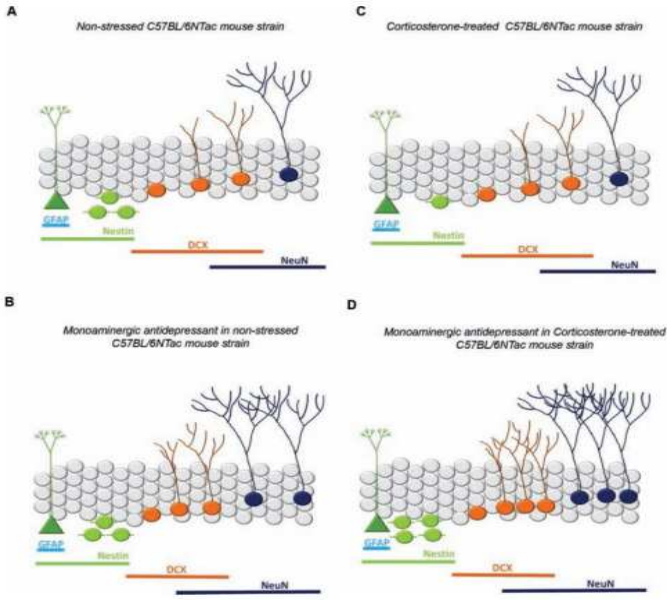

Figura 4. El tratamiento antidepresivo estimula la neurogénesis y la maduración dendrítica. Anatomía y estadios funcionales durante la diferenciación y maduración neuronal, incluyendo la glía radial (verde), progenitores neuronales (verde claro), neuronas granulares inmaduras (naranja) y neuronas maduras (azul), en ratones *wild-type* no estresados no tratados (a) o tratados (b), como también en ratones *wild-type* estresados no tratados (c) o tratados (d). Notar el efecto de la administración de corticosterona (modelo estrés crónico) en la proliferación de los progenitores y el efecto del tratamiento antidepresivo en el número y arborización de las neuronas granulares inmaduras y maduras. Adaptado de David et al., 2010.

el DG sino también el número de nuevas neuronas potenciando además la arborización dendrítica de las mismas (ver figura 4) (Madsen et al., 2000; Malberg and Duman, 2003; Toda et al., 2008; David et al., 2009; Inta et al., 2013). De modo que, una de las características fundamentales de un tratamiento antidepresivo crónico es que sea capaz de promover la neurogénesis y la supervivencia de las nuevas neuronas así como generar contactos sinápticos funcionales en áreas cerebrales que incluyen el HPC y PFC. Esto, en parte se logra a través de la señalización mediada por BDNF y activación del receptor TrkB (Santarelli et al., 2003; Li et al., 2008).

Estudios post-mortem en pacientes con depresión víctimas de suicidio han mostrado una reducción de la expresión de BDNF y TrkB en la PFC e HPC (Dwivedi et al., 2003; Karege et al., 2005; Pandey et al., 2008). Contrariamente, pacientes que reciben tratamiento antidepresivo no presentan niveles disminuidos de BDNF en la PFC o HPC en comparación a los controles en el momento de morir (Chen et al., 2001, Karege et al., 2005). Además, los niveles plasmáticos de BDNF en pacientes con depresión y que no reciben tratamiento son inferiores comparados con sujetos controles y pacientes medicados (Shimizu et al., 2003; Lee et al., 2007; Lee et al., 2008). Estudios de neuroimagen han establecido una correlación entre la reducción del volumen hipocampal con la frecuencia de los episodios depresivos y el tiempo que la depresión permanece sin tratar (Drevets, 2001; Videbech and Ravnkilde, 2004). Aunque en parte esto podría ser consecuencia de la reducción del volumen glial

(Czéh and Lucassen, 2007), estudios histológicos han mostrado que pacientes con depresión que reciben tratamiento antidepresivo tienen mayor número de progenitores neuronales (células positivas por nestina y Ki-67) que los individuos no tratados o los sujetos controles (Boldrini et al., 2009, 2012).

1.1.4. Hipótesis Glutamatérgica

Durante los últimos años se han ido acumulando evidencias del sistema glutamatérgico como diana de la fisiopatología del estrés, depresión y tratamiento antidepresivo (Paul and Skolnick, 2003; Sanacora et al., 2003; Duman et al., 2016). Hace ya más de 20 años se observó que el uso crónico de antagonistas del receptor glutamatérgico NMDA en roedores tiene efectos antidepresivos (Trullas and Skolnick, 1990; Skolnick et al., 1996). Además, se ha descrito una reducción de la densidad glial en áreas cerebrales tales como la PFC o AMG en pacientes con depresión (Ongür el al., 1998; Cotter et al., 2002; Hamidi et al., 2004), hecho que altera la homeostasia de la neurotransmisión glutamatérgica. Aunque se requiere la activación de los receptores NMDA para facilitar la plasticidad sináptica, el exceso de glutamato extracelular produciría efectos neurotóxicos, activando entre otros al receptor metabotrópico de glutamato 2/3 (mGluR2/3; *metabotropic glutamate receptor 2/3*) que inhibe la propia neurona presináptica y activando también los receptores NMDA extrasinápticos que favorecen la reducción de la arborización (Kugaya and Sanacora, 2005). La atrofia de las neuronas y la pérdida de sinapsis glutamatérgicas contribuirían a la sintomatología de la depresión (Duman et al., 2016).

Más evidencias de la relación entre depresión con sistema glutamatérgico y PFC se han obtenido con el uso de antidepresivos de acción rápida en seres humanos. Por ejemplo, se han observado respuestas antidepresivas muy rápidas con la DBS en el área de Broodmann 25 de la PFC (Mayberg et al., 2005; Puigdemont et al., 2012), área con alta conectividad con muchas áreas subcorticales incluyendo los núcleos monoaminérgicos. Estudios preclínicos aplicando DBS en la mPFC han mostrado también efecto antidepresivo en roedores, hecho que se acompaña con la elevación de la neurotransmisión glutamatérgica y monoaminérgica (Hamani et al., 2010; Perez-Caballero et al., 2014; Jiménez-Sánchez et al., 2016a, 2016b).

Efectos antidepresivos muy rápidos se han obtenido también con la administración intravenosa o intranasal del antagonista no competitivo del receptor NMDA ketamina en pacientes con depresión resistentes a tratamiento (Berman et al., 2000; Zarate et al., 2006, 2012; Diazgranados et al., 2010; Lapidus et al., 2014). Se cree que el mecanismo de acción de la ketamina sería promover la neurotransmisión glutamatérgica. Esto podría suceder indirectamente mediante el bloqueo de los receptores NMDA en las interneuronas GABAérgicas, desinhibiendo así la actividad de las neuronas piramidales y la transmisión glutamatérgica (ver figura 5) (Homayoun and Moghaddam, 2007; Li et al., 2010). El aumento de glutamato, activaría entonces los receptores AMPA quienes a través de la señalización con BDNF activarían mTORC1, incrementando la síntesis de proteínas requeridas para la formación de nuevas sinapsis. De esta manera, la rápida inducción de la sinaptogénesis revertiría la pérdida de conexiones y arborización sináptica descrita en los individuos con depresión, rehabilitando así la función de la PFC e incrementando su conectividad con otras estructuras límbicas (Duman and Aghajanian, 2012; Kang et al., 2012; Murrough et al., 2015).

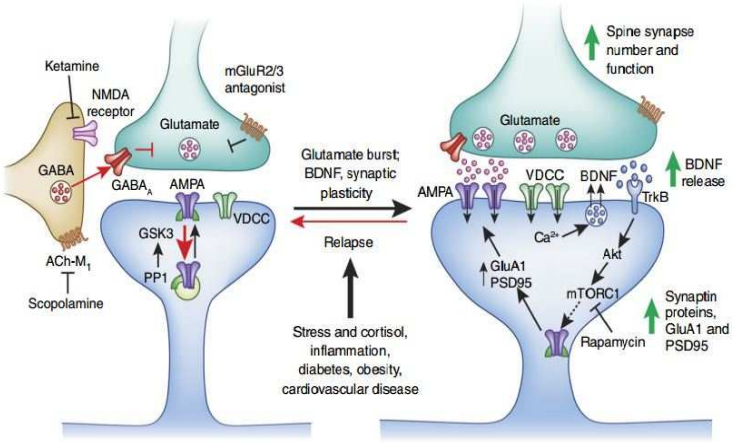

Figura 5. Mecanismo de acción de la ketamina a nivel del PFC. La ketamina causaría un aumento del glutamato sináptico mediante el bloqueo de los receptores NMDA en neuronas GABAérgica, desinhibiendo las neuronas glutamatérgicas. El glutamato liberado estimularía los receptores AMPA en neuronas postsinápticas y activando canales de voltaje dependientes de Ca^{2+} (VDCC). Esto induce la liberación de BDNF y activación de TrkB y Akt, activando la señalización mTORC1 conduciendo a un incremento de la síntesis de proteínas necesarias para la formación y maduración de las sinapsis, como PSD95 o GluA1. La escopolamina, a través del bloqueo del receptor colinérgico muscarínico M_1, también induciría desinhibición glutamatérgica y efecto antidepresivo de acción rápida. Adaptado de Duman et al., 2016.

1.2. Modelos animales de depresión asociados a estrés

El estrés es un factor importante que subyace la sintomatología depresiva y juega un papel clave en la manifestación de los primeros episodios. Aun así, es difícil pensar que la exposición a situaciones de estrés como el dolor o el miedo en roedores pueda generar la vasta complejidad y variabilidad de la depresión humana. Más complicado resulta imitar síntomas como los pensamientos recurrentes de muerte o sentimientos de culpa. Sin embargo y a pesar de ello, síntomas como la anhedonia o pérdida de placer e incluso alteración de la neurogénesis y disminución de la expresión de factores neurotróficos pueden desarrollarse en animales de experimentación sometidos a factores estresantes.

A grandes rasgos, la sintomatología de tipo "depresiva" que desarrollan los animales sometidos a diferentes modelos de depresión asociados a estrés crónico incluye bajo estado anímico y anhedonia. El bajo estado anímico puede ser evaluado mediante el test de suspensión de la cola (TST; *tail suspension test*) en ratón o el test de natación forzada (FST; *forced swim test*) en rata y ratón. En ellos, los roedores con síntomas de tipo depresivo presentan un mayor tiempo de inmovilidad que los "no deprimidos", reflejando así la menor capacidad de lucha frente a situaciones inescapables (Cryan and Holmes, 2005; Cryan et al., 2005a, 2005b). Además, el TST y el FST también son modelos de estrés agudo ampliamente aceptados como herramientas para evaluar la eficacia de gran cantidad de tratamientos antidepresivos (Porsolt et al., 1977; Steru et al., 1985; Cryan and Slattery, 2007; O'Leary and Cryan, 2013). Por otra parte, la anhedonia en los roedores puede ser evaluada mediante la prueba de la preferencia por la sacarosa, en el que el animal puede elegir consumir agua normal o agua azucarada (Eagle et al., 2016).

Experiencias estresantes durante el desarrollo temprano pueden producir efectos de larga duración en el cerebro humano y en la capacidad de responder al estrés en la

vida adulta. De hecho, el maltrato físico y emocional durante la infancia se ha vinculado a un mayor riesgo de padecer depresión en el adulto (Heim and Nemeroff, 2001; Kaufman and Charney, 2001; Vythilingam et al., 2002). En un intento de obtener un modelo animal capaz de contemplar estas situaciones, los roedores pueden ser sometidos a condiciones de estrés prenatal o de separación materna que conducen al desarrollo de efectos tipo depresivos cuando alcanzan la madurez (Kaufman et al., 2000). En el primero de ellos, la hembra gestante es expuesta a un factor de estrés como la inmovilidad repetida durante varias semanas, mientras que el segundo caso la progenie se separa intermitentemente de la madre durante las 2 o 3 primeras semanas de vida (Pryce and Feldon, 2003; Maccari and Morley-Fletcher, 2007). Estas intervenciones inducen un comportamiento de tipo depresivo y cambios fisiopatológicos en la camada, como por ejemplo incremento de los niveles de CRH y ACTH, y disminución de los niveles del RNA mensajero (mRNA; messenger RNA) de BDNF en la PFC (Alonso et al., 1991; Ladd et al., 1996; Francis et al., 1999; Maccari et al., 2003; Roceri et al., 2004; Pollak et al., 2010).

Por otro lado, la exposición repetida a situaciones de estrés en la edad adulta es uno de los factores de mayor predisposición a la depresión. Los modelos animales de estrés crónico incluyen: descarga eléctrica en las patas, inmovilización crónica, estrés leve crónico impredecible (UCMS; *unpredictable chronic mild stress*), indefensión aprendida, paradigma del residente-intruso y consumo crónico de corticosterona (Overmier and Seligman, 1967; Willner, 1997; Rasmusson et al., 2002; Cryan and Slattery, 2007; Veena et al., 2009; Gourley and Taylor, 2009; Chaouloff, 2013). Los modelos de descarga eléctrica en las patas y de inmovilización crónica se logran después de una presentación repetida del mismo factor estresante a lo largo de varios días o semanas. Estos producen, por ejemplo, depleción de los niveles de monoaminas, atrofia de las dendritas en la PFC y el HPC así como disminución de la neurogénesis y de la expresión de BDNF en el DG del HPC (Weiss et al., 1981; Rasmusson et al., 2002; Pham et al., 2003; Cook and Wellman, 2004; Murakami et al., 2005). De modo similar, en el UCMS, los animales se exponen diariamente a un factor estresante que cambia cada día de modo aleatorio. Esto produce efectos de tipo depresivo como anhedonia, incremento del tiempo de inmovilidad en el TST y el FST,

incremento de los niveles de glucocorticoides y BDNF en suero o reducción de la neurogénesis en el DG del HPC, entre otros (Muscat and Willner, 1992; Alonso et al., 2004; Mineur et al., 2006; Jindal et al., 2013). Este modelo ha sido originalmente evaluado en ratas, de modo que la literatura disponible, aunque abundante para rata es relativamente limitada en ratón. Además, los resultados a veces son contradictorios, complicando establecer un perfil claro de este modelo en ratón. Estas discrepancias se pueden atribuir en parte al hecho que las distintas cepas de ratón presentan diferente susceptibilidad al UCMS (Mineur et al., 2006; Nollet et al., 2013).

En el modelo de indefensión aprendida, se someten los animales a un estímulo eléctrico inescapable que, una vez habituados, hace que desarrollen cierta indefensión que se pone de manifiesto cuando fracasan al intentar escapar cuando sí podrían hacerlo. Se trata de un modelo validado especialmente para ratas produciendo síntomas de tipo depresivo como déficits cognitivos, anhedonia y reducción de la expresión de BDNF en el HPC (Willner, 1991; Vollmayr et al., 2001; Song et al., 2006; Enkel et al., 2010), siendo menos caracterizado en ratones (Vollmayr and Henn, 2001; Chourbaji et al., 2005).

El paradigma del residente-intruso se basa en el hecho que un animal establece una territorialidad en un espacio (residente) y ataca al animal desconocido introducido (intruso). Los intrusos muestran un comportamiento defensivo en respuesta a los ataques. La exposición repetida del mismo intruso a distintos residentes cada día es una tipo de estés social que induce efectos de tipo depresivo en rata y ratón como incremento del tiempo de inmovilidad en el FST, anhedonia, hiperactividad del eje HPA y disminución de la proliferación en el DG del HPC (Kudryavtseva et al., 1991; Rygula et al., 2006; Yap et al., 2006; Becker et al., 2008).

Sin bien todos estos modelos logran reproducir algunos de los síntomas depresivos en ratones, todos ellos se basan en el estrés ambiental y requieren de una manipulación del entorno, generando una gran variabilidad de protocolos entre laboratorios que dificulta su replicación (David et al., 2010). De este modo, el modelo

por consumo crónico de corticosterona, es más fácilmente replicable. La corticosterona es una hormona producida en las glándulas adrenales en respuesta al estrés y los niveles plasmáticos de la misma se encuentran elevados en varios de los modelos de roedores de depresión como la inmovilización crónica, el paradigma del residente-intruso o el FST. Además, estudios en seres humanos ponen de manifiesto que la depresión habitualmente está asociada a la disfunción del eje HPA con la consecuente alteración de los niveles de cortisol (Gold and Chrousos, 1985; Murphy, 1991; Holsboer, 2001; Holsboer and Ising, 2008; Vreeburg et al., 2009). La administración exógena de corticosterona ha sido validada y utilizada como modelo de estrés crónico y depresión (Ardayfio and Kim, 2006; Gourley et al., 2008, 2009; Murray et al., 2008; David et al., 2009, 2010). El tratamiento crónico con bajas dosis de corticosterona (35 mg/mL en disolución con en el agua de bebida) es suficiente para inducir cambios histológicos, morfológicos y comportamentales similares a la depresión clínica, tales como la atrofia de las dendritas de la PFC, la disminución de los niveles de factores tróficos y de neuroplasticidad en el HPC, la reducción de la proliferación y neurogénesis del DG o los efectos de tipo depresivo en diferentes paradigmas de comportamiento (Wellman, 2001; Ardayfio and Kim, 2006; Gourley et al., 2008, 2009; Murray et al., 2008; David et al., 2009, 2010). Además, el fenotipo molecular y comportamental desarrollado por estos animales es sensible a la reversión con un tratamiento antidepresivo crónico, pero no agudo (David et al., 2009). En la presente Tesis se ha utilizado el modelo por consumo crónico de corticosterona en ratón para investigar el efecto antidepresivo de moléculas de RNA pequeñas de interferencia (siRNA; *small interfering RNA*) conjugadas.

1.3. Sistema serotoninérgico

La 5-HT juega un papel fundamental en el cerebro humano. Controla funciones fisiológicas como el sueño, la alimentación, la regulación de la temperatura y la conducta sexual. Asimismo participa en la modulación del dolor e interviene en un gran número de comportamientos incluyendo agresión, impulsividad, atención, toma de decisiones, recompensa y funciones cognitivas. La disfunción del sistema serotoninérgico ha sido implicada en esquizofrenia, ansiedad, depresión, adicción a drogas, enfermedad de Parkinson y autismo (Abi-Dargham et al., 1997; Huot et al., 2011; Nakamura, 2013).

Aunque el sistema serotoninérgico está formado solamente por aproximadamente 250.000 neuronas concentradas en su mayoría en el núcleo del rafe dorsal (DR; *dorsal raphe nucleus)*, sus axones inervan extensamente la corteza y el sistema límbico, liberando 5-HT de modo paracrino y haciendo pocos contactos sinápticos (de Montigny, 1977; Jacobs and Azmitia, 1992; Blier and de Montigny, 1999; Adell et al., 2002; Celada et al., 2013). La 5-HT se cree es el más ancestral de los neurotransmisores habiéndose identificado en el cnidario *Renilla koellikeri* (Umbriaco et al., 1990).

1.3.1. Anatomía y conectividad del sistema serotoninérgico

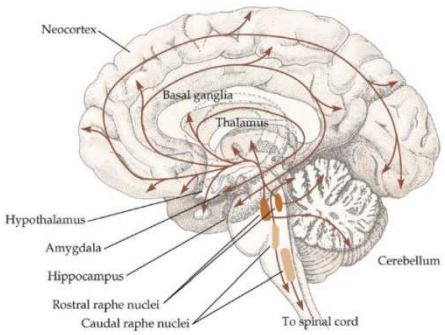

Figura 6. Representación de los subsistemas serotoninérgicos rostrales (naranja) y caudales (naranja claro) y sus respectivas proyecciones ascendentes y descendentes en el cerebro humano.

En los mamíferos, el sistema serotoninérgico está formado por nueve núcleos que se dividen en dos subsistemas: el rostral que proyecta hacia el prosencéfalo y el caudal que proyecta hacia el tronco cerebral y médula espinal (ver figura 6). El subsistema rostral, de interés en la presente Tesis, está formado por 4 núcleos: el núcleo caudal linear, el DR, el núcleo del rafe medial (MR; *median raphe*

nucleus) y la región supralemniscal (Jacobs and Azmitia, 1992; Piñeyro and Blier, 1999). Solo el DR contiene más del 50% de las neuronas serotoninérgicas del cerebro humano y murino. Las neuronas del núcleo caudal linear así como las de la región supralemniscal pueden considerase una extensión del segundo mayor núcleo serotoninérgico, el MR, por compartir un origen común en el neurodesarrollo y proyectar hacia las mismas áreas cerebrales (Jacobs and Azmitia, 1992; Piñeyro and Blier, 1999; Baker et al., 1990).

A nivel morfológico se pueden distinguir dos poblaciones axonales serotoninérgicas dependiendo del núcleo de origen. Las que proceden del DR presentan varicosidades axonales pequeñas de menos de 1 µm de diámetro y las que lo hacen del MR muestran varicosidades más grandes del orden de 2 a 5 µm de diámetro (Kosofsky and Molliver, 1987; Törk, 1990). Además de las diferencias morfológicas, las proyecciones del DR y del MR presentan también distinta sensibilidad a derivados de anfetaminas (Mamounas et al., 1991). Por consiguiente, se distinguen dos subsistemas serotoninérgicos rostrales con propiedades y distribución cerebral diferenciada, según se originen en el DR o el MR. Cada uno de los dos núcleos/subsistemas inerva áreas cerebrales específicas. A grandes rasgos, las áreas corticales reciben más inervación serotoninérgica del DR que del MR (Kosofsky and Molliver, 1987; Mamounas et al., 1991; McQuade and Sharp, 1997).

La actividad eléctrica de las neuronas serotoninérgicas se caracteriza por ser de modo tónico con un patrón de descarga regular de 1-5 espigas/s (Aghajanian and Vandermaelen, 1982). No obstante, esta actividad no es siempre igual, sino que sufre cambios durante el ciclo de sueño-vigilia, siendo más lenta durante el sueño profundo y prácticamente inexistente durante la fase REM. La actividad de las neuronas serotoninérgicas está fuertemente regulada por las aferencias que recibe (ver figura 7). Una de las principales procede de la

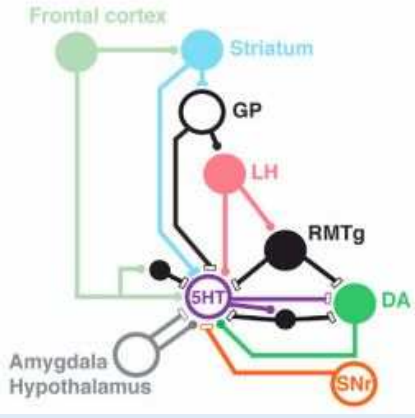

Figura 7. Modelo de las aferencias que reciben las neuronas serotoninérgicas. Las aferencias excitadoras están representadas con círculo y las inhibidoras con rectángulos. Adaptado de Pollak Dorocic et al., 2014.

PFC. Se cree que las proyecciones glutamatérgicas de la corteza infralímbica en roedores hacen sinapsis preferentemente con interneuronas GABAérgicas del DR (Hajos el al., 1999; Celada el al., 2001), de modo que la desinhibición glutamatérgica de la PFC a consecuencia de la hiperpolarización de interneuronas GABAérgicas corticales por las propias fibras serotoninérgicas (Santana et al., 2004), disminuiría la actividad serotoninérgica.

Otras aferencias que controlan la actividad de las neuronas serotoninérgicas del DR son las fibras noradrenérgicas procedentes del locus cerúleo (LC; *locus coeruleus*). Estudios preclínicos en roedores mostraron que la activación de los receptores α_1 adrenérgicos localizados en los cuerpos neuronales serotoninérgicos incrementa la función de las neuronas serotoninérgicas. Por el contrario, la administración de prazosin, antagonista selectivo α_1 adrenérgico, inhibe la actividad de las neuronas serotoninérgicas así como la liberación de 5-HT en los núcleos del rafe (Vandermaelen and Aghajanian, 1983; Bortolozzi and Artigas, 2003). También son de destacar las proyecciones de la habénula lateral hacia el DR (Aghajanian and Wang, 1977; Peyron et al., 1998a). Aunque los primeros estudios sugirieron que las proyecciones de la habénula lateral excitaban las neuronas GABAérgicas en el DR inhibiendo así las neuronas serotoninérgicas (Park, 1987; Varga et al., 2003), nuevas técnicas de trazado han identificado aferencias glutamatérgicas de la habénula lateral contactando directamente con las neuronas serotoninérgicas (PollaK Dorocic et al., 2014). Otra aferencia importante es la proveniente desde el Hyp (Peyron et al., 1998b; Adell et al., 2002; Celada et al., 2002). Se describió que diferentes poblaciones de neuronas hipotalámicas que contienen DA, hipocretinas o neuropéptidos (vasopresina, oxitocina o melanina) proyectan hacia el sistema serotoninérgico (PollaK Dorocic et al., 2014). Además, hay que destacar las aferencias originadas en la sustancia negra y área tegmental ventral o las procedentes de la AMG (Kalén et al., 1988; Kirouac et al., 2004; PollaK Dorocic et al., 2014). En general, todas las aferencias que reciben las neuronas serotoninérgicas, tienen un papel en la regulación del tono serotoninérgico y en última instancia sobre la liberación de 5-HT.

La síntesis de 5-HT está regulada por la disponibilidad del aminoácido triptófano y por la actividad de la enzima TPH_2, isoforma específica del cerebro (Walther et al., 2003). Una vez sintetizada, la 5-HT se almacena en vesículas sinápticas mediante el transportador vesicular de monoaminas 2 (VMAT2; *vesicular monoamine transporter 2*). Durante la neurotransmisión, la llegada de los potenciales de acción a los terminales y varicosidades axonales despolariza la membrana celular favoreciendo la entrada de calcio hacia el interior de la célula. Éste activa la fusión de las vesículas con la membrana celular favoreciendo la liberación de 5-HT al espacio sináptico y activación de los receptores. El cese del estímulo se logra por la degradación de 5-HT a través de las enzimas monoamino oxidasas (MAO; *monoamine oxidase*), principalmente la isoforma A, o por la recaptación del neurotransmisor al interior de la neurona serotoninérgica mediante el SERT.

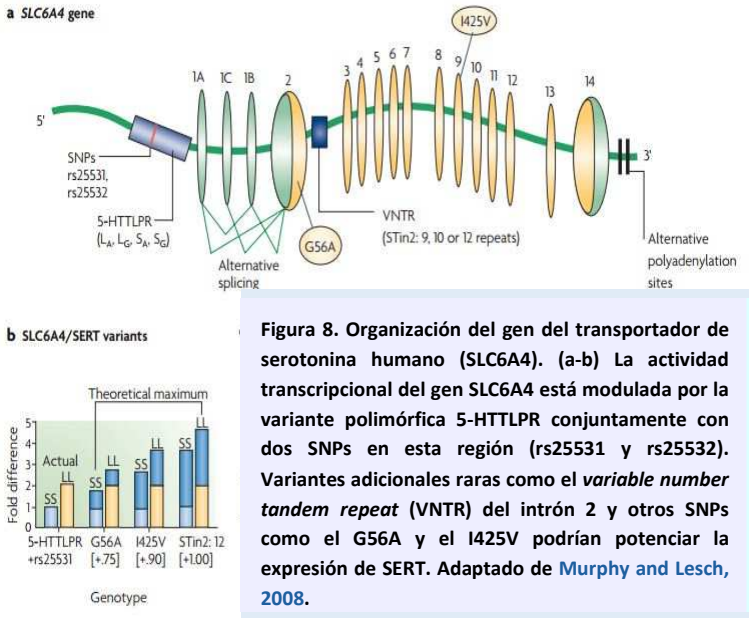

Figura 8. Organización del gen del transportador de serotonina humano (SLC6A4). (a-b) La actividad transcripcional del gen SLC6A4 está modulada por la variante polimórfica 5-HTTLPR conjuntamente con dos SNPs en esta región (rs25531 y rs25532). Variantes adicionales raras como el *variable number tandem repeat* (VNTR) del intrón 2 y otros SNPs como el G56A y el I425V podrían potenciar la expresión de SERT. Adaptado de Murphy and Lesch, 2008.

El hecho de que más del 90% de los antidepresivos disponibles en clínica tienen el SERT como diana molecular primaria pone de manifiesto la importancia de este transportador en la regulación de la neurotransmisión serotoninérgica y en la fisiopatología y tratamiento de la depresión. Prueba de ello es la existencia del polimorfismo 5-HTTLPR en su zona promotora (ver figura 8), dónde la variante corta S, a diferencia del alelo L, ha sido asociada a una menor resiliencia al estrés y depresión (Caspi et al., 2003). Además, el alelo S conlleva resistencias al tratamiento antidepresivo con SSRIs como la paroxetina o el escitalopram (Murphy et al., 2004; Outhred et al., 2014).

Se ha descrito en roedores que alrededor del 90% de la expresión del mRNA del SERT tiene lugar en las neuronas serotoninérgicas mientras que el 10% restante tiene lugar en neuronas no serotoninérgicas y en células gliales (Pickel and Chan, 1999). La proteína SERT se localiza tanto en los cuerpos neuronales como en los axones serotoninérgicos (Blakely et al., 1994; Qian et al., 1995; Murphy et al., 2008). El tratamiento crónico con SSRIs favorece la internalización del transportador SERT disminuyendo los sitios de unión en la membrana celular sin alterar los niveles de expresión de su mRNA (Benmansour et al., 1999, 2002; Samuvel et al., 2005; Lau et al., 2008). Mientras que los SSRIs modulan la actividad de la proteína quinasa C (PKC; *protein kinase C*) fosforilando el SERT e induciendo su internalización, la 5-HT protege de esta fosforilación (Qian et al., 1997; Ramamoorthy and Blakely, 1999). Además, se ha descrito que el tratamiento crónico con el SSRI fluoxetina aumenta la expresión del micro RNA (miRNA; *micro RNA*) 16 (miR-16) en el DR de ratón, que a su vez inhibe la traducción del SERT (Baudry et al., 2010). Así, la disminución de la fracción activa del SERT reduce la recaptación de 5-HT que en última instancia incrementará la señalización postsináptica mediada por receptores de 5-HT.

Existen al menos 16 genes de receptores de 5-HT en mamíferos: 5-$HT_{1A/B/D/E/F}$, 5-$HT_{2A/B/C}$, 5-$HT_{3A/B/C}$, 5-HT_4, 5-$HT_{5A/B}$, 5-HT_6 y 5-HT_7 (Hoyer and Martin, 1997; Barnes and Sharp, 1999). Excepto el receptor 5-HT_3, que es un canal iónico, el resto de los receptores serotoninérgicos son metabotrópicos y por lo tanto acoplados a proteínas G de señalización intracelular. Uno de los más abundantes en el cerebro y con un rol fundamental en la depresión y la acción antidepresiva es el receptor 5-HT_{1A}. Este receptor se expresa presinápticamente en las neuronas serotoninérgicas actuando como autoreceptor manteniendo la homeostasia de la neurotransmisión

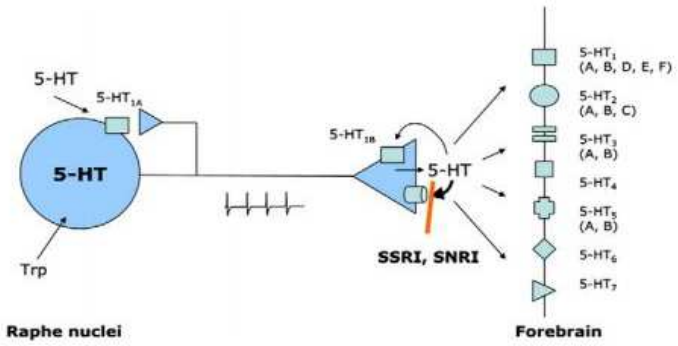

Figura 9. Localización de los receptores serotoninérgicos. La 5-HT ejerce su función mediante la estimulación de sus múltiples receptores, presentes todos en la neurona postsináptica. Además, el receptor 5-HT_{1A} y 5-HT_{1B} están también presentes en la neurona presináptica, el primero en la zona somatodendrítica y el segundo en los terminales axonales. Adaptado de Artigas, 2013.

serotoninérgica y, postsinápticamente como heteroreceptor en áreas de proyección incluyendo PFC, HPC, AMG, septum, entre otras (ver figura 9) (Pazos and Palacios, 1985; Sotelo et al., 1990; Pompeiano et al., 1992; Amargós-Bosch et al., 2004; Santana et al., 2004; de Almeida and Mengod, 2008).

Estudios postmortem y de neuroimagen en seres humanos han revelado una mayor densidad del autoreceptor 5-HT_{1A} en pacientes con depresión en comparación con sujetos control (Stockmeier et al., 1998; Parsey et al., 2006). El aumento de la densidad del autoreceptor 5-HT_{1A} también se ha descrito en los portadores del alelo G del SNP G(-1019)C, haciéndolos más susceptibles a la depresión y peor respondedores a los antidepresivos de tipo SSRI (Lemonde et al., 2003; Serretti et al., 2004; Neff et al., 2009).

A nivel molecular, el 5-HT_{1A} es un receptor de tipo inhibitorio que disminuye la producción de adenosina monofosfato cíclico (cAMP; *cyclic adenosine monophosphate*) y la actividad de la proteína quinasa A (PKA; *protein kinase A*). Esta señalización inhibe canales de calcio, disminuyendo su concentración intracelular, y promueve la apertura de los canales de potasio rectificadores internos acoplados a proteína G (GIRK; *G protein-coupled inwardly-rectifying potassium channel*) y de los canales de potasio semejantes a TWIK "1" (TREK1; *TWIK-related* K^+ *channel* 1), hiperpolarizando la neurona (Araneda and Andrade, 1991; Bayliss et al., 1995; Barnes and Sharp, 1999; Lanfumey and Hamon, 2000; Gordon and Hen, 2006; Mathie, 2007; Polter and Li, 2010; Ye et al., 2015). Debido a su doble localización (pre- y postsináptica), los agonistas de este receptor tienen un efecto dual sobre la neurotransmisión serotoninérgica. Actuando a nivel presináptico, inhiben la actividad eléctrica de las neuronas serotoninérgicas y reducen la liberación de 5-HT, mientras que actuando a nivel postsináptico en las áreas de proyección, estos agonistas mimetizan el efecto de la 5-HT liberada potenciando la neurotransmisión serotoninérgica.

1.3.2. Regulación del sistema serotoninérgico

Además de las diferentes aferencias que controlan la actividad de los núcleos del rafe, el propio sistema serotoninérgico controla la actividad del mismo mediante un sistema de autocontrol de inhibición negativo. Para ello, los axones serotoninérgicos contralaterales hacen sinapsis sobre las propias neuronas serotoninérgicas. El autoreceptor 5-HT_{1A} tiene un papel primordial en este mecanismo de autoregulación que ayuda a mantener la homeostasia del sistema (Piñeyro and Blier, 1999; Lanfumey and Hamon, 2000; Altieri et al., 2013; Artigas, 2013). Durante los periodos de vigilia, las neuronas serotoninérgicas descargan de modo lento y regular. Cuando se produce una activación excesiva de estas neuronas, como ocurre por ejemplo durante una situación estresante, el aumento de la 5-HT liberada por los axones contralaterales incrementa la actividad del autoreceptor 5-HT_{1A}. Esto hiperpolariza las neuronas serotoninérgicas normalizando del patrón de descarga (Adell et al., 1997; Artigas, 2013).

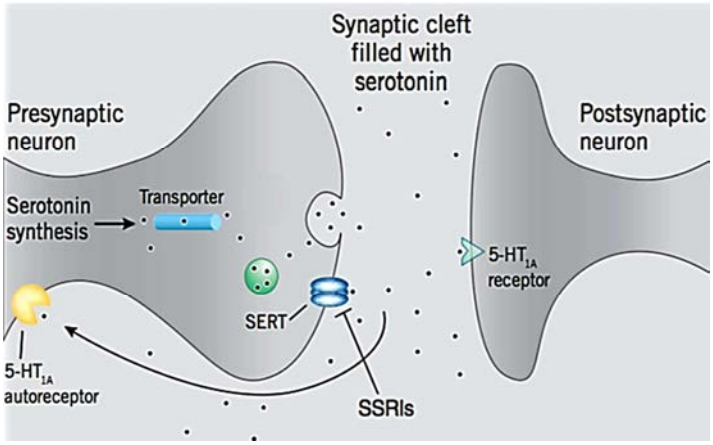

Figura 10. Sinapsis serotoninérgica y control por un mecanismo de inhibición negativo. En condiciones normales, la 5-HT empaquetada en vesículas es transportada y liberada al espacio sináptico, donde difunde hacia la membrana postsináptica uniéndose a los receptores de 5-HT. Parte de la 5-HT liberada también se une al autoreceptor 5-HT_{1A} activando el mecanismo de autoinhibición que conlleva a una reducción de la liberación de 5-HT. El bloqueo farmacológico del SERT incrementa la concentración sináptica de 5-HT aumentando la actividad del autoreceptor, hecho que reduce más el tono serotoninérgico limitando la acción antidepresiva. Adaptado de Fulmer, 2010.

La presencia de este mecanimo fisiológico de autoregulación tiene un impacto negativo sobre el mecanismo de acción de los fármacos antidepresivos de tipo serotoninérgico. El bloqueo farmacológico del SERT (tratamientos con SSRIs, SNRIs o TCAs), incrementa la fracción activa de 5-HT en el cerebro, sobre todo en los núcleos del rafe. Esto activa el autoreceptor 5-HT_{1A} que reduce rápidamente la actividad del sistema serotoninérgico, atenuando así el incremento de la concentración de 5-HT en las áreas de proyección (ver figura 10)

(Artigas et al., 1996; Piñeyro and Blier, 1999). El control que el receptor 5-HT_{1A} somatodendrítico ejerce sobre el tono serotoninérgico, ha llevado a hipotetizar que su activación es la responsable del retraso en la acción clínica de los fármacos antidepresivos (Blier and de Montigny, 1994; Artigas et al., 1996; Gardier et al., 1996). Solo después del tratamiento prolongado con SSRIs se produciría la desensibilización del autoreceptor 5-HT_{1A}, logrando un aumento marcado y sostenido de la concentración de 5-HT y, alcanzando ahora sí, la respuesta terapéutica (Blier and de Montigny, 1994; Blier et al., 1998). En este sentido y con el fin de acelerar y mejorar la eficacia de los tratamientos antidepresivos, se propuso en los años 90 la combinación de éstos con el antagonista del receptor 5-HT_{1A} pindolol, evitando de este modo el *feedback* negativo mediado por el autoreceptor (Artigas, 1993; Artigas et al., 1994; Portella et al., 2011). No obstante, para la acción antidepresiva es necesaria la activación del receptor 5-HT_{1A} postsináptico, hecho que limita la utilidad de estos antagonistas (Haddjeri et al., 1998).

Otro receptor con un rol destacado en la homeostasis del sistema serotoninérgico es el receptor 5-HT_{1B}, que como el 5-HT_{1A} se localiza pre- y postsinápticamente regulando negativamente la formación de cAMP. A diferencia del autoreceptor 5-HT_{1A}, el receptor 5-HT_{1B} presináptico se localiza en el axón, inhibiendo la síntesis y liberación de 5-HT de forma local (Artigas, 2013; Sari, 2014).

1.4. Sistema noradrenérgico

Con solo 15.000 neuronas noradrenérgicas en la especie humana, este sistema está involucrado en funciones tales como la regulación de la atención, la adquisición de la información sensorial, la flexibilidad cognitiva, la plasticidad sináptica a largo plazo y la recuperación de memoria remota, entre otras (Berridge and Waterhouse, 2003; Sara and Bouret, 2012). Esto hace del sistema noradrenérgico uno de los principales candidatos responsables de algunos de los síntomas de la depresión como la dificultad de concentración, la fatiga y los trastornos del sueño. Del mismo modo que el sistema serotoninérgico, la arborización de los axones del sistema noradrenérgico permite inervar prácticamente todo el prosencéfalo (Loughlin et al., 1986).

El sistema noradrenérgico de los mamíferos está formado por siete núcleos. EL LC, que se extiende a ambos lados de la zona ventrolateral del cuarto ventrículo, es el principal núcleo y contiene toda la población de neuronas noradrenérgicas que proyectan hacia el prosencéfalo (ver figura 11) (Dahlstroem and Fuxe, 1964; Moore and Bloom, 1979; Foote et al., 1983; Sara, 2015).

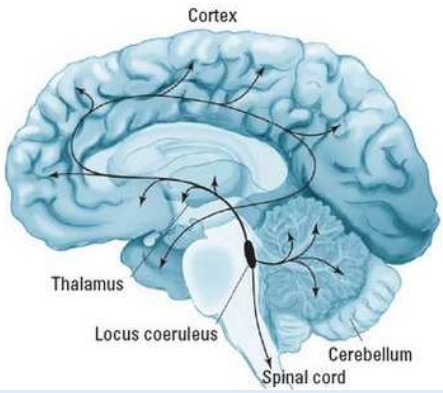

Figura 11. Esquema de las proyecciones de las neuronas noradrenérgicas del LC en el cerebro de humanos.

Las neuronas noradrenérgicas del LC descargan de modo tónico con un patrón de descarga regular y constante de 0.5-5 espigas/s similar a las neuronas serotoninérgicas (Moore and Bloom, 1979; Foote et al., 1983). Sin embargo, a diferencia de estas últimas, las neuronas noradrenérgicas también pueden hacer descargas fásicas de 2 a 3 potenciales de acción produciendo una mayor liberación de NE (Rajkowski et al., 2004). Además, la actividad noradrenérgica se ve modificada con cada fase del sueño. Durante el sueño profundo el patrón de descarga se enlentece, deteniéndose durante la fase REM. Esta actividad del LC varía en anticipación a cada fase del sueño (Aston-Jones and Bloom, 1981).

Las principales aferencias hacia el LC provienen de dos núcleos reticulares: i) proyecciones inhibitorias procedentes del hipogloso prepósito relacionadas con el estado vegetativo, y ii) proyecciones excitadoras desde el núcleo paragigantocelular vinculadas a funciones autónomas e integradoras de estímulos (Aston-Jones et al., 1991). Otras aferencias son: glutamatérgicas de la PFC que participan en los procesos cognitivos superiores como la memoria de trabajo (Jodo and Aston-Jones, 1997) y las serotoninérgicas desde el DR y el MR (Cedarbaum and Aghajanian, 1978). El LC también recibe proyecciones procedentes del PVN y la AMG (Cedarbaum and Aghajanian, 1978; Wallace et al., 1992; Reyes et al., 2005). Por otro lado, una densa colección de neuronas GABAérgicas en la zona pericoerular inerva el LC (Aston-Jones et al., 2004). Además, se han identificado en el LC neuropéptidos como vasopresina, somatostatina, neuropéptido Y, encefalina, neurotensina, CRH, galanina y orexinas, que actúan modulando la actividad de las neuronas noradrenérgicas (Olpe and Steinmann, 1991; Kiyashchenko et al., 2002).

Como previamente se describió, las conexiones eferentes desde el LC dan lugar a una extensa arborización por todo el CNS. Destacan áreas cerebrales como la corteza que exhiben altas densidades de varicosidades noradrenérgicas (Jones and Moore, 1977; Moore and Bloom, 1979; Foote et al., 1983; Agster et al., 2013). Así las cortezas cingular y frontal, seguidas de la visual, la auditiva y la sensomotriz, contienen las mayores concentraciones de NE (Levitt and Moore, 1978). No obstante, hay áreas cerebrales que reciben muy escasa inervación noradrenérgica como los ganglios basales (cuerpo estriado y globo pálido) y el NAc.

El precursor en la biosíntesis de NE es el aminoácido tirosina, que por acción de las enzimas tirosina hidroxilasa (TH; *tyrosine hydroxylase*) y DOPA descarboxilasa dan lugar a DA. Está es captada por VMAT2 e internalizada dentro de las vesículas sinápticas y transformada a NE por acción de la dopamina beta-hidroxilasa (DBH; *dopamine beta-hydroxylase*) (ver figura 12) (Rush and Geffen, 1980). La despolarización del terminal sináptico induce la fusión de las vesículas con las membranas celulares y la liberación de NE a la hendidura sináptica. La terminación de la neurotransmisión sucede por la recaptación de NE a través del transportador de

noradrenalina (NET; *norepinephrine transporter*) y por la degradación de la NE, preferentemente por la isoforma A de la MAO.

Del mismo modo que el SERT, el NET pertenece a la familia de transportadores con doce dominios transmembrana dependientes de Na^+/Cl^-. Dicho transportador se encuentra anclado en la membrana plasmática a nivel del soma, dendritas y terminales axonales de las neuronas noradrenérgicas. El bloqueo del NET a fin de inhibir la recaptación de NE es el objetivo de muchos fármacos antidepresivos. Así los TCAs y los SNRI (Benmansour et al., 2004) tienen alta afinidad por SERT y NET, mientras que los antidepresivos inhibidores selectivos de la recaptación de noradrenalina (NERI; *norepinephrine reuptake inhibitor*), siendo reboxetina su prototipo, inhiben selectivamente el NET (Gould et al., 2003).

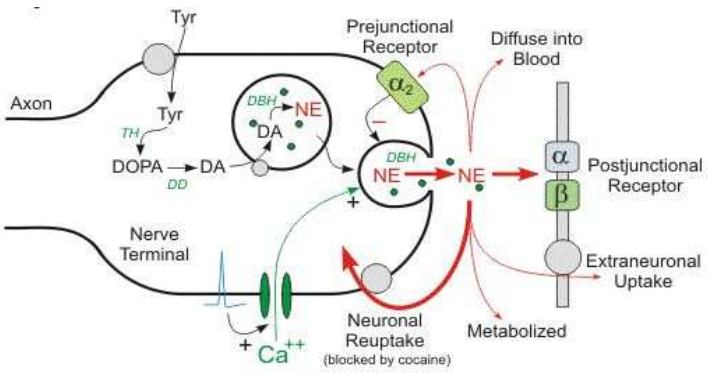

Figura 12. Representación esquemática de la síntesis y liberación de NE. La NE es sintetizada en una serie de pasos enzimáticos que incluyen la actividad de la TH, DOPA descarboxilasa y DBH, éste último ocurre dentro de las vesículas sinápticas. Una vez liberada al espacio sináptico, la NE se une y activa los receptores adrenérgicos. La señal de terminación de la señalización NE sucede con la recaptación del neurotransmisor a través del NET y su degradación por la isoforma A de la MAO.

La NE ejerce su efecto por unión y activación de sus receptores. Los receptores adrenérgicos son receptores metabotrópicos que pertenecen a tres familias según su homología, perfil farmacológico y mecanismo de señalización intracelular: $\alpha_{1A,\ 1B,\ 1D}$, los $\alpha_{2A,\ 2B,\ 2C}$ y los $\beta_{1,\ 2,\ 3}$ (Lefkowitz and Caron, 1988; Harrison et al., 1991; Bylund et al., 1994). El agonismo de los receptores α_1 adrenérgicos induce la activación de la fosfolipasa C (PLC; *fosfolipase C*) produciendo inositol trifosfato (IP_3; *inositol trisphosphate*) y diacilglicerol (DAG; *diacylglycerol*) como segundos mensajeros (Burch et al., 1986). Por otro lado, la activación de los receptores α_2 adrenérgicos inhibe la formación cAMP y la actividad de PKA, reduciendo la actividad de los canales de Ca^{+2} dependientes de voltaje, la apertura de los canales de potasio o la activación de la bomba Na^+/H^+ (North and Yoshimura, 1984; Sweatt et al., 1985;

Lipscombe et al., 1989). Los tres miembros de tipo β están acoplados a proteína G_s, estimulando la producción de cAMP. Los receptores α_1 y β se localizan a nivel postsináptico, mientras que los α_2 se encuentra en la neurona presináptica a nivel de terminales, soma y dendritas y también en la neurona postsináptica e incluso en glía (Aoki et al., 1994; Lee et al., 1998).

Estudios postmortem en cerebros humanos han mostrado que pacientes con depresión víctimas de suicido presentan mayor densidad de los receptores adrenérgicos α_1 y α_2 en la PFC que el grupo control (Meana et al., 1992; Arango et al., 1993). Además, estudios preclínicos de comportamiento (TST y FST) y neuroquímicos realizados en roedores indican que los receptores α_1 participan en la respuesta de la terapia antidepresiva (Cunha et al., 2013; Citó et al., 2015). No obstante, los receptores α_2 han recibido mayor atención como dianas antidepresivas potenciales debido a que son capaces de regular de modo inhibitorio la liberación de NE (Starke, 1987). Estudios de microdiálisis *in vivo* en roedores han descrito que la administración local de fármacos agonistas del receptor α_2 adrenérgico (clonidina, medetomidina, UK 14,304) en la PFC disminuye la liberación de NE. Contrariamente, la administración de fármacos antagonistas (atipamezol, idazoxan) produjo un incremento de la concentración extracelular de NE (Dennis et al., 1987; Dalley and Standord, 1995). Esto indicaría que el autoreceptor α_2 adrenérgico localizado en las terminales tiene un efecto inhibitorio sobre la concentración de NE. También se ha mostrado mediante técnicas de microdiálisis *in vivo* que la administración intra-LC de fármacos agonistas (clonidina, UK 14,304) o antagonistas (BRL44408) para el receptor α_2 adrenérgico disminuye o incrementa, respectivamente, la concentración de NE en la corteza cingulada (Mateo and Meana, 1999). En general, lo datos indicarían el efecto inhibitorio del receptor α_2 adrenérgico de expresión presináptica y su rol modulador de la actividad eléctrica de las neuronas noradrenérgicas del LC. De hecho, entre los tratamientos actuales para la depresión se incluyen dos antagonistas del receptor α_2 como son la mirtazapina y la mianserina (Pinder and Van Delft, 1983; Anttila and Leinonen, 2001; Langer, 2015). Aun así, del mismo modo que el receptor 5-HT_{1A}, parece ser necesaria la activación del receptor α_2 adrenérgico de expresión

postsináptica para lograr el efecto antidepresivo (Vega-Rivera et al., 2013; Ishola et al., 2014).

1.5. Tratamientos Antidepresivos

Antes del descubrimiento de los primeros psicofármacos como los TCAs y los MAOIs no se disponía de herramientas terapéuticas eficaces para el tratamiento de los trastornos del estado del ánimo. La introducción de los mismos en la década de 1950 se considera uno de los grandes avances de la medicina del siglo XX comparándose incluso con el descubrimiento de los antibióticos. A pesar de la gran incidencia e impacto socioeconómico de la depresión así como de la enorme cantidad de recursos destinados al desarrollo de nuevas terapias, desafortunadamente los fármacos antidepresivos disponibles presentan una limitada eficacia dejando una elevada proporción de pacientes con depresión resistentes a tratamientos.

1.5.1. Fármacos antidepresivos monoaminérgicos

Los fármacos antidepresivos monoaminérgicos tienen como finalidad incrementar la neurotransmisión monoaminérgica, principalmente 5-HT y NE. Dentro de la primera generación de fármacos antidepresivos, el desarrollo de la iproniazida, generada originalmente para el tratamiento de la tuberculosis, fue el primer fármaco de la familia de los MAOIs. Estos actúan bloqueando una o ambas isoformas (A y/o B) de la MAO y así incrementan los niveles de 5-HT. Más tarde, la imipramina, desarrollada primero como un fármaco antihistamínico y antipsicótico, fue el primer compuesto de la familia de los TCAs que actúa bloqueando los transportadores SERT y NET inhibiendo la recaptación de 5-HT y NE, respectivamente.

Aun hoy estas dos familias de drogas continúan utilizándose para tratar la depresión. Sin embargo, han quedado relegadas a segundas o terceras líneas de tratamiento debido a los efectos secundarios que producen y a la introducción de los fármacos antidepresivos de segunda generación, mucho más seguros y tolerables.

Los SSRI y los SNRI son los fármacos antidepresivos más prescritos y de primera elección para el tratamiento de la depresión (Rush et al., 2006). Los primeros actúan bloqueando selectivamente el SERT, aumentando la fracción sináptica de 5-HT activa,

mientras que los segundos son de acción dual bloqueando el SERT y NET, aumentando los niveles extracelulares de ambos neurotransmisores 5-HT y NE en el espacio sináptico (ver figura 13). Aún y siendo estos los fármacos antidepresivos más prescritos, sus ratios de respuesta y remisión son de aproximadamente del 60% y 40%, respectivamente (Tollefson and Holman, 1994; Stahl, 2000; Thase et al., 2001). Además, estudios naturalísiticos como el STAR*D (*Sequenced Treatment Alternatives to Relieve Depression*) revelaron que los ratios de respuesta y remisión son substancialmente menores (del 47% y 28%, respectivamente) después de ocho semanas de tratamiento con el SSRI citalopram (Trivedi et al., 2006a). Estrategias de complementación con drogas no dirigidas al SERT (buspirona, bupropión) en pacientes no respondedores a los SSRI obtuvieron ratios de remisión similares (Rush et al., 2006a; Trivedi et al., 2006b). El estudio STAR*D también mostró que la tasa de remisión total incrementa hasta el 67% después de un año con cuatro tratamientos secuenciados con diferentes fármacos antidepresivos (Rush et al., 2006b). Estas cifras, que reflejan la práctica clínica diaria, indican que casi un tercio de los pacientes con depresión tratados no responden adecuadamente a los tratamientos habituales.

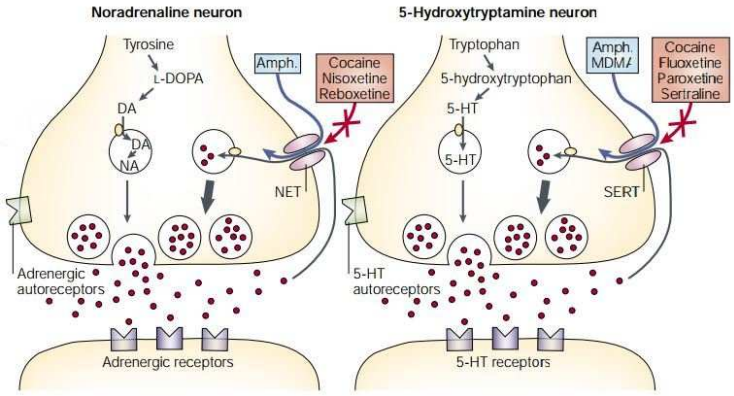

Figura 13. Representación esquemática de los terminales sinápticos de NE y 5-HT. El NET y el SERT están localizados en la membrana presináptica, donde recaptan el neurotransmisor liberado. La mayor parte de los fármacos antidepresivos de uso clínico actúan bloqueando estos dos transportadores, incrementando la fracción activa de los respectivos neurotransmisores en la sinapsis. Adaptado de Torres et al., 2003.

Una segunda limitación de los tratamientos antidepresivos actuales es su lentitud de acción. Ensayos controlados con SSRIs o SNRIs muestran que los fármacos activos se diferencian significativamente del placebo después de dos o más semanas de tratamiento, alcanzando una diferencia máxima entre las seis y las ocho semanas de tratamiento (Tollefson and Holman, 1994; Stahl, 2000; Thase et al., 2001).

Otros fármacos monoaminérgicos incluyen los NERI (reboxetina, atomoxetina, etc.), que actúan como inhibidores de la recaptación de NE al bloquear selectivamente el NET y los antidepresivos atípicos mirtazapina y mianserina, antagonistas de los receptores 5-HT_2, α_2 adrenérgico e histaminérgico 1, que incrementan la neurotransmisión serotoninérgica y noradrenérgica (Pinder and Van Delft, 1983; Anttila and Leinonen, 2001). También los antagonistas del receptor 5-HT_{1A} pueden mejorar los efectos clínicos de los antidepresivos evitando la activación del *feedback* negativo mediado por el autoreceptor 5-HT_{1A} (Artigas, 1993). Estudios clínicos observaron que el antagonista doble de los receptores 5-HT_{1A} y β adrenérgico pindolol acelera la respuesta antidepresiva en pacientes con depresión no tratados (Artigas et al., 1994, 1996; Blier and Bergeron, 1995; Perez et al., 1997). Otros estudios clínicos han mostrado que los antipsicóticos atípicos (antagonistas de los receptores de dopamina D2 y 5-HT_{2A}) incrementan la respuesta clínica de los SSRI en pacientes resistentes a tratamiento (Shelton et al., 2001; Barbee et al., 2004; Berman et al., 2007; Carvalho et al., 2009).

A nivel preclínico también se ha estudiado la acción de otros compuestos sobre receptores de 5-HT diferentes a los mencionados hasta ahora. Así por ejemplo, se ha observado que el antagonista del receptor 5-HT_{1B} CP94253 y los agonistas del receptor 5-HT_{2B} (BW723C86) y 5-HT_{2C} (WAY161503, RO60-0175 y RO60-0332) disminuyen el tiempo de inmovilidad en el FST (Cryan and Lucki, 2000; Tatarczynska et al., 2004; Diaz et al., 2012). También se ha comprobado que el antagonista del receptor 5-HT_3 ondansetron potencia el incremento de la concentración extracelular de 5-HT producida por el SSRI citalopram en el prosencéfalo de rata (Mork et al., 2012). Otro estudio preclínico en ratas mostró que los agonistas del receptor 5-HT_4 RS67333 y prucalopride disminuyen la inmovilidad en el FST y modifican parámetros, considerados marcadores de la acción antidepresiva, como son la desensibilización del autoreceptor 5-HT_{1A}, el incremento de la fosforilación de CREB y la neurogénesis en el HPC (Lucas et al., 2007). También se han observado efectos antidepresivos en rata y ratón de antagonistas del receptor 5-HT_6 (SB399885) y 5-HT_7 (SB269970), como por ejemplo la reducción de la inmovilidad en el TST y el FST (Wesolowska et al., 2006; Wesolowska and Nikiforuk, 2007).

En conjunto, aunque los estudios de agonistas y antagonistas arriba mencionados sugieren que los receptores de 5-HT pueden ser dianas potenciales de nuevos fármacos antidepresivos, su modulación individual no ofrece los beneficios farmacológicos de los tratamientos con los SSRIs y SNRIs. En este sentido, se están desarrollando fármacos antidepresivos que además de bloquear el SERT presentan múltiples afinidades para distintos receptores de 5-HT, como por ejemplo la vilazodona (inhibidor del SERT y agonista parcial del receptor 5-HT_{1A}) y la vortioxetina (inhibidor del SERT, agonista parcial del receptor 5-HT_{1A} y antagonista de los receptores 5-HT_3, 5-HT_{1B} y 5-HT_7) (Artigas, 2015).

A pesar de la gran variedad de estrategias monoaminérgicas disponibles para tratar la depresión, solo una pequeña proporción de los pacientes responden a estos tratamientos, lo que en conjunto, plantea la necesidad de desarrollar nuevas estrategias terapéuticas que superen las limitaciones de los fármacos de acción monoaminérgica actuales: baja eficacia y lentitud de acción.

1.5.2. Otras terapias para el tratamiento de la depresión

Los tratamientos para la depresión más comunes incluyen los fármacos antidepresivos descritos en el apartado anterior, la psicoterapia y la combinación de ambos. Se ha demostrado la utilidad de la psicoterapia para tratar casos de depresión poco severos evitando así el uso de fármacos (Weissman et al., 1979; Kovacs et al., 1981; Rush and Thase, 1998; Hollon et al., 2002). Aunque la combinación de fármacos antidepresivos y psicoterapia proporciona solo cierta mejoría, en algunos pacientes la terapia combinada es mucha más efectiva que la medicación o la psicoterapia solas (Weissman et al., 1979; Thase et al., 1997; Keller et al., 2000; Nemeroff et al., 2003).

Otro tipo de terapia antidepresiva menos frecuente, aunque de rápido efecto antidepresivo son las manipulaciones del ciclo sueño-vigilia, incluyendo deprivaciones del sueño parciales o totales. Se cree que el efecto terapéutico de esta práctica puede ser debido a un reajuste en la homeostasis del ciclo sueño-vigilia (Wirz-Justice and Van den Hoofdakker, 1999; Wirz-Justice, 2006).

En depresiones severas resistentes a tratamientos farmacológicos se puede recurrir a intervenciones como la ECT (Nobler et al., 2000; Khlid et al., 2008; Dukart, 2014), la estimulación magnética transcranial (Levkovitz et al., 2009; Rosenberg et al., 2011; Gaynes et al., 2014; Janicak and Dokucu, 2015) y la terapia magnética convulsiva, que combina aspectos terapéuticos de las dos anteriores (Lisanby et al., 2000; Kayser et al., 2011, 2015), o bien a intervenciones invasivas que requieren cirugía cerebral como la estimulación del nervio vagal (Nahas et al., 2005; Dorr and Debonnel, 2006; Schlaepfer et al., 2008; Shah et al., 2014) y la DBS (Mayberg et al., 2005; McNeely et al., 2008; Malone et al., 2009; Kennedy et al., 2011; Puigdemont et al., 2012). Aunque todas estas intervenciones ofrecen una oportunidad de mejora para aquellos pacientes resistentes a tratamiento, hay que tener presente su limitada disponibilidad y la falta de datos de eficacia a largo plazo, por lo que el paciente se enfrenta a una terapia de ensayo-error (Bewernick and Schlaepfer, 2015).

Otros tratamientos antidepresivos experimentales que aparecen en la literatura son: antagonistas de los receptores κ de opioides, agonistas y antagonistas del receptor CB_1 de cannabinoides, inhibidores de las histonas deacetilasas, antagonistas del receptor de CRH 1, antagonistas de los receptores de glucocorticoides, antagonistas del receptor V1b de vasopresina y antagonistas del receptor NK_1 del neuropéptido P, entre otros (Berton and Nestler, 2006; Artigas, 2015).

1.5.3. Fármacos experimentales de acción rápida

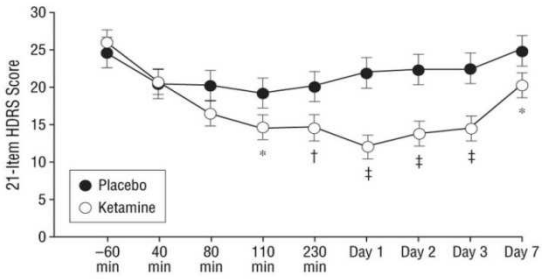

Figura 14. Efectos antidepresivos muy rápidos del tratamiento con ketamina. Puntuación en la escala de Hamilton 21 a lo largo de una semana de pacientes con depresión tratados con ketamina o placebo. Una sola dosis de ketamina intravenosa es suficiente para producir efecto antidepresivo en tan solo 2 horas después de su administración y de hasta 7 días de duración. Adaptado de Zarate et al., 2006.

Ensayos clínicos han constatado que la administración intravenosa o intranasal de una única dosis subanestésica del antagonista no competitivo del receptor NMDA ketamina, produce efectos antidepresivos en pocas horas y que pueden permanecer por una semana en pacientes con depresión unipolar

o bipolar resistentes a otros tratamientos (ver figura 14) (Berman et al., 2000; Zarate et al., 2006, 2012; Diazgranados et al., 2010; Lapidus et al., 2014). Se cree que el mecanismo de acción implica el bloqueo preferencial del receptor NMDA presente en las interneuronas GABAérgicas, desinhibiendo así la transmisión glutamatérgica (Homayoun and Moghaddam, 2007) y favoreciendo la plasticidad neuronal y sinaptogénesis en la PFC y circuitos cerebrales implicados en emoción y cognición (Li et al., 2010; Duman and Aghajanian, 2012). Sin embargo, el efecto psicotomimético de la ketamina precede la acción antidepresiva, lo que pone en duda la utilidad de la ketamina en la práctica clínica.

Actualmente, existen ensayos clínicos con otros antagonistas del receptor NMDA como lanicemina (Zarate et al., 2013; Sanacora et al., 2014) o antagonistas selectivos de la subunidad NR2B del receptor NMDA (CP-101.606 o Ro 25-6981) (Duman et al., 2012), con el fin de lograr efectos terapéuticos similares a la ketamina evitando los efectos adversos. Además, se está evaluando también la combinación de ketamina con bajas dosis de sales de litio a fin de obtener efectos antidepresivos rápidos con menores efectos adversos (Ghasemi et al., 2010; Liu et al., 2013; Duman, 2014).

Recientemente se han reportado también efectos antidepresivos rápidos con una única dosis de escopolamina intravenosa en pacientes con depresión unipolar o bipolar (Furey and Drevets, 2006; Drevets and Furey, 2010). Este fármaco es un antagonista del receptor muscarínico tipo M1 de acetilcolina, y como en el caso de la ketamina, se propone que las acciones antidepresivas de la escopolamina son mediadas por las neuronas GABAérgicas en la PFC (Wohleb et al., 2016). El antagonismo del receptor M1 sobre las neuronas GABAérgicas, permitiría la deshibición de las neuronas piramidales glutamatérgicas resultando en un incremento de la liberación y señalización mediada por glutamato y por consiguiente la aparición de la respuesta antidepresiva.

Aunque se requieren muchos más estudios preclínicos y clínicos asociados a estos fármacos, las propiedades antidepresivas tan rápidas ponen en relieve la importancia del sistema glutamatérgico en la búsqueda de nuevas dianas para el desarrollo de fármacos antidepresivos eficaces y de acción rápida.

La farmacología antidepresiva tiene gran necesidad de nuevas dianas y estrategias que, además de ser más eficaces y de acción más rápida que las drogas monoaminérgicas actuales, deberían también estar libres de los efectos secundarios adversos como los psicotomiméticos y disociativos de la ketamina. La presente Tesis aborda el desarrollo de nuevas estrategias terapéuticas en depresión basadas en el uso del RNA interferente (RNAi; *RNA interference*) para regular la expresión de dianas clásicas como el receptor 5-HT_{1A} y el SERT o nuevas dianas con potencial antidepresivo como el canal de potasio sensor de ácido semejante a TWIK "3" (TASK3; *TWIK-related acid-sensing* K^+ *channel 3*).

1.6. Canales de Potasio

La versatilidad de la actividad eléctrica neuronal está regulada en gran parte por la expresión de diferentes clases de canales de potasio. Estos, agrupan 79 genes que codifican para una subunidad transmembrana conductora del ion, o subunidad α (http://www.genenames.org/cgi-bin/genefamilies/set/183). Acorde con su homología y aspectos funcionales, se dividen en cuatro familias: 1) **canales de potasio activados por voltaje** (Kv; *voltage-gated potassium channels*), que se abren en respuesta a la despolarización de la membrana contribuyendo así a la repolarización y terminación del potencial de acción (flujo de corriente desde el interior hacia el exterior celular), 2) **canales de potasio activados por calcio** (KCa; *calcium-activated potassium channel*), sensibles al incremento del Ca^{2+} intracelular, 3) **canales de potasio rectificadores internos** (Kir; *inwardly rectifying potassium channels*) activos a potenciales por debajo del potencial de equilibrio y regulados por moduladores de la actividad celular tales como las proteínas G (subfamilia GIRK), nucleótidos o poliaminas (flujo de corriente desde el exterior hacia el interior) y, 4) la familia de **canales de potasio con dos dominios de poro** (K_{2P}; *two-pore domain potassium channel*) de interés en la presente Tesis. Esta última familia recibe su nombre en base a la diferente topología respecto a las otras familias: mientras todos los miembros de las diferentes familias presentan un único dominio de poro (P) en cada subunidad α, los canales K_{2P} contienen dos (ver figura 15). Cualquier canal de potasio para ser funcional ha de contener cuatro dominios P para formar el poro conductor de potasio (Doyle et al., 1998). Por consiguiente, los canales K_{2P} dimerizan, hecho que los distingue y caracteriza frente a las otras familias de canales que tetramerizan (Lesage

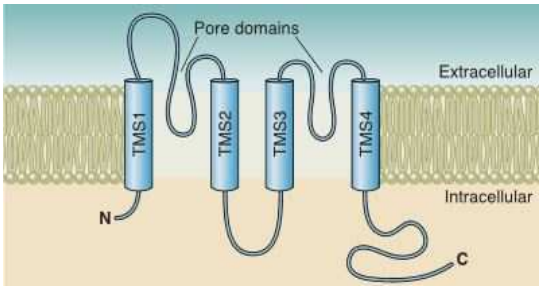

Figura 15. Representación esquemática de la topología de una subunidad K_{2P}. Los segmentos transmembrana se indican con cilindros azules (TMS1-4). Adaptado de Enyedi and Czirják, 2010.

and Lazdunski, 2000; Talley and Bayliss, 2002; Berg et al., 2004; Hwang et al, 2014; Levitz et al., 2016).

Los canales K_{2P} se expresan de modo abundante en el CNS, tanto en células gliales como en las neuronas (Talley et al., 2001; Trimmer, 2015). Éstos generan corrientes débiles que contribuyen a establecer el potencial de reposo de la membrana regulando la excitabilidad de las neuronas (Aller et al., 2005). A nivel de la glía participan, por ejemplo, en la modulación de la liberación de glutamato astrocítico contribuyendo a la homeostasia de la neurotransmisión glutamatérgica (Woo et al., 2012). A nivel funcional, los canales K_{2P} responden a una gran variedad de estímulos fisiológicos como el pH interno, neurotransmisores, segundos mensajeros acoplados a receptores de membrana que señalizan a través de proteína G (cAMP, IP_3, Ca^{2+}, PKA y PKC), temperatura, lípidos celulares (fosfolípidos, lisofosfolípidos, ácidos grasos insaturados, etc.), así como otros estímulos no fisiológicos incluidos los anestésicos volátiles (cloroformo, halotano, isoflurano) y los agentes farmacológicos (riluzol, fluoxetina) (Patel et al., 1998; Lesage and Lazdunski, 2000; Maingret et al., 2000; Talley et al., 2000; Bayliss et al., 2001; Talley and Bayliss, 2002; Berg et al., 2004; Kennard et al., 2005; Mathie, 2007; Cadaveira-Mosquera et al., 2011; Xi et al., 2011).

En mamíferos, la familia K_{2P} está formada por 15 miembros divididos en 6 subfamilias: 1) canales de potasio rectificadores internos débiles con dominio de poro en tándem (TWIK; *tandem pore domain weak inwardly rectifying K^+ channel*), incluyen TWIK1, TWIK2 y KCNK7; 2) canales de potasio TASK, incluyen TASK1, TASK3 y TASK5; 3) canales de potasio TREK, incluyen TREK1, TREK2 y TRAAK; 4) canales de potasio activados por alcalinidad semejantes a TWIK (TALK; *TWIK-related alkaline-activated K^+ channel*), incluyen TALK1, TALK2 y TASK2; 5) canales de potasio inhibidos por halotano semejantes a

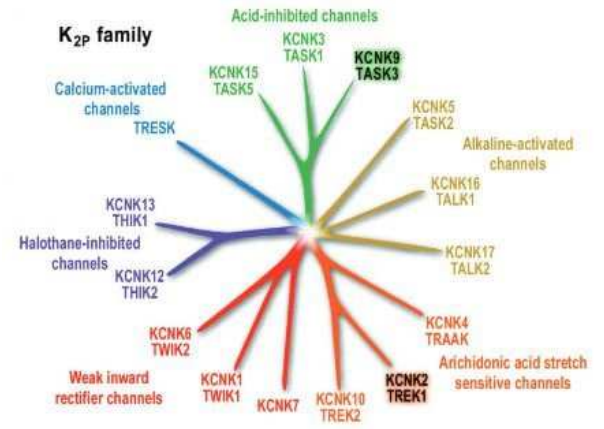

Figura 16. Familia de los canales K_{2P}. Los 15 miembros están clasificados en seis subfamilias diferentes simbolizadas con ramas de diferente color. Adaptado de Borsotto et al., 2015.

TWIK (THIK; *TWIK-related halothane-inhibited K^+ channel*), incluyen THIK1 y THIK2; y 6) canales de potasio de médula espinal semejantes a TWIK (TRESK; *TWIK-related spinal cord K^+ channel*) formado por un único miembro denominado igual que la subfamilia (ver figura 16) (Enyedi and Czirják, 2010). En condiciones fisiológicas todos ellos funcionan como rectificadores abiertos (flujo de corriente desde el interior hacia el exterior según gradiente de concentración) a excepción de TWIK1 y TWIK2, que lo hacen como rectificadores internos (Lesage et al., 1996; Honoré, 2007; Chen et al., 2014). Por otro lado, algunos canales como el TREK1 o TASK3, están constitutivamente abiertos en reposo, cerrándose en respuesta a la activación de receptores acoplados a proteína G, (Dupart et al., 1997; Talley et al., 2000; Bayliss et al., 2001; Mathie, 2007). Otros miembros de la familia K_{2P}, inactivos en reposo, requieren de un estímulo para abrirse (Patel et al., 1998; Maingret et al., 2000).

En los últimos años, estudios realizados en primates no humanos y en seres humanos han sugerido que los canales TASK3 y TREK1 podrían contribuir a la fisiopatología de la depresión (ver figura 17) (Perlis et al., 2008; Dillon et al., 2010; Bogdan et al., 2011; Borsotto et al., 2015). En modelos animales se ha mostrado que ambos genotipos de ratones nulos para los canales TREK1 o TASK3 (*knockout)* muestran comportamientos de tipo antidepresivo (Heurteaux et al., 2006; Bayliss and Barrett, 2008; Gotter et al., 2011). Utilizando paradigmas comportamentales, tales como FST, TST o test de supresión de la ingesta por novedad (NSFT; *novelty suppressed feeding test*), se ha observado que los ratones *knockout* para estos canales son más resistentes a mostrar síntomas de tipo depresivo que los controles, comportándose de modo similar a aquellos ratones tratados con fluoxetina o paroxetina (Heurteaux et al., 2006; Gotter et al., 2011). Se ha observado también que

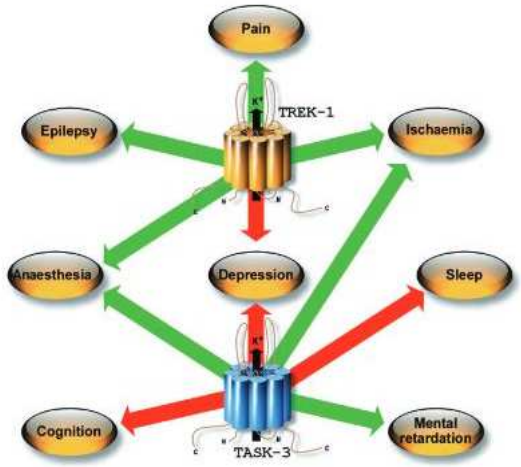

Figura 17. Esquema representado el rol de los canales TREK1 y TASK3 en diferentes procesos fisiológicos y patológicos. Las flechas verdes y rojas indican la apertura o cierre del canal, respectivamente, implicado en cada proceso. Notar que ambos canales TREK1 y TASK3 ejercen una influencia positiva en depresión cuando permanecen cerrados. Adaptado de Borsotto et al., 2015.

ratones *knockout* para TREK1 muestran una respuesta de tipo ansiosa en el campo abierto (OF; *open field*) (Mirkovic et al., 2012). Asimismo, se ha descrito que ratones deficientes para el canal TASK3 presentan alteraciones en el ciclo sueño-vigilia, supresión del sueño REM e incremento de la temperatura corporal (Gotter et al., 2011), signos característicos del estado de ánimo elevado y de la acción antidepresiva (Wirz-Justice, 2006).

Ambos canales, TREK1 y TASK3, se expresan en la PFC y el HPC (Fink et al., 1996; Talley et al., 2001), áreas cerebrales implicadas en los aspectos cognitivos de la depresión como los problemas de memoria, sentimiento de culpa o la desesperación. También se encuentran expresados en AMG e Hyp, áreas cerebrales involucradas con la memoria emocional y la anhedonia descritas en depresión (Maingret et al., 2000; Talley et al., 2001; Nestler et al., 2002). Además, los canales TREK1 y TASK3 se expresan de modo abundante en los núcleos monoaminérgicos del DR y LC, precisamente en las neuronas serotoninérgicas y noradrenérgicas (Talley et al., 2001; Marinc et al., 2011).

En el caso del canal TREK1, mucho más documentado que el canal TASK3, se ha observado que la fluoxetina bloquea directamente el canal, sugiriendo que parte del mecanismo de acción de este fármaco involucra a TREK1 (Kennard et al., 2005; Sandoz et al., 2011; Xi et al., 2011). En este sentido, se han desarrollado otros compuestos que antagonizan selectivamente TREK1 tales como SID1900 y spadin con potencial antidepresivo (Mazella et al., 2010; Borsotto et al., 2015; Ye et al., 2015). Se ha descrito que estos compuestos producen respuestas de tipo antidepresivas en el FST y TST, aumentan la frecuencia de

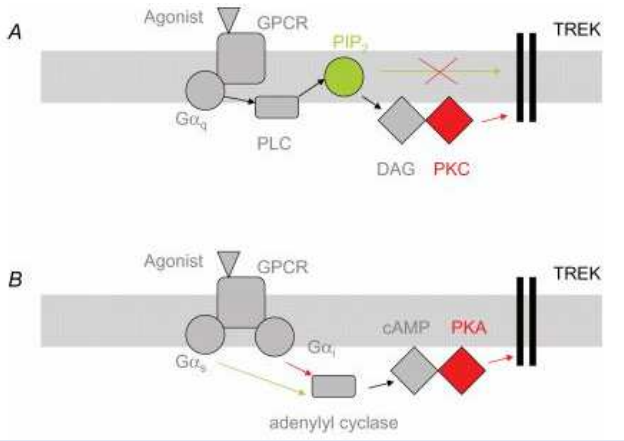

Figura 18. Diferentes tipos de proteína G actúan sobre los canales TREK para regular su actividad. (a) La inhibición de los canales TREK por la activación de la proteína G_q esta mediada por PKC o por la depleción de PIP_2. (b) La actividad de los canales TREK puede ser incrementada o disminuida por G_i y G_s, respectivamente, por la modulación de los niveles intracelulares de cAMP. Adaptado de Mathie, 2007.

descarga de las neuronas serotoninérgicas en el DR y estimulan la neurogénesis en el HPC de ratones (Mazella et al., 2010; Ye et al., 2015). Además, ambos compuestos (SID1900 y spadin) incrementaron la señalización PKA-CREB-BDNF en el HPC, PFC y DR, efecto mayor en presencia del agonista del receptor 5-HT_{1A} 7-(dipropilamino)-5,6,7,8-tetrahidronaftalen-1-ol (8-OH-DPAT; *7-(Dipropylamino)-5,6,7,8-tetrahydronaphthalen-1-ol*) y revertido por el antagonista WAY100635 (Ye et al., 2015). En concordancia con esta sinergia con el receptor 5-HT_{1A}, se conoce que TREK1 está regulado por neurotransmisores que inducen fluctuaciones de cAMP a través de receptores acoplados a proteína G_i o G_s (Fink et al., 1996; Patel et al., 1998; Bang et al., 2000; Lesage et al., 2000; Bockenhauer et al., 2001; Heurteaux et al., 2006) como también por aquellos que activan proteína G_q (ver figura 18) (Fink et al., 1996; Lesage and Lazdunski, 2000; Lesage et al., 2000; Czirjak and Enyedi, 2002; Chemin et al., 2003; Enyeart et al., 2005; Lopes et al., 2005; Murbartián et al., 2005).

Con respecto al canal TASK3, se han descrito algunos compuestos capaces de inhibir de modo no selectivo el canal TASK3 como por ejemplo el Zn^{2+} y el rojo rutenio así como agonistas cannabinoides como la anandamida, la metanandamida y el WIN212-2 (Maingret et al., 2001; Czirják and Enyedi, 2002, 2003; Berg et al., 2004; Veale et al., 2007b; Mathie et al., 2010). Varios estudios han observado que los agonistas cannabinoides producen efectos de tipo antidepresivo en modelos murinos, como reducción de la inmovilidad en el TST y FST, aumento de la neurogénesis en el DG del HPC, así como incremento de la frecuencia de descarga de las neuronas serotoninérgicas del DR y noradrenérgicas del LC (Gobbi et al., 2005; Jiang et al., 2005; Zhong et al., 2014). No obstante, el bloqueo de TASK3 con estas drogas no selectivas, puede inducir efectos adversos como ataxia y otras alteraciones del movimiento. Aunque se ha identificado un antagonista selectivo para TASK3 (con base 5,6,7,8-tetrahidropirido[4,3-d]pirimidina) capaz de modular los patrones del sueño en modelos murinos de electroencefalograma (Coburn et al., 2012), su potencial como fármaco antidepresivo aún necesita ser validado.

A nivel de la señalización, parece que TASK3 es inhibido por la activación de receptores acoplados a proteína G_q (Mathie, 2007). Aunque la secuencia de eventos

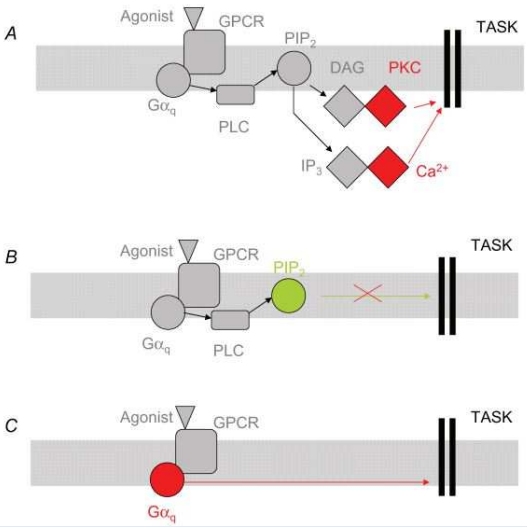

Figura 19. Hipótesis que relacionan la inhibición del canal TASK3 con la proteína G_q. (a) La inhibición de TASK3 esta mediada por uno o más productos de la hidrólisis de PIP_2. (b) PIP_2 mantiene TASK3 abierto. La llegada de estímulo produce su hidrólisis e inhibición. (c) Gαq actúa directamente sobre TASK3 inhibiéndolo. Adaptado de Mathie, 2007.

subsecuentes a la activación de la proteína G_q que lleva a la inhibición del canal no está bien establecida, estudios *in vitro* han sugerido que puede ser inhibido por PKC (Vega-Saenz de Miera et al., 2001; Veale et al., 2006a), directamente por la proteína G_q (Chen et al., 2006) o por la hidrólisis del fosfatidilinositol 4,5-bifosfato ($PIP_{2;}$ *phosphatidylinositol 4,5-bisphosphate*) (ver figura 19) (Lopes et al., 2005). No obstante, otros estudios han encontrado resultados opuestos, no detectando inhibición de TASK3 mediada por PKC u obteniendo su inhibición independiente de PIP_2 (Kim et al., 2000; Meadows and Randall, 2001; Chemin et al., 2003; Chen et al., 2006). Por otro parte, también se ha observado que TASK3 puede ser inhibido cuando el pH desciende por debajo de 6.4 y también, aunque más débilmente, por la acción de la PKA (Meadows and Randall, 2001; Berg et al., 2004).

El conocimiento acerca de la modulación fisiológica de TASK3 es limitado. Esto es consecuencia, en parte, de la escasa disponibilidad de compuestos selectivos para este canal. Además, los canales K_{2P} tienen una distribución ubica en el cerebro y TASK3 no es la excepción. Los canales K_{2P} de potasio mantienen el potencial de reposo de membrana, vital para el mantenimiento de la homeostasia celular. Si lo que se desea es modular la expresión/función del canal TASK3 en un área cerebral o población neuronal concreta, se deberá diseñar y generar nuevas estrategias basadas por ejemplo en el RNAi, uno de los objetivos principales de la presente Tesis.

1.7. RNA de interferencia

Como se ha mencionado previamente, la depresión es un trastorno complejo que resulta de la interacción de factores neurobiológicos, genéticos, culturales y ambientales. Existen evidencias crecientes que la depresión se asocia con: i) alteraciones de la plasticidad estructural y sináptica, ii) patologías relacionada con el estrés y sistema inmunitario, y iii) en cierta medida, polimorfismos genéticos (Peña et al, 2014; Ota and Duman, 2013; Sequeira and Turecki, 2006). El procesamiento aberrante de la información a través de redes celulares en los circuitos del estado de ánimo y la cognición puede conducir a alteraciones de la plasticidad sináptica y estructural, lo que lleva al final a la aparición de los síntomas de la depresión. Las investigaciones realizadas durante la última década han permitido identificar mecanismos epigenéticos como efectores importantes para regular los programas de la expresión de genes asociados con depresión, acción antidepresiva y la resistencia a la depresión en modelos animales (Sun et al., 2013).

Más recientemente, los RNAs pequeños no codificantes (ncRNAs; *non-coding RNA*) endógenos, entre ellos los miRNAs, han surgido como reguladores post-transcripcionales de la expresión génica. Los miRNAs juegan un papel en casi todos los procesos biológicos, tales como la proliferación celular, el desarrollo, la diferenciación, y la muerte celular programada. Más de 1400 miRNAs han sido ya identificados, cada uno de los cuales puede regular la expresión de un gran número de moléculas diferentes de mRNA**,** evidenciando su papel crucial como determinantes de la homeostasia celular (Lin y Gregory, 2015). Los miRNAs pueden no sólo evitar la traducción de su mRNA diana o promover su degradación, sino que también pueden actuar como activadores de la traducción o incluso impedir la transcripción mediante la unión a promotores de genes (Krol et al., 2010). Dada la complejidad celular y transcripcional del sistema nervioso, no es sorprendente que aproximadamente el 75% de los miRNAs identificados se expresen en el cerebro en comparación con otros tejidos (Kosik, 2006).

Los primeros estudios de localización han mostrado que los miRNAs se expresan en diferentes áreas del cerebro. Sin embargo, el uso de las nuevas tecnologías ha permitido identificar la distribución cerebral de los miRNAs a nivel celular y subcelular. Por ejemplo, utilizando técnicas de inmunoprecipitación en ratones transgénicos, a los que mediante el sistema Cre/Lox se ha introducido un epítopo a la proteína Ago2 en un tipo neuronal concreto, ha sido posible identificar el perfil de expresión de aproximadamente 480 miRNA en neuronas glutamatérgicas y en diferentes subtipos de interneuronas GABAérgicas de la PFC (He et al., 2012). Del mismo modo, los transcritos de miRNAs se procesan no solo dentro del núcleo sino también en las dendritas, estando altamente enriquecidos en las sinapsis (Smalheiser, 2014).

Los miRNAs cerebrales contribuyen tanto al desarrollo del cerebro como a la función neuronal, incluyendo procesos como la neurogénesis, diferenciación neuronal y sinaptogénesis, ofreciendo muchas oportunidades para modular "finamente" las propiedades funcionales de las subpoblaciones neuronales (Mercer et al, 2008; Sun et al., 2015). Por otra parte, los miRNAs juegan un papel crítico en la determinación del destino celular de las neuronas y la glía mediante la supresión de genes específicos. De este modo, ambos miR-124 y miR-29 se encuentran entre los miRNAs mejor estudiados y se ha demostrado que regulan la diferenciación de los progenitores en las vías neuronales o gliales. Mientras el miR-124 y el miR-128 se expresan principalmente en las neuronas, el miR-23, el miR-26 y el miR-29 se producen en grandes cantidades en los astrocitos (Krichevsky et al., 2006; Makeyev et al., 2007; Sun et al, 2015). La desregulación del miR-124 se ha relacionado con la neurodegeneración, trastornos de la inmunidad del CNS y el estrés entre otros (Sun et al., 2015). Algunos miRNAs están implicados en funciones neurológicas tales como el aprendizaje y la memoria. Así, se ha sugerido que el miR-132, el miR-134 y el miR-let-7 desempeñan un papel crucial en la formación y la plasticidad de las sinapsis, mientras que otros como el miR-124a y el miR-125b se han asociado con el crecimiento de los axones (Vo et al., 2005;. Schratt et al, 2006). Los datos actualmente disponibles indican que los miRNAs pueden ser importantes reguladores celulares que contribuyen a la función cerebral normal y patológica (Alural et al 2016;

Dwivedi, 2016). Los cambios en la expresión y la función de los miRNAs están implicados en la fisiopatología del trastorno depresivo así como en las acciones antidepresivas. Dada la necesidad crítica de descubrir nuevos marcadores diagnósticos y tratamientos para la depresión, es imprescindible ampliar el foco de los estudios genómicos para incluir el papel de los ncRNAs: miRNAs y siRNAs. Estos últimos representan el objetivo central de la presente Tesis.

1.7.1. Mecanismo RNAi

El RNAi es un proceso endógeno implicado en la defensa celular contra las infecciones virales, en el control de la expresión y la movilidad de los transposones y, en la regulación de la expresión génica endógena (Hannon, 2002). Evolutivamente conservado desde las plantas hasta los mamíferos, fue originalmente identificado en *C. Elegans* por Andrew Fire y Craig Mello, descubrimiento que les valió el Premio Nobel de Fisiología o Medicina en el año 2006 (Fire et al., 1998; Elbashir et al., 2001).

A grandes rasgos, el RNAi se refiere al proceso por el cual moléculas de RNA de doble hebra (dsRNA; *double-stranded RNA*), como miRNAs y siRNAs, silencian un gen diana a través de la degradación específica del mRNA o del bloqueo de la traducción. Concretamente, los genes que codifican los miRNAs son transcritos por la RNA polimerasa II generando los miRNA primarios (pri-miRNAs; *primary miRNA*) de entre 50 y 120 nucleótidos de largo (Lee et al., 2004). Entonces, y aún en el núcleo, los pri-miRNAs son escindidos a precursor de miRNA (pre-miRNA; *precursor-miRNA*) por un complejo multiproteico que incluye DGCR8 y la ribonucleasa Drosha (Lee et al., 2003). Los pre-miRNAs son ahora reconocidos por la exportina 5 y transportados al citoplasma, donde la endoribonucleasa Dicer y la proteína TRBP generan ya los miRNAs maduros (Park et al., 2011), en otras palabras, moléculas de RNA de cadena simple (ssRNA; *single-stranded RNA)* de aproximadamente 22 bases (Bartel, 2004). Finalmente, el miRNA maduro es integrado al complejo silenciador inducido por RNA (RISC; *RNA-induced silencing complex*) en una serie de pasos en que se incorporan las proteínas Ago2, GW182 y FMRP (Im and Kenny, 2012), formando un complejo capaz de reconocer e inhibir el mRNA diana. Según el grado de complementariedad del

mRNA diana con la hebra del miRNA, el silenciamiento puede ser por degradación del mRNA (complementariedad perfecta) o represión de la traducción (complementariedad imperfecta) (ver figura 20) (Humphreys et al., 2005).

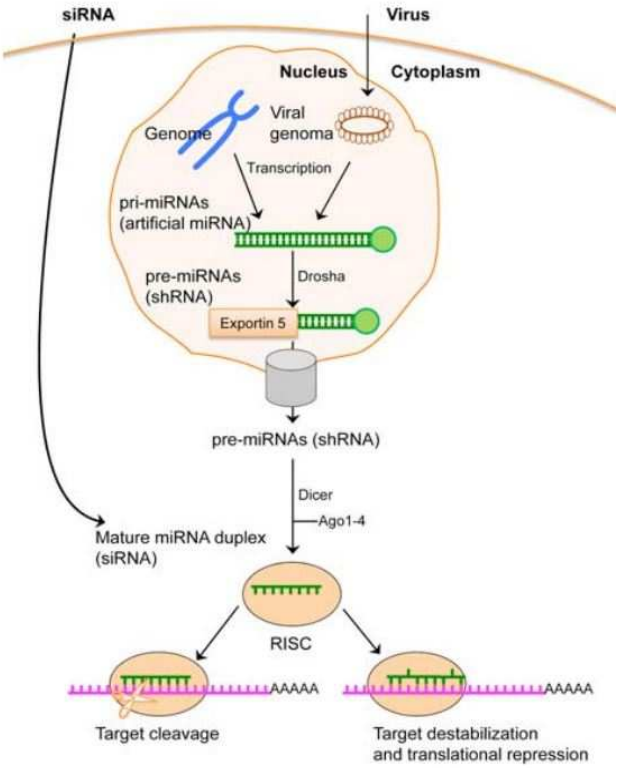

Figura 20. Representación esquemática del mecanismo bioquímico del RNAi. Brevemente, los genes que codifican para miRNAs son transcritos a pri-miRNAs, escindidos por el complejo Drosha-DGCR8 a pre-miRNA y traslocados al citosol por la exportina 5. En el citoplasma celular, Dicer escinde el pre-miRNA formando el miRNA funcional que es incorporado al RISC en una secuencia de eventos regulados por Dicer, Ago2 y otras proteínas reguladoras. Finalmente, el miRNA guía todo el complejo ribonucleoproteico al mRNA diana por interacción de complementariedad de bases conduciendo a la desestabilización y represión de la traducción o provocando la degradación del mRNA. La inhibición de la expresión génica puede ser manipulada externamente cuando una molécula de siRNA sintético alcanza el compartimiento intracelular después de su aplicación. Adaptado de Bortolozzi et al., 2014.

La maquinaria que forma el sistema RNAi puede ser manipulada mediante la introducción de siRNAs exógenos, o mediante la transfección de vectores que codifican para RNAs cortos en horquilla (shRNA; *short hairpin RNA*), así como otros vectores basados en miRNAs (ver figura 20) (Brummelkamp et al., 2002; Paddison et al., 2002; Silva et al., 2005; Stegmeier et al., 2005; Gao and Zhang, 2007; Boudreau et al., 2011; Boudreau and Davidson, 2012). Por lo tanto, el RNAi puede ser utilizado en neurociencia con dos enfoques diferentes. En primer lugar, el RNAi puede servir como una herramienta biológica para entender el papel de los diferentes genes candidatos que han sido implicados en la neurobiología de los trastornos neuropsiquiátricos. En segundo lugar, el RNAi puede ser utilizado como una herramienta terapéutica para silenciar los genes diana en el proceso de la enfermedad. Sin embargo, a pesar de su potencial terapéutico prometedor, la utilidad *in vivo* del RNAi está limitada principalmente por nuestra capacidad para introducir los siRNAs en el área de interés, siendo este uno de los grandes desafíos de la presente Tesis.

1.7.2. Consideraciones para el uso *in vivo* de siRNAs

Los siRNAs son moléculas de dsRNA sintéticas de 21-23 pares de bases diseñadas específicamente para silenciar la expresión de genes diana. Estos dsRNAs son procesados por la maquinaria RNAi endógena después de ser introducidos en las células (ver figura 20). A diferencia de los miRNAs, la hebra antisentido del siRNA presenta una complementariedad de bases perfecta con el mRNA diana, de modo que provoca la degradación del mRNA. Debido a que pueden silenciar de manera eficiente y específica la expresión de genes, los siRNAs se convierten en herramientas útiles para estudiar la función de genes individuales, tanto *in vitro* como *in vivo,* y representan una nueva clase de terapia atractiva especialmente para pacientes con trastornos cerebrales y otras enfermedades no tratables con la farmacología disponible (Ozcan et al., 2015).

A pesar de las ventajas que ofrecen los siRNAs para el tratamiento potencial de las enfermedades cerebrales, aún quedan muchos retos por resolver, incluyendo: 1) los efectos *off-target*, 2) la degradación rápida de las moléculas de siRNAs, 3) la generación de respuesta inmune, 4) la captación celular *in vivo* limitada, y 5) la selectividad celular. El diseño racional de secuencias de siRNAs, el desarrollo de modelos predictivos basados en algoritmos de segunda generación, la presencia de modificaciones químicas y la utilización de nanoportadores ofrecen oportunidades significativas para superar algunos de los problemas anteriores.

Aunque los siRNAs están diseñados para reconocer una diana específica, también podrían silenciar a un número desconocido de genes no deseados. Estos efectos *off-target* pueden ocurrir de dos maneras. Por un lado, los siRNAs pueden presentar una complementariedad imperfecta con un mRNA, diferente a su diana, manteniendo la capacidad de reprimir su traducción (Snove et al., 2004). Los miRNAs reconocen sus dianas principalmente por complementariedad de bases con sus regiones *seed* (nucleótidos 2-8). La complementariedad con el resto de nucleótidos es menos importante para el reconocimiento. Debido a que los siRNAs son prácticamente idénticos a los miRNAs, estos pueden reconocer otros mRNAs con su región *seed* produciendo la represión de un número impredecible de mRNAs. Por otro lado, los

siRNAs pueden introducirse en vías de miRNAs endógenos y reprimir la expresión de uno o más mRNAs por unión con sus regiones 3' no traducidas (3'UTR; *3' untranslated region*) (Doench et al., 2003). Se están invirtiendo muchos esfuerzos, incluyendo modificaciones químicas de las secuencias de siRNAs y variaciones en su diseño, para limitar el riesgo de efectos *off-target* sin reducir la potencia del siRNA.

En cuanto a la eficacia de los siRNAs, las primeras investigaciones mostraron que no todos los siRNAs son equipotentes. Se describió que distintos siRNAs dirigidos a diferentes regiones de la misma secuencia de mRNA tienen diferentes eficacias, y que solamente una pequeña fracción de los siRNAs son funcionales en células de mamífero. Por ejemplo, entre diferentes siRNAs seleccionados aleatoriamente, se observó que el 58-78% de estos inducen un silenciamiento con una eficacia superior al 50% y que solo un 11-18% de ellos produce silenciamientos del orden del 90-95% (Chalk et al., 2004). El diseño de la primera generación de siRNAs validados se focalizó en características específicas del propio siRNA como el contenido en guanina-citosina y la termolabilidad general, con poca o ninguna consideración respecto la estructura del mRNA diana. Más recientemente se han desarrollado nuevos algoritmos de segunda generación para el diseño de moléculas de siRNA teniendo en cuenta además, la estructura del mRNA diana para maximizar la potencia de silenciamiento de una región en particular (Rettig and Behlke, 2012; Ozcan et al., 2015).

Por otra parte, se ha reportado que el mecanismo de RNAi está implicado en la respuesta inmune. Varios estudios han revelado que los siRNAs pueden activar la inmunidad innata mediante la inducción de la expresión del interferón, incluso a dosis muy bajas (Judge et al., 2005; Robbins et al., 2008). La proteína quinasa R (PKR; *protein kinase R*) y tres vías de señalización de receptores semejantes a toll (TLR; *toll-like receptors*) pueden estar implicadas en la activación inmunológica de los siRNAs, independientemente de su secuencia. Además, la propia secuencia del siRNA puede estimular la producción de citoquinas proinflamatorias a través de la activación de los receptores TLR7 y TLR8. Algunas secuencias de oligonucleótidos como 5'-UGUGU-3' (Judge et al., 2005) o 5'-GUCCUUCAA-3' (Hornung et al., 2005) así como el contendido

en uridina de las secuencias de siRNAs han sido identificadas como inductoras inmunológicas. Ciertas modificaciones químicas en los siRNAs tales como las 2'-O-metilaciones se usan para prevenir la activación del sistema inmune.

Otros factores como la resistencia frente a la actividad enzimática nucleasa, el tiempo de vida media, la biodistribución y la captación celular son variables necesarias a tener en cuenta para el diseño adecuado de siRNAs de uso terapéutico (Behlke, 2008; Gaglioni and Messere, 2010). Concretamente, junto a la cinética de excreción rápida, la susceptibilidad a la degradación por nucleasas es un problema importante que limita el tiempo de mida media de las moléculas de siRNA en plasma (Bartlett and Davis, 2007; Volkov et al., 2009). Se han descrito algunas modificaciones químicas como la introducción de fosfotionatos que protegen a los siRNAs de la degradación por nucleasas sin interferir con la eficiencia del siRNA. Además otras modificaciones incluyen la conjugación con ligandos hidrofóbicos (por ej. colesterol) que junto a los fosfotionatos aumentan la interacción de los siRNAs con las proteínas presentes en el suero favoreciendo el tiempo de vida media (Braasch et al., 2004; Soutschek et al., 2004; Behlke, 2008; Ozpolat et al., 2010).

Otro aspecto importante consiste en la captación de los siRNAs por parte de las células diana así como la llegada a su lugar de acción en el citosol o el núcleo (Juliano et al., 2008). Se han documentado varias estrategias para dirigir los siRNAs hacia el cerebro utilizando lípidos catiónicos, complejos poliméricos o endocitosis mediada por anticuerpo (Song et al., 2005; Vornlocher, 2006; Ozpolat et al., 2010). Otra estrategia es utilizar la endocitosis mediada por receptor/transportador para favorecer la acumulación selectiva de siRNAs conjugados en las células diana que expresan el receptor/transportador de manera específica y abundante en la superficie celular (Juliano et al., 2008; artículos de la presente Tesis). El desarrollo y caracterización de esta última aproximación tecnológica para dirigir *in vivo* las moléculas de siRNAs hacia las neuronas monoaminérgicas, principalmente serotoninérgicas, ha sido el trabajo central de la presente Tesis.

1.7.3. Desarrollo preclínico de terapias antidepresivas basadas en siRNAs

Varios estudios preclínicos en modelos de roedores han sugerido la posibilidad de regular la expresión de genes en las neuronas monoaminérgicas implicados en los trastornos del estado de ánimo y cognitivos utilizando moléculas exógenas de siRNA (Shishkina et al., 2004; Thakker et al, 2004, 2005; Salahpour et al., 2007; artículos de la presente Tesis). Algunos de estos genes, que codifican para los transportadores de monoaminas (SERT, DAT, NET), son reguladores clave de la neurotransmisión dopaminérgica, noradrenérgica y serotoninérgica ya que controlan la fracción activa de estas monoaminas (detallado en los apartados 1.3 y 1.4). Estos transportadores también están implicados en la fisiopatología y el tratamiento farmacológico de los trastornos neuropsiquiátricos como el trastorno por déficit de atención con hiperactividad, la dependencia a las drogas, la enfermedad de Parkinson y los trastornos del estado de ánimo, incluyendo la ansiedad y la depresión. Como se ha descrito anteriormente, los SSRI y los SNRI son tratamientos de primera elección para el trastorno depresivo mayor, pero muestran limitaciones importantes en cuanto a la eficacia y rapidez de acción (Trivedi et al., 2006a). Dado el papel clave de los transportadores en el control de la neurotransmisión de monoaminas en el cerebro, los trabajos de Thakker y colaboradores (Takker et al., 2004, 2005) fueron pioneros al silenciar los transportadores DAT y SERT utilizando RNAi *in vivo*. En estos estudios, la administración intracerebroventricular de siRNAs no modificados químicamente dirigidos contra DAT o SERT a 400 µg/día durante dos semanas redujo específicamente los niveles de los mRNAs de DAT y SERT aproximadamente un 30% en comparación con el grupo control. Los ratones *knockdown* para SERT mostraron respuestas antidepresivas similares al tratamiento con el SSRI citalopram en el FST (Thakker et al., 2005). Además, la reducción de la expresión de SERT fue similar a la observada previamente en un estudio inicial usando plásmidos que contienen una secuencia de oligonucleótido antisentido parcial contra el gen del SERT (reducción del 28% observada 7 días después de la infusión intra-DR del plásmido) (Fabre et al., 2000).

Otros estudios, han utilizado siRNAs para investigar el papel de genes clave implicados en la fisiopatología y tratamiento de la depresión en circuitos que no están directamente relacionados con la señalización monoaminérgica. A continuación, se resumen algunas de estas dianas, que incluyen neuropéptidos, receptores de glutamato y factores tróficos entre otros, algunos de los cuales carecen de farmacología adecuada.

Las dinorfinas son péptidos opioides endógenos que se sintetizan a partir de la proteína precursora prodinorfina, la cual se cree participa en la regulación de los estados de ánimo negativos y la neuroplasticidad asociada con la adicción (Carlezon and Thomas, 2009). Así la transfección de un shRNA para silenciar la prodinorfina en el NAc de rata redujo el comportamiento de tipo depresivo en el FST, aunque el mismo tratamiento no alteró el comportamiento de tipo ansioso en el laberinto en cruz elevado (EPM; *elevated plus maze*) (Cohen et al., 2014). La galanina es otro neuropéptido implicado en la regulación del estado de ánimo (Juhasz et al., 2014). Se ha observado que ratones con sobreexpresión de galanina muestran un incremento del tiempo de inmovilidad en el FST (Kuteeva et al., 2005). El silenciamiento mediante siRNAs de los receptores de galanina 1 o 2 fue suficiente para prevenir el aumento del tiempo de inmovilidad observado en el FST tras la administración de galanina. (Millón et al., 2014).

Dos intervenciones no farmacológicas para la depresión, la ECT y la DBS, están asociadas con un aumento de la liberación de adenosina y la estimulación de los receptores purinérgicos A1 (Bekar et al., 2008; Sadek et al., 2011). Se ha observado que la administración del agonista del receptor A1 CCPA conlleva efectos de tipo antidepresivo en el FST. Por el contrario, los ratones *knockout* para este receptor presentaron un fenotipo depresivo con incremento de la inmovilidad en el TST, anhedonia en la prueba de preferencia por la sacarosa y mostraron resistencia al efecto antidepresivo de la terapia por deprivación del sueño evaluados en el FST y el TST (Hines et al., 2013; Serchov et al., 2015). Por otro lado, se conoce que algunos tratamientos antidepresivos incrementan la expresión de homer1a en la mPFC de ratón (Conti et al., 2007; Sun et al., 2011), proteína implicada en la etiología de la depresión (Rietschel et al., 2010). La administración local de siRNAs para silenciar

homer1a en la mPFC de ratón aumentó el comportamiento de tipo depresivo en el FST y evitó el efecto antidepresivo de la terapia por deprivación del sueño y los tratamientos con imipramina y ketamina asociados a la activación del receptor A1 (Serchov et al., 2015).

Otra diana de interés en cognición y el estado emocional es el receptor metabotrópico de glutamato 7 (mGlu7; *metabotropic glutamate receptor 7*) (Ohishi et al., 1995; Kinoshita et al., 1998). Se ha sugerido que el receptor mGlu7 podría ser clave en la modulación de la respuesta sináptica glutamatérgica y la neurotransmisión GABAérgica (Kinoshita et al., 1998; Kosinski et al., 1999). La generación del ratón *knockout* o el silenciamiento mediante siRNAs contra el receptor mGlu7 han indicado que participa en procesos tales como la ansiedad, el miedo, la memoria espacial y la respuesta hormonal al estrés (Frendt et al., 2008; O'Connor et al., 2010).

Del mismo modo, algunos síntomas de la depresión pueden ser inducidos en seres humanos bloqueando la enzima acetilcolinesterasa (AChE; *acetylcholinesterase*) (Risch et al., 1981; Furey and Drevets, 2006; Mineur et al., 2013). Se ha observado que la infusión hipocampal de un shRNA contra la AChE utilizando un vector vírico induce comportamientos de tipo ansioso en el OF y en la caja luz-oscuridad (DLB; *dark-light box*), como también de tipo depresivo en el TST y el FST, comportamientos que fueron revertidos por el SSRI fluoxetina (Mineur et al., 2013).

Se ha descrito disminución de los niveles de BDNF en el HPC en víctimas de suicidio y pacientes con depresión (Dwivedi et al., 2003). Además, investigaciones preclínicas mostraron una relación directa entre la reducción de la neurogénesis en el HPC y comportamientos de tipo depresivo (Santarelli et al., 2003). Utilizando el mecanismo de RNAi se confirmó que la reducción *in vivo* la expresión de BDNF en regiones específicas del HPC disminuye la diferenciación neuronal, induce anhedonia en la prueba de preferencia por la sacarosa y reduce el tiempo de inmovilidad en el FST (Taliaz et al., 2010). Estos resultados respaldan la hipótesis neurotrófica de la depresión.

Finalmente, otras dianas implicadas en depresión o en el desarrollo de nuevas terapias antidepresivas son la fosfodiesterasa 4 (PDE4; *phosphodiesterase 4*) (Wang et al., 2013) y la calcineurina (Mineur et al., 2014). Así, la infusión de vectores virales empaquetados con un shRNA contra la PDE4 en la PFC de rata produjo efectos antidepresivos en el FST y TST, así como mejoras de la cognición en laberinto de agua de Morris similares a los producidos por el inhibidor prototipo de PDE4 rolipram. También, el silenciamiento de calcineurina en la AMG de ratón mediante un shRNA produjo incrementos del comportamiento de tipo ansioso en el EPM, DLB y OF, así como comportamientos de tipo depresivo en el FST.

En conjunto, todas estas investigaciones pueden facilitar el desarrollo de nuevos enfoques para el tratamiento del trastorno depresivo y otras enfermedades relacionadas mediante el silenciamiento génico inducido por RNAi.

2. Hipótesis y Objetivos

La hipótesis de trabajo de la presente Tesis plantea que los niveles de expresión del autoreceptor 5-HT_{1A}, el SERT y el canal de potasio TASK3 en las neuronas serotoninérgicas podrían determinar la vulnerabilidad al estrés y por ende, la susceptibilidad a la depresión y/o respuesta antidepresiva en modelos murinos.

El objetivo principal es determinar las consecuencias moleculares, histológicas, neuroquímicas y comportamentales asociadas a la modulación post-transcripcional de los genes 5-HT_{1A}, SERT y TASK3 en las neuronas serotoninérgicas y, este último, también en las neuronas noradrenérgicas mediante la estrategia de RNAi. El silenciamiento específico de genes individuales en áreas cerebrales concretas y/o poblaciones neuronales selectivas contribuirá a entender el rol funcional del gen en estudio y permitirá desarrollar nuevas terapias antidepresivas que superen las limitaciones actuales.

Los objetivos concretos son:

1- Analizar la capacidad (o viabilidad) de disminuir el nivel de expresión de genes *in vivo* localizados en neuronas monoaminérgicas utilizando moléculas de siRNAs aplicadas localmente en áreas cerebrales, de modo intracerebroventricular, o administradas por vía intranasal.

2- Reducir *in vivo* la expresión del autoreceptor 5-HT_{1A} localizado en los núcleos del rafe de ratón utilizando moléculas de siRNA sin modificar o conjugadas químicamente con un ligando que favorece el direccionamiento hacia las neuronas serotoninérgicas. Examinar les consecuencias funcionales en una situación de estrés y analizar la potencialidad como estrategia antidepresiva.

3- Reducir *in vivo* la expresión del SERT en los núcleos del rafe de ratón utilizando moléculas de siRNA sin modificar o conjugadas químicamente para favorecer la acumulación en las neuronas serotoninérgicas. Examinar las consecuencias funcionales sobre diferentes variables antidepresivas en ratones *wild-type* y en un modelo murino de depresión asociado a estrés. Comparar los efectos antidepresivos con aquellos inducidos por el tratamiento con el SSRI fluoxetina.

4- Reducir selectivamente la expresión del canal de potasio TASK3 en neuronas serotoninérgicas o en neuronas noradrenérgicas utilizando una secuencia de siRNA contra TASK3 conjugada químicamente y administrada por vía intranasal. Estudiar los efectos funcionales sobre el sistema serotoninérgico o noradrenérgico con el fin de evaluar su relevancia y potencial como diana antidepresiva.

3. Materiales y Métodos

En esta sección se describen de modo general los materiales y métodos utilizados en la presente tesis. Información más detallada y específica de los mismos se encuentra en la sección de materiales y métodos en los respectivos artículos de esta Tesis.

3.1. Animales

Se utilizaron ratones macho C57Bl/6J entre 10 y 15 semanas de edad suministrados por la empresa Charles River. En los trabajos 1 y 2 se utilizaron también ratones *knockout* para el receptor 5-HT_{1A} procedentes de la Universidad de Princeton (Parks et al., 1998) con el mismo fondo genético C57Bl/6J. A partir de ellos, generamos una colonia estable mantenida en el estabulario de la Facultad de Medicina de la Universidad de Barcelona.

Los animales fueron estabulados en una habitación con temperatura controlada (22 ± 2 ºC), con un ciclo de 12 horas de luz/oscuridad y acceso libre a comida y agua. El cuidado y tratamiento de los animales se realizó según las directrices éticas habituales (regulación europea L35/118/12/1986) y de conformidad con el comité de ética de la Universidad de Barcelona.

3.2. siRNAs: síntesis y tratamiento

La síntesis y purificación de los siRNAs (sin modificar o conjugados químicamente) fue efectuada por la compañía nLife Therapeutics S.L (Granada, España) según patente PCT/EP2011/056270. En el caso de los siRNAs conjugados, la hebra sentido fue modificada introduciendo un grupo amino en la posición 5'-C6, y posteriormente se llevó a cabo la condensación con el grupo éster succinato de la sertralina o reboxetina (sertralina/reboxetina-NH-CH2C(=O)NH(CH2)5COO-succinato). Las hebras de oligonucleótidos conjugadas se purificaron por cromatografía líquida de alta resolución (HPLC; *high-performance liquid chromatography*) en fase reversa. Las fracciones de oligonucleótidos de longitud correcta fueron desaladas, liofilizadas y caracterizadas por espectrometría de masas MALDI-TOF. Las cadenas complementarias de oligonucleótidos fueron anilladas, purificadas utilizando HPLC y finalmente, liofilizadas. La tabla 1 resume los siRNAs utilizados en los diferentes

trabajos de la presente Tesis haciendo referencia al tipo de conjugación, secuencias de las hebras sentido y antisentido, protocolo de administración y dosis empleadas.

Tabla 1: Secuencias de siRNAs

siRNA	Conjugación	Hebra sentido SS/ antisentido AS	Vía de administración	Tratamientos	Trabajo
1A-siRNA1 *	-	SS: CGAUACUGGCCUCUCCAACTT AS: GGUGCUCAACAAGUGGACUTT	Local/ DR	2 dosis: 0.18 o 0.7 nmol·día^{-1} (2.5 o 10 µg·día^{-1})	1, 2
1A-siRNA2 *	-	SS: GGUGCUCAACAAGUGGACUTT AS: AGUCCACUUGUUGAGCACCTT			
1A-siRNA3 *	-	SS: GGAAGAGUGUAGGGCUUACTT AS: GUAAGCCCUACACUCUUCCTT	i.c.v./ D3V	1 dosis: 2.1 nmol·día^{-1} (30 µg·día^{-1})	1
1A-siRNA4 *	-	SS: CGAUGGAAGUUUAAACCUCTT AS: GAGGUUUAAACUUCCAUCGTT			
C-1A-siRNA1 *	Sertralina	SS: CGAUACUGGCCUCUCCAACTT AS: GGUGCUCAACAAGUGGACUTT	Local/ DR	2 dosis: 0.7 nmol·día^{-1} (10 µg·día^{-1})	
C-1A-siRNA2 *	Sertralina	SS: GGUGCUCAACAAGUGGACUTT AS: AGUCCACUUGUUGAGCACCTT	i.c.v./ D3V	1 dosis: 2.1 nmol·día^{-1} (30 µg·día^{-1})	1
C-1A-siRNA3 *	Sertralina	SS: GGAAGAGUGUAGGGCUUACTT AS: GUAAGCCCUACACUCUUCCTT			
C-1A-siRNA4 *	Sertralina	SS: CGAUGGAAGUUUAAACCUCTT AS: GAGGUUUAAACUUCCAUCGTT	i.n.	1 dosis: 2.1 o 7 nmol·día^{-1} (30 o 100 µg·día^{-1})	
SERT-siRNA	-	SS: GCUAGCUACAACAAGUUCATT AS: UGAACUUGUUGUAGCUAGCTT	Local/ DR	2, 4 o 7 dosis: 0.7 nmol·día^{-1} (10 µg·día^{-1})	3
C-SERT-siRNA	Sertralina	SS: GCUAGCUACAACAAGUUCATT AS: UGAACUUGUUGUAGCUAGCTT	i.n.	1, 4 o 7 dosis: 2.1 nmol·día^{-1} (30 µg·día^{-1})	4
TASK3-siRNA	-	SS: CCGGGCUACCGUCCACACCTT AS: GGUGUGGACGGUAGCCCGGTT	Local/ DR o LC	2 dosis: 0.7 nmol·día^{-1} (10 µg·día^{-1})	5
Ser-TASK3-siRNA	Sertralina	SS: CCGGGCUACCGUCCACACCTT AS: GGUGUGGACGGUAGCCCGGTT	i.n.	7 dosis: 2.1 o 5.3 nmol·día^{-1} (30 o 75 µg·día^{-1})	5
Reb-TASK3-siRNA	Reboxetina	SS: CCGGGCUACCGUCCACACCTT AS: GGUGUGGACGGUAGCCCGGTT	i.n.	7 dosis: 5.3 nmol·día^{-1} (75 µg·día^{-1})	5
NS-siRNA	-	SS: AGUACUGCUUACGAUACGGTT AS: CCGUAUCGUAAGCAGUACUTT	Local/ DR o LC	2, 4 o 7 dosis: 0.18 o 0.7 nmol·día^{-1} (2.5 o 10 µg·día^{-1})	1, 2, 3, 5
NS-siRNA	-	SS: AGUACUGCUUACGAUACGGTT AS: CCGUAUCGUAAGCAGUACUTT	i.c.v./ D3V	1 dosis: 2.1 nmol·día^{-1} (30 µg·día^{-1})	1
C-NS-siRNA**	Sertralina	SS: AGUACUGCUUACGAUACGGTT AS: CCGUAUCGUAAGCAGUACUTT	Local/ DR	2 dosis: 0.7 nmol·día^{-1} (10 µg·día^{-1})	1
C-NS-siRNA**	Sertralina	SS: AGUACUGCUUACGAUACGGTT AS: CCGUAUCGUAAGCAGUACUTT	i.c.v./ D3V	1 dosis: 2.1 nmol·día^{-1} (30 µg·día^{-1})	1
C-NS-siRNA**	Sertralina	SS: AGUACUGCUUACGAUACGGTT AS: CCGUAUCGUAAGCAGUACUTT	i.n.	1 dosis: 2.1 nmol·día^{-1} (30 µg·día^{-1})	1, 4, 5
Reb-NS-siRNA	Reboxetina	SS: AGUACUGCUUACGAUACGGTT AS: CCGUAUCGUAAGCAGUACUTT	i.n.	7 dosis: 5.3 nmol·día^{-1} (75 µg·día^{-1})	5
β-Gal-128	-	SS: CUACACAAAUCAGCGAUUU AS: GAUGUGUUUAGUCGCUAAA	Local/ DR	2 dosis: 0.7 nmol·día^{-1} (10 µg·día^{-1})	1
Cy3-C-NS-siRNA	Sertralina Cy3	SS: AGUACUGCUUACGAUACGGTT AS: CCGUAUCGUAAGCAGUACUTT	i.c.v./ D3V	1 dosis: 2.1 nmol·día^{-1} (30 µg·día^{-1})*	1
A488-C-NS-siRNA**	Sertralina Alexa 488	SS: AGUACUGCUUACGAUACGGTT AS: CCGUAUCGUAAGCAGUACUTT	i.n.	4 dosis: 2.1 nmol·día^{-1} (30 µg·día^{-1})	4, 5
A488-Reb-NS-siRNA	Reboxetina Alexa 488	SS: AGUACUGCUUACGAUACGGTT AS: CCGUAUCGUAAGCAGUACUTT	i.n.	4 dosis: 2.1 nmol·día^{-1} (30 µg·día^{-1})	5
A488-NS-siRNA	Alexa 488	SS: AGUACUGCUUACGAUACGGTT AS: CCGUAUCGUAAGCAGUACUTT	i.n.	4 dosis: 2.1 nmol·día^{-1} (30 µg·día^{-1})	5

1A-siRNA: siRNA contra el receptor 5-HT$_{1A}$; SERT-siRNA: siRNA contra el SERT; TASK3-siRNA: siRNA contra el TASK3; NS-siRNA: siRNA sin homología por ningún mRNA; β-Gal-128: siRNA contra la β-galactosidasa; DR: núcleo del rafe dorsal; D3V: tercer ventrículo dorsal; LC: locus cerúleo; i.c.v.: intracerebroventricular; i.n.: intranasal; *1A-siRNA(1-4) y C-1A-siRNA(1-4) fueron administrados en combinación a concentraciones equimolares y a la dosis total indicada en la tabla; **En el trabajo 5 la conjugación con sertralina esta descrita como Ser-NS-siRNA o A488-Ser-NS-siRNA

Los siRNAs fueron administrados por infusión intracerebral o por vía intranasal. Para la infusión intracerebral, los ratones fueron anestesiados con pentobarbital (40 $mg \cdot kg^{-1}$, intraperitoneal - i.p.) y sometidos a cirugía estereotáxica con el fin de implantarles una microcánula capilar de sílica con un diámetro externo e interno de 110 y 40 µm, respectivamente. Acorde con cada experimento, la microcánula fue implantada en el DR (coordenadas en mm: anteroposterior-AP, -4.5; mediolateral-ML, -1.0; dorsoventral-DV, -4.4 con un ángulo lateral de 20 ºC), en el LC (AP, -5.2; ML, -0.9; DV, -3.5) o en el tercer ventrículo dorsal (D3V; *dorsal third ventricle*: AP, -2.0; ML, 0; DV, -2.1). Los siRNAs fueron disueltos en 1 o 2.5 µl de líquido cefalorraquídeo artificial (aCSF; *artificial cerebrospinal fluid*: 125 mM NaCl, 2.5 mM KCl, 1.26 mM $CaCl_2 \cdot 2H_2O$ and 1.18 mM $MgCl_2 \cdot 6H_2O$) según fueron administrados intra-DR/LC o en el D3V, respectivamente. La microinfusión se llevó a cabo 24 horas después de la cirugía mediante una bomba de infusión (modelo WPI, SP220i) a 0.5 $\mu l \cdot min^{-1}$ en animal despierto. En el caso de la administración intranasal, los ratones fueron anestesiados con isoflurano al 2% por inhalación y colocados en posición supina. Una gota de 5 µl de siRNA disuelto en tampón fosfato salino (PBS; *phosphate-buffered saline*) fue aplicada alternativamente en cada narina. El volumen total administrado fue de 10 µl para cada dosis. Para los diferentes tratamientos (intracerebral o intranasal), los ratones recibieron una única dosis de siRNA por día. Un resumen de los diferentes protocolos de administración y dosis de siRNAs utilizados se detallan en la tabla 1.

3.3. Tratamientos farmacológicos

Fluoxetina fue preparada en solución salina y administrada a 10 o 20 mg/kg/día i.p. una vez al día. Los protocolos de administración se resumen en la tabla 2. En el trabajo 1, fluoxetina fue utilizada como control positivo de efecto antidepresivo en los paradigmas comportamentales FST y TST. En los trabajos 3 y 4, fluoxetina fue utilizada para comparar la eficacia de los tratamientos antidepresivos: silenciamiento del mRNA de SERT con siRNAs en comparación al bloqueo farmacológico del SERT.

La función del autoreceptor 5-HT_{1A} en ratones puede examinarse mediante la evaluación de la respuesta de hipotermia inducida por el agonista del receptor 5-HT_{1A} 8-OH-DPAT (Martin et al., 1992). Para ello, los ratones fueron individualizados 20 minutos antes de la prueba. La temperatura rectal se midió usando una sonda y un termómetro digital. En primer lugar se tomaron dos medidas correspondientes a la temperatura basal. A continuación, los animales fueron tratados con 8-OH-DPAT (1 $mg \cdot kg^{-1}$, i.p.) (ver tabla 2), momento a partir del cual se midió la temperatura rectal cada 15 minutos durante 2 h.

Tabla 2: Tratamientos

Fármaco	Tratamiento	Trabajo
Fluoxetina	Dosis única de 10 $mg \cdot kg^{-1}$ i.p.	**1**
Fluoxetina	4, 7 o 15 dosis a 20 $mg \cdot kg^{-1}$ i.p. durante 4, 7 o 15 días	**3**
Fluoxetina	7 o 28 dosis a 10 $mg \cdot kg^{-1}$ i.p. durante 7 o 28 días	**4**
8-OH-DPAT	Dosis única de 1 $mg \cdot kg^{-1}$ i.p.	**1, 2**
Corticosterona	15 días a 6.6 $mg \cdot kg^{-1}$ + 3 días a 2.7 $mg \cdot kg^{-1}$ + 10 o 31 días a 1.1 $mg \cdot kg^{-1}$ vía oral	**4**
BrdU	4 dosis a 75 $mg \cdot kg^{-1}$ i.p. cada 2 horas en un único día	**3, 4**

BrdU: bromodesoxiuridina; 8-OH-DPAT: 7-(dipropilamino)-5,6,7,8-tetrahidronaftalen-1-ol; i.p.: intraperitoneal

Los tratamientos agudos con fármacos en experimentos de microdiálisis se describen en apartado 3.7.

3.4. Modelos animales experimentales

Modelo de depresión: en el trabajo 4 se utilizó el modelo de estrés asociado al consumo crónico de corticosterona (Gourley et al., 2009). La corticosterona fue disuelta en agua mineral comercial. La solución de corticosterona (pH 7.0-7.4) fue presentada a los animales en substitución al agua de bebida durante los días y a las concentraciones indicados en la tabla 2. Brevemente, los animales recibieron corticosterona equivalente a una dosis diaria de 6.6 $mg \cdot kg^{-1}$ durante 15 días, seguido de 2.7 $mg \cdot kg^{-1}$ durante 3 días y luego 1.1 mg/kg^{-1} durante 10 o 31 días hasta la finalización del experimento. El tratamiento antidepresivo con fluoxetina o siRNAs se

inició el día 22 post-exposición de corticosterona y se mantuvo durante 7 o 28 días hasta la finalización del tratamiento.

Modelo de proliferación celular: para la determinación del número de células en fase de mitosis se utilizó bromodesoxiuridina (BrdU; *bromodeoxyuridine*) como marcador exógeno (Nowakowski et al., 1989). La BrdU es un nucleótido sintético análogo a la timidina que se incorpora al DNA durante el proceso de replicación celular. En los trabajos 3 y 4, BrdU fue disuelta en solución salina y los ratones recibieron 4 inyecciones de BrdU a 75 $mg \cdot kg^{-1}$, i.p. cada 2 h el último día de tratamiento con fluoxetina o siRNA (ver tabla 2) (Santarelli et al., 2003). Los ratones fueron sacrificados y su cerebro extraído y procesado para inmunohistoquímica (IHC; *immunohistochemistry*) utilizando un anticuerpo contra la BrdU (ver apartado 3.6).

3.5. Métodos bioquímicos y moleculares

Determinación de los niveles de corticosterona en plasma: éstos fueron analizados al finalizar los diferentes tratamientos en el modelo de estrés crónico por consumo de corticosterona. Las extracciones de sangre se efectuaron a la misma hora por punción cardíaca y usando citrato trisódico como anticoagulante. A continuación, se obtuvo el plasma mediante centrifugación (1000 g, 15 minutos) y se congeló a -80ºC. La detección de los niveles de corticosterona se realizó por radioinmunoensayo utilizando un kit comercial y un contador de partículas gamma para medir la radioactividad en las muestras.

PCR cuantitativa: con el objetivo de cuantificar los niveles de mRNAs específicos en diferentes áreas cerebrales (trabajos 1 y 2), los ratones se sacrificaron y el cerebro fue extraído y colocado sobre una placa metálica enfriada con hielo. Secciones del cerebro medio de 1 mm de espesor conteniendo el DR fueron diseccionadas usando una matriz de cerebro de ratón. Inmediatamente, los tejidos fueron congelados en hielo seco y almacenados a -80ºC. El RNA total se extrajo utilizando una solución de Trizol. Luego, se disolvió a una concentración de 0.5 µg/µl en agua libre de RNasas. Previo tratamiento con DNasas para eliminar los restos de DNA genómico, se procedió a la transcripción inversa para generar DNA a partir de los mRNAs. La PCR

cuantitativa se realizó utilizando la tecnología SYBR Green para medir la cantidad de DNA inicial en tiempo real. Los cebadores utilizados se detallan en la tabla 3. La cuantificación se realizó mediante el programa AbiPrism SDS 2.1 y los datos de cada muestra se normalizaron con la cantidad del gen de referencia interna ciclofilina A. Los resultados se expresan como el promedio ± s.e.m. de la relación unitaria en comparación al tratamiento control.

Tabla 3: Cebadores

Gen o mRNA	Cebador anverso	Cebador reverso	Trabajo
Ciclofilina A	GATGAGAACTTCATCCTAAAGCATACA	TCAGTCTTGGCAGTGCAGATAAA	**1, 2**
5-HT_{1A}	CCGTGAGAGGAAGACAGTGAAGAC	GTGAGAGGAAGACAGTGAAGAC	**1, 2**
5-HT_{1B}	TCTCACCAACCTCTCCCACAAC	GTCCGATACACCGTAGCGATTAC	**1, 2**
SERT	CTCATCTTCACCATTATCTACTTCAG	CTCACCAGCAGGACAGAAAG	**1, 2**
TNFα	GCAGTCTGTGTCTGCTGGGAT	CGCAGAACGGGATGAAGC	**1, 2**
IFNγ	CCCACAGGTCCAGCGCCAAG	CCCACCCCGAATCAGCAGCG	**1, 2**
BAX	AGCGAGTGTCTCCGGCGAATTG	TCTGATCAGCTCGGGCACTTTAG	**1**

5-HT_{1A}: receptor de serotonina 1A; 5-HT_{1B}: receptor de serotonina 1B; SERT: transportador de serotonina; TNFα: factor de necrosis tumoral alfa; IFNγ: interferón gamma; BAX: proteína X asociada a Bcl-2

Western blot: esta técnica se utilizó con el objetivo de cuantificar la proteína TASK3 en el trabajo 5. Los ratones fueron sacrificados y el cerebro extraído y colocado sobre una placa metálica enfriada con hielo. Diferentes áreas cerebrales incluyendo mPFC, HPC, DR y LC fueron diseccionadas utilizando una matriz de ratón e inmediatamente congeladas en hielo seco y almacenadas a -80ºC. Las diferentes áreas fueron homogenizadas y sonicadas para la extracción de las proteínas totales utilizando un tampón de lisis (50 mM Tris-Base, 150 mM NaCl, 0.5% deoxicolato de sodio, 0.1% SDS, 1% Tritón X-100). Seguidamente, se cuantificaron las proteínas totales utilizando el kit BCA y se añadió el tampón de carga Laemmli y el agente desnaturalizante β-mercaptoetanol para la electroforesis. Se procedió a cargar 5 µg de cada extracto proteico en un gel comercial de tris/glicina en gradiente de concentración 4-20%. Finalizada la electroforesis, las proteínas fueron transferidas a una membrana de PVDF. Después, la membrana fue lavada, bloqueada con leche durante 2 h e incubada con el anticuerpo primario durante 24 h a 4ºC (ver tabla 4).

Tabla 4: Anticuerpos primarios utilizados en la Tesis

Anticuerpo	Fabricante	Referencia	Dilución	Técnica	Trabajo
anti-TASK3	Fabricación propia	-	1:500	WB	**5**
anti-β-actina	Sigma-Aldrich	A1978-200UL	1:4000	WB	**5**
anti-TPH_2	Millipore	AB1541	1:100 1:2500 1:2000	IF IF IHC +ISH	**1** **4, 5** **5**
anti-SERT	ImmunoStar	24330	1:2500	IHC	**3, 4**
anti-BrdU	Roche	11170376001	1:600	IHC	**3, 4**
anti-Ki-67	Abcam	ab16667	1:5000	IHC	**3, 4, 5**
anti-NeuroD	Santa Cruz	sc-1084	1:200	IHC	**3, 4**
anti-DCX	Santa Cruz	sc-8066	1:200	IHC	**3, 4, 5**
anti-NeuN	Millipore	MAB377	1:1000	IHC	**3, 4**
anti-GFAP	Dako	Z 0334	1:1000	IHC	**3, 4, 5**
anti-IBA-1	Wako	019-197741	1:1000	IHC	**3, 4, 5**
anti-Rab5	Abcam	ab18211	1:500	IF	**4, 5**
anti-Rab7	Sigma-Aldrich	R8779-200UL	1:2000	IF	**4, 5**
anti-TH	Abcam	ab112	1:1250 1:5000	IF IHC +ISH	**5** **5**

TASK3: canal de potasio sensor de ácido semejante a TWIK "3"; TPH_2: triptófano hidroxilasa 2; SERT: transportador de serotonina; BrdU: bromodesoxiuridina; DCX: doblecortina; GFAP: proteína ácida fibrilar glial; Rab5; proteína semejante a Ras "5"; Rab7; proteína semejante a Ras "7"; TH: tirosina hidroxilasa; IF: inmunofluorescencia; IHC (dip): inmunohistoquímica sobre porta dipeado en emulsión fotográfica; IHC: inmunohistoquímica; WB: *western blot*

A continuación, la membrana fue incubada 1 h con el anticuerpo secundario conjugado con la enzima peroxidasa a fin de detectar las proteínas mediante un sistema de quimioluminiscencia basado en el luminol. Las bandas inmunoreactivas detectadas fueron digitalizadas, analizadas y cuantificadas mediante densitometría con el programa ImageJ (1.49g) como soporte. La cantidad de proteína de interés en cada una de las muestras fue normalizada en relación a la cantidad del control interno β-actina. Los resultados se expresan como el promedio ± s.e.m. de la relación porcentual en comparación al tratamiento control.

3.6. Métodos histológicos

Hibridación *in situ* (ISH; *in situ hybridization*): en todos los trabajos se utilizó esta técnica para determinar la eficacia y selectividad de los siRNAs para silenciar el mRNA diana. Para ello, los ratones fueron sacrificados con una sobredosis de pentobarbital. Inmediatamente después el cerebro fue extraído, congelado en hielo seco y almacenado a -80ºC. Secciones coronales de tejido cerebral de 14 µm de espesor fueron cortadas mediante un micrótomo de congelación (Microm HM500 OM), colocadas en portaobjetos tratados con 3-aminopropil-trietoxisilano y preservadas a -20ºC. Las sondas de oligonucleótidos contra los mRNAs de interés fueron marcadas en el extremo 3' con ^{33}P-dATP mediante una enzima deoxinucleotidil transferasa terminal. En la tabla 5 se indican las secuencias de las sondas de oligonucleótido utilizadas en la presente Tesis.

Para el procedimiento de la ISH, los tejidos fueron fijados con paraformaldehido (PFA; *paraformaldehyde*) al 4% y tratados con la proteasa pronasa para facilitar la accesibilidad de la sonda al mRNA de interés. A continuación, los tejidos fueron cubiertos con el tampón de hibridación que contiene aproximadamente 1.5 nM de la sonda de oligonucleótido radioactiva y fueron incubados en cajas humedecidas a 42ºC durante 24 h. Después, las secciones hibridadas fueron lavadas y expuestas a una película fotográfica durante 1-4 semanas.

A continuación, los autoradiogramas fueron analizados y la densidad óptica relativa (ROD; *relative optical density*) en el área cerebral de interés fue obtenida utilizando un analizador de imágenes asistido por ordenador (MCID). El fondo y las inespecificidades fueron sustraídas. Las RODs se evaluaron en dos o tres secciones adyacentes por duplicado para cada ratón y se promediaron para obtener los valores individuales. El analizador se usó también para la obtención de las imágenes en un pseudocolor proporcional a las RODs. Las imágenes en blanco y negro fueron tomadas en un microscopio Leica Wild 420 equipado con una cámara Nikon DXM1200F conectada al programa ACT-1. Los datos se expresan como el promedio ± s.e.m. de los porcentajes de las RODs en comparación al grupo tratado con el vehículo.

Tabla 5: Sondas de oligonucleótidos

Gen o mRNA	GenBank	Secuencia de las sondas	Bases mRNA homólogas	Trabajo
5-HT$_{1A}$	NM_012585.1	CTGGGACGCTGTGGTGTTGTTGCCCTGGCCAAAACTGAACACATCCAT CCTGTTCTCAGCACAGCGCCTCCAGTCCCCACTACCTGGCTGTCCGTT TCGGCGGCAGAACTTGCACTTGATTATCTTCTTAAAAGCGTTTTGAAA	1-48 763-810 1219-1266	1, 2 1, 2 1, 2
5-HT$_{1A}$	NM_008308	TCAGCGGCAGAACTTGCACTTGATGATCTTCTTAAAAGCGTTTTGAAA	1780-1827	3, 4, 5
SERT	NM_010484.1	GGGGGACGTGGAATGCAGCGTCCAGGTGATGTTGTCCTGGGCGAAGTA	820-863	3, 4, 5
TPH$_2$	NM_173391	GATATGAAGCATGTTGACATGTTTTTCCTGGAATAGTCTAAGTGCTTTCA	360-410	3, 4
Ki-67	NM_001081117	GACCTTCCCCATCAGGGTCAGCACAGAAGCTATCTCTTGAGGCTCGCCTT	603-653	3
BDNF	NM_007540	ACCCATGGGATTACACTTGGTCTCGTAGAAATACTGCTTCAGTTGGCCTT	1188-1238	3, 4, 5
VEGF	NM_001025250	GTGCCCCCGTGCCCTGGCCTTGCTTGCTCCCCGGCAGGCAAAAGGACTTC	2217-2267	3, 4, 5
ARC	NM_018790	AGCTCTGCTCTTCTTCACTGGTATGAATCACTGCTGGGGGCCAGGAGG	1990-2040	3, 4, 5
CREB	NM_009952	ATTCAAAATTTTCCTGTAGGAAGGCCTCCTTGAAAGGATTTCCCTTCGTT	593-643	3
TrkB	NM_001025074	CGTGCAGATGGCAGACCACAATTGGGTATCTGCAGGTTCGCCAGGGGCAT	1075-1124	4
PSD95	D50621	GGCCTGCACCAGGTAAGCTATTTGCACCGCGAGGATCAGT	76-120	4
Neuritina	NM_153529	CACATATCTTTCGCCCCTTCCTGGCAATCCGTAAGAGCTG	408-448	4
TASK3	NM_001033876	GCACAGGGTTCTGCCGTATTTCCTGAGGAAGTACATGGCGTGGTGCCTCT	839-888	5
TASK1	NM_010608	CATCGTCCCTCCCGGGTCCTCGCCGGCCCTCCGGCGTCTCCGGCCGCGGC	101-150	5
TREK1	NM_001159850	TTATTGCTGCCACTATTTGCTGGATGAGTTCGTCCAGCTCGGTGGAGTTG TCCACCTTCAGTTCGTGGGGAGATGTTTCCAAATCCTATGGTTGTGATAA AGATGATACGAATCTTCGTCTGACTAACATTCCACTTAATAAATGTGTCT ACCACAGGCTTGTAGAAGTCCAGATATTCAATGTCTGATCCACCTGCCAC	592-641 726-775 889-938 1082-1131	5 5 5 5
NET	NM_009209	GTAACACAGTTGATGGAGCTGGTCAGTAGAGCATCCCTGTAACAGTTGTT	1210-1259	5
α_2	NM_NC_000085	TCTCCCGGTTTTGCCTCCCGCGCCAGCGCGACGCTTTGGCGCCCCCGCCG	2137-2186	5

5-HT$_{1A}$: receptor de serotonina 1A; SERT: transportador de serotonina; TPH$_2$: triptófano hidroxilasa 2; BDNF: factor neurotrófico derivado del cerebro; VEGF: factor de crecimiento endotelial vascular; ARC: proteína asociada al citoesqueleto regulada por actividad; CREB: proteína de unión a elemento de respuesta al cAMP; TrkB: receptor tropomiosina quinasa B; PSD95: proteína de densidad postsináptica 95; TASK3: canal de potasio sensor de ácido semejante a TWIK "3"; TASK1: canal de potasio sensor de ácido semejante a TWIK "1"; TREK1: canal de potasio semejante a TWIK "1"; NET: transportador de noradrenalina; α_2: receptor α_2 adrenérgico

Autoradiografía de receptores y transportadores: esta técnica fue utilizada en los trabajos 1, 2, 3 y 4 para evaluar los sitios de unión a los receptores 5-HT$_{1A}$ y 5-HT$_{1B}$, los transportadores SERT y NET así como para examinar el acople funcional del receptor 5-HT$_{1A}$ a la proteína G. En la tabla 6 se indican los radioligandos utilizados en cada caso y las condiciones experimentales.

Tabla 6: Experimentos de autoradiografía

Auto-radiografía	Radioligando	Pre-incubación	Incubación	Lavados en tampón enfriado en hielo	Tiempo de exposición	Blanco	Trabajo
5-HT$_{1A}$	^{3}H-8-OH-DPAT (1 nM)	Tampón A 30 min	Tampón A 60 min	2 x 5 min	60 días	5-HT (10 µM)	**1, 2, 3, 4**
5-HT$_{1B}$	^{125}I-cianopindolol (0.1 nM)	Tampón B 10 min	Tampón B 120 min	2 x 15 min	1 día	5-HT (10 µM)	**1, 2**
SERT	^{3}H-citalopram (1.5 nM)	Tampón C 15 min	Tampón C 60 min	2 x 10 min	45 días	fluoxetina (1 µM)	**1, 2, 3, 4**
NET	^{3}H-nisoxetina (3 nM)	Tampón D 15 min	Tampón D 240 min	3 x 5 min	90 días	mazindol (10 µM)	**3, 4**
5-HT$_{1A}$ acoplado a proteína G	^{35}S-GTPγS (0.04 nM)	Tampón E 30 min	Tampón E 120 min	2 x 15 min	2 días	GTPγS (10 µM)	**3, 4**

5-HT$_{1A}$: receptor de serotonina 1A; 5-HT$_{1B}$: receptor de serotonina 1B; SERT: transportador de serotonina; NET: transportador de noradrenalina; Tampón A: Tris-HCl 170 mM, $CaCl_2$ 4 mM, ácido ascórbico 0.01%, pargilina 10 µM, pH=7.6; Tampón B: Tris-HCl 170 mM, NaCl 150 mM, 8-OH-DPAT 100 nM, isoproterenol 30 nM, pH=7.4; Tampón C: Tris-HCl 50 mM, NaCl 120 mM, KCl 5 mM, pH=7.6; Tampón D: Tris-HCl 50 mM, NaCl 300 mM, KCl 5 mM, pH 7.4; Tampón E: Tris-HCl 50 mM, EGTA 0.2 mM, $MgCl_2$ 3mM, NaCl 100 mM, DTT 1 mM, GDP 2 mM, adenosina desaminase 10 mU/ml, 8-OH-DPAT 10 µM, (WAY100635 10 µM)*, pH 7.7; *añadido al buffer solo en los tejidos para evaluar el blanco de actividad

Brevemente, los tejidos fueron preincubados e incubados a temperatura ambiente con los tampones correspondientes y durante los tiempos indicados en la tabla 6. Una vez lavados, para eliminar el exceso de radioligando no unido, los tejidos se sumergieron en agua destilada helada y se secaron rápidamente bajo una corriente de aire fría. Finalmente, los tejidos se expusieron a una película fotográfica junto con microescalas estándares de ^{3}H o ^{14}C. Los autoradiogramas obtenidos fueron analizados del mismo modo descrito para la técnica de ISH, con la diferencia que el equipo de análisis fue calibrado con los estándares de ^{3}H o ^{14}C para obtener la concentración de proteína (fmol·mg^{-1}) a partir de las RODs.

Inmunohistoquímica: esta técnica fue utilizada en los trabajos 1, 3, 4 y 5 para determinar la densidad de fibras inmunoreactivas al SERT o el recuento de células positivas a ciertos marcadores. Los ratones fueron anestesiados con pentobarbital y perfundidos durante 20 minutos con PFA 4% disuelto en PBS. Transcurrida la perfusión, los cerebros fueron extraídos y post-fijados 24 h en PFA 4% a 4ºC. A continuación fueron sometidos a un gradiente de sacarosa 10-30% durante 3 días a 4ºC. Finalmente los cerebros fueron congelados por inmersión en isopentano a -35ºC y almacenados a -80ºC. Se obtuvieron cortes coronales de tejido cerebral

conteniendo bulbos olfatorios, HPC, AMG, DR/MR y LC de 30 µm de espesor utilizando un micrótomo de congelación. Las diferentes secciones fueron sumergidas en una solución de criopreservación y almacenadas a -20ºC hasta su posterior uso. La IHC se realizó con la técnica de flotación libre (*free-floating*) colocando un solo tejido por pocillo en placas de 48 pocillos. En primer lugar, se eliminó la solución de criopreservación con sucesivos lavados de PBS y se inactivaron las peroxidasas endógenas con una solución de H_2O_2 al 1.5%. A continuación, se realizaron lavados con el detergente Tritón al 0.2% disuelto en PBS para mantener las membranas permeabilizadas y, se procedió a aplicar la solución de bloqueo con suero de la especie animal en que se sintetizó el anticuerpo secundario. Tras 2 h con la solución de bloqueo, se lavó y se añadió el anticuerpo primario dejándolo durante 24 h incubando a 4ºC. La tabla 4 muestra una relación de los anticuerpos utilizados en la presente Tesis así como información relevante de los mismos.

Finalizados los lavados posteriores a la incubación con el anticuerpo primario, los tejidos se incubaron durante 1 h con el anticuerpo secundario conjugado con biotina, seguido de otra incubación de 1 h con una solución de biotina y estreptavidina para generar una amplificación de la señal permitiendo de este modo la detección de proteínas con bajos niveles de expresión. Finalmente, después de varios lavados, el revelado se realizó por incubación con una solución de 3,3'-diaminobencidina (DAB; *3,3'-diaminobenzidine*). A continuación, los tejidos fueron montados sobre portaobjetos tratados con gelatina utilizando el medio de montaje Entellan. Los tejidos fueron visualizados y fotografiados con un microscopio Nikon Eclipse E1000 equipado con una cámara Nikon DXM1200F conectada al el programa ACT-1. Las imágenes fueron procesadas con Photoshop utilizando los mismos valores de contraste y brillo. Los datos se expresan como el promedio ± s.e.m. de la densidad de fibras o número células inmunoreactivas en relación absoluta o relativa porcentual al tratamiento control.

Inmunofluorescencia (IF; *immunofluorescence*): esta técnica fue utilizada en los trabajos 1, 4 y 5 para el estudio de la localización y distribución cerebral de las moléculas de siRNAs conjugadas. El procedimiento de obtención de los cortes de

tejido fue similar al detallado en el método de IHC. La IF se realizó en *free-floating* colocando un solo tejido por pocillo en placas de 48 pocillos. Brevemente, tras eliminar la solución de criopreservación con Tritón al 0.2% disuelto en PBS se aplicó la solución de bloqueo con suero de la especie animal en que se sintetizó el anticuerpo secundario. Tras 2 h de incubación, se lavó y se añadió el anticuerpo primario dejándolo durante 24 h incubando a 4ºC (ver tabla 4). Una vez lavado el anticuerpo primario, los tejidos se incubaron 1 h con el anticuerpo secundario conjugado al fluorocromo Alexa555 (rojo) o Alexa 647 (lila). Los núcleos fueron visualizados con el colorante DAPI o YOYO. Tras ser lavados, los tejidos fueron montados sobre portaobjetos tratados con gelatina, secados y deshidratados. Los tejidos fueron visualizados y fotografiados con un microscopio confocal Leica TCS SP5. Las imágenes fueron procesadas con Photoshop utilizando los mismos valores de contraste y brillo. En el análisis cuantitativo del trabajo 4 los datos se expresan como el promedio ± s.e.m. del número de células dobles positivas (TPH_2 y siRNA) según la densidad intracelular de siRNA.

Hibridación *in situ* + inmunohistoquímica: en el trabajo 5, se utilizó una combinación de técnicas de ISH y IHC para colocalizar el mRNA del canal de potasio TASK3 en tipos celulares serotoninérgicos identificados con el marcador TPH_2 o noradrenérgicos utilizando el marcador TH. Para ello, acabada la ISH contra el mRNA de TASK3, las secciones (14 µm) hibridadas y montadas sobre portaobjetos fueron dipeadas en emulsión fotográfica y expuestas durante 2 semanas a 4ºC. Tras el revelado, los tejidos fueron sometidos a un protocolo de IHC como el descrito anteriormente adaptando la dilución del anticuerpo primario a la nueva condición (ver tabla 4). Los tejidos fueron visualizados y fotografiados con un microscopio Nikon Eclipse E1000 equipado con una cámara Nikon DXM1200F conectada al el programa ACT-1. Las imágenes fueron procesadas con Photoshop utilizando los mismos valores de contraste y brillo. Los resultados se expresan como el promedio ± s.e.m. del número de células dobles positivas (TASK3 y TPH_2 o TH) o de la densidad intracelular del mRNA de TASK3 en células positivas para TPH_2 o TH expresado como porcentajes en relación al grupo control.

3.7. Métodos neuroquímicos

Microdiálisis intracerebral: este procedimiento fue utilizado en los trabajos de la presente Tesis para determinar las concentraciones extracelulares de los neurotransmisores 5-HT, NE y DA en diferentes áreas cerebrales. Para ello los ratones fueron anestesiados con pentobarbital (40 $mg \cdot kg^{-1}$, i.p.) y sometidos a cirugía estereotáxica con el fin de implantarles una sonda de diálisis en las siguientes áreas cerebrales: mPFC (AP, 2.2; ML, -0.2; DV, -3.4), cuerpo estriado (AP, 0.5; ML, -1.7; DV, -4.5) o HPC (AP,-3.0; ML, -3.0; DV, -4.0). Los experimentos se llevaron a cabo entre las 24 y 72 h posteriores a la cirugía en animal despierto y en libre movimiento. Durante el experimento se perfundió aCSF a través de la sonda de diálisis mediante una bomba de infusión de precisión (modelo WPI, SP220i). Para la evaluación de 5-HT, el aCSF fue perfundido a 2 $\mu l \cdot min^{-1}$ obteniendo muestras de dializado cada 30 minutos. Cuando el experimento de microdiálisis de 5-HT se llevó a cabo simultáneamente con el paradigma comportamental TST, el aCSF fue perfundido a 5 $\mu l \cdot min^{-1}$ obteniendo muestras cada 6 minutos. Para la determinación de NE y DA, el aCSF fue perfundido a 1 o 1.64 $\mu l \cdot min^{-1}$ obteniendo muestras cada 35 o 20 minutos, respectivamente. La concentración de 5-HT, NE o DA fue determinada mediante HPLC (Hewlett Packard 1049) con detección electroquímica a +0.6, +0.3 o +0.75 V, respectivamente.

Con el fin de estudiar el efecto del silenciamiento de genes sobre la concentración extracelular de 5-HT, NE o DA en diferentes áreas cerebrales, los fármacos fueron administrados i.p. o bien de modo local por diálisis reversa a través de la sonda. La tabla 7 muestra los fármacos utilizados en la presente Tesis detallando la vía de administración y la concentración. Los niveles basales de monoaminas fueron calculados como el promedio de las cuatro muestras iniciales libres de fármacos, a excepción del experimento simultáneo de microdiálisis y TST en que se utilizaron de siete a diez muestras basales. La verificación de la correcta posición de la sonda de diálisis en el área cerebral de interés fue llevada a cabo mediante la tinción de cresil de violeta. Los resultados se expresan como el promedio ± s.e.m de los niveles del neurotransmisor en el dializado expresado como porcentaje respecto a los niveles basales.

Tabla 7: Fármacos utilizados en los experimentos de microdiálisis

Diálisis	Fármaco	Mecanismo de acción	Administración	Concentración /dosis	Trabajo
5-HT	Fluoxetina	SSRI	i.p.	20 $mg \cdot kg^{-1}$	**1, 2, 3, 5**
	Citalopram	SSRI	d.r.	1 µM	**1, 2, 3, 4, 5**
	Citalopram	SSRI	d.r.	1-10-50 µM	**3, 4**
	Sertralina	SSRI	i.p.	20 $mg \cdot kg^{-1}$	**1**
	8-OH-DPAT	Agonista 5-HT_{1A}	i.p.	0.5 $mg \cdot kg^{-1}$	**1, 2, 3, 4**
	8-OH-DPAT	Agonista 5-HT_{1A}	i.p.	1 $mg \cdot kg^{-1}$	**5**
	Veratridina	Agente despolarizante	d.r.	50 µM	**3, 5**
NE	Reboxetina	NERI	i.p	20 $mg \cdot kg^{-1}$	**5**
	Clonidina	Agonista α_2	i.p.	0.3 $mg \cdot kg^{-1}$	**5**
	Desipramina	TCA	d.r.	1 µM	**5**
DA	BAYx3702	Agonista 5-HT_{1A}	d.r.	3 µM	**2**

5-HT: serotonina; NE: noradrenalina; DA: dopamina; 8-OH-DPAT: 7-(dipropilamino)-5,6,7,8-tetrahidronaftalen-1-ol; SSRI: inhibidor selectivo de la recaptación de serotonina; NERI: inhibidor selectivo de la recaptación de noradrenalina; TCA: antidepresivo tricíclico; i.p.: intraperitoneal; d.r.: diálisis reversa a través de la sonda

3.8. Métodos comportamentales

Los ratones fueron evaluados entre las 10:00 a.m. y 15:00 p.m. y al menos 24 h después de los tratamientos con fluoxetina o moléculas de siRNA. Aquellos animales sometidos a más de una prueba comportamental, se dejaron descansar entre 1 y 2 días entre las diferentes pruebas. El día de la evaluación los animales fueron transportados a la sala de comportamiento donde permanecieron 1 h antes de iniciar la prueba. El experimentador que realizó las pruebas ignora el tratamiento que ha recibido cada animal.

Campo abierto: esta prueba permite la evaluación de la actividad motora del animal en respuesta a un ambiente nuevo. Esta se realizó en una caja cuadrada abierta por la parte superior de 35 x 35 x 40 cm iluminada indirectamente para evitar reflejos y sombras. El suelo fue cubierto con una base de plástico, opaca e intercambiable, reemplazada para cada animal. El tiempo de actividad y la distancia total recorrida incluyendo movimientos rápidos (velocidad > 10.5 $cm \cdot s^{-1}$) y lentos (velocidad entre 3-10.5 $cm \cdot s^{-1}$) fueron registrados de modo automático durante 15 minutos utilizando una camera conectada a un ordenador (Videotrack). Los resultados se expresan como el promedio ± s.e.m del tiempo de actividad en segundos y la distancia recorrida en cm.

Prueba de preferencia por la sacarosa: este paradigma examina el consumo de soluciones palatables, como por ejemplo, agua enriquecida con sacarosa. La disminución del consumo y la indiferencia o menor preferencia por el agua con sacarosa es indicativa de anhedonia (pérdida de interés o satisfacción) en roedores. Durante la prueba, los ratones tuvieron libre acceso a dos botellas durante 8 horas, una con solución con sacarosa al 1% y otra con agua normal. La posición de las botellas en la jaula se cambió a las 4 h. El consumo de agua normal y de agua con sacarosa fue registrado al final del experimento. El consumo de sacarosa fue calculado como la cantidad de sacarosa consumida (mg) por gramo de peso corporal. La preferencia para la sacarosa se calculó como el porcentaje de solución con sacarosa consumida respecto la cantidad total de líquido ingerido. El criterio de anhedonia se considera cuando los valores de preferencia para la sacarosa bajan del 55%. Los resultados se expresan como el promedio ± s.e.m.

Laberinto en cruz elevado: se trata de un laberinto con cuatro brazos de 16 x 5 cm en cruz que permite evaluar el comportamiento de tipo ansioso en los roedores. Dos de los brazos están cerrados y los otros dos permanecen abiertos. La prueba expone al animal a un conflicto entre el miedo innato de los roedores a las áreas abiertas contra el deseo de explorar nuevos ambientes. Los ratones fueron colocados en la zona central del laberinto enfrente de uno de los brazos abiertos. La prueba tuvo una duración de 5 minutos durante los cuales se registraron el número de entradas en los brazos abiertos y el tiempo de permanencia en ellos. Los resultados se expresan como el promedio ± s.e.m del porcentaje del tiempo de permanencia y del número de entradas a los brazos abiertos en relación al grupo control.

Test de enterramiento de cánicas (MBT; *marble burying test*): esta prueba puede ser usada como un indicador del comportamiento de tipo ansioso. Los ratones presentan ciertos comportamientos característicos de especie como es el hecho de excavar, actividad muy sensible a lesiones hipocampales y fármacos que actúan sobre el sistema serotoninérgico (Deacon, 2006). Los ratones se colocaron individualmente en cajas cuadradas de 25 x 25 cm iluminadas indirectamente para evitar reflejos y sombras con 25 esferas de vidrio equidistantes sobre 5 cm de viruta fina de madera

estéril. Transcurridos 30 minutos, el ratón se devuelve a su jaula hogar y se contabilizan aquellas esferas enterradas al menos en sus dos terceras partes con viruta de madera. Los resultados se expresan como el promedio ± s.e.m del valor absoluto del número de cánicas enterradas.

Test de supresión de la ingesta por novedad: se trata de una prueba que permite valorar el comportamiento de tipo ansioso en los ratones así como evaluar la eficacia de los tratamientos antidepresivos crónicos (Samuels and Hen, 2011). Este paradigma comportamental se basa en un conflicto en el que compiten el impulso de comer y el miedo a aventurarse hacia el centro de una caja iluminada. El aparato de NSFT consiste en una caja de 35 x 35 cm fuertemente iluminada con el suelo cubierto por 2 cm de viruta de madera. 24 h antes de la prueba se retiró toda la comida de la jaula hogar. El día de la prueba, un trozo de comida fue colocado sobre una plataforma de papel blanco en el centro de la caja e iluminado con 1100 luxes. Durante la realización de la prueba, el ratón fue colocado en una esquina de la caja momento a partir del cual se empezó a contar el tiempo. La variable principal que se registró es la latencia a comer definida como el tiempo en segundos que el animal necesita para morder un trozo de comida con la ayuda de las patas delanteras mientras está sentado sobre las traseras. Inmediatamente después, el animal fue trasladado a su jaula y entorno habitual registrándose el tiempo de latencia a comer en su jaula así como la cantidad de alimento consumido durante 5 minutos. Además, cada ratón fue pesado al inicio de la deprivación y antes de la prueba a fin de evaluar el porcentaje de pérdida de peso. Todas estas variables secundarias (latencia a comer en su jaula, alimento consumido y porcentaje de pérdida de peso) se evaluaron como control interno del experimento. Los resultados se expresan como el promedio ± s.e.m de la variable principal de latencia en segundos y en un análisis de supervivencia.

Test de natación forzada: descrito originalmente por Porsolt y colaboradores (Porsolt et al., 1977), es un paradigma comportamental ampliamente utilizado para evaluar la vulnerabilidad al estrés así como para llevar a cabo un *screening* de fármacos antidepresivos. En él, los roedores son forzados a nadar en un entorno confinado del que instintivamente intentan escapar. Después de intentos fallidos, los animales

adoptan una postura flotante de inmovilidad, una actitud de desesperación o de tipo depresivo. Durante su realización, los ratones fueron introducidos en un cilindro transparente de 15 cm de diámetro, 30 cm de alto y 3.5 litros de agua a 25ºC un total de 6 minutos, tiempo durante el cual se registró el tiempo de inmovilidad en fracciones de 2 minutos. Los resultados se expresan como el promedio ± s.e.m del tiempo de inmovilidad en segundos de cada uno de los tres bloques de 2 minutos y como el tiempo de inmovilidad total en segundos.

Test de suspensión de la cola: del mismo modo que el FST, el TST se utiliza para evaluar la vulnerabilidad al estrés así como para llevar a cabo el *screening* de los fármacos antidepresivos. Durante la prueba los animales inútilmente intentan escapar de una situación adversa hasta que experimentan desesperación y se inmovilizan. Durante la prueba, los ratones fueron suspendidos a 30 cm de una superficie lisa no reflectante mediante una cinta adhesiva colocada aproximadamente a 1 cm de la punta de la cola. La prueba tiene una duración total de 6 minutos durante los cuales se contabiliza el tiempo de inmovilidad. En los trabajos 2 y 5, se registró de modo simultáneo la liberación de 5-HT en la mPFC durante la ejecución del TST (ver apartado 3.7). Los resultados de TST se expresan como el promedio ± s.e.m del tiempo de inmovilidad en segundos.

3.9. Análisis estadístico

Los datos fueron analizados utilizando los programas estadísticos de GraphPad Prism 6.0 o STATISTICS. Los análisis estadísticos realizados incluyeron la prueba T de Student y ANOVAs de una, dos y tres vías seguidas por los post-hoc Newman-Keuls o Tukey, según fuera apropiado. En el NSFT se utilizó el análisis de supervivencia de Kaplan-Meier y el logrank (Mantel-Cox) para evaluar las diferencias entre los grupos experimentales, debido a que los resultados no cumplían los criterios de una distribución normal (Samuels and Hen, 2011). El nivel de significación se fijó en $p < 0.05$ (dos colas).

4. Resultados

4.1. Trabajo 1

Selective siRNA-mediated suppression of 5-HT$_{1A}$ autoreceptors evokes strong anti-depressant-like effects

A Bortolozzi, A Castañé, J Semakova, N Santana, G Alvarado, R Cortés, A Ferrés-Coy, G Fernández, MC Carmona, M Toth, JC Perales, A Montefeltro and F Artigas

Molecular Psychiatry. 2012 Jun; 17(6):612-623

La mayor parte de los fármacos antidepresivos prescritos, los SSRI, actúan inhibiendo el SERT. Esto conduce a incrementos de la concentración extracelular del neurotransmisor 5-HT que lleva a la activación de los receptores serotoninérgicos postsinápticos, entre ellos el receptor 5-HT$_{1A}$, necesarios para la manifestación de la mejora clínica. Sin embargo, la activación simultánea del autoreceptor 5-HT$_{1A}$ disminuye la actividad de las neuronas serotoninérgicas y la liberación de 5-HT, efecto contrario al deseado de un fármaco SSRI. Solo después de tratamientos prolongados con SSRI en los que se desensibiliza este mecanismo de autoregulación inhibitorio junto a cambios neuroplásticos se obtiene la respuesta terapéutica. En este trabajo presentamos una nueva estrategia antidepresiva basada en la administración aguda de siRNAs para suprimir el mecanismo de retroalimentación negativo mediado por el autoreceptor 5-HT$_{1A}$. En este trabajo se desarrolló una molécula de siRNA contra el receptor 5-HT$_{1A}$ (1A-siRNA) conjugada con sertralina (C-1A-siRNA) para direccionar y concentrar las moléculas de siRNA en las neuronas serotoninérgicas que expresan de modo abundante el SERT, por el que sertralina tiene una elevada afinidad. Nuestras hipótesis de trabajo fueron: 1) la conjugación con sertralina permitiría la acumulación selectiva del siRNA en neuronas serotoninérgicas y 2) el silenciamiento selectivo del autoreceptor 5-HT$_{1A}$ desencadenaría efectos antidepresivos debido al incremento del tono serotoninérgico, preservando la actividad del receptor 5-HT$_{1A}$ postsináptico.

Los resultados confirmaron que la administración intracerebroventricular del C-1A-siRNA en ratones no solo permitió la acumulación selectiva de esta molécula en las neuronas serotoninérgicas del DR, sino que además redujo la expresión y función del autoreceptor 5-HT_{1A} sin alterar la expresión/función del mismo receptor a nivel postsináptico. Los ratones presentaron respuestas de tipo antidepresivo en el TST y el FST, sin desencadenar comportamientos de ansiedad en el EPM. Además, la administración de C-1A-siRNA incrementó los niveles extracelulares de 5-HT inducidos por el SSRI fluoxetina. Interesantemente, resultados similares se obtuvieron después de la administración intranasal del C-1A-siRNA.

Estos resultados constatan que el C-1A-siRNA tiene la capacidad de silenciar selectivamente el autoreceptor 5-HT_{1A} *in vivo*, abriendo un extenso abanico de posibilidades terapéuticas silenciando variantes alélicas de este receptor u otros genes asociadas a resistencias farmacológicas y aproximando, por vez primera, la tecnología basada en RNAi a la terapia de las enfermedades neuropsiquiátricas.

Molecular Psychiatry (2012) 17, 612–623

www.nature.com/mp

ORIGINAL ARTICLE

Selective siRNA-mediated suppression of 5-HT$_{1A}$ autoreceptors evokes strong anti-depressant-like effects

A Bortolozzi[1,2,3], A Castañé[1,3,8], J Semakova[4,8], N Santana[1,3], G Alvarado[5], R Cortés[1,6], A Ferrés-Coy[1,2], G Fernández[5], MC Carmona[5], M Toth[7], JC Perales[4], A Montefeltro[5] and F Artigas[1,3]

[1]*Department of Neurochemistry and Neuropharmacology, IIBB - CSIC - IDIBAPS, Barcelona, Spain;* [2]*Institut d'Investigacions Biomèdiques August Pi i Sunyer (IDIBAPS), Barcelona, Spain;* [3]*Centro de Investigación Biomédica en Red de Salud Mental (CIBERSAM), Madrid, Spain;* [4]*Department of Physiological Sciences II, School of Medicine, Bellvitge, University of Barcelona, Barcelona, Spain;* [5]*n-Life Therapeutics, S.L., La Coruña, Spain;* [6]*Centro de Investigación Biomédica en Red de Enfermedades Neurodegenerativas (CIBERNED), Madrid, Spain and* [7]*Department of Pharmacology, Weill Medical College, Cornell University, New York, NY, USA*

Depression is a major health problem worldwide. Most prescribed anti-depressants, the selective serotonin reuptake inhibitors (SSRI) show limited efficacy and delayed onset of action, partly due to the activation of somatodendritic 5-HT$_{1A}$-autoreceptors by the excess extracellular serotonin (5-HT) produced by SSRI in the raphe nuclei. Likewise, 5-HT$_{1A}$ receptor (5-HT$_{1A}$R) gene polymorphisms leading to high 5-HT$_{1A}$-autoreceptor expression increase depression susceptibility and decrease treatment response. In this study, we report on a new treatment strategy based on the administration of small-interfering RNA (siRNA) to acutely suppress 5-HT$_{1A}$-autoreceptor-mediated negative feedback mechanisms. We developed a conjugated siRNA (C-1A-siRNA) by covalently binding siRNA targeting 5-HT$_{1A}$ receptor mRNA with the SSRI sertraline in order to concentrate it in serotonin axons, rich in serotonin transporter (SERT) sites. The intracerebroventricular (i.c.v.) infusion of C-1A-siRNA to mice resulted in its selective accumulation in serotonin neurons. This evoked marked anti-depressant-like effects in the forced swim and tail suspension tests, but did not affect anxiety-like behaviors in the elevated plus-maze. In parallel, C-1A-siRNA administration markedly decreased 5-HT$_{1A}$-autoreceptor expression and suppressed 8-OH-DPAT-induced hypothermia (a pre-synaptic 5-HT$_{1A}$R effect in mice) without affecting post-synaptic 5-HT$_{1A}$R expression in hippocampus and prefrontal cortex. Moreover, i.c.v. C-1A-siRNA infusion augmented the increase in extracellular serotonin evoked by fluoxetine in prefrontal cortex to the level seen in 5-HT$_{1A}$R knockout mice. Interestingly, intranasal C-1A-siRNA administration produced the same effects, thus opening the way to the therapeutic use of C-1A-siRNA. Hence, C-1A-siRNA represents a new approach to treat mood disorders as monotherapy or in combination with SSRI.
Molecular Psychiatry (2012) **17**, 612–623; doi:10.1038/mp.2011.92; published online 2 August 2011

Keywords: anti-depressant drug design; anxiety; major depression; serotonin neurons; small-interfering RNA; 5-HT$_{1A}$ receptors

Introduction

Major depression is a severe and heterogeneous psychiatric disease with high, increasing prevalence and socio-economic impact.[1–3] The serotonergic system is implicated in the etiology and treatment of mood disorders.[2] Most prescribed anti-depressants, the selective serotonin (5–HT) reuptake inhibitors (SSRI) and the dual 5-HT and norepinephrine reuptake inhibitors block physiological reuptake mechanisms in serotonergic axons, and thereby increase extracellular 5-HT concentration to activate post-synaptic 5-HT receptors (5-HT$_{1A}$R) required for clinical effects. However, this process is severely compromised by the simultaneous activation of somatodendritic 5-HT$_{1A}$-autoreceptors in the mid-brain raphe nuclei. 5-HT$_{1A}$-autoreceptor activation reduces serotonergic activity and forebrain 5-HT release, an effect contrary to that required for therapeutic response.[4–6]

Hence, the limited clinical efficacy of 5-HT-enhancing drugs and their delayed action are partly due to this negative feedback mechanism. Upon chronic treatment, 5-HT$_{1A}$-autoreceptors desensitize, leading to the recovery of serotonergic activity and 5-HT release.[5,6] Individuals with elevated density or activity of 5-HT$_{1A}$-autoreceptors are more susceptible

Correspondence: Professor F Artigas or Dr A Bortolozzi, Department of Neurochemistry and Neuropharmacology, IIBB-CSIC-IDIBAPS, 08036 Barcelona, Spain.
E-mails: fapnqi@iibb.csic.es or abbnqi@iibb.csic.es
[8]These authors contributed equally to this work.
Received 19 January 2011; revised 20 June 2011; accepted 21 June 2011; published online 2 August 2011

to mood disorders and respond poorly to anti-depressants.[7–9]

5-HT$_{1A}$R antagonists might thus be useful to improve anti-depressant therapy by preventing the 5-HT$_{1A}$-autoreceptor-mediated negative feedback. However, the activation of post-synaptic 5-HT$_{1A}$R is a necessary step for anti-depressant effects,[10] which limits the usefulness of this strategy. Thus, unlike the non-selective 5-HT$_{1A}$R/ß-adrenoceptor antagonist pindolol[11,12] (with a preferential action at 5-HT$_{1A}$-autoreceptors),[13,14] the selective 5-HT$_{1A}$R antagonist DU-125530 does not enhance clinical fluoxetine effects (Scorza *et al.*, in preparation).

In this study, we report on a new anti-depressant strategy, based on the use of small-interfering RNA (siRNA) targeted to serotonin neurons, to selectively reduce the expression and function of pre-synaptic (but not post-synaptic) 5-HT$_{1A}$R. We have developed a conjugated 5-HT$_{1A}$R siRNA (C-1A-siRNA) directed to serotonin neurons, by covalently binding 5-HT$_{1A}$R siRNA molecules to the SSRI sertraline. Our working hypotheses were: a) the presence of sertraline would allow the selective accumulation of C-1A-siRNA in serotonin neurons and b) the selective 5-HT$_{1A}$-autoreceptor silencing would have anti-depressant effects due to the increased signaling and preservation of post-synaptic 5-HT$_{1A}$R activity.

Materials and methods

Animals

Male C57BL/6J mice (Charles River) and male homozygous 5-HT$_{1A}$R knockout (1A-KO) mice on the same background[15] were used. Mice (10–15-week old) were housed under controlled conditions (22 ± 1 °C; 12 h light/dark cycle) with food and water available *ad libitum*. Animal procedures were conducted in accordance with standard ethical guidelines (European Union regulations L35/118/12/1986) and approved by the local ethical committee.

siRNAs

Four unmodified siRNAs (nt: 633-651, 852-870, 1889-1907 and 2167-2185, GenBank accession #NM_008308) targeting the 5-HT$_{1A}$R (1A-siRNA1 to 1A-siRNA4) were chosen for *in vivo* studies and administered as a mixture, containing an equal amount of each siRNA duplex. In addition, an unrelated siRNA duplex with no homology to mouse genome was used as negative control (nonsense siRNA — ns-siRNA). All siRNAs, consisted of two complementary 21-nucleotide RNA strand with 3′dTdT overhangs and were prepared according to the manufacturer's protocol (Ambion, Madrid, Spain). Conjugated siRNA against 5-HT$_{1A}$R (C-1A-siRNA) and conjugated nonsense siRNA (C-ns-siRNA) were synthesized by nLife Therapeutics, S.L. (La Coruña, Spain) as described (International patent application PCT/EP2011/056270). Each specific siRNA sequence against 5-HT$_{1A}$R (1A-siRNA1 to 1A-siRNA4) and ns-siRNA was designed to carry a substitution in each 5′-end strand (Figure 1a). Conjugated single-strand oligonucleotides were purified by reverse-phase high-performance liquid chromatography. Fractions containing full-length oligonucleotides were pooled, desalted, lyophilized and characterized by MALDI-TOF. Complementary strands were annealed in an isotonic RNA-annealing buffer (100 mM potassium acetate, 30 mM HEPES-KOH pH = 7.4, 2 mM magnesium acetate), pre-incubated by 1 min at 90 °C, centrifuged for 15 s and incubated 1 h at 37 °C. Annealed products were high-performance liquid chromatography purified and siRNA-containing fractions were lyophilized. Purity was >92%. Similarly to unmodified siRNAs, conjugated siRNAs were used *in vivo* as a mixture consisting of an equal amount of each C-1A-siRNA.

For experiments involving localization of C-1A-siRNA after intracerebroventricular (i.c.v.) infusion, each C-1A-siRNA molecule was additionally bound to biotin in the anti-sense strand. This was performed by a biotinylation reaction of the conjugate's OH-free end in its terminal C18 spacer.

We used a second strategy to generate a construct with a stronger stability against ribonucleases by the standard phosporamidite chemistry[16,17] as described (International patent application PCT/EP2011/056270). A sertraline-conjugated ns-oligonucleotide (single-strand 18-mer oligonucleotide nonsense sequence, with 2′-O-methyl ribonucleotides at positions 1–3 and 16–18, and a DNA gap of 12 nucleobases) was synthesized with a Cy3 label at 3′ attached by a phosphodiester linkage. This was coupled to sertraline to examine the penetration into serotonin neurons after i.c.v. infusion.

A siRNA targeting β-galactosidase (β-Gal-128) bearing a motif eliciting interferon production was also used.[18] Stock solutions of all siRNAs were prepared by re-suspension of the lyophilized product in RNAse-free water and stored at −20 °C until use. siRNA sequences are shown in Supplementary Table S1.

Treatments

Intracerebral siRNA infusion. Mice were anesthetized (pentobarbital, 40 mg kg^{-1}, i.p.) and silica capillary microcannulae (110 µm-OD, 40 µm-ID; Polymicro Technologies, Madrid, Spain) were stereotaxically implanted into dorsal raphe nucleus (DR; coordinates in mm: anteroposterior-AP, -4.5; mediolateral-ML, -1.0; dorsoventral-DV, -4.4; with a lateral angle of 20°) or in dorsal third ventricle (D3V; AP, -2.0; ML, 0; DV, -2.1).[19] Some animals were also implanted with a microdialysis probe in medial prefrontal cortex (mPFC) (see below). siRNA microinfusion was performed with a perfusion pump at 0.5 µl min^{-1} 20–24 h after surgery in awake mice. siRNAs targeting 5-HT$_{1A}$R, β-galactosidase or nonsense were prepared in artificial cerebrospinal fluid (125 mM NaCl, 2.5 mM KCl, 1.26 mM $CaCl_2$ and 1.18 mM $MgCl_2$ with 5% glucose) and infused at doses of 10 or 30 µg of siRNA per mouse. Intra-DR siRNA infusion was repeated 24 h later

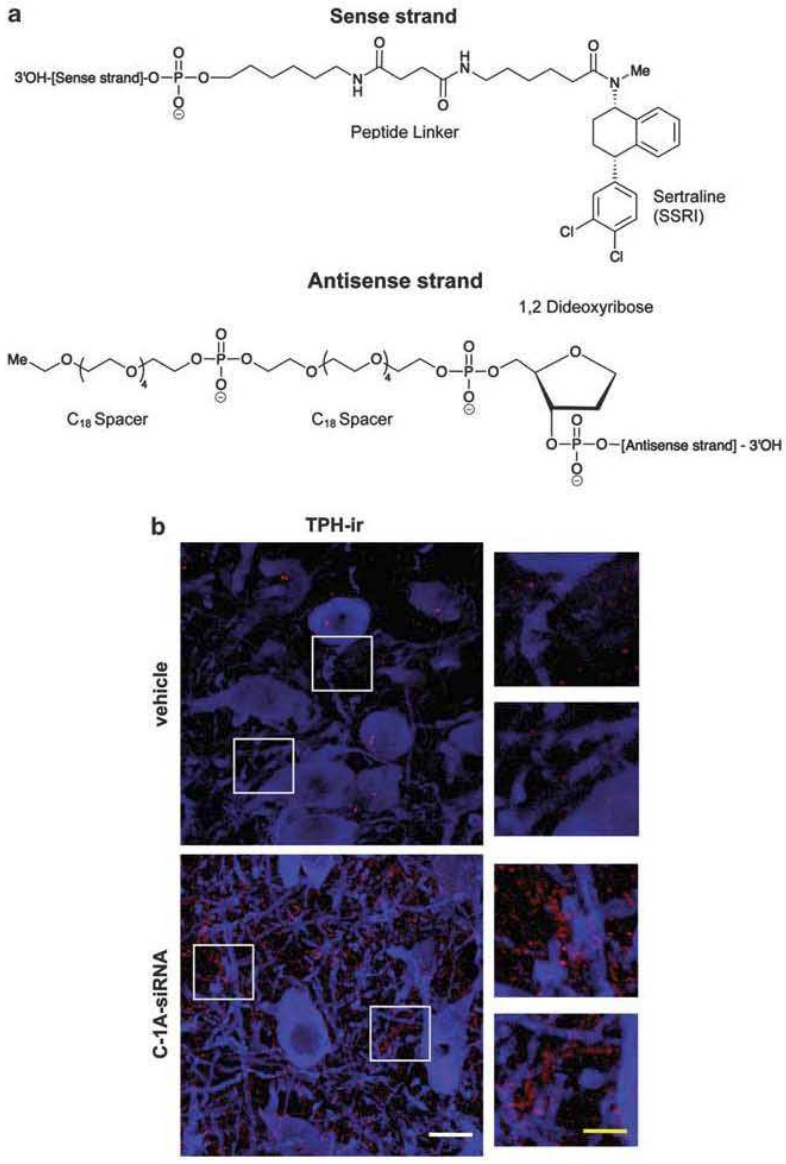

Figure 1 (**a**) Chemical structure of conjugated 5-HT$_{1A}$R-small-interfering RNA (siRNA) (C-1A-siRNA). C-1A-siRNA construct comprising specific siRNA sequences directed against 5-HT$_{1A}$R with chemical conjugation in each 5′-end strand. The sense strand was amino-modified by performing a 5′-C6 amino modification and condensation with a succinimide active ester of sertraline (sertraline-NH-CH2C(= O)NH(CH2)5COO-succinimide) making up the peptide linker of the conjugate (sertraline-NH-CH2C(= O)NH(CH2)5COO-sense strand-3′OH). A phosphoramidite derivative of 1′,2′-dideoxyribose molecule (dSpacer CE Phosphoramidite: 5′-O-Dimethoxytrityl-1′,2′-Dideoxyribose-3′-((2-cyanoethyl)-(N,N-diisopropyl))phosphoramidite) and two phosphoramidite C18 spacer arms (Spacer Phosphoramidite 18: 18-O-Dimethoxytritylhexaethyleneglycol, 1-((2-cyanoethyl)-(N,N-diisopropyl)) phosphoramidite) were covalently coupled to the complementary antisense strand by phosphodiester linkages. (**b**) Selective accumulation of C-1A-siRNA in raphe serotonin neurons. Mice received a single intracerebroventricular infusion of vehicle or biotin-labeled C-1A-siRNA (30 μg) into the dorsal third ventricle, and were killed 48 h post-administration ($n = 3$ mice per group). Laser confocal images of TPH-immunoreactive serotonin neurons (blue) showing the immune-localized biotin-labeled C-1A-siRNA (red). Right-hand panels are high-magnification photomicrographs of the frames in the left. Scale bars: white = 60 μm, yellow = 25 μm.

(1-μl aliquots; two administrations in total), while i.c.v. infusion was performed only once into the D3 V (2.5-ul aliquots). Controls and 1A-KO mice received aCSF.

Intranasal siRNA administration. Pentobarbital-anesthetized mice were positioned lying on their backs. Phosphate buffered saline (PBS) or conjugated

siRNAs (C-ns-siRNA and C-1A-siRNA prepared in PBS) were slowly dropped alternatively into each nostril with a micropipette tip in 5-µl aliquots. Total administered doses were 30 or 100 µg of conjugated siRNAs.

RNA isolation and quantitative RT-PCR analysis
After 24–48 h the last administration of vehicle or siRNA, mice were killed and brains were removed. Midbrain sections containing the raphe nuclei (1-mm thick) were dissected out using a Mouse Brain Matrix (Ted Pella, Madrid, Spain), quickly frozen on dry ice and stored at −80 °C. Total RNA was isolated with Trizol solution (Invitrogen, Barcelona, Spain). Complementary DNA synthesis was performed using Retro-tools two step kits (Biotools B & M labs SA, Madrid, Spain). Quantitative RT-PCR (7900HT Fast Real-Time PCR System, Applied Biosystems, Madrid, Spain) was performed using Power SYBR Green PCR Master Mix (Applied Biosystems) in 20 µl of reaction mix. Cycle threshold values were calculated using AbiPrism SDS 2.1 software (Applied Biosystems). Data were normalized to the amount of cyclophilinA cDNA. Results were expressed as the unitary ratio versus vehicle controls. Primer sequences are given in Supplementary Table S1.

Tissue preparation for in situ *hybridization and receptor autoradiography*
Mice were killed by pentobarbital overdose and the brains rapidly removed, frozen on dry ice and stored at −20 °C. Tissue sections, 14-µm thick, were cut using a microtome-cryostat (HM500 OM, Microm, Walldorf, Germany), thaw-mounted onto 3-amino-propyltriethoxysilane-coated slides (Sigma-Aldrich, Madrid, Spain) and kept at −20 °C until use.

In situ *hybridization*
For 5-HT$_{1A}$R mRNA, three oligonucleotides were used simultaneously, complementary to bases: 1–48, 763–810 and 1219–1266 (GenBank accession #NM_012585). These probes were synthesized with a 380 Applied Biosystem DNA synthesizer. Labeling of the probes and *in situ* hybridization procedures were carried out as described previously.[20–22] Hybridized sections were exposed to Biomax MR film (Kodak, Sigma-Aldrich, Madrid, Spain) for 2–3 weeks with intensifying screens.

Receptor autoradiography
The autoradiographic binding assays for 5-HT$_{1A}$ and 5-HT$_{1B}$ receptors and serotonin transporter (SERT)[20,23,24] were performed using the following radioligands: (a) [^{3}H]-8-OH-DPAT (233 Cimmol $^{-1}$), (b) [^{125}I]-cyanopindolol (2200 Cimmol $^{-1}$) and (c) [^{3}H]-citalopram (70 Cimmol $^{-1}$), respectively (Amersham-GE Healthcare, Barcelona, Spain and Perkin-Elmer, Madrid, Spain). 8-OH-DPAT, isoproterenol, pargyline and 5-HT were from Sigma-Aldrich, and fluoxetine was from Tocris. Experimental conditions are summarized in Supplementary Table S2. Tissues were exposed to Biomax MR film (Kodak) together with ^{3}H-Microscales standards (Amersham-GE Healthcare). All experimental and control brains within a group were processed in duplicate and exposed to films as a batch.

Films were analyzed by microdensitometry using a computer-assisted image analyzer (AIS, Imaging Research, St Catherines, Ontario, Canada). 5-HT$_{1A}$R mRNA and 5-HT$_{1B}$ binding sites in selected brain regions were measured in the respective autoradiograms to obtain relative optical densities. For 5-HT$_{1A}$R and SERT binding, the system was calibrated with ^{3}H-Microscales standards to obtain fmol mg $^{-1}$ protein equivalents from relative optical densities data. AIS system was also used to acquire pseudocolor images. Black and white photographs were taken from autoradiograms using a Wild 420 microscope (Leica, Heerbrugg, Germany) equipped with a Nikon DXM1200 F digital camera and ACT-1 Nikon software, Soft Imaging System Gmbh, Münster, Germany. Images were processed with Photoshop (Adobe Systems, Mountain View) by using identical values for contrast and brightness.

Immunohistochemistry
Animals were killed by a pentobarbital overdose and perfused with 4% paraformaldehyde in sodium-phosphate buffer (pH = 7.4). Brains were dissected, post-fixed 24 h at 4 °C in the same solution and then placed in 30% sucrose in PBS for 3 days at 4 °C. After cryopreservation, brains were embedded with gelatin, frozen and sectioned in a cryostat (30 µm coronal). Free-floating sections were washed and permeabilized with PBS-Triton 0.3%, blocked with BlockAid (Invitrogen) plus 0.3% Triton for 2 h at 23 °C and then incubated with NeutrAvidin (Invitrogen) 0.0125 mg ml $^{-1}$ in blocking solution (1 h, 23 °C). Sections were than washed and incubated overnight (4 °C) with biotinylated rabbit anti-donkey antibody (Abcam, Madrid, Spain) diluted 1:200, washed and incubated (2 h, 23 °C) with Cy3-conjugated donkey anti-rabbit antibody (Rockland, Barcelona, Spain) diluted 1:200 in blocking solution. This was followed by additional blocking with 10% donkey serum (Sigma-Aldrich) in PBS-Triton 0.3%, 1 h, 23 °C and overnight incubation with anti-tryptophan hydroxylase antibody (1:100; Chemicon-Millipore, Billerica, MA, USA) diluted in 3% of donkey serum in PBS-Triton 0.3%. Excess of primary antibody was washed and sections were incubated 2 h, 23 °C with Alexa-Fluor 647-conjugated donkey anti-sheep antibody (Invitrogen) diluted 1:200 and YOYO-1 (Invitrogen) diluted 1:5000 in 3% of donkey serum in PBS-Triton 0.3%. Finally, sections were mounted with Mowiol (Calbiochem, San Diego, CA, USA). Samples were analyzed using a Leica spectral confocal microscope; (Wetzlar, Germany) data were sequentially collected from each channel, merged by Leica Confocal Software (Wetzlar, Germany) and 3D projections (maximal, average and transparent) were made from z-series. Pictures were generated using Photoshop.

Intracerebral microdialysis
Extracellular 5-HT concentration was measured by *in vivo* microdialysis as previously described.[20] Briefly, one concentric dialysis probe (cuprophan; 1 mm-long) was implanted in mPFC (AP, 2.2; ML, -0.2; DV, -3.4)[19] of pentobarbital-anaesthetized mice. Experiments were performed 48–72 h after surgery. To assess 8-OH-DPAT effects on extracellular 5-HT, 1 μM citalopram (SSRI; Lundbeck A/S, Valby, Copenhagen) was added to artificial cerebrospinal fluid.[25] The artificial cerebrospinal fluid was pumped at 2.0 μl min $^{-1}$ (WPI model sp220i) and 30-min samples were collected. 5-HT concentrations were analyzed by high-performance liquid chromatography-amperometric detection (Hewlett-Packard 1049; +0.6 V, Palo Alto, CA, USA) with detection limits of 1.5 fmol sample $^{-1}$. Baseline 5-HT levels were calculated as the average of the four pre-drug samples. Correct probe placement was verified using cresyl-violet staining.

Behavioral and physiological assessments
Mice were tested at 24–72 h after treatments. Elevated plus-maze (EPM) and tail suspension tests (TST) were always conducted in this order, with 1 day between tests. All tests were performed between 1000 and 1500 hours. On test days, animals were transported to the dimly illuminated behavioral laboratory and were left undisturbed for at least 1 h before testing.

8-OH-DPAT-induced hypothermia. Body temperature was measured intrarectally using a lubricated probe inserted ~2 cm and a digital thermometer (AZ9882, Panlab, Barcelona, Spain). Mice were singly housed in clean cages for 20 min before measurements, and then two baseline temperature measurements were taken. After 10 min, animals received 8-OH-DPAT 1 mg kg $^{-1}$ i.p., and body temperature was recorded every 15 min for a total of 120 min. Data are presented as a change from the final baseline measurement.

Elevated plus maze. The EPM was performed using a cross maze with 16 × 5 cm arms illuminated from the top (100 lux). Mice were placed in the central area, facing one of the open arms and the time and number of entries into open and closed arms in 5 min were recorded (video camera system, Smart, Panlab). Results were expressed as the percentage of time and number of entries into the open arms.

Tail suspension test. Mice were suspended 30 cm above the bench by adhesive tape placed approximately 1 cm from the tip of the tail. Mice were monitored and recorded using a video camera system (Smart, Panlab), and the time spent immobile was recorded for 6 min.

Forced swim test (FST). Mice were individually placed into a clear cylinder (15 cm diameter, 30 cm height) containing 20 cm of water maintained at 24–25 °C, essentially as described by Porsolt *et al.*[26] In this test, time of immobility was scored in 2-mm bins for a total of 6 min using a video camera system (Smart, Panlab).

Statistical analysis
Data are expressed as means ± s.e.m. Data were analyzed with Student's *t*-test, one- or two-way analysis of variance, as appropriate, followed by post-hoc test (Newman–Keuls). The level of significance was set at $P < 0.05$ (two tailed).

Results

Selective silencing of 5-HT$_{1A}$-autoreceptor expression
The potential of siRNA-based gene silencing *in vivo* has been limited by the lack of safe delivery to specific target cells.[27] Previously,[28] we established that local infusion of four siRNA sequences directed toward 5-HT$_{1A}$R (1A-siRNA) into the mice DR reduced 5-HT$_{1A}$-autoreceptor expression and function without affecting post-synaptic 5-HT$_{1A}$R, evoking a robust and rapid antidepressant-like effect. We therefore used the same 1A-siRNA sequences to construct C-1A-siRNA. Sense and antisense strands were chemically conjugated in each 5′-end strand, whereas the sense strand was covalently bound to the SSRI-sertraline (Figure 1a). This modification was intended to direct C-1A-siRNA molecules to 5-HT axons, extremely rich in axonal varicosities (>10^6 per mm^3),[29] expressing SERT, for which sertraline shows very high affinity (Ki = 0.29 nM, http://kidb.case.edu/pdsp.php).

Figure 2 Selective 5-HT$_{1A}$-autoreceptor silencing by intracerebroventricular infusion of C-1A-small-interfering RNA (siRNA). (**a**) Representative coronal brain sections showing the C-1A-siRNA-induced reduction of 5-HT$_{1A}$R expression in raphe nuclei assessed by *in situ* hybridization and [^{3}H]-8-OH-DPAT binding. (**b**) Representative coronal brain sections showing [^{3}H]-8-OH-DPAT binding to 5-HT$_{1A}$R in medial prefrontal cortex (mPFC) and hippocampus (HPC). Scale bars: white = 2 mm, black = 500 μm. (**c**) Effect of C-1A-siRNA (30 μg) on 5-HT$_{1A}$R mRNA and binding in dorsal raphe nucleus (DR) ($n = 3$–5). One-way analysis of variance revealed a group effect on 5-HT$_{1A}$R mRNA ($F_{4,15} = 7.15$, $P < 0.01$) and 5-HT$_{1A}$R binding ($F_{4,13} = 5.04$, $P < 0.05$). $^*P < 0.05$, $^{**}P < 0.01$ versus the rest of experimental groups. (**d**) Post-synaptic 5-HT$_{1A}$R binding in mPFC and HPC was not affected by any treatment ($n = 3$–4). (**e**) The 5-HT$_{1A}$R agonist, 8-OH-DPAT (1 mg kg^{-1}, i.p.) reduced body temperature in vehicle and conjugated nonsense siRNA (C-ns-siRNA), but not in C-1A-siRNA and 1A-KO mice. Pretreatment (3 h) with sertraline (20 mg kg^{-1}, i.p.) blocked C-1A-siRNA (30 μg) effect on 5-HT$_{1A}$-autoreceptor silencing ($n = 5$–8). One-way analysis of variance, $F_{5,31} = 25.35$, $P < 0.001$. (**f**) 8-OH-DPAT (0.5 mg kg^{-1}, i.p.) decreased extracellular serotonin in controls, but not in C-1A-siRNA and 1A-KO groups. Pretreatment (3 h) with sertraline (20 mg kg^{-1}, i.p.) prevented the effect of C-1A-siRNA ($n = 5$–8, $F_{6,38} = 15.74$, $P < 0.001$). $^{***}P < 0.001$ versus control groups, $^{\#\#\#}P < 0.001$ versus C-1A- siRNA. Values are mean ± s.e.m.

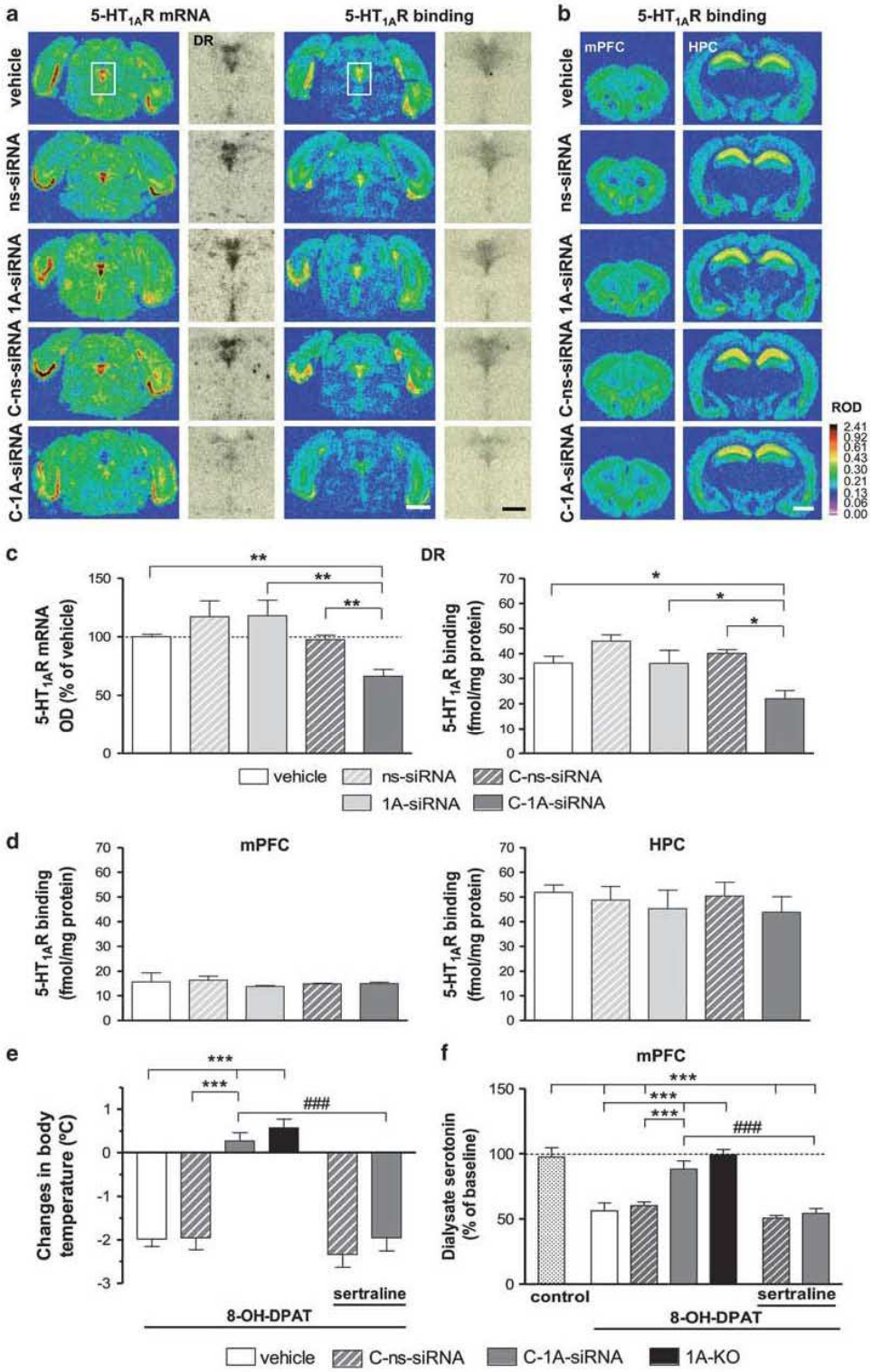
a
5-HT1AR mRNA
5-HT1AR binding
DR
vehicle
ns-siRNA
1A-siRNA
C-ns-siRNA
C-1A-siRNA
b
5-HT1AR binding
mPFC
HPC
ROD
2.41
0.92
0.61
0.43
0.30
0.21
0.13
0.06
0.00
c
5-HT1AR mRNA OD (% of vehicle)
DR
5-HT1AR binding (fmol/mg protein)
vehicle
ns-siRNA
C-ns-siRNA
1A-siRNA
C-1A-siRNA
d
mPFC
HPC
5-HT1AR binding (fmol/mg protein)
e
Changes in body temperature (ºC)
8-OH-DPAT
sertraline
f
mPFC
Dialysate serotonin (% of baseline)
control
8-OH-DPAT
sertraline
vehicle
C-ns-siRNA
C-1A-siRNA
1A-KO

After 48 h stereotaxic infusion in the D3 V (30 μg per mouse, as in receptor expression and functional experiments; see below), the C-1A-siRNA construct was detected in midbrain serotonergic neuropil, rich in dendrites and initial axonal segments (Figure 1b, Supplementary Figure S1). In contrast, C-1A-siRNA was undetectable in dorsal hippocampal neurons, located much closer to the infusion site (Supplementary Figure S2). Additional experiments using a Cy3-coupled, sertraline-conjugated -18-mer oligonucleotide (see Material and methods) showed that 24 h after its infusion into the D3 V (30 μg), the Cy3-labeled oligonucleotide was found in the cytoplasm of TPH-positive midbrain serotonin neurons (Supplementary Figure S3).

Next, we evaluated whether the i.c.v. infusion of C-1A-siRNA could selectively silence the *5-HT$_{1A}$R* gene in 5-HT neurons, as observed after local infusion of unmodified 1A-siRNA.[28] Mice were stereotaxically injected into D3 V with: (a) vehicle, (b) unmodified nonsense siRNA (ns-siRNA), (c) unmodified 1A-siRNA, (d) C-ns-siRNA or (e) C-1A-siRNA (30 μg of each siRNA). Histological examination at 1–3 days post-administration revealed that 5-HT$_{1A}$R mRNA and binding densities were significantly decreased in the dorsal (40% versus control) and median raphe (30%) nuclei of C-1A-siRNA-treated mice (Figure 2a, c and Supplementary Figure S4).

A similar decrease was produced by intra-DR infusion of the same unmodified 1A-siRNA sequences (Supplementary Figure S5). Likewise, local 1A-siRNA and C-1A-siRNA infusion reduced comparably 5-HT$_{1A}$R binding density in the DR (Supplementary Figure S6), indicating that sertraline conjugation did not alter 1A-siRNA capacity to knockdown 5-HT$_{1A}$R.

In contrast, C-1A-siRNA infusion into D3 V did not affect post-synaptic 5-HT$_{1A}$R density in forebrain (Figure 2b, d and Supplementary Figure S7a), nor that of other genes expressed by 5-HT neurons (SERT and 5-HT$_{1B}$R) of the same mice (Figure 3a–c). Likewise, C-1A-siRNA sequences did not upregulate inflammatory cytokines (tumor necrosis factor α and interferon-γ) or apoptotic genes (*BAX*), while the immunostimulatory activity of β-galactosidase-siRNA sequence (used as positive control) dramatically increased tumor necrosis factor α and interferon-γ expression (Figure 3d–f), indicating that 5-HT$_{1A}$-autoreceptor silencing was specifically mediated by an RNA interference (RNAi) mechanism.

Effects of C-1A-siRNA on serotonergic function

The physiological consequences of 5-HT$_{1A}$-autoreceptor silencing were examined using the hypothermia response induced by the selective 5-HT$_{1A}$R agonist, 8-OH-DPAT, an effect mediated exclusively by presynaptic 5-HT$_{1A}$R in mice.[30] C-1A-siRNA-treated mice did not show hypothermia, nor did constitutive 5-HT$_{1A}$R knockout mice (1A-KO), while control groups displayed the expected hypothermic response (Figure 2e, Supplementary Figure S8a). We next investigated the consequences of 5-HT$_{1A}$-autoreceptor knockdown on serotonergic function. Baseline extracellular 5-HT concentration in mPFC did not differ among experimental groups (Supplementary Table S3). However, 8-OH-DPAT administration (0.5 mg kg^{-1}, i.p.) reduced extracellular 5-HT concentration in mPFC of vehicle (56% of baseline) and C-ns-siRNA-treated mice (60%), but not in C-1A-siRNA-treated (88%) and 1A-KO mice (99%) (Figure 2f, Supplementary Figure S8b).

To assess the involvement of SERT as a gate for the accumulation of C-1A-siRNA in 5-HT neurons, mice were pretreated with sertraline (20 mg kg^{-1}, i.p.; 3 h before the i.c.v. C-1A-siRNA infusion). These mice displayed the fall in 5-HT release and body temperature as did controls, whereas those treated with C-1A-siRNA alone did not respond to 8-OH-DPAT in both experimental approaches (Figure 2e-f, Supplementary Figure S8). This indicates that C-1A-siRNA requires functional SERT sites to silence 5-HT$_{1A}$-autoreceptor expression.

C-1A-siRNA evokes anti-depressant-like responses

To explore the behavioral effects of 5-HT$_{1A}$-autoreceptor knockdown, we examined the anti-depressant- and anxiety-like responses using the FST, tail suspension test (TST) and EPM paradigm. Mice infused with C-1A-siRNA (30 μg) into the D3 V displayed a marked reduction of immobility time in FST compared with controls (Figure 4a). Moreover, C-1A-siRNA-treated mice showed a significantly lower immobility than controls in the TST, as did 1A-KO mice (Figure 4b). A quantitative difference between both groups was noted, likely due to the partial knockdown of 5-HT$_{1A}$-autoreceptors in C-1A-siRNA-treated mice and total absence in 1A-KO mice. Fluoxetine administration (10 mg kg^{-1}, i.p.), used as a positive control, also reduced immobility in the FST and TST (Figure 4a and b). In contrast, control and C-1A-siRNA-treated mice behaved comparably in the EPM, with equal number of entries and time spent in the open arms. 1A-KO mice showed a clear anxiogenic profile, as previously described[15,31] (Figure 4c). At the neurochemical level, fluoxetine (20 mg kg^{-1}, i.p.) increased extracellular 5-HT concentration in mPFC significantly more in C-1A-siRNA (272% of baseline) and 1A-KO mice (230%) than in controls (vehicle: 138%; C-ns-siRNA: 150%), indicating that C-1A-siRNA-induced reduction in 5-HT$_{1A}$-autoreceptors augments SSRI effects (Figure 4d).

Intranasal C-1A-siRNA administration reduces 5-HT$_{1A}$-autoreceptor expression and induces anti-depressant effects

The above findings support the potential of C-1A-siRNA as a new anti-depressant strategy, either as monotherapy or in combination with 5-HT-enhancing drugs. However, its therapeutic use is limited by the lack of a suitable route to brain. We therefore examined the potential of the non-invasive intranasal route, as described before.[32–34] Intranasal C-1A-siRNA administration (30 μg per mouse, as in i.c.v. studies)

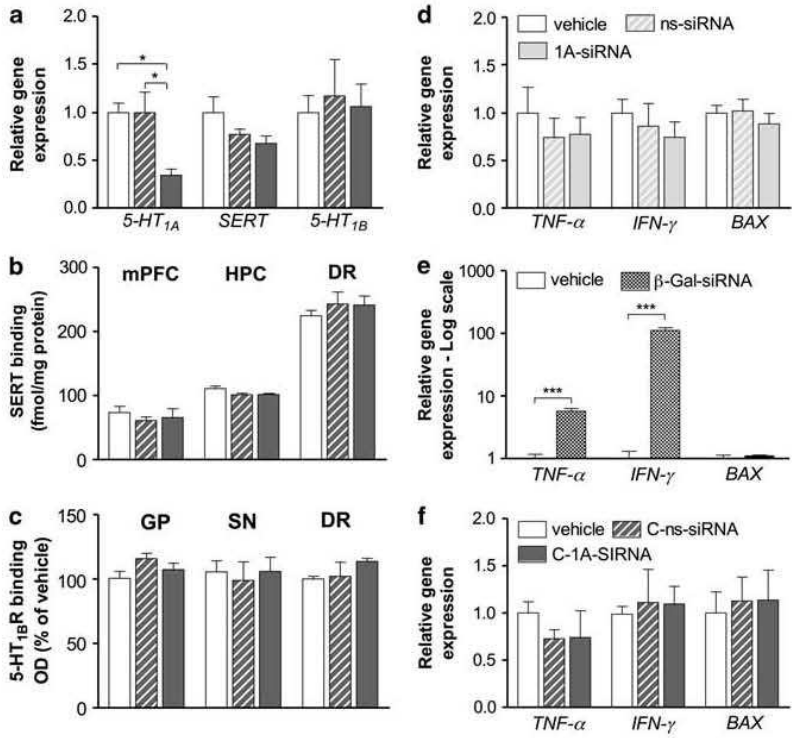

Figure 3 (**a–c**) Unchanged serotonin transporter (SERT) and 5-HT$_{1B}$R expression after 5-HT$_{1A}$-autoreceptors silencing. Mice received: (**a**) vehicle, (**b**) C-ns-small-interfering RNA (siRNA) or (**c**) C-1A-siRNA (30 μg) into D3 V and were killed 24 h after administration ($n = 5–7$). (**a**) The levels of the mRNAs encoding 5-HT$_{1A}$, SERT and 5-HT$_{1B}$ (serotonin pathway) were evaluated in midbrain raphe nuclei by RT-qPCR. One-way analysis of variance showed a group effect on 5-HT$_{1A}$R mRNA levels ($F_{2,13} = 6.06$, $P < 0.05$). $^*P < 0.05$ versus vehicle and conjugated nonsense siRNA (C-ns-siRNA). (**b**) Quantitative autoradiography of [^{3}H]-citalopram binding showed no differences on SERT density in the different brain areas for each treatment. (**c**) Bar graph showing no differences in 5-HT$_{1B}$R density evaluated by [^{125}I]-cyanopindolol binding in the different brain areas. mPFC-medial prefrontal cortex; HPC-hippocampus; DR-dorsal raphe nucleus; GP-globus pallidus; SN-substantia nigra. (**d–f**) Unmodified 1A-siRNA and C-1A-siRNA sequences did not induce inflammatory and apoptotic responses. (**d**) Mice received intra-DR: (i) vehicle, (ii) unmodified ns-siRNA or (iii) unmodified 1A-siRNA (10 μg by 2 consecutive days, 20 μg in total) and were killed 24 h after administration. mRNA levels of tumor necrosis factor α (TNFα) and interferon-γ (IFNγ) (pro-inflammatory cytokines) and BAX (apoptosis pathway) were evaluated in midbrain raphe nuclei by RT-qPCR ($n = 4–6$). (**e**) Immunostimulatory β-Gal-siRNA was used as a positive control. Mice received intra-DR: (i) vehicle, or (ii) β-Gal-siRNA (10 μg by 2 consecutive days, 20 μg in total) and were killed 24 h after administration. TNFα and IFNγ mRNA levels were significantly upregulated in midbrain after β-Gal-siRNA infusion ($n = 3–6$, Student's *t*-test, $^{***}P < 0.001$). (**f**) Bar graphs showing no differences in TNFα, IFNγ and BAX mRNA levels of mice infused with: (i) vehicle, (ii) C-ns-siRNA or (iii) C-1A-siRNA (30 μg) into D3 V and killed 24 h after administration ($n = 5–7$). Values are mean ± s.e.m.

reduced 5-HT$_{1A}$R mRNA and binding density (27%) in the DR, but not in post-synaptic sites in the same mice (Figure 5a–d, Supplementary Figure S7b). Unlike in controls (vehicle and C-ns-siRNA), 8-OH-DPAT administration did not reduce body temperature and 5-HT release in mice treated intranasally with C-1A-siRNA (Figure 5e and f).

Given the smaller effect size of 30 μg intranasal C-1A-siRNA on 5-HT$_{1A}$-autoreceptor expression—compared with i.c.v. infusion—we conducted behavioral experiments using 30 and 100 μg of intranasal C-1A-siRNA. Both doses significantly reduced immobility in the TST, with a greater effect of the 100 μg dose (Figure 5g). Similarly, intranasal C-1A-siRNA (100 μg) evoked a reduction of immobility time in the FST, which was significantly lower than that seen in controls (Figure 5h). Neither dose affected anxiety-like behavior as assessed with EPM test (data not shown).

Discussion

The present findings show that C-1A-siRNA can be used to efficiently and selectively silence 5-HT$_{1A}$-autoreceptor expression and function *in vivo*. This represents a new therapeutic approach in neuropsychopharmacology, based on the use of RNAi. Hence, i.c.v. and intranasal C-1A-siRNA infusion (i) reduced 5-HT$_{1A}$-autoreceptor expression, without affecting that of post-synaptic 5-HT$_{1A}$R, (ii) suppressed the hypothermia and fall in 5-HT release induced by 8-OH-DPAT; (iii) evoked a marked anti-depressant-

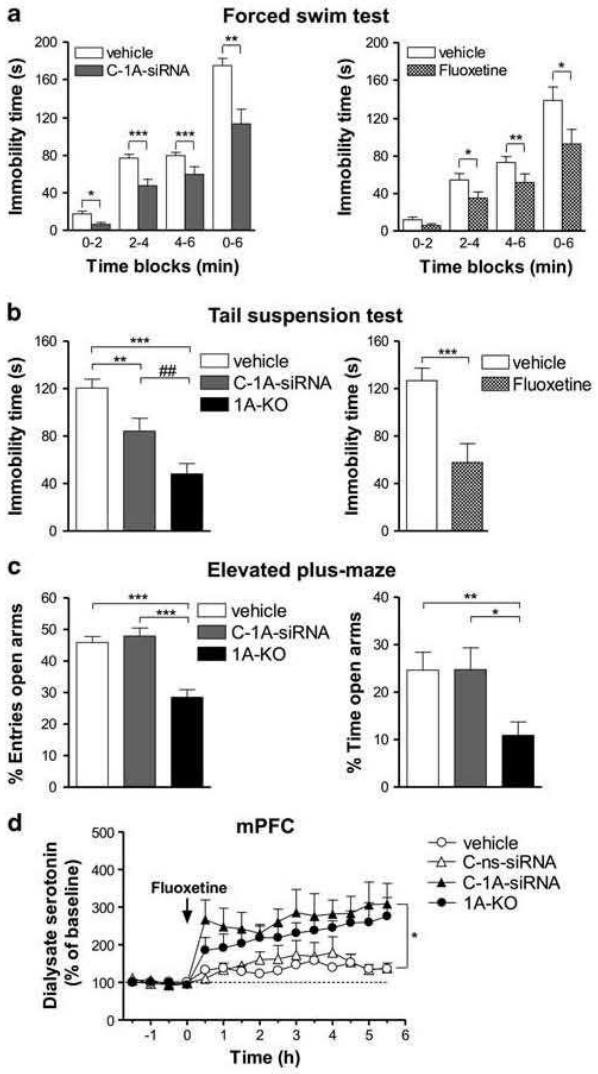

Figure 4 C-1A-small-interfering RNA (siRNA) evokes anti-depressant-like responses and potentiates the neurochemical effect of fluoxetine. **(a)** Mice infused with 30 μg C-1A-siRNA in the dorsal third ventricle (D3 V) displayed a decreased immobility in the forced swim test (FST) ($n=14$–15). Two-way analysis of variance showed a significant effect of group ($F_{1,27}=12.98$, $P<0.001$), time ($F_{2,54}=150.05$, $P<0.0001$) and interaction ($F_{2,54}=3.18$, $P<0.05$). A significantly greater reduction of the immobility in C-1A-siRNA-treated mice versus controls was observed for the total period (0–6 min) ($P<0.01$; Student's *t*-test). A comparable anti-depressant response was observed after acute selective serotonin reuptake inhibitors fluoxetine administration to control C57BL/6J mice (10 mg kg^{-1}, i.p. 30 min before FST) ($n=12$–13). Effect of group ($F_{1,23}=5.18$, $P<0.05$) and time ($F_{2,46}=66.94$, $P<0.0001$). Student's *t*-test was used to assess the action of fluoxetine for the total observation period (0–6 min). $^{*}P<0.05$, $^{**}P<0.01$, $^{***}P<0.001$ versus respective controls. **(b)** C-1A-siRNA-treated mice also showed a reduced immobility in the tail suspension test (TST), as did constitutive 1A-KO mice ($n=12$–18). One-way analysis of variance showed a significant effect of group ($F_{2,47}=18.64$, $P<0.001$). Acute fluoxetine administration (10 mg kg^{-1}, i.p. 1 h before TST) produced a similar anti-depressant response ($n=7$). $^{**}P<0.01$, $^{***}P<0.001$ versus vehicle mice, $^{\#\#}P<0.01$ versus C-1A-siRNA mice. **(c)** Unlike 1A-KO mice, vehicle and C-1A-siRNA mice behaved similarly in the elevated plus-maze ($n=12$–18). One-way analysis of variance indicated a group effect on entries ($F_{2,43}=24.18$, $P<0.001$) and time in open arms ($F_{2,42}=4.56$, $P<0.05$). $^{*}P<0.05$, $^{**}P<0.01$, $^{***}P<0.001$ versus vehicle and C-1A-siRNA groups. **(d)** Acute fluoxetine (20 mg kg^{-1}, i.p.) increased extracellular serotonin in mPFC of C-1A-siRNA and 1A-KO mice significantly more than in vehicle and conjugated nonsense siRNA (C-ns-siRNA) groups ($n=4$–6). Effect of group ($F_{3,17}=4.78$, $P<0.05$), time ($F_{14,238}=19.40$, $P<0.001$) and interaction ($F_{42,238}=2.57$, $P<0.001$). $^{*}P<0.05$ versus control groups. Values are mean ± s.e.m.

Figure 5 Intranasal C-1A-small-interfering RNA (siRNA) silences 5-HT$_{1A}$-autoreceptors and evokes anti-depressant-like responses. **(a)** Representative coronal brain sections showing the C-1A-siRNA-induced reduction of 5-HT$_{1A}$R expression in raphe nuclei by *in situ* hybridization and [^{3}H]-8-OH-DPAT binding. **(b)** Representative coronal brain sections showing [^{3}H]-8-OH-DPAT binding to 5-HT$_{1A}$R in medial prefrontal cortex (mPFC) and hippocampus (HPC). Scale bars: white = 2 mm, black = 500 μm. **(c)** Bar graphs showing the effects of intranasal C-1A-siRNA (30 μg) administration on 5-HT$_{1A}$R mRNA and binding in dorsal raphe nucleus (DR) ($n=3$–6). One-way analysis of variance showed a significant effect of group on 5-HT$_{1A}$R mRNA ($F_{2,9}=12.41$, $P<0.01$) and 5-HT$_{1A}$R binding ($F_{2,8}=37.98$, $P<0.001$). $^{*}P<0.05$, $^{**}P<0.01$ versus control groups. **(d)** Unchanged densities of post-synaptic 5-HT$_{1A}$R binding in all experimental groups ($n=3$–6). **(e)** Systemic 8-OH-DPAT administration (1 mg kg^{-1}, i.p.) did not evoke hypothermia in C-1A-siRNA-treated (30 μg) mice ($n=5$–7). Two-way analysis of variance showed a significant effect of group ($F_{2,13}=34.21$, $P<0.001$), time ($F_{4,52}=59.30$, $P<0.001$) and interaction ($F_{8,52}=10.89$, $P<0.001$). $^{***}P<0.001$ versus control groups. **(f)** Reduced extracellular serotonin in mPFC of controls, but not in C-1A-siRNA mice after 8-OH-DPAT administration (0.5 mg kg^{-1}, i.p.) ($n=4$–6). Significant effect of group ($F_{2,12}=8.22$, $P<0.01$), time ($F_{14,168}=7.56$, $P<0.001$) and interaction ($F_{28,168}=2.28$, $P<0.001$). $^{**}P<0.01$ versus controls. **(g)** Single intranasal C-1A-siRNA administration (30 or 100 μg) evoked a dose-dependent decreased immobility in the tail suspension test ($n=10$–15). One-way analysis of variance showed a significant effect of group ($F_{2,34}=8.70$, $P<0.001$). $^{*}P<0.05$, $^{***}P<0.001$ versus vehicle. **(h)** Mice treated intranasally with C-1A-siRNA (100 μg) displayed a reduced immobility time in the forced swim test compared with vehicle-treated controls ($n=13$–16). Two-way analysis of variance showed a significant effect of group ($F_{1,27}=9.27$, $P<0.01$) and time ($F_{2,54}=102.95$, $P<0.0001$). Student's *t*-test was used to assess the action of C-1A-siRNA for the total observation period (0–6 min). $^{**}P<0.01$ versus vehicle. Values are mean ± s.e.m.

like response in the FST and TST, and (iv) augmented the SSRI-induced elevation of extracellular 5-HT.

siRNAs are effective, safe and well tolerated in mice and non-human primates. Although they are used therapeutically in other medical areas, their applicability to brain diseases has been hampered by the difficulty to target selected neuronal populations and by the lack of adequate delivery methods.[27] The present results represent a major advance in this field given the selective targeting of 5-HT$_{1A}$R expressed in 5-HT neurons after i.c.v. and intranasal administration. Although further investigations are required to

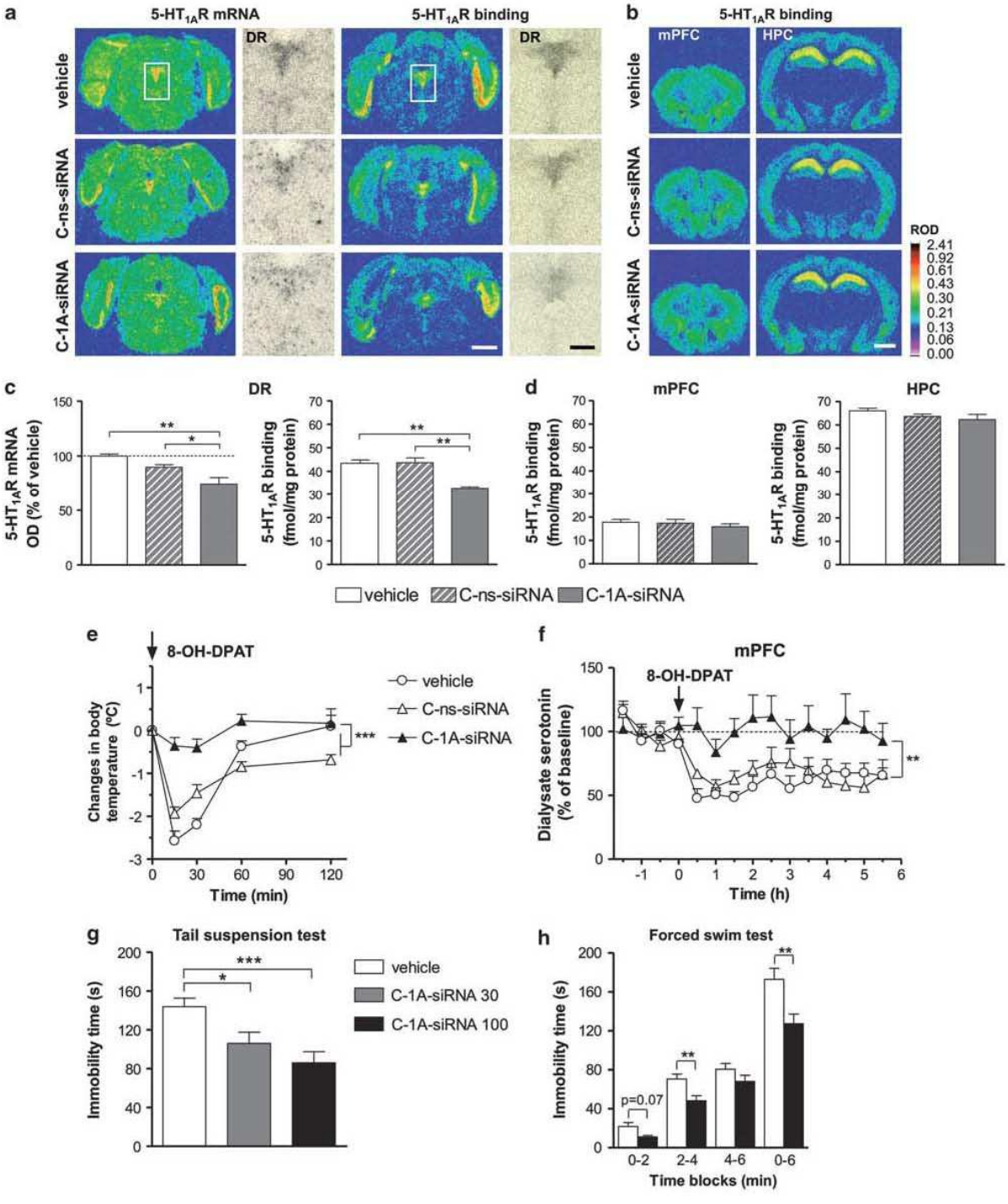

examine the exact mechanism(s) used by C-1A-siRNA to accumulate into 5-HT neurons, available evidence suggests that C-1A-siRNA can be internalized via SERT, similarly to SSRI[35] to reach the somatodendritic region of serotonergic neurons via retrograde axonal transport. This view is supported by (i) the selective presence of sertraline-conjugated C-1A-siNA and the C-ns-oligonucleotide in midbrain serotonergic neuropil and cell bodies, respectively, (ii) its selective action on 5-HT$_{1A}$-autoreceptors (far from the infusion site), (iii) the lack of effect on hippocampal 5-HT$_{1A}$R, much closer to the D3V, and (iv) the prevention of C-1A-siRNA effects by prior SERT blockade. The present procedure offers unprecedented efficacy and cellular selectivity, compared with previous siRNA conjugation methods used *in vivo*.[27,36–38] Hence, the 40% knockdown of 5-HT$_{1A}$-autoreceptors produced by single-point administration of 30 μg C-1A-siRNA is comparable to previous results using prolonged infusion of unmodified siRNA to silence monoamine transporters (400 μg day ^{1} for 1–2 weeks; 2.8–5.6 mg in total, that is 90–180-fold the dose used herein).[39,40]

Our results agree with previous observations on the detrimental role of 5-HT$_{1A}$ autorerceptors in depression. Human neuroimaging studies have associated high 5-HT$_{1A}$-autoreceptor levels with a poor amygdale reactivity.[41] Likewise, genetic studies link 5-HT$_{1A}$R mutations leading to high levels of 5-HT$_{1A}$-autoreceptors with higher incidence of mood disorders and poorer response to anti-depressants.[7] In rodents, disruption of the 5-HT$_{1A}$-autoreceptor-mediated negative feedback with 5-HT$_{1A}$R antagonists enhances SSRI effects.[5,6] Clinically, the non-selective 5-HT$_{1A}$R antagonist pindolol augments and accelerates SSRI effects, likely by a preferential interaction with 5-HT$_{1A}$-autoreceptors.[11,12,42] The present data support that C-1A-siRNA could be used to acutely suppress 5-HT$_{1A}$-autoreceptor function, without the need to wait for anti-depressant-induced desensitization, thus optimizing anti-depressant action.

Our results also agree with those found recently using conditional knockout mice for pre-synaptic 5-HT$_{1A}$R.[43] Both studies indicate that the selective, yet partial, reduction of 5-HT$_{1A}$-autoreceptor expression with unchanged post-synaptic 5-HT$_{1A}$R expression evokes anti-depressant-like behavior and augments SSRI effects. Interestingly, the RNAi strategy can be applied in adult mice, without the unwanted neurodevelopmental effects associated to 5-HT$_{1A}$R suppression.[44] Although further improvements are required, the intranasal route offers a first potential way for C-1A-siRNA delivery to brain. This route allowed the same effects than the i.c.v. infusion, yet with a slightly smaller effect size, likely due to the dilution of C-1A-siRNA during brain entry. Once crossed the semi-permeable nasal blood–brain barrier, C-1A-siRNA molecules may reach the dense plexus of serotonergic axons in outer layers of the olfactory bulb, anatomically connected with olfactory regions.[45]

In summary, our results show for the first time the feasibility of using RNAi strategies for the treatment of mood disorders. The excellent cellular selectivity and efficacy obtained with acute C-1A-siRNA treatment indicate that this may be a new approach to treat mood disorders and open the way to develop RNAi-based therapeutic classes to silence genes, or variant alleles refractory to classical pharmacological treatments.

Conflict of interest

The authors declare no conflict of interest.

Acknowledgments

We thank Leticia Campa for skillful work with HPLC equipment, and Verónica Paz and Noemí Jurado for technical assistance. This study was supported by grants from Spanish Ministry of Science and Innovation SAF2007-62378 and CDTI, with the participation of the DENDRIA Consortium; from Spanish Ministry of Health, Instituto de Salud Carlos III PI10/00290 and Centro de Investigación Biomédica en Red de Salud Mental, CIBERSAM; and a research contract CSIC-IDIBAPS with NEDKEN, SL-nLife Therapeutics, SL Support from the Innovative Medicines Initiative Joint Undertaking (IMI) under Grant Agreement N° 115008 (NEWMEDS) is also acknowledged. IMI is a public-private partnership between the European Union and the European Federation of Pharmaceutical Industries and Associations. AB is supported by the Research stabilization Program of the Health Department of the Generalitat de Catalunya. AM is a cofounder and board member of nLife Therapeutics, SL GA, GF and MCC are employees of nLife Therapeutics, SL.

References

1 Andlin-Sobocki P, Jönsson B, Wittchen HU, Olesen J. Cost of disorders of the brain in Europe. *Eur J Neurol* 2005; **12**: 1–27.
2 Krishnan V, Nestler EJ. The molecular neurobiology of depression. *Nature* 2008; **455**: 894–902.
3 Murray CJL, López AD. Alternative projections of mortality and disability by cause 1990–2020: Global Burden of Disease Study. *Lancet* 1997; **34**: 1498–1504.
4 Piñeyro G, Blier P. Autoregulation of serotonin neurons: role in antidepressant drug action. *Pharmacol Rev* 1999; **51**: 533–591.
5 Blier P, de Montigny C. Current advances and trends in the treatment of depression. *Trends Pharmacol Sci* 1994; **15**: 220–226.
6 Artigas F, Romero L, de Montigny C, Blier P. Acceleration of the effect of selected antidepressant drugs in major depression by 5-HT$_{1A}$ antagonists. *Trends Neurosci* 1996; **19**: 378–383.
7 Lemonde S, Turecki G, Bakish D, Du L, Hrdina PD *et al*. Impaired repression at 5-hydroxytryptamine$_{1A}$ receptor gene polymorphism associated with major depression and suicide. *J Neurosci* 2003; **23**: 8788–8799.
8 Neff CD, Abkevich V, Packer JC, Chen Y, Potter J *et al*. Evidence for HTR1A and LHPP as interacting genetic risk factors in major depression. *Mol Psychiatry* 2009; **14**: 621–630.
9 Stockmeier CA, Shapiro LA, Dilley GE, Kolli TN, Friedman L *et al*. Increase in serotonin-1A autoreceptors in the midbrain of suicide

victims with major depression-postmortem evidence for decreased serotonin activity. *J Neurosci* 1998; **18**: 7394–7401.
10 Haddjeri N, Blier P, de Montigny C. Long-term antidepressant treatments result in a tonic activation of forebrain 5-HT$_{1A}$ receptors. *J Neurosci* 1998; **18**: 10150–10156.
11 Artigas F, Peréz V, Alvaréz E. Pindolol induces a rapid improvement of depressed patients treated with serotonin reuptake inhibitors. *Arch Gen Psychiatry* 1994; **51**: 248–251.
12 Artigas F, Celada P, Laruelle M, Adell A. How does pindolol improve antidepressant action? *Trends Pharmacol Sci* 2001; **22**: 224–228.
13 Martinez D, Hwang D, Mawlawi O, Slifstein M, Kent J *et al*. Differential occupancy of somatodendritic and postsynaptic 5HT(1A) receptors by pindolol: a dose-occupancy study with [11C]WAY 100635 and positron emission tomography in humans. *Neuropsychoparmacology* 2001; **24**: 209–229.
14 Serrats J, Artigas F, Mengod G, Cortés R. An autoradiographic study of the influence of pindolol upon [35S]GTPgammaS binding in rat, guinea pig and human brain. *Int J Neuropsychopharmacol* 2004; **7**: 27–34.
15 Parks CL, Robinson PS, Sibille E, Shenk T, Toth M. Increased anxiety of mice lacking the serotonin1A receptor. *Proc Natl Acad Sci USA* 1998; **95**: 10734–10739.
16 McBride LJ, Caruthers MH. An investigation of several deoxynucleoside phosphoramidites useful for synthesizing deoxyoligonucleotides. *Tetrahedron Lett* 1983; **24**: 245–248.
17 Kurreck J, Wyszko E, Gillen C, Erdmann VA. Design of antisense oligonucleotides stabilized by locked nucleic acids. *Nucleic Acids Res* 2002; **30**: 1911–1918.
18 Judge AD, Sood V, Shaw JR, Fang D, McClintock K, MacLachlan I. Sequence-dependent stimulation of the mammalian innate immune response by synthetic siRNA. *Nat Biotechnol* 2005; **23**: 457–462.
19 Franklin KBJ, Paxinos G. *The Mouse Brain in Stereotaxic Coordinates*,, Compact 3rd edn Academic Press: New York, USA, 2008.
20 Amargós-Bosch M, Bortolozzi A, Puig MV, Serrats J, Adell A *et al*. Co-expression and *in vivo* interaction of serotonin1A and serotonin2A receptors in pyramidal neurons of prefrontal cortex. *Cereb Cortex* 2004; **14**: 281–299.
21 Pompeiano M, Palacios JM, Mengod G. Distribution and cellular localization of mRNA coding for 5-HT$_{1A}$ receptor in the rat brain: correlation with receptor binding. *J Neurosci* 1992; **12**: 440–453.
22 Santana N, Bortolozzi A, Serrats J, Mengod G, Artigas F. Expression of serotonin1A and serotonin2A receptors in pyramidal and GABAergic neurons of the rat prefrontal cortex. *Cereb Cortex* 2004; **14**: 1100–1109.
23 D'Amato RJ, Largent BL, Snowman AM, Snyder SH. Selective labeling of serotonin uptake sites in rat brain by [^{3}H]citalopram contrasted to labeling of multiple sites by [^{3}H]imipramine. *J Pharmacol Exp Ther* 1987; **242**: 364–371.
24 Pazos A, Palacios JM. Quantitative autoradiographic mapping of serotonin receptors in the rat brain. I. Serotonin-1 receptors. *Brain Res* 1985; **346**: 205–230.
25 Adell A, Celada P, Abellán MT, Artigas F. Origin and functional role of the extracellular serotonin in the midbrain raphe nuclei. *Brain Res Rev* 2002; **39**: 154–180.
26 Porsolt RD, Bertin A, Jalfre M. Behavioural despair in rats and mice: strain differences and the effects of imipramine. *European J Pharmacol* 1978; **51**: 291–294.
27 Baker M. RNA intereference: homing in on delivery. *Nature* 2010; **464**: 1225–1228.
28 López-Gil X, Bortolozzi A, Castañé A, Santana N, Cortés R *et al*. Selective *in vivo* knockdown of mouse presynaptic 5-HT$_{1A}$ receptors using RNA interference,. 39th Annual Meeting of the Society for Neuroscience 2009; abstract 342.7.
29 Beaudet A, Descarries L. Quantitative data on serotonin nerve terminals in adult rat neocortex. *Brain Res* 1976; **111**: 301–309.
30 Martin KF, Phillips I, Hearson M, Prow MR, Heal DJ. Characterization of 8-OH-DPAT-induced hypothermia in mice as a 5-HT$_{1A}$ autoreceptor response and its evaluation as a model to selectively identify antidepressants. *Br J Pharmacol* 1992; **107**: 15–21.
31 Ramboz S, Oosting R, Amara DA, Kung HF, Blier P *et al*. Serotonin receptor 1A knockout: an animal model of anxiety-related disorder. *Proc Natl Acad Sci USA* 1998; **95**: 14476–14481.
32 Illum L. Transport of drugs from the nasal cavity to the central nervous system. *Eur J Pharm Sci* 2000; **11**: 1–18.
33 Marks DR, Tucker K, Cavallin MA, Mast TG, Fadool DA. Awake intranasal insulin delivery modifies protein complexes and alters memory, anxiety, and olfactory behaviors. *J Neurosci* 2009; **29**: 6734–6751.
34 Yamada M, Chiba T, Sasabe J, Terashita K, Aiso S, Matsuoka M. Nasal Colivelin treatment ameliorates memory impairment related to Alzheimer's disease. *Neuropsychopharmacology* 2008; **33**: 2020–2032.
35 Ramamoorthy S, Blakely RD. Phosphorylation and sequestration of serotonin transporters differentially modulated by psychostimulants. *Science* 1999; **285**: 763–766.
36 Kumar P, Wu H, McBride JL, Jung KE, Kim MH *et al*. Transvascular delivery of small interfering RNA to the central nervous system. *Nature* 2007; **448**: 39–43.
37 Song E, Zhu P, Lee SK, Chowdhury D, Kussman S *et al*. Antibody mediated *in vivo* delivery of small interfering RNAs via cell-surface receptors. *Nat Biotechnol* 2005; **23**: 709–717.
38 Soutschek J, Akinc A, Bramlage B, Charisse K, Constien R *et al*. Therapeutic silencing of an endogenous gene by systemic administration of modified siRNAs. *Nature* 2004; **432**: 173–178.
39 Thakker DR, Natt F, Hüsken D, Maier R, Müller M *et al*. Neurochemical and behavioral consequences of widespread gene knockdown in the adult mouse brain by using nonviral RNA interference. *Proc Natl Acad Sci USA* 2004; **101**: 17270–17275.
40 Thakker DR, Natt F, Hüsken D, van der Putten H, Maier R *et al*. siRNA-mediated knockdown of the serotonin transporter in the adult mouse brain. *Mol Psychiatry* 2005; **10**: 782–789.
41 Fakra E, Hyde LW, Gorka A, Fisher PM, Muñoz KE *et al*. Effects of HTR1A C(-1019)G on amygdala reactivity and trait anxiety. *Arch Gen Psychiatry* 2009; **66**: 33–40.
42 Ballesteros J, Callado LF. Effectiveness of pindolol plus serotonin uptake inhibitors in depression: a meta-analysis of early and late outcomes from randomized controlled trials. *J Affect Disord* 2004; **79**: 137–147.
43 Richardson-Jones JW, Craige CP, Guiard BP, Stephen A, Metzger KL *et al*. 5-HT$_{1A}$ autoreceptor levels determine vulnerability to stress and response to antidepressants. *Neuron* 2010; **65**: 40–52.
44 Gleason G, Liu B, Bruening S, Zupan B, Auerbach A *et al*. The serotonin1A receptor gene as a genetic and prenatal maternal environmental factor in anxiety. *Proc Natl Acad Sci USA* 2010; **107**: 7592–7597.
45 McLean JH, Shipley MT. Serotonergic afferents to the rat olfactory bulb: I. Origins and laminar specificity of serotonergic inputs in the adult rat. *J Neurosci* 1987; **7**: 3016–3028.

Supplementary Information accompanies the paper on the Molecular Psychiatry website (http://www.nature.com/mp)

Supplementary Information for

Selective siRNA-mediated suppression of 5-HT_{1A} autoreceptors evokes strong antidepressant-like effects

Analía Bortolozzi[1,2,3a], Anna Castañé[1,3b], Jana Semakova[5b], Noemí Santana[1,3], Gabriel Alvarado[6], Roser Cortés[1,4], Albert Ferrés-Coy[1,2], Gerónimo Fernández[6], María C Carmona[6], Miklos Toth[7], José C Perales[5], Andrés Montefeltro[6], Francesc Artigas[1,3a]

[a]Correspondence should be addressed to Prof. Francesc Artigas or Dr. Analía Bortolozzi, IIBB-CSIC-IDIBAPS, 08036 Barcelona, Spain. E-mail: fapnqi@iibb.csic.es (F.A.); abbnqi@iibb.csic.es (A.B.).

[b]Anna Castañé and Jana Semakova have contributed equally to this study.

This PDF file includes:

Figures and legends S1 to S8

Tables S1 to S3

Supplementary Figures and Legends

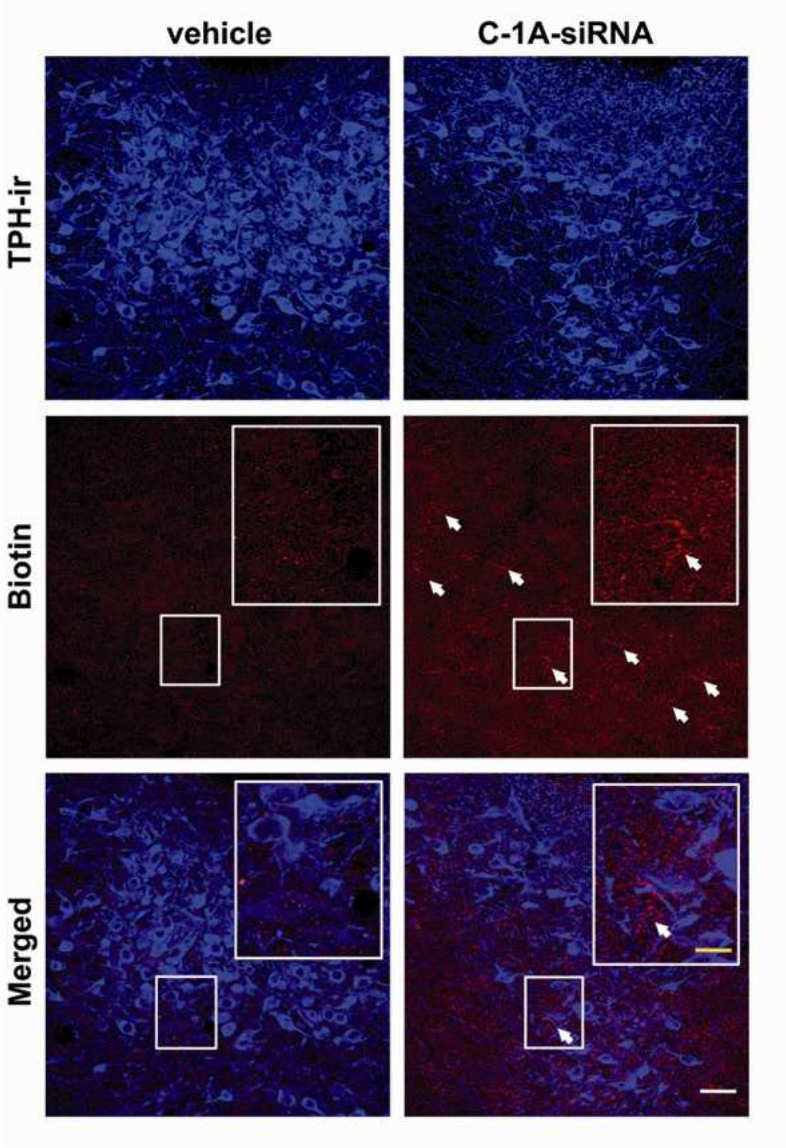

Figure S1. Enrichment of C-1A-siRNA molecules in the midbrain raphe nuclei. Mice were infused with vehicle or biotin-labeled C-1A-siRNA (30µg) into the dorsal third ventricle and were killed 48h post-administration (*n*=3 mice/group). Laser confocal images show TPH-immunoreactive serotonin neurons (blue), immune-localized biotin-labeled C-1A-siRNA (red, marked by arrows) and merged of biotin-labeled C-1A-siRNA and TPH-immunoreactive cells in coronal sections containing raphe nuclei. Upper right insets are enlargements of the small frames close to the center of each image. Scale bars: white=40µm and yellow=20µm.

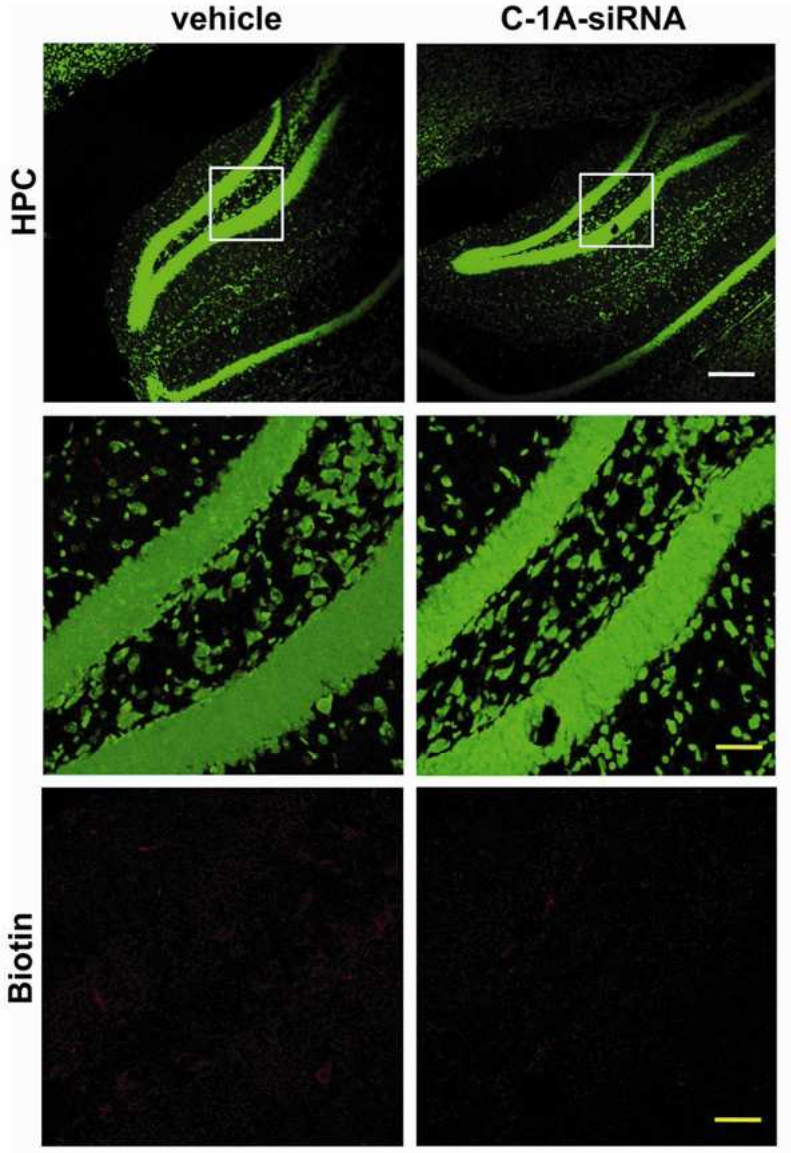

Figure S2. Absence of C-1A-siRNA molecules in the dorsal hippocampus. Laser confocal images show immune-localized nuclei in hippocampus (green) of mice received vehicle or biotin-labeled C-1A-siRNA (30µg) into dorsal third ventricle 48h before (*n*=3 mice/group, the same mice than in Figure 1b and Supplementary Figure S1). Higher magnification views of the boxed areas are shown in the middle panels. Images revealed the lack of biotin-labeled C-1A-siRNA (red) in hippocampus near to the application site. Scale bars: white=200µm and yellow=40µm.

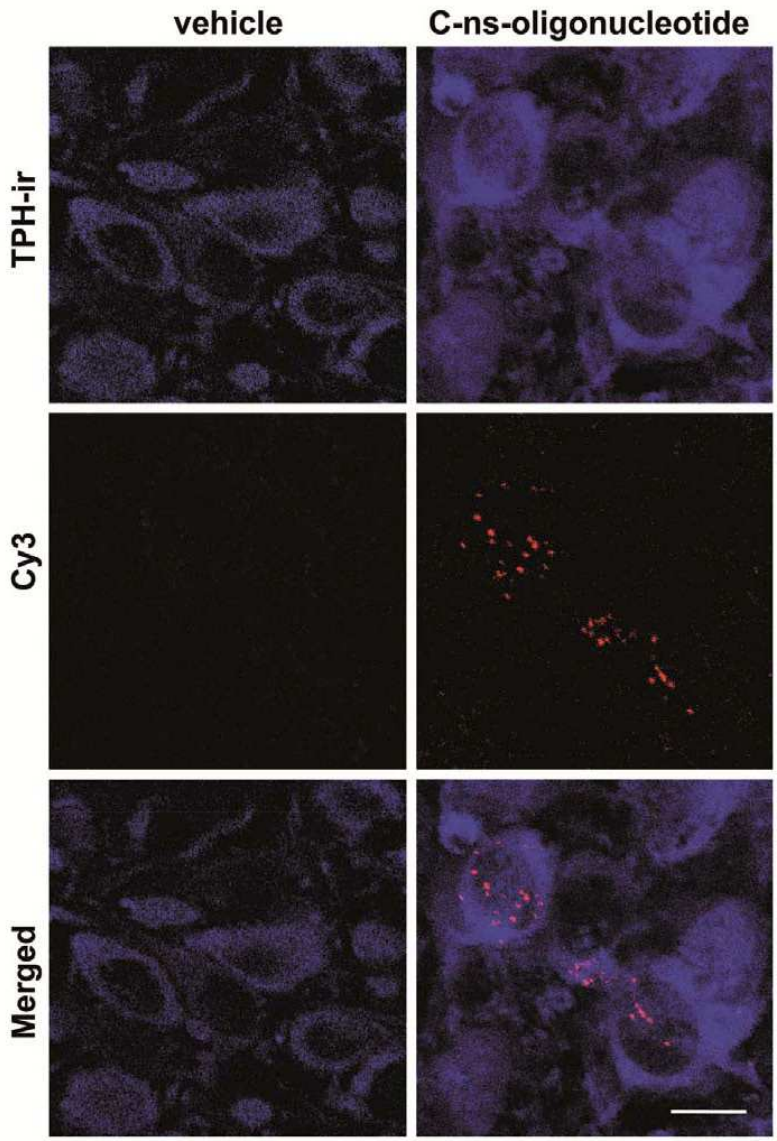

Figure S3. Presence of a sertraline-conjugated nonsense oligonucleotide (C-ns-oligonucleotide) in dorsal raphe serotonin neurons. Vehicle or Cy3-labeled C-ns-oligonucleotide (30µg) were applied i.c.v. into the dorsal third ventricle (D3V) and mice were killed 24h post-administration (*n*=2/treatment). Laser confocal images show TPH-immunoreactive serotonin neurons (blue), Cy3 fluorescence (red) and merged of Cy3-labeled C-ns-oligonucleotide and TPH-immunoreactive cells in coronal sections containing the dorsal raphe nucleus. Cy3 fluorescence appears in the neuronal cytoplasm as distinct bodies (red-pink color). Scale bars: 16 µm.

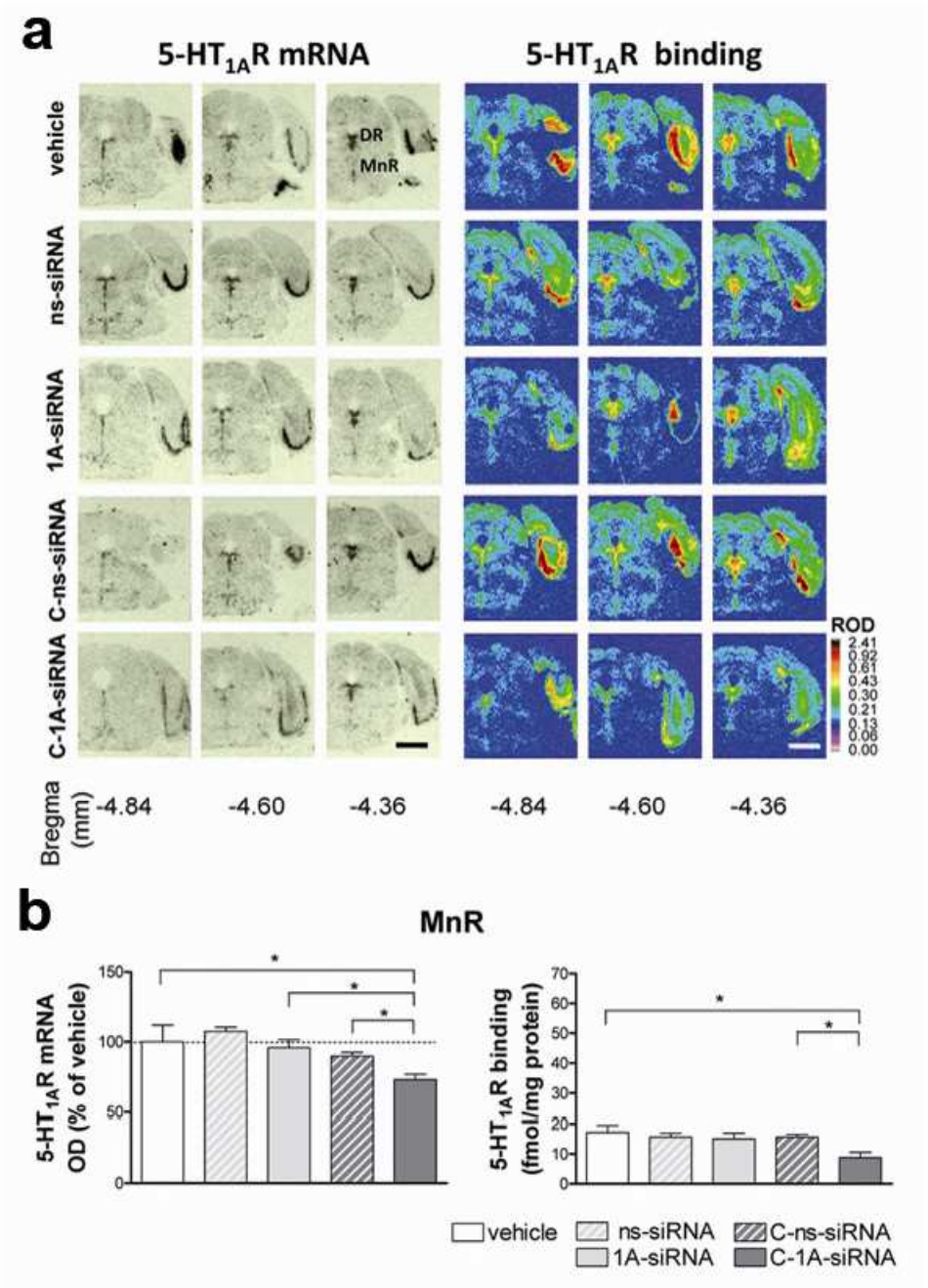

Figure S4. Selective 5-HT_{1A}-autoreceptor silencing by intracerebroventricular infusion of C-1A-siRNA. Mice were infused into the dorsal third ventricle with: *a*) vehicle, *b*) unmodified ns-siRNA, *c*) unmodified 1A-siRNA, *d*) C-ns-siRNA, or *e*) C-1A-siRNA (30µg of each siRNA). **(a)** Representative images of in situ hybridization and [^{3}H]-8-OH-DPAT binding by 5-HT_{1A}R in coronal section of mouse raphe nuclei at different anteroposterior coordinates (AP: -4.84 to -4.36

mm, taken from bregma). Note the reduction of 5-HT_{1A}R expression for each raphe nuclei section in C-1A-siRNA-treated mice. **(b)** Bar graph showing the effects of C-1A-siRNA infusion on 5-HT_{1A}R mRNA and binding in MnR (n=3-4 mice/group). One-way ANOVA showed a main effect of group for 5-HT_{1A}R mRNA ($F_{4,10}$=6.86, P<0.01) and 5-HT_{1A}R binding ($F_{4,14}$=3.59, P<0.05). *P<0.05 versus vehicle, C-ns-siRNA and unmodified 1A-siRNA. Values are mean ± s.e.m. DR, dorsal raphe nucleus; MnR, median raphe nucleus. Scale bars: 2mm (white and black).

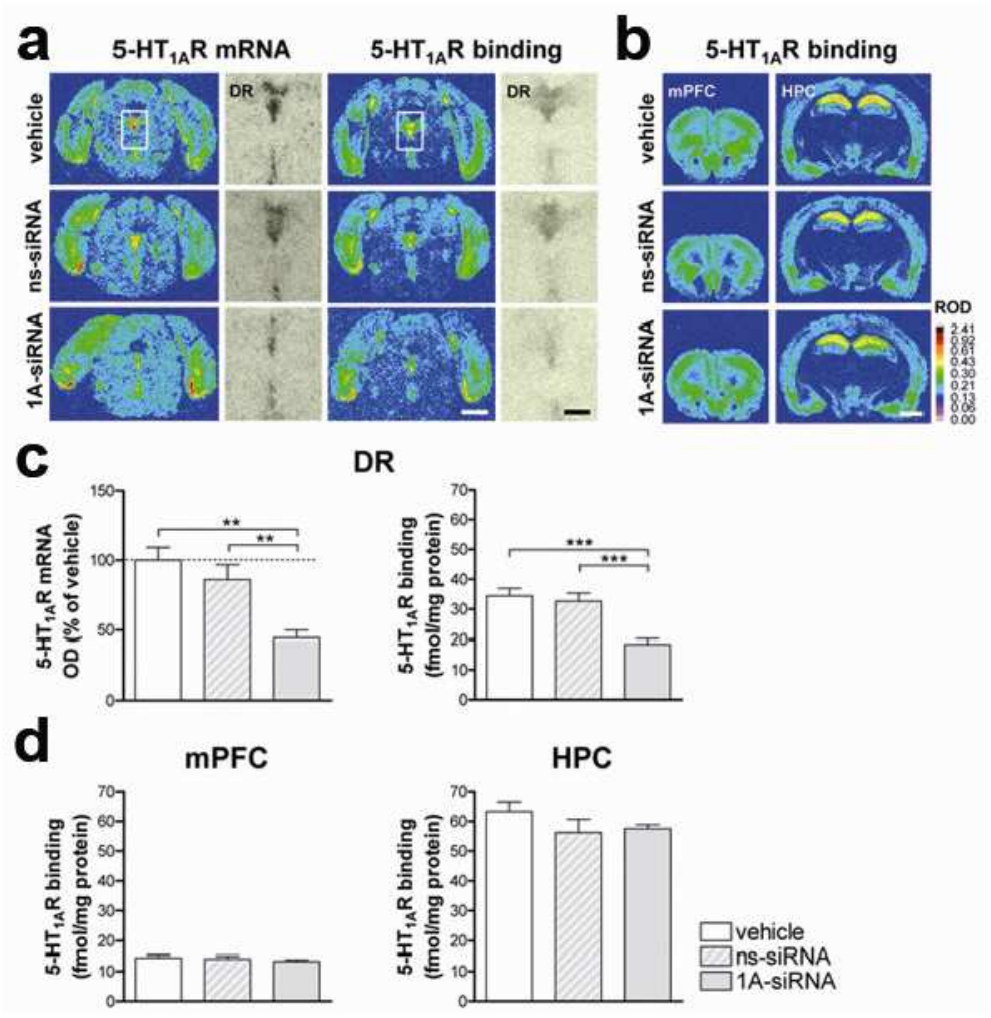

Figure S5. Selective 5-HT_{1A}-autoreceptor silencing by intra-DR infusion of unmodified 1A-siRNA. Mice were locally infused with: *a*) vehicle, *b*) ns-siRNA, or *c*) 1A-siRNA (10µg by 2 consecutive days, 20µg in total) into DR (n=4-6 mice/group). (**a**) Representative coronal brain sections showing 5-HT_{1A}R expression in the raphe nuclei assessed by in situ hybridization and [^{3}H]-8-OH-DPAT binding. Note the reduction of DR 5-HT_{1A}R density by intra-DR 1A-siRNA infusion. (**b**) Brain sections showing unaltered [^{3}H]-8-OH-DPAT binding to 5-HT_{1A}R in the mPFC and HPC of the same mice. (**c**) Effects of local 1A-siRNA infusion on 5-HT_{1A}R mRNA and binding in the DR. One-way ANOVA showed effect of group for 5-HT_{1A}R mRNA ($F_{2,10}$=10.49, P<0.01) and 5-HT_{1A}R binding ($F_{2,12}$=34.10, P<0.001). **P<0.01, ***P<0.001 versus vehicle and ns-siRNA. (**d)**

No group differences were detected on the postsynaptic 5-HT_{1A}R binding in the mPFC and HPC of the same mice. Values are mean ± s.e.m. DR, dorsal raphe nucleus; mPFC, medial prefrontal cortex; HPC, hippocampus. Scale bars: white=2mm, black=500µm.

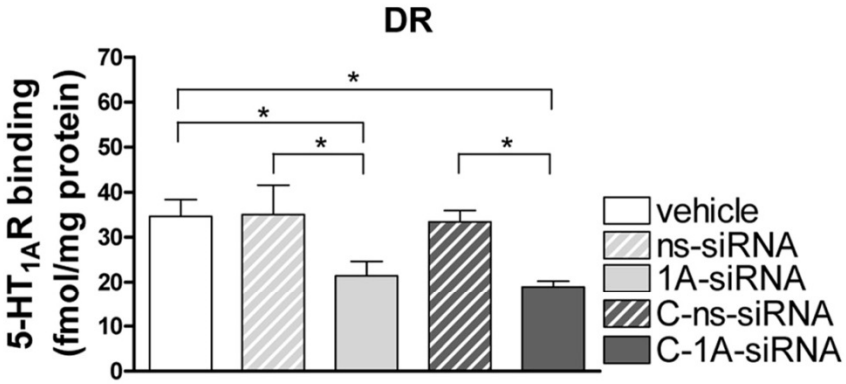

Figure S6. Chemical conjugation of C-1A-siRNA did not change the capability of the siRNA component to knockdown 5-HT_{1A}-autoreceptors. Mice received: *a*) vehicle, *b*) unmodified ns-siRNA, *c*) unmodified 1A-siRNA, *d*) C-ns-siRNA or *e*) C-1A-siRNA locally into the dorsal raphe nucleus (DR; 10µg by 2 consecutive days, 20µg in total). Quantitative autoradiography of [^{3}H]-8-OH-DPAT binding in the DR showed that both unmodified 1A-siRNA and sertraline-conjugated C-1A-siRNA induced a comparable decrease of 5-HT_{1A}-autoreceptor density in this brain area (n=4 mice/group). One-way ANOVA showed an effect of group on 5-HT_{1A}R binding ($F_{4,11}$=5.00, P<0.05). *P<0.05 versus vehicle, ns-siRNA and C-ns-siRNA. Values are mean ± s.e.m.

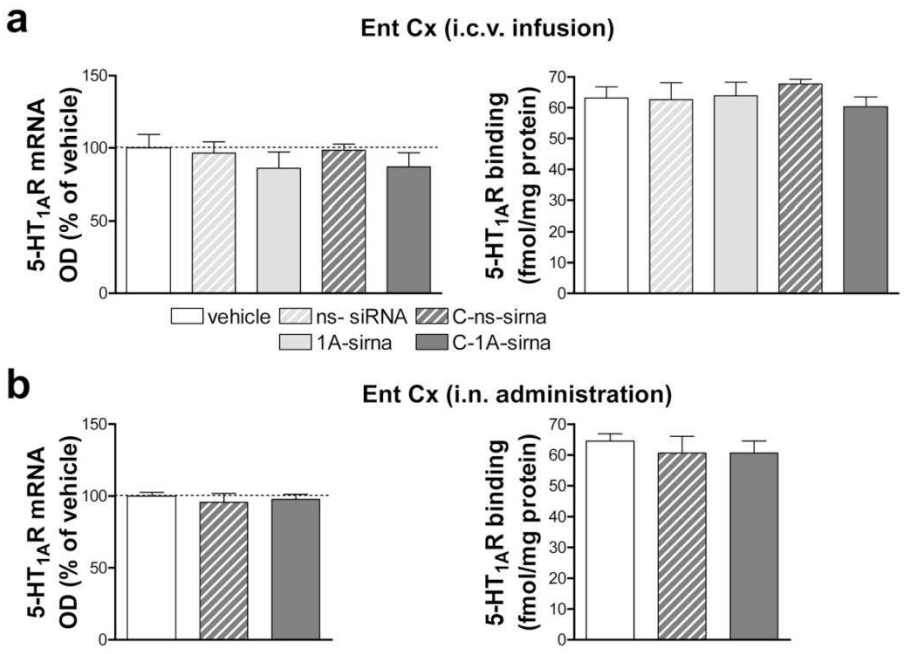

Figure S7. Postsynaptic 5-HT_{1A}R expression in entorhinal cortex (Ent Cx) was not affected by any C-1A-siRNA treatment. **(a)** Mice were infused into the dorsal third ventricle (D3V) with: *a*) vehicle, *b*) unmodified ns-siRNA, *c*) unmodified 1A-siRNA, *d*) C-ns-siRNA, or *e*) C-1A-siRNA (30µg of each siRNA). Bar graphs showing the effects of C-1A-siRNA i.c.v. infusion on 5-HT_{1A}R mRNA and binding in Ent Cx (*n*=4-5 mice/group). **(b)** Bar graphs showing the effects of intranasal C-1A-siRNA (30µg) administration on 5-HT_{1A}R mRNA and binding in Ent Cx (*n*=4 mice/group). Values are mean ± s.e.m.

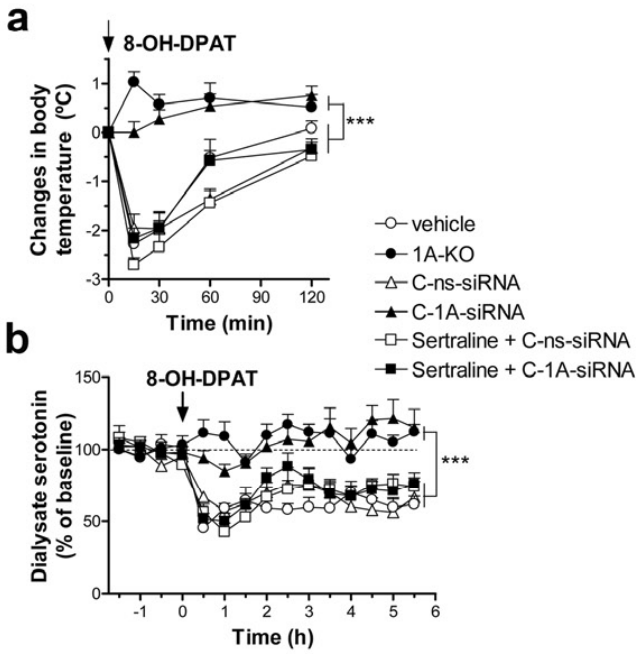

Figure S8. C-1A-siRNA requires a functional serotonin transporter to silence 5-HT_{1A}-autoreceptors. Mice received: *a*) vehicle, *b*) C-ns-siRNA, or *c*) C-1A-siRNA (30µg) into the dorsal third ventricle. Two additional groups of mice were injected with SSRI sertraline (20mgkg^{-1}, i.p.) 3h before the intracerebroventricular infusion of C-ns-siRNA or C-1A-siRNA. 1A-KO mice was used as positive control (*n*=6-8 mice/group). **(a)** The systemic administration of selective 5-HT_{1A}R agonist, 8-OH-DPAT (1 mgkg^{-1}, i.p.) induced the expected hypothermia response in vehicle and C-ns-siRNA, but not in C-1A-siRNA and 1A-KO mice. Sertraline pre-treatment prevented the effect of C-1A-siRNA and 8-OH-DPAT-evoked hypothermic response was shown as did controls. Two-way ANOVA showed effect of group ($F_{5,31}$=33.40), time ($F_{4,124}$=71.78) and interaction ($F_{20,124}$=11.79). ***P<0.01 versus vehicle, C-ns-siRNA and sertraline + C-siRNA (ns and 1A). **(b)** 8-OH-DPAT administration (0.5 mgkg^{-1}, i.p.) reduced extracellular serotonin concentration in the medial prefrontal cortex (mPFC) of vehicle and ns-C-siRNA, but not in C-1A-siRNA and 1A-KO mice. Sertraline pre-treatment prevented the effect of C-1A-siRNA. Two-way ANOVA showed effect of group ($F_{5,32}$=14.85), time ($F_{14,448}$=16.55) and interaction ($F_{70,448}$=3.35). ***P<0.01 versus vehicle, C-ns-siRNA and sertraline + C-siRNA (ns and 1A). Values are mean ± s.e.m.

Supplementary Tables

Table S1. Sequences of siRNAs and primers used

siRNAs	forward	reverse
1A-siRNA1	CGAUACUGGCCUCUCCAACTT	GGUGCUCAACAAGUGGACUTT
1A-siRNA2	GGUGCUCAACAAGUGGACUTT	AGUCCACUUGUUGAGCACCTT
1A-siRNA3	GGAAGAGUGUAGGGCUUACTT	GUAAGCCCUACACUCUUCCTT
1A-siRNA4	CGAUGGAAGUUUAAACCUCTT	GAGGUUUAAACUUCCAUCGTT
ns-siRNA	AGUACUGCUUACGAUACGGTT	CCGUAUCGUAAGCAGUACUTT
β-Gal-siRNA	CUACACAAAUCAGCGAUUU	GAUGUGUUUAGUCGCUAAA
Primers		
Cyclophilin A	GATGAGAACTTCATCCTAAAGCATACA	TCAGTCTTGGCAGTGCAGATAAA
5-HT$_{1A}$	CCGTGAGAGGAAGACAGTGAAGAC	GTGAGAGGAAGACAGTGAAGAC
5-HT$_{1B}$	TCTCACCAACCTCTCCCACAAC	GTCCGATACACCGTAGCGATTAC
SERT	CTCATCTTCACCATTATCTACTTCAG	CTCACCAGCAGGACAGAAAG
TNFα	GCAGTCTGTGTCTGCTGGGAT	CGCAGAACGGGATGAAGC
IFNγ	CCCACAGGTCCAGCGCCAAG	CCCACCCCGAATCAGCAGCG
BAX	AGCGAGTGTCTCCGGCGAATTG	TCTGATCAGCTCGGGCACTTTAG

Table S2. Summary of the conditions for labeling serotonin receptors and transporter in the present work

Protein	Ligand	[Ligand] (nM)	Buffer	Pre-incubation (RT, min)	Incubation buffer	Incubation protocol (RT, min)	Washing protocol (i.c.b., min)	Exposure time	Blank
5-HT_{1A}R	[^{3}H]-8-OH-DPAT	1.0	A	30	A + 10µM pargyline	60	2 x 5	60 days	10µM serotonin
5-HT_{1B}R	[^{125}I]-cyanopindolol	0.1	B	10	B + 100nM 8-OH-DPAT + 30nM isoproterenol	120	2 x 15	1 day	10µM serotonin
SERT	[^{3}H]-citalopram	1.5	C	15	C	60	2 x 10	45 days	1µM fluoxetine

RT, room temperature; i.c.b., ice-cold buffer; Buffer A: 170mM Tris-HCl, 4mM $CaCl_2$, 0.01% ascorbic acid, pH=7.6; Buffer B: 170mM Tris-HCl, 150mM NaCl, pH=7.4; Buffer C: 50mM Tris-HCl, 120mM NaCl, 5mM KCl, pH=7.6.

Table S3. Basal serotonin dialysate values in medial prefrontal cortex of mice

Group	aCSF Serotonin	aCSF + citalopram Serotonin
vehicle	7.6 ± 0.5	20.0 ± 2.9
C-ns-siRNA	6.2 ± 0.4	22.8 ± 3.6
C-1A-siRNA	6.4 ± 0.9	21.1 ± 2.7
1A-KO	6.9 ± 1.0	18.1 ± 1.2

Data are means ± s.e.m expressed as fmol per 30µl dialysate. *n*=5-11 mice per groups.

aCSF, artificial cerebrospinal fluid

aCSF + citalopram, artificial cerebrospinal fluid containing 1µM citalopram

4.2. Trabajo 2

Acute 5-HT$_{1A}$ autoreceptor knockdown increases antidepressant responses and serotonin release in stressful conditions

A Ferrés-Coy, N Santana, A Castañé, R Cortés, MC Carmona, M Toth, A Montefeltro, F Artigas and A Bortolozzi

Psychopharmacology (Berl). 2013 Jan; 225(1):61-74

El estrés es un factor ambiental ampliamente asociado con los trastornos del estado del ánimo. La exposición a situaciones estresantes durante el desarrollo, la niñez o incluso en la edad adulta puede predisponer a la depresión y la ansiedad. Estudios de neuroimagen han mostrado que individuos con una expresión elevada del autoreceptor 5-HT$_{1A}$ podrían presentar una menor resiliencia frente a situaciones estresantes así como una menor respuesta a los fármacos antidepresivos SSRI. En el trabajo anterior desarrollamos un siRNA contra el receptor 5-HT$_{1A}$ conjugado con sertralina y mostramos que la administración intracerebroventricular o intranasal del mismo en ratones: 1) favorece su acumulación selectiva en neuronas serotoninérgicas, 2) reduce la expresión y función del autoreceptor 5-HT$_{1A}$ y 3) produce respuestas de tipo antidepresivo. Continuando con estos hallazgos, en este trabajo utilizamos moléculas de siRNA contra el receptor 5-HT$_{1A}$ sin conjugar aplicadas localmente en el DR bajo la hipótesis de trabajo que la reducción selectiva del autoreceptor 5-HT$_{1A}$ podría incrementar la resiliencia durante situaciones de estrés mediante la facilitación del tono serotoninérgico.

Los resultados mostraron que la infusión local y aguda del 1A-siRNA en el DR de ratón reduce selectivamente la expresión y función del receptor 5-HT$_{1A,}$ efecto restringido a la zona de aplicación. Estos efectos persistieron hasta el día 6 post-administración, recuperándose a continuación hasta alcanzar el nivel de expresión basal del receptor 5-HT$_{1A}$. Además, la concentración basal extracelular de 5-HT en la mPFC no se

modificó entre los diferentes tratamientos. Sin embargo, los ratones tratados con las moléculas de 1A-siRNA mostraron respuestas de tipo antidepresivo en el TST y FST. Básicamente, estos efectos fueron acompañados por un incremento significativo de la liberación de 5-HT en la mPFC durante la ejecución de la prueba de TST.

Estos datos, junto con el primer trabajo, indican que la supresión aguda del autoreceptor 5-HT_{1A} produce respuestas de tipo antidepresivo, seguramente mediadas por la mayor capacidad de las neuronas serotoninérgicas de liberar 5-HT en situaciones de estrés.

Psychopharmacology (2013) 225:61–74
DOI 10.1007/s00213-012-2795-9

ORIGINAL INVESTIGATION

Acute 5-HT_{1A} autoreceptor knockdown increases antidepressant responses and serotonin release in stressful conditions

Albert Ferrés-Coy · Noemí Santana · Anna Castañé · Roser Cortés · María C. Carmona · Miklos Toth · Andrés Montefeltro · Francesc Artigas · Analía Bortolozzi

Received: 20 March 2012 / Accepted: 25 June 2012 / Published online: 21 July 2012

Abstract
Rationale Identifying the etiological factors in anxiety and depression is critical to develop more efficacious therapies. The inhibitory serotonin$_{1A}$ receptors (5-HT_{1A}R) located on 5-HT neurons (autoreceptors) limit antidepressant responses and their expression may be increased in treatment-resistant depressed patients.
Objectives Recently, we reported that intranasal administration of modified small interference RNA (siRNA) molecules targeting 5-HT_{1A}R in serotonergic neurons evoked antidepressant-like effects. Here we extended this finding using marketed siRNAs against 5-HT_{1A}R (1A-siRNA) to reduce directly the 5-HT_{1A} autoreceptor expression and evaluate its biological consequences under basal conditions and in response to stressful situations.
Methods Adult mice were locally infused with vehicle, nonsense siRNA, and 1A-siRNA into dorsal raphe nucleus (DR). 5-HT_{1A}R knockout mice (1A-KO) were also used. Histological approaches, in vivo microdialysis, and stress-related behaviors were performed to assess the effects of 5-HT_{1A} autoreceptor knockdown.
Results Intra-DR 1A-siRNA infusion selectively reduced 5-HT_{1A}R mRNA and binding levels and canceled 8-OH-DPAT-induced hypothermia. Basal extracellular 5-HT in medial prefrontal cortex (mPFC) did not differ among treatments. However, 1A-siRNA-treated mice displayed less immobility in the tail suspension and forced swim tests, as did 1A-KO mice. This was accompanied by a greater increase in prefrontal 5-HT release during tail suspension test. Moreover, intra-DR 1A-siRNA infusion augmented the increase of extracellular 5-HT in mPFC evoked by fluoxetine, up to the level in 1A-KO mice.
Conclusion Together with our previous report, the present results indicate that acute suppression of 5-HT_{1A} autoreceptor

Electronic supplementary material The online version of this article (doi:10.1007/s00213-012-2795-9) contains supplementary material, which is available to authorized users.

A. Ferrés-Coy · N. Santana · A. Castañé · R. Cortés · F. Artigas · A. Bortolozzi (✉)
Department of Neurochemistry and Neuropharmacology,
IIBB–CSIC–IDIBAPS,
C/ Roselló 161, 6th floor,
08036 Barcelona, Spain
e-mail: abbnqi@iibb.csic.es

A. Bortolozzi
Institut d'Investigacions Biomèdiques August Pi i Sunyer (IDIBAPS),
Barcelona, Spain

A. Ferrés-Coy · N. Santana · A. Castañé · F. Artigas · A. Bortolozzi
Centro de Investigación Biomédica en Red de Salud Mental (CIBERSAM),
Madrid, Spain

R. Cortés
Centro de Investigación Biomédica en Red de Enfermedades Neurodegenerativas (CIBERNED),
Madrid, Spain

M. C. Carmona · A. Montefeltro
n-Life Therapeutics, S.L.,
A Coruña, Spain

M. Toth
Department of Pharmacology, Weill Medical College,
Cornell University,
New York, NY, USA

expression evokes robust antidepressant-like effects, likely mediated by an increased capacity of serotonergic neurons to release 5-HT in stressful conditions.

Keywords 5-HT_{1A} receptor · Antidepressant effects · Depression · RNA interference · Serotonin · Stress

Abbreviations

1A-KO	5-HT_{1A}R knockout mice
5-HT	Serotonin
5-HT_{1A}R	Serotonin$_{1A}$ receptors
aCSF	Artificial cerebrospinal fluid
DA	Dopamine
DR	Dorsal raphe nucleus
EPM	Elevated plus maze
FST	Forced swim test
mPFC	Medial prefrontal cortex
ns-siRNA	Nonsense siRNA
SERT	Serotonin transporter
siRNA	Small interference RNA
SSRIs	Selective serotonin reuptake inhibitors
TST	Tail suspension test

Introduction

Major depression is a severe and heterogeneous psychiatric syndrome with high prevalence and socio-economic impact (Andlin-Sobocki et al. 2005; Murray and López 1997). The serotonergic system has been implicated in the etiology and treatment of depression and other mood disorders (Krishnan and Nestler 2008). Serotonin$_{1A}$ receptor (5-HT_{1A}R) plays a key inhibitory role in brain function due to its coupling to inward-rectifying K^+ channels (Andrade et al. 1986; Innis and Aghajanian 1987). It is located presynaptically (as autoreceptor) on serotonergic neurons in the raphe nuclei and postsynaptically on glutamatergic and GABAergic neurons in corticolimbic areas (Pompeiano et al. 1992; Riad et al. 2000; Santana et al. 2004). Negative feedback inhibition of serotonergic activity is mediated by activation of 5-HT_{1A} autoreceptors (Innis and Aghajanian 1987; Piñeyro and Blier 1999), which reduces the discharge rate of serotonergic neurons and terminal serotonin (5-HT) release (Artigas et al. 1996; Blier and deMontigny 1994).

Antidepressant drugs, including the selective 5-HT reuptake inhibitors (SSRIs), markedly increase extracellular 5-HT in the raphe nuclei, thus acutely activating this negative feedback (Adell and Artigas 1991; Romero and Artigas 1997). Upon chronic treatment, 5-HT_{1A} autoreceptors desensitize, leading to the recovery of serotonergic activity and increased 5-HT release (Artigas et al. 1996; Blier and deMontigny 1994). Likewise, 5-HT_{1A}R knockout mice display enhanced neurochemical responses to SSRIs (Bortolozzi et al. 2004; Knobelman et al. 2001). Prevention of this negative feedback with the non-selective 5-HT_{1A}R antagonist pindolol augments antidepressant effects (Artigas et al. 1994; Portella et al. 2011). However, the clinical applicability of selective 5-HT_{1A}R antagonists is limited by their comparable action at pre- and postsynaptic 5-HT_{1A}R and the need to preserve postsynaptic 5-HT_{1A}R activation for clinical effects (Haddjeri et al. 1998).

Furthermore, differences in 5-HT_{1A}R expression are associated with affective disorders and antidepressant response. Hence, individuals with high 5-HT_{1A} autoreceptor expression, including those with a functional polymorphism in the promoter region of *Htr1a* gene, are more susceptible to depression and suicide and respond poorly to antidepressant therapy (Fakra et al. 2009; Lemonde et al. 2003; Neff et al. 2009; Stockmeier et al. 1998; Sullivan et al. 2009).

The study of the relative role of the different 5-HT_{1A}R populations in the pathophysiology and treatment of psychiatric disorders has been limited by the lack of pharmacological and genetic tools selective for pre- and postsynaptic 5-HT_{1A}R (Gleason et al. 2010). Richardson-Jones et al. (2010) reported antidepressant-like responses in transgenic mice with a moderate reduction of 5-HT_{1A} autoreceptors.

Small interference RNA (siRNA) is effective, safe, and well tolerated in mice and non-human primates (Heidel et al. 2004; Kumar et al. 2007; Li et al. 2005; Thakker et al. 2004, 2005). We recently reported that sertraline-conjugated siRNA molecules (Patent PCT/EP2011/056270) designed to silence the 5-HT_{1A}R mRNA only in 5-HT neurons evoke antidepressant-like effects in mice (Bortolozzi et al. 2012). Here, we extend these findings using unmodified siRNA molecules against 5-HT_{1A}R under the working hypothesis that selective siRNA-induced 5-HT_{1A} autoreceptor reduction would increase resilience to stressful situations through an increase of the serotonergic tone.

Material and methods

Animals

Male homozygous 5-HT_{1A}R knockout (1A-KO) (Parks et al. 1998) and wild-type mice on the same background (C57BL/6J) were used. Mice (9–12 weeks old) were housed under controlled conditions (22±1 °C; 12 h light/dark cycle). Food and water were provided ad libitum. All animal procedures were conducted in accordance with the standard ethical guidelines (European Union regulations L35/118/12/1986) and approved by the local ethical committee of the School of Medicine, University of Barcelona.

siRNAs and treatments

Four siRNAs targeting the 5-HT_{1A}R (1A-siRNA1 to 1A-siRNA4) (nt 633–651, 852–870, 1,889–1,907, and 2,167–2,185, GenBank accession #NM_008308) were chosen and infused as a mixture, containing an equal amount of each siRNA duplex. Additionally, an unrelated siRNA duplex with no homology to mouse genome was used as negative control (nonsense siRNA—ns-siRNA). The siRNA sequences are shown in Table 1. All siRNAs were dissolved following the manufacturer's protocol (Ambion, Madrid, Spain) and stored at −30 °C until use.

Mice were anesthetized (pentobarbital, 40 mg/kg, i.p.) and silica capillary microcannulae (110 μm OD and 40 μm ID; Polymicro Technologies, Madrid, Spain) were stereotaxically implanted into the dorsal raphe nucleus (DR; coordinates in mm: AP -4.5; ML -1.0; DV -4.4; with a lateral angle of 20°) (Franklin and Paxinos 2008). Some animals were also implanted with a microdialysis probe in medial prefrontal cortex (mPFC) (see below). Microinfusion experiments were conducted 24 h after surgery in awake mice using a precision pump at a rate of 0.5 μl/min (WPI model sp220i, Aston, Stevenage, UK). A mixture of the four 1A-siRNAs were prepared in artificial cerebrospinal fluid (aCSF) (125 mM NaCl, 2.5 mM KCl, 1.26 mM $CaCl_2$, and 1.18 mM $MgCl_2$ with 5 % glucose) and administered at the doses of 2.5 or 10 μg of 1A-siRNA per mouse into DR (1 ul aliquots). Nonsense siRNA was infused at the same doses. Intra-DR siRNA infusion was repeated 24 h later (two administrations in total). Controls and 1A-KO mice were subjected to the same experimental procedure and received aCSF.

RNA isolation and quantitative RT-PCR analysis

Mice were killed 24 h after treatments. The brain was removed and placed on an ice-cold plate. Midbrain sections (1 mm thick) containing the raphe nuclei were dissected out using a Mouse Brain Matrix (Ted Pella, Madrid, Spain), quickly frozen on dry ice, and stored at −80 °C. Total RNA was isolated with Trizol solution and rehydrated in 10 μl RNAse-free water to a final RNA concentration of 0.5 μg/μl. Quantitative RT-PCR was made as previously described (Bortolozzi et al. 2012). The primers used are summarized in Table 1.

In situ hybridization and receptor autoradiography

Mice were killed by pentobarbital overdose, and the brains rapidly removed, frozen on dry ice, and stored at −20 °C. Tissue sections, 14 μm thick, were cut using a microtome cryostat (HM500 OM, Microm, Walldorf, Germany), thaw-mounted onto 3-aminopropyltriethoxysilane-coated slides (Sigma-Aldrich, Madrid, Spain), and kept at −20 °C until use.

For 5-HT_{1A}R mRNA, three oligonucleotides were used simultaneously, complementary to bases 1–48, 763–810, and 1,219–1,266 (GenBank accession #NM_012585). Probes labeling and in situ hybridization procedures were carried out as described previously (Bortolozzi et al. 2012; Santana et al. 2004).

The autoradiographic binding assays for 5-HT_{1A} and 5-HT_{1B} receptors and serotonin transporter (SERT) (Amargós-Bosch et al. 2004; Bortolozzi et al. 2012; D'Amato et al. 1987; Pazos and Palacios 1985) were performed using the following radioligands: [^{3}H]-8-OH-DPAT (233 Ci/mmol), [^{125}I]-cyanopindolol (2,200 Ci/mmol), and [^{3}H]-citalopram (70 Ci/mmol), respectively (Perkin-Elmer, Madrid, Spain). 8-OH-DPAT, isoproterenol, pargyline, and serotonin were obtained from Sigma-Aldrich and fluoxetine was from Tocris (Avonmouth, UK). Experimental conditions are summarized in Table 2. The films were analyzed by microdensitometry using a previously described method (Bortolozzi et al. 2012).

Table 1 Sequences of siRNAs and primers used for RT-PCR

	Forward	Reverse
siRNAs		
1A-siRNA1	CGAUACUGGCCUCUCCAACTT	GGUGCUCAACAAGUGGACUTT
1A-siRNA2	GGUGCUCAACAAGUGGACUTT	AGUCCACUUGUUGAGCACCTT
1A-siRNA3	GGAAGAGUGUAGGGCUUACTT	GUAAGCCCUACACUCUUCCTT
1A-siRNA4	CGAUGGAAGUUUAAACCUCTT	GAGGUUUAAACUUCCAUCGTT
ns-siRNA	AGUACUGCUUACGAUACGGTT	CCGUAUCGUAAGCAGUACUTT
Primers		
Cyclophilin A	GATGAGAACTTCATCCTAAAGCATACA	TCAGTCTTGGCAGTGCAGATAAA
5-HT_{1A}	CCGTGAGAGGAAGACAGTGAAGAC	GTGAGAGGAAGACAGTGAAGAC
5-HT_{1B}	TCTCACCAACCTCTCCCACAAC	GTCCGATACACCGTAGCGATTAC
SERT	CTCATCTTCACCATTATCTACTTCAG	CTCACCAGCAGGACAGAAAG
TNFα	GCAGTCTGTGTCTGCTGGGAT	CGCAGAACGGGATGAAGC
IFNγ	CCCACAGGTCCAGCGCCAAG	CCCACCCCGAATCAGCAGCG

Table 2 Experimental procedures for labeling serotonin receptors and transporter

Protein	Ligand	[Ligand] (nM)	Buffer	Pre-incubation (RT, min)	Incubation buffer	Incubation protocol (RT, min)	Washing protocol (i.c.b., min)	Exposure time	Blank
5-HT_{1A}R	[^{3}H]-8-OH-DPAT	1.0	A	30	A + 10 μM pargyline	60	2×5	60 days	10 μM serotonin
5-HT_{1B}R	[^{125}I]-cyanopindolol	0.1	B	10	B + 100 nM 8-OH-DPAT + 30 nM isoprotere-nol	120	2×15	1 day	10 μM serotonin
SERT	[^{3}H]-citalopram	1.5	C	15	C	60	2×10	45 days	1 μM fluoxetine

Buffer A: 170 mM Tris–HCl, 4 mM $CaCl_2$, 0.01 % ascorbic acid, pH 7.6; buffer B: 170 mM Tris–HCl, 150 mM NaCl, pH 7.4; buffer C: 50 mM Tris–HCl, 120 mM NaCl, 5 mM KCl, pH 7.6

RT room temperature, *i.c.b.* ice-cold buffer

Intracerebral microdialysis

Extracellular 5-HT and dopamine (DA) concentrations were measured by in vivo microdialysis as previously described (Amargós-Bosch et al. 2004; Díaz-Mataix et al. 2005). Briefly, one concentric dialysis probe equipped with a Cuprophan membrane (2 mm long) was implanted in mPFC (AP +2.2; ML −0.2; DV −3.4) (Franklin and Paxinos 2008) of anesthetized mice. Microdialysis experiments were performed 24 h after treatments. In experiments examining the change in 5-HT release to 8-OH-DPAT administration or to stress (tail suspension test, TST), 1 μM citalopram (SERT inhibitor; Lundbeck, Valby, Copenhagen) was added to aCSF (Adell et al. 2002). The probes were continuously perfused (WPI model sp220i) with aCSF, and the dialysate was collected every 20 min for DA and every 6 or 30 min for 5-HT. Monoamine concentrations were analyzed by HPLC-amperometric detection (Hewlett Packard-1049, Palo Alto, CA, USA) at +0.75 and +0.60 V for DA and 5-HT, respectively, with detection limits of 2 fmol/sample. Baseline monoamine levels were calculated as the average of four pre-drug samples or ten pre-TST samples, respectively. Following sample collection, brains were removed and sectioned to ensure proper probe placement after cresyl-violet staining.

Behavioral and physiological testing

Mice were tested at 24 h after treatments. All tests were performed between 10:00 a.m. and 14:00 p.m. On test days, animals were transported to the dimly illuminated behavioral laboratory and were left undisturbed for at least 1 h before testing. Animals did not undergo more than one behavioral assay.

Elevated plus-maze test (EPM)

EPM was performed using a cross maze with 16×5 cm arms illuminated from the top (100 lx). Mice were placed in the central area, facing one of the open arms, and the time and number of entries into open and closed arms in 5 min were recorded (video camera system, Smart, Panlab, Barcelona, Spain). Results were expressed as the percentage of time and number of entries into the open arms.

Tail suspension test

Mice were suspended 30 cm above the bench by adhesive tape placed approximately 1 cm from the tip of the tail. Mice were monitored and recorded using a video camera system (Smart, Panlab), and the time spent immobile was recorded for 6 min. In an additional group, the mPFC 5-HT concentration was simultaneously measured during TST paradigm by in vivo microdialysis (see above).

Forced swim test (FST)

Mice were individually placed into a clear cylinder (15 cm diameter, 30 cm height) containing 20 cm of water maintained at 24–25 °C, essentially as described by Porsolt et al. (1978). In this test, immobility of the mouse was scored in 2 min bins for a total of 6 min using a video camera system (Smart, Panlab).

8-OH-DPAT-induced hypothermia

Body temperature was measured intrarectally using a lubricated probe inserted ~2 cm and a digital thermometer (AZ9882, Panlab) as previously described (Bortolozzi et al. 2012). Mice received 8-OH-DPAT 1 mg/kg i.p. and body

temperature was recorded every 15 min for a total of 120 min.

Statistical analysis

Data are expressed as means ± SEM. One- or two-way ANOVA was used to compare data from mRNA expression, autoradiography, and neurochemical and behavioral analyses in the experimental groups, as appropriate, followed by post hoc test (Newman–Keuls). Student's *t* test was used to identify significant difference in the FST. The level of significance was set at $p<0.05$ (two-tailed).

Results

Selective silencing of presynaptic 5-HT_{1A}R expression by local 1A-siRNA infusion into mice DR

We first examined the feasibility of reducing directly 5-HT_{1A} autoreceptor expression in the DR of adult mice by local infusion of 1A-siRNA molecules. The 1A-siRNA mixture was applied in a volume of 1 μl at two concentrations (2.5 or 10 mg/ml solution) on two consecutive days, giving a total amount of 1A-siRNA of 5 and 20 μg (0.3 and 1.4 nmol, respectively).

In situ hybridization experiments revealed that the local infusion of 5 and 20 μg 1A-siRNA evoked a dose-dependent decrease of 5-HT_{1A}R mRNA levels in the DR at 1 day post-administration (to 82±6 and 44±5 % of the vehicle-treated group). Mice treated with 20 μg 1A-siRNA had a significant reduction of 5-HT_{1A}R mRNA compared to vehicle or ns-siRNA-treated mice (Fig. 1a, b). Two-way ANOVA showed significant effects of group [$F(2, 13)=16.08$, $p<0.001$] and group-by-dose interaction [$F(2, 13)=6.41$, $p<0.05$]. Further, quantitative densitometric analysis of [^{3}H]-8-OH-DPAT binding also revealed a reduction of DR 5-HT_{1A}R density in mice treated with 5 or 20 μg 1A-siRNA (to 70±5 and 50±5 % of vehicle-treated mice) compared with that in control groups (vehicle and ns-siRNA) (Fig. 1a, b). Two-way ANOVA showed a significant effect of group [$F(2, 45)=16.95$, $p<0.001$], but no effect of dose nor interaction group-by-dose. The suppression of presynaptic 5-HT_{1A}R in the DR was observed at the three anteroposterior coordinates examined.

Intra-DR 1A-siRNA administration did not alter 5-HT_{1A}R expression in the median raphe nucleus (MnR), indicating a restricted siRNA diffusion after local application with capillary microcannula (Fig. 1c, Supplementary Fig. S1). Likewise, 5-HT_{1A}R density in forebrain areas rich in 5-HT_{1A}R, such as the prefrontal cortex, hippocampal formation, and entorhinal cortex, remained also unaffected (Fig. 1d, e).

Furthermore, we examined the expression of potentially unintended targets by measuring mRNA and binding densities of two related genes that are localized in serotonergic neurons: SERT and 5-HT_{1B}R. Neither SERT and 5-HT_{1B}R mRNAs nor their respective binding sites were affected by intra-DR 1A-siRNA infusion (Fig. 2a–e). Moreover, 1A-siRNA application did not change the mRNA expression of pro-inflammatory cytokines such as *TNF-α* (relative gene expression: control, 1.0±0.2; ns-siRNA 0.7±0.2; 1A-siRNA, 0.8±0.2; $n=5–6$) and *INF-γ* (relative gene expression: control, 1.0±0.1; ns-siRNA 0.9±0.2; 1A-siRNA, 0.7±0.2; $n=5–6$) in the raphe nuclei.

We next evaluated the time course of 1A-siRNA effects in vivo. We infused the highest dose (20 μg/mice) of 1A-siRNA into the DR, and groups of mice were killed at different times after the last siRNA injection. Autoradiographic binding experiments revealed that the DR 5-HT_{1A}R density was significantly lower in 1A-siRNA-treated mice than in the respective control groups 1 and 3 days post-administration, with a recovery of 5-HT_{1A}R density to control values at 6 and 12 days post-administration (Fig. 3a, b). One-way ANOVA showed a significant effect of group at day 1 [$F(2, 10)=15.62$, $p<0.001$] and day 3 [$F(2, 13)=10.32$, $p<0.01$] after infusion.

Altered agonist response in 5-HT_{1A} autoreceptor knockdown mice

To directly confirm the in vivo functional impact of DR 5-HT_{1A}R suppression indicated by autoradiography (Fig. 3a, b), we assessed the hypothermic response mediated by the activation of presynaptic 5-HT_{1A}R in mice (Martin et al. 1992). We administered the 5-HT_{1A}R agonist, 8-OH-DPAT (1 mg/kg, i.p.), to control (vehicle and ns-siRNA), 1A-siRNA-treated mice, and constitutive 1A-KO mice. Vehicle and ns-siRNA-treated mice displayed the expected hypothermic response to 8-OH-DPAT, which was absent in 1A-siRNA-treated mice at days 1–3 and was recovered at days 6–12 post-administration, in agreement with the change in 5-HT_{1A} autoreceptors levels. 1A-KO mice showed no hypothermic response at any time (Fig. 3c). Significant differences were observed at day 1: effect of group [$F(3, 24)=28.78$, $p<0.001$], time [$F(4, 96=13.53)$, $p<0.001$], and interaction [$F(12, 96)=10.15$, $p<0.001$]; day 3: effect of group [$F(3, 28=3.56)$, $p<0.05$], time [$F(4, 112)=54.13$, $p<0.001$], and interaction [$F(12, 112)=2.05$, $p<0.05$]; day 6: effect of time [$F(4, 108)=61.17$, $p<0.001$] and interaction [$F(12, 108)=2.19$, $p<0.05$]; and day 12: effect of time [$F(4, 136)=75.72$, $p<0.001$].

We next examined how decreased 5-HT_{1A} autoreceptor expression induced by intra-DR 1A-siRNA infusion translated into a distal regulation of 5-HT and DA release in the forebrain. We performed pharmacological studies in the mPFC of freely moving mice using microdialysis. No difference was observed in baseline 5-HT and DA

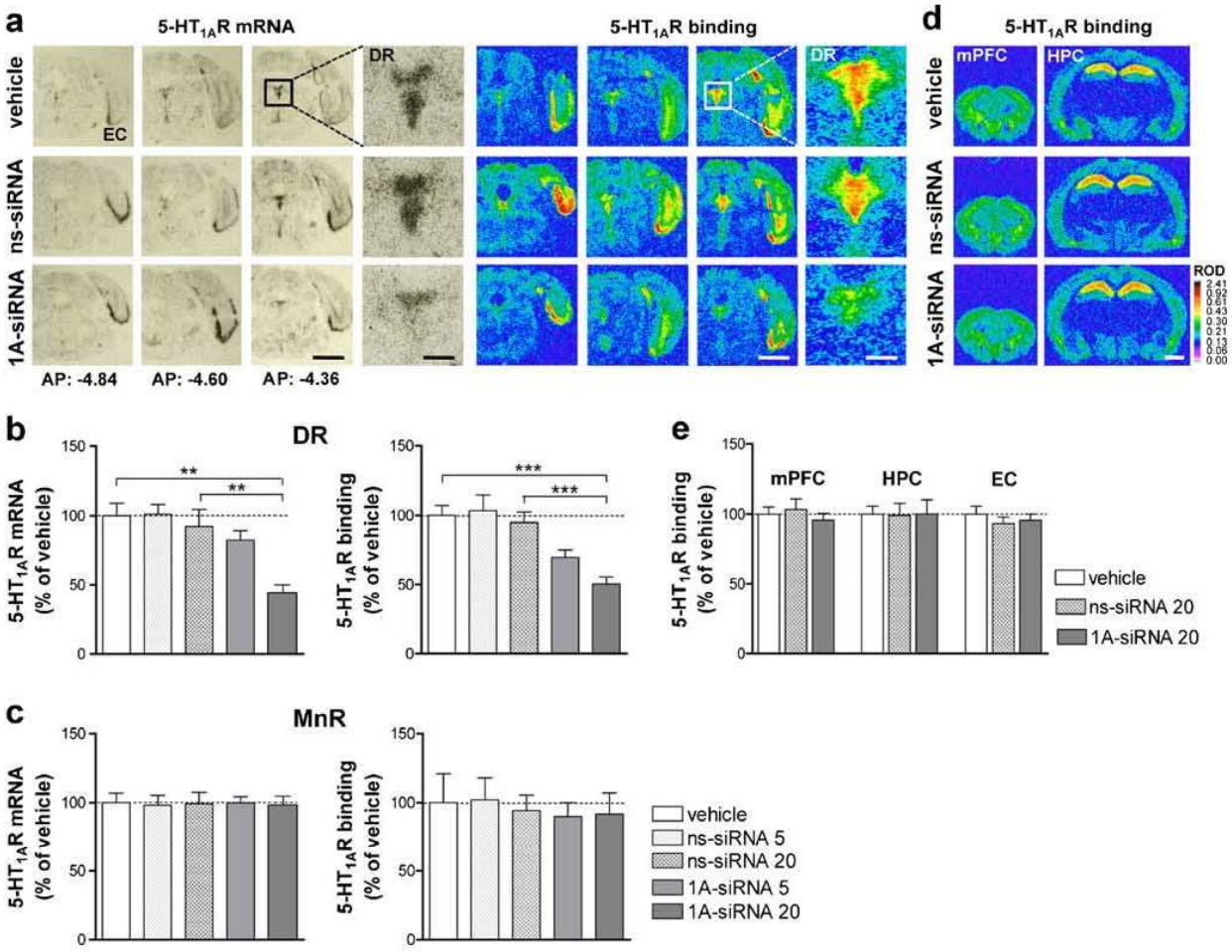

Fig. 1 Selective 5-HT$_{1A}$ autoreceptor silencing by 1A-siRNA infused into the dorsal raphe nucleus (DR). Mice received (1) vehicle, (2) ns-siRNA, or (3) 1A-siRNA (5 or 20 μg; 2×2.5 or 2×10 μg, respectively) into DR and were killed 24 h after administration. **a** Representative coronal brain sections showing the 1A-siRNA (20 μg)-induced reduction of 5-HT$_{1A}$R expression in DR at different anteroposterior coordinates (AP −4.84 to −4.36 mm, taken from bregma) assessed by in situ hybridization and [^{3}H]-8-OH-DPAT binding. The *boxes* delimit areas of DR shown at higher magnification. *Scale bars*: low magnification=2 mm, high magnification=500 μm. **b** Densitometric quantification of 5-HT$_{1A}$R mRNA and binding in DR (n=5–8 mice/group, relative optical density was evaluated in two adjacent DR sections at the three AP levels (see above) of each mouse and averaged to obtain individual values). Note the decreased 5-HT$_{1A}$ autoreceptor expression in mice treated with the higher dose of 1A-siRNA. $^{**}p<0.01$, $^{***}p<0.001$ versus vehicle and ns-siRNA-treated mice. **c** No group differences were detected for presynaptic 5-HT$_{1A}$R expression in the median raphe nucleus (MnR) (n=5–8 mice/group). **d** Representative coronal brain sections showing [^{3}H]-8-OH-DPAT binding to 5-HT$_{1A}$R in medial prefrontal cortex (mPFC) and dorsal hippocampus (HPC). *Scale bar*=2 mm. **e** Postsynaptic 5-HT$_{1A}$R binding in mPFC, HPC, and entorhinal cortex (EC) was not affected by any treatment (n=5–6). Values are mean ± SEM

concentration between the various groups of mice (Table 3). The 5-HT$_{1A}$R agonist 8-OH-DPAT (0.5 mg/kg, i.p.) reduced extracellular 5-HT concentration to ~40 % of baseline in mPFC of control groups, but not in 1A-siRNA-treated or 1A-KO mice [effect of group, $F(3, 21)=11.29$, $p<0.01$; time, $F(14, 294)=4.40$, $p<0.001$; and time-by-group interaction, $F(42, 294)=3.57$, $p<0.001$] (Fig. 4a).

Postsynaptic 5-HT$_{1A}$R in mPFC is involved in the control of mesocortical dopamine (DA) activity and local DA release (Díaz-Mataix et al. 2005). To confirm the absence of functional changes on mPFC 5-HT$_{1A}$R by intra-DR 1A-siRNA infusion, we assessed the effect of the selective 5-HT$_{1A}$R agonist, BAYx3702 on extracellular DA in mPFC of these mice. Local BAYx3702 infusion at 3 μM by reverse dialysis increased DA concentration in mPFC of vehicle, ns-siRNA, and 1A-siRNA-treated mice to a similar extent, with no effect on 1A-KO mice [effect of group, $F(3, 12)=10.02$, $p<0.01$; time, $F(14, 168)=17.80$, $p<0.001$; and time-by-group interaction, $F(42, 168)=2.74$, $p<0.001$, without

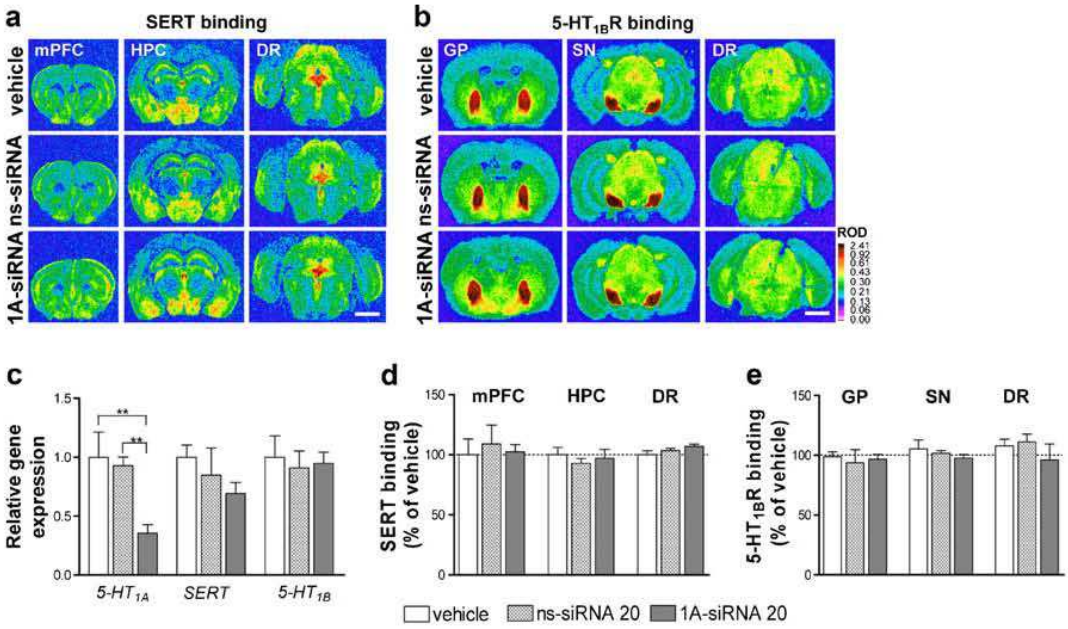

Fig. 2 Unchanged expression of the serotonin transporter (SERT) and 5-HT_{1B}R after 5-HT_{1A} autoreceptor silencing. Mice received (1) vehicle, (2) ns-siRNA, or (3) 1A-siRNA (20 μg, 2×10 μg) into dorsal raphe nucleus (DR) and were killed 24 h after treatments (n=5–8 mice/group). **a** Representative images showing [^{3}H]-citalopram binding to SERT in coronal section of medial prefrontal cortex (mPFC), dorsal hippocampus (HPC), and DR. **b** Brain sections containing the globus pallidus (GP), substantia nigra (SN), and DR showing [^{125}I]-cyanopindolol binding to 5-HT_{1B}R. *Scale bar*=2 mm. **c** The levels of the mRNAs encoding 5-HT_{1A}, SERT, and 5-HT_{1B} were assessed in midbrain raphe nuclei by RT-PCR. Unlike 5-HT_{1A}R expression, 1A-siRNA infusion did not change the mRNA levels of SERT and 5-HT_{1B}R. $^{**}p<0.01$ versus vehicle and ns-siRNA-treated mice. **d** Quantitative autoradiography of [^{3}H]-citalopram binding showed no differences on SERT density in the different brain areas for each treatment. **e** *Bar graph* showing no differences in 5-HT_{1B}R expression evaluated by [^{125}I]-cyanopindolol binding in the different brain areas. Values are mean ± SEM

post hoc differences between 1A-siRNA-treated mice and controls] (Fig. 4b). These results are consistent with the above 5-HT_{1A}R binding data and indicate that intra-DR 1A-siRNA infusion did not alter cortical 5-HT_{1A}R expression and function.

Unchanged anxiety-like behavior and altered response to depression/stress-related paradigms in 5-HT_{1A} autoreceptor knockdown mice

To evaluate the role of presynaptic 5-HT_{1A}R in anxiety-like behavior in adulthood, we used the EPM paradigm. Vehicle and 1A-siRNA-treated mice showed similar behavioral responses during exposure to the EPM, whereas 1A-KO mice exhibited an anxiety-like behavior (Fig. 5a). One-way ANOVA indicated a significant effect of group for entries [$F(2, 35)=25.77$, $p<0.001$] and for time in open arms [$F(2, 35)=3.83$, $p<0.05$], without post hoc differences between 1A-siRNA and vehicle-treated mice. The number of entries in closed arms was similar between vehicle and 1A-siRNA groups, indicating a lack of effects of 1A-siRNA on locomotor activity. Thus, acute changes of 5-HT_{1A} autoreceptor expression in adulthood do not evoke anxiety-like responses, consistent with findings showing a developmental role of 5-HT_{1A}R in the establishment of anxiety-related circuitry (Gleason et al. 2010; Gross et al. 2002; see, however, Richardson-Jones et al. 2011).

Additional to its role in anxiety, several studies suggest that 5-HT_{1A}R levels influence behavioral resilience to stressful situations, i.e., individuals with higher 5-HT_{1A}R expression are more susceptible to depression and suicide (Lemonde et al. 2003; Neff et al. 2009). We therefore examined the potential antidepressant-like responses evoked by intra-DR 1A-siRNA application in adult mice using two depression-related stress paradigms: TST and FST. In both tests, immobility is scored as a measure of behavioral despair (Lucki 1997). In TST, 1A-siRNA-treated and 1A-KO mice showed a greater propensity to escape and a shorter immobility time than vehicle controls [effect of group, $F(2, 36)=25.25$, $p<0.001$] (Fig. 5b). The intrinsic decreased immobility shown by 5-HT_{1A} autoreceptor knockdown mice in the TST was comparable to that exhibited by control mice after antidepressant treatments (Bortolozzi et al. 2012; Cryan et al. 2005).

Likewise, mice treated with intra-DR infusion of 1A-siRNA were more active and displayed a reduced

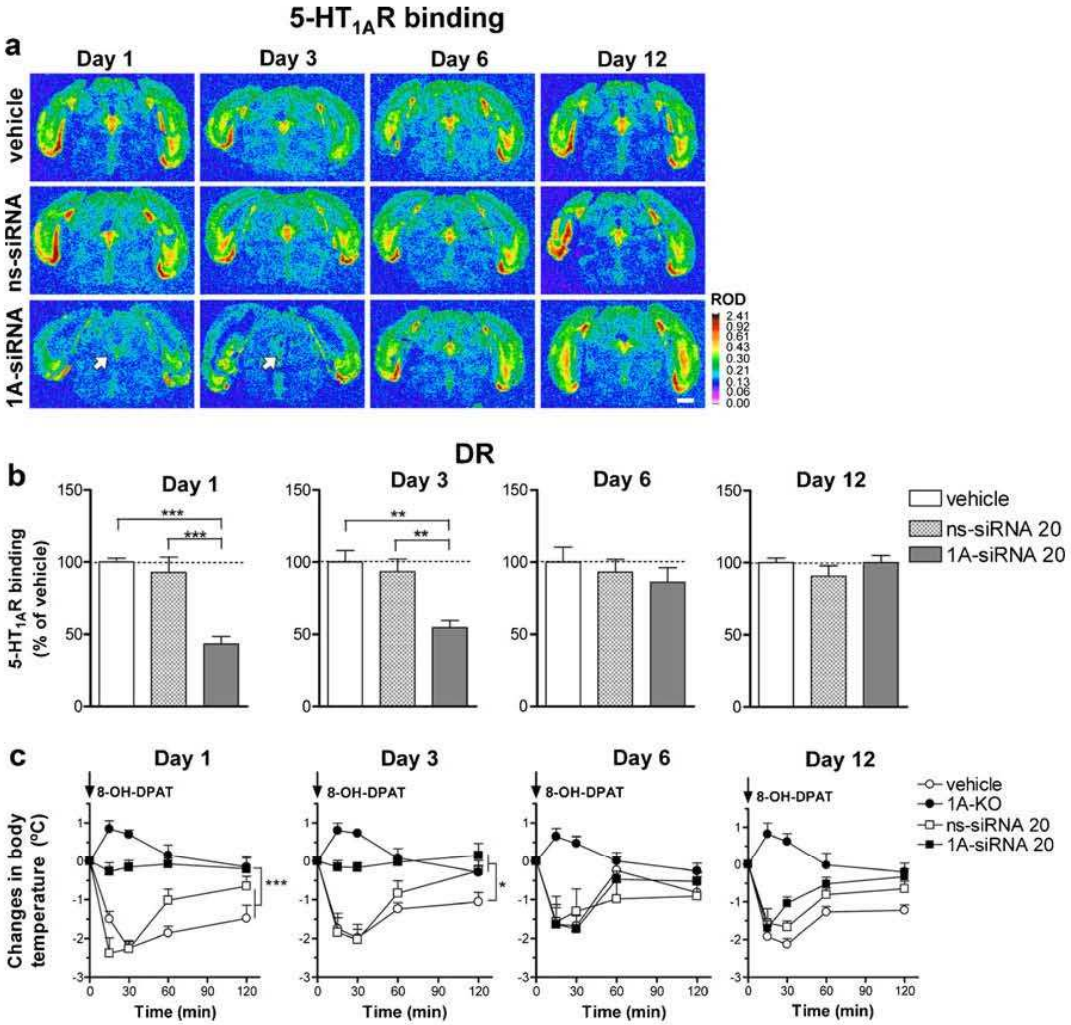

Fig. 3 Time course of 5-HT_{1A} autoreceptor suppression in the DR after local 1A-siRNA infusion. **a** Brain sections containing the raphe nuclei showing [^{3}H]-8-OH-DPAT binding to 5-HT_{1A}R from mice that received vehicle, ns-siRNA, or 1A-siRNA (20 μg) into the dorsal raphe nucleus (DR) and were killed at 1, 3, 6, and 12 days post-administration. The *arrows* indicate the decreased 5-HT_{1A}R density in DR of mice treated with 1A-siRNA and sacrificed at days 1 and 3 post-infusion. *Scale bar*=2 mm. **b** *Bar graphs* showing a significant reduction of [^{3}H]-8-OH-DPAT binding to 5-HT_{1A}R in DR of 1A-siRNA-treated mice compared with their respective controls at days 1 and 3 post-administration. Conversely, no difference was detected at days 6 and 12 post-administration (n=4–7 mice/group, relative optical density was evaluated in two adjacent DR sections at three anteroposterior levels of each mouse and averaged to obtain individual values). $^{**}p<0.01$, $^{***}p<0.001$ versus vehicle and ns-siRNA-treated mice. **c** Time course of the hypothermic response to the 5-HT_{1A}R agonist 8-OH-DPAT (1 mg/kg, i.p.). Hypothermia was abolished in 5-HT_{1A} autoreceptor knockdown mice at days 1 and 3. Constitutive 1A-KO mice, also lacking 8-OH-DPAT-induced hypothermia, were used as positive controls (n=6–10 mice/group). $^{*}p<0.05$, $^{***}p<0.001$ versus vehicle and ns-siRNA-treated mice. Values are mean ± SEM

immobility than vehicle mice in the FST (Fig. 5c). A comparable antidepressant response was observed after acute SSRI fluoxetine administration (Bortolozzi et al. 2012; Cryan et al. 2005). Two-way ANOVA showed a significant effect of group [$F(1, 18)=16.88$, $p<0.001$] and time [$F(2, 36)=81.73$, $p<0.001$]. Thus, while low 5-HT_{1A} autoreceptor expression in adulthood does not alter anxiety-like behavior, it elicits a more active response in depression-related tasks such as the TST and the FST.

Increased serotonin levels in 5-HT_{1A} autoreceptor knockdown mice under a depression/stress-related paradigm and in response to fluoxetine

Given the increased resilience to stressful factors in 1A-siRNA-treated mice and the inhibitory control of 5-HT_{1A} autoreceptors on serotonergic function, we next examined whether this effect was associated to an increased forebrain 5-HT release. We performed in vivo microdialysis in mPFC

Table 3 Basal serotonin and dopamine dialysate values in the medial prefrontal cortex of mice

Groups	aCSF		aCSF+citalopram	
	Serotonin (fmol/30 min)	Dopamine (fmol/20 min)	Serotonin (fmol/30 min)	Serotonin (fmol/6 min)
Vehicle	7.6±0.5 (5)	5.3±0.9 (5)	20.0±2.9 (5)	6.3±0.6 (6)
ns-siRNA	6.1±0.7 (7)	5.5±0.9 (5)	15.6±3.7 (7)	7.6±1.3 (5)
1A-siRNA	5.2±0.9 (6)	5.4±1.1 (5)	15.2±3.7 (7)	9.2±1.4 (7)
1A-KO	6.9±1.0 (4)	6.0±1.3 (5)	18.1±1.2 (6)	n.e.

Data are mean ± SEM of the number of animals shown in parentheses. For DA assessing, the aCSF was pumped at 1.5 μl/min and dialysate was collected every 20 min. For 5-HT assessing, the microdialysis probes were perfused with appropriate aCSF at 1.5 or 5.0 μl/min and dialysates were collected every 30 or 6 min, respectively

aCSF artificial cerebrospinal fluid, *aCSF + citalopram* artificial cerebrospinal fluid containing 1 μM citalopram, *n.e.* not examined

simultaneously during the performance of the TST. Despite no significant difference was detected in prefrontal 5-HT concentration at baseline between groups (Table 3), the dialysate 5-HT increased twofold in 5-HT_{1A} autoreceptor knockdown mice under TST-induced behavioral despair (Fig. 6a). Two-way ANOVA showed significant effect of time [$F(18, 270)=5.35$, $p<0.001$] and time-by-group interaction [$F(36, 270)=1.91$, $p<0.01$]. In parallel, 1A-siRNA-treated mice showed a shorter immobility time than vehicle and ns-siRNA-treated mice [effect of group, $F(2, 15)=4.99$, $p<0.05$] (Fig. 6b).

Finally, we examined whether the 1A-siRNA-induced changes in 5-HT_{1A} autoreceptor expression translated into an enhancement of the neurochemical response to an SSRI, as previously observed with the pharmacological blockade of 5-HT_{1A}R (Artigas et al. 1996; Romero and Artigas 1997). Mice received a single fluoxetine injection (20 mg/kg, i.p.), which increased extracellular 5-HT concentration in mPFC of all groups, but significantly more in 1A-siRNA-treated and 1A-KO mice [effect of group, $F(3, 17)=6.45$, $p<0.01$; time, $F(14, 238)=17.62$, $p<0.001$; and time-by-group interaction, $F(42, 238)=3.44$, $p<0.001$] (Fig. 7).

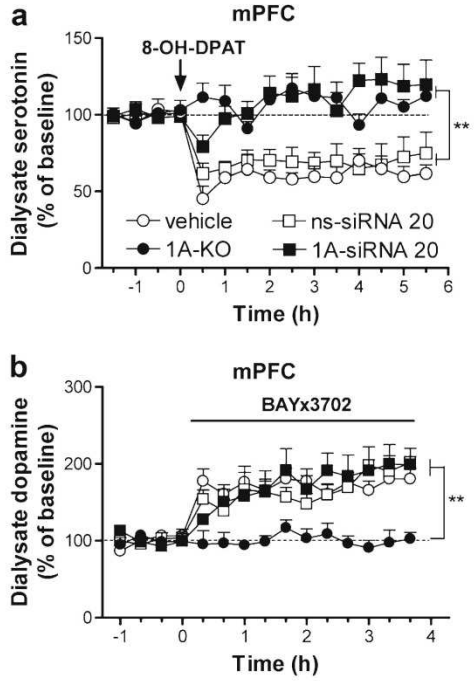

Fig. 4 Neurochemical consequences of 1A-siRNA-induced 5-HT_{1A} autoreceptor knockdown. **a** Acute 8-OH-DPAT administration (0.5 mg/kg, i.p.) did not reduce extracellular serotonin concentration in medial prefrontal cortex (mPFC) of 1A-siRNA-treated mice and 1A-KO mice (n=5–7 mice/group). **$p<0.01$ versus vehicle and ns-siRNA-treated mice. **b** Local activation of postsynaptic 5-HT_{1A}R in mPFC by the infusion of 3 μM BAYx3702 by reverse dialysis increased extracellular dopamine concentration in vehicle, ns-siRNA, and 1A-siRNA-treated mice, but not in 1A-KO mice (n=4 mice/group). **$p<0.01$ versus vehicle, ns-siRNA, and 1A-siRNA groups. Values are mean ± SEM

Discussion

In agreement with our recent observations (Bortolozzi et al. 2012), the present study shows that direct suppression of presynaptic 5-HT_{1A}R expression in the DR in adulthood is sufficient to impact on reactivity to stress/depression-related behavior without affecting anxiety-like response. Both sets of independent results are entirely comparable and show that 1A-siRNA is a powerful tool for the efficient and selective silencing of the 5-HT_{1A} autoreceptor expression in vivo in rodent brain. This procedure provides a number of advances over more classical transgenic mice approaches. First, it allows for spatial and temporal specificity, neither of which is possible using constitutive KO mice. Indeed, we evaluated the effect of 5-HT_{1A} autoreceptor changes on anxiety- and depression-like behaviors in adulthood leaving aside neurodevelopment problems due to the lack of 5-HT_{1A}R (Gleason et al. 2010; Gross et al. 2002; Heisler et al. 1998; Parks et al. 1998; Ramboz et al. 1998). Second, the siRNA strategy allows for the examination of the physiological role of receptors/transporters and the subsequent adaptive

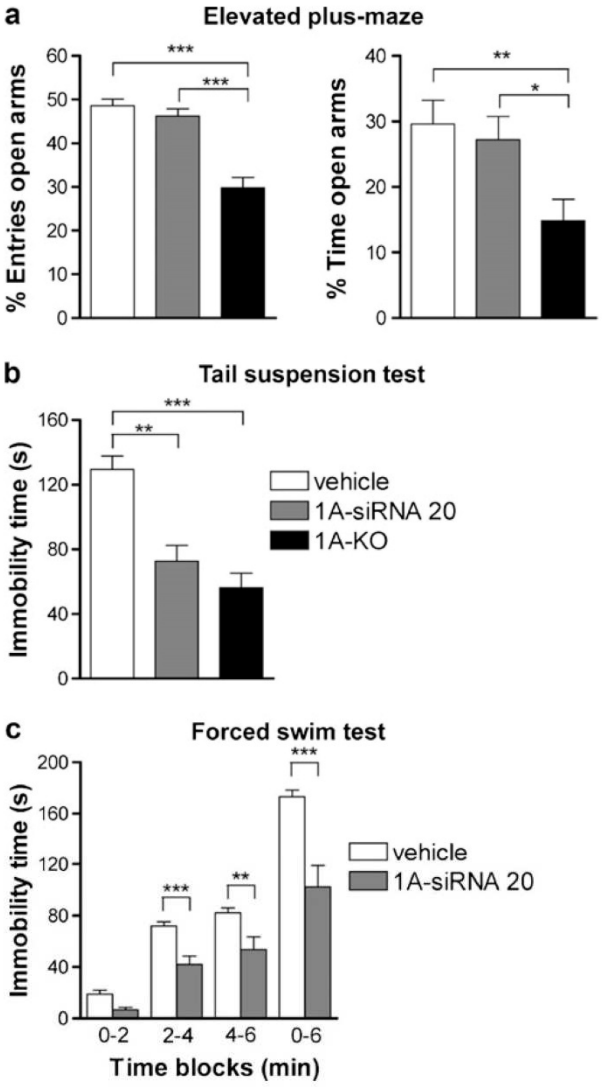

Fig. 5 Behavioral consequences of 1A-siRNA-induced 5-HT_{1A} autoreceptor knockdown. Mice were infused with 20 μg (2×10 μg) 1A-siRNA into dorsal raphe nucleus (DR) and behavioral tests were conducted 24 h after administration. Control and 1A-KO mice received vehicle into DR and were subjected to the same experimental procedure. **a** Anxiety-like behavior. Unlike 1A-KO mice, vehicle and 1A-siRNA-treated mice showed a similar anxiety-like behavior in the elevated plus maze (EPM), with no differences in the percentage of entries and time spent in open arms (n=12–13 mice/group). *p<0.05, **p<0.01, ***p<0.001 versus vehicle and 1A-siRNA-treated mice. **b**, **c** Antidepressant-like behaviors. **b** 1A-siRNA-treated mice displayed a reduced immobility in the tail suspension test (TST), as did constitutive 1A-KO mice (n=12–13 mice/group). **p<0.01, ***p<0.001 versus vehicle-treated mice. **c** 1A-siRNA-treated mice also showed a decreased immobility in the forced swim test (FST) (n=10 mice/group). **p<0.01, ***p<0.001 versus vehicle-treated mice. Values are mean ± SEM

temporal changes induced on other genes in response to the reduced expression of the target gene (Bortolozzi et al. 2011).

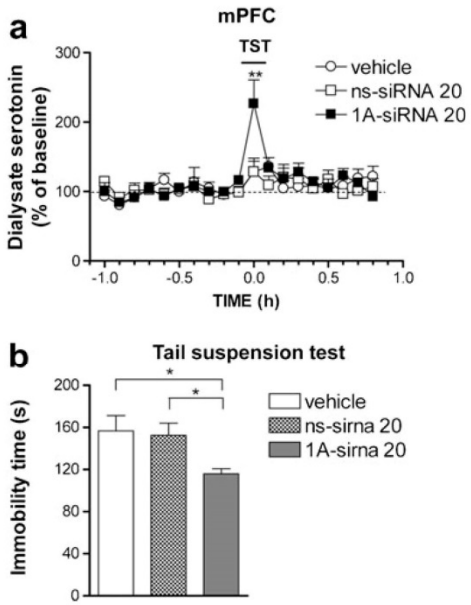

Fig. 6 Increased extracellular serotonin (5-HT) concentration in 5-HT_{1A} autoreceptor knockdown mice under a depression-related stress paradigm. **a** Extracellular 5-HT levels were measured by in vivo microdialysis in medial prefrontal cortex (mPFC) of mice treated with vehicle, ns-siRNA, or 1A-siRNA (20 μg; 2×10 μg, respectively) during acute stress induced by tail suspension test (TST). Note that 5-HT_{1A} autoreceptor knockdown mice showed a larger increase of 5-HT release in mPFC than control groups (n=5–7 mice/group). **p< 0.01 versus vehicle and ns-siRNA-treated mice. **b** In parallel, 1A-siRNA-treated mice displayed a reduced immobility in the TST (n= 5–7 mice/group). *p<0.05 versus vehicle and ns-siRNA-treated mice. Values are mean ± SEM

Pharmacological or molecular approaches—and siRNAs are no exception (Moss and Taylor 2003; Sledz et al. 2003)—have unintended off-target effects. Some genes containing sequences with incomplete complementarity may be unintentionally silenced by mRNA cleavage (Dykxhoorn

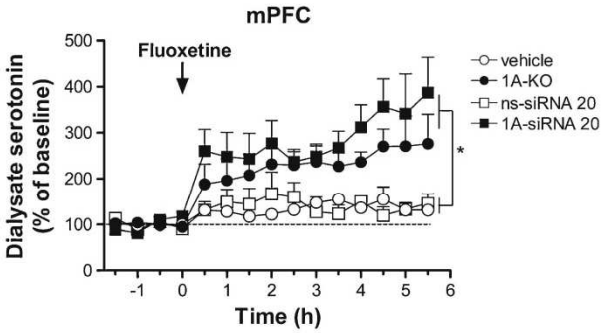

Fig. 7 Enhance neurochemical response to a SSRI fluoxetine in 5-HT_{1A} autoreceptor knockdown mice. Acute fluoxetine administration (20 mg/kg, i.p.) increased the extracellular serotonin (5-HT) concentration in mPFC of 1A-siRNA-treated mice and 1A-KO mice at the same level (n=4–7 mice/group). *p<0.05 versus vehicle and ns-siRNA-treated mice. Values are mean ± SEM

and Lieberman 2006). Although the rules for predicting in vivo off-target gene regulation are still poorly known, the present results support a specific effect of 1A-siRNA on 5-HT_{1A} autoreceptor expression restricted to the application site (DR) (Supplementary Fig. S1). Hence, presynaptic 5-HT_{1A}R in the MnR and forebrain postsynaptic 5-HT_{1A}R were unaffected by intra-DR 1A-siRNA application. Moreover, the same amount of nonsense siRNA infused into the DR did not evoke any change in the 5-HT_{1A} autoreceptor density. Additionally, other genes expressed by serotonergic neurons, such as SERT or 5-HT_{1B}R, were unmodified by this approach. It is possible that siRNAs could alter the cellular homeostasis by triggering immune and inflammatory pathways (Judge et al. 2005; Moss and Taylor 2003; Sledz et al. 2003). However, the 1A-siRNA sequences used herein did not induce pro-inflammatory genes (*TNFα*, *INFγ*) as previously described by β-galactosidase-siRNA (Bortolozzi et al. 2012). The absence of non-specific effects is likely due to the use of low siRNA concentrations, compared with other in vivo brain studies (Thakker et al. 2004, 2005).

A lower density of 5-HT_{1A} autoreceptor was observed at 1 and 3 days post-administration of 1A-siRNA and it was recovered at 6 days. This is consistent with the turnover of 5-HT_{1A}R obtained after its chemical inactivation by N-ethoxycarbonyl-2-ethoxy-1,2-dihydroquinoline (EEDQ) (Gozlan et al. 1994). Interestingly, there was a close temporal parallelism between the changes in receptor expression and the functional status of 5-HT_{1A} autoreceptor in response to the 5-HT_{1A}R agonist 8-OH-DPAT. However, the magnitude of the effects was markedly different. Thus, a decrease of 5-HT_{1A} autoreceptor density (44 %) was sufficient to prevent 8-OH-DPAT-mediated responses (fall in extracellular 5-HT and hypothermia), making 1A-siRNA-treated mice to partially behave as constitutive 1A-KO mice. However, the last showed a hyperthermia response following 8-OH-DPAT injection, likely due to the anxious-like response in 1A-KO mice (Heisler et al. 1998; Parks et al. 1998; Pattij et al. 2002; Ramboz et al. 1998). The "reserve" pool presence of presynaptic 5-HT_{1A}R was suggested after irreversible EEDQ effect on GPCRs (Bohmaker et al. 1992; Cox et al. 1993). Our results, using an entirely different strategy, support the existence of different functional 5-HT_{1A} autoreceptor pools and suggest that newly synthesized 5-HT_{1A} autoreceptors are functionally active receptors that mediate the 8-OH-DPAT agonist response.

In coincidence with previous findings (Amargós-Bosch et al. 2004; Bortolozzi et al. 2004, 2012; He et al. 2001; Knobelman et al. 2001; Ramboz et al. 1998; Richardson-Jones et al. 2010), the basal extracellular 5-HT concentration was similar in controls and 1A-siRNA-treated and 1A-KO mice. This also agrees with the absence of major alterations in the firing rate of DR serotonergic neurons in 1A-KO mice (Amargós-Bosch et al. 2004; Richer et al. 2002) and provides further support to the view that 5-HT_{1A} autoreceptors are not tonically activated under physiological conditions (Johnson et al. 2002; Mannoury la Cour et al. 2001). Actually, 5-HT_{1A} autoreceptors play the role of "safety valves" to maintain the slow and regular discharge of serotonergic

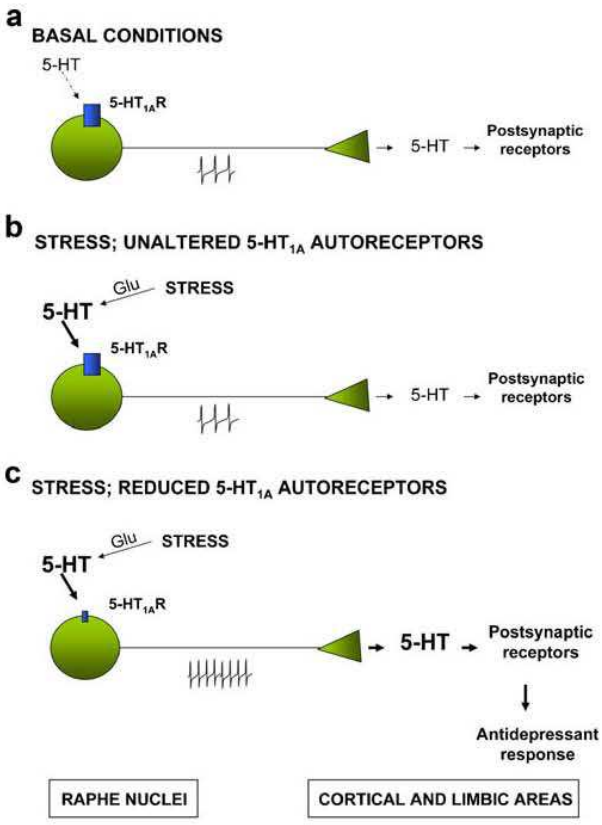

Fig. 8 Schematic representation of the balance between presynaptic 5-HT_{1A}R activation in the raphe nuclei and 5-HT release by nerve terminals in cortical and limbic areas. **a** In basal conditions, the balance between excitatory and inhibitory inputs onto DR serotonergic neurons (Celada et al. 2001) keeps the extracellular 5-HT concentration in the vicinity of serotonergic cell bodies and dendrites below the concentration required to activate 5-HT_{1A} autoreceptors. **b** In conditions of increased excitatory inputs, such as during stress, 5-HT release increases in the DR (either somatodendritic or from the dense network of 5-HT axons within the raphe nuclei; Adell et al. 1997, 2002). The subsequent 5-HT_{1A} autoreceptor activation and neuronal hyperpolarization keeps serotonergic cell firing low (typically ~1 Hz) and regular, with no effect on firing-dependent terminal 5-HT release. **c** In a situation of low density or sensitivity of 5-HT_{1A} autoreceptors (illustrated by a small size of the 5-HT_{1A} autoreceptors symbol), the above negative feedback does not occur and increased excitatory inputs onto serotonergic neurons translate into a greater terminal 5-HT release in corticolimbic areas that helps to increase resilience to stress (e.g., lower immobility in TST and FST). Similarly, the excess of extracellular 5-HT evoked by SERT blockade with fluoxetine cannot activate the 5-HT_{1A} autoreceptor-mediated negative feedback (Artigas et al. 1996), resulting in a greater extracellular 5-HT concentration in forebrain, as shown in the preceding figure

neurons in conditions of high excitatory input (Celada et al. 2001) such as during stressful conditions (Adell et al. 1997). In non-stressful conditions, 5-HT release remains at concentrations below those required to activate 5-HT_{1A} autoreceptors. This may explain the apparent contradiction between decreased presynaptic 5-HT_{1A}R expression and unchanged 5-HT levels in mPFC. Only when 5-HT_{1A} autoreceptors are markedly activated by the excess 5-HT induced by SSRIs, the difference in terminal 5-HT levels is evident. Thus, the increase of mPFC 5-HT evoked by fluoxetine was augmented in mice treated with 1A-siRNA to reach the values seen in 1A-KO mice, as previously observed using SSRI + 5-HT_{1A}R antagonists (Artigas et al. 1996; Romero and Artigas 1997; Scorza et al. 2012).

Moreover, 1A-siRNA-treated mice showed a marked reduction in immobility versus control mice in standard depression-related stress tests, indicating that the suppression of 5-HT_{1A} autoreceptors evoked antidepressant-like effects, which were similar to those exhibited by constitutive 1A-KO mice when examined (TST). Hence, the increased 5-HT release in mPFC (and likely other forebrain areas) obtained by down-regulated 5-HT_{1A} autoreceptor expression would enhance resilience to stressful conditions, as seen here with 1A-siRNA-treated mice in the TST (see scheme in Fig. 8). This view is also consistent with the increased raphe firing rate in a model of 5-HT_{1A} autoreceptor transgenic mice under chronic stress (Richardson-Jones et al. 2010).

The ~44 % knockdown of 5-HT_{1A} autoreceptor found herein after acute 1A-siRNA infusion was comparable to that reported after prolonged administration of high siRNA concentrations in the brain (Thakker et al. 2004, 2005). Likewise, the functional consequences of 1A-siRNA-induced 5-HT_{1A} autoreceptor knockdown are comparable with previous pharmacological and clinical observations using 5-HT_{1A}R antagonists which attributed a key role to presynaptic 5-HT_{1A}R in antidepressant therapy (Artigas et al. 1994; Ballesteros and Callado 2004; Portella et al. 2011; Scorza et al. 2012). However, unlike pindolol, selective 5-HT_{1A}R antagonists do not discriminate between pre- and postsynaptic 5-HT_{1A}R, a lack of regional selectivity that can limit their therapeutic use in SSRI combination studies due to the need to enhance presynaptic serotonergic function without blocking postsynaptic 5-HT_{1A}R (Ballesteros and Callado 2004; Haddjeri et al. 1998; Scorza et al. 2012). In view of these limitations, a siRNA-based approach may uncover valid therapeutic strategies, provided that appropriate cellular targeting can be achieved. Indeed, there is a considerable effort in developing improved siRNA delivery and gene silencing in vivo (Baker 2010; Kumar et al. 2007; Song et al. 2005; Soutschek et al. 2004). Thus, our efforts are directed to achieving a selective targeting of genes expressed in serotonergic neurons (Bortolozzi et al. 2012).

Neuroimaging studies have associated high 5-HT_{1A} autoreceptor density in humans with a poor reactivity of the amygdala, a brain region important for responses to stress and threatening stimuli (Fakra et al. 2009). Further, genetic studies link 5-HT_{1A}R mutations leading to high levels of 5-HT_{1A} autoreceptor with higher incidence to mood disorders and poorer response to antidepressants (Lemonde et al. 2003; Neff et al. 2009; Stockmeier et al. 1998). Our results agree with the hypothesis that 5-HT_{1A} autoreceptors have a critical role in the treatment of major depression (Bortolozzi et al. 2012; Richardson-Jones et al. 2010), and they provide support for optimizing therapeutic interventions on the basis of the heterogeneity of patients with regard to function of the 5-HT system.

In summary, together with our recently reported work (Bortolozzi et al. 2012), the present study indicates that selective 5-HT_{1A} autoreceptor suppression prevents the self-inhibitory effects of DR 5-HT_{1A}R activation. The prevention of this physiological negative feedback evokes antidepressant-like responses, likely mediated by an increased capacity of serotonergic neurons to release 5-HT in stressful conditions and also augments the neurochemical effects of fluoxetine. Overall, these observations hold promise for the development of a new class of therapeutics that harnesses the RNAi mechanism to regulate gene expression in serotonergic neuron and help to unveil the complex relationship between stress and the 5-HT system.

Acknowledgments This research was supported by grants from the Spanish Ministry of Science and Innovation SAF2007-62378 (to F.A.) and CDTI, with the participation of the DENDRIA Consortium (to A.B.); from Instituto de Salud Carlos III PI10/00290 (to A.B.) and Centro de Investigación Biomédica en Red de Salud Mental (CIBERSAM); and a research contract CSIC-IDIBAPS with NEDKEN, S.L.-nLife Therapeutics. Structural funds of the European Union, through the National Applied Research Projects (R+D+I 2008/11) and from the Catalan Government (grant 2009SGR220), are also acknowledged. We gratefully acknowledge Leticia Campa for her assisting with the HPLC equipment and Verónica Paz for technical assistance.

Conflict of interest F.A. has received consulting and educational honoraria on antidepressant drugs from Eli Lilly and Lundbeck. A.M. is a cofounder and board member of nLife Therapeutics S.L. M.C.C. is an employee on nLife Therapeutics S.L. The rest of the authors report no biomedical financial interests or potential conflicts of interest.

References

Adell A, Artigas F (1991) Differential effects of clomipramine given locally or systemically on extracellular 5-HT in raphe nuclei and frontal cortex. Naunyn-Schmiedeberg's Arch Pharmacol 343:237–244

Adell A, Casanovas JM, Artigas F (1997) Comparative study in the rat of the actions of different types of stress on the release of 5-HT in raphe nuclei and forebrain areas. Neuropharmacology 36:735–741

Adell A, Celada P, Abellán MT, Artigas F (2002) Origin and functional role of the extracellular serotonin in the midbrain raphe nuclei. Brain Res Rev 39:154–180

Amargós-Bosch M, Bortolozzi A, Puig MV, Serrats J, Adell A, Celada P, Toth M, Mengod G, Artigas F (2004) Co-expression and in vivo interaction of serotonin$_{1A}$ and serotonin$_{2A}$ receptors in pyramidal neurons of prefrontal cortex. Cereb Cortex 14:281–299

Andlin-Sobocki P, Jönsson B, Wittchen HU, Olesen J (2005) Cost of disorders of the brain in Europe. Eur J Neurol 12:1–27

Andrade R, Malenka RC, Nicoll RA (1986) G-protein couples serotonin and GABAB receptors to the same channels in hippocampus. Science 234:1261–1265

Artigas F, Peréz V, Alvaréz E (1994) Pindolol induces a rapid improvement of depressed patients treated with serotonin reuptake inhibitors. Arch Gen Psychiatry 51:248–251

Artigas F, Romero L, deMontigny C, Blier P (1996) Acceleration of the effect of selected antidepressant drugs in major depression by 5-HT$_{1A}$ antagonists. Trends Neurosci 19:378–383

Baker M (2010) Homing in on delivery. Nature 464:1225–1228

Ballesteros J, Callado LF (2004) Effectiveness of pindolol plus serotonin uptake inhibitors in depression: a meta-analysis of early and late outcomes from randomized controlled trials. J Affect Disord 79:137–147

Blier P, deMontigny C (1994) Current advances and trends in the treatment of depression. Trends Pharmacol Sci 15:220–226

Bohmaker K, Bordi F, Meller E (1992) The effects of pertussis toxin on dopamine D2 and serotonin 5-HT$_{1A}$ autoreceptor-mediated inhibition of neurotransmitter synthesis: relationship to receptor reserve. Neuropharmacology 31:451–459

Bortolozzi A, Amargós-Bosch M, Toth M, Artigas F, Adell A (2004) In vivo efflux of serotonin in the dorsal raphe nucleus of 5-HT$_{1A}$ receptor knockout mice. J Neurochem 88:1373–1379

Bortolozzi A, Valdizán E, Ferrés-Coy A, Pilar MF, Vargas V, Vidal R, Cortés R, Pazos A, Montefeltro A, Artigas F (2011) siRNA-induced reduction of the expression of the serotonin transporter gene as a new antidepressant strategy. 41st Annual Meeting of the Society for Neuroscience, Abstract 907.03

Bortolozzi A, Castañé A, Semakova J, Santana N, Alvarado G, Cortés R, Ferrés-Coy A, Fernández G, Carmona MC, Toth M, Perales JC, Montefeltro A, Artigas F (2012) Selective siRNA-mediated suppression of 5-HT$_{1A}$ autoreceptors evokes strong antidepressant-like effects. Mol Psychiatry 17:612–623

Celada P, Puig MV, Casanovas JM, Guillazo G, Artigas F (2001) Control of dorsal raphe serotonergic neurons by the medial prefrontal cortex: Involvement of serotonin-1A, GABA(A), and glutamate receptors. J Neurosci 21:9917–9929

Cox RF, Meller E, Waszczak BL (1993) Electrophysiological evidence for a large receptor reserve for inhibition of dorsal raphe neuronal firing by 5-HT$_{1A}$ agonists. Synapse 14:297–304

Cryan JF, Mombereau C, Vassout A (2005) The tail suspension test as a model for assessing antidepressant activity: review of pharmacological and genetic studies in mice. Neurosci Biobehav Rev 29:571–625

D'Amato RJ, Largent BL, Snowman AM, Snyder SH (1987) Selective labeling of serotonin uptake sites in rat brain by [^{3}H]citalopram contrasted to labeling of multiple sites by [^{3}H]imipramine. J Pharmacol Exp Ther 242:364–371

Díaz-Mataix L, Scorza MC, Bortolozzi A, Toth M, Celada P, Artigas F (2005) Involvement of 5-HT$_{1A}$ receptors in prefrontal cortex in the modulation of dopaminergic activity: role in atypical antipsychotic action. J Neurosci 25:10831–10843

Dykxhoorn DM, Lieberman J (2006) Knocking down disease with siRNAs. Cell 126:231–235

Fakra E, Hyde LW, Gorka A, Fisher PM, Muñoz KE, Kimak M, Halder I, Ferrell RE, Manuck SB, Hariri AR (2009) Effects of HTR1A C(-1019)G on amygdala reactivity and trait anxiety. Arch Gen Psychiatry 66:33–40

Franklin KBJ, Paxinos G (2008) The mouse brain in stereotaxic coordinates, compact 3rd edition. Academic, New York

Gleason G, Liu B, Bruening S, Zupan B, Auerbach A, Mark W, Oh JE, Gal-Toth J, Lee F, Toth M (2010) The serotonin$_{1A}$ receptor gene as a genetic and prenatal maternal environmental factor in anxiety. Proc Natl Acad Sci USA 107:7592–7597

Gozlan H, Laporte AM, Thibault S, Schechter LE, Bolaños F, Hamon M (1994) Differential effects of N-ethoxycarbonyl-2-ethoxy-1,2-dihydroquinoline (EEDQ) on various 5-HT receptor binding sites in the rat brain. Neuropharmacology 33:423–431

Gross C, Zhuang X, Stark K, Ramboz S, Oosting R, Kirby L, Santarelli L, Beck S, Hen R (2002) Serotonin1A receptor acts during development to establish normal anxiety-like behavior in the adult. Nature 416:396–400

Haddjeri N, Blier P, deMontigny C (1998) Long-term antidepressant treatments result in a tonic activation of forebrain 5-HT$_{1A}$ receptors. J Neurosci 18:10150–10156

He M, Sibille E, Benjamin D, Toth M, Shippenberg T (2001) Differential effects of 5-HT1A receptor deletion upon basal and fluoxetine-evoked 5-HT concentrations as revealed by in vivo microdialysis. Brain Res 902:11–17

Heidel JD, Hu S, Liu XF, Triche TJ, Davis ME (2004) Lack of interferon response in animals to naked siRNAs. Nat Biotechnol 22:1579–1582

Heisler LK, Chu HM, Brennan TJ, Danao JA, Bajwa P, Parsons LH, Tecott LH (1998) Elevated anxiety and antidepressant-like responses in serotonin 5-HT$_{1A}$ receptor mutant mice. Proc Natl Acad Sci USA 95:15049–15054

Innis RB, Aghajanian GK (1987) Pertussis toxin blocks 5-HT$_{1A}$ and GABA$_B$ receptor-mediated inhibition of serotonergic neurons. Eur J Pharmacol 143:195–204

Johnson DA, Gartside SE, Ingram CD (2002) 5-HT$_{1A}$ receptor mediated autoinhibition does not function at physiological firing rates: evidence from in vitro electrophysiological studies in the rat dorsal raphe nucleus. Neuropharmacology 43:959–965

Judge AD, Sood V, Shaw JR, Fang D, McClintock K, MacLachlan I (2005) Sequence-dependent stimulation of the mammalian innate immune response by synthetic siRNA. Nat Biotechnol 23:457–462

Knobelman DA, Hen R, Blendy JA, Lucki I (2001) Regional patterns of compensation following genetic deletion of either 5-hydroxytryptamine(1A) or 5-hydroxytryptamine(1B) receptor in the mouse. J Pharmacol Exp Ther 298:1101–1107

Krishnan V, Nestler EJ (2008) The molecular neurobiology of depression. Nature 455:894–902

Kumar P, Wu H, McBride JL, Jung KE, Kim MH, Davidson BL, Lee SK, Shankar P, Manjunath N (2007) Transvascular delivery of small interfering RNA to the central nervous system. Nature 448:39–43

Lemonde S, Turecki G, Bakish D, Du L, Hrdina PB, Bown CD, Sequeira A, Kushwaha N, Morris SJ, Basak A, Ou XM, Albert PR (2003) Impaired repression at a 5-hydroxytryptamine$_{1A}$ receptor gene polymorphism associated with major depression and suicide. J Neurosci 23:8788–8799

Li BJ, Tang Q, Cheng D, Qin C, Xie FY, Wei Q, Xu J, Liu Y, Zheng BJ, Woodle MC, Zhong N, Lu PY (2005) Using siRNA in prophylactic and therapeutic regimens against SARS coronavirus in Rhesus macaque. Nat Med 11:944–951

Lucki I (1997) The forced swimming test as a model for core and component behavioral effects of antidepressant drugs. Behav Pharmacol 8:523–532

Mannoury la Cour C, Boni C, Hanoun N, Lesch KP, Hamon M, Lanfumey L (2001) Functional consequences of 5-HT transporter gene disruption on 5-HT$_{1A}$ receptor-mediated regulation of dorsal raphe and hippocampal cell activity. J Neurosci 21:2178–2185

Martin KF, Phillips I, Hearson M, Prow MR, Heal DJ (1992) Characterization of 8-OH-DPAT-induced hypothermia in mice as a 5-

HT_{1A} autoreceptor response and its evaluation as a model to selectively identify antidepressants. Br J Pharmacol 107:15–21

Moss EG, Taylor JM (2003) Small-interfering RNAs in the radar of the interferon system. Nat Cell Biol 5:771–772

Murray CJL, López AD (1997) Alternative projections of mortality and disability by cause 1990–2020: Global Burden of Disease Study. Lancet 349:1498–1504

Neff CD, Abkevich V, Packer JC, Chen Y, Potter J, Riley R, Davenport C, DeGrado Warren J, Jammulapati S, Bhathena A, Choi WS, Kroeger PE, Metzger RE, Gutin A, Skolnick MH, Shattuck D, Katz DA (2009) Evidence for HTR1A and LHPP as interacting genetic risk factors in major depression. Mol Psychiatry 14:621–630

Parks CL, Robinson PS, Sibille E, Shenk T, Toth M (1998) Increased anxiety of mice lacking the $serotonin_{1A}$ receptor. Proc Natl Acad Sci USA 95:10734–10739

Pattij T, Groenink L, Hijzen TH, Oosting RS, Maes RA, van der Gugten J, Olivier B (2002) Autonomic changes associated with enhanced anxiety in 5-HT(1A) receptor knockout mice. Neuropsychopharmacology 27:280–390

Pazos A, Palacios JM (1985) Quantitative autoradiographic mapping of serotonin receptors in the rat brain. I. Serotonin-1 receptors. Brain Res 346:205–230

Piñeyro G, Blier P (1999) Autoregulation of serotonin neurons: role in antidepressant drug action. Pharmacol Rev 51:533–591

Pompeiano M, Palacios JM, Mengod G (1992) Distribution and cellular localization of mRNA coding for $5\text{-}HT_{1A}$ receptor in the rat brain: correlation with receptor binding. J Neurosci 12:440–453

Porsolt RD, Bertin A, Jalfre M (1978) Behavioural despair in rats and mice: strain differences and the effects of imipramine. Eur J Pharmacol 51:291–294

Portella MJ, de Diego-Adeliño J, Ballesteros J, Puigdemont D, Oller S, Santos B, Álvarez E, Artigas F, Pérez V (2011) Can we really accelerate and enhance the selective serotonin reuptake inhibitor antidepressant effect? A randomized clinical trial and a meta-analysis of pindolol in nonresistant depression. J Clin Psychiatry 72:962–969

Ramboz S, Oosting R, Amara DA, Kung HF, Blier P, Mendelsohn M, Mann JJ, Brunner D, Hen R (1998) Serotonin receptor1A knockout: an animal model of anxiety-related disorder. Proc Natl Acad Sci USA 95:14476–14481

Riad M, Garcia S, Watkins KC, Jodoin N, Doucet E, Langlois X, el Mestikawy S, Hamon M, Descarries L (2000) Somatodendritic localization of $5\text{-}HT_{1A}$ and preterminal axonal localization of $5\text{-}HT_{1B}$ serotonin receptors in adult rat brain. J Comp Neurol 417:181–194

Richardson-Jones JW, Craige CP, Guiard BP, Stephen A, Metzger KL, Kung HF, Gardier AM, Dranovsky A, David DJ, Beck SG, Hen R, Leonardo ED (2010) $5\text{-}HT_{1A}$ autoreceptor levels determine vulnerability to stress and response to antidepressants. Neuron 65:40–52

Richardson-Jones JW, Craige CP, Nguyen TH, Kung HF, Gardier AM, Dranovsky A, Guiard BP, Beck SG, Hen R, Leonardo ED (2011) Serotonin-1A autoreceptors are necessary and sufficient for the normal formation of circuits underlying innate anxiety. J Neurosci 31:6008–6018

Richer M, Hen R, Blier P (2002) Modification of serotonin neuron properties in mice lacking 5-HT1A receptors. Eur J Pharmacol 435:195–203

Romero L, Artigas F (1997) Preferential potentiation of the effects of serotonin uptake inhibitors by $5\text{-}HT_{1A}$ receptor antagonists in the dorsal raphe pathway: role of somatodendritic autoreceptors. J Neurochem 68:2593–2603

Santana N, Bortolozzi A, Serrats J, Mengod G, Artigas F (2004) Expression of $serotonin_{1A}$ and $serotonin_{2A}$ receptors in pyramidal and GABAergic neurons of the rat prefrontal cortex. Cereb Cortex 14:1100–1109

Scorza MC, Lladó-Pelfort L, Oller S, Cortés R, Puigdemont D, Portella MJ, Pérez-Egea R, Alvarez E, Celada P, Pérez V, Artigas F (2012) Preclinical and clinical characterization of the selective serotonin-1A receptor antagonist DU-125530 for antidepressant treatment. Br J Pharmacol. doi:10.1111/j.1476-5381.2011.01770.x

Sledz CA, Holko M, de Veer MJ, Silverman RH, Williams BR (2003) Activation of the interferon system by short-interfering RNAs. Nat Cell Biol 5:834–839

Song E, Zhu P, Lee SK, Chowdhury D, Kussman S, Dykxhoorn DM, Feng Y, Palliser D, Weiner DB, Shankar P, Marasco WA, Lieberman J (2005) Antibody mediated in vivo delivery of small interfering RNAs via cell-surface receptors. Nat Biotechnol 23:709–717

Soutschek J, Akinc A, Bramlage B, Charisse K, Constien R, Donoghue M, Elbashir S, Geick A, Hadwiger P, Harborth J, John M, Kesavan V, Lavine G, Pandey RK, Racie T, Rajeev KG, Röhl I, Toudjarska I, Wang G, Wuschko S, Bumcrot D, Koteliansky V, Limmer S, Manoharan M, Vornlocher HP (2004) Therapeutic silencing of an endogenous gene by systemic administration of modified siRNAs. Nature 432:173–178

Stockmeier CA, Shapiro LA, Dilley GE, Kolli TN, Friedman F, Rajkowska G (1998) Increased $serotonin_{1A}$ autoreceptors in the midbrain of suicide victims with major depression—postmortem evidence for decreased serotonin activity. J Neurosci 18:7394–7401

Sullivan GM, Ogden RT, Oquendo MA, Kumar JS, Simpson N, Huang YY, Mann JJ, Parsey RV (2009) Positron emission tomography quantification of serotonin-1A receptor binding in medication-free bipolar depression. Biol Psychiatry 66:223–230

Thakker DR, Natt F, Hüsken D, Maier R, Müller M, van der Putten H, Hoyer D, Cryan JF (2004) Neurochemical and behavioral consequences of widespread gene knockdown in the adult mouse brain by using nonviral RNA interference. Proc Natl Acad Sci USA 101:17270–17275

Thakker DR, Natt F, Hüsken D, van der Putten H, Maier R, Hoyer D, Cryan JF (2005) siRNA-mediated knockdown of the serotonin transporter in the adult mouse brain. Mol Psychiatry 10:782–789

Supplementary Material

Acute 5-HT_{1A} autoreceptor knockdown increases antidepressant responses and serotonin release in stressful conditions

Albert Ferrés-Coy[1,3], Noemí Santana[1,3], Anna Castañé[1,3], Roser Cortés[1,4], María C Carmona[5], Miklos Toth[6], Andrés Montefeltro[5], Francesc Artigas[1,3], Analía Bortolozzi[1,2,3]

[1]Department of Neurochemistry and Neuropharmacology, IIBB - CSIC - IDIBAPS, Barcelona, Spain

[2]Institut d'Investigacions Biomèdiques August Pi i Sunyer (IDIBAPS), Barcelona, Spain

[3]Centro de Investigación Biomédica en Red de Salud Mental (CIBERSAM), Madrid, Spain.

[4]Centro de Investigación Biomédica en Red de Enfermedades Neurodegenerativas (CIBERNED), Madrid, Spain

[5]n-Life Therapeutics, S.L., La Coruña, Spain

[6]Department of Pharmacology, Weill Medical College, Cornell University, NY, USA

Correspondence should be addressed to Dr. Analía Bortolozzi; Dept of Neurochemistry and Neuropharmacology, IIBB-CSIC-IDIBAPS. C/ Roselló 161, 6th floor, 08036 Barcelona, Spain. Phone: +3493-363 8300; Fax: +3493-363 8301; e-mail: abbnqi@iibb.csic.es

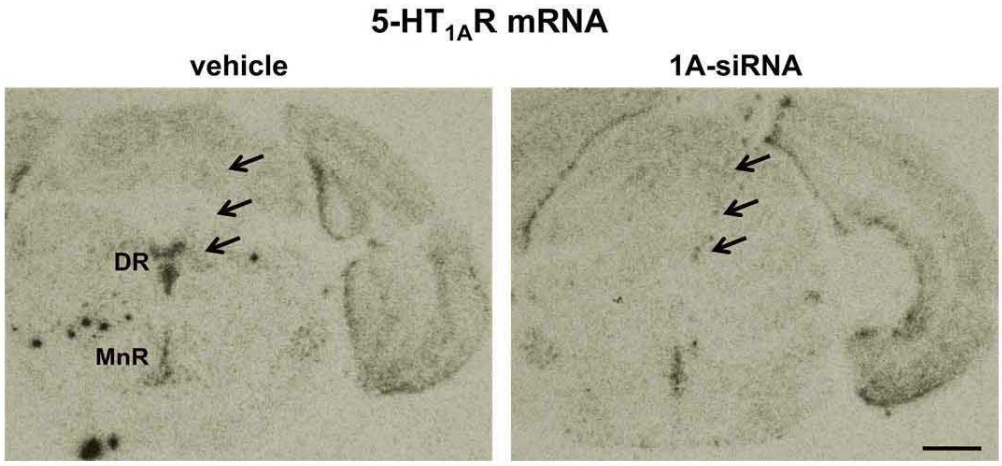

Supplementary Figure S1. Representative coronal brain sections showing 1A-siRNA-induced reduction of 5-HT_{1A}R expression in dorsal raphe nucleus (DR) assessed by in situ hybridization. The arrows indicate the track left by the microinfusion capillary microcannula. Note that the lack of effect on 5-HT_{1A}R expression in medial raphe nucleus (MnR) indicating that 1A-siRNA effect is restricted to the site of application site. Note also the minimal tissue damage produced by the microcannula. Scale bar: 1 mm

4.3. Trabajo 3

RNAi-mediated serotonin transporter suppression rapidly increases serotonergic neurotransmission and hippocampal neurogenesis

A Ferrés-Coy, F Pilar-Cuéllar, R Vidal, V Paz, M Masana, R Cortés, MC Carmona, L Campa, A Pazos, A Montefeltro, EM Valdizán, F Artigas and A Bortolozzi

Translational Psychiatry. 2013 Jan; 15;3e211

El SERT tiene un papel fundamental en la neurotransmisión serotoninérgica, pues controla la fracción activa de 5-HT en la sinapsis. Además, el SERT es la diana principal de los fármacos antidepresivos SSRI, de primera elección en la práctica clínica. Los tratamientos con SSRI promueven la internalización del SERT de la membrana plasmática al citosol, sin alterar la expresión del mRNA del SERT. Este hecho junto con la pérdida de la función del autoreceptor 5-HT_{1A} favorece la neurotransmisión serotoninérgica en el cerebro contribuyendo a la acción terapéutica de los SSRI. Sin embargo, estos efectos suceden después de tratamientos prolongados con SSRI. En el presente trabajo nos preguntamos si el silenciamiento de la expresión del SERT mediante siRNAs podría ser una estrategia terapéutica más rápida y efectiva que el clásico bloqueo farmacológico con SSRI.

Los resultados indicaron que la infusión local de una secuencia no conjugada de siRNA contra el SERT (SERT-siRNA) en el DR de ratón reduce selectivamente los niveles de mRNA y proteína del SERT. Este efecto no fue observado después del tratamiento con el SSRI fluoxetina indicando diferencias en el mecanismo de regulación del SERT entre ambos tratamientos. Además, el tratamiento con el SERT-siRNA durante 4 días modificó variables consideradas marcadores de acción antidepresiva en ratones que incluyeron: 1) incremento de la concentración de 5-HT en áreas cerebrales de proyección, 2) reducción de la expresión y función del autoreceptor 5-HT_{1A}, 3) incremento de la neurogénesis y 4) la expresión de genes

relacionados con la neuroplasticidad en el HPC. Efectos similares fueron observados después de 15 días de tratamiento con fluoxetina.

Conjuntamente con los trabajos previos, este estudio ilustra el potencial terapéutico de las estrategias basadas en RNAi para el tratamiento de la depresión. En particular, nuestros datos indican la relevancia de la modulación post-transcripcional del SERT como una nueva aproximación terapéutica para desarrollar antidepresivos de acción rápida.

Citation: Transl Psychiatry (2013) 3, e211; doi:10.1038/tp.2012.135

www.nature.com/tp

RNAi-mediated serotonin transporter suppression rapidly increases serotonergic neurotransmission and hippocampal neurogenesis

A Ferrés-Coy[1,2], F Pilar-Cuellar[2,3], R Vidal[2,3], V Paz[1,2], M Masana[1,2,7], R Cortés[1,4], MC Carmona[5], L Campa[1,2], Á Pazos[2,3], A Montefeltro[5], EM Valdizán[2,3], F Artigas[1,2] and A Bortolozzi[1,2,6]

Current antidepressants, which inhibit the serotonin transporter (SERT), display limited efficacy and slow onset of action. Here, we show that partial reduction of SERT expression by small interference RNA (SERT-siRNA) decreased immobility in the tail suspension test, displaying an antidepressant potential. Moreover, short-term SERT-siRNA treatment modified mouse brain variables considered to be key markers of antidepressant action: reduced expression and function of 5-HT_{1A}-autoreceptors, elevated extracellular serotonin in forebrain and increased neurogenesis and expression of plasticity-related genes (*BDNF, VEGF, Arc*) in hippocampus. Remarkably, these effects occurred much earlier and were of greater magnitude than those evoked by long-term fluoxetine treatment. These findings highlight the critical role of SERT in serotonergic function and show that the reduction of SERT expression regulates serotonergic neurotransmission more potently than pharmacological blockade of SERT. The use of siRNA-targeting genes in serotonin neurons (SERT, 5-HT_{1A}-autoreceptor) may be a novel therapeutic strategy to develop fast-acting antidepressants.
Translational Psychiatry (2013) **3,** e211; doi:10.1038/tp.2012.135; published online 15 January 2013

Introduction

Despite the high prevalence of depression and its considerable socioeconomic impact, its pathophysiological mechanisms remain poorly understood.[1–3] Serotonin (5-HT) participates in the etiology and treatment of major depression, being the selective serotonin reuptake inhibitors (SSRIs), the most common antidepressant therapy. However, SSRIs need to be administered for long time periods before clinical improvement emerges, and fully remit depressive symptoms in only one third of patients.[4–6]

The serotonin transporter (SERT) is a key regulator of serotonergic neurotransmission, as it controls the active fraction of 5-HT. In the brain, SERT is localized to raphe 5-HT neurons at somatodendritic and terminal levels.[7–9] SERT blockade by SSRIs (showing nM affinity for SERT)[10] initiates the chain of events leading eventually to clinical improvement. Long-term SSRI treatment promotes an internalization of SERT from the cell surface in 5-HT neurons without affecting SERT mRNA expression.[11–15] In addition to loss of 5-HT_{1A}-autoreceptor function,[16–18] SERT down-regulation may enhance forebrain 5-HT neurotransmission contributing to the therapeutic action of SSRIs.[19,20]

Polymorphic variations in SERT transcriptional region—leading to reduced SERT expression and function—are involved in multiple neuropsychiatric disorders, including major depression,[21–25] and in the clinical response to SSRI.[26,27] SERT-knockout mice were generated to gain further insight into the role of SERT in the pathophysiology and treatment of depression.[28,29] However, these mice showed depression-related behaviors attributable to the developmental changes that result from SERT early-life absence and the perturbed 5-HT function.[30–32] Thus, while SERT-knockout mice represent a useful model to investigate disorders involving genetic alterations in SERT during early life, they are less appropriate to study downstream changes of 5-HT transmission secondary to SERT blockade in adulthood.

RNA interference (RNAi) has a critical role in regulating gene expression.[33,34] It also provides new alternatives to pharmacological treatments to modulate brain neurotransmission through the use of exogenous small interference RNA (siRNA). Recent studies have shown the feasibility to silence the expression of critical genes in 5-HT neurons, such as SERT and the 5-HT_{1A}-autoreceptor.[18,35] Given the above limitations of SERT-knockout mice, here we evaluated the specificity and selectivity of partial SERT suppression in adult mice, following short-term SERT-siRNA treatment. We examined downstream changes on brain variables linked to antidepressant efficacy and compared SERT-siRNA effects with those of a standard SSRI (fluoxetine) treatment. The results indicate that the post-transcriptional regulation of

[1]Department of Neurochemistry and Neuropharmacology, IIBB-CSIC, IDIBAPS, Barcelona, Spain; [2]Centro de Investigación Biomédica en Red de Salud Mental (CIBERSAM), ISCIII, Madrid, Spain; [3]Institute of Biomedicine and Biotechnology of Cantabria (IBBTEC; UC-CISC-SODERCAN), Santander, Spain; [4]Centro de Investigación Biomédica en Red de Enfermedades Neurodegenerativas (CIBERNED), ISCIII, Madrid, Spain; [5]nLife Therapeutics, S.L., Granada, Spain and [6]Institut d'Investigacions Biomèdiques August Pi i Sunyer (IDIBAPS), Barcelona, Spain
Correspondence: Dr A Bortolozzi, Deparment of Neurochemistry and Neuropharmacology, IIBB-CSIC-IDIBAPS, Barcelona 08036, Spain.
E-mail: abbnqi@iibb.csic.es
[7]Current address: Max Planck Institute of Psychiatry, Munich D-80804, Germany
Keywords: BDNF; fast-acting antidepressants; neurogenesis; RNAi; serotonin; SERT transporter
Received 24 July 2012; revised 8 November 2012; accepted 10 November 2012

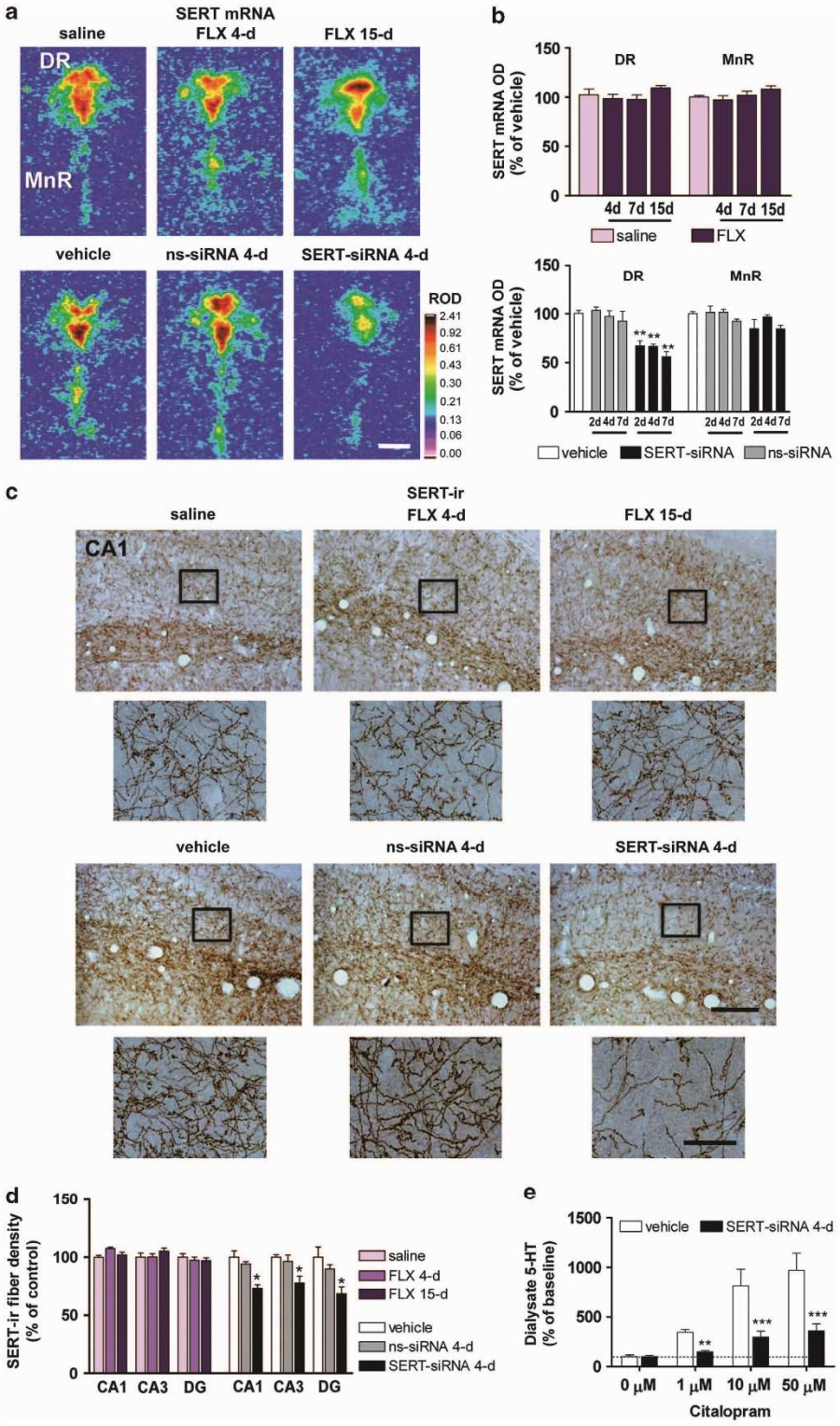
a
SERT mRNA
saline
FLX 4-d
FLX 15-d
DR
MnR
vehicle
ns-siRNA 4-d
SERT-siRNA 4-d
ROD
2.41
0.92
0.61
0.43
0.30
0.21
0.13
0.06
0.00
b
SERT mRNA OD (% of vehicle)
DR
MnR
4d 7d 15d
saline
FLX
2d 4d 7d
vehicle
SERT-siRNA
ns-siRNA
c
SERT-ir
CA1
d
SERT-ir fiber density (% of control)
CA1 CA3 DG
e
Dialysate 5-HT (% of baseline)
0 μM 1 μM 10 μM 50 μM
Citalopram

SERT may constitute a target for fast-acting antidepressants, thus bringing RNAi closer to the clinic as a potential therapy for major depression.

Materials and methods

Animals. Male C57BL/6J mice (10–14 weeks; Charles River, Lyon, France) were housed under controlled conditions (22 ± 1 °C; 12 h light/dark cycle) with food and water available *ad libitum*. Animal procedures were conducted in accordance with standard ethical guidelines (EU regulations L35/118/12/1986) and approved by the local ethical committee.

Drug/siRNA treatments. SERT-targeting siRNA (nt:1230–1250, GenBank accession NM_010484) and an unrelated siRNA with no homology to mouse genome (nonsense siRNA, ns-siRNA) were used (Life Technology, Madrid, Spain). The siRNA sequences are shown in Supplementary Table S1.

Mice were anesthetized (pentobarbital, 40 mg kg $^{-1}$, intraperitoneally, i.p.) and silica capillary microcannula (110 μm-outer diameter (OD), 40 μm-inner diameter (ID); Polymicro Technologies, Madrid, Spain) were stereotaxically implanted into the dorsal raphe nucleus (DR; coordinates in mm: anteroposterior, −4.5; mediolateral, −1.0; dorsoventral, −4.4; with a lateral angle of 20°).[36] Local siRNA microinfusion was performed with a perfusion pump at 0.5 μl min $^{-1}$ 24 h after surgery in awake mice as described previously.[18] siRNAs were prepared in artificial cerebrospinal fluid (125 mM NaCl, 2.5 mM KCl, 1.26 mM $CaCl_2$ and 1.18 mM $MgCl_2$ with 5% glucose) and infused intra-DR once daily at the dose of 10 μg μl $^{-1}$ (0.7 nmol per dose). Mice received two dose in 2 consecutive days, or four dose in 5 days (days 1, 2, 4 and 5), and were killed on 3rd or 6th day, respectively. An additional group of mice received seven dose in 9 days (days 1, 2, 3, 5, 6, 8 and 9) and was killed on 10th-day. In the last group, only *in situ* hybridization and autoradiography studies were performed (see below). Control mice received artificial cerebrospinal fluid.

Fluoxetine (Tocris, Madrid, Spain) was prepared in saline and was administered once daily at 20 mg kg $^{-1}$ dose, i.p. for 4, 7 or 15 days. Mice were killed on 5th, 8th or 16th day, respectively. Control mice received saline.

In situ hybridization and autoradiographic studies

Tissue preparation. Mice were killed by pentobarbital overdose and brains rapidly removed, frozen on dry ice and stored at −80 °C. Tissue sections (14 μm thick-coronal) were cut using a microtome-cryostat (HM500-OM, Microm, Walldorf, Germany), thaw-mounted onto 3-aminopropyltriethoxysilane (Sigma-Aldrich, Madrid, Spain)-coated slides and kept at −20 °C until use.

In situ hybridization. Antisense oligoprobes [^{33}P]-labeling and *in situ* hybridization procedures were carried out as described previously.[18] Mouse SERT, 5-HT_{1A}R, tryptophan hydroxylase 2, Ki-67, brain-derived neurotrophic factor (BDNF), vascular endothelial growth factor (VEGF), activity-regulated cytoskeletal protein (Arc), and cAMP response element binding protein (CREB) probes were synthesized by IBA-GmbH (Göttingen, Germany). Details can be found in the Supplementary Information.

Receptor autoradiography. The autoradiographic binding assays for 5-HT_{1A}R, SERT and norepinephrine transporter were performed using the following radioligands: (a) [^{3}H]-8-OH-DPAT (233 Ci mmol $^{-1}$), (b) [^{3}H]-citalopram (70 Ci mmol $^{-1}$) and (c) [^{3}H]-nisoxetine (85 Ci mmol $^{-1}$), respectively (Perkin-Elmer, Madrid, Spain).[18,37] Experimental conditions are summarized in Supplementary Table S2.

5-HT_{1A}R-stimulated [^{35}S]GTPγS autoradiography. Labeling of DR sections with [^{35}S]GTPγS was performed as described previously.[38] Autoradiograms were analyzed and the relative optical densities (ROD) were obtained using a computer-assisted image analyzer (AIS, Imaging Research, St Catherines, Ontario, Canada). Details are shown in Supplementary information.

5-Bromo-2′-deoxyuridine administration. 5-Bromo-2′-deoxyuridine was purchased from Sigma-Aldrich (Madrid, Spain) and dissolved in saline solution. Mice were injected with 4×75 mg kg $^{-1}$ 5-Bromo-2′-deoxyuridine every 2 h, i.p., the last day of antidepressant treatments. Mice were killed 24 h later.

Immunohistochemistry. Animals were deeply anesthetized with pentobarbital and transcardially perfused with 4% paraformaldehyde in sodium-phosphate buffer (pH = 7.4). Brains were collected, post-fixed 24 h at 4 °C in the same solution, and then placed in gradient sucrose or phosphate-buffered saline 10–30% for 2 days at 4 °C. After

Figure 1 Serotonin transporter-small interference RNA (SERT-siRNA) treatment, but not fluoxetine (FLX), downregulates SERT mRNA and protein levels. Mice were infused with two-, four- or seven-dose SERT- or nonsense siRNA (ns-siRNA) (10 μg–0.7 nmol per day) or vehicle into the dorsal raphe nucleus (DR). Other groups of mice were treated with 4, 7 or 15-day FLX (20 mg kg $^{-1}$ per day, intraperitoneally) or saline. (**a**) Representative coronal brain sections showing reduced SERT expression in the DR of mice treated with SERT-siRNA (four dose), but not with FLX, as assessed by *in situ* hybridization. Scale bar = 500 μm. (**b**) Bar graphs showing no differences in SERT mRNA level in DR and median raphe nucleus (MnR) of FLX-treated mice. However, SERT-siRNA at different doses significantly reduced SERT mRNA level exclusively in DR ($n = 5$–10 mice per group). Two-way analysis of variance revealed a significant effect of group ($F_{2,33} = 59.32$, $P < 0.001$). (**c**) Representative images of SERT-immunoreactive (SERT-ir) axons in the hippocampal CA1 region. Short-term SERT-siRNA treatment (four dose) significantly decreased the target SERT protein density as compared with vehicle and ns-siRNA-treated mice. In contrast, FLX treatment did not alter SERT-ir axon density. Box insets represent regions of high-magnification photomicrographs. Scale bars: lower magnification = 100 μm and high magnification = 20 μm. (**d**) SERT-ir fiber density in different hippocampal subfields including CA1, CA2, CA3 and dentate gyrus (DG) was measured and expressed as the percentage of the density in the respective vehicle-treated mice ($n = 4$–6 mice per group). Two-way ANOVA showed an effect of group ($F_{2,11} = 11.16$, $P < 0.01$). (**e**) Local citalopram (SSRI) infusion by reverse dialysis induced a concentration-dependent increase of extracellular 5-HT in caudate putamen (CPu) of vehicle-treated mice ($n = 7$). However, this effect was lesser marked in SERT-siRNA-treated mice ($n = 9$). Two-way ANOVA showed an effect of group ($F_{1,14} = 17.17$, $P < 0.0001$), concentration ($F_{3,42} = 27.06$, $P < 0.0001$) and group-by-concentration interaction ($F_{3,42} = 7.72$, $P < 0.0001$). $^*P < 0.05$, $^{**}P < 0.01$, $^{***}P < 0.001$ compared with vehicle and ns-siRNA-treated mice. Values are mean ± s.e.m.

cryopreservation, 30-μm-thick free-floating coronal brain sections were processed for immunohistochemical visualization of SERT, BdrU, Ki-67, NeuroD, NeuN, Doublecortin (DCX), GFAP and IBA-1 by using the biotin-labeled antibody procedure. Details are shown in Supplementary Information.

Intracerebral microdialysis. Extracellular serotonin concentration was measured by *in vivo* microdialysis.[18,39] Details are shown in the Supplementary Information.

Tail suspension test. Mice were moved from the housing room to the testing area in their home cages and allowed to adapt to the new environment for at least 1 h before testing. Mice were suspended 30 cm above the bench by adhesive tape placed ~1 cm from the tip of the tail. The total duration of immobility during a 6 min test was measured.

Statistical analysis. Data are expressed as means ± s.e.m. Data were analyzed with Student's *t*-test, one- two- or three-way analysis of variance as appropriate followed by *post-hoc* test (Newman-Keuls). The level of significance was set at $P<0.05$.

Results

***In vivo* characterization of SERT knockdown in mice.** We first examined the feasibility to acutely suppress in vivo SERT expression in raphe 5-HT neurons using a SERT-siRNA. Mice were locally infused with: (a) vehicle, (b) ns-siRNA or (c) SERT-siRNA (10 μg per dose) into DR for 2 consecutive days using a protocol similar to that inducing 5-HT_{1A}-autoreceptor knockdown.[18,40] Histological analysis revealed a significant decrease of SERT expression in DR—but not in median raphe nucleus (MnR)—of SERT-siRNA-treated mice (SERT mRNA and binding levels were 63 ± 4% and 70 ± 8%, respectively versus vehicle and ns-siRNA-treated mice). Neither treatment altered the raphe expression of norepinephrine transporter, 5-HT_{1A}R and tryptophan hydroxylase 2 (Supplementary Figure S1a–d).

Next, we evaluated the potential neurotoxic effects of SERT-siRNA infusion by immunohistochemical staining for NeuN, GFAP and IBA-1 (neuronal, astrocyte and microglial markers, respectively). Compared with control groups (ns-siRNA and vehicle), SERT-siRNA-treated mice showed no loss of NeuN-positive neurons in DR. In addition, a mild increase in DR GFAP was noted in all experimental groups, likely due to the reactive astrogliosis secondary to the microcannula implant. Likewise, IBA-1-stained sections in each group showed no increase in activated microglia, except for within the injection tracts (Supplementary Figure S2a–c).

The functional impact of siRNA-induced acute SERT reduction was assessed by *in vivo* microdialysis in caudate putamen (CPu), a forebrain area exclusively innervated by DR 5-HT fibers.[41] Local 50 μM veratridine application produced a similar increase of extracellular 5-HT in CPu of all groups, indicating that SERT knockdown did not alter the impulse-dependent 5-HT release. However, 1 μM citalopram (SSRI) infusion by reverse dialysis increased 5-HT concentration in CPu of vehicle (170 ± 27% of baseline) and ns-siRNA-treated mice (180 ± 15%), but not of SERT-siRNA-treated mice (83 ± 8%), reflecting a decreased SERT expression/function in the latter group (Supplementary Figure S3a). In addition, fluoxetine administration (SSRI; 20 mg kg^{-1}, i.p.) enhanced extracellular 5-HT in CPu of vehicle-treated mice (8.0 ± 1.0 fmol per fraction), reaching the basal values in SERT-siRNA-treated mice (10.0 ± 0.6 fmol per fraction) (Supplementary Figure S3b). Next, the efficacy of SERT-siRNA infusion was tested in the tail suspension test, a highly reliable predictor of clinical antidepressant potential.[42,43] Mice treated with SERT-siRNA showed a significant reduction of the immobility time compared with control groups (Supplementary Figure S3c).

Different regulation of SERT mRNA and protein levels after SERT-siRNA or fluoxetine treatment. Following verification the effectiveness of SERT suppression by acute SERT-siRNA, we evaluated the effect on SERT regulation after short-term SERT-siRNA administration and its time course. Mice were infused intra-DR with four- or seven-dose

Figure 2 (**a–f**) Short-term serotonin transporter-small interference RNA (SERT-siRNA) treatment, but not fluoxetine (FLX), reduces 5-HT_{1A}-autoreceptor expression and function. Mice were infused with four or seven dose SERT- or nonsense siRNA (ns-siRNA; 10 μg per day) or vehicle into dorsal raphe nucleus (DR). Other groups of mice were treated with 4, 7 or 15-day FLX (20 mg kg^{-1} per day, intraperitoneally (i.p.) or saline. (**a**) Representative coronal midbrain sections showing [^{3}H]-8-OH-DPAT binding to 5-HT_{1A}R in DR. The arrow indicates the decreased DR 5-HT_{1A}R density in SERT-siRNA-treated mice (four dose). Scale bar = 2 mm. (**b**) Bar graphs showing no differences in DR 5-HT_{1A}R mRNA levels of vehicle- and FLX-treated mice. However, SERT-siRNA significantly reduced 5-HT_{1A}R mRNA level in DR compared with vehicle and ns-siRNA groups ($n=3$–5 mice per group). Two-way analysis of variance (ANOVA) revealed an effect of group ($F_{2,15}=22.59$, $P<0.001$). (**c**) Quantitative [^{3}H]-8-OH-DPAT binding showed a decreased DR 5-HT_{1A}R density after SERT-siRNA treatment, but not with FLX ($n=4$–7). Two-way ANOVA showed a significant effect of group ($F_{2,15}=20.69$, $P<0.001$). (**d**) Autoradiograms of coronal midbrain sections of mice showing 5-HT_{1A}R 8-OH-DPAT agonist-stimulated [^{35}S]GTPγS binding. Scale bar = 500 μm. (**e**) FLX induced a decreased DR 8-OH-DPAT-stimulated [^{35}S]GTPγS binding from days 7 to 15 of treatment ($n=5$–8). Two-way ANOVA showed an effect of group ($F_{3,25}=11.40$, $P<0.001$). However, SERT-siRNA produced a fast 5-HT_{1A}-autoreceptor desensitization detected after four dose treatment ($n=4$–8). Two-way ANOVA revealed an effect of group ($F_{2,31}=10.47$, $P<0.001$). (**f**) The 5-HT_{1A}R agonist 8-OH-DPAT (0.5 mg kg^{-1}, i.p.) decreased extracellular 5-HT concentration in ventral hippocampus (HPC) of saline- and FLX-treated mice (4-day), but not after 15-day FLX treatment ($n=5$–9). Two-way ANOVA showed an effect of group ($F_{2,18}=41.32$, $P<0.0001$), time ($F_{10,180}=13.96$, $P<0.001$) and interaction ($F_{20,180}=4.41$, $P<0.001$). Similarly, 8-OH-DPAT had no effect on ventral HPC 5-HT release in SERT-siRNA-treated mice (four-dose), unlike to control groups ($n=4$). Two-way ANOVA showed an effect of group ($F_{2,8}=23.13$, $P<0.0001$), time ($F_{10,80}=6.38$, $P<0.001$) and interaction ($F_{20,80}=4.41$, $P<0.001$). (**g–h**) Time course of the increase in extracellular 5-HT levels in forebrain. Mice received an intra-DR infusion of two or four dose siRNA or vehicle. Microdialysis experiments were performed on the 3rd or 6th day, respectively. In addition, groups of mice were treated with FLX (20 mg kg^{-1} per day, i.p.) or saline and microdialysis experiments were performed 24 h after the last administration on 2nd, 3rd, 4th, 5th, 7th, 8th and 16th day. (**g**) FLX treatment significantly increased extracellular 5-HT levels in caudate putamen (CPu) from six dose onwards, compared with saline-treated mice ($F_{13,80}=7.43$, $P<0.0001$; $n=7$–10 mice per group). In contrast, SERT-siRNA-treated mice displayed a larger and faster increase in CPu 5-HT levels, which was significantly different from control already after two-dose treatment ($F_{5,60}=32.52$, $P<0.0001$; $n=7$–12 mice per group). (**h**) Long-term FLX treatment (15 dose) also increased 5-HT levels in ventral HPC compared with saline-treated mice ($F_{3,20}=39.93$, $P<0.0001$; $n=4$–9). SERT-siRNA-treated mice (four dose) also showed a rapid and significant increase of HPC 5-HT levels relative to vehicle and ns-siRNA-treated mice ($F_{2,18}=14.51$, $P<0.001$; $n=4$–9 mice). ^^$P<0.01$, ^^^$P<0.001$ versus saline-treated mice; *$P<0.05$, **$P<0.01$, ***$P<0.001$ versus vehicle and ns-siRNA-treated mice. Values are mean ± s.e.m.

SERT- or ns-siRNA (10 μg per dose) or vehicle during 5 and 9 days, respectively. The effects on SERT expression were compared with those in mice treated with fluoxetine (20 mg kg^{-1} per day, i.p.) or saline for 4, 7 or 15 days.

Short-term SERT-siRNA infusion evoked a regionally selective (only in DR) and dose-dependent reduction of SERT mRNA expression. This reduction was not observed in control mice (vehicle and ns-siRNA) nor in any of the fluoxetine-treated groups (Figures 1a and b). As SERT is localized in the somatodendritic and terminal regions of raphe 5-HT neurons,[7] [^{3}H]-citalopram autoradiography was performed to quantify SERT-binding sites in different brain regions along the rostro-caudal axis. Repeated SERT-siRNA infusion, but not ns-siRNA, significantly reduced SERT binding by ~30%–40% in most brain regions analyzed. Differences in the extent of the reduction likely reflect the DR/MnR origin of serotonergic fibers in each region (Supplementary Figure S4).

In contrast, a specific [^{3}H]-citalopram signal was undetectable in fluoxetine-treated mice (4, 7 or 15 days), likely owing to the long half-life of fluoxetine. Additional SERT autoradiography binding was performed in fluoxetine-treated mice (4 or 7-day) and subjected to a 48–96 h washout before killed to reduce fluoxetine serum concentrations.[13,44] Even in these conditions, a specific [^{3}H]-citalopram binding was not observed (data not shown).

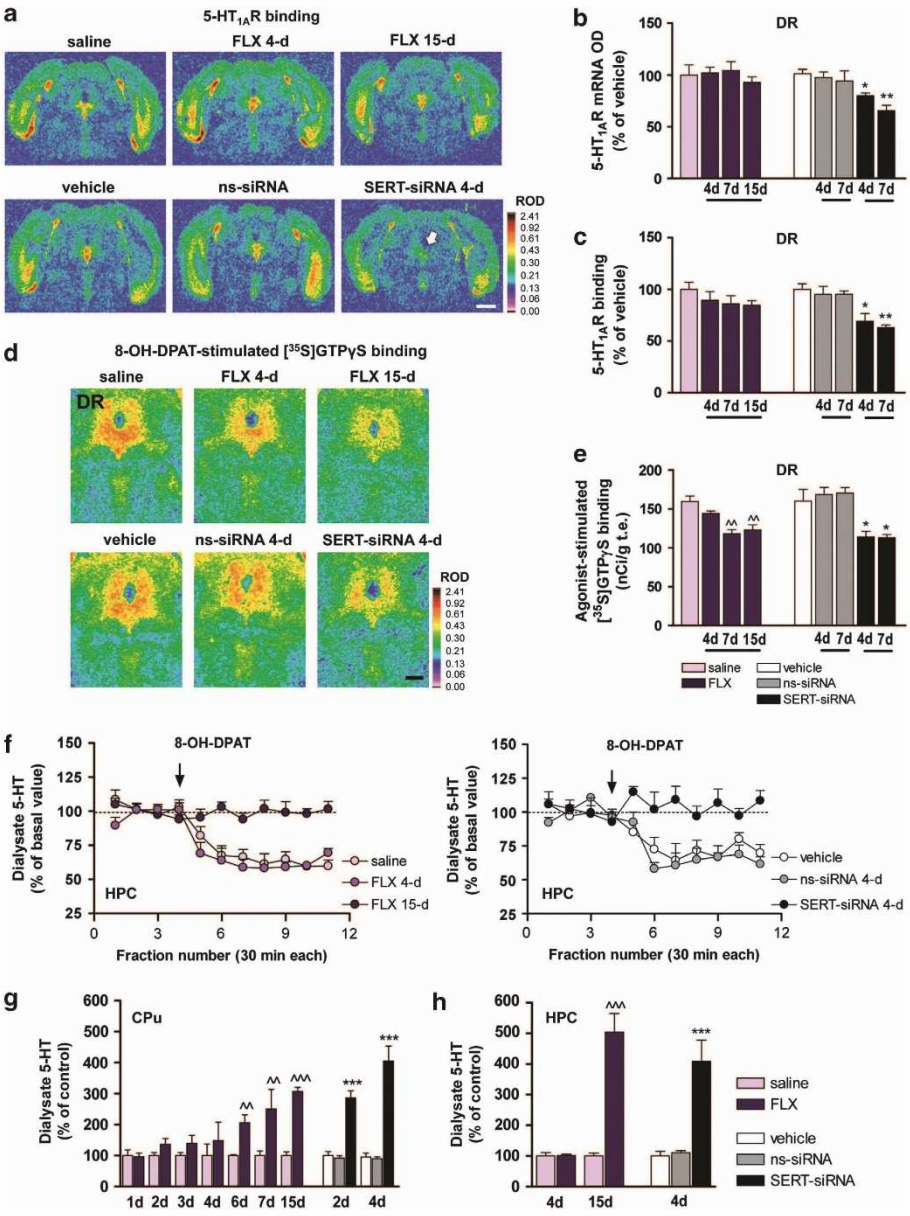

Next, we examined the density of SERT-containing fibers in several brain areas, including different hippocampus (HPC) subfields (Figure 1c and Supplementary Figure S5) where neurogenesis was evaluated (see below). Short-term SERT-siRNA treatment (four dose) caused a rapid and significant decrease of SERT-immunolabeling in different HPC areas relative to vehicle- and ns-siRNA-treated mice. However, SERT-immunolabeling was equal in fluoxetine-treated mice and their respective controls (Figures 1c and d). The presence of an immunohistochemical SERT signal in fluoxetine-treated mice indicates that the lack of specific [^{3}H]-citalopram binding was due to competence with fluoxetine present in the tissue sections. Likewise, these data highlight the different mechanism of regulation of SERT expression. Thus, whereas SERT-siRNA-induced post-transcriptional changes lead to SERT mRNA knockdown and a subsequent fall in protein density, we did not find an effect of fluoxetine on SERT expression, as previously reported.[45,46]

In agreement with this partial SERT suppression, a decreased SERT function was observed in SERT-siRNA-treated mice (four dose). Hence, local application of citalopram (1–10–50 μM) produced much smaller increases of extracellular 5-HT in the CPu relative to vehicle controls (Figure 1e).

Short-term SERT-siRNA treatment, but not fluoxetine, reduces 5-HT$_{1A}$-autoreceptor expression and function. The functional down-regulation of presynaptic 5-HT$_{1A}$R (5-HT$_{1A}$-autoreceptors) is required for the clinical antidepressant action.[16,38,47,48] Indeed, the degree of 5-HT$_{1A}$R-mediated inhibition of 5-HT by SSRIs has been used as a reliable index of their sensitivity.[49,50] As expected, 5-HT$_{1A}$-autoreceptor expression was unchanged in any of the fluoxetine-treated groups (Figures 2a–c). However, 7 and 15-day fluoxetine administration (but not 4-day) attenuated 8-OH-DPAT-stimulated [^{35}S]GTPγS binding in the DR, indicating a decrease in G-protein coupling efficiency of 5-HT$_{1A}$R (Figures 2d and e). In contrast, a short-term SERT-siRNA treatment significantly reduced 5-HT$_{1A}$-autoreceptor expression and produced a concomitant loss of function as assessed by [^{35}S]GTPγS binding (Figures 2a–e).

Likewise, the 5-HT$_{1A}$R agonist 8-OH-DPAT (0.5 mg kg^{-1}, i.p.) significantly decreased 5-HT release in the HPC of vehicle (62 ± 4% of baseline) and mice treated with fluoxetine for 4 days (61 ± 4%), but not in those treated for 15 days (99 ± 2%) (Figure 2f). Interestingly, 8-OH-DPAT did not reduce hippocampal 5-HT release in four-dose SERT-siRNA-treated mice (103 ± 5% of baseline), unlike in control groups (vehicle: 70 ± 3% and ns-siRNA: 65 ± 2%) (Figure 2f). This indicates a very fast attenuation of 5-HT$_{1A}$-autoreceptor sensitivity in SERT-siRNA-treated mice, as observed after long-term pharmacological blockade of SERT.[47,51]

Time course of forebrain extracellular 5-HT concentration after SERT-siRNA or fluoxetine treatment. We next assessed the kinetics of extracellular 5-HT levels after SERT-siRNA or fluoxetine treatment using *in vivo* microdialysis. Basal extracellular 5-HT levels in CPu and HPC of control mice were: 3.4 ± 0.3 fmol per fraction (n = 49) and 1.7 ± 0.1 fmol (n = 9) per fraction, respectively. Further, baseline 5-HT levels of mice implanted with a silica microcannula into DR were: 3.9 ± 0.4 fmol per fraction (CPu, n = 25) and 2.4 ± 0.5 fmol per fraction (HPC, n = 10). No significant differences were detected between groups.

Repeated fluoxetine administration induced a progressive and significant increase of 5-HT levels in CPu from days 6 to 15 of treatment compared to their respective saline-treated controls (Figure 2g). SERT-siRNA-treated mice displayed a larger and faster increase in CPu 5-HT levels, which was not seen in control groups. Extracellular 5-HT in CPu of mice treated with four doses of SERT-siRNA was greater than after 15-day fluoxetine administration (Figure 2g). Similar results were seen in HPC, where SERT-siRNA (four doses) increased extracellular 5-HT to the same extent than a 15-day treatment with fluoxetine (Figure 2h). Regional differences are likely owing to the greater contribution of DR axons in CPu versus HPC.[52]

SERT-siRNA treatment induces faster adult neurogenesis than fluoxetine. We then addressed whether the above temporal differences between SERT-siRNA and fluoxetine translated into the proliferative activity in dentate gyrus (DG), a key feature of antidepressant treatments. To this end, mice were injected with the proliferation marker BdrU on the last day of the antidepressant treatments. Twenty-four hours later, BdrU incorporation was quantified in DG. Remarkably, SERT-siRNA (four dose) significantly enhanced the number of BdrU-labeled cells to 144 ± 8% of vehicle-treated mice. No effect was observed in ns-siRNA-treated mice (Figures 3a and b). Detailed morphological analysis revealed that these cells were grouped in clusters, suggesting an acute induction of mitotic activity. Such clusters of BdrU-positive cells were detectable after 15-day (but not 4-day) fluoxetine treatment (BdrU-positive cells:

Figure 3 Serotonin transporter (SERT) silencing accelerates neural proliferation in the adult hippocampus compared with fluoxetine (FLX). Mice were infused with four dose SERT- or nonsense siRNA (ns-siRNA; 10 μg per day) or vehicle into dorsal raphe nucleus (DR). Other groups of mice were treated with 4 or 15-day FLX (20 mg kg^{-1} per day, intraperitoneally) or saline. (**a**) Representative images showing an increased number of 5-Bromo-2′-deoxyuridine (BdrU)-positive cells in the dentate gyrus (DG) of FLX-treated mice (15-day) or serotonin transporter-small interference RNA (SERT-siRNA)-treated mice (four dose) compared with their respective control mice. Box insets frame regions of high-magnification photomicrographs shown below. Scale bars: lower magnification = 100 μm and high magnification = 20 μm. (**b**) Cell proliferation was assessed by the number of BdrU-positive cells (n = 5–8 mice) and Ki-67-positive cells (n = 5–9 mice) in the granule cell layer. Quantitative analysis indicated a significant increase in both BdrU- and Ki-67-positive cell number for longer treatment with FLX (BdrU: $F_{2,20}$ = 53.16; Ki-67: $F_{2,17}$ = 20.72) or SERT-siRNA (BdrU: $F_{2,13}$ = 14.10; Ki-67: $F_{2,18}$ = 6.26). (**c**) Representative coronal brain sections showing Ki-67 expression in DG assessed by *in situ* hybridization. Scale bar = 100 μm. (**d**) Bar graph showing increased Ki-67 mRNA levels in DG following FLX (15-day) and SERT-siRNA (four dose) treatment as compared with respective control groups (n = 3–4 mice). One-way analysis of variance revealed a significant effect of group ($F_{4,11}$ = 9.73, P < 0.01). ^P < 0.05, ^^^P < 0.001 versus saline-treated mice; *P < 0.05, **P < 0.01 versus vehicle and ns-siRNA-treated mice. Values are mean ± s.e.m.

91 ± 5 and 229 ± 16% following 4- and 15-day fluoxetine relative to saline group) (Figures 3a and b). Moreover, we confirmed the effects on neural progenitor cell proliferation, assessing the intrinsic Ki-67 expression in DG.[53,54] Both Ki-67 mRNA level and Ki-67-positive cells were significantly increased in the DG of SERT-siRNA- and fluoxetine-treated mice following 4 and 15-day of administration, respectively, compared with their control groups (Figures 3b–d).

In addition, an increase in NeuroD-positive cells was seen in the subgranular cell layer of DG after four-dose SERT-

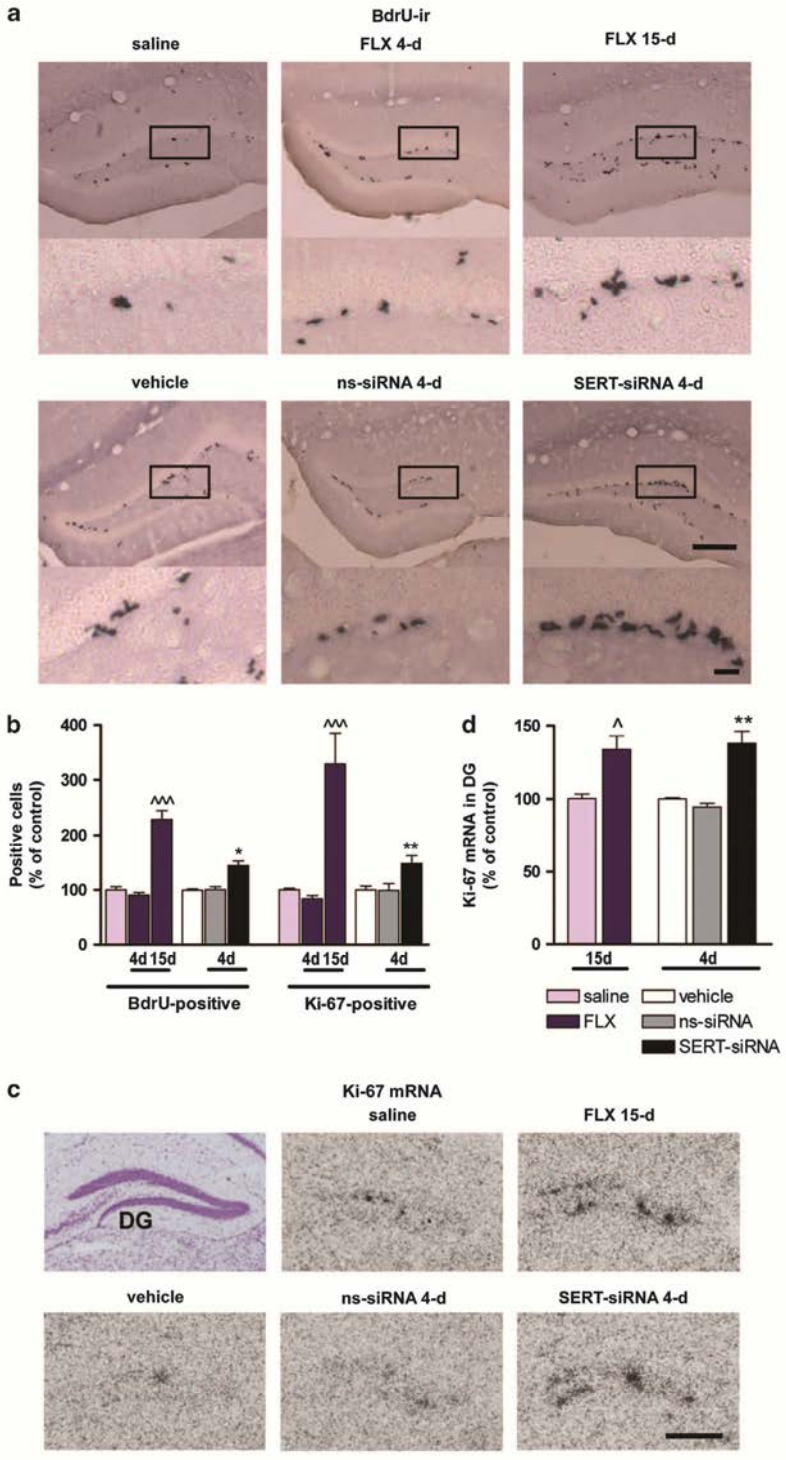

siRNA treatment (129 ± 5% of vehicle), whereas fluoxetine administration (15-day) led to a slight, but non-significant increase in the number of immature neurons (NeuroD-positive cells: 115 ± 10% of vehicle) (Figures 4a and b). To assess whether SERT-siRNA regulates neuronal cell migration, DCX-immunostaining was performed. SERT-siRNA treatment (four-dose) significantly enhanced the number of DCX-positive cells in the DG (137 ± 9% of vehicle) compared with control groups. Similar data were obtained after 15-day fluoxetine administration (DCX-positive cells: 121 ± 4% of vehicle) (Figures 4c and d).

Short-term SERT-siRNA treatment, but not fluoxetine, enhances hippocampal plasticity-associated gene expression. As the final step of the present study, we assessed whether SERT-siRNA (four dose) was able to increase the hippocampal expression of trophic factors such as BDNF and VEGF, which are known to be enhanced only after prolonged (2–3 weeks) antidepressant treatments.[55–57] We also examined the effects on the expression of the immediate early gene Arc and the transcription factor CREB, which are also regulated by chronic antidepressant treatments and contribute to the antidepressant efficacy.[58,59] We found that SERT-siRNA infusion (four dose) robustly and significantly increase BDNF mRNA levels in the different hippocampal areas (CA1: 134 ± 9%, CA3: 144 ± 9% and DG: 122 ± 2% of vehicle) (Figure 5a). A 15-day fluoxetine treatment (but not 4-day) increased BDNF mRNA expression only in DG (151 ± 25%). Likewise, SERT-siRNA (four dose) significantly enhanced VEGF expression in all HPC subfields (~125%), as produced by 15-day fluoxetine treatment (Figure 5b).

Furthermore, SERT-siRNA (four dose) significantly upregulated the Arc mRNA expression in CA1 and DG (~135%), an effect that was observed in DG only after 15-day fluoxetine treatment (190 ± 27%) (Figure 5c). In contrast to these changes, neither SERT-siRNA nor fluoxetine altered hippocampal CREB mRNA expression (Figure 5d).

Discussion

The present study shows that partial RNAi-based reduction of SERT expression in mouse DR has dramatic effects on serotonergic neurotransmission. Short-term SERT-siRNA treatment evoked a number of changes in behavioral, neurochemical and cellular variables predictive of therapeutic antidepressant activity, such as (i) reduced immobility time in the tail suspension test, (ii) increased extracellular 5-HT concentration, (iii) downregulated 5-HT_{1A}-autoreceptor expression/function, (iv) enhanced hippocampal neurogenesis and (v) increased hippocampal expression of plasticity-associated genes. Remarkably, these changes occurred much earlier and were in general of greater magnitude than those evoked by long-term SSRI-fluoxetine administration. Together with earlier reports,[18,35,40] this study illustrates the therapeutic potential of siRNA-based strategies in the treatment of major depression. In particular, our data highlight the relevance of post-transcriptional SERT regulation as a new therapeutic approach to develop fast-acting antidepressants.

We previously showed that unmodified siRNA infusion into the mouse DR and also, intracerebroventricular or intranasal administration of a conjugated siRNA can efficiently and selectively reduce 5-HT_{1A}-autoreceptor expression in 5-HT neurons, thus evoking antidepressant responses.[18,40] Here, we suppressed SERT expression, another key mechanism controlling brain serotonergic transmission. RNAi-induced reduction of SERT level triggers remarkable effects on serotonergic function, faster and more efficient than those produced by the pharmacological SERT blockade. Thus, forebrain 5-HT concentration was increased three- and four-fold by two and four doses of SERT-siRNA, respectively, an effect similar to that found after 2-week fluoxetine treatment at a daily dose showing ~90% SERT occupancy.[60] The robust effect on extracellular 5-HT, compared with the relatively modest change in SERT expression (consistent with its half-life, ~3 days),[61] suggests that functional SERT derives from newly synthesized pools.

As expected from the increased serotonergic function, resulting from the decreased SERT level, mice treated with very small SERT-siRNA (1.4 nmol) showed a marked reduction of immobility in the tail suspension test, a behavioral response evoked by antidepressant drugs.[18,42] An earlier study also found antidepressant-like effects in the forced swim test but after a prolonged intracerebroventricular SERT-siRNA infusion during 2-week at a higher dose (31 nmol per day).[35] Overall, this indicates that SERT knockdown in adulthood significantly improves the resilience to stress, thus contributing to the antidepressant action.

The fast increase of extracellular 5-HT observed in SERT knockdown mice likely accounts for the rapid desensitization of 5-HT_{1A}-autoreceptors, a key characteristic of antidepressant drugs. Indeed, 5-HT_{1A}-autoreceptor stimulation by the excess 5-HT produced by SSRIs reduces raphe 5-HT neuronal firing and, consequently, 5-HT neurotransmission in forebrain.[16] Only after successful 5-HT_{1A}-autoreceptor desensitization, 5-HT neuron activity and terminal 5-HT release are recovered.[17,47] In agreement with these previous studies, fluoxetine desensitized 5-HT_{1A}-autoreceptors after 2-week treatment. Interestingly, short-term SERT-siRNA

Figure 4 Serotonin transporter (SERT) silencing rapidly increases the number of NeuroD- and DCX-positive cells in hippocampus. Mice were infused with four dose SERT- or nonsense siRNA (ns-siRNA; 10 μg per day) or vehicle into dorsal raphe nucleus (DR). Other groups of mice were treated with 4 or 15-day fluoxetine (FLX; 20 mg kg^{-1} per day, intraperitoneally) or saline. (**a**) Immunohistochemical images showing NeuroD-positive progenitors in the dentate gyrus (DG) of mice. Box insets represent regions of high-magnification photomicrographs. Scale bars: lower magnification = 100 μm and high magnification = 20 μm. (**b**) Quantitative analysis indicated a significant increase in the number of NeuroD-positive cells in serotonin transporter-small interference RNA (SERT-siRNA)-treated mice (four dose) compared with vehicle and ns-siRNA-treated mice (n = 5–9 mice). One-way analysis of variance (ANOVA) showed an effect of group ($F_{2,11}$ = 5.87, P < 0.05). (**c**) Representative photomicrographs showing DCX-positive cells, bearing a complex dendritic morphology in the DG of mice. Scale bar = 20 μm. (**d**) Quantitative analysis revealed a significant increase in the number of DCX-positive cells in both 15-day FLX ($F_{2,29}$ = 7.71, P < 0.01) and four dose SERT-siRNA-treated mice ($F_{2,18}$ = 5.94, P < 0.05) (n = 6–10). ^^P < 0.01 versus saline-treated mice; *P < 0.05, **P < 0.01 versus vehicle and ns-siRNA-treated mice. Values are mean ± s.e.m.

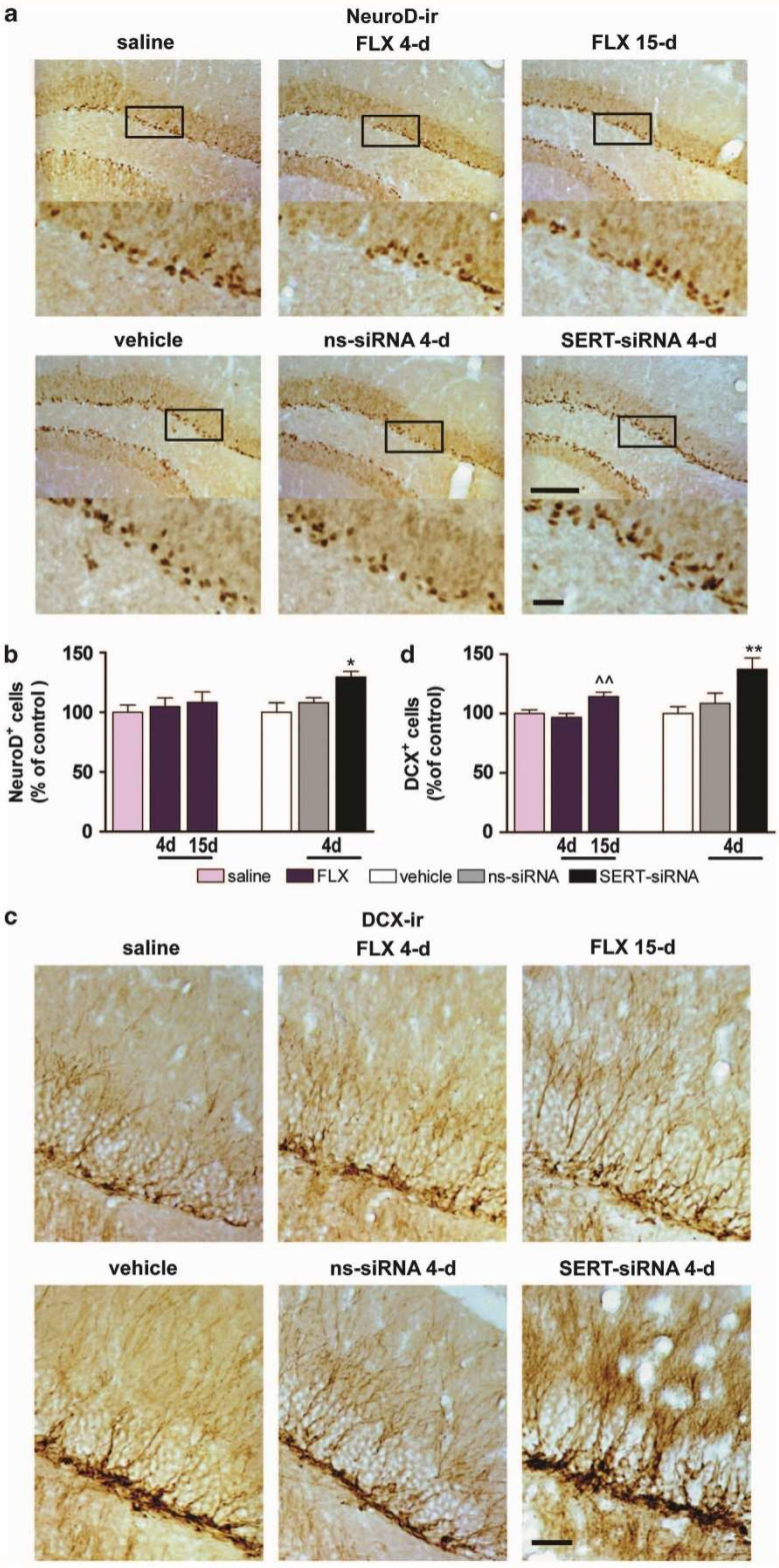
a
NeuroD-ir
saline
FLX 4-d
FLX 15-d
vehicle
ns-siRNA 4-d
SERT-siRNA 4-d
b
NeuroD+ cells (% of control)
150
100
50
0
*
4d 15d
4d
d
DCX+ cells (%of control)
^^
**
saline
FLX
vehicle
ns-siRNA
SERT-siRNA
c
DCX-ir
saline
FLX 4-d
FLX 15-d
vehicle
ns-siRNA 4-d
SERT-siRNA 4-d

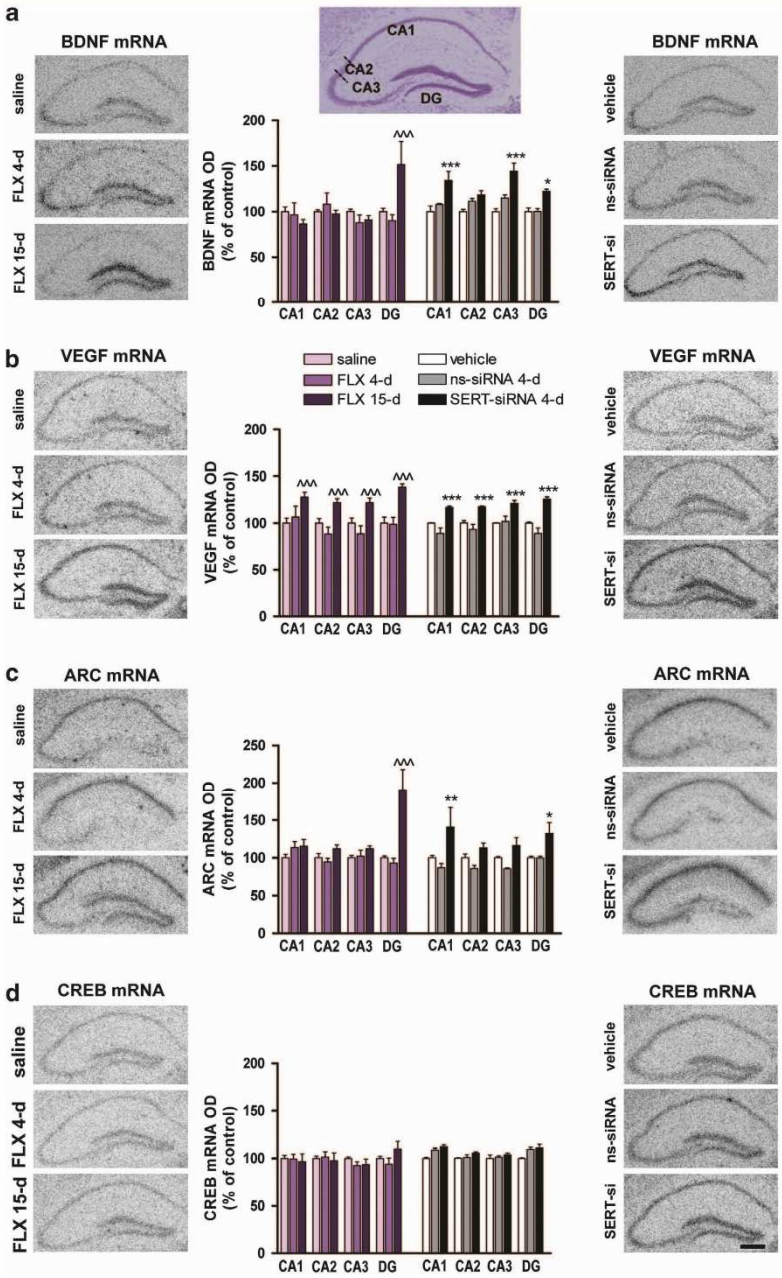

Figure 5 Serotonin transporter (SERT) silencing enhances hippocampal plasticity-associated gene expression. Mice were infused with four dose SERT- or nonsense siRNA (ns-siRNA; 10 μg per day) or vehicle into dorsal raphe nucleus (DR). Other groups of mice were treated with 4 or 15-day fluoxetine (FLX; 20 mg kg^{-1} per day, intraperitoneally) or saline. (**a**–**d**) Representative autoradiograms of hippocampal sections of mice are shown for (**a**) brain-derived neurotrophic factor (BDNF), (**b**) vascular endothelial growth factor (VEGF), (**c**) activity-regulated cytoskeletal protein (Arc) and (**d**) cAMP response element binding protein (CREB) mRNA expression. Scale bar = 100 μm. Densitometric analyses were performed in different hippocampal regions: CA1, CA2, CA3 and dentate gyrus (DG), shown in the cresyl violet-stained section (top). Levels of mRNA for each gene are shown in the bar graphs next to the representative autoradiograms ($n = 4$–5 mice). (**a**) BDNF mRNA levels in DG were significantly increased after 15-day FLX treatment compared with saline-treated mice (two-way analysis of variance (ANOVA): effect of region $F_{3,33} = 5.76$ and interaction group-by-region $F_{6,33} = 7.86$). However, serotonin transporter-small interference RNA (SERT-siRNA) treatment (four dose) increased BDNF expression in CA1, CA3 and DG compared with respective control groups (significant effect of group $F_{2,8} = 18.03$ and region $F_{3,24} = 4.33$). (**b**) VEGF mRNA levels were augmented in all hippocampal subfields after FLX (15-day) or SERT-siRNA (four dose) treatments compared with respective control groups (two-way ANOVA; FLX: effect of group $F_{2,10} = 10.11$, region $F_{3,30} = 12.80$ and interaction $F_{6,30} = 4.54$; SERT-siRNA: effect of group $F_{2,8} = 17.32$, region $F_{3,24} = 5.00$ and interaction $F_{6,24} = 5.42$). (**c**) Arc mRNA levels in DG were significantly increased following FLX (15-day) compared with saline-treated mice (two-way ANOVA: effect of group $F_{2,11} = 9.30$, region $F_{3,33} = 4.93$ and interaction group-by-region $F_{6,33} = 7.75$). SERT-siRNA treatment (four dose) increased Arc expression in CA1 and DG compared with respective control groups (significant effect of group $F_{2,13} = 11.53$, region $F_{3,39} = 6.77$ and interaction $F_{6,39} = 4.05$). (**d**) CREB mRNA levels were unchanged following any treatment. $^{\wedge\wedge\wedge}P < 0.001$ versus saline-treated mice; $^{*}P < 0.05$, $^{**}P < 0.01$, $^{***}P < 0.001$ versus vehicle and ns-siRNA-treated mice. Values are mean ± s.e.m.

treatment fully disrupts the 5-HT_{1A}-autoreceptor function and—unlike fluoxetine—decreases their expression in DR, thus hastening the adaptive presynaptic mechanisms in serotonergic neurotransmission.

The fast-acting antidepressant potential of SERT-siRNA was further confirmed by its ability to increase neurogenesis and to activate the expression of plasticity gene in the adult mouse HPC. It is well accepted that antidepressants share the common property to positively modulate cellular growth and plasticity in mood-related brain areas. Indeed, plasticity-associated gene expression and neurogenesis are considered to be specific markers of antidepressant action.[56–59] However, these effects require prolonged (for example, >2 weeks) administration of antidepressants drugs.[62–64] One of the more relevant findings of the present study is the observation that short-term SERT-siRNA treatment increased hippocampal progenitor proliferation using two different markers (5-Bromo-2′-deoxyuridine and Ki-67), an effect produced only after 15-day pharmacological SERT blockade. This was accompanied by an increase in the number of NeuroD- and DCX-positive cells, whose morphological complexity suggests that the integration of immature neurons into hippocampal networks may be accelerated by SERT-siRNA. In parallel, SERT-siRNA (four dose)—but not fluoxetine—, also enhanced the expression of trophic factors such as BDNF and VEGF, as well as that of the activity-dependent *Arc* gene in several HPC subfields. Neuronal activity recruits latent stem/progenitor cells in the adult HPC, increasing the expression of trophic factors.[65] Therefore, these could serve to link neuronal activity to structural plasticity in the hippocampal neurogenic niche. Future experiments will examine whether this neurogenic effect is required for the antidepressant-like responses elicited by SERT-siRNA treatment.

In conclusion, our results show that siRNA-induced selective SERT knockdown evokes a number of behavioral, neurochemical and cellular responses predictive of clinical antidepressant activity. Notably, these effects occur after short-term SERT-siRNA treatment and are remarkably faster and—in most instances—more effective than those elicited by persistent SERT blockade with the SSRI fluoxetine. Together with previous observations,[18,35,40] the present data support the usefulness of RNAi strategies, stimulating serotonergic transmission as a new therapeutic class overcoming the two main limitations of current pharmacological treatments, that is, limited efficacy and slowness of action.

Conflict of interest

FA has received consulting and educational honoraria on antidepressant drugs from Eli Lilly and Lundbeck. AM is a cofounder and board member of nLife Therapeutics S.L. MCC is an employee of nLife Therapeutics S.L. The rest of authors report no biomedical financial interests or potential conflicts of interest.

Acknowledgements. This research was supported by grants from Spanish Ministry of Science and Innovation—CDTI, with the participation of the DENDRIA Consortium; from Instituto de Salud Carlos III PI10/00290 and Centro de Investigación Biomédica en Red de Salud Mental (CIBERSAM, P91C). Structural funds of the European Union, through the National Applied Research Projects (R+D+I 2008/11) and from the Catalan Government (grant 2009SGR220) are also acknowledged. We gratefully thank to Mireia Galofré and Esther Ruiz-Bronchal for technical support and, Anna Castañé for advice in behavioral test.

1. Kessler RC, Chiu WT, Demler O, Merikangas KR, Walters EE. Prevalence, severity, and comorbidity of 12-month DSM-IV disorders in the National Comorbidity Survey Replication. *Arch Gen Psychiatry* 2005; **62**: 617–627.
2. Krishnan V, Nestler EJ. The molecular neurobiology of depression. *Nature* 2008; **455**: 894–902.
3. Smith K. Trillion-dollar brain drain. *Nature* 2011; **478**: 15.
4. Wong ML, Licinio J. Research and treatment approaches to depression. *Nature Rev Neurosci* 2001; **2**: 343–351.
5. Rush AJ, Trivedi MH, Wisniewski SR, Nierenberg AA, Stewart JW, Warden D *et al.* Acute and longer-term outcomes in depressed outpatients requiring one or several treatment steps: a STAR*D report. *Am J Psychiatry* 2006; **163**: 1905–1917.
6. Trivedi MH, Fava M, Wisniewski SR, Thase ME, Quitkin F, Warden D *et al.* Medication augmentation after the failure of SSRIs for depression. *N Engl J Med* 2006; **354**: 1243–1252.
7. Blakely RD, De Felice LJ, Hartzell HC. Molecular physiology of norepinephrine and serotonin transporters. *J Exp Biol* 1994; **196**: 263–281.
8. Pickel VM, Chan J. Ultrastructural localization of the serotonin transporter in limbic and motor compartments of the nucleus accumbens. *J Neurosci* 1999; **19**: 7356–7366.
9. Quin Y, Melikian HE, Rye DB, Levey AI, Blakely RD. Identification and characterization of antidepressant-sensitive serotonin transporter proteins using site-specific antibodies. *J Neurosci* 1995; **15**: 1261–1274.
10. Torres GE, Gainetdinov RR, Caron MG. Plasma membrane monoamine transporters: structure, regulation and function. *Nature Rev Neurosci* 2003; **4**: 13–25.
11. Baudry A, Mouillet-Richard S, Schneider B, Launay JM, Kellermann O. miR-16 targets the serotonin transporter: a new facet for adaptive responses to antidepressants. *Science* 2010; **329**: 1537–1541.
12. Benmansour S, Cecchi M, Morilak DA, Gerhardt GA, Javors MA, Gould GG *et al.* Effects of chronic antidepressant treatments on serotonin transporter function, density, and mRNA level. *J Neurosci* 1999; **19**: 10494–10501.
13. Benmansour S, Owens WA, Cecchi M, Morilak DA, Frazer A. Serotonin clearance in vivo is altered to a greater extent by antidepressant-induced downregulation of the serotonin transporter than by acute blockade of this transporter. *J Neurosci* 2002; **22**: 6766–6772.
14. Lau T, Horschitz S, Berger S, Bartsch D, Schloss P. Antidepressant-induced internalization of the serotonin transporter in serotonergic neurons. *FASEB J* 2008; **22**: 1702–1714.
15. Piñeyro G, Blier P, Dennis T, de Montigny C. Desensitization of the neuronal 5-HT carrier following its long-term blockade. *J Neurosci* 1994; **14**: 3036–3047.
16. Artigas F, Celada P, Laruelle M, Adell A. How does pindolol improve antidepressant action? *Trends Pharmacol Sci* 2001; **22**: 224–228.
17. Blier P, de Montigny C. Current advances and trends in the treatment of depression. *Trends Pharmacol Sci* 1994; **15**: 220–226.
18. Bortolozzi A, Castañé A, Semakova J, Santana N, Alvarado G, Cortés R *et al.* Selective siRNA-mediated suppression of 5-HT_{1A} autoreceptors evokes strong anti-depressant-like effects. *Mol Psychiatry* 2012; **17**: 612–623.
19. Frazer A, Benmansour S. Delayed pharmacological effects of antidepressants. *Mol Psychiatry* 2002; **7**: S23–S28.
20. Zhao Z, Zhang HT, Bootzin E, Millan MJ, O'Donnel JM. Association of changes in norepinephrine and serotonin transporter expression with the long-term behavioral effects of antidepressant drugs. *Neuropsychopharmacology* 2009; **34**: 1467–1481.
21. Anguelova M, Benkelfat C, Turecki G. A systematic review of association studies investigating genes coding for serotonin receptors and the serotonin transporter: II. Suicidal behavior. *Mol Psychiatry* 2003; **8**: 646–653.
22. Caspi A, Sugden K, Moffitt TE, Taylor A, Craig IW, Harrington H *et al.* Influence of life stress on depression: moderation by a polymorphism in the 5-HTT gene. *Science* 2003; **301**: 386–389.
23. Hu XZ, Lipsky RH, Zhu G, Akhtar LA, Taubman J, Greenberg BD *et al.* Serotonin transporter promoter gain-of-function genotypes are linked to obsessive compulsive disorder. *Am J Hum Genet* 2006; **78**: 815–826.
24. Lesch KP, Bengel D, Heils A, Sabol SZ, Greenberg BD, Petri S *et al.* Association of anxiety-related traits with a polymorphism in the serotonin transporter gene regulatory region. *Science* 1996; **274**: 1527–1531.
25. Murphy DL, Lesch KP. Targeting the murine serotonin transporter: insights into human neurobiology. *Nat Rev Neurosci* 2008; **9**: 85–96.
26. Smeraldi E, Zanardi R, Benedetti F, Di Bella D, Perez J, Catalano M. Polymorphism within the promoter of the serotonin transporter gene and antidepressant efficacy of fluvoxamine. *Mol Psychiatry* 1998; **3**: 508–511.
27. Zanardi R, Serretti A, Rossini D, Franchini L, Cusin C, Lattuada E *et al.* Factors affecting fluvoxamine antidepressant activity: influence of pindolol and 5-HTTLPR in delusional and nondelusional depression. *Biol Psychiatry* 2001; **50**: 323–330.
28. Holmes A, Yang RJ, Murphy DL, Crawley JN. Evaluation of antidepressant-related behavioral responses in mice lacking the serotonin transporter. *Neuropsychopharmacology* 2002; **27**: 914–923.

29. Lira A, Zhou M, Castanon N, Ansorge MS, Gordon JA, Francis JH *et al.* Altered depression-related behaviors and functional changes in the dorsal raphe nucleus of serotonin transporter-deficient mice. *Biol Psychiatry* 2003; **54**: 960–971.
30. Ansorge MS, Zhou M, Lira A, Hen R, Gingrich JA. Early-life blockade of the 5-HT transporter alters emotional behavior in adult mice. *Science* 2004; **306**: 879–881.
31. Holmes A, Murphy DL, Crawley JN. Abnormal behavioral phenotypes of serotonin transporter knockout mice: parallels with human anxiety and depression. *Biol Psychiatry* 2003; **54**: 953–959.
32. Oh JE, Zupan B, Gross S, Toth M. Paradoxical anxiogenic response of juvenile mice to fluoxetine. *Neuropsychopharmacology* 2009; **34**: 2197–2207.
33. Davidson BL, Boudreau RL. RNA interference: a tool for querying nervous system function and an emerging therapy. *Neuron* 2007; **53**: 781–788.
34. He L, Hannon GJ. MicroRNAs: small RNAs with a big role in gene regulation. *Nat Rev Genet* 2004; **5**: 522–531.
35. Thakker DR, Natt F, Hüsken D, van der Putten H, Maier R, Hoyer D *et al.* siRNA-mediated knockdown of the serotonin transporter in the adult mouse brain. *Mol Psychiatry* 2005; **10**: 782–789.
36. Franklin KBJ, Paxinos G. *The Mouse Brain in Stereotaxic Coordinates*. Academic Press: New York, USA, 2008.
37. Hebert C, Habimana A, Elie R, Reader TA. Effects of chronic antidepressant treatments on 5-HT and NA transporters in rat brain: an autoradiographic study. *Neurochem Int* 2001; **38**: 63–74.
38. Castro ME, Díaz A, Del Olmo E, Pazos A. Chronic fluoxetine induces opposite changes in G-protein coupling at pre and postsynaptic 5-HT_{1A} receptors in rat brain. *Neuropharmacology* 2003; **4**: 93–101.
39. Amargós-Bosch M, Bortolozzi A, Puig MV, Serrats J, Adell A, Celada P *et al.* Co-expression and in vivo interaction of serotonin1A and serotonin2A receptors in pyramidal neurons of prefrontal cortex. *Cerebral Cortex* 2004; **14**: 281–299.
40. Ferrés-Coy A, Santana N, Castañé A, Cortés R, Carmona MC, Toth M *et al.* Acute 5-HT1A autoreceptor knockdown increases antidepressant responses and serotonin release in stressful conditions. *Psychopharmacology (Berl)* advance online publication, 21 July 2012 (e-pub ahead of print); PMID:22820867.
41. Azmitia EC, Segal M. An autoradiographic analysis of the differential ascending projections of the dorsal and median raphe nuclei in the rat. *J Comp Neurol* 1978; **179**: 641–667.
42. Cryan JF, Mombereau C, Vassout A. The tail suspension test as a model for assessing antidepressant activity: review of pharmacological and genetic studies in mice. *Neurosci Biobehav Rev* 2005; **29**: 571–625.
43. Nestler EJ, Gould E, Manji H, Buncan M, Duman RS, Greshenfeld HK *et al.* Preclinical models: status of basic research in depression. *Biol Psychiatry* 2002; **52**: 503–528.
44. Hirano K, Kimura R, Sugimoto Y, Yamada J, Uchida S, Kato Y *et al.* Relationship between brain serotonin transporter binding, plasma concentration and behavioural effect of selective serotonin reuptake inhibitors. *Br J Pharmacol* 2005; **144**: 695–702.
45. Ramamoorthy S, Blakely RD. Phosphorylation and sequestration of serotonin transporters differentially modulated by psychostimulants. *Science* 1999; **285**: 763–766.
46. Samuvel DJ, Jayanthi LD, Bhat NR, Ramamoorthy S. A role of for p38 mitogen-activated protein kinase in the regulation of the serotonin transporter: evidence for distinct cellular mechanisms involved in transporter surface expression. *J Neurosci* 2005; **25**: 29–41.
47. Artigas F, Romero L, de Montigny C, Blier P. Acceleration of the effect of selected antidepressant drugs in major depression by 5-HT_{1A} antagonists. *Trends Neurosci* 1996; **19**: 378–383.
48. Hensler JG. Differential regulation of 5-HT_{1A} receptor-G protein interactions in brain following chronic antidepressant administration. *Neuropsychopharmacology* 2002; **26**: 565–573.
49. Arborelius L, Hawks BW, Owens MJ, Plotsky PM, Nemeroff CB. Increased responsiveness of presumed 5-HT cells to citalopram in adult rats subjected to prolonged maternal separation relative to brief separation. *Psychopharmacology* 2004; **176**: 248–255.
50. Romero L, Artigas F. Preferential potentiation of the effects of serotonin uptake inhibitors by 5-HT_{1A} receptor antagonists in the dorsal raphe pathway: role of somatodendritic autoreceptors. *J Neurochem* 1997; **68**: 2593–2603.
51. Piñeyro G, Blier P. Autoregulation of serotonin neurons: role in antidepressant drug action. *Neuropsychopharmacology* 1999; **21**: 91S–98S.
52. McQuade R, Sharp T. Functional mapping of dorsal and median raphe 5-hydroxytryptamine pathways in forebrain of the rat using microdialysis. *J Neurochem* 1997; **69**: 791–796.
53. Kee N, Sivalingam S, Boonstra R, Wojtowicz JM. The utility of Ki-67 and BrdU as proliferative markers of adult neurogenesis. *J Neurosci Methods* 2002; **115**: 97–105.
54. Scholzen T, Gerdes J. The Ki-67 protein: from the known and the unknown. *J Cell Physiol* 2000; **182**: 311–322.
55. Dias BG, Banerjee SB, Duman RS, Vaidya VA. Differential regulation of brain derived neurotrophic factor transcripts by antidepressant treatments in the adult rat brain. *Neuropharmacology* 2003; **45**: 553–563.
56. Nibuya M, Morinobu S, Duman RS. Regulation of BDNF and trkB mRNA in rat brain by chronic electroconvulsive seizure and antidepressant drug treatments. *J Neurosci* 1995; **15**: 7539–7547.
57. Warner-Schmidt JL, Duman RS. VEGF is an essential mediator of the neurogenic and behavioral actions of antidepressants. *Proc Natl Acad Sci USA* 2007; **104**: 4647–4652.
58. Nibuya M, Nestler EJ, Duman RS. Chronic antidepressant administration increases the expression of cAMP response element binding protein (CREB) in rat hippocampus. *J Neurosci* 1996; **16**: 2365–2372.
59. Pei Q, Zetterström TS, Sprakes M, Tordera R, Sharp T. Antidepressant drug treatment induces Arc gene expression in the rat brain. *Neuroscience* 2003; **121**: 975–982.
60. Wong DT, Bysmaster FP, Reid LR, Fuller RW, Perry KW. Inhibition of serotonin uptake by optical isomers of fluoxetine. *Drug Dev Res* 1985; **6**: 397–403.
61. Kimmel H, Vicentic A, Kuhar MJ. Neurotransmitter transporters synthesis and degradation rates. *Life Sci* 2001; **68**: 2181–2185.
62. Sahay A, Hen R. Adult hippocampal neurogenesis in depression. *Nat Neurosci* 2007; **10**: 1110–1115.
63. Santarelli L, Saxe M, Gross C, Surget A, Battaglia F, Dulawa S *et al.* Requirement of.hippocampal neurogenesis for the behavioral effects of antidepressants. *Science* 2003; **301**: 805–809.
64. Schmidt HD, Duman RS. The role of neurotrophic factors in adult hippocampal neurogenesis, antidepressant treatments and animal models of depressive-like behavior. *Behav Pharmacol* 2007; **18**: 391–418.
65. Walker TL, White A, Black DM, Wallace RH, Sah P, Bartlett PF. Latent stem and progenitor cells in the hippocampus are activated by neural excitation. *J Neurosci* 2008; **28**: 5240–5247.

Supplementary Information accompanies the paper on the Translational Psychiatry website (http://www.nature.com/tp)

Revised Manuscript 2012TP000122-T

Supplementary information

RNAi-mediated serotonin transporter suppression rapidly increases serotonergic neurotransmission and hippocampal neurogenesis

A Ferrés-Coy[1,3], F Pilar-Cuellar[2,3], R Vidal[2,3], V Paz[1,3], M Masana[1,3,a], R Cortés[1,4], MC Carmona[5], L Campa[1,3], Á Pazos[2,3], A Montefeltro[5], EM Valdizán[2,3], F Artigas[1,3] and A Bortolozzi[1,3,6,b]

Inventory of supplementary information

Supplementary figure legends

Figure S1 Selective mouse SERT silencing by SERT-siRNA. Mice received an intra-dorsal raphe (DR) infusion of 2 doses of SERT- or ns-siRNA (10µg - 0.7nmol per day) or vehicle and were killed 24h post-infusion. **(a)** Representative coronal brain sections showing SERT-siRNA-induced reduction of SERT expression in DR as assessed by *in situ* hybridization and [^{3}H]-citalopram binding. Scale bar= 500µm. **(b)** Effect of SERT-siRNA (2-dose) on SERT mRNA and binding in DR and median raphe nucelus (MnR) (n=4-6 mice). One-way ANOVA revealed an effect of group on SERT mRNA ($F_{2,7}$=22.71, P<0.01) and SERT binding ($F_{2,10}$=4.69, P<0.05). **(c)** Representative coronal midbrain sections showing: (i) [^{3}H]-nisoxetine binding to the norepinephrine transporter (NET), (ii) [^{3}H]-8-OH-DPAT binding to 5-HT$_{1A}$R and, (iii) tryptophan hydroxylase-2 (TPH2; the synthesizing enzyme of 5-HT) mRNA density in DR assessed by *in situ* hybridization. Scale bars= 2mm and 500µm. **(d)** Bar graphs showing no differences in NET and 5-HT$_{1A}$R binding sites and TPH2 mRNA levels in DR (n=3-5). *P<0.05, **P<0.01 compared to vehicle and ns-siRNA-treated mice. Values are mean ± s.e.m.

Figure S2 Immunohistochemical assessment of cellular viability in the midbrain region after SERT-siRNA infusion. Mice were infused with 2-dose SERT- or ns-siRNA (10µg per day) or vehicle into dorsal raphe nucleus (DR) and were killed 24h post-infusion (n=4 mice). **(a-c)** Adjacent, 30-µm-thick sections through the midbrain raphe nuclei were stained with neuronal (NeuN, **a**), astrocytic (GFAP, **b**), or microglial (IBA-1, **c**) markers. Frame with continuous lines in the low magnification photomicrographs shows DR area used for high magnification photomicrographs in

panels **a, b and c** (top). The rectangle with dashed lines in the low magnification photomicrographs shows the corresponding paralemniscial nucleus (PN) region used for high magnification photomicrographs in panel **c** (below). **(a)** Coronal DR sections stained for NeuN show no signs of neuron loss in the different mouse groups, except near the cannula tract. **(b)** Tissue DR sections from mice in all treatment groups labeled with GFAP exhibit a slight reactive astrogliosis. **(c)** Tissue sections stained with the microglial marker IBA-1 exhibits no intensity differences in PN between all groups. However, an increased immunoreactivity was observed along the cannula tract. Note also the large tissue damage outside DR produced by the cannula, together with the minimal lesion in the DR provoked by the silica capillary. Scale bars in **(a)** and **(c)**= 200μm, and in (**b**)= 50μm.

Figure S3 Neurochemical and antidepressant-like effects after SERT-siRNA-induced SERT suppression. Mice were infused with 2-dose SERT- or ns-siRNA (10μg per day) or vehicle into dorsal raphe nucleus (DR). Microdialysis experiments were performed 24h after the last infusion. **(a)** Local application of veratridine (50μM) increased the extracellular 5-HT levels in the caudate putamen (CPu) to the same extent in all groups (n=4-6). Two-way ANOVA showed an effect of time ($F_{5,55}$=60.85, P<0.001). However, infusion of citalopram (SSRI; 1μM) by reverse-dialysis increased CPu 5-HT concentration in vehicle and ns-siRNA-treated mice, but not in SERT-siRNA-treated mice, revealing the loss of SERT function. Two-way ANOVA showed an effect of group ($F_{2,11}$=12.52, P<0.01), time ($F_{8,88}$=13.23, P<0.001) and interaction group-by-time ($F_{16,88}$=3.58; P<0.001). **(b)** Acute fluoxetine administration (20 $mgkg^{-1}$, i.p.) increased extracellular 5-HT concentration in CPu of vehicle-infused mice, reaching those of basal extracellular levels in SERT-siRNA-treated mice (n=4-6

mice). Two-way ANOVA of fraction 1 to fraction 15 showed an effect of time ($F_{14,112}$=2.16, P<0.05) and group-by-time interaction ($F_{14,112}$=5.13, P<0.0001). **(c)** Mice infused with SERT-siRNA into DR displayed a decreased immobility in the tail suspension test (TST) as compared to control groups (n=14 mice/group). One-way ANOVA showed a significant effect of group (F2,39=4.05, P<0.05). *P<0.05 versus vehicle and ns-siRNA-treated mice. Values are mean ± s.e.m.

Figure S4 Short-term SERT-siRNA treatment evoked a widespread reduction of SERT-binding sites in mouse brain. Mice were infused with 2, 4 or 7-dose SERT- or ns-siRNA (10µg by day) or vehicle into DR and were killed 24h post-infusion. **(a)** Representative autoradiograms of [^{3}H]-citalopram binding showing the SERT-siRNA-induced down-regulation of SERT binding sites in different brain regions following a 4-dose treatment. Open boxes in the cresyl violet-stained sections (top) mark the approximate areas where densitometric analyses were performed. Medial prefrontal cortex (mPFC), caudate putamen (CPu), septum (Sep), hippocampus (HPC), hypothalamus (HYP), amygdala (Amyg), dorsal raphe nucleus (DR) and median raphe nucleus (MnR). Scale bar= 2mm. **(b)** Densitometric analyses of specific SERT binding is shown as percentage of binding in the corresponding region of vehicle-infused mice (n=5-10). Three-way ANOVA (group, region and time) showed an effect of group ($F_{2,39}$=71.37, P<0.001), region ($F_{7,273}$=4.82, P<0.001) and group-by-region interaction ($F_{14,273}$=4.04, P<0.001). *P<0.05, **P<0.01 versus vehicle and ns-siRNA-treated mice. Values are mean ± s.e.m.

Figure S5 SERT-siRNA treatment, but not fluoxetine, reduces SERT-immunoreactivity in forebrain**.** Mice were infused with 4-dose SERT- or ns-siRNA (10µg by day) or vehicle into dorsal raphe nucleus (DR). Other groups of mice were treated with 4 or 15-day fluoxetine (FLX; 20 $mg \cdot kg^{-1}day^{-1}$, i.p.) or saline. All mice were killed 24h post-infusion. **(a)** Representative brain sections showing SERT-immmunoreativity (SERT-ir) axons in the piriform cortex (Pir) and amygdala (Amyg) of mice. Note that short-duration SERT-siRNA treatment (4-dose) decreased the density of SERT-ir fibers as compared to vehicle and ns-siRNA-treated mice (*n*=4-6 mice). However, neither fluoxetine treatment altered SERT-ir density (*n*=4-6). Boxes represent regions of high-magnification photomicrographs. Scale bars: lower magnification= 100µm and high magnification= 20µm. **(b)** SERT-ir fiber density in Pir and Amyg was measured and expressed as the percentage of the density in the respective vehicle-treated mice (*n*=4-6 mice/group). **P*<0.05 versus vehicle and ns-siRNA-treated mice. Values are mean ± s.e.m.

Figure S6 Secondary antibody (AB) controls. Immunostaining was conducted without the primary antibody. With no primary antibody to bind the secondary antibody, no labeling should be seen. The secondary antibody control was run in parallel with each experiment. Scale bars= 100µm.

Supplementary Figures

Figure S1

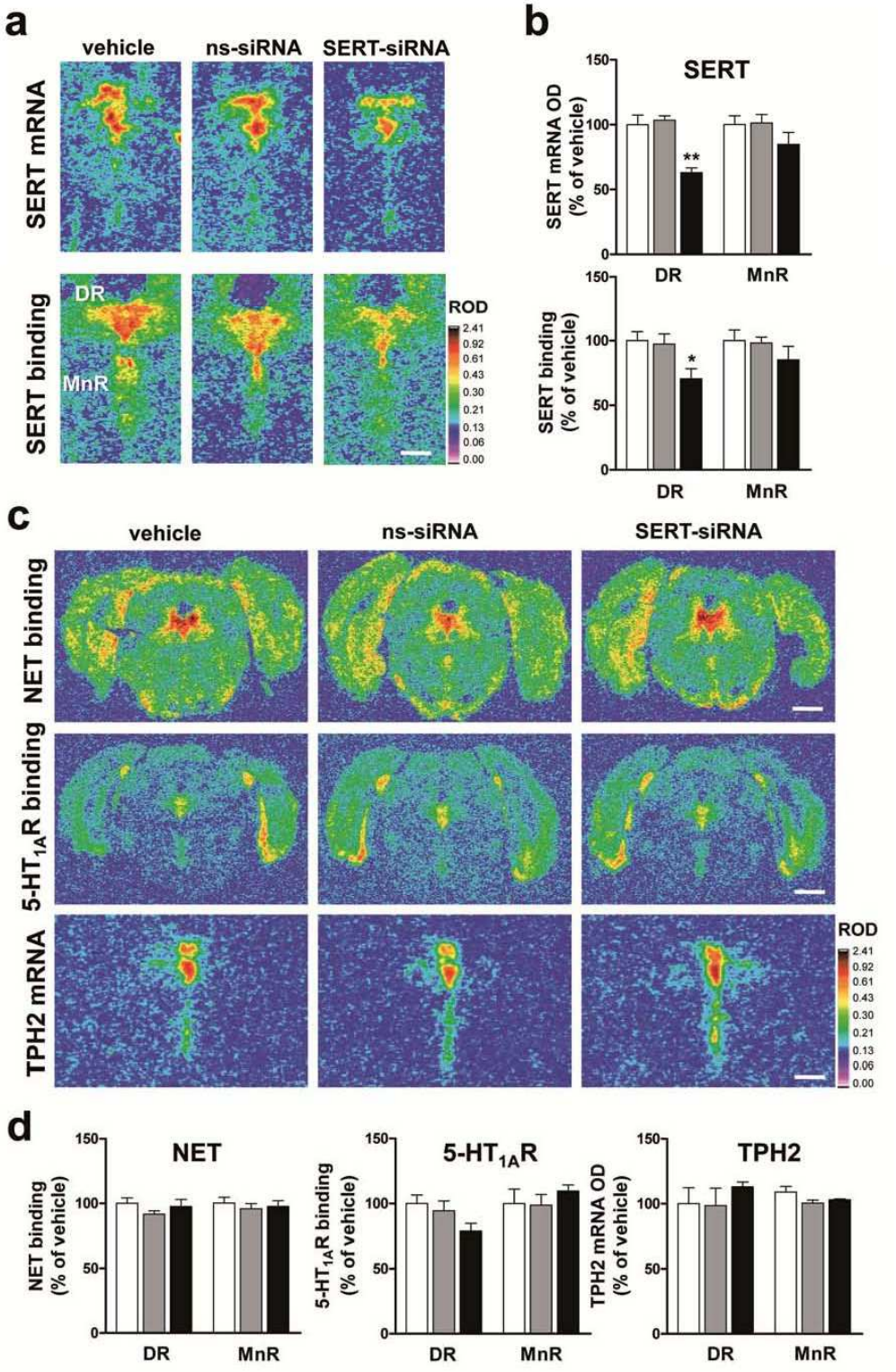

Figure S2

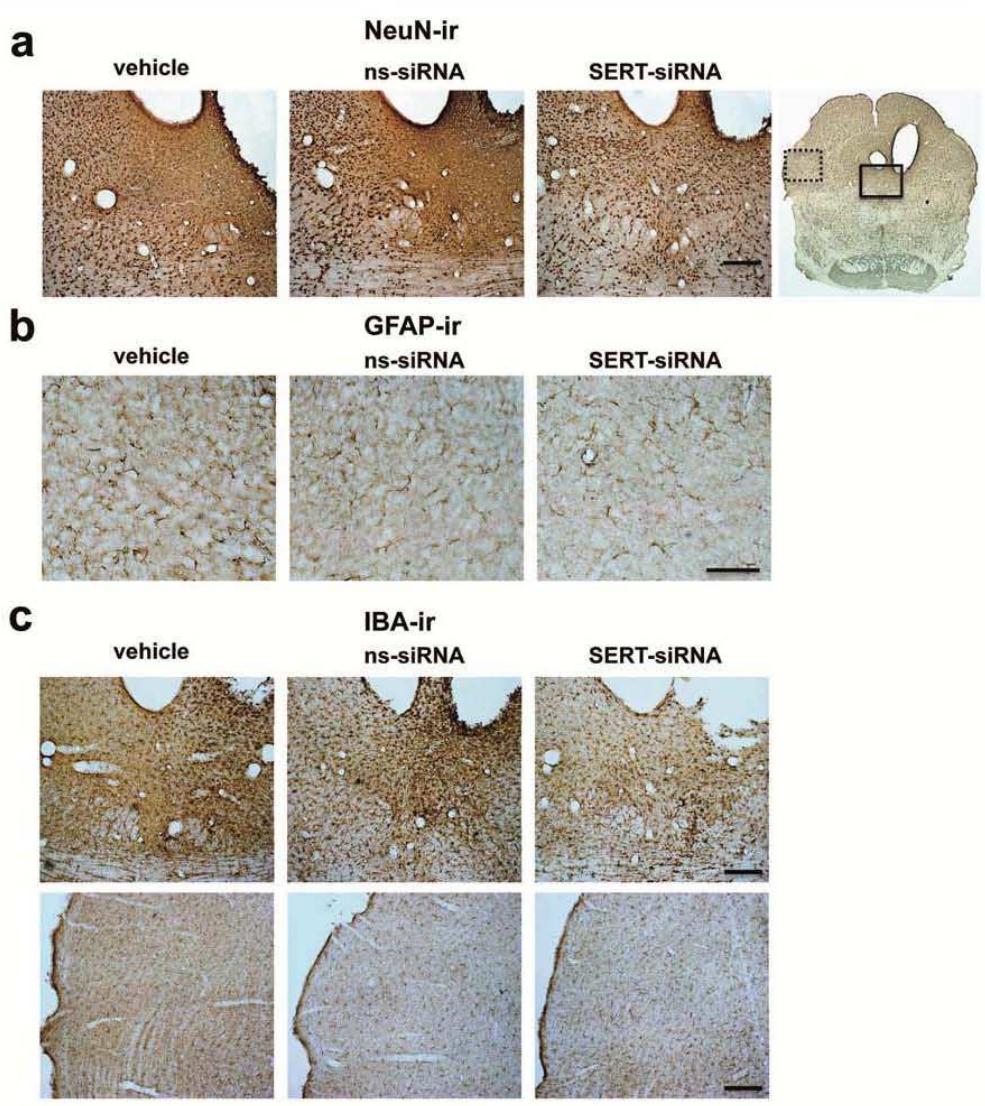
a
NeuN-ir
vehicle
ns-siRNA
SERT-siRNA
b
GFAP-ir
vehicle
ns-siRNA
SERT-siRNA
c
IBA-ir
vehicle
ns-siRNA
SERT-siRNA

Figure S3

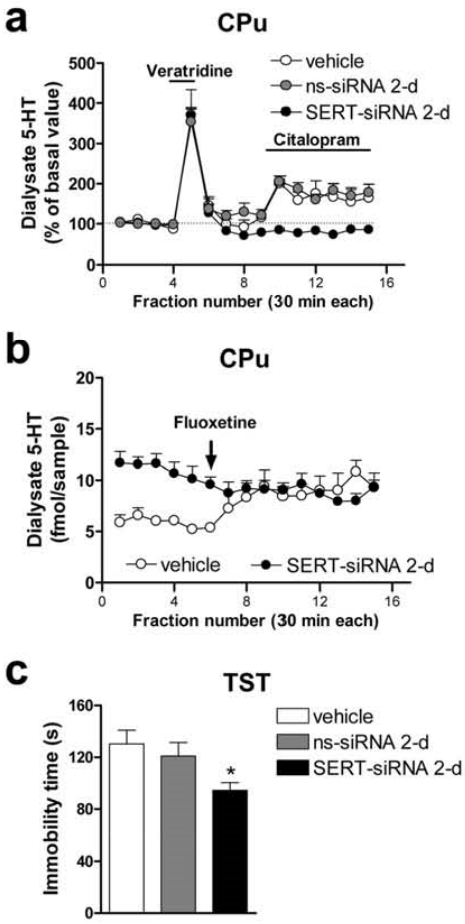
a
CPu
Veratridine
vehicle
ns-siRNA 2-d
SERT-siRNA 2-d
Citalopram
Dialysate 5-HT (% of basal value)
Fraction number (30 min each)
b
CPu
Fluoxetine
Dialysate 5-HT (fmol/sample)
vehicle
SERT-siRNA 2-d
Fraction number (30 min each)
c
TST
vehicle
ns-siRNA 2-d
SERT-siRNA 2-d
Immobility time (s)
*

Revised Manuscript 2012TP000122-T

Figure S4

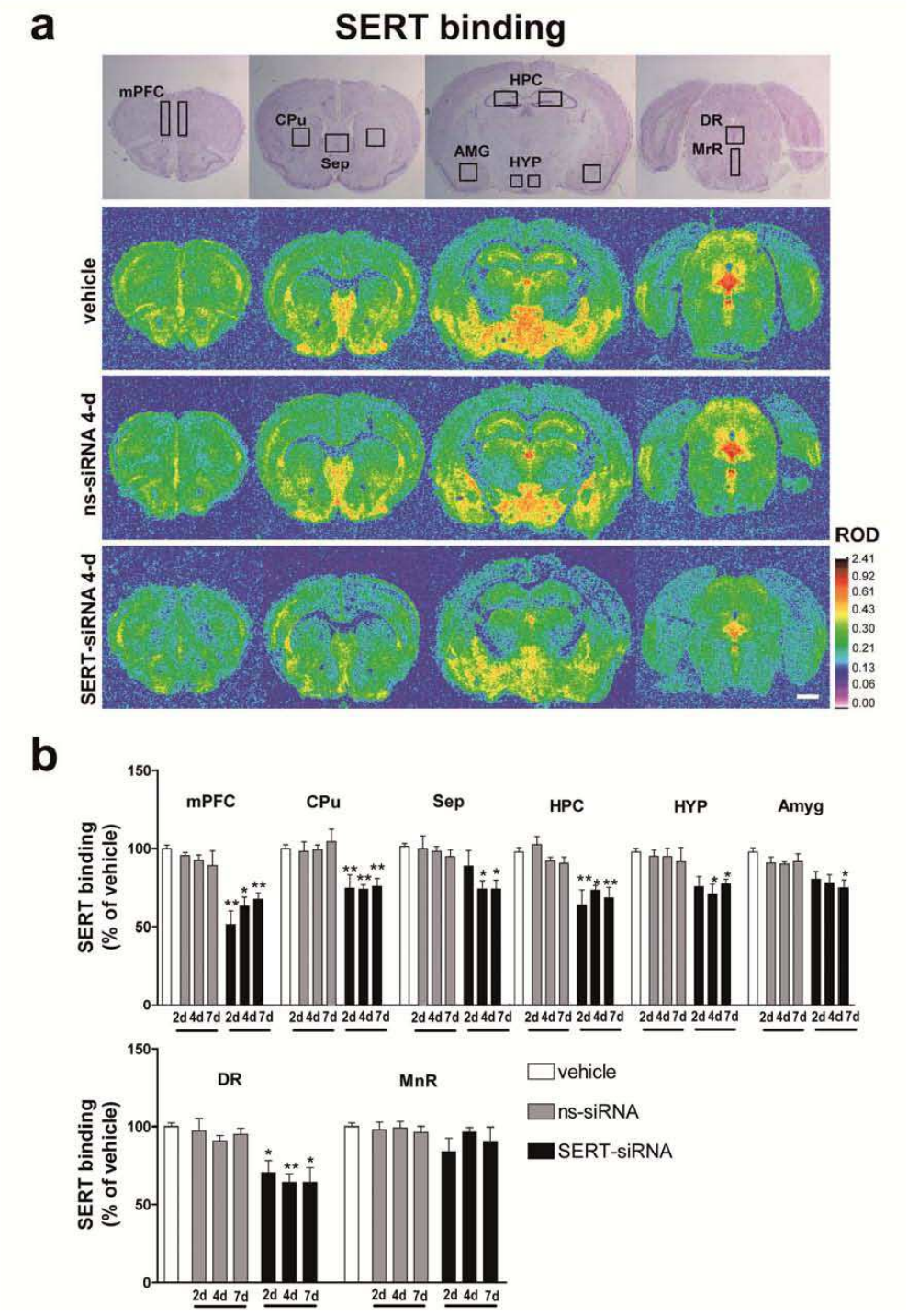

Figure S5

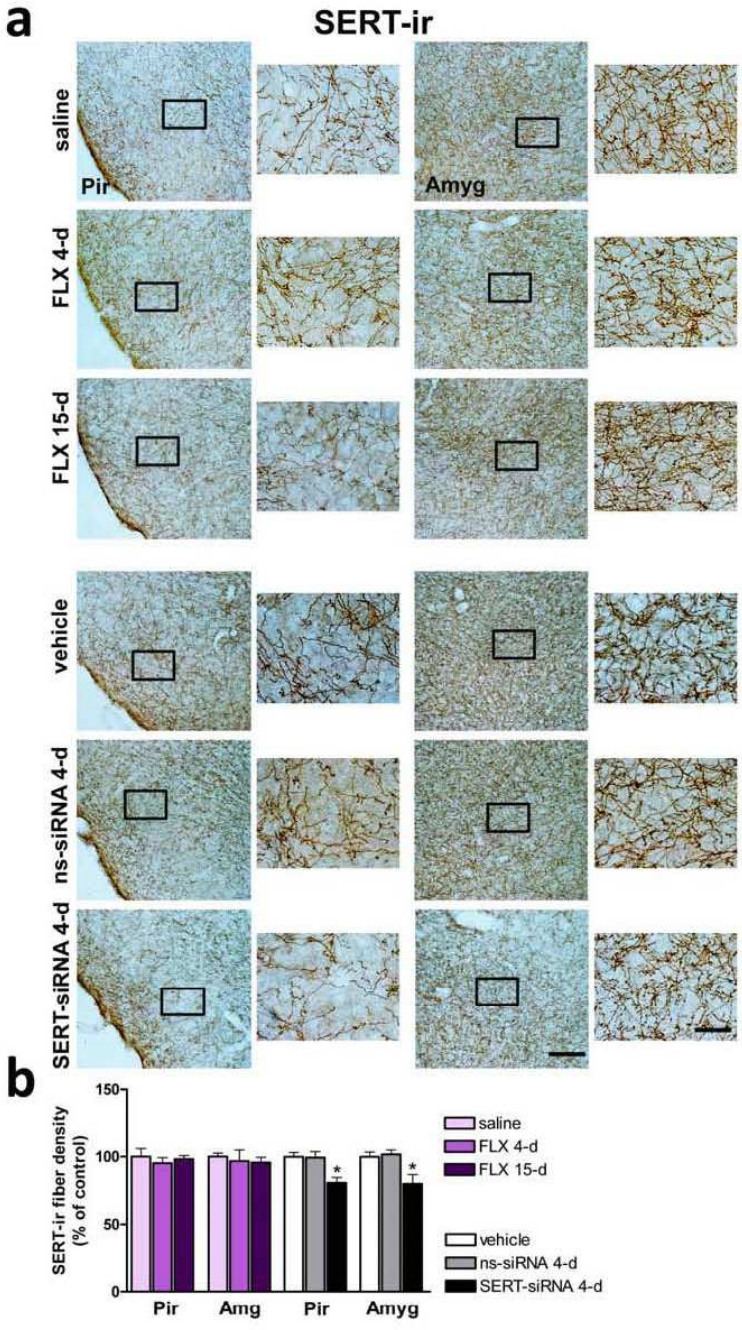
a
SERT-ir
saline
FLX 4-d
FLX 15-d
vehicle
ns-siRNA 4-d
SERT-siRNA 4-d
Pir
Amyg
b
SERT-ir fiber density (% of control)
150
100
50
0
saline
FLX 4-d
FLX 15-d
vehicle
ns-siRNA 4-d
SERT-siRNA 4-d
Pir
Amg
Pir
Amyg

Figure S6

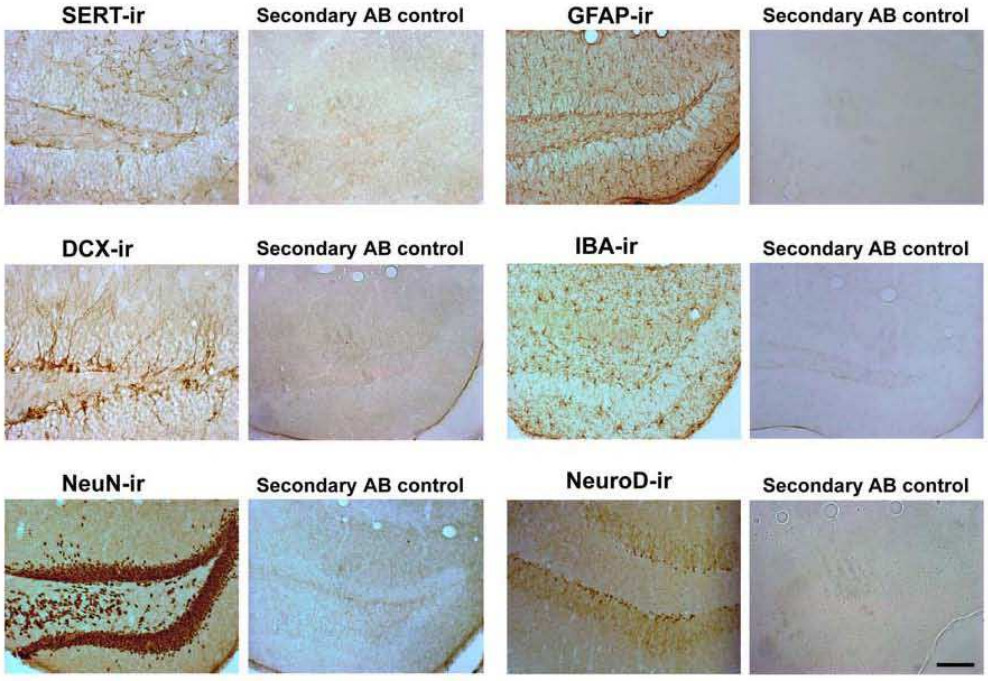
SERT-ir
Secondary AB control
GFAP-ir
Secondary AB control
DCX-ir
Secondary AB control
IBA-ir
Secondary AB control
NeuN-ir
Secondary AB control
NeuroD-ir
Secondary AB control

Supplementary Tables

Table S1. Sequences of siRNA molecules used

siRNA	forward	reverse
SERT-siRNA	GCUAGCUACAACAAGUUCATT	UGAACUUGUUGUAGCUAGCTT
ns-siRNA	AGUACUGCUUACGAUACGGTT	CCGUAUCGUAAGCAGUACUTT

Table S2. Summary of the conditions for labeling 5-HT_{1A}R, SERT and NET in the present work

Protein	Ligand	[nM]	Buffer	Preincubation (RT, min)	Incubation Buffer	Incubation Protocol (RT, min)	Washing Protocol (IC, min)	Exposure (days)	Blank
5-HT_{1A}	[^{3}H]-8-OH-DPAT	1.0	A	30	A + 10µM pargyline	60	2 x 5	60	10µM serotonin
SERT	[^{3}H]-citalopram	1.5	B	15	B	60	2 x 10	45	1µM fluoxetine
NET	[^{3}H]-nisoxetine	3.0	C	15	C	240	3 x 5	90	10µM mazindol

RT, room temperature; IC, ice-cold buffer; **Buffer A**: 170mM Tris-HCl, 4mM CaCl2, 0.01% ascorbic acid, pH 7.6; **Buffer B**: 50mM Tris-HCl, 120mM NaCl, 5mM KCl, pH 7.6; **Buffer C**: 50mM Tris-HCl, 300mM NaCl, 5mM KCl, pH 7.4.

Supplementary experimental procedures

***In situ* hybridization**

Oligodeoxyribonucleotide probes for mouse SERT, 5-HT_{1A}R, tryptophan hydroxylase 2 (TPH2), Ki-67, brain derived neurotrophic factor (BDNF), vascular endothelial growth factor (VEGF), activity regulated cytoskeletal protein (Arc), and cAMP response element binding protein (CREB) mRNAs were synthesized by IBA-GmbH (Göttingen, Germany). Antisense oligoprobes were complementary to bases: SERT/820-863 (GenBank accession NM_010484.1), 5-HT_{1A}R/1780-1827 (NM_008308), TPH2/360-410 (NM_173391), Ki-67/603-653 (NM_001081117), BDNF/1188-1238 (NM_007540), VEGF/2217-2267 (NM_001025250), Arc/1990-2040 (NM_018790) and, CREB/593-643 (NM_009952), respectively. The oligonucleotides were individually labeled (2 pmol) at the 3'-end with [^{33}P]-dATP (>2500 Cimmol^{-1}; DuPont-NEN, Boston, MA) using terminal deoxynucleotidyltransferase (TdT, Calbiochem, La Jolla, CA). The labeled oligoprobes were purified using QIAquick Nucleotide Removal Kit (QIAGEN GmbH, Hilden, Germany).

Sections were hybridized as described previously.[18,66] Briefly, frozen tissue sections were first brought to room temperature, fixed for 20min at 4ºC in 4% paraformaldehyde in phosphate-buffered saline (1xPBS: 8mM Na_2HPO_4, 1.4mM KH_2PO_4, 136mM NaCl, and 2.6mM KCl), washed for 5 min in 3xPBS at room temperature, twice for 5min each in 1x PBS, and incubated for 2min at 21ºC in a solution of predigested pronase (Calbiochem, San Diego, CA) at a final concentration of 24 UmL^{-1} in 50mM Tris-HCl, pH 7.5, and 5mM EDTA. The enzymatic activity was stopped by immersion for 30s in 2mgml^{-1} glycine in 1xPBS. Tissues were finally rinsed in 1xPBS and dehydrated through a graded series of ethanol. For

hybridization, the radioactively labeled probes were diluted in a solution containing 50% formamide, 4x standard saline citrate, 1x Denhardt's solution, 10% dextran sulfate, 1% sarkosyl, 20mM phosphate buffer, pH 7.0, 250 μgml^{-1} yeast tRNA, and 500 μgml^{-1} salmon sperm DNA. The final concentrations of radioactive probes in the hybridization buffer were in the same range (~1.5 nM). Tissue sections were covered with hybridization solution containing the labeled probes, overlaid with Nescofilm coverslips (Bando Chemical Ind., Kobe, Japan), and incubated overnight at 42ºC in humid boxes. Sections were then washed 4 times (45 min each) in a buffer containing 0.6M NaCl and 10mM Tris-HCl (pH 7.5) at 60ºC. Hybridized sections were exposed to Biomax-MR film (Kodak, Sigma-Aldrich, Madrid, Spain) for 1-4 weeks with intensifying screens. For specificity control, adjacent sections were incubated with an excess (50x) of unlabelled probes. The cytoarchitecture of different mouse brain areas were analyzed in an adjacent series of cresyl-violet stained frozen sections.

Receptor autoradiography

The autoradiographic binding assays for 5-HT_{1A}R, SERT and norepinephrine transporter (NET) were performed using the following radioligands: (a) [^{3}H]-8-OH-DPAT (233 $Cimmol^{-1}$), (b) [^{3}H]-citalopram (70 $Cimmol^{-1}$) and, (c) [^{3}H]-nisoxetine (85 $Cimmol^{-1}$), respectively (Perkin-Elmer, Madrid, Spain) as described previously. [37,67,68] 8-OH-DPAT, isoproterenol, mazindol, pargyline and serotonin were from Sigma-Aldrich (Madrid, Spain). The experimental conditions for incubation with each radioligand are summarized in **Table S2**. After incubation and washing, tissues were dipped in distilled ice-cold water and dried rapidly under a cold air stream. Tissues were exposed to Biomax-MR film together with ^{3}H-Microscales standards

(Amersham-GE Healthcare, Barcelona, Spain) at 4ºC for 1-3 month. All experimental and control brains within a group were processed in duplicate and exposed to films as a batch.

5-HT_{1A}R-stimulated [^{35}S]GTPγS autoradiography

Coronal dorsal raphe (DR) sections were pre-incubated for 30min at 25ºC in a buffer containing 50mM Tris–HCl, 0.2mM EGTA, 3mM $MgCl_2$, 100mM NaCl, 1mM DTT and 2mM GDP (pH 7.7). Slides were subsequently incubated for 2h in the same buffer containing adenosine deaminase (10mU/ml) with [^{35}S]GTPγS (0.04nM) and consecutive sections were incubated with (+)-8-OHDPAT (10^{-5}M) alone or in the presence of WAY100635 (10^{-5}M). Nonspecific binding was determined in the presence of 10μM GTPγS. Sections were exposed to autoradiographic film (Biomax-MR) together with ^{14}C-polymer standards at 4ºC for two days.

Quantitative image analysis of film autoradiograms

Autoradiograms were analysed and the relative optical densities (ROD) were obtained using a computer assisted image analyser (AIS, Imaging Research, St Catherines, Ontario, Canada). For 5-HT_{1A}R, SERT and NET binding sites, the system was calibrated with ^{3}H-Microscales standards to obtain fmolmg^{-1} protein equivalents from ROD data. For [^{35}S]GTPγS experiments, a standard curve was prepared using ^{14}C-standars. The data were corrected for the specific activity of [^{35}S]GTPγS at the calibration date and the decay factor of ^{35}S. ROD were evaluated in two or three adjacent sections by duplicate of each mouse and averaged to obtain individual values. For assess the SERT, 5-HT_{1A}R and TPH2 expression in the DR,

ROD were analysed at three antero-posterior levels of DR by duplicate (AP: -4.24 to -4.72)[36] for each mouse.

AIS system was also used to acquire pseudocolor images. Black and white photographs were taken from autoradiograms using a Wild 420 macroscope (Leica, Heerbrugg, Germany) equipped with Nikon DXM1200F digital camera and ACT-1 Nikon software (Soft Imaging System Gmbh, Münster, Germany). Images were processed with Photoshop (Adobe Systems, Mountain View) by using identical values for contrast and brightness.

Immunohistochemistry (IHC)

To confirm siRNA silencing of targeted SERT expression, the SERT protein was detected using immunohistochemistry (IHC). The SERT is a large transmembrane protein localized to serotonergic axon terminals in the forebrain, and has been shown to be an excellent presynaptic, structural marker of 5-HT axons.[69,70] IHC staining was performed using standard avidin-biotin-peroxidase techniques. Briefly, brain sections were treated with 1x PBS, 100% methanol and 30% H_2O_2 for 30 min. After incubation in 3% normal goat serum (Vector Laboratories, Burlingame, CA) in PBS/Triton 0.2% for 120 min, the sections were incubated for 4 days in rabbit anti-SERT (1:2500; ImmunoStar, Inc, Hudson, WI) at 4°C. After washing with PBS, sections were incubated in biotinylated goat anti-rabbit IgG (1:200; Vector Laboratories) made in 1% PBS for 1h. After incubation with 1% avidin biotin complex (Vectastain Elite ABC Kit, Vector laboratories) for 1h, sections were washed and reacted for visualization using diaminobenzidine tetrahydrochloride (DAB) solution in a peroxidase reaction to produce a brown reaction product. Sections were mounted in Entellan (Electron Microscopy Sciences). Images were captured by using a Nikon Eclipse E1000

microscope (Nikon, Tokyo, Japan) equipped with bright- and dark-field condensers for transmitted light and a digital camera (DXM1200 3.0, ACT-1 software, Nikon). Axons were visualized at a magnification of 20x objective, yielding excellent resolution of bright and well-delineated axons. The images were contrast by histogram stretching followed by thresholding to convert to a binary image using ImageJ Software. For each mouse, measurements were taken from three coronal brain sections and, six different microscope fields were analyzed in each section.

For BdrU IHC was performed as previously described.[71-73] Briefly, 30-µm-thick, free floating coronal hippocampus sections were incubated for 2h in 50% formamide/2× SSC at 65°C, followed by incubation in 2N HCl for 30 min. Then sections were incubated for 10 min in 0.1M borate buffer. After washing in PBS, sections were incubated in 1% H_2O_2 in PBS for 30 min to inactive endogenous peroxidase activity. After several rinses in PBS, sections were incubated in PBS/0.2% Triton X-100/5% goat serum (PBS–TS) for 30 min and then incubated with monoclonal mouse anti-BrdU (1:600; Roche Diagnostics, Barcelona, Spain) overnight at 4°C. After several rinses in PBS–TS, sections were incubated for 2h with biotinylated goat anti-mouse Fab Fragment IgG secondary antibody (1:200; Jackson ImmunoResearch Laboratories, Inc., US-PA), followed by amplification with avidin–biotin complex (Vector Laboratories). For quantification of BrdU+ cells, one every sixth section throughout the hippocampus was processed and counted under a light microscope (Carl Zeiss Axioskop 2 Plus) at 40x and 100x magnification. The total number of BrdU+ cells per section were determined and multiplied by 6 to obtain the total number of BrdU+ cells per hippocampus.

Ki-67 IHC was carried out in adjacent sections to those used in the BdrU labeling studies. IHC visualization of cell proliferation by Ki-67 has been validated

against the BdrU labeling technique elsewhere,[53] showing high correlations between the two methods. After several rinses in PBS, endogenous peroxidase activity was inactivated and the sections were rinsed in PBS and the antigen was retrieved by heating at 80ºC in 10 mM citric acid, pH 9.0 for 30 min. After several washes in PBS, block for 30 min in blocking solution (50mM Tris–HCl, 150mM NaCl, 0.1% Triton X-100, pH 7.4), containing 1% donkey serum and 1% BSA). Incubate with rabbit anti-Ki-67 (1:5000, Abcam plc, Cambridge, UK) overnight at 4°C. Sections were washed with PBS, incubated with biotinylated donkey anti-rabbit secondary antibody (1:200; Jackcon ImmunoResearch Laboratories, Inc., US) for 2h, and the signal was amplified with avidin–biotin complex (Vector Laboratories). Ki-67+ cells were labeled using DAB as chromogen (Vector Laboratories). The quantification of Ki67+ cells was performed as described for BrdU+ cells.

To evaluate adult neurogenesis, we also used a primary goat polyclonal anti-NeuroD-antibody (1:200, sc-1084, Santa Cruz Biotechnology, Santa Cruz, CA) and a primary goat polyclonal anti-DCX-antibody (Doublecortin; 1:200; sc-8066, Santa Cruz Biotechnology). After endogenous peroxidase inhibition and washes, pre-incubation and incubation were carried out in a 1x PBS/Triton 0.2% solution containing 10% and 3% normal donkey serum (Millipore), respectively. Both primary antibodies, anti-NeuroD and anti-DCX, were incubated overnight a 4ºC, followed by incubation with biotinylated donkey anti-goat (1:200, sc-2042, Santa Cruz Biotechnology), and subsequent incubation in ABC solution (Vector Laboratories) according to the manufacturer's instructions. The color reaction was performed by incubation with DAB solution. The sections were mounted onto gelatin-coated slides, embedded and investigated on a Nikon Eclipse E1000 microscope (Nikon, Tokyo, Japan) using 20x and 40x objectives. For each marker and mouse, between three consecutive

sections containing the hippocampal structures and six different microscope fields were analyzed in each section.

For IHC visualization of neurons (NeuN, 1:1000, Millipore, Madrid, Spain), reactive astrocytes (GFAP, 1:1000, DAKO, Barcelona, Spain), or microglia (IBA-1, 1:1,000; WAKO, Irvine, CA), we used a biotin-labeled antibody procedure. Following endogenous peroxidase inhibition and washes, tissues were blocked for 2h in 3% normal goat serum, and primary antibody incubations were carried out overnight at 4ºC. Sections were incubated in goat anti-rabbit or anti-mouse biotinylated IgG secondary antibodies (1:200; Vector Laboratories, Burlingame, CA) for 1h at room temperature and subsequent incubation in ABC solution. Sections were mounted onto gelatin-coated slides with Entellan. Images were captured by using a Nikon Eclipse E1000 microscope (Nikon, Tokyo, Japan) equipped with a digital camera (DXM1200 3.0, Nikon) and ACT-1 software (Nikon). Figures were assembled in Adobe Photoshop (Adobe Systems, San Jose, CA); only contrast and brightness were adjusted to optimize the images. The secondary antibody controls were run in parallel with each experiment (Figure S6).

Intracerebral microdialysis

Extracellular serotonin (5-HT) concentration was measured by *in vivo* microdialysis as previously described.[18,39] Briefly, one concentric dialysis probe (Cuprophan; 1.5 mm-long) was implanted in caudate putamen (CPu; AP, 0.5; ML, -1.7; DV, -4.5) or ventral hippocampus (vHPC; AP, -3.0; ML, -3.0; DV, -4.0)[36] of pentobarbital-anaesthetized mice. Experiments were performed 24-48h after surgery. Veratridine, a voltage-dependent Na+ channel opening agent, was from Tocris Bioscience (Bristol, UK). To assess 8-OH-DPAT effects on extracellular 5-HT, 1µM SSRI-

citalopram (Lundbeck A/S, Valby, Copenhagen) was added to artificial cerebrospinal fluid (CSF).[74] The aCSF was pumped (WPI model, SP220i) at 2.0 μlmin^{-1} and 30-min samples were collected. 5-HT concentrations were analyzed by high-performance liquid chromatography-amperometric detection (+0.6V; Hewlett Packard 1049, Palo Alto, CA, USA) with detection limits of 1.5 fmolsample^{-1}. Baseline 5-HT levels were calculated as the average of the four pre-drug samples. Correct probe placement was verified using cresyl-violet staining.

Supplementary references

66. Santana N, Bortolozzi A, Serrats J, Mengod G, Artigas F. Expression of serotonin1A and serotonin2A receptors in pyramidal and GABAergic neurons of the rat prefrontal cortex. *Cerebral Cortex* 2004; **14**: 1100-1109.

67. D'Amato RJ, Largent BL, Snowman AM, Snyder SH. Selective labeling of serotonin uptake sites in rat brain by [3H]citalopram contrasted to labeling of multiple sites by [3H]imipramine. *J Pharmacol Exp Ther* 1987; **242**: 364-371.

68. Pazos A, Palacios JM. Quantitative autoradiographic mapping of serotonin receptors in the rat brain. I. Serotonin-1 receptors. *Brain Res* 1985; **346**: 205-230.

69. Qian Y, Melikian HE, Rye DB, Levey AI, Blakely RD. Identification and characterization of antidepressant-sensitive serotonin transporter proteins using site-specific antibodies. *J Neurosci* 1995; **15**: 1261–1274.

70. Sur C, Betz H, Schloss P. Immunocytochemical detection of the serotonin transporter in rat brain. *Neuroscience* 1996; **73**: 217–231.

71. Mostany R, Valdizán EM, Pazos A. A role for nuclear beta-catenin in SNRI antidepressant-induced hippocampal cell proliferation. *Neuropharmacol* 2008; **55**:18-73.

72. Pilar-Cuéllar F, Vidal R, Pazos A. Subchronic treatment with fluoxetine and ketanserin increases hippocampal brain-derived neurotrophic factor, β-catenin and antidepressant-like effects. *Br J Pharmacol* 2012; **165**: 1046-1057.

73. Pascual-Brazo J, Castro E, Díaz A, Valdizán EM, Pilar-Cuéllar F, Vidal R, Treceño B, Pazos A. Modulation of neuroplasticity pathways and antidepressant-like behavioural responses following the short-term (3 and 7 days) administration

of the 5-HT_4 receptor agonist RS67333. *Int J Neuropsychopharmacol* 2012; **15**: 631-643.

74. Adell A, Celada P, Abellán MT, Artigas F. Origin and functional role of the extracellular serotonin in the midbrain raphe nuclei. *Brain Res Rev* 2002; **39**: 154–180.

4.4. Trabajo 4

Therapeutic antidepressant potential of a conjugated siRNA silencing the serotonin transporter after intranasal administration

A Ferrés-Coy, M Galofré, F Pilar-Cuéllar, R Vidal, V Paz, E Ruiz-Bronchal, L Campa, A Pazos, JR Caso, JC Leza, G Alvarado, A Montefeltro, EM Valdizán, F Artigas and A Bortolozzi

Molecular Psychiatry. 2016 Mar; 21(3):328-338

Estrategias de RNAi han sido previamente utilizadas para evocar respuestas de tipo antidepresivo en animales de experimentación. Sin embargo, una de las principales limitaciones de su uso *in vivo* se relaciona con la limitada capacidad que disponemos para dirigir los oligonucleótidos hacia sistemas o poblaciones neuronales específicas. En el presente trabajo, integramos la tecnología desarrollada en los estudios 1 y 3 y, generamos un siRNA contra el SERT conjugado con sertralina (C-SERT-siRNA) para facilitar su acumulación en neuronas serotoninérgicas después de la administración intranasal. Además nos preguntamos si la molécula de C-SERT-siRNA sería capaz de revertir el comportamiento de tipo depresivo del modelo murino asociado al consumo crónico de corticosterona.

Los resultados mostraron que la administración intranasal del C-SERT-siRNA disminuye la expresión y función del SERT, produciendo respuestas de tipo antidepresivo en ratón más rápido que aquellas inducidas por fluoxetina. Estas respuestas incluyeron: 1) incremento de la concentración de 5-HT en áreas de proyección como el cuerpo estriado y el HPC, 2) desensibilización del autoreceptor 5-HT_{1A}, 3) aceleración de la proliferación de precursores neuronales, 4) incremento de la expresión de factores tróficos y, 5) incremento de la complejidad dendrítica en el HPC. Además, mientras que la fluoxetina requiere un tratamiento de 28 días, solo siete días de tratamiento con el C-SERT-siRNA fueron suficientes para revertir el

comportamiento de tipo depresivo exhibido por los ratones expuestos al consumo crónico de corticosterona.

Los presentes resultados demuestran la factibilidad de evocar respuestas de tipo antidepresivo utilizando estrategias de RNAi apropiadas para dirigir las moléculas de oligonucleótidos hacia poblaciones neuronales específicas, abriendo así nuevas vías/horizontes para futuros estudios traslacionales.

Molecular Psychiatry (2016) 21, 328–338

www.nature.com/mp

OPEN

ORIGINAL ARTICLE

Therapeutic antidepressant potential of a conjugated siRNA silencing the serotonin transporter after intranasal administration

A Ferrés-Coy[1,2,3], M Galofré[1,2,3], F Pilar-Cuéllar[3,4], R Vidal[3,4], V Paz[1,2,3], E Ruiz-Bronchal[1,2,3], L Campa[1,2,3], Á Pazos[3,4], JR Caso[3,5], JC Leza[3,5], G Alvarado[6], A Montefeltro[6], EM Valdizán[3,4], F Artigas[1,2,3] and A Bortolozzi[1,2,3]

Major depression brings about a heavy socio-economic burden worldwide due to its high prevalence and the low efficacy of antidepressant drugs, mostly inhibiting the serotonin transporter (SERT). As a result, ~80% of patients show recurrent or chronic depression, resulting in a poor quality of life and increased suicide risk. RNA interference (RNAi) strategies have been preliminarily used to evoke antidepressant-like responses in experimental animals. However, the main limitation for the medical use of RNAi is the extreme difficulty to deliver oligonucleotides to selected neurons/systems in the mammalian brain. Here we show that the intranasal administration of a sertraline-conjugated small interfering RNA (C-SERT-siRNA) silenced SERT expression/function and evoked fast antidepressant-like responses in mice. After crossing the permeable olfactory epithelium, the sertraline-conjugated-siRNA was internalized and transported to serotonin cell bodies by deep Rab-7-associated endomembrane vesicles. Seven-day C-SERT-siRNA evoked similar or more marked responses than 28-day fluoxetine treatment. Hence, C-SERT-siRNA (i) downregulated 5-HT_{1A}-autoreceptors and facilitated forebrain serotonin neurotransmission, (ii) accelerated the proliferation of neuronal precursors and (iii) increased hippocampal complexity and plasticity. Further, short-term C-SERT-siRNA reversed depressive-like behaviors in corticosterone-treated mice. The present results show the feasibility of evoking antidepressant-like responses by selectively targeting neuronal populations with appropriate siRNA strategies, opening a way for further translational studies.

Molecular Psychiatry (2016) **21,** 328–338; doi:10.1038/mp.2015.80; published online 23 June 2015

INTRODUCTION

Major depressive disorder (MDD) is a severe, chronic and life-threatening disease with a high incidence; affecting ca. 120 million people worldwide.[1–3] The midbrain serotonin (5-hydroxytryptamine (5-HT)) system has a critical role in many brain functions, including mood control. Derangements of serotonin pathway are involved in MDD, and most antidepressant drugs aim to increase serotonergic function.[4] Serotonin transporter (SERT) is a key player in MDD, by controlling the active 5-HT fraction and, being the target of most prescribed antidepressant drugs, the selective serotonin reuptake inhibitors (SSRI) and the selective serotonin and norepinephrine reuptake inhibitors (SNRI).[5,6] These drugs need to be administered for long time before clinical improvement emerges, and they fully remit depressive symptoms in only one-third of patients leaving a large proportion of people with partial or incomplete clinical responses.[7,8] For these reasons, there is an urgent need to improve antidepressant treatments.

Chronic—but not acute—SSRI treatments elicit a series of neurobiological changes relevant for antidepressant activity. Hence, chronic SSRI treatments downregulates SERT, increasing forebrain serotonergic neurotransmission and neuronal plasticity in the hippocampus,[9–12] although the precise mechanisms involved remain uncertain. Likewise, chronic SSRI treatments internalize SERT and reduce SERT-binding sites without affecting SERT mRNA levels.[9,10,13,14] In particular, fluoxetine (FLX) promotes the biogenesis of microRNA-16, resulting in a downstream repression of SERT levels in mouse 5-HT neurons, accompanied by antidepressant-like effects in the chronic mild stress and forced-swim animal models.[15]

Altogether, these data uncover the functional significance of SERT downregulation in mediating antidepressant responses. The identification of intracellular networks underlying SERT downregulation may be a new target for the development of fast-acting antidepressants. Hence, exogenous small interfering RNAs (siRNAs) have been preliminarily investigated as potential therapeutic tools to silence the expression of critical genes in 5-HT neurons.[16–18] Intracerebral treatments with siRNA against SERT—or their related antisense oligonucleotides—significantly decreased SERT expression and function in the rodent brain and evoked cellular and behavioral responses predictive of clinical antidepressant activity.[16,17,19] Despite these exciting prospects, the utility of RNA interference (RNAi)-based silencing strategies for MDD treatment is severely compromised by the extreme difficulty to deliver oligonucleotide sequences to their neuronal functional sites, due to the need to cross several biological barriers after administration and the evident complexity of the mammalian brain.[20,21]

Here we have used targeted delivery of a sertraline ligand-conjugated siRNA directed against SERT (C-SERT-siRNA) to

[1]Institut d'Investigacions Biomèdiques August Pi i Sunyer (IDIBAPS), Barcelona, Spain; [2]Department of Neurochemistry and Neuropharmacology, IIBB-CSIC (Consejo Superior de Investigaciones Científicas), Barcelona, Spain; [3]Centro de Investigación Biomédica en Red de Salud Mental (CIBERSAM), ISCIII, Madrid, Spain; [4]Institute of Biomedicine and Biotechnology of Cantabria (IBBTEC; UC-CISC-SODERCAN), Santander, Spain; [5]Department of Pharmacology, School of Medicine, Universidad Complutense and IIS Hospital 12 de Octubre, Madrid, Spain and [6]n-Life Therapeutics, S.L., Granada, Spain. Correspondence: Dr A Bortolozzi, Department of Neurochemistry and Neuropharmacology, IIBB-CSIC-IDIBAPS, Rosselló 161, 6th floor, Barcelona 08036, Spain.
E-mail: abbnqi@iibb.csic.es
Received 10 October 2014; revised 27 March 2015; accepted 6 May 2015; published online 23 June 2015

downregulate SERT expression selectively in raphe 5-HT neurons. We show that C-SERT-siRNA silenced SERT expression/function and evoked fast and robust antidepressant-like responses after intranasal (i.n.) administration in mice. Moreover, it reversed the depressive-like behavior in corticosterone-treated mice due to the increased 5-HT signaling and synaptic plasticity. These results highlight the potential of RNAi-based antidepressant therapies targeting genes linked to antidepressant responses, such as SERT or the 5-HT_{1A}-autoreceptor[18] through a clinically feasible (i.n.) administration route.

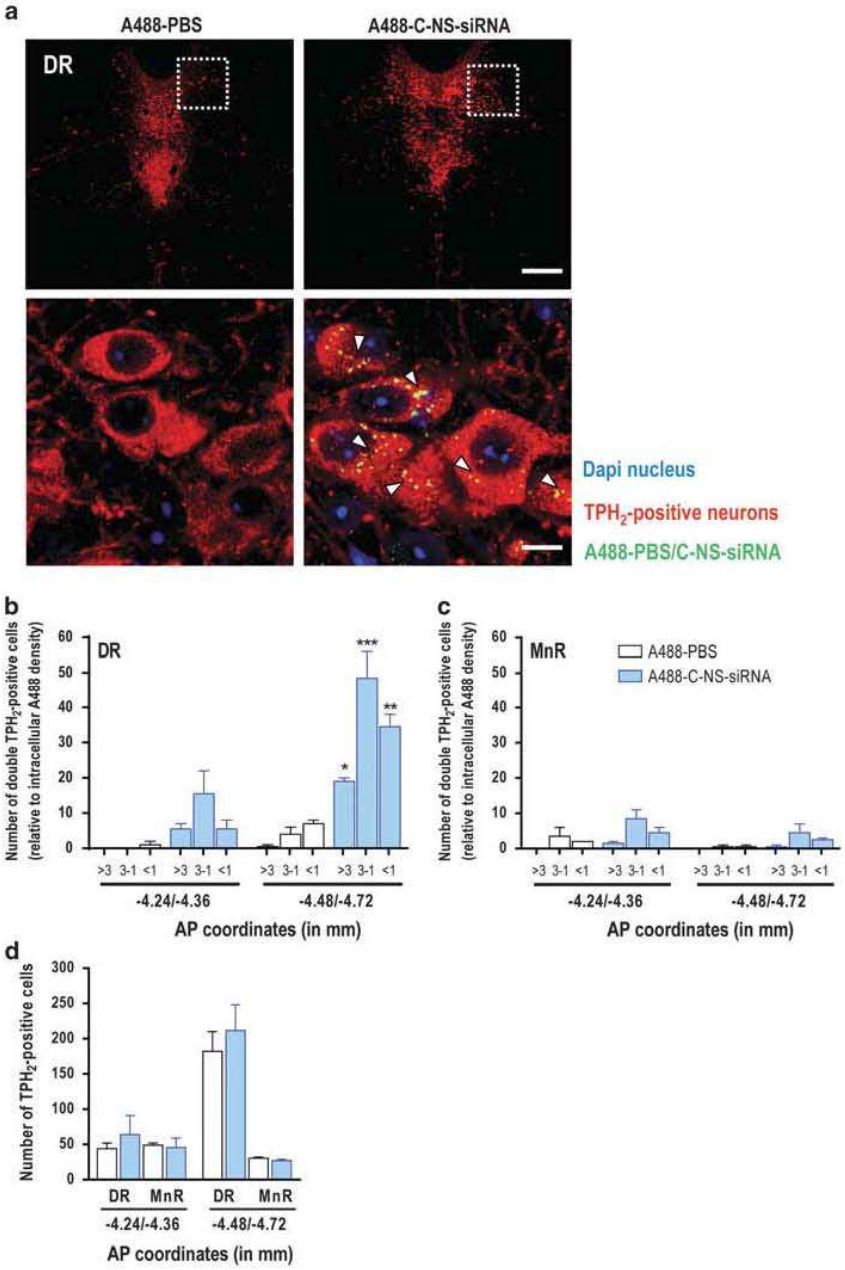

Figure 1. Selective accumulation of sertraline-conjugated nonsense-siRNA (C-NS-siRNA) in tryptophan hydroxylase2-positive (TPH_2-positive) 5-hydroxytryptamine (5-HT) neurons after intranasal administration. Mice were intranasally administered with alexa488 phosphate-buffered saline (PBS) (A488-PBS) or alexa488-labeled C-NS-siRNA (A488-C-NS-siRNA) at 30 µg day^{-1} during 4 days and were killed 6 h postadministration ($n = 2$ mice/group). (**a**) Confocal images showing co-localization of A488-C-NS-siRNA (yellow) in dorsal raphe nucleus (DR) 5-HT neurons (TPH_2-positive, red) identified with white arrowheads. Cell nuclei were stained with DAPI (4,6-diamidino-2-phenylindole; blue). Bottom row are high-magnification photomicrographs of the frames in top row. Scale bars: low = 200 µm, high = 10 µm. (**b** and **c**) Histograms show the distribution profile of the abundance of A488-C-NS-siRNA (expressed as fluorescence units, ranges shown below the abscissa axis) in TPH_2-positive neurons. Note the greater number of TPH_2-positive cells co-localized with A488-C-NS-siRNA in the DR compared with median raphe nucleus (MnR). Range: >3, 3–1 and <1 represent relative unit of intracellular A488 density. (**d**) Number of TPH_2-positive cells in the DR and MnR of mice. AP coordinates (in mm): −4.24/−4.36 and −4.48/−4.72 from bregma ($n = 2$ mice/group). $^*P < 0.05$, $^{**}P < 0.01$, $^{***}P < 0.001$ versus A488-PBS-treated mice. Data are mean ± s.e.m.

MATERIALS AND METHODS

Animals

Male C57BL/6J mice (10–14 weeks; Charles River, Lyon, France) were housed under controlled conditions (22 ± 1 °C; 12-h light/dark cycle) with food and water available *ad libitum*. Animal procedures were conducted in accordance with standard ethical guidelines (EU regulations L35/118/12/1986) and approved by the local ethical committee.

Conjugated siRNA synthesis

The synthesis and purification of sertraline-conjugated siRNA directed against SERT (C-SERT-siRNA, nt: 1230–1250, GenBank accession NM_010484) and sertraline-conjugated nonsense siRNA (C-NS-siRNA) molecules were performed by nLife Therapeutics S.L. (Granada, Spain).[18] Details are shown in Supplementary Information.

To study *in vivo* intracellular distribution and incorporation of conjugated siRNA into 5-HT neurons, C-NS-siRNA was additionally labeled with alexa488 in the antisense strand (A488-C-NS-siRNA). We used C-NS-siRNA instead of C-SERT-siRNA to examine the brain distribution after i.n. administration because C-SERT-siRNA reduces SERT expression (see Results section), this compromising the penetration of new doses into 5-HT neurons through SERT. Along these lines, we assumed that the main factor conferring the neuronal target selectivity was the presence of covalently bound sertraline rather than the oligonucleotide sequence. Stock solutions of all siRNAs were prepared in RNAse-free water and stored at − 20 °C until use. Sequences are shown in Supplementary Table S1.

Treatments

For i.n. administration, mice were slightly anesthetized by 2% isoflurane inhalation and placed in a supine position.[18] A 5-µl drop of phosphate-buffered saline (PBS) or conjugated siRNA (C-NS-siRNA and C-SERT-siRNA) was applied alternatively to each nostril once daily. A total of 10 µl of solution containing 30 µg (2.1 nmol day $^{-1}$) of conjugated siRNA was delivered for 1, 4 or 7 days, and mice were killed at 1, 3, 7 or 15 days after last administration. To evaluate the C-SERT-siRNA efficacy on SERT knockdown, mice were i.n. treated with the C-SERT-siRNA at 10, 30 or 100 µg day $^{-1}$ (0.7, 2.1 or 7 nmol day $^{-1}$, respectively) during 7 days and were killed 24 h after last administration.

FLX (Tocris, Madrid, Spain) was administered once daily at 10 mg kg $^{-1}$, intraperitoneally (i.p.), for 7 or 28 days. Mice were killed at 24 h after last administration. Control mice received saline.

Corticosterone (Cortico, Sigma-Aldrich, Madrid, Spain) was dissolved in commercial mineral water and brought to a pH 7.0–7.4 with HCl. Group-housed mice were presented with Cortico solution for 28 or 49 days at: 30 µg ml $^{-1}$ during 15 days (resulting in a dose of approximately 6.6-mg kg $^{-1}$ day $^{-1}$, p.o.), followed by 15 µg ml $^{-1}$ (2.7 mg kg $^{-1}$ day $^{-1}$) during

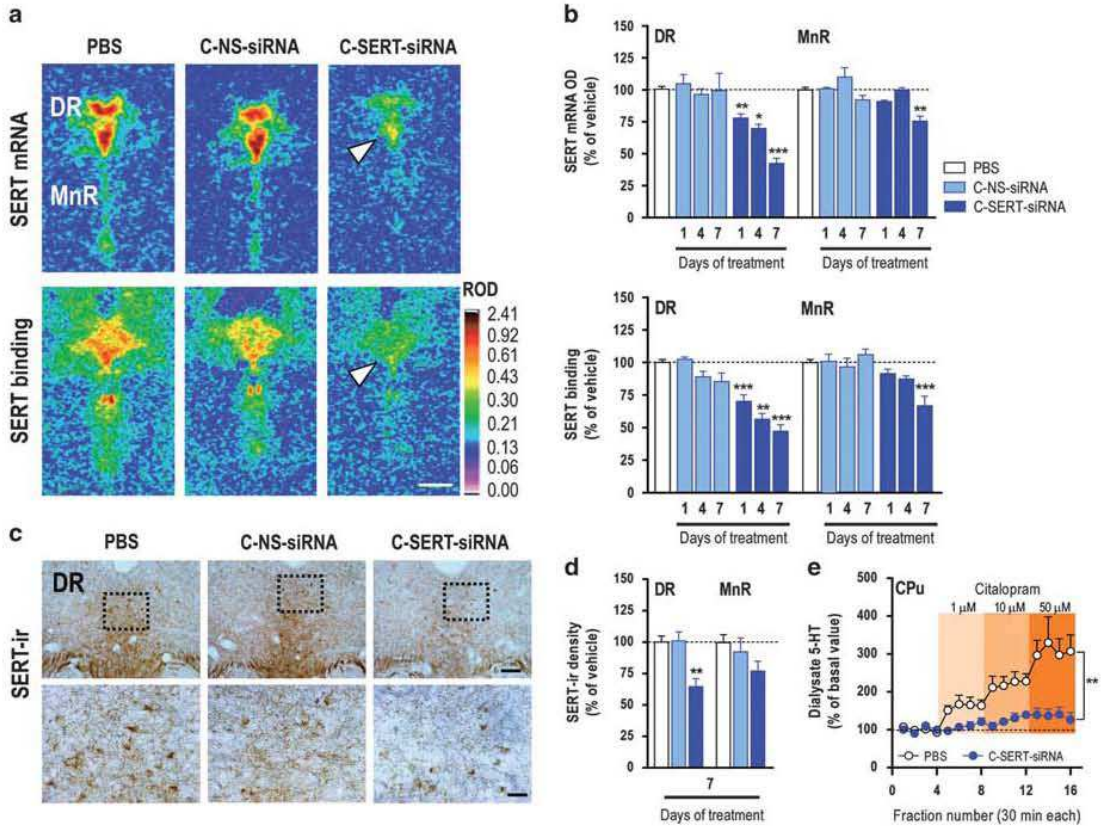

Figure 2. Intranasal sertraline-conjugated serotonin transporter small interfering RNA (SERT-siRNA) (C-SERT-siRNA) treatment downregulates SERT expression. Mice received intranasally: phosphate-buffered saline (PBS), sertraline-conjugated nonsense-siRNA (C-NS-siRNA) or C-SERT-siRNA at 30 µg day^{-1} (2.1 nmol day^{-1}) during 1, 4 or 7 days. (**a**) Coronal brain sections showing reduced SERT mRNA and binding site levels in the dorsal raphe nucleus (DR) (AP coordinates: −4.48 to −4.72 in mm) of mice treated with C-SERT-siRNA (7-day). Scale bar: 500 µm. (**b**) Effects of C-SERT-siRNA on SERT mRNA and binding site densities in the DR and median raphe nucleus (MnR) ($n = 3$–8 mice/group; $^{*}P < 0.05$, $^{**}P < 0.01$, $^{***}P < 0.001$ versus PBS- and C-NS-siRNA-treated mice). (**c**) Immunohistochemistry images showing the expression of SERT protein (SERT-ir) in mouse DR. Bottom row are high-magnification photomicrographs of the frames in top row. Scale bars: low = 100 µm, high = 20 µm. (**d**) C-SERT-siRNA treatment (7-day) decreased DR SERT protein density versus PBS- and C-NS-siRNA-treated mice ($n = 3$–5 mice/group; $^{**}P < 0.01$). (**e**) Local selective serotonin reuptake inhibitor citalopram infusion by reverse-dialysis induced concentration-dependent increases of extracellular 5-hydroxytryptamine (5-HT) in the caudate putamen (CPu) of PBS-treated mice more than in C-SERT-siRNA-treated mice ($n = 7$–8 mice/group; $^{**}P < 0.01$ versus PBS). Data are mean ± s.e.m.

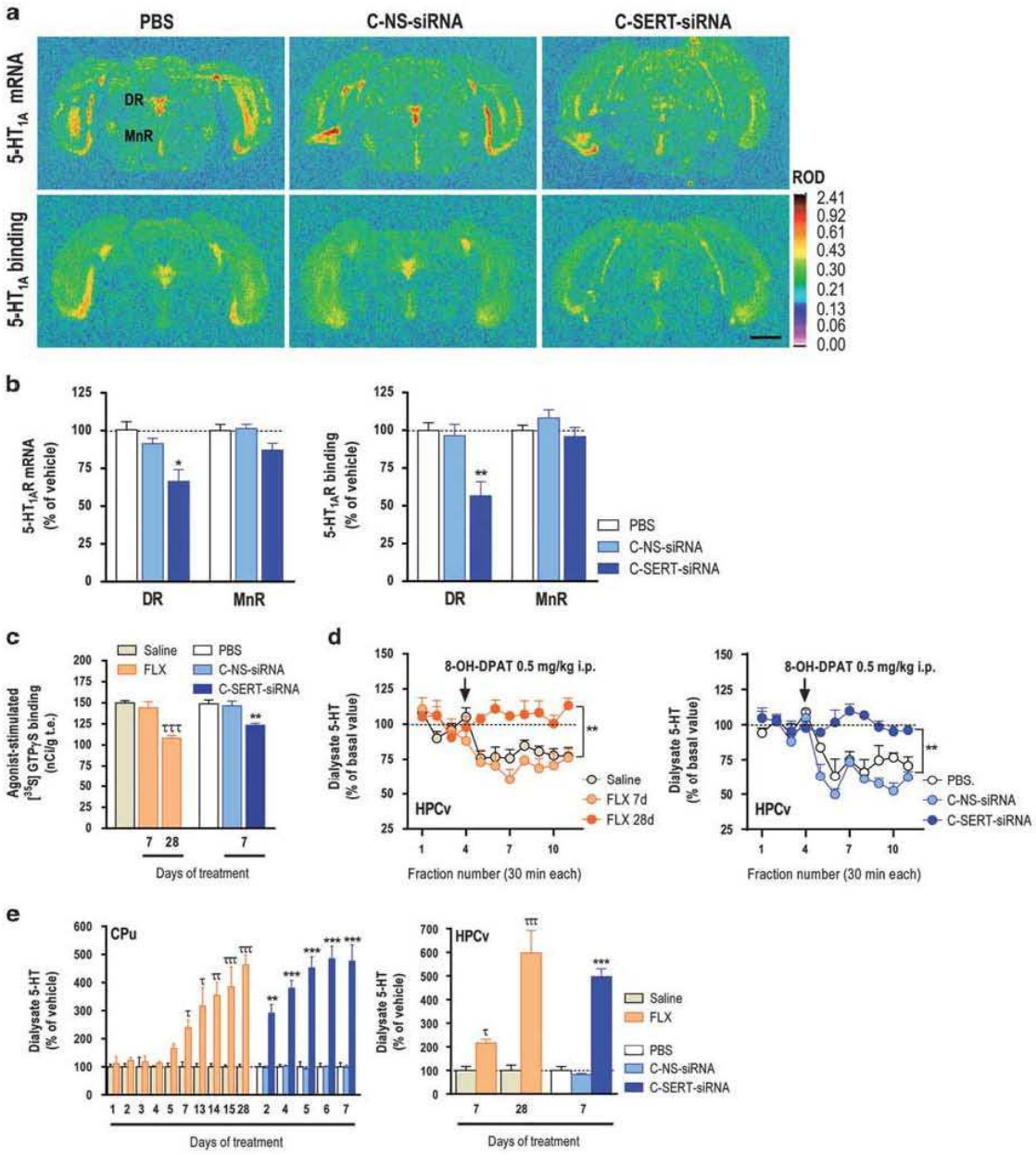

Figure 3. RNA interference-induced serotonin transporter (SERT) suppression reduces 5-hydroxytryptamine 1A (5-HT_{1A})-autoreceptor expression/function and rapidly enhances the forebrain 5-HT transmission. Mice were intranasally administered with: phosphate-buffered saline (PBS), sertraline-conjugated nonsense-small interfering RNA (siRNA) (C-NS-siRNA) or sertraline-conjugated SERT-siRNA (C-SERT-siRNA) at 30 μg day^{-1} during 7-day treatment. Other groups of mice were treated with saline or fluoxetine (FLX) at 10 mg kg^{-1} day^{-1}, intraperitoneally during 7- or 28-day treatment. (**a**) Representative coronal brain sections showing reduced 5-HT_{1A} receptor mRNA and binding site levels in the dorsal raphe nucleus (DR) of C-SERT-siRNA-treated mice. Scale bar: 2 mm. (**b**) Effects of C-SERT-siRNA on 5-HT_{1A} receptor mRNA and binding site densities in the DR and median raphe nucleus (MnR) of mice ($n = 3$–4 mice/group; $^{*}P < 0.05$, $^{**}P < 0.01$ compared with PBS- and C-NS-siRNA-treated mice). (**c**) Effects of C-SERT-siRNA and FLX on 5-HT_{1A}-autoreceptor function. C-SERT-siRNA (7-day) decreased 5-HT_{1A} receptor-mediated 8-OH-DPAT-stimulated [^{35}S]GTPγS binding in the DR, whereas FLX (7-day) was without effect ($n = 3$–4 mice/group; $^{**}P < 0.01$ versus PBS- and C-NS-siRNA-treated mice). FLX reduced 5-HT_{1A}-autoreceptor function after 28-day treatment ($n = 3$–4 mice/group; $^{\tau\tau\tau}P < 0.001$ versus saline and FLX 7-day). (**d**) 8-OH-DPAT did not reduce 5-HT release in the ventral hippocampus (HPCv) of C-SERT-siRNA-treated mice (7-day), unlike control groups ($n = 3$–4 mice/group; $^{**}P < 0.01$ versus PBS and C-NS-siRNA). However, 8-OH-DPAT decreased hippocampal 5-HT concentration in saline- and FLX-treated 7-day mice but not in 28-day FLX-treated mice ($n = 5$–8 mice/group; $^{\tau\tau}P < 0.01$ versus saline and FLX 7-day). (**e**) Intranasal C-SERT-siRNA treatment increased extracellular 5-HT levels in CPu more rapidly than FLX ($n = 4$–10 mice/group; $^{**}P < 0.01$, $^{***}P < 0.001$ versus PBS and C-NS-siRNA; $^{\tau}P < 0.05$, $^{\tau\tau}P < 0.01$, $^{\tau\tau\tau}P < 0.001$ versus saline). Significant differences versus their respective control mice occurred after 2-day C-SERT-siRNA and after 7-day FLX treatment. Similar temporal differences were observed in HPCv ($n = 3$-6 mice/group; $^{***}P < 0.001$ versus PBS and C-NS-siRNA; $^{\tau}P < 0.05$, $^{\tau\tau\tau}P < 0.001$ versus saline). Data are mean ± s.e.m.

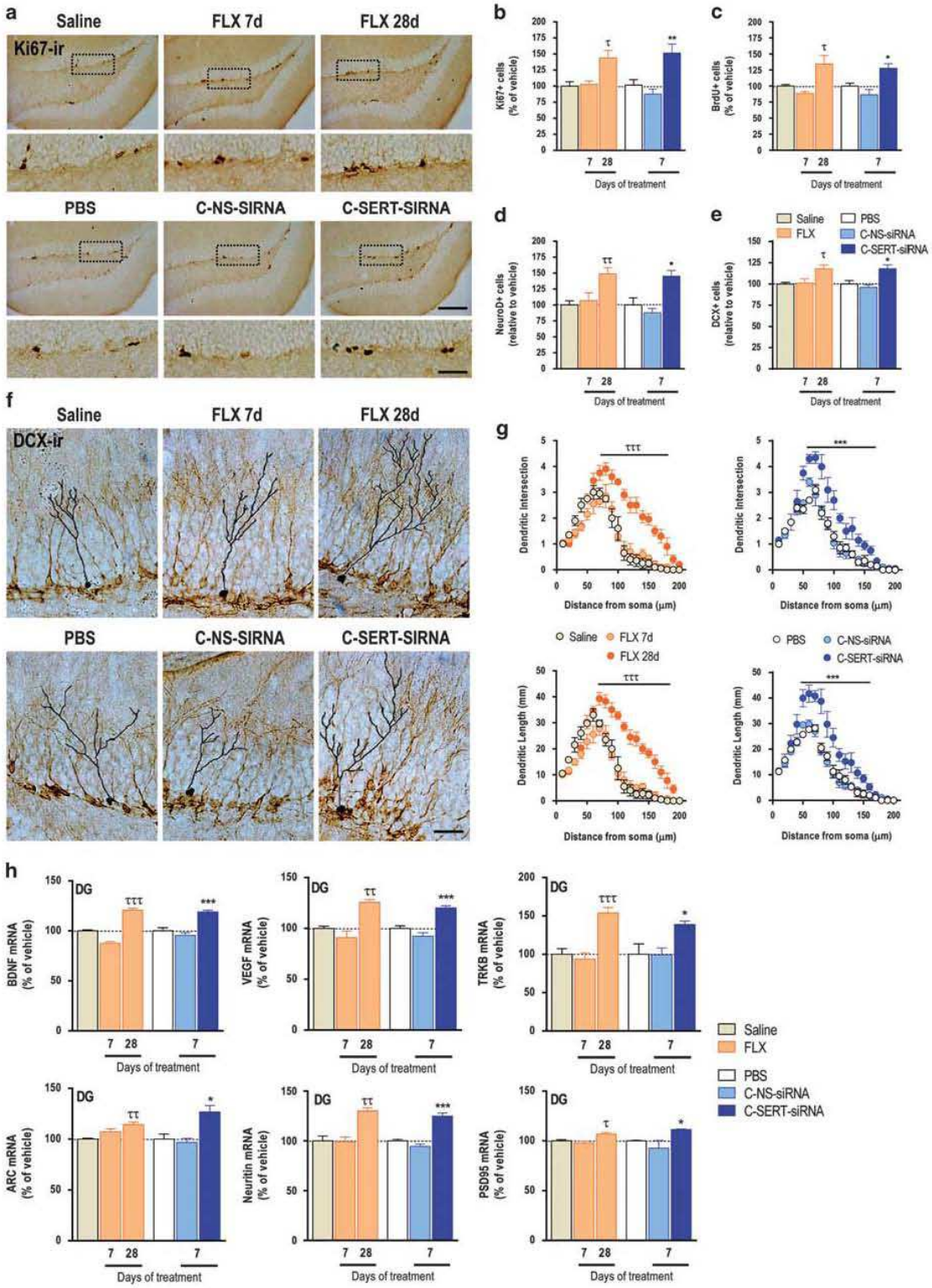

3 days and 7.5 μg ml^{-1} (1.1 mg kg^{-1} day^{-1}) during 10 or 31 days to allow a gradual recovery of endogenous corticosterone plasma level.[22,23] Cortico solutions were no more than 3 days old and mantained in opaque bottles to protect it from light. From day 21, one group of animals treated with Cortico received daily i.n. PBS, C-NS-siRNA or C-SERT-siRNA for 7 days. Another group of mice treated with Cortico received i.p. injections of saline or FLX for 7 or 28 days (Supplementary Figure S1).

Plasma corticosterone levels

Posttreatment corticosterone was measured in plasma obtained from blood samples after cardiac puncture at 1500–1600 hours using trisodium citrate as anticoagulant. After blood centrifugation at 1000 *g* for 15 min, all plasma samples were stored at −80 °C before assay by using a commercially available kit by radioimmunoassay of ^{125}I-labeled rat corticosterone (Coat-A-Count, Siemens, Healthcare Diagnostics, Berkeley, CA, USA). A gamma counter (Perkin Elmer Wallac Wizard 1470, Turku, Finland) was used to measure radioactivity of the samples.[24]

In situ hybridization

Mice were killed by pentobarbital overdose, and the brains were rapidly removed, frozen on dry ice and stored at −80 °C. Coronal tissue sections (14-μm thick) were cut using a microtome-cryostat (HM500-OM, Microm, Walldorf, Germany), thaw-mounted onto 3-aminopropyltriethoxysilane (Sigma-Aldrich)-coated slides and kept at −20 °C until use. Antisense oligoprobes were complementary to bases: SERT/820-863 (GenBank accession NM_010484.1), serotonin1A receptor-5-HT$_{1A}$R/1780-1827 (NM_008308), tryptophan hydroxylase-2 (TPH$_2$)/360-410 (NM_173391), brain-derived neurotrophic factor (BDNF)/1188-1238 (NM_007540), vascular endothelial growth factor (VEGF)/2217-2267 (NM_001025250), activity-regulated cytoskeletal protein (ARC)/1990-2040 (NM_018790), TRKB receptor/1075-1124 (NM_001025074), PSD-95/76-120 (D50621), and neuritin/408-448 (NM_153529), respectively (Göttingen, Germany). Oligonucleotides were individually labeled (2 pmol) at the 3'-end with [^{33}P]-dATP (>2500 Ci mmol^{-1}; DuPont-NEN, Boston, MA, USA) using terminal deoxynucleotidyl-transferase (TdT, Calbiochem, La Jolla, CA, USA). Sections were hybridized as previously described.[17,18,25] Details are shown in Supplementary Information.

Autoradiographic studies

The autoradiographic binding assays for 5-HT$_{1A}$R, SERT and norepinephrine transporter were performed using the following radioligands: (a) [^{3}H]-8-OH-DPAT (233 Ci mmol^{-1}), (b) [^{3}H]-citalopram (70 Ci mmol^{-1}) and (c) [^{3}H]-nisoxetine (85 Ci mmol^{-1}), respectively (Perkin-Elmer, Madrid, Spain) as described previously.[17] The experimental conditions are summarized in Supplementary Table S2. For 5-HT$_{1A}$R-stimulated [^{35}S]GTPγS autoradiography, coronal dorsal raphe nucleus (DR) sections were labeled with 0.04 nM [^{35}S]GTPγS.[17] Details are shown in Supplementary Information.

Quantitative image analysis of film autoradiograms

Autoradiograms were analyzed and relative optical densities (ROD) were obtained using a computer-assisted image analyzer (MCID, Mering, Germany). The system was calibrated with ^{3}H- or ^{14}C-microscales standards to obtain fmol mg^{-1} protein equivalents from ROD data. The slide background and non-specific densities were subtracted. ROD were evaluated in two or three adjacent sections by duplicate of each mouse and averaged to obtain individual values. MCID system was also used to acquire pseudocolor images. Black and white photographs were taken from autoradiograms using a Wild 420 microscope (Leica, Heerbrugg, Germany) equipped with Nikon DXM1200F digital camera and ACT-1 Nikon software (Soft Imaging System Gmbh, Münster, Germany). Images were processed with Photoshop (Adobe Systems, Mountain View, CA, USA) by using identical values for contrast and brightness.

5-Bromo-2'-deoxyuridine (BrdU) administration

BrdU was purchased from Sigma-Aldrich and dissolved in saline solution. The last day of antidepressant treatment, mice were injected with 4×75-mg kg^{-1} BrdU, i.p., every 2h and were killed 24h later in according to Santarelli *et al.*[11]

Immunohistochemistry

Mice were anesthetized with pentobarbital and transcardially perfused with 4% paraformaldehyde in sodium–phosphate buffer (pH 7.4). Brains were collected, postfixed 24 h at 4 °C in the same solution and then placed in gradient sucrose 10–30% for 3 days at 4 °C. After cryopreservation, serial 30-μm thick sections were cut through the olfactory bulbs, the hippocampal formation, amygdala and the midbrain raphe nuclei. Immunohistochemical procedure was performed for SERT, BrdU, Ki-67, NeuroD, NeuN, Doublecortin (DCX), glial fibrillary acidic protein (GFAP) and Iba-1 using biotin-labeled antibody procedure.[17] Details are shown in Supplementary Information.

Confocal fluorescence microscopy

Intracellular C-NS-siRNA distribution in 5-HT neurons was examined by confocal microscopy using a Leica TCS SP5 laser scanning confocal microscope (Leica Microsystems Heidelberg GmbH, Manheim, Germany) equipped with a DMI6000 inverted microscope, blue diode (405 nm), Argon (458/476/488/496/514), diode-pumped solid state (561 nm) and HeNe (594/633nm) lasers. After i.n. administration with Alexa488 labeled C-NS-siRNA at 30 μg day^{-1} during 4 days, mice were killed and their brain were extracted and processed for immunofluorescence. Details are shown in Supplementary Information.

Intracerebral microdialysis

Extracellular 5-HT concentration was measured by *in vivo* microdialysis as previously described.[17,18,25] Briefly, one concentric dialysis probe (Cuprophan; 1.5-mm long) was implanted in caudate putamen (CPu; coordinates in mm: AP, 0.5; ML, −1.7; DV, −4.5) or ventral hippocampus (vHPC; AP, −3.0; ML, −3.0; DV, −4.0)[26] of pentobarbital-anaesthetized mice. Experiments were performed 24–48h after surgery. To assess 8-OH-DPAT effects on extracellular 5-HT, 1 μM SSRI citalopram (Lundbeck A/S, Valby, Copenhagen, Denmark) was added to artificial cerebrospinal fluid. Artificial cerebrospinal fluid was pumped (WPI model, SP220i) at 2.0 μl min^{-1} and 30-min samples were collected. 5-HT concentrations were analyzed by high-performance liquid chromatography amperometric detection (+0.6V; Hewlett Packard 1049, Palo Alto, CA, USA) with 3-fmol detection limits. Baseline 5-HT levels were calculated as the average of four predrug samples.

Figure 4. Intranasal administration of sertraline-conjugated serotonin transporter small interfering RNA (SERT-siRNA) (C-SERT-siRNA) accelerates the proliferation of cellular precursors and dendrite complexity in the hippocampus. (**a**) Representative images showing an increased number of Ki67-positive cells in the dentate gyrus (DG) of C-SERT-siRNA (7-day) or fluoxetine-treated mice (FLX, 28-day) versus their respective control mice. Bottom row shows high-magnification photomicrographs of the top row frames. Scale bars: low = 100 μm and high = 20 μm. (**b** and **c**) Short-term C-SERT-siRNA (7-day) or long-term FLX (28-day) treatments increased similarly the number of DG Ki-67-positive cells (n = 5–10 mice/group) and 5-bromo-2'-deoxyuridine (BrdU)-positive cells (n = 6–10 mice/group). $^*P < 0.05$, $^{**}P < 0.01$ versus phosphate-buffered saline (PBS) and sertaline-conjugated nonsense-siRNA (C-NS-siRNA); $^{\tau}P < 0.05$ versus saline and FLX 7-day treatment. (**d** and **e**) Short-term C-SERT-siRNA treatment or chronic FLX administration increased similarly the number of immature neurons identified with NeuroD (n = 4–10 mice/group) or doublecortin (DCX; n = 5-11 mice/group) markers ($^*P < 0.05$ versus PBS and C-NS-siRNA; $^{\tau}P < 0.05$, $^{\tau\tau}P < 0.01$ versus saline and FLX 7-day treatment). (**f**) Representative images and traces from Sholl analyses of DCX-positive cells bearing a complex dendritic morphology in the DG of mice in the different treatment group. Scale bar: 20 μm. (**g**) Effects of C-SERT-siRNA (7-day) or FLX (28-day) treatments on dendritic intersection numbers and dendritic length of DCX-positive neurons (n = 4 mice/group, 5 cells/mouse; $^{***}P < 0.001$ versus PBS and C-NS-siRNA; $^{\tau\tau\tau}P < 0.001$ versus saline and FLX 7-day). (**h**) Levels of mRNA for the following genes: BDNF, VEGF, TRKB, ARC, Neuritin, and PSD95 in the DG were analyzed by densitometry and are shown in the bar graphs (n = 3–10 mice/group; $^*P < 0.05$, $^{***}P < 0.001$ versus PBS and C-NS-siRNA; $^{\tau}P < 0.05$, $^{\tau\tau}P < 0.01$, $^{\tau\tau\tau}P < 0.001$ versus saline and FLX 7-day treatment). Values are mean ± s.e.m.

Behavioral studies

All mice were tested at 24h after treatments. All tests were performed between 1000 and 1500 hours. Behavioral assessments were examined with at least an interval of 1–2 days between tests. They were conducted in the following order: (1) open field test, (2) sucrose preference test, (3) novelty suppressed-feeding test, and (4) tail suspension test. On test days, animals were transported to a dimly illuminated behavioral room and were left undisturbed for at least 1 h before testing. Behavioral tests were conducted by an experimenter blind to mouse treatments. Details are shown in Supplementary Information.

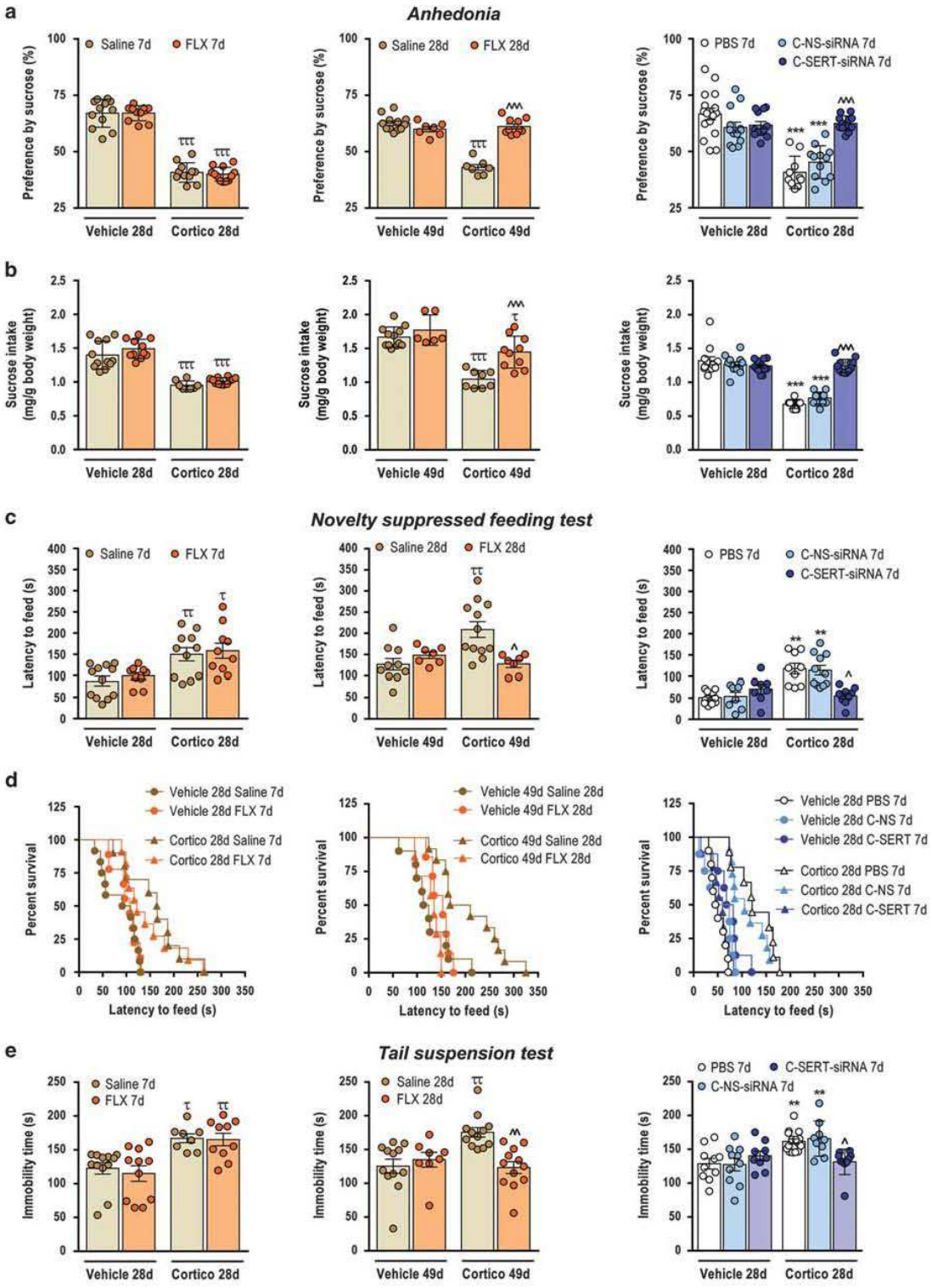

Statistical analyses

All results are given as mean ± s.e.m. Data were analyzed using GraphPad Prism 6.0 (GraphPad, San Diego, CA, USA). Statistical analyses were performed by two-tailed Student's *t*-test and one-way or two-way analysis of variance followed by Tukey's *post-hoc* test as appropriate. In novelty suppressed-feeding test, we used the Kaplan–Meier survival analysis due to the lack of normal distribution of the data. Animals that did not eat during the 10-min testing period were discarded. Mantel–Cox log-rank test was used to evaluate differences between experimental groups, as described by Samuels and Hen.[27] Differences were considered significant when $P < 0.05$. Completed statistical analyses are summarized in Supplementary Table S3.

RESULTS

Sertraline-conjugated siRNA is internalized into 5-HT neurons by endocytosis after i.n. administration

We used a previously developed strategy of transporter-mediated neuronal delivery of siRNA, in which the SSRI sertraline—which selectively binds to SERT—was chemically conjugated to the oligonucleotide.[18] The working hypothesis was that the presence of sertraline would allow the selective enrichment of this conjugated siRNA in 5-HT neurons, where the targeted transporter (SERT) is differentially expressed.[28] As first evidence in support of this mechanism, we previously showed that sertraline pretreatment (20 mg kg^{-1}, i.p.) prevented the effects of sertraline-conjugated siRNA, indicating that conjugated siRNA molecules enter 5-HT neurons via SERT.[18]

For localization purposes, we synthesized an alexa488-labeled sertraline-conjugated nonsense-siRNA (A488-C-NS-siRNA). Confocal fluorescence microscopy revealed that A488-C-NS-siRNA was intracellularly detected in TPH_2-positive midbrain 5-HT neurons after i.n. administration (Figure 1a). Confocal analysis showed that A488-C-NS-siRNA molecules were more efficiently uptaken by TPH_2-positive neurons in the DR than in median raphe nucleus (MnR) (Figures 1b and d and Supplementary Figure S2). In addition, A488-C-NS-siRNA was absent in cells of brain areas close to the application site (olfactory bulbs) or to brain ventricles (hippocampus) (Supplementary Figure S3), supporting that surface SERT expression is a requirement for oligonucleotide uptake and internalization. Sertraline-conjugated siRNA was possibly accumulated in 5-HT cells perhaps by endocytosis and entered in a complex network of trafficking pathways as vesicles containing A488-C-NS-siRNA co-localized with Rab5 (early endosome marker) and Rab7 (late endosome marker) (Supplementary Figure S4). Further studies are needed to fully characterize the route used by sertraline-conjugated siRNA molecules to reach raphe 5-HT neurons.

Sertraline-conjugated SERT-siRNA induces selective and safe suppression of SERT expression

We first examined the effect of i.n. C-SERT-siRNA administration (30 µg day^{-1}) on SERT expression. SERT mRNA and binding site levels were significantly lower in the raphe nuclei of C-SERT-siRNA-treated mice compared with control groups (PBS- and C-NS-siRNA-treated mice), with a maximal reduction after 7-day treatment. Immunohistochemistry analysis confirmed these results at the protein level (Figures 2a and d and Supplementary Figure S5). C-SERT-siRNA suppressed SERT expression more markedly in the DR than in MnR, as supported by the higher intracellular density of oligonucleotide in DR 5-HT neurons (Figure 1). We then evaluated the dose-related effects of C-SERT-siRNA (10–30–100 µg day^{-1} during 7 days, i.n.) on SERT expression in the DR. All doses significantly decreased SERT mRNA expression 24 h after last administration, with no significant differences between doses, despite a slightly greater reduction at 30 and 100 µg day^{-1} (Supplementary Figure S6). Next we assessed the temporal pattern of SERT decrease. For this purpose, mice were i.n. administered with C-SERT-siRNA at 30 µg day^{-1} during 7 days and killed at different times after last administration. SERT mRNA level in the DR was significantly lower in C-SERT-siRNA-treated mice that in the control group at 1 and 3 days postadministration, with a recovery of SERT expression to control values at 7 and 15 days postadministration (Supplementary Figure S7). These values agree with data in the literature indicating a short half-life of SERT.[19]

The reduced SERT expression was accompanied by a decreased function, as assessed by intracerebral microdialysis in the CPu, a DR-innervated area. Hence, i.n. C-SERT-siRNA treatment (30 µg day^{-1}, 7-day) doubled basal extracellular 5-HT levels in the CPu versus PBS-treated mice (9.9 ± 1.6 and 4.7 ± 0.7 fmol fraction^{-1}, respectively; $n = 7$-8; $P < 0.01$) and provoked a lesser response of the SSRI citalopram to increase extracellular 5-HT (Figure 2e).

C-SERT-siRNA (30 µg day^{-1}, 7-day, i.n.) did not induce neuronal degeneration (NeuN-positive), astrogliosis (GFAP-positive) nor immune responses (Iba-1-positive) (Supplementary Figure S8). Similarly, 7-day C-SERT-siRNA did not alter TPH_2 mRNA levels in 5-HT neurons nor the binding density of [^{3}H]-nisoxetine, which recognizes norepinephrine transporter (Supplementary Figure S9). Altogether, these data support the specificity and safety of C-SERT-siRNA effects.

RNAi-based SERT suppression rapidly attenuates 5-HT_{1A}-autoreceptor expression/function and enhances forebrain 5-HT transmission

Concurrently, 7-day C-SERT-siRNA treatment reduced 5-HT_{1A}-autoreceptor expression and function in mouse (Figures 3a and d), as also described after DR infusion of a unmodified SERT-siRNA in mouse or SERT antisense-plasmid in rat.[17,19] C-SERT-siRNA diminished 5-HT_{1A}-autoreceptor mRNA level in the DR at both doses tested (30 and 100 µg day^{-1}), but not 10 µg day^{-1}, 24 h after last siRNA administration (Supplementary Figures S10a and b). Decreased 5-HT_{1A}-autoreceptor response is necessary for the clinical antidepressant action, as 5-HT_{1A}-autoreceptor activation by the excess 5-HT produced by SSRI/SNRI in the DR reduces

Figure 5. Short-term intranasal (i.n.) treatment with sertraline-conjugated serotonin transporter small interfering RNA (SERT-siRNA) (C-SERT-siRNA) efficiently attenuates the behavioral deficits in a stress-induced depression model. Grouped-housed male C57BL/6J mice were presented during 28 or 49 days with vehicle (non-stressed mice) or corticosterone (stressed mice) in the presence or absence of an antidepressant treatment (C-SERT-siRNA 30 µg day^{-1}, i.n. or fluoxetine (FLX) 10 mg kg^{-1} day^{-1}, intraperitoneally) during the last 7 or 28 days of the corticosterone regimen. (**a** and **b**) Short-term C-SERT-siRNA reversed the reduction of sucrose intake and preference in the corticosterone-induced anhedonia ($n = 10$–16 mice/group; $^{***}P < 0.001$ versus non-stressed mice; $^{\wedge\wedge\wedge}P < 0.001$ versus corticosterone-stressed mice treated with phosphate-buffered saline (PBS) or sertraline-conjugated nonsense-siRNA (C-NS-siRNA)). FLX induced a similar recovery after 28-day, but not after 7-day, treatment ($n = 7$–12 mice/group; $^{\tau\tau\tau}P < 0.001$ versus non-stressed mice; $^{\wedge\wedge\wedge}P < 0.001$ versus corticosterone-stressed mice treated with saline. (**c**) Effect on novelty suppressed feeding test (NSFT). Seven-day C-SERT-siRNA, but not 7-day FLX, reversed the increased latency to feed in corticosterone-treated mice ($n = 8$–12 mice/group; $^{**}P < 0.01$ versus non-stressed mice; $^{\wedge}P < 0.05$ versus corticosterone-stressed mice treated with PBS or C-NS-siRNA). Similar effects were elicited by 28-day FLX administration ($n = 7$–12 mice/group; $^{\tau\tau}P < 0.01$ versus non-stressed mice; $^{\wedge}P < 0.05$ versus corticosterone-stressed mice treated with saline). (**d**) Survival analysis of NSFT data. (**e**) C-SERT-siRNA (7-day) or FLX (28-day), but not FLX 7-day, decreased the immobility time in the tail suspension test (TST) in cortico-stressed mice ($n = 8$–15 mice/group). $^{**}P < 0.01$, $^{***}P < 0.001$, $^{\tau}P < 0.05$, $^{\tau\tau}P < 0.01$ versus their non-stressed mice, respectively; $^{\wedge}P < 0.05$, $^{\wedge\wedge}P < 0.01$ versus cortico-stressed mice treated with saline, PBS or C-NS-siRNA, respectively. Values are mean ± s.e.m.

5-HT neuronal activity and 5-HT release, thus counteracting the facilitation of 5-HT transmission induced by SERT blockade.[29–31] This inhibitory feedback is an essential component of the delayed therapeutic action of antidepressant drugs. Long-term FLX treatment (10 mg kg^{-1}, 28-day, but not 7-day, i.p.) attenuated 5-HT_{1A}-autoreceptor-mediated activation of G-proteins as expected[32] and prevented the effect of 8-OH-DPAT (selective 5-HT_{1A} receptor agonist) to reduce hippocampal 5-HT release. In contrast, 7-day C-SERT-siRNA administration (30 μg day^{-1}) was sufficient to downregulate 5-HT_{1A}-autoreceptors and to avoid the 8-OH-DPAT effect on 5-HT release (Figures 3c and d). Neither treatment modified the hippocampal [^{35}S]GTP-γ-S binding in the presence of 8-OH-DPAT (Supplementary Figure S10c). The reduction in SERT expression/function, together with the 5-HT_{1A}-autoreceptor downregulation, increased extracellular 5-HT concentration in the CPu and hippocampus more rapidly and markedly than after FLX (Figure 3e). The present results indicate that cellular changes—classically associated to long-term SSRI treatment—can be achieved after only 1 week of i.n. C-SERT-siRNA administration. These observations suggest that SSRI and C-SERT-siRNA distinctly regulate the molecular mechanisms controlling SERT function, resulting in a more rapid and efficient increase of presynaptic 5-Ht function with the RNAi strategy.

Sertraline-conjugated SERT-siRNA rapidly increases and facilitates maturation of newborn cells

The clinical antidepressant action is also associated with neural stem cell proliferation, neurogenesis and the establishment of new synaptic contacts in brain circuits controlling motivation, emotion and cognition.[33,34] Treatments with C-SERT-siRNA (30 μg day^{-1}, 7-day) or FLX (10 mg kg^{-1}, 28-day, but not 7-day) markedly increased the number of Ki67- and BrdU-labeled progenitor cells in the dentate gyrus of hippocampus (Figures 4a–c, Supplementary Figure S11a, Supplementary Table S4). In addition, 7-day C-SERT-siRNA promoted significantly the generation of NeuroD- and DCX-expressing neurons faster than FLX (28-day) (Figures 4d and e, Supplementary Figure S11b, Supplementary Table S4). Dendritic morphology of newborn cells was comparable after 7-day C-SERT-siRNA and 28-day FLX treatments, as indicated by Sholl analysis on DCX-positive neurons with tertiary dendrites, the number of intersections and dendrite length (Figures 4f and g). These data support that RNAi-induced SERT knockdown rapidly enhances neuronal plasticity in hippocampus as a result of the increased 5-HT signaling.

These cellular changes were accompanied by a higher activation of neuroplasticity-associated genes in the hippocampus. Seven-day C-SERT-siRNA or 28-day FLX treatments increased comparably the expression of BDNF and its TRKB receptor as well as VEGF and ARC essentially in the dentate gyrus (Figure 4h and Supplementary Figure S12). Likewise, mRNA neuritin and PSD95 levels, two critical downstream mediators of antidepressant/BDNF-induced plasticity[35–37] were selectively increased in the dentate gyrus of both the mice groups. However, a 7-day FLX regime was without effect on these variables (Figure 4).

Short-term sertraline-conjugated SERT-siRNA efficiently attenuates the behavioral alterations in the corticosterone depression model

Finally, we confirmed the potential therapeutic benefit of the RNAi-induced downregulation of SERT expression in a stress-related model of depression: the corticosterone model—a well-established stress inducer.[12,22] Despite displaying plasma corticosterone levels and open field behavior similar to controls, mice exposed to a low oral dosage of corticosterone for 28 or 49 days showed a persistent depressive-like behavior, characterized by reduced sucrose preference, increased latency in the novelty suppressed feeding paradigm and increased immobility time in the tail suspension test (Supplementary Figure S13). These depressive-like behaviors were reversed to the same extent by 7-day i.n. C-SERT-siRNA (30 μg day^{-1}) and by 28-day FLX (10 mg kg^{-1}) treatments (Figure 5). In contrast, 7-day FLX did not evoke any antidepressant-like effects.

DISCUSSION

Here we show that C-SERT-siRNA evokes very fast (7-day) and robust antidepressant-like responses in control and corticosterone-treated mice, comparable than those evoked by a 28-day FLX treatment. Prior studies using RNAi strategies to elicit antidepressant-like responses in rodents used unmodified siRNA sequences directed against SERT or 5-HT_{1A} receptors.[16,17,25] The study confirms and extends our previous observations on the use of sertraline-conjugated siRNA sequences to silence genes in 5-HT neurons.[18] The design of the conjugated siRNA allows its selective enrichment in 5-HT neurons after i.n. administration, opening new ways for the therapeutic use of RNAi strategies to treat mood disorders, which may overcome the limitations of standard antidepressant treatments, that is, slow clinical action and low efficacy.

As a consequence of the fast and effective SERT downregulation, 7-day C-SERT-siRNA treatment (i) reduced 5-HT_{1A}-autoreceptor expression/function, (ii) facilitated forebrain serotonin neurotransmission, (iii) accelerated the proliferation of neuronal precursors, (iv) increased the expression of growth factors (for example, BDNF, VEGF) and genes promoting neurite outgrowth (for example, neuritin, PSD95) and (v) increased hippocampal dendritic complexity and synaptic plasticity. All these variables are predictive of clinical antidepressant action. In addition, short-term C-SERT-siRNA treatment normalized stress-induced depressive-like behaviors, which were only sensitive to 28-day FLX treatment. Interestingly, the above actions were produced by the i.n. administration of very small doses (2.1 nmol day^{-1}) of C-SERT-siRNA illustrating the effectiveness of the present RNAi strategy.

The precise mechanism(s) used by C-SERT-siRNA reach 5-HT neurons are not fully understood. Unlike other strategies used for oligonucleotide delivery to target neuronal populations,[38,39] here we used a transporter (SERT)-mediated process to target a selective gene (SERT) expressed in 5-HT neurons, as previously used to silence 5-HT_{1A}-autoreceptors.[18] Paradoxically, this approach could limit the extent of the intracellular C-SERT-siRNA accumulation, as the conjugated siRNA enters 5-HT neurons via SERT.[18] However, the present results indicate that the remaining expression of SERT—even after 7-day C-SERT-siRNA treatment—is sufficient to evoke a very large increase of presynaptic serotonergic function.

Moreover, as trans-nasal oligonucleotide delivery to brain is mediated by extracellular mechanisms,[40–42] it is also possible that C-SERT-siRNA can use this extracellular pathway before being taken up by serotonergic terminals and transported back to cell bodies in the midbrain. This view is showed by the association of the conjugated siRNA to Rab7, supporting traffic via late endomembrane compartments.

The present results indicate that C-SERT-siRNA is preferentially accumulated into DR (versus MnR) 5-HT neurons. Anatomical and functional differences between the two 5-HT subsystems have been reported.[43–45] In particular, SERT expression is greater in DR than in MnR and DR-innervated areas are more sensitive to the action of SSRI,[40] which suggests a preferential uptake of C-SERT-siRNA by DR axons.

Consistent with previous findings using intra-raphe SERT-siRNA infusion,[17] i.n. C-SERT-siRNA treatment triggered a complex cascade of signaling events that ultimately results in downregulation of SERT and also 5-HT_{1A}-autoreceptors on midbrain serotonin neurons. As both mechanisms tightly control the active 5-HT fraction, their downregulation by C-SERT-siRNA dramatically increased the extracellular 5-HT levels in the forebrain in a faster

way than that produced by the pharmacological SERT blockade with FLX. The intracellular mechanisms by which short-term C-SERT-siRNA or chronic SSRI treatments downregulate SERT and 5-HT_{1A} receptor levels to increase the serotonergic neurotransmission are still poorly known. Recent reports suggest a role for altered patterns of gene expression in mediating the long-term therapeutic effects of SSRIs, focusing on the potential involvement of microRNAs as fine-tuners and on–off switches of gene expression.[15,46] Hence, miR-135 levels were upregulated after single and chronic FLX administrations,[47] suggesting that this microRNA may act as an endogenous homeostatic mechanism to maintain the physiological balance between SERT and 5-HT_{1A}-autoreceptors.

Similarly to intra-raphe SERT-siRNA application,[17] the short-term i.n. administration of C-SERT-siRNA—but not FLX—evoked hippocampal postsynaptic responses to the enhanced serotonergic signaling, which are predictive of clinical antidepressant effects. These responses included the proliferation of progenitor cells, stimulation of dendritic branching, acceleration of the maturation of immature DCX neurons and increased expression of spine/synapse markers. Moreover, these postsynaptic changes were accompanied by the reversal of the behavioral deficits caused by prolonged corticosterone exposure. The C-SERT-siRNA ability to increase synaptic plasticity may be mediated by an enhancement of BDNF/TRKB signaling, among others that were upregulated after 7-day C-SERT-siRNA treatment. Activation of their downstream signaling pathways was shown to enhance maturation and dendritic development.[48] Induction of neuritin and PSD95 are also indicative of an increased synapse formation and function.[37] However, additional antidepressant mechanisms may be involved, resulting from the enhanced 5-HT neurotransmission in other brain areas implicated in MDD, such as the ventromedial prefrontal cortex.

In conclusion, our findings indicate that RNAi-based SERT repression elicits faster and more effective antidepressant-like actions than persistent SERT blockade with FLX. Enhancing serotonin signaling through downregulation of SERT expression evokes standard antidepressant responses, promotes the generation of new hippocampal neurons, increases synaptic plasticity and counteracts behavioral deficits in a stress-induced depression model. Furthermore, the study has a high translational value due to the use of a clinically feasible (i.n.) administration route.[40–42] This opens new therapeutic perspectives for the treatment of mood disorders, including MDD.

CONFLICT OF INTEREST

FA has received consulting and educational honoraria on antidepressant drugs from Lundbeck and he is PI of grants from Lundbeck. He is also a member of the advisory board of Neurolixis Inc. AB and FA are authors of the patent WO/2011/131693 for the siRNA and ASO (antisense oligonucleotides) molecules and the targeting approach related to this work. GA and AM are board members of nLife Therapeutics S.L. The rest of authors declare no competing financial interest.

ACKNOWLEDGMENTS

We thank María Calvo, Elisenda Coll and Anna Bosch for outstanding technical support in the Confocal microscopy unit (CCiT-UB) and María C Carmona for advice on design of small RNA and oligonucleotide molecules. This work was supported by grants from CDTI—Spanish Ministry of Science and Innovation—DENDRIA contribution, 'nLife all rights reserved' (to AB and FA); Instituto de Salud Carlos III PI10/00290 and PI13/01390 (to AB), PI/10/0123 (to JCL) and Centro de Investigación Biomédica en Red de Salud Mental (CIBERSAM); NARSAD Independent Investigator Grant from the Brain & Behavior Research Foundation Grant 20003 (to AB); Ministry of Economy and Competitiveness SAF2012-35183 (to FA) and SAF2011-25020 (to AP); and Generalitat de Catalunya, Secretaria d'Universitat i Recerca del Departament d'Economia i Coneixement (SGR2014) Catalan Government Grant 2009SGR220 (to FA). Some of these grants are co-financed by the European Regional Development Fund 'A way to build Europe'. AF-C is a recipient of a fellowship from Spanish Ministry of Education, Culture and Sport.

REFERENCES

1 Wong ML, Licinio J. Research and treatment approaches to depression. *Nat Rev Neurosci* 2001; **2**: 343–351.
2 Belmaker RH, Agam G. Major depressive disorder. *N Engl J Med* 2008; **358**: 55–68.
3 Krishnan V, Nestler EJ. The molecular neurobiology of depression. *Nature* 2008; **455**: 894–902.
4 Stockmeier CA. Involvement of serotonin in depression: evidence from postmortem and imaging studies of serotonin receptors and the serotonin transporter. *J Psychiatry Res* 2003; **37**: 357–373.
5 Blakely RD, De Felice LJ, Hartzell HC. Molecular physiology of norepinephrine and serotonin transporters. *J Exp Biol* 1994; **196**: 263–281.
6 Quin Y, Melikian HE, Rye DB, Levey AI, Blakely RD. Identification and characterization of antidepressant-sensitive serotonin transporter proteins using site-specific antibodies. *J Neurosci* 1995; **15**: 1261–1274.
7 Rush AJ, Trivedi MH, Wisniewski SR, Nierenberg AA, Stewart JW, Warden D *et al.* Acute and longer-term outcomes in depressed outpatients requiring one or several treatment steps: a STAR*D report. *Am J Psychiatry* 2006; **163**: 1905–1917.
8 Trivedi MH, Fava M, Wisniewski SR, Thase ME, Quitkin F, Warden D *et al.* Medication augmentation after the failure of SSRIs for depression. *N Engl J Med* 2006; **354**: 1243–1252.
9 Benmansour S, Cecchi M, Morilak DA, Gerhardt GA, Javors MA, Gould GG *et al.* Effects of chronic antidepressant treatments on serotonin transporter function, density, and mRNA level. *J Neurosci* 1999; **19**: 10494–10501.
10 Benmansour S, Owens WA, Cecchi M, Morilak DA, Frazer A. Serotonin clearance in vivo is altered to a greater extent by antidepressant-induced downregulation of the serotonin transporter than by acute blockade of this transporter. *J Neurosci* 2002; **22**: 6766–6772.
11 Santarelli L, Saxe M, Gross C, Surget A, Battaglia F, Weisstaub N *et al.* Requirement of hippocampal neurogenesis for the behavioral effects of antidepressants. *Science* 2003; **301**: 805–809.
12 David DJ, Samuels BA, Rainer Q, Wang JW, Marsteller D, Mendez I *et al.* Neurogenesis-dependent and -independent effects of fluoxetine in an animal model of anxiety/depression. *Neuron* 2009; **62**: 479–493.
13 Samuvel DJ, Jayanthi LD, Bhat NR, Ramamoorthy S. A role for p38 mitogen-activated protein kinase in the regulation of the serotonin transporter: evidence for distinct cellular mechanisms involved in transporter surface expression. *J Neurosci* 2005; **25**: 29–41.
14 Lau T, Horschitz S, Berger S, Bartsch D, Schloss P. Antidepressant-induced internalization of the serotonin transporter in serotonergic neurons. *FASEB J* 2008; **22**: 1702–1714.
15 Baudry A, Mouillet-Richard S, Schneider B, Launay JM, Kellermann O. miR-16 targets the serotonin transporter: a new facet for adaptive responses to antidepressants. *Science* 2010; **329**: 1537–1541.
16 Thakker DR, Natt F, Hüsken D, van der Putten H, Maier R, Hoyer D *et al.* siRNA-mediated knockdown of the serotonin transporter in the adult mouse brain. *Mol Psychiatry* 2005; **10**: 782–789.
17 Ferrés-Coy A, Pilar-Cuéllar F, Vidal R, Paz V, Masana M, Cortés R *et al.* RNAi-mediated serotonin transporter suppression rapidly increases serotonergic neurotransmission and hippocampal neurogenesis. *Transl Psychiatry* 2013; **15**: e211.
18 Bortolozzi A, Castañé A, Semakova J, Santana N, Alvarado G, Cortés R *et al.* Selective siRNA-mediated suppression of 5-HT_{1A} autoreceptors evokes strong anti-depressant-like effects. *Mol Psychiatry* 2012; **17**: 612–623.
19 Fabre V, Boutrel B, Hanoun N, Lanfumey L, Fattaccini CM, Demeneix B *et al.* Homeostatic regulation of serotonergic function by the serotonin transporter as revealed by nonviral gene transfer. *J Neurosci* 2000; **20**: 5065–5075.
20 Juliano R, Bauman J, Kang H, Ming X. Biological barriers to therapy with antisense and siRNA oligonucleotides. *Mol Pharm* 2009; **6**: 686–695.
21 Boudreau RL, Rodríguez-Lebrón E, Davidson BL. RNAi medicine for the brain: progresses and challenges. *Hum Mol Genet* 2011; **20**: 21–27.
22 Gourley SL, Taylor JR. Recapitulation and reversal of a persistent depression-like syndrome in rodents. *Curr Protoc Neurosci* 2009; **Chapter 9**: Unit 9.32.
23 Gourley SL, Kiraly DD, Howell JL, Olausson P, Taylor JR. Acute hippocampal brain-derived neurotrophic factor restores motivational and forced swim performance after corticosterone. *Biol Psychiatry* 2008; **64**: 884–890.
24 Pérez-Nievas BG, García-Bueno B, Caso JR, Menchén L, Leza JC. Corticosterone as a marker of susceptibility to oxidative/nitrosative cerebral damage after stress exposure in rats. *Psychoneuroendocrinol* 2007; **32**: 703–711.
25 Ferrés-Coy A, Santana N, Castañé A, Cortés R, Carmona MC *et al.* Acute 5-HT_{1A} autoreceptor knockdown increases antidepressant responses and serotonin release in stressful conditions. *Psychopharmacology (Berl)* 2013; **225**: 61–74.
26 Franklin KBJ, Paxinos G. *The Mouse Brain in Stereotaxic Coordinates*. Academic Press: New York, NY, USA, 2008.

27 Samuels BA, Hen R. Novelty-suppressed feeding in the mouse. In: Gould TD (ed). *Mood and Anxiety Related Phenotypes in Mice: Characterization Using Behavioral Tests, Volume II*. Springer: New York, NY, USA, 2011; pp 107–121.
28 Torres GE, Gainetdinov RR, Caron MG. Plasma membrane monoamine transporters: structure, regulation and function. *Nat Rev Neurosci* 2003; **4**: 13–25.
29 Artigas F, Romero L, de Montigny C, Blier P. Acceleration of the effect of selected antidepressant drugs in major depression by 5-HT_{1A} antagonists. *Trends Neurosci* 1996; **19**: 378–383.
30 Pérez V, Gilaberte I, Faries D, Alvarez E, Artigas F. Randomised, double-blind, placebo-controlled trial of pindolol in combination with fluoxetine antidepressant treatment. *Lancet* 1997; **349**: 1594–1597.
31 Artigas F, Celada P, Laruelle M, Adell A. How does pindolol improve antidepressant action? *Trends Pharmacol Sci* 2001; **22**: 224–228.
32 Hensler JG. Differential regulation of 5-HT_{1A} receptor-G protein interactions in brain following chronic antidepressant administration. *Neuropsychopharmacology* 2002; **26**: 565–573.
33 Duman RS, Aghajanian GK. Synaptic dysfunction in depression: potential therapeutic targets. *Science* 2012; **338**: 68–72.
34 Duman RS, Voleti B. Signaling pathways underlying the pathophysiology and treatment of depression: novel mechanisms for rapid-acting agents. *Trends Neurosci* 2012; **35**: 47–56.
35 El-Husseini AE, Schnell E, Chetkovich DM, Nicoll RA, Bredt DS. PSD-95 involvement in maturation of excitatory synapses. *Science* 2000; **290**: 1364–1368.
36 Hu X, Ballo L, Pietila L, Viesselmann C, Ballweg J, Lumbard D *et al*. BDNF-induced increase of PSD-95 in dendritic spines requires dynamic microtubule invasions. *J Neurosci* 2011; **31**: 15597–15603.
37 Son H, Banasr M, Choi M, Chae SY, Licznerski P, Lee B *et al*. Neuritin produces antidepressant actions and blocks the neuronal and behavioral deficits caused by chronic stress. *Proc Natl Acad Sci USA* 2012; **109**: 11378–11383.
38 Ming X, Rowshon Alan Md, Fisher M, Yan Y, Chen X, Juliano RL *et al*. Intracellular delivery of an antisense oligonucleotide via endocytosis of a G protein-coupled receptor. *Nucleic Acids Res* 2010; **38**: 6567–6576.
39 Juliano RL, Carver K, Cao C, Ming X. Receptors, endocytosis, and trafficking: the biological basis of targeted delivery of antisense and siRNA oligonucleotides. *J Drug Targeting* 2013; **21**: 27–43.
40 Dhuria SV, Hanson LR, Frey WH. Intranasal delivery to the central nervous system: mechanisms and experimental considerations. *J Pharm Sci* 2010; **99**: 1654–1673.
41 Lochhead JJ, Thorne RG. Intranasal delivery of biologics to the central nervous system. *Adv Drug Deliv Rev* 2012; **64**: 614–628.
42 Renner DB, Frey WH 2nd, Hanson LR. Intranasal delivery of siRNA to the olfactory bulbs of mice via the olfactory nerve pathway. *Neurosci Lett* 2012; **513**: 193–197.
43 Mamounas LA, Mullen CA, O'hearn E, Molliver ME. Dual serotoninergic projections to forebrain in the rat: Morphologically distinct 5-HT axon terminals exhibit differential vulnerability to neurotoxic amphetamine derivatives. *J Comp Neurol* 1999; **314**: 558–586.
44 Brown P, Molliver ME. Dual serotonin (5-HT) projections to the nucleus accumbens core and shell: relation of the 5-HT transporter to amphetamine-induced neurotoxicity. *J Neurosci* 2000; **20**: 1952–1963.
45 Hervás I, Queiroz CMT, Adell A, Artigas F. Role of uptake inhibition and autoreceptor activation in the control of 5-HT release in the frontal cortex and dorsal hippocampus of the rat. *Br J Pharmacol* 2000; **130**: 160–166.
46 Lopez JP, Lim R, Cruceanu C, Crapper L, Fasano C, Labonte B *et al*. miR-1202 is a primate-specific and brain-enriched microRNA involved in major depression and antidepressant treatment. *Nat Med* 2014; **20**: 764–768.
47 Issler O, Haramati S, Paul ED, Maeno H, Navon I, Zwang R *et al*. MicroRNA 135 is essential for chronic stress resiliency, antidepressant efficacy, and intact serotonergic activity. *Neuron* 2014; **83**: 344–360.
48 Wang JW, David DJ, Monckton JE, Battaglia F, Hen R. Chronic fluoxetine stimulates maturation and synaptic plasticity of adult-born hippocampal granule cells. *J Neurosci* 2008; **28**: 1374–1384.

Supplementary Information accompanies the paper on the Molecular Psychiatry website (http://www.nature.com/mp)

Supplementary Information for

Therapeutic antidepressant potential of a conjugated siRNA silencing the serotonin transporter after intranasal administration

Albert Ferrés-Coy[1,2,3], Mireia Galofré[1,2,3], Fuencisla Pilar-Cuéllar[3,4], Rebeca Vidal[3,4], Verónica Paz[1,2,3], Esther Ruiz-Bronchal[1,2,3], Letizia Campa[1,2,3], Ángel Pazos[3,4], Javier R Caso[3,5], Juan C Leza[3,5], Gabriel Alvarado[6], Andrés Montefeltro[6], Elsa M Valdizán[3,4], Francesc Artigas[1,2,3] and Analia Bortolozzi[1,2,3*]

The PDF file includes:

Materials and Methods

Conjugated siRNA synthesis

The synthesis and purification of sertraline-conjugated siRNA directed against serotonin transporter-[SERT] (C-SERT-siRNA, nt: 1230–1250, GenBank accession NM_010484) and sertraline-conjugated nonsense-siRNA (C-NS-siRNA) molecules were performed by nLife Therapeutics S.L. (Granada, Spain) as previously reported.[18] In brief, siRNA (sense and antisense strands) synthesis was performed using ultra mild-protected phosphoramidites (Glen Research, Sterling, VA, USA) and H-8 DNA/RNA Automatic synthesizer (K&A Laborgeraete GbR, Schaafheim, Germany). Sense strand was amino-modified by performing a 5'-C6 amino modification and condensation with a succinimide active ester of sertraline (sertraline-NH-CH2C(=O)NH(CH2)5COO-succinimide) making up the peptide linker of the conjugate (sertraline-NH-CH2C(=O)NH(CH2)5COO-sense strand-3'OH). Conjugated single strand oligonucleotides were purified by high performance liquid chromatography using a RP-C18 column (4.6x150 mm, 5 µm) under a linear gradient condition of acetonitrile shifting the concentration from 5% to 35% for 30min in 100mM TEAA (pH 7.0). The molecular weights of the siRNA strands and the conjugate were confirmed by MALDI-TOF mass spectrometry (Ultraflex, Bruker Daltonics). The yield of the conjugates was spectrophotometrically calculated on the basis of absorbance at 260nm wavelength. Complementary strands were annealed in an isotonic RNA-annealing buffer (100mM potassium acetate, 30mM HEPES pH 7.4, 2mM magnesium acetate), pre-incubated by 1min at 90ºC, centrifuged for 15s and incubated 1h at 37ºC. Duplex RNA formation was confirmed using 20% polyacrylamide gel electrophoresis (PAGE, 30mA, 60min) and visualized by silver staining (DNA Silver stain kit, GE Healthcare, Piscataway, NJ). Sequences are shown in **Supplementary Table S1**.

In situ hybridization

Frozen tissue sections were first brought to room temperature, fixed for 20min at 4ºC in 4% paraformaldehyde in phosphate-buffered saline (1xPBS: 8mM Na_2HPO_4, 1.4mM KH_2PO_4, 136mM NaCl, and 2.6mM KCl), washed for 5min in 3xPBS at room temperature, twice for 5min each in 1xPBS, and incubated for 2min at 21ºC in a solution of predigested pronase (Calbiochem, San Diego, CA) at a final concentration of 24 U/mL in 50mM Tris-HCl, pH 7.5, and 5mM EDTA. The enzymatic activity was stopped by immersion for 30s in 2 mg/ml glycine in 1xPBS. Tissues were finally rinsed in 1xPBS and dehydrated through a graded series of ethanol. For hybridization, the radioactively labeled probes were diluted in a solution containing 50% formamide, 4x standard saline citrate, 1x Denhardt's solution, 10% dextran sulfate, 1% sarkosyl, 20mM phosphate buffer, pH 7.0, 250 $\mu g \cdot ml^{-1}$ yeast tRNA, and 500 $\mu g \cdot ml^{-1}$ salmon sperm DNA. The final concentrations of radioactive probes in the hybridization buffer were in the same range (~1.5 nM). Tissue sections were covered with hybridization solution containing the labeled probes, overlaid with Nescofilm coverslips (Bando Chemical Ind., Kobe, Japan), and incubated overnight at 42ºC in humid boxes. Sections were then washed 4 times (45min each) in a buffer containing 0.6M NaCl and 10mM Tris-HCl (pH 7.5) at 60ºC. Hybridized sections were exposed to Biomax-MR film (Kodak, Sigma-Aldrich, Madrid, Spain) for 1-4 weeks with intensifying screens. For specificity control, adjacent sections were incubated with an excess (50x) of unlabelled probes. The cytoarchitecture of different mouse brain areas were analyzed in an adjacent series of cresyl-violet stained frozen sections.

Autoradiographic studies

The autoradiographic binding assays for 5-HT_{1A}R, SERT and norepinephrine transporter (NET) were performed using the following radioligands: (a) [^{3}H]-8-OH-DPAT (233 $Ci \cdot mmol^{-1}$), (b) [^{3}H]-citalopram (70 $Ci \cdot mmol^{-1}$) and, (c) [^{3}H]-nisoxetine (85 $Ci \cdot mmol^{-1}$), respectively (Perkin-Elmer, Madrid, Spain) as described previously.[17] 8-OH-DPAT, isoproterenol,

mazindol, pargyline and serotonin were from Sigma-Aldrich. The experimental conditions for incubation with each radioligand are summarized in **Supplementary Table S2**. After incubation and washes, tissues were dipped in distilled ice-cold water and dried rapidly under a cold air stream. Tissues were exposed to Biomax-MR film together with ^{3}H-Microscales standards (Amersham-GE Healthcare, Barcelona, Spain) at 4ºC for 1-3 month. All experimental and control brains within a group were processed in duplicate and exposed to films as a batch.

For 5-HT_{1A}R-stimulated [^{35}S]GTPγS autoradiography, coronal dorsal raphe nucleus (DR) sections were pre-incubated for 30min at 25ºC in a buffer containing 50mM Tris–HCl, 0.2mM EGTA, 3mM $MgCl_2$, 100mM NaCl, 1mM DTT and 2mM GDP (pH 7.7). Slides were subsequently incubated for 2h in the same buffer containing 10mU·ml^{-1} adenosine deaminase with 0.04nM [^{35}S]GTPγS and consecutive sections were incubated with 10^{-5}M 8-OHDPAT alone or in the presence of 10^{-5}M WAY-100,635. Nonspecific binding was determined in the presence of 10μM GTPγS. Sections were exposed to autoradiographic film (Biomax-MR) together with ^{14}C-polymer standards at 4ºC for two days.[17]

Immunohistochemistry

For SERT staining, brain sections were treated with 1x PBS, 100% methanol and 30% H_2O_2 for 30min. After incubation in 3% normal goat serum (Vector Laboratories, Burlingame, CA) in 0.2% PBS/Triton for 120min, the sections were incubated for 4 days in rabbit anti-SERT (1:2500; ref.: 24330 ImmunoStar, Inc, Hudson, WI) at 4°C. After washing with PBS, sections were incubated in biotinylated goat anti-rabbit IgG (1:200; ref.: BA-1000 Vector Laboratories) for 1h. After incubation with 1% avidin biotin complex (Vectastain Elite ABC Kit, Vector laboratories) for 1h, sections were washed and reacted for visualization using diaminobenzidine tetrahydrochloride (DAB) solution in a peroxidase reaction to produce a brown reaction product. Sections were mounted in Entellan (Electron Microscopy Sciences). Images were captured at a magnification of 20x by using a Nikon Eclipse E1000 microscope (Nikon, Tokyo, Japan) equipped with bright- and dark-field condensers for transmitted light

and a digital camera (DXM1200 3.0, ACT-1 software, Nikon). For each mouse, measurements were taken from five consecutive coronal brain sections and, two areas per section were delineated using ImageJ Software. Optical density was obtained as the logarithmic ratio between SERT-ir intensity in dorsal raphe nucleus, hippocampus or amygdala and an adjacent area as background.

BrdU staining was performed as previously described.[17] Free floating coronal hippocampus sections were incubated for 2h in 50% formamide/2x SSC at 65°C, followed by incubation in 2N HCl for 30min. Then sections were incubated for 10min in 0.1M borate buffer. After washing in PBS, sections were incubated in 1% H_2O_2 in PBS for 30min to inactive endogenous peroxidase activity. After several rinses in PBS, sections were incubated in PBS/0.2% Triton X-100/5% goat serum (PBS–TS) for 30min and then incubated with monoclonal mouse anti-BrdU (1:600; ref.: 11170376001 Roche Diagnostics, Barcelona, Spain) overnight at 4°C. After several rinses in PBS–TS, sections were incubated for 2h with biotinylated goat anti-mouse Fab Fragment IgG secondary antibody (1:200; ref.: 115-066-006 Jackson ImmunoResearch Laboratories, Inc., US-PA), followed by amplification with avidin–biotin complex (Vector Laboratories). For quantification of $BrdU^+$ cells, one every sixth section throughout the hippocampus was processed and counted under a light microscope (Carl Zeiss Axioskop 2 Plus) at 40x and 100x magnification. The total number of $BrdU^+$ cells per section were determined and multiplied by 6 to obtain the total number of $BrdU^+$ cells per hippocampus.

Ki-67 staining was carried out in sections adjacent to those used in the BrdU labeling studies. Sections were prepared as above including the inactivation of endogenous peroxidase activity, washing in PBS and retrieving of the antigen by heating at 80ºC in 10 mM citric acid, pH 9.0 for 30min. The sample were then incubated with rabbit anti-Ki-67 (1:5000, ref.: ab16667 Abcam, Cambridge, UK) overnight at 4°C, washed with PBS, incubated with biotinylated donkey anti-rabbit secondary antibody (1:200; ref.: 711-065-152 Jackcon ImmunoResearch Laboratories, Inc., US) for 2h, and the signal was amplified with avidin–biotin complex (Vector Laboratories). $Ki\text{-}67^+$ cells were labeled using DAB as

chromogen (Vector Laboratories). The quantification of $Ki67^+$ cells was performed as described for $BrdU^+$ cells.

Goat anti-NeuroD (1:200; sc-1084, Santa Cruz Biotechnology, Santa Cruz, CA) and goat anti-Doublecortin (DCX; 1:200; ref.: sc-8066, Santa Cruz Biotechnology) were used as neurogenesis markers. After endogenous peroxidase inhibition and washes, pre-incubation and incubation were carried out in a 1x PBS/Triton 0.2% solution containing 10% and 3% normal donkey serum (Millipore), respectively. Primary antibodies were incubated overnight at 4ºC, followed by incubation with biotinylated donkey anti-goat (1:200; ref.: sc-2042, Santa Cruz Biotechnology), and subsequent incubation in ABC solution (Vector Laboratories) according to the manufacturer's instructions. The color reaction was performed by incubation with DAB solution. The sections were mounted onto gelatin-coated slides, embedded and investigated on a Nikon Eclipse E1000 microscope (Nikon, Tokyo, Japan) using 20x and 40x objectives. Labeled cells ($NeuroD^+$ or DCX^+ neurons) were counting in three consecutive sections containing the hippocampal structures and six different microscope fields were analyzed in each section. In addition, DCX^+ cells were subcategorized according to their dendritic morphology. Four randomly selected DCX^+ cells per mouse (a total of 120 neurons) with tertiary relatively un-truncated dendritic branches were traced using NeuronJ plugin v1.4.2. Dendritic length and number of intersections (branch point) were evaluated using ImageJ (v1.47n) Software and Sholl Analysis plugin (v1.0).

For immunohistochemical identification of neurons (NeuN; 1:1000; ref.: MAB377, Merck Millipore, Madrid, Spain), reactive astrocytes (GFAP; 1:1000; ref.: Z0334, DAKO, Barcelona, Spain), or microglia (Iba-1; 1:1,000; ref.: 019-197741, WAKO, Irvine, CA), we used a biotin-labeled antibody procedure. Following endogenous peroxidase inhibition and washes, tissues were blocked for 2h in 3% normal goat serum, and primary antibody incubations were carried out overnight at 4ºC. Sections were incubated in goat anti-rabbit (1:200; ref.: BA-1000, Vector Laboratories, Burlingame, CA) or goat anti-mouse (1:200; ref.: sc-2039, Santa Cruz Biotechnology) biotinylated IgG secondary antibodies for 1h at room temperature and subsequent incubation in ABC solution. Sections were mounted onto

gelatin-coated slides with Entelan. Images were captured by using a Nikon Eclipse E1000 microscope (Nikon, Tokyo, Japan) equipped with a digital camera (DXM1200 3.0, Nikon) and ACT-1 software (Nikon). Figures were assembled in Adobe Photoshop (Adobe Systems, San Jose, CA); only contrast and brightness were adjusted to optimize the images.

Confocal fluorescence microscopy

Brain sections were rinsed with PBS/Triton 0.2%, incubated with 10% normal serum from secondary antibody host and treated with primary antibodies: sheep anti-TPH_2 (1:2500; ref.: AB1541, Merck Millipore), rabbit anti-Rab5 (1:500; ref.: ab18211, Abcam) or mouse anti-Rab7 (1:2000; ref.: R8779-200UL, Sigma-Aldrich). Sections were then incubated at 4ºC overnight, rinsed and treated with respectively secondary Alexa555-conjugated antibodies (1:500, A-20000, Life Technologies) for 120min. After subsequent washes, the section were dehydrated and mounted in the anti-fading agent Prolong Gold with DAPI (Life Technologies). DAPI, Alexa488 and Alexa555 images were acquired sequentially using 405, 488 and 561 laser lines, AOBS (Acoustic Optical Beam Splitter) as beam splitter and emission detection ranges 415- 480, 500-550 and 571-625 nm, respectively and, the confocal pinhole set at 1 Airy units. Images were acquired at 400Hz in a 1024 x 1024 pixels format. Images were composed using NIH ImageJ 1.49g software ((http://rsbweb.nih.gov/ij/). Images were acquired from two sections containing both DR and MnR at AP coordinates (in mm) of -4.24/-4.36 and -4.48/-4.72 from bregma for each mouse. For co-localization analysis, the confocal images were processed with the co-localization highlighter plugin, and only TPH_2-positive cells with a threshold of more than 10 pixels co-localizing with A488-C-NS-siRNA or A488-PBS were taken into account.

Behavioral studies

Open field. This test was performed as described previously.[49] Briefly, motor activity was measured in four Plexiglas open field boxes 35x35x40 cm indirectly illuminated (25-40 luxes) to avoid reflection and shadows. The floor of the open field was covered with an

interchangeable opaque plastic base that was replaced for each animal. Motor activity was recorded during 15min by a camera connected to a computer (Videotrack, View Point, Lyon France). We automatically measured the following variables: horizontal locomotor and exploratory activity, defined as the total distance moved in cm including fast/large (speed > 10.5 $cm \cdot s^{-1}$) and slow/short movements (speed 3-10.5 $cm \cdot s^{-1}$), and the activation time, i.e., the time (sec) spent in movement.

Sucrose preference test. During this test, mice were given a free choice between two bottles, one with 1% sucrose solution and another with regular water, for 8h between 09:00-17:00h. To prevent the possible effects of a side-preference in drinking behavior, the position of the bottles in the cage was switched after 4h during the test. No previous food or water deprivation was applied before the test. The consumption of water and sucrose solution was assessed simultaneously in control and experimental groups by weighing the bottles. The sucrose intake was calculated as an amount of consumed sucrose in mg per gram body weight. The preference for sucrose was calculated as a percentage of consumed sucrose solution of the total amount of liquid drunk. A decrease of sucrose preference below 55%, measured at 28 days of chronic CORT exposure, was taken as the criterion for anhedonia.[50]

Novelty suppressed feeding. NSF is a conflict test that elicits competing motivations: the drive to eat and the fear of venturing into the center of the brightly lit arena. The NSF test was carried out during a 10 min period as previously described.[7,8] The testing apparatus consisted of a plastic box (35x35x20 cm), the floor of which was covered with approximately 2 cm of wooden bedding for each animal. 24h prior to behavioral testing, all food was removed from the home cage. At the time of testing, a single pellet of food was placed on a white paper platform in the center of the box directly illuminated with 1100 luxes. An animal was placed in a corner of the box, and a stopwatch was immediately started. The latency to eat (defined as the mouse sitting on its haunches and biting the pellet with the use of forepaws) was timed. Immediately afterwards, the animal was transferred to its home cage and, the latency to feed and the amount of food consumed by the mouse in the subsequent 5

min was measured. Each mouse was weighed before food deprivation and before testing to assess the percentage of body weight loss.

Tail suspension test. Mice were suspended 30 cm above the bench by adhesive tape placed approximately 1 cm from the tip of the tail. The total duration of immobility during a 6min test was measured.[17,18,25]

REFERENCES

49. Scorza MC, Castañé A, Bortolozzi A, Artigas F. Clozapine does not require 5-HT1A receptors to block the locomotor hyperactivity induced by MK-801 Clz and MK-801 in KO1A mice. *Neuropharmacol.* 2010; **59**: 112-120.
50. Strekalova T, Spanagel R, Bartsch D, Henn FA, Gass P. Stress-induced anhedonia in mice is associated with deficits in forced swimming and exploration. *Neuropsychopharmacol.* 2004; **29**: 2007–2017.

Supplementary Figures

Figure S1 Experimental timeline of corticosterone exposure and antidepressant treatments. Group-housed male C57BL/6J mice were presented during 28 or 49 days with vehicle or corticosterone at: 30 $\mu g \cdot ml^{-1}$ for 15 days, followed by 15 $\mu g \cdot ml^{-1}$ for 3 days and 7.5 $\mu g \cdot ml^{-1}$ for 10 or 31 days in the presence or absence of an antidepressant treatment (sertraline-conjugated SERT-siRNA -C-SERT-siRNA- 30 $\mu g \cdot day^{-1}$, i.n. or fluoxetine -FLX- 10 $mg \cdot kg^{-1} \cdot day^{-1}$, i.p.) during the last 7 or 28 days of the corticosterone regimen. We investigated whether the behavioral changes resulting from chronic corticosterone exposure were reversed by treatment with C-SERT-siRNA or FLX. The same animal was successively tested in the sucrose preference, novelty suppressed feeding and tail suspension tests and then, sacrificed to obtain blood samples by cardiac puncture and the brain for neuroplasticity analysis.

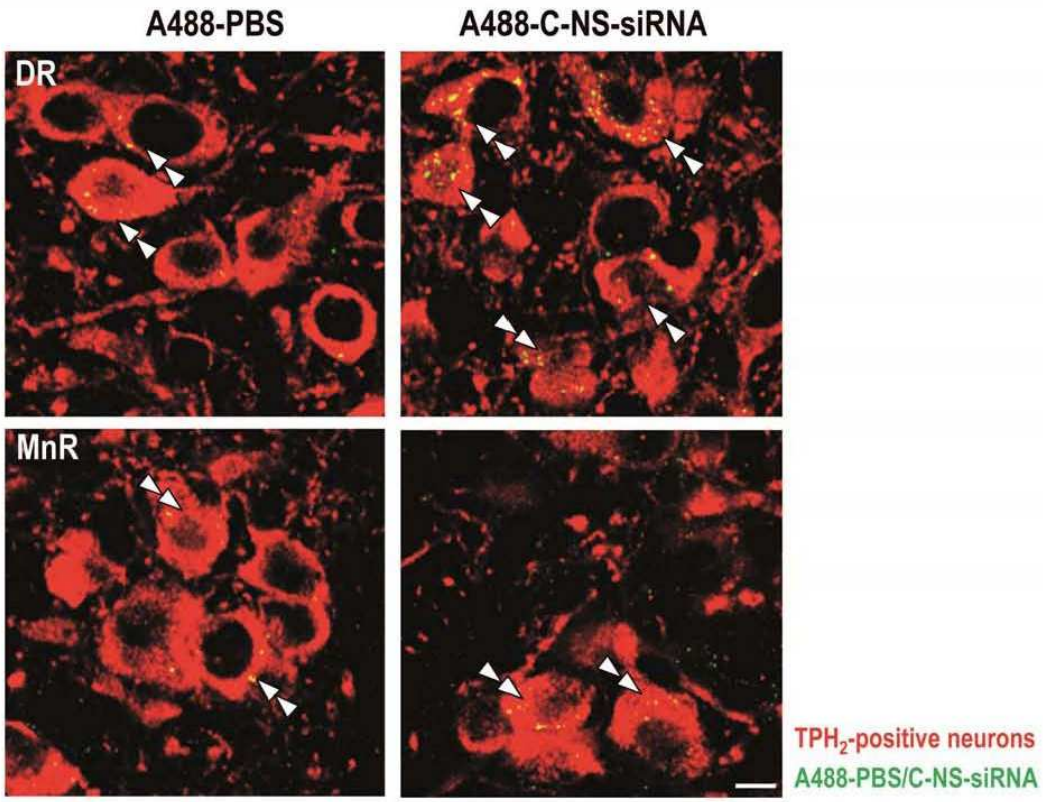

Figure S2 Preferential accumulation of sertraline-conjugated nonsense-siRNA (C-NS-siRNA) molecules in serotonin neurons of mouse DR. Mice were intranasally administered with alexa488 PBS (A488-PBS) or alexa488-labeled C-NS-siRNA (A488-C-NS-siRNA) at 30 µg·day^{-1} during 4-day, and were killed 6h post-administration (*n*=2 mice/group). Confocal images showing co-localization of A488-PBS or A488-C-NS-siRNA (yellow) in DR and MnR 5-HT neurons (TPH_2-positive, red) identified with double white arrowheads. Scale bars: 10 µm.

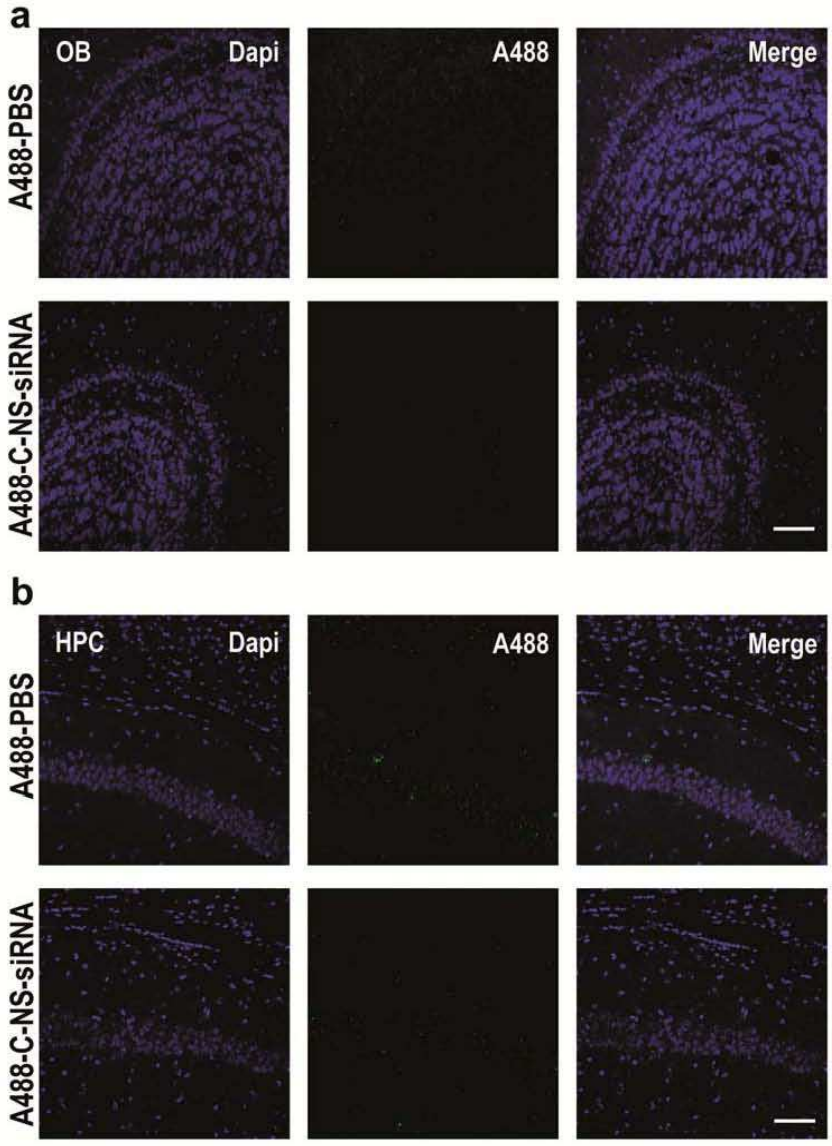

Figure S3 Absence of sertraline-conjugated nonsense-siRNA (C-NS-siRNA) molecules in: **(a)** olfactory bulbs - OB and, **(b)** dorsal hippocampus - HPC of treated mice. Laser confocal images show cell nuclei stained with Dapi (blue) in OB and HPC of mice treated intranasally with vehicle or Alexa488-labeled C-NS-siRNA (A488-C-NS-siRNA) at 30 µg·day^{-1} during 4 days (n=3 mice/group, the same mice than in Figure 1). Scale bars: 50 µm.

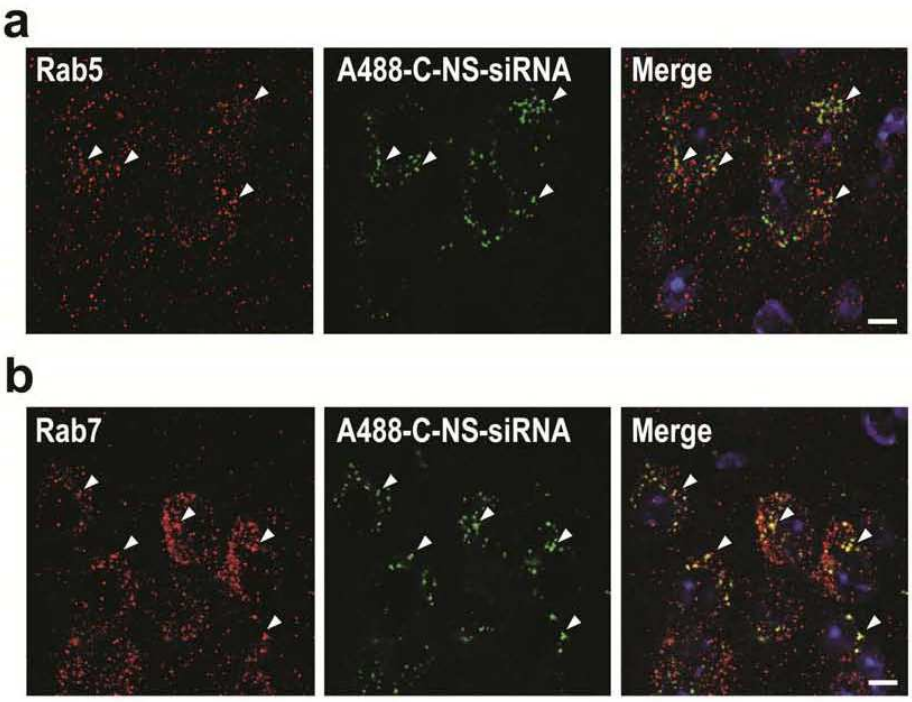

Figure S4 Co-localization of alexa488-labeled sertraline-conjugated nonsense-siRNA (A488-C-NS-siRNA) with markers of endomembrane compartments. **(a)** Selected vesicles showing co-localization (yellow) between Rab5 (early endosome marker, red) with A488-C-NS-siRNA (green) in DR neurons. Scale bar: 10 µm. **(b)** Selected vesicles showing co-localization (yellow) between Rab7 (late endosome marker, red) with A488-C-NS-siRNA (green) in DR neurons. Vesicles are marked with white arrowheads. Scale bar: 10 µm.

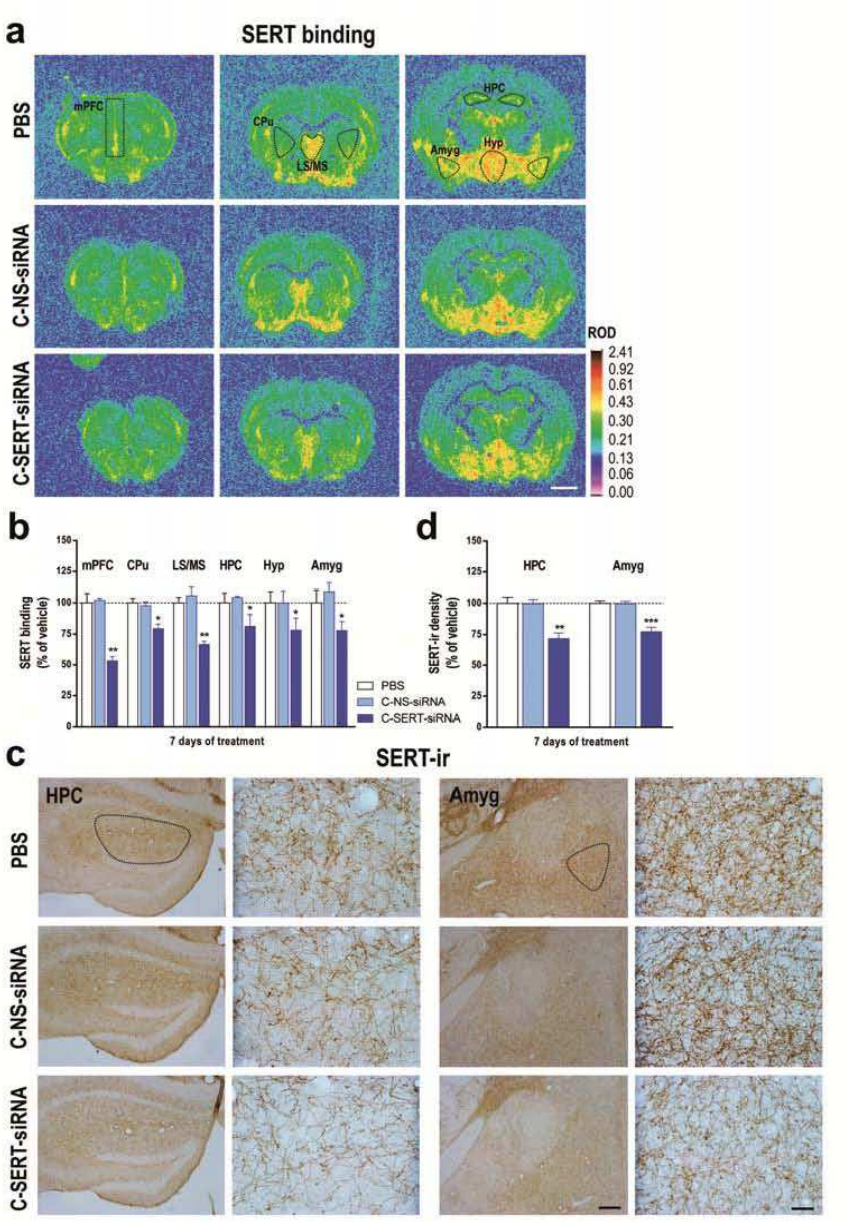

Figure S5 Down-regulation of SERT binding sites and protein levels in mouse brain following sertraline-conjugated SERT-siRNA (C-SERT-siRNA). **(a)** Representative coronal brain sections showing reduced SERT binding levels in forebrain regions of mice treated with C-SERT-siRNA for 7-day. Solid line contours mark the approximate areas where densitometric analyses were performed. Medial prefrontal cortex (mPFC), caudate putamen (CPu), lateral and medial septal nuclei (LS/MS), hippocampus (HPC), hypothalamus (HYP) and, amygdala (Amyg). Scale bar: 2 mm. **(b)** Densitometric analysis of specific SERT binding is presented as % binding in the corresponding region of PBS-treated mice (n=4-10 mice/group; $^{*}P<0.05$, $^{**}P<0.01$ compared to PBS and C-NS-siRNA). **(c)** Representative images of SERT-immunoreative (SERT-ir) fibers in forebrain regions such as HPC and

Amyg. Images in the right hand are high-magnification photomicrographs of the frames in left hand row. Scale bars: low=100 µm, high=20 µm. **(d)** C-SERT-siRNA treatment (7-day) decreased the target SERT protein density as compared to PBS- and C-NS-siRNA-treated mice (n=6 mice/group; **P<0.01, ***P<0.001 versus PBS and C-NS-siRNA). Bars represent mean ± s.e.m.

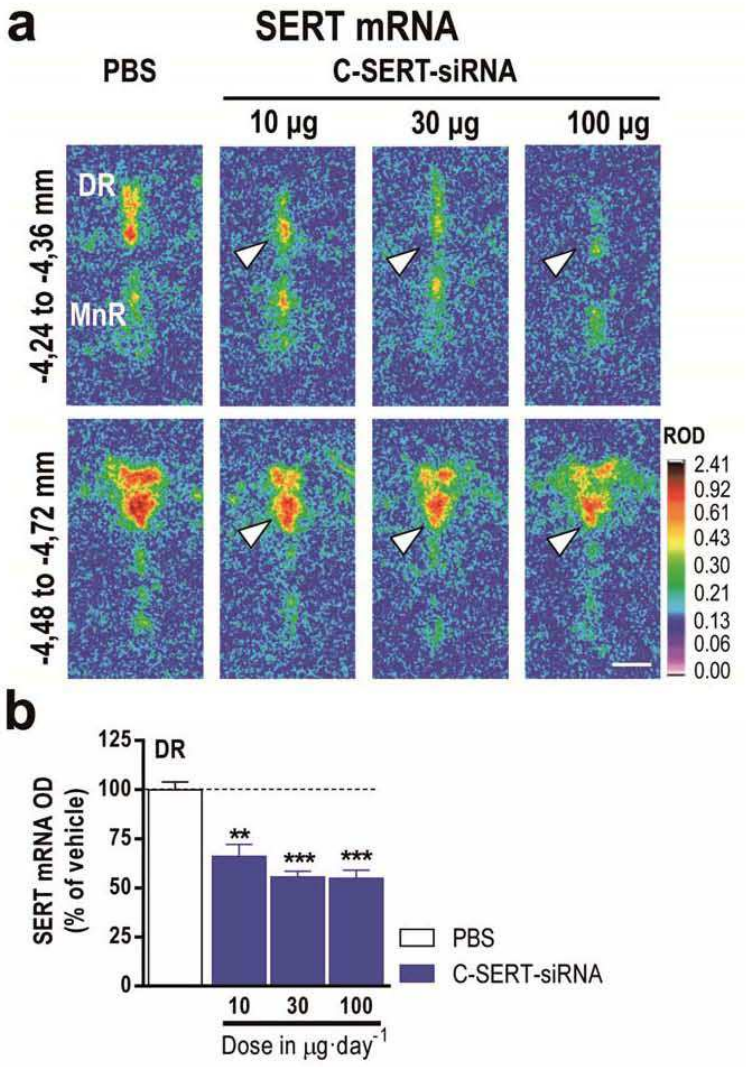

Figure S6 Dose-related effects of sertraline-conjugated SERT-siRNA (C-SERT-siRNA) on SERT mRNA level in mouse DR. Mice received intranasally: PBS or C-SERT-siRNA at 10-30-100 µg·day^{-1} (0.7, 2.1 or 7 nmol·day^{-1}, respectively) during 7 days and were killed 24h after last administration. **(a)** Coronal brain sections showing reduced SERT mRNA levels in the DR (AP coordinates from bregma: -4.24/-4.36 to -4.48/-4.72 in mm) of mice treated with C-SERT-siRNA (7-day) indicated with white arrowheads. Scale bar: 500 µm. **(b)** Effects of different doses of C-SERT-siRNA on SERT mRNA densities in the DR of mice (n=3-5 mice/group; $^{**}P$<0.01, $^{***}P$<0.001 versus PBS-treated mice). Bars represent mean ± s.e.m.

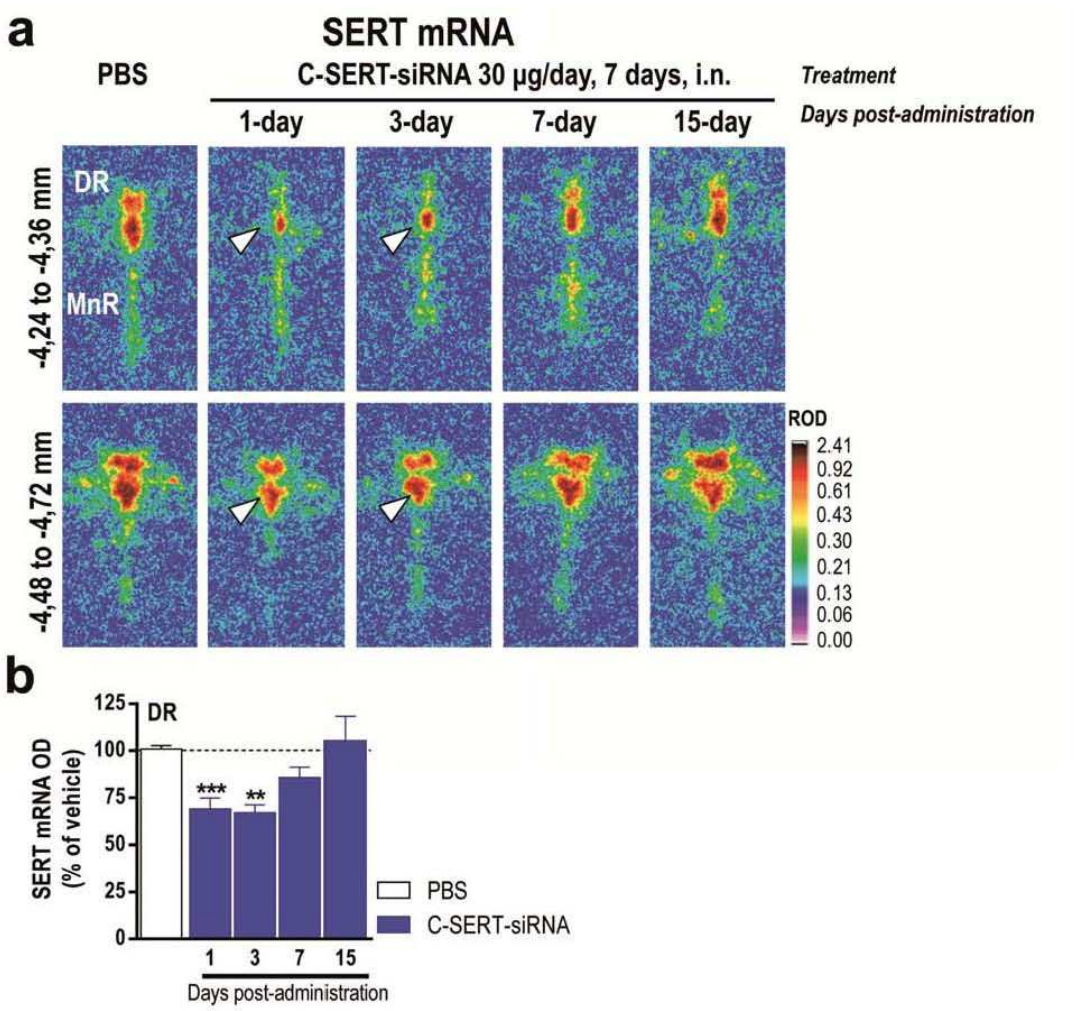

Figure S7 Time course of SERT suppression in the DR after intranasal sertraline-conjugated SERT-siRNA (C-SERT-siRNA) administration. Mice received intranasally: PBS or C-SERT-siRNA at 30 µg·day^{-1} (2.1 nmol·day-1) during 7 days and were killed at 1, 3, 7 and 15 days post-administration. **(a)** Brain sections containing the raphe nuclei showing SERT mRNA density at two AP coordinates from bregma: -4.24/-4.36 to -4.48/-4.72 in mm. The arrows indicate the decreased SERT expression in the DR of mice treated with C-SERT-siRNA and sacrificed at days 1 and 3 post-treatment. Scale bar: 500 µm. **(b)** Bar graphs showing a significant reduction of SERT mRNA density in the DR of C-SERT-siRNA-treated mice compared with PBS-treated mice. Conversely, no difference was detected at days 7 and 15 post-administration (n=3-5 mice/group; $^{**}P$<0.01, $^{***}P$<0.001 versus PBS). Bars represent mean ± s.e.m.

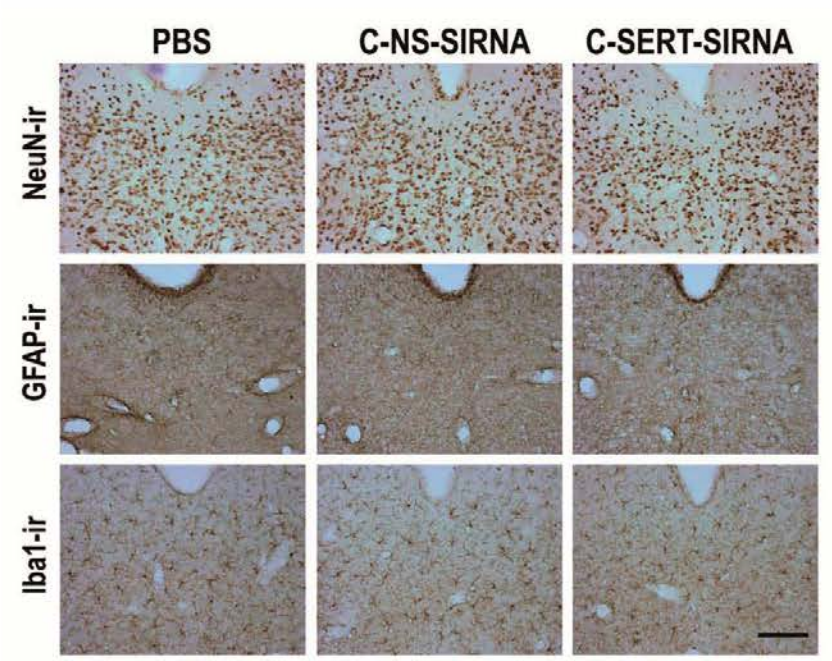

Figure S8 Immunohistochemical assessment of cellular viability in the raphe nuclei after intranasal administration of sertraline-conjugated SERT-siRNA (C-SERT-siRNA). Mice received intranasally PBS, C-NS-siRNA or C-SERT-siRNA at 30 μg·day^{-1} during 7 days (n=4 mice/group). Adjacent 30-μm-thick sections through the midbrain raphe nuclei were stained with neuronal NeuN, astrocytic GFAP or, microglial Iba1 markers. No differences were found between all experimental groups for any of the markers. Scale bar: 100 μm.

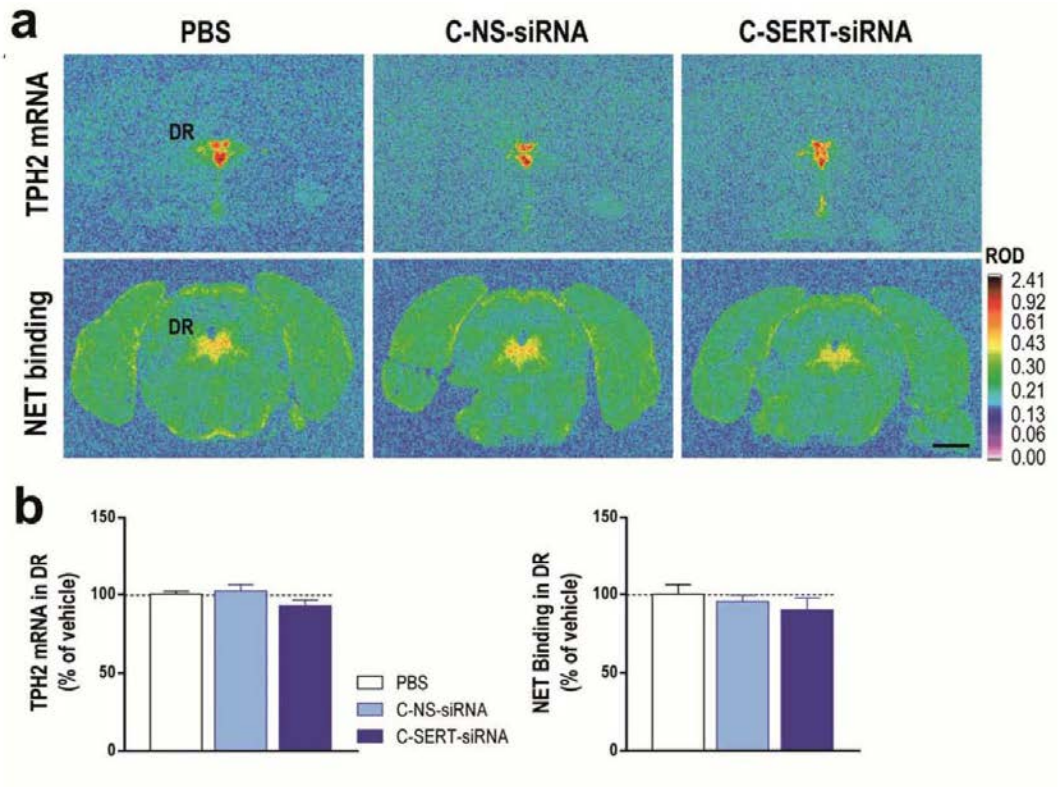

Figure S9 Selectively of SERT expression silencing after intranasal administration of sertraline-conjugated SERT-siRNA (C-SERT-siRNA). Mice received intranasally PBS, sertraline-conjugated nonsense-siRNA (C-NS-siRNA) or C-SERT-siRNA at 30 μg·day^{-1} during 7-day. **(a)** Representative coronal midbrain sections showing tryptophan hydroxylase-2 (TPH2, rate-limiting enzyme for 5-HT synthesis) mRNA density and [^{3}H]-nisoxetine binding to the norepinephrine transporter (NET) in the dorsal raphe nuclei (DR). Scale bar: 2 mm. **(b)** Bar graphs showing no differences in TPH2 mRNA levels and NET binding sites in the DR (*n*=3-4 mice/group). Values are mean ± s.e.m.

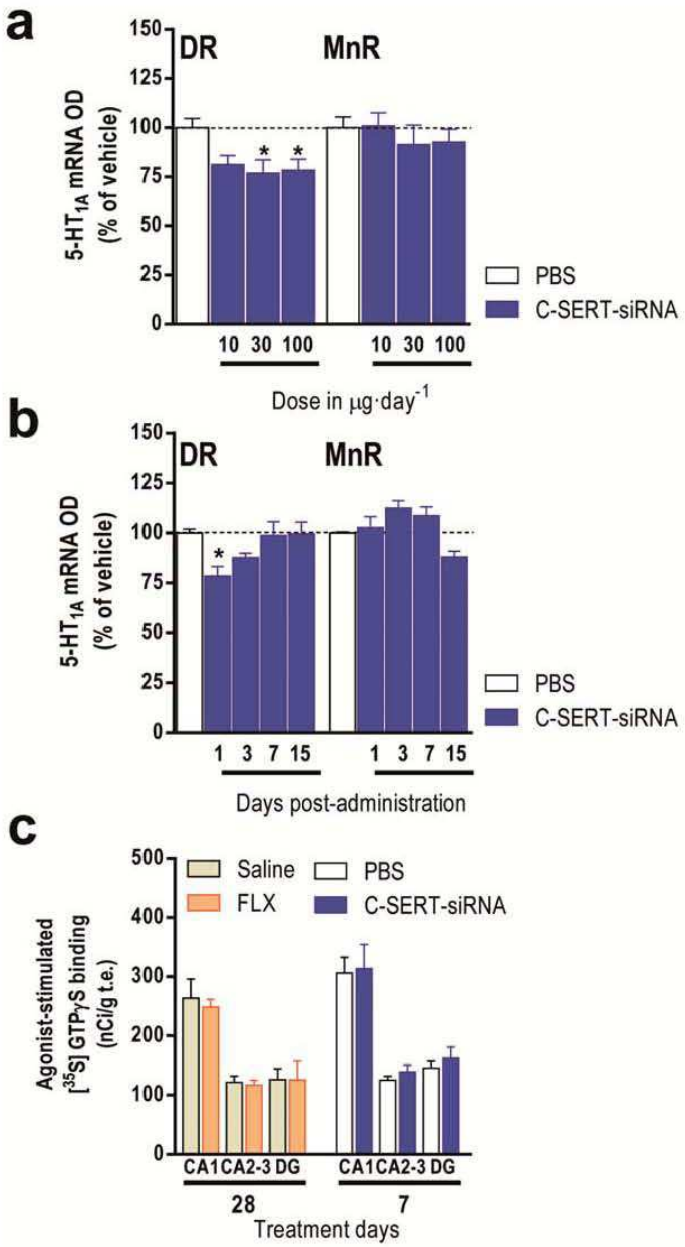

Figure S10 (a) Bar graphics showing effects of different doses of sertraline-conjugated SERT-siRNA (C-SERT-siRNA) on 5-HT_{1A} mRNA densities in the mouse DR and MnR (n=3-5 mice/group; *P<0.05 versus PBS-treated mice). Mice received intranasally PBS or C-SERT-siRNA at 10-30-100 µg·day^{-1} during 7-day and were killed a 24h after last administration. **(b)** Bar graphs showing a significant reduction of 5-HT_{1A} mRNA density in the DR of C-SERT-siRNA-treated mice (30 µg·day^{-1}, 7-day) versus PBS-treated mice at 1 day post-administration. Conversely, no difference was detected at days 3, 7 and 15 post-administration (n=3-12 mice/group; *P<0.05 versus PBS). **(c)** Effects of C-SERT-siRNA (30 µg·day^{-1}, 7-day) and FLX (10 mg·Kg^{-1}, 28-day) on post-synaptic 5-HT_{1A} receptor function in the hippocampus (n=5-10 mice/group). Values are mean ± s.e.m.

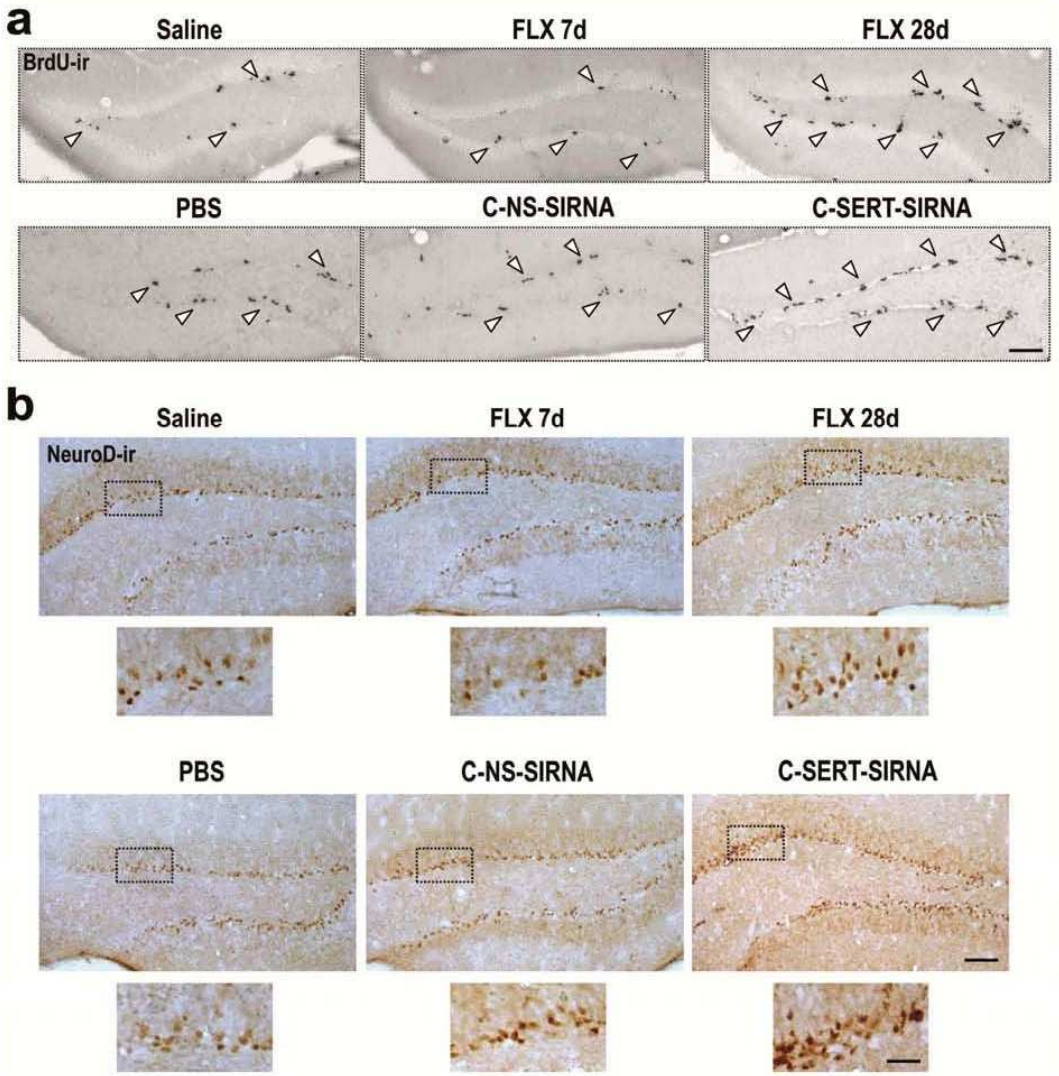

Figure S11 Short-term sertraline-conjugated SERT-siRNA (C-SERT-siRNA) stimulates the proliferation of cell precursors and immature neurons. Mice were intranasally administered with: PBS, sertraline-conjugated nonsense-siRNA (C-NS-siRNA) or C-SERT-siRNA at 30 µg·day during 7-day. Other groups of mice were treated with saline or fluoxetine (FLX) at 10 mg·kg·day, i.p. during 7- or 28-day. **(a)** Representative images showing an increased number of BrdU-positive cells in the dentate gyrus (DG) of C-SERT-siRNA (7-day) or FLX-treated mice (28-day), but not FLX 7-day, compared to their respective control mice. White arrowheads mark some BrdU-positive cells. Scale bar: 100 µm. **(b)** Immunohistochemical images showing NeuroD-positive progenitors in the DG of mice. Bottom row are high-magnification photomicrographs of the frames in top row. Scale bars: low=100 µm and high=20 µm.

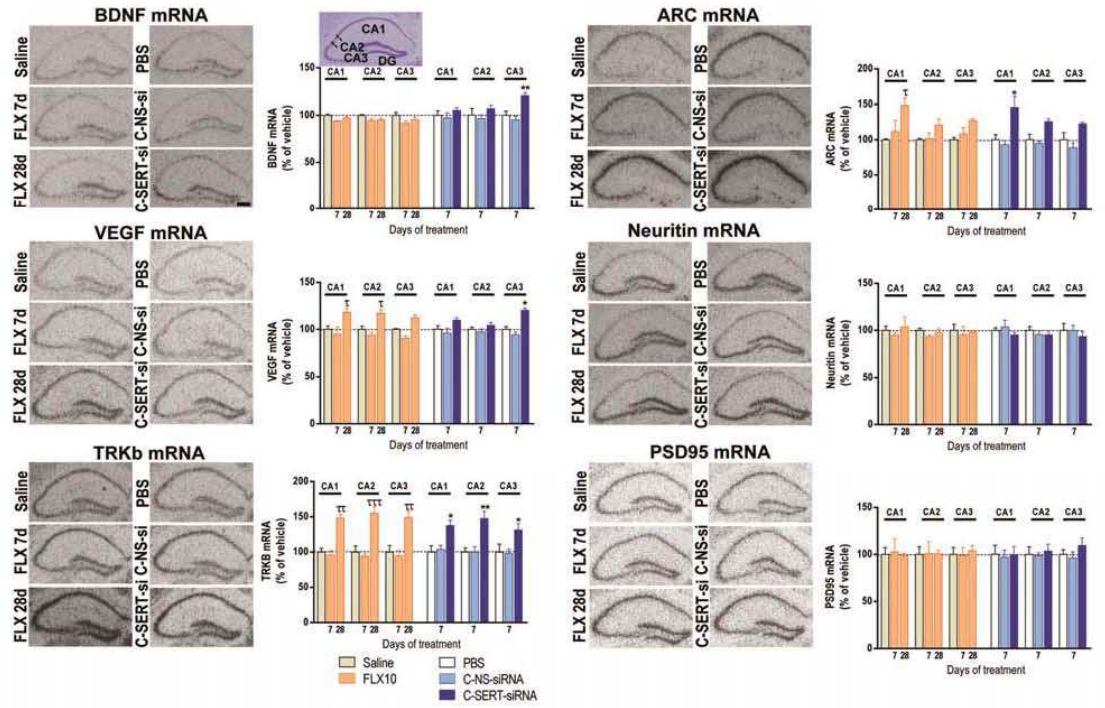

Figure S12 Expression of neuroplasticity genes in the different mouse hippocampal subfields including CA1, CA2 and CA3. Mice were intranasally administered with: PBS, sertraline-conjugated nonsense-siRNA (C-NS-siRNA) or C-SERT-siRNA at 30 μg·day^{-1} during 7-day. Other groups of mice were treated with saline or fluoxetine (FLX) at 10 mg·kg^{-1}·day^{-1}, i.p. during 7- or 28-day. Representative autoradiograms of hippocampal sections of mice are shown BDNF, VEGF, TRKB, ARC, Neuritin and PSD95 mRNA expression. Scale bar: 100 μm. Densitometric analyses were performed in different hippocampal regions: CA1, CA2 and CA3 shown in the cresyl violet-stained section (top). Levels of mRNA for each gene are shown in the bar graphs next to the representative autoradiograms (n=3-8 mice/group; *P<0.05, **P<0.01 versus PBS and C-NS-siRNA; $^{\tau}P$<0.05, $^{\tau\tau}P$<0.01, $^{\tau\tau\tau}P$<0.001 versus saline FLX 7-day). Values are mean ± s.e.m.

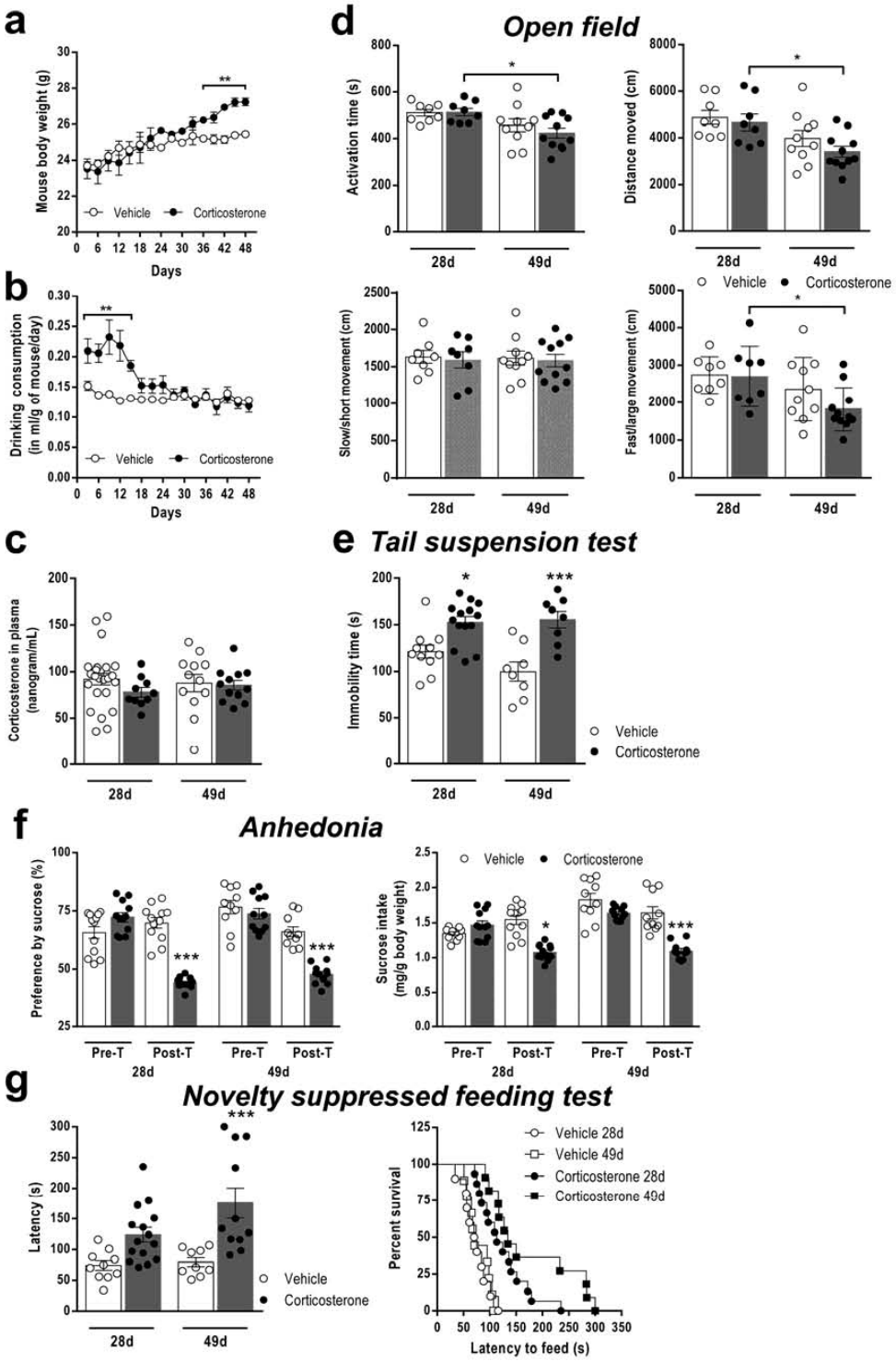
a
Mouse body weight (g)
Vehicle
Corticosterone
Days
b
Drinking consumption (in ml/g of mouse/day)
Vehicle
Corticosterone
Days
c
Corticosterone in plasma (nanogram/mL)
28d
49d
d
Open field
Activation time (s)
Distance moved (cm)
Slow/short movement (cm)
Fast/large movement (cm)
Vehicle
Corticosterone
28d
49d
e
Tail suspension test
Immobility time (s)
Vehicle
Corticosterone
f
Anhedonia
Preference by sucrose (%)
Sucrose intake (mg/g body weight)
Pre-T
Post-T
28d
49d
g
Novelty suppressed feeding test
Latency (s)
Vehicle
Corticosterone
Percent survival
Vehicle 28d
Vehicle 49d
Corticosterone 28d
Corticosterone 49d
Latency to feed (s)

Figure S13 Effects of chronic corticosterone exposure on body weight, drinking of the corticosterone solution, plasma corticosterone levels and behavioral assessments. **(a)** Corticosterone-exposed mice showed an increase of body weight from day 36 onwards (n=2-6 groups of 5 mice/each; $^{**}P<0.01$ versus vehicle-exposed mice). **(b)** Fifteen-day corticosterone treatment (30 µg/ml) increased the consumption of the corticosterone solution, yet drinking returned to control values after reducing corticosterone dosage (15 and 7.5 $\mu g \cdot ml^{-1}$) (n=2-16 groups of 5 mice/each; $^{**}P<0.01$ versus vehicle-exposed mice). **(c)** Plasma corticosterone levels did not differ between groups (n=12-24 mice/group). **(d)** Effects of the two corticosterone regimes (28- or 49-day) on locomotor activity in the open field test. No differences were observed in the activation time, distance moved, slow/short and fast/large movement between vehicle and corticosterone-exposed mice (n=8-11 mice/group). However, a significant effect of corticosterone regimen was detected in the corticosterone group for activation time, distance moved and fast/large movements ($^{*}P<0.05$). **(e)** Effects of the two corticosterone regimes (28- or 49-day) on tail suspension test (n=8-15 mice/group; $^{*}P<0.05$, $^{***}P<0.001$ versus vehicle-exposed mice). **(f)** Effects of the two corticosterone regimes (28- or 49-day) on anhedonia. Results are expressed as mean of % preference by sucrose or mean of sucrose intake (n=10-12 mice/group; $^{***}P<0.001$ versus vehicle-exposed mice). No difference in sucrose preference before corticosterone pre-treatment (at baseline measurement) was observed. **(g)** Effects of the two corticosterone regimes (28- or 49-day) on the novelty suppressed feeding test. Results are expressed as mean of latency to feed (in seconds) or cumulative survival (n=9-15 mice/group; $^{***}P<0.001$ versus vehicle-exposed mice). No differences were detected in the feeding drive of each mouse after returning the animal to the familiar environment in the home cage, immediately after the test. Values are mean ± s.e.m.

Supplementary Tables

Table S1. Sequences of siRNA molecules used

siRNA	forward	Reverse
SERT-siRNA	GCUAGCUACAACAAGUUCATT	UGAACUUGUUGUAGCUAGCTT
NS-siRNA	AGUACUGCUUACGAUACGGTT	CCGUAUCGUAAGCAGUACUTT

Table S2. Summary of the conditions for labeling 5-HT_{1A}R, SERT and NET in the present work

Protein	Ligand	[nM]	Buffer	Pre-Inc (RT, min)	Inc Buffer	Inc (RT, min	Washing (min)	Exposure (days)	Blank
5-HT_{1A}	[^{3}H]-8-OH-DPAT	1.0	A	30	A +10µM pargyline	60	2 x 5	60	10µM serotonin
SERT	[^{3}H]-citalopram	1.5	B	15	B	60	2 x 10	45	1µM fluoxetine
NET	[^{3}H]-nisoxetine	3.0	C	15	C	240	3 x 5	90	10µM mazindol

RT, room temperature; IC, ice-cold buffer; **Buffer A**: 170mM Tris-HCl, 4mM $CaCl_2$, 0.01% ascorbic acid, pH 7.6; **Buffer B**: 50mM Tris-HCl, 120mM NaCl, 5mM KCl, pH 7.6; **Buffer C**: 50mM Tris-HCl, 300mM NaCl, 5mM KCl, pH 7.4.

Table S3. Summary of complete statistical analyses

Excel file

Table S4. Number of immunoreactive-positive cells in the different treatments

Treatments	Total Ki67-positive cells	Total BrdU-positive cells	NeuroD-positive cells/mm^2	DCX-positive cells/mm^2
Saline 7d	2196 ± 283	3882 ± 385	122 ± 12	99 ± 3
FLX 7d	2264 ± 122	3599 ± 162	130 ± 15	100 ± 5
Saline 28d	1195 ± 83	3242 ± 78	91 ± 9	85 ± 2
FLX 28d	1719 ± 138*	4368 ± 433*	131 ± 12*	100 ± 4*
PBS 7d	2639 ± 229	3826 ± 106	134 ± 15	145 ± 6
C-NS-siRNA 7d	2077 ± 333	3755 ± 200	128 ± 17	141± 4
C-SERT-siRNA 7d	3830 ± 347*ττ	5481 ± 292**ττ	194 ± 12*τ	171 ± 7*ττ

Mice were intranasally administered with: PBS, sertraline-conjugated nonsense-siRNA (C-NS-siRNA) or sertraline-conjugated SERT-siRNA (C-SERT-siRNA) at 30 μg·day^{-1} during 7-day. Other groups of mice were treated with saline or fluoxetine (FLX) at 10 mg·kg^{-1}·day^{-1}, i.p. during 7- or 28-day (n=5-11 mice/group; *P<0.05, **P<0.01 versus saline or PBS, respectively; τP<0.05, ττP<0.01 versus C-NS-siRNA). Values are mean ± s.e.m.

Procedure/Paradigm	Measurement	Statistical test	Comparison	Stastistics	Degrees of freedom	p	Figure
Confocal analysis	Intracelular A488 density in TPH2-positive cells (DR)	One-way ANOVA		F=22.54	11, 12	<0.0001****	1b
	Intracelular A488 density in TPH2-positive cells (MnR)	One-way ANOVA		F=3.460	11, 12	<0.05*	1c
In situ hybridization	SERT mRNA (DR)	Two-way ANOVA	Factor 1 Group Factor 2 Time Interaction (F1 x F2)	F=56.73 F=4.698 F=5.927	2, 32 2, 32 4, 32	<0.001*** <0.05* <0.01**	2b
	SERT mRNA (MnR)	Two-way ANOVA	Factor 1 Group Factor 2 Time Interaction (F1 x F2)	F=7.379 F=13.07 F=3.525	2, 37 2, 37 4, 37	<0.01** <0.001*** <0.05*	
Autoradiography	SERT binding (DR)	Two-way ANOVA	Factor 1 Group Factor 2 Time Interaction (F1 x F2)	F=66.61 F=4.20 F=1.039	2, 32 2, 32 4, 32	<0.001*** <0.05* >0.145	
	SERT binding (MnR)	Two-way ANOVA	Factor 1 Group Factor 2 Time Interaction (F1 x F2)	F=12.52 F=0.6104 F=3.865	2, 30 2, 30 4, 30	<0.001*** >0.05 <0.05*	
Immunohistochemistry	SERT protein (DR) SERT protein (MnR	One-way ANOVA		F=12.28 F=1.86	2, 9 2, 8	<0.01** >0.05	2d
Microdialysis	Dialysate 5-HT	Two-way ANOVA	Factor 1 Group Factor 2 Concentration Interaction (F1 x F2)	F=12.05 F=13.77 F=6.724	1, 13 15, 195 15, 195	<0.01** <0.001*** <0.0001****	2e
In situ hybridization	5-HT1A mRNA (DR) 5-HT1A mRNA (MnR)	One-way ANOVA		F=9.326 F=4.192	2, 9 2, 9	<0.01** 0.0517	3b
Autoradiography	5-HT1A binding site (DR) 5-HT1A binding site (MnR)			F=9.467 F=1.463	2, 8 2, 8	<0.01** >0.05	
Autoradiography	GTPγS binding in DR (FLX group) GTPγS binding in DR (C-SERT-siRNA group)	One-way ANOVA		F=30.72 F=13.78	2, 8 2, 7	<0.001*** <0.01**	3c
Microdialysis	Dialysate 5-HT in HPCv (8-OH-DAPT effect in FLX	Two-way ANOVA	Factor 1 Group Factor 2 Time Interaction (F1 x F2)	F=18.94 F=5.61 F=2.96	2, 15 10, 150 20, 150	<0.001*** <0.001*** <0.001***	3d
	Dialysate 5-HT in HPCv (8-OH-DAPT effect in C-SERT-siRNA group)	Two-way ANOVA	Factor 1 Group Factor 2 Time Interaction (F1 x F2)	F=53.15 F=11.94 F=4.081	2, 8 10, 80 20, 80	<0.001*** <0.001*** <0.001***	
Microdialysis	Dialysate 5-HT in Cpu (Time course in FLX group)	Two-way ANOVA	Factor 1 Group Factor 2 Time Interaction (F1 x F2)	F=63.84 F=12.10 F=12.11	1, 76 9, 76 9, 76	<0.001*** <0.001*** <0.001***	3e
	Dialysate 5-HT in Cpu (Time course in C-SERT-siRNA group)	Two-way ANOVA	Factor 1 Group Factor 2 Time Interaction (F1 x F2)	F=211.2 F=2.638 F=2.645	2, 64 4, 64 8, 64	<0.001*** <0.05* <0.01**	
	Dialysate 5-HT in HPCv (FLX group)	Two-way ANOVA	Factor 1 Group Factor 2 Time Interaction (F1 x F2)	F=47.58 F=18.40 F=18.38	1, 19 1, 19 1, 19	<0.001*** <0.001*** <0.001***	
	Dialysate 5-HT in HPCv (C-SERT-siRNA group)	One-way ANOVA		F=141.5	2, 8	<0.001***	
Proliferation and neurogenesis	Ki67+ cells BrdU+ cells NeuroD+ cells DCX+ cells	One-way ANOVA		F=7.957 F=6.976 F=6.596 F=6.163	5, 48 5, 46 5, 28 5, 31	<0.001*** <0.001*** <0.001*** <0.001***	4b 4c 4d 4e
Maturation index	Dendritic intersections (FLX group)	Two-way ANOVA	Factor 1 Group Factor 2 Distance from soma Interaction (F1 x F2)	F=133.7 F=67.0 F=5.764	2, 100 19, 100 38, 100	<0.001*** <0.001*** <0.001***	4g
	Dendritic intersections (C-SERT-siRNA group)	Two-way ANOVA	Factor 1 Group Factor 2 Distance from soma Interaction (F1 x F2)	F=82.15 F=95.53 F=3.061	2, 180 19, 180 38, 180	<0.001*** <0.001*** <0.001***	
	Dendritic length (FLX group)	Two-way ANOVA	Factor 1 Group Factor 2 Distance from soma Interaction (F1 x F2)	F=168.2 F=78.33 F=6.030	2, 180 19, 180 38, 180	<0.001*** <0.001*** <0.001***	
	Dendritic length (C-SERT-siRNA group)	Two-way ANOVA	Factor 1 Group Factor 2 Distance from soma Interaction (F1 x F2)	F=85.31 F=100.7 F=3.101	2, 100 19, 100 38, 180	<0.001*** <0.001*** <0.001***	
Gene expression in DG	BDNF mRNA VEGF mRNA TRKB mRNA ARC mRNA Neuritin mRNA PSD95 mRNA (FLX group)	One-way ANOVA		F=121.3 F=17.65 F=9.57 F=10.08 F=18.09 F=6.737	2, 9 2, 9 2, 9 2, 9 2, 8 2, 20	<0.001*** <0.001*** <0.001*** <0.01** <0.01** <0.05*	4h
	BDNF mRNA VEGF mRNA TRKB mRNA			F=27.11 F=31.92 F=6.644	2, 10 2, 10 2, 10	<0.001*** <0.001*** <0.05*	

	ARC mRNA Neuritin mRNA PSD95 mRNA (C-SERT siRNA group)	One-way ANOVA		F=9,612 F=30.03 F=6.319	2, 10 2, 9 2, 11	<0.01** <0.001*** <0.05*	
Anhedonia	Preference by sucrose (FLX group, 7-day)	Two-way ANOVA	Factor 1 Pre-treatment Factor 2 Treatment Interaction (F1 x F2)	F=414.6 F=0.0826 F=0.0812	1, 42 1, 42 1, 42	<0.001*** >0.05 >0.05	5a
	Preference by sucrose (FLX group, 28-day)	Two-way ANOVA	Factor 1 Pre-treatment Factor 2 Treatment Interaction (F1 x F2)	F=64.78 F=46.25 F=82.92	1, 32 1, 32 1, 32	<0.001*** <0.001*** <0.001***	
	Preference by sucrose (C-SERT-siRNA group, 7-day)	Two-way ANOVA	Factor 1 Pre-treatment Factor 2 Treatment Interaction (F1 x F2)	F=58.94 F=10.89 F=19.21	1, 69 2, 69 2, 69	<0.001*** <0.001*** <0.001***	
	Sucrose intake (FLX group, 7-day)	Two-way ANOVA	Factor 1 Pre-treatment Factor 2 Treatment Interaction (F1 x F2)	F=120.1 F=3.676 F=0.1111	1, 39 1, 39 1, 39	<0.001*** >0.05 >0.05	5b
	Sucrose intake (FLX group, 28-day)	Two-way ANOVA	Factor 1 Pre-treatment Factor 2 Treatment Interaction (F1 x F2)	F=54.27 F=15.44 F=5.35	1, 32 1, 32 1, 32	<0.001*** <0.001*** <0.05*	
	Sucrose intake (C-SERT-siRNA group, 7-day)	Two-way ANOVA	Factor 1 Pre-treatment Factor 2 Treatment Interaction (F1 x F2)	F=172.3 F=29.68 F=45.75	1, 66 2, 66 2, 66	<0.001*** <0.001*** <0.001***	
Novelty suppressed feeding	Latency to feed (FLX group, 7-day)	Two-way ANOVA	Factor 1 Pre-treatment Factor 2 Treatment Interaction (F1 x F2)	F=19.44 F=0.6123 F=0.01298	1, 38 1, 38 1, 38	<0.001*** >0.05 >0.05	5c
		Kaplan-Meier survival analysis				<0.01**	5d
	Latency to feed (FLX group, 28-day)	Two-way ANOVA	Factor 1 Pre-treatment Factor 2 Treatment Interaction (F1 x F2)	F=0.1540 F=0.9203 F=20.29	1, 31 1, 31 1, 31	>0.05 >0.05 <0.001***	5c
		Kaplan-Meier survival analysis				<0,01**	5d
	Latency to feed (C-SERT-siRNA group, 7-day)	Two-way ANOVA	Factor 1 Pre-treatment Factor 2 Treatment Interaction (F1 x F2)	F=5.028 F=0.0012 F=16,35	1, 53 2, 53 2, 53	<0.05* >0.05 <0.001***	5c
		Kaplan-Meier survival analysis				<0.001***	5d
Tail suspension test	Immobility time (FLX group, 7-day)	Two-way ANOVA	Factor 1 Pre-treatment Factor 2 Treatment Interaction (F1 x F2)	F=24.39 F=0.2405 F=0.097	1, 37 1, 37 1, 37	<0.001*** >0.05 >0.05	5e
	Immobility time (FLX group, 28-day)	Two-way ANOVA	Factor 1 Pre-treatment Factor 2 Treatment Interaction (F1 x F2)	F=5.121 F=5.121 F=10.78	1, 40 1, 40 1, 40	<0.05* <0.05* <0.01**	
	Immobility time (C-SERT siRNA, 7-day)	Two-way ANOVA	Factor 1 Pre-treatment Factor 2 Treatment Interaction (F1 x F2)	F=13.20 F=1,317 F=6.511	1, 57 2, 57 2, 57	<0.001*** >0.05 <0.01**	
Autoradiography	SERT binding (mPFC) SERT binding (CPu) SERT binding (LS/MS) SERT binding (HPC) SERT binding (Hyp) SERT binding (Amyg)	One-way ANOVA		F=10.10 F=6.605 F=12.86 F=11.70 F=8.479 F=15.13	2, 15 2, 15 2, 15 2, 14 2, 14 2, 9	<0.01** <0.05* <0.01** <0.05* <0.05* <0.01**	S5b
Immunohistochemistry	SERT protein (HPC) SERT protein (Amyg)	One-way ANOVA		F=13.86 F=23.59	2, 15 2, 15	<0.01** <0.001***	S5d
In situ hybridization	SERT mRNA (DR)	One-way ANOVA		F=20,15	3, 14	<0.0001****	S6b
In situ hybridization	SERT mRNA (DR)	One-way ANOVA		F=8,89	4, 28	<0.0001****	S7b
In situ hybridization Autoradiography	TPH2 mRNA (DR) NET binding (DR)	One-way ANOVA		F=2.267 F=0.616	2, 9 2, 6	>0.05 >0.05	S9b
In situ hybridization	5-HT$_{1A}$ mRNA (DR) 5-HT$_{1A}$ mRNA (MnR)	One-way ANOVA		F=4.64 F=0.479	3, 12 3, 15	<0,05* >0,05	S10a
	5-HT$_{1A}$ mRNA (DR) 5-HT$_{1B}$ mRNA (MnR)	One-way ANOVA		F=3,731 F=7,523	4, 24 4, 21	<0,05* <0,05*	S10b
Autoradiography	GTPγS binding in Hippocampus (FLX group) GTPγS binding in Hippocampus (C-SERT siRNA group)	One-way ANOVA		F=14,00 F=14,08	5, 24 5, 54	<0,0001**** <0,0001****	S10c
	BDNF mRNA	Two-way ANOVA	Factor 1 Group FLX Factor 2 Area Interaction (F1 x F2)	F=0.6934 F=7.993 F=0.2473	2, 27 2, 27 4, 27	>0.05 <0.01** >0.05	
			Factor 1 Group C-SERT-siRNA Factor 2 Area Interaction (F1 x F2)	F=9.411 F=0.8932 F=1.442	2, 30 2, 30 4, 30	<0.001*** >0.05 >0.05	
			Factor 1 Group FLX Factor 2 Area	F=25.66 F=0.6050	2, 27 2, 27	<0.001*** >0.05	

Gene expression in the hippocampus	VEGF mRNA	Two-way ANOVA	Interaction (F1 x F2)	F=0.1592	4, 27	>0.05	S12
			Factor 1 Group C-SERT-siRNA	F=20.22	2, 30	<0.001***	
			Factor 2 Area	F=1,471	2, 30	>0.05	
			Interaction (F1 x F2)	F=2,882	4, 30	<0.05*	
	TRKb mRNA	Two-way ANOVA	Factor 1 Group FLX	F=50.32	2, 27	<0.001***	
			Factor 2 Area	F=0.05593	2, 27	>0.05	
			Interaction (F1 x F2)	F=0.1021	4, 27	>0.05	
			Factor 1 Group C-SERT-siRNA	F=23.00	2, 30	<0.001***	
			Factor 2 Area	F=0.4009	2, 30	>0.05	
			Interaction (F1 x F2)	F=0.3572	4, 30	>0.05	
	ARC mRNA	Two-way ANOVA	Factor 1 Group FLX	F=13.16	2, 27	<0.001***	
			Factor 2 Area	F=1.982	2, 27	>0.05	
			Interaction (F1 x F2)	F=0.9167	4, 27	>0,05	
			Factor 1 Group C-SERT-siRNA	F=20.52	2, 27	<0.001***	
			Factor 2 Area	F=1.028	2, 27	>0.05	
			Interaction (F1 x F2)	F=0.0149	4, 27	>0.05	
	Neuritin mRNA	Two-way ANOVA	Factor 1 Group FLX	F=3.080	2, 24	>0.05	
			Factor 2 Area	F=0.5855	2, 24	>0.05	
			Interaction (F1 x F2)	F=0.4337	4, 24	>0.05	
			Factor 1 Group C-SERT-siRNA	F=4.744	2, 27	<0.05*	
			Factor 2 Area	F=0.7946	2, 27	>0.05	
			Interaction (F1 x F2)	F=0.9265	4, 27	>0.05	
	PSD95 mRNA	Two-way ANOVA	Factor 1 Group FLX	F=0.06946	2, 45	>0.05	
			Factor 2 Area	F=0.007348	2, 45	>0.05	
			Interaction (F1 x F2)	F=0.3151	4, 45	>0.05	
			Factor 1 Group C-SERT-siRNA	F=3.236	2, 35	>0.05	
			Factor 2 Area	F=0.5238	2, 35	>0.05	
			Interaction (F1 x F2)	F=0.8558	4, 35	>0.05	
Mouse body weight		Two-way ANOVA	Factor 1 Pre-treatment	F=36.95	1, 88	<0.001***	S13a
			Factor 2 Time	F=29.01	15, 88	<0.001***	
			Interaction (F1 x F2)	F=6.056	15, 88	<0.001***	
Drinking consumption		Two-way ANOVA	Factor 1 Pre-treatment	F=25.62	1, 320	<0.001***	S13b
			Factor 2 Time	F=5.016	15, 320	<0.001***	
			Interaction (F1 x F2)	F=3.901	15, 320	<0.001***	
Corticosterone levels		Two-way ANOVA	Factor 1 Pre-treatment	F=1.173	1, 54	>0,05	S13c
			Factor 2 Time	F=0.046	1, 54	>0,05	
			Interaction (F1 x F2)	F=0.6173	1, 54	>0,05	
Open field	Activaction time	Two-way ANOVA	Factor 1 Pre-treatment	F=0.6905	1, 33	>0,05	S13d
			Factor 2 Time	F=11.42	1, 33	<0.01**	
			Interaction (F1 x F2)	F=0.8918	1, 33	>0,05	
	Distance moved		Factor 1 Pre-treatment	F=1.579	1, 33	>0,05	
			Factor 2 Time	F=11.88	1, 33	<0.01**	
			Interaction (F1 x F2)	F=0.3226	1, 33	>0,05	
	Slows/short movement		Factor 1 Pre-treatment	F=0.1544	1, 33	>0,05	
			Factor 2 Time	F=0.01911	1, 33	>0,05	
			Interaction (F1 x F2)	F=0.002833	1, 33	>0,05	
	Fast/large movement		Factor 1 Pre-treatment	F=1.567	1, 33	>0,05	
			Factor 2 Time	F=7.282	1, 33	<0.05*	
			Interaction (F1 x F2)	F=1.163	1, 33	>0,05	
Tail suspension test	Immobility time	Two-way ANOVA	Factor 1 Pre-treatment	F=30.10	1, 37	<0.001***	S13e
			Factor 2 Time	F=1.407	1, 37	>0.05	
			Interaction (F1 x F2)	F=2.338	1, 37	>0.05	
Anhedonia	Preference by sucrose	Two-way ANOVA	Factor 1 Pre-treatment	F=175.2	1, 41	<0.001***	S13f
			Factor 2 Time	F=0.003165	1, 41	>0.05	
			Interaction (F1 x F2)	F=4.774	1, 41	>0.05	
	Sucrose intake		Factor 1 Pre-treatment	F=77.4	1, 41	<0.001***	
			Factor 2 Time	F=0.5138	1, 41	>0.05	
			Interaction (F1 x F2)	F=0.5138	1, 41	>0.05	
Novelty suppressed feeding	Latency to feed	Two-way ANOVA	Factor 1 Pre-treatment	F=22.60	1, 41	<0.001***	S13g
			Factor 2 Time	F=3.433	1, 41	>0.05	
			Interaction (F1 x F2)	F=2.269	1, 41	>0.05	
		Kaplan-Meier survival analysis				<0.001***	

4.5. Trabajo 5

Selective knockdown of TASK3 potassium channel in monoamine neurons evoke robust antidepressant-like effects

A Ferrés-Coy, N Fullana, JE Ortega, E Ruiz-Bronchal, V Paz, A Montefeltro, JJ Meana, F Artigas and A Bortolozzi

Articulo manuscrito

La farmacología actual para el tratamiento de la depresión resulta inadecuada, por lo que existe una necesidad urgente de descubrir nuevas dianas terapéuticas y desarrollar tratamientos más efectivos y de acción rápida. Recientemente, el canal de potasio TASK3, miembro de la familia K_{2P}, ha sido identificado como posible nueva diana en depresión. Se ha observado que ratones *knockout* para TASK3 presentan cambios asociados con los trastornos del estado del ánimo y la acción antidepresiva como son la reducción del sueño REM y comportamientos de tipo antidepresivo en el FST y el TST. En este último trabajo nos preguntamos si el silenciamiento del TASK3 en el DR o el LC de ratón podría incrementar la neurotransmisión monoaminérgica y lograr efectos de tipo antidepresivo. Para ello, se empleó una secuencia de siRNA contra el TASK3 (TASK3-siRNA) conjugada con sertralina (Ser-TASK3-siRNA) o reboxetina (Reb-TASK3-siRNA) para silenciar específicamente el canal TASK3 en neuronas serotoninérgicas o noradrenérgicas, respectivamente.

Los resultados confirmaron que el tratamiento intranasal con el Ser-TASK3-siRNA o el Reb-TASK3-siRNA disminuye la expresión del canal TASK3 selectivamente en las neuronas serotoninérgicas del DR o noradrenérgicas del LC. Además, el silenciamiento de TASK3 evocó respuestas antidepresivas que incluyeron: 1) facilitación de la liberación de 5-HT o NE en la corteza prefrontal de ratones, 2) incremento de la proliferación y neuroplasticidad hipocampal y, 3) disminución de la inmovilidad y tiempo de latencia en el TST y NSFT, respectivamente. Estos efectos

fueron más marcados después de la reducción de la expresión de TASK3 inducida por siRNAs en neuronas serotoninérgicas que en noradrenérgicas. Finalmente, el tratamiento con el Ser-TASK3-siRNA produjo mayor resiliencia a una situación de estrés, permitiendo una mayor liberación de 5-HT cuando el animal fue sometido a un modelo de estrés agudo como el TST.

En conjunto, los datos sugieren que la pérdida de la función de TASK3 en las neuronas monoaminérgicas facilita su actividad, incrementa la neurotransmisión y evoca respuestas antidepresivas en ratones confirmando TASK3 como una nueva diana para el desarrollo de estrategias terapéuticas antidepresivas.

Selective knockdown of TASK3 potassium channel in monoamine neurons evoke robust antidepressant-like effects

Albert Ferrés-Coy[1,2,3], Neus Fullana[1,2,3], Jorge E Ortega[3,5], Esther Ruiz-Bronchal[1,2,3], Verónica Paz[1,2,3], Andrés Montefeltro[4], Javier J Meana[3,5], Francesc Artigas[1,2,3] and Analia Bortolozzi[1,2,3*]

[1]Department of Neurochemistry and Neuropharmacology, IIBB-CSIC (Consejo Superior de Investigaciones Científicas), Barcelona, Spain.
[2]Institut d'Investigacions Biomèdiques August Pi i Sunyer (IDIBAPS), Barcelona, Spain.
[3]Centro de Investigación Biomédica en Red de Salud Mental (CIBERSAM), ISCIII, Madrid, Spain.
[4]n-Life Therapeutics, S.L., Granada, Spain
[5]Department of Pharmacology, University of Basque Country UPV/EHU and BioCruces Institute, Bizkaia, Spain

*Corresponding author. E-mail: abbnqi@iibb.csic.es

ABSTRACT

Major depressive disorder (MDD) is a chronic, recurring and potentially life-threatening mental illness. Its high socio-economic impact is partly due to the slowness of action and limited efficacy of current antidepressant treatments, based on monoamine reuptake inhibition. Therefore, there is an urgent need to develop faster-acting and more effective treatments. Recently, TWIK-related acid-sensing K+ channel 3 (TASK3) protein (KCNK9), member of two-pore domain (K_{2P}) potassium channel family, has been identified as a potential target in depression. Here, we examined the effects of the selective reduction of TASK3 expression in serotonin (5-HT) and norepinephrine (NE) neurons in dorsal raphe (DR) and locus coeruleus (LC), respectively. We assessed the ability of a small interfering RNA (siRNA) sequence directed against TASK3 (TASK3-siRNA) to down-regulate TASK3 expression by local stereotaxic infusion into DR or LC (10 µg/day for 2-day) of C57Bl/6J mice. TASK3 mRNA levels were reduced to 69±4% (DR) and 84±4% (LC) of control groups. Further, TASK3-siRNA was conjugated to cell-specific ligands, sertraline (serotonin transporter -SERT- inhibitor) or reboxetine (norepinephrine transporter -NET- inhibitor) to promote their selective delivery to monoaminergic neurons. Sertraline- and reboxetine-conjugated, fluorescence-labeled siRNAs (30 µg/day for 4-day) were found in TPH_2^+ (DR) and TH^+ (LC) cells but not in other brain regions. Moreover, a 7-day intranasal treatment with Ser-TASK3-siRNA or Reb-TASK3-siRNA selectively reduced TASK3 mRNA density in 5-HT or NE neurons, respectively. Specifically, TASK3 knockdown in DR i) evoked antidepressant-like effects in the tail suspension (TST) and novelty suppressed feeding (NSFT) tests, ii) desensitized $5\text{-}HT_{1A}$ autoreceptors, iii) augmented the effect of fluoxetine on forebrain extracellular 5-HT, and iiii) increased plasticity-associated gene expression. Similar effects, yet of lower effect size were found in NE neurons. Overall, these results support that loss of function of TASK3 channels in monoamine neurons markedly enhances their activity and evokes antidepressant-like effects in mice, supporting the validity of TASK3 as a new target in antidepressant drug development.

Keywords: RNAi; depression; new antidepressant target; K_{2P} channel; intranasal delivery

Running title: Intranasal delivery of conjugated TASK3-siRNA

INTRODUCTION

Major depressive disorder (MDD) is a severe and highly prevalent psychiatric disease with a very high socioeconomic impact.[1,2] Its treatment is mainly based on monoamine (serotonin, 5-HT and norepinephrine, NE) reuptake inhibitors. These drugs show a slow onset of clinical action and limited efficacy, which results in a high percentage of MDD patients with poor or no responses, thus reducing quality of life and increasing suicide risk.[3-5] The reasons for the limited efficacy of SSRI (selective serotonin reuptake inhibitors) and SNRI (serotonin and norepinephrine reuptake inhibitors) are manifold, including presynaptic and postsynaptic adaptive mechanisms of monoamine neurotransmission, as well as genetic factors resulting in a large interindividual variability.[6]

RNAi strategies have been successfully used to evoke antidepressant-like effects in rodents.[7] Hence, the intracerebroventricular (i.c.v.) or intranasal (i.n.) administration of SSRI-conjugated siRNA (small interfering RNA) directed against the serotonin transporter (SERT) or 5-HT_{1A} autoreceptors induced robust antidepressant-like effects in mice,[8,9] mimicking the effects of the local siRNA application in the midbrain raphe nuclei.[10,11] The presence of the SSRI sertraline in the conjugated siRNA molecule allows its accumulation by serotonergic neurons and the selective targeting of genes expressed by these neurons. Interestingly, 1-week intranasal administration of small amounts (2.1 $nmol \cdot day^{-1}$) of a sertraline-conjugated siRNA directed against SERT evoked antidepressant-like responses and changed pre- and postsynaptic variables predictive of clinical antidepressant activity (autoreceptor sensitivity, extracellular 5-HT, hippocampal neurogenesis, trophic factor expression, etc.) to the same extent than 1-month of treatment with 10 $mg \cdot kg^{-1} \cdot day^{-1}$ fluoxetine.[9] On the other hand, the knockdown of 5-HT_{1A} autoreceptors also evoked rapid antidepressant-like effects in mice,[8,10] an action likely due to the ability of serotonergic neurons to increase their activity and release 5-HT in forebrain during stressful situations, thus increasing resilience to stress.

Recently, the TWIK-related acid-sensing K+ channel 3 (TASK3) protein (KCNK9), member of two-pore domain (K_{2P}) potassium channel family,[12] has been identified as a new potential target in depression.[13,14] Deletion of TASK3 in mice markedly reduced REM sleep and evoked antidepressant-like effects, suggesting that TASK3 channel blockers may have clinical antidepressant actions. TASK3 mRNA shows a widespread distribution in rodent brain, being abundantly expressed in the cerebral cortex, the hippocampus, thalamic and hypothalamic nuclei and the cerebellum as well as in 5-HT and NE neurons of the dorsal raphe (DR) and locus coeruleus (LC), respectively.[15,16] TASK3 channels subserve a variety of physiological functions and largely contribute to the background K currents, acting also as extracellular pH sensors.[17] Here we examined the effects of the selective reduction of the expression of TASK3 channels in these neuronal groups, under the working hypothesis that the reduced expression/function of constitutively active TASK3 channels would enhance monoamine cell function. This effect would result from an increased excitation/inhibition balance on monoamine neurons following the reduced outflow of K^+ ions, in a manner similar to that produced by 5-HT_{1A} autoreceptor knockdown in the case of 5-HT neurons. On the other hand, the selective reduction of TASK3 function in 5-HT or NE neurons would avoid potential side effects of TASK3 channel blockers (e.g., memory and/or motor problems) resulting from their interaction with TASK3 channels in forebrain areas, as well as in cerebellum.

MATERIALS AND METHODS

Animals

Male C57BL/6J mice (10–14 weeks; Charles River, Lyon, France) were housed under controlled conditions (22±1ºC; 12h light/dark cycle) with food and water available *ad-libitum*. Animal procedures were conducted in accordance with standard ethical guidelines (EU regulations L35/118/12/1986) and approved by the local ethical committee.

Drugs

All reagents used were of analytical grade and were obtained from Merck (Germany). 5-HT oxalate, NE, bitartrate, (±)-8-hydroxi-2(dipropylamino)tetralin hydrobromide (8-OH-DPAT), and clonidine were from Sigma-Aldrich-RBI (Madrid, Spain). Moreover, fluoxetine, reboxetine, desipramine and citalopram hydrobromide were purchased from Tocris (Madrid, Spain). To assess local effects in the microdialysis experiments, drugs were dissolved in artificial cerebrospinal fluid (aCSF, in mM: NaCl, 125; KCl, 2.5; $CaCl_2$, 1.26 and $MgCl_2$, 1.18) and, administered by reverse dialysis at the stated concentrations (uncorrected for membrane recovery). All other drugs were dissolved in saline or aCSF, as required. Concentrated solutions (1mM; pH adjusted to 6.5–7 with NaHCO3 when necessary) were stored at -80ºC and working solutions were prepared daily by dilution in aCSF.

siRNA synthesis

The synthesis and purification of naked and conjugated siRNA targeting TASK3 potassium channel (TASK3-siRNA, nt: 1056–1075, GenBank accession NM_001033876) and nonsense siRNA (NS-siRNA) were performed by nLife therapeutics S.L. (Granada, Spain). Both TASK3-siRNA and scrambled (non-sense) siRNA (NS-siRNA) sequences were conjugated with the SSRI sertraline (Ser-TASK3-siRNA and Ser-NS-siRNA) as described for the selective targeting of 5-HT neurons.[8,9] The TASK3 siRNA was also conjugated with the

selective NE reuptake inhibitor reboxetine (Reb-TASK3-siRNA and Reb-NS-siRNA) to target NE neurons. Details are shown in the Supplementary Information.

To study *in vivo* intracellular distribution and incorporation of conjugated siRNA into 5-HT or NE neurons, Ser-NS-siRNA and Reb-NS-siRNA were additionally labeled with Alexa488 in the antisense strand (A488-Ser-NS-siRNA and A488-Reb-NS-siRNA). Control groups were administered with Alexa488-PBS (A488-PBS) and non-conjugated (naked) NS-siRNA (A488-NS-siRNA).[9] Stock solutions of all siRNAs were prepared in RNAse-free water and stored at -20ºC until use. Sequences are shown in **Supplementary Table S1**.

Treatments

In order to compare the efficiency of the intranasal administration of the sertraline-conjugated siRNA with that of an unmodified siRNA locally applied in the monoamine nuclei, different groups of mice were administered intracerebrally or intranasally.

For intracerebral naked siRNA infusion (TASK3-siRNA and NS-siRNA), mice were anesthetized (pentobarbital, 40 $mg \cdot kg^{-1}$, intra-peritoneally, i.p.) and silica capillary microcannula (110 µm-outer diameter (OD), 40 µm-inner diameter (ID); Polymicro Technologies, Madrid, Spain) were stereotaxically implanted into the DR (coordinates in mm: AP, -4.5; ML, -1.0; DV, -4.1) or LC (coordinates in mm: AP, -5.20; ML, -0.9; DV, -3.5).[18] Local siRNA microinfusion was performed 24 h after surgery in awake mice using a precision minipump at a 0.5 $\mu l \cdot min^{-1}$ as previously described.[8,10,11] siRNAs were prepared in a RNase-free aCSF with 5 % glucose and infused intra-DR or intra-LC once daily at the dose of 10 $\mu g \cdot \mu l^{-1}$(0.7 nmol per dose). Mice received two doses in 2 consecutive days. Control mice received aCSF. Mice were sacrificed 24 h after last infusion.

For i.n. administration, mice were slightly anesthetized by 2% isoflurane inhalation and placed in a supine position.[8,9] A 5 µl-drop of phosphate buffered saline (PBS) or conjugated siRNAs (Ser- or Reb-NS-siRNA or Ser- or Reb-TASK3-siRNA) was applied alternatively to each nostril once daily. A total of 10 µl of solution containing 30 or 75 µg (2.1 or 5.3

nmol·day^{-1}) of conjugated siRNA was delivered for 7 days and mice were sacrificed between 3-4 days after last administration.

***In situ* hybridization and quantitative image analysis of film autoradiograms**

Mice were killed by pentobarbital overdose and brains were rapidly removed, frozen on dry ice and stored at -80ºC. Coronal tissue sections (14 µm-thick) were cut using a microtome-cryostat (HM500-OM, Microm, Walldorf, Germany), thaw-mounted onto 3-aminopropyltriethoxysilane (Sigma-Aldrich, St. Louis, MO, USA)-coated slides and kept at -20ºC until use. Antisense oligoprobes were complementary to bases: TASK3/839-888 (GenBank accession NM_001033876), TWIK-related acid-sensitive K+ channel 1-TASK1/101-150 (NM_010608), TWIK-related potassium channel 1-TREK1/592-641, 726-775, 889-938, 1082-1131 (NM_001159850/NM_010607), SERT/820-863 (NM_010484.1), serotonin-1A receptor-5-HT$_{1A}$R/1780-1827 (NM_008308), NET/1210-1259 (NM_009209), α2-adrenoreceptor-Adra2/2137-2186 (NM_NC_000085), brain derived neurotrophic factor-BDNF/1188-1238 (NM_007540), vascular endothelial growth factor-VEGF/2217-2267 (NM_001025250), activity regulated cytoskeletal protein-ARC/1990-2040 (NM_018790), respectively (Göttingen, Germany). Oligonucleotides were individually labeled (2 pmol) at the 3'-end with [^{33}P]-dATP (>2500 Ci·mmol^{-1}; DuPont-NEN, Boston, MA) using terminal deoxynucleotidyltransferase (TdT, Calbiochem, La Jolla, CA). Sections were hybridized as previously described.[8-11] Films were analyzed and relative optical densities (ROD) were obtained using a computer assisted image analyzer (MCID, Mering, Germany). The slide background and non-specific densities were subtracted. ROD were evaluated in two or three adjacent sections by duplicate of each mouse and averaged to obtain individual values. MCID system was also used to acquire pseudocolor images. Black and white photographs were taken from autoradiograms using a Wild 420 microscope (Leica, Heerbrugg, Germany) equipped with Nikon DXM1200F digital camera and ACT-1 Nikon software (Soft Imaging System Gmbh, Münster, Germany). Images were processed with Photoshop (Adobe Systems, Mountain View) by using identical values for contrast and brightness. Additionally,

TASK3 hybridized slides were then dipped into Ilford K5 nuclear emulsion (Ilford, Mobberly, Chesire, UK) diluted 1:1 with distilled water. They were exposed in the dark at 4°C for 2 weeks, and finally developed in Kodak D19 (Kodak, Rochester, NY, USA) for 5 min, and fixed in Ilford Hypam fixer (Ilford). Details of image acquisition and quantification analysis of dipped TASK3 slides are shown in the Supplementary Information.

Immunohistochemistry

Mice were anesthetized with pentobarbital and transcardially perfused with 4% paraformaldehyde in sodium-phosphate buffer (pH 7.4). Brains were collected, post-fixed 24h at 4ºC in the same solution, and then placed in gradient sucrose 10–30% for 3 days at 4ºC. After cryopreservation, serial 30 µm-thick sections were cut of the hippocampal formation, the midbrain raphe nuclei and LC. Immunohistochemical procedure was performed for doublecortin (DCX), glial fibrillary acidic protein (GFAP), Iba-1, Ki-67, tyrosine hydroxylase (TH) and tryptophan hydroxylase 2 (TPH_2) using biotin-labeled antibody procedure.[9,11] Details are shown in the Supplementary Information.

Confocal fluorescence microscopy

Intracellular Ser- and Reb-NS-siRNA distribution in 5-HT and NE neurons was examined by confocal microscopy using a Leica TCS SP5 laser scanning confocal microscope (Leica Microsystems Heidelberg GmbH, Manheim, Germany) equipped with a DMI6000 inverted microscope, blue diode (405nm), Argon (458/476/488/496/514), diode pumped solid state (561nm) and HeNe (594/633nm) lasers. After i.n. administration with Alexa488 labeled Ser- or Reb-NS-siRNA at 30 $\mu g \cdot day^{-1}$ during 4 days, mice were sacrificed and their brain were extracted and processed for immunofluorescence. Details are shown in the Supplementary Information.

TASK3 antibody production and purification

The anti-TASK3 antibody was raised against a synthetic peptide corresponding to amino acid CGDHRLHLRRKSI of the C terminus from the protein KCNK9. The peptide synthesis and production of antibodies has been performed by the platform of Production of Biomolecules of the ICTS "NANBIOSIS", more specifically by the Unit U2: Custom Antibody Service at the Institut de Quimica Avançada de Catalunya (IQAC-CSIC) and Unit U3: Synthesis of peptide Unit (Parc Cientific de Barcelona & Universidad de Barcelona (UB)) from of the CIBER in Bioengineering, Biomaterials & Nanomedicne (CIBER-BBN). The BSA and HCH were conjugated to CGDHRLHLRRKSI peptide using a heterobifunctional crosslinker N-hydroxysuccinimide maleimidopropionate (N-SMP).[19] The conjugation was carried out firstly by the addition of N-SMP (0.41 mg) in DMF (50 µL) to a solution of BSA or HCH (10 mg) dissolved in PBS (950 µL). The reaction was stirred for two hours at room temperature. The activated protein was purified by size exclusion chromatography. The eluted fractions were collected and was reacted by the addition of the BF1 peptide (5 mg) dissolved in a H2O:ACN mixture (1:1, 200 µL). The mixture was kept under stirring overnight at 4ºC. The final conjugates were purified by dialysis, lyophilized and stored freeze-dried at -20ºC. In order to evaluate the degree of conjugation for SMP and CGDHRLHLRRKSI conjugation the mass spectra was acquired using a MALD-TOF MS technique. The hapten density was 9 and 3 for BSA-SMP and BSA-SMP- CGDHRLHLRRKSI conjugate, respectively.

The antisera obtained by immunizing female white New Zealand rabbits with CGDHRLHLRRKSI -HCH. Evolution of the antibody titer was assessed on a non-competitive indirect ELISA, by measuring the binding of serial dilutions of the different antisera to microtiter plates coated with a fixed concentration of CGDHRLHLRRKSI -BSA (1 mg mL−1). After 6 immunizations, the animals were exsanguinated, and the blood was collected in vacutainer tubes provided with a serum separation gel. Antisera were obtained by centrifugation at 4 °C for 10 min at 4000 rpm, and stored at −80 °C in the presence of 0.02% NaN_3. Unless otherwise indicated, working aliquots were stored at 4 °C. The antiserum obtained was affinity-purified by a HiTrap NHS-activated column. The purified antibody was characterized by Western blot analysis (**Supplementary Figure S1**).

Western Blot

Mice were killed by pentobarbital overdose and brains were rapidly removed. The medial prefrontal cortex (mPFC), hippocampus (HPC), DR and LC were dissected out using a Mouse Brain Matrix (Ted Pella, Madrid, Spain), quickly frozen on dry ice and stored at -80ºC. Each sample was homogenized (Miccra D-1 homogenizer, Miccra GmbH, Müllheim, Deutschland) and sonicated (Labsonic M ultrasonic homogenizer, Sartorius, Göttingen, Germany) with RIPA buffer (50 mM Tris-Base, 150 mM NaCl, 0.5 % sodium deoxycholate, 0.1 % SDS and 1 % Triton X-100) containing a protease inhibitor cocktail (cOmplete Protease; Roche, Indianapolis, IN, USA). Protein extracts were quantified following the BCA method (Pierce BCA Protein Assay Kit, Thermo Fisher Scientific Inc., Rockford, IL, USA). Then, 5 μg of each protein extract were mixed with loading buffer (Laemmli Sample Buffer, Bio-Rad, Hercules, CA, USA) plus β-mercaptoethanol, heated at 95ºC for 5 min, loaded onto a 4-20 % precast gel (Mini-Protean TGX, Bio-Rad) and electrophoresed. Next, proteins were transferred onto a 0.2 μm PVDF membrane (Trans-Blot Turbo Mini PVDF Transfer Pack, Bio-Rad), which was subsequently rinsed, blocked with milk and incubated overnight at 4ºC with a rabbit anti-TASK3 antibody (1:500). Finally, the membrane was incubated with a horseradish peroxidase-conjugated donkey anti-rabbit secondary antibody (1:2500, Sigma Aldrich) and proteins were detected with a chemiluminiscence detection system based on the luminol reaction (SuperSignal West Pico, Thermo Fisher Scientific Inc.). The immunoreactive bands were digitalized (Molecular Imager VersaDoc MP 5000, Bio-Rad) and a densitometry analysis was performed using ImageJ (1.49g) software. TASK3 protein levels were normalized to that of β-actine.

Intracerebral microdialysis

Extracellular 5-HT and NE concentrations were measured by *in vivo* microdialysis as previously described.[8-11,20-22] Briefly, one concentric dialysis probe (Cuprophan; 1.5 mm-long)

was implanted mPFC (coordinates in mm: AP, 2.2; ML, -0.2; DV, -3.4)[18] of anaesthetized mice. Experiments were performed 24-72 h after surgery.

In experiments involving 5-HT, aCSF was pumped (WPI model, SP220i) at 2.0 or 5.0 $\mu l \cdot min^{-1}$ and 30-min or 6-min samples were collected, respectively. 1 µM citalopram was added to aCSF of experiments examining the change in 5-HT release after 8-OH-DPAT administration or during stressful procedures (tail suspension test, TST). 5-HT concentrations were analyzed by high performance liquid chromatography (HPLC) with electrochemical amperometric detection (+0.6V; Hewlett Packard 1049, Palo Alto, CA, USA) with 3-fmol detection limits.

For the analysis of NE in dialysate samples, mice were connected to a fraction collection system for freely moving animals (Raturn; BASi, Indianapolis, USA).[23] The input tube of the dialysis probe was connected to a syringe pump (BeeHive and BabyBee; BASi, Indianapolis, USA), which delivered artificial cerebrospinal fluid 2($aCSF_2$: 148 mM NaCl, 2.7 mM KCl, 1.2 mM CaCl2, and 0.85 mM MgCl2; pH 7.4) pumped at a flow rate of 1 $\mu L\ min^{-1}$. Samples were collected every 35 min. In experiments evaluating NE release in response to clonidine administration, 1 µM desipramine was added to $aCSF_2$. NE concentrations were analyzed by HPLC with amperometric detection (VT-03 cell, Decade II, Antec Leyden, Holland) at an oxidizing potential of 0.300 mV. The mobile phase (50 mM fosforic acid, 0.1 mM EDTA, 8 mM sodium chloride, 500 mg L−1 sodium octyl sulfate, pH 6, and 16% methanol) was filtered, degassed (Hewlett-Packard model 1100 degasser), and delivered at a flow rate of 0.2 mL/min by a Hewlett- Packard model 1100 pump.

Baseline 5-HT or NE levels were calculated as the average of the four pre-drug samples or seven pre-TST samples.

Behavioral studies

All tests were performed between 10:00 and 15:00h. Behavioral assessments were performed 24h after last dose with a minimal interval of one day between tests. All mice were evaluated in two behavioral paradigms including novelty suppressed-feeding test (NSFT) and

TST or NSFT and marble burying test (MBT). On test days, animals were transported to a dimly illuminated behavioral room and were left undisturbed for at least 1 h before testing. In an additional group, the mPFC 5-HT concentration was simultaneously measured during TST paradigm by *in vivo* microdialysis (see above). Behavioral tests were conducted by an experimenter blind to mouse treatments. Details are shown in the Supplementary Information.

Statistical analyses

All results are given as mean ± s.e.m. Data were analyzed using GraphPad Prism 6.0 (San Diego, CA). Statistical analyses were performed by two-tailed Student's *t*-test and one-way or two-way ANOVA followed by Tukey's *post-hoc* test as appropriate. In NSF test, we used the Kaplan-Meier survival analysis due to the lack of normal distribution of the data. Animals that did not eat during the 10min testing period were discarded. Mantel-Cox log-rank test was used to evaluate differences between experimental groups, as described by Samuels and Hen (2011).[24] Differences were considered significant when $P<0.05$.

RESULTS

Localization of sertraline- and reboxetine-conjugated siRNA in DR and LC after i.n. administration

In order to target 5-HT neurons of he DR we used a previously developed strategy, in which the SSRI sertraline was chemically conjugated to the oligonucleotide molecule.[8,9] This strategy allowed the selective enrichment of this sertraline-conjugated siRNA in raphe 5-HT neurons, which selectively express SERT.[25] We then hypothesized that the presence of the selective NE reuptake inhibitor (NERI) reboxetine would allow the selective delivery of conjugated siRNA molecules to NE neurons of the LC, where the norepinephrine transporter (NET) is selectively expressed.[26]

To assess the presence of the conjugated siRNA molecules in DR and LC neurons, after i.n. administration, four groups of mice were treated once daily with: (a) A488-PBS, (b) A488-NS-siRNA, (c) A488-Ser-NS-siRNA or (d) A488-Reb-NS-siRNA (2.1 nmol per dose) during 4 consecutive days. Mice were killed 6 h after last dose. Confocal fluorescence procedures revealed the presence of double-conjugated molecules in DR and LC. Hence, A488-Ser-NS-siRNA was detected in TPH_2^+ neurons of DR and A488-Reb-NS-siRNA was present in TH^+ neurons of LC. Both molecules were absent in the HPC region, which is closer the application site and to the 3rd ventricle (**Figures 1a and b**).

Although the transport mechanisms employed by 5-HT and NE neurons to transport the conjugated siRNA molecules to the cell bodies are not fully known, it is likely that endosomal networks are involved, since conjugated A488-siRNAs colocalized with the late endosomal marker Rab7 (**Figures 1c and d**).

Sertraline- and reboxetine-conjugated TASK3-siRNA selectively suppress TASK3 expression into 5-HT and NE neurons, respectively

We previously examined whether a naked TASK3-siRNA sequence was able to decrease *in vivo* TASK3 expression in DR and LC. To this end, mice were daily treated intra-DR or intra-

LC with 1 μl of: (a) vehicle, (b) NS-siRNA or (c) TASK3-siRNA (10 μg -0.7 nmol- per dose) for 2 consecutive days. siRNAs were applied through out a stereotaxically implanted silica capillary microcannula, as described in Methods. *In situ* hybridization experiments revealed a reduction of TASK3 mRNA to 69.4 ± 3.8 % of control values in DR and to 82.3 ± 2.1 % of control values in LC versus vehicle and NS-siRNA (**Supplementary Figure S2**).

We then examined the effect of i.n. Ser-TASK3-siRNA on DR TASK3 expression. Ser-TASK3-siRNA (2.1 nmol·day^{-1}) was administered i.n. during 7 days. Two control groups were used, administered respectively with PBS or Ser-NS-siRNA. *In situ* hybridization experiments revealed a reduction of TASK3 mRNA to 89.2 ± 2.2 % of control groups without affecting TASK3 expression in other brain regions, such as LC, or the expression of other genes expressed by 5-HT neurons, including TASK3-family related genes (**Supplementary Figure S3**). A small, but not significant reduction of the expression of 5-HT$_{1A}$ receptors was noted.

Given the small reduction of TASK3 expression, further experiments were performed with a higher daily dose (75 μg·day^{-1}; 5.25 nmol·day^{-1}) also administered during 7 days. New histological experiments showed that TASK3 mRNA was reduced to 83.3 ± 2.5 % of control (PBS) levels in the DR by this dose, without altering TASK3 expression in the hippocampal formation (CA1 and DG) or mPFC (**Figures 2b and c**). A more detailed analysis, in which dipped TASK3 hybridized sections were immunostained using a specific 5-HT neuron marker (TPH$_2$), showed a specific and greater reduction of TASK3 expression in 5-HT neurons along DR antero-posterior axis (**Figures 2a and b**). Western blot analysis confirmed these silencing at the protein level (**Figures 2d and e**).

Similarly, we studied the effect of i.n. Reb-TASK3-siRNA administration on LC TASK3 expression, using the same administration protocol (5.25 nmol·day^{-1} for 7 days). This evoked a selective reduction of TASK3 mRNA in the LC, without affecting TASK3 mRNA in other areas such as DR, CA1, DG and mPFC nor the expression of NET, α2-adrenoreceptor and, TASK1 and TREK1 potassium channels in LC (**Figures 2g and h, Supplementary Figure S4**). The co-localization analysis showed that Reb-TASK3-siRNA significantly reduced the

intracellular density of TASK3 mRNA in NE TH^+ neurons of LC (**Figures 2f and g**). Identical data were obtained in Western blot analysis (**Figures 2i and j**).

Neither treatment with Ser-TAK3-siRNA nor Reb-TASK3-siRNA induced neuronal degeneration, as evidenced by the same number of TPH_2^+ or TH^+ neurons in all experimental groups (**Supplementary Table S2**). In addition, we did not observe astrogliosis (GFAP) nor immune responses (Iba-1) (**Supplementary Figure S4**).

Seven-day treatment with Ser-TASK3-siRNA evoked neurochemical, behavioral and cellular changes predictive of antidepressant activity

First of all, for the purpose of evaluate the neurochemical impact of seven-day treatment with Ser-TASK3-siRNA (75 $\mu g \cdot day^{-1}$), we performed 5-HT microdialysis experiment in mPFC. Although there were no differences in baseline levels of 5-HT (**Supplementary Table S3**) nor veratridine-stimulated 5-HT values (data not shown), the reduction of TASK3 channel in 5-HT neurons diminished $5\text{-}HT_{1A}$ autoreceptor response as assessed by the dampened effect of 8-OH-DPAT 1 mg/kg i.p. administration on 5-HT release (**Figure 3a**). Moreover, Ser-TASK3-siRNA treatment enhanced the increase of extracellular 5-HT levels produced by acute administration of fluoxetine 20 mg/kg i.p. in the mPFC (**Figure 3b**).

Secondly, we used different rodent paradigms to assess the antidepressant-like behavior. The daily treatment with Ser-TASK3-siRNA (7 days, 75 $\mu g \cdot day^{-1}$) decreased the latency to feed in the NSFT and the immobility time in the TST compared to the control groups (**Figures 3c and d**), but there were no differences in the forced swimming test (data not shown), all paradigms predictive of the antidepressant effect in mice. In addition, TASK3 silencing in DR did not evoke significant changes in anxiety behavior versus PBS-treated mice using the MBT (**Figure 3e**).

Finally, mobilization of neural stem cells to create new granule neurons in the DG with novel functional synaptic contacts has been associated with antidepressant action.[27] Here, intranasal treatment with Ser-TASK3-siRNA (7 days, 75 $\mu g \cdot day^{-1}$) increased $Ki\text{-}67^+$ and DCX^+

cells in de DG of HPC in comparison with the control group (**Figures 3f and g**). Enlarge proliferative and neurogenic activity described co-occurred with a higher expression of neuroplasticity-associated genes, such as BDNF, ARC, and VEGF, in different subregions of the HPC (**Figures 3h and i**).

Seven-day treatment with Reb-TASK3-siRNA evoked a slight antidepressant-like effect

Next, with Reb-TASK3-siRNA molecule, we evaluated all the same key markers of antidepressant activity that we studied before with sertraline-conjugated siRNA. Here, we use an identical i.n. administration protocol of 75 $\mu g \cdot day^{-1}$ for one week. Reduction of TASK3 channel expression in the TH^+ neurons of LC did not modify the baseline of NE concentration nor enhanced the reboxetine effect in the mPFC (**Figure 4b**, **Supplementary Table S3**). Nevertheless, we observed a significant clonidine effect on cortical NE suggesting a lower functional $\alpha 2$-adrenoreceptor activity of TASK3 knockdown mice (**Figure 4a**).

Regarding to behavior paradigms, the selective reduction of TASK3 in NE neurons triggered a reduced immobility time in the TST, but did not produce significant differences in the NSFT and MBT compared with PBS-treated mice (**Figures 4c-e**).

Although any significant increase was observed neither in Ki-67^+ nor DCX^+ cells of TASK3 knockdown animals compared with PBS-treated mice, it could be appreciated a strong tendency with Ki-67 immunoreactivity (**Figures 4f and g**). Concerning neuroplasticity-associated genes, we stated an increase in BDNF, ARC and VEGF expression produced by Reb-TASK3-siRNA treatment versus control group (**Figures 4h and i**).

To sum up, reduction of TASK3 channel expression in the TH^+ neurons of LC did not produce antidepressant-like effects to the same extent as those observed when TASK3 expression is disrupted in 5-HT neurons.

Disturbed TASK3 expression in DR 5-HT neurons increase 5-HT release in response to a depression/stress-related paradigm

Considering the increased resilience of Ser-TASK3-siRNA-treated mice in the NSFT and TST and the putative connection between TASK3 channel and 5-HT_{1A} autoreceptor, as was evidenced by 8-OH-DPAT dampened effect, we next examined whether this effect was associated with a facilitated forebrain 5-HT release. We performed 5-HT *in vivo* microdialysis in mPFC simultaneously during the performance of the TST, as previously reported.[10] Even though no differences were observed in baseline levels of 5-HT between Ser-TASK3-siRNA and PBS treatment, TASK3 knockdown mice developed a twofold increase of 5-HT release when exposed to the TST stress (**Figure 5a**, **Supplementary Table S3**). Moreover, this facilitation of 5-HT neurotransmission was accompanied by a significance decreased immobility time in the TST versus PBS-treated mice (**Figure 5b**).

DISCUSSION

The present study shows that a siRNA-induced knockdown of TASK3 expression, a member of the two-pore potassium channels, in 5-HT or NE neurons, induces immediate and robust antidepressant-like responses in mice. We used a conjugated siRNA, in which naked siRNA molecules were covalently bound to the SSRI sertraline in order to selectively target 5-HT neurons after i.n. administration. As observed in previous studies,[8,9] this procedure resulted in the selective accumulation of sertraline-conjugated TASK3 siRNA molecules (Ser-TASK3-siRNA) in raphe 5-HT neurons. Here we extend this methodology to LC NE neurons by covalently binding siRNA molecules to the selective NET inhibitor reboxetine. As observed for the Ser-TASK3-siRNA, Reb-TASK3-siRNA molecules were identified in LC NE neurons after i.n. administration. Although the precise transport mechanism of the conjugated siRNA molecules to the cell bodies of 5-HT and NE neurons are still poorly known, it is possible that they undergo retrograde axonal transport via endosomes after their selective accumulation by the dense network of forebrain 5-HT or NE axons, as suggested by their association with the late endosomal marker Rab7.

The administration of the conjugated TASK3-siRNA resulted in a significant reduction of TASK3 mRNA in 5-HT and NE neurons, as evidenced by Western blots and *in situ* hybridization experiments, without altering TASK3 expression in other areas rich in TASK3, such as mPFC and HPC, much closer to the application site. The extent of the reduction in 5-HT neurons was slightly lower than that of other genes expressed by this neuronal group, such as the 5-HT_{1A} autoreceptor or SERT.[8,9] This difference is unlikely to be accounted for by the conjugated siRNA dose, since similar daily doses of all siRNAs were used, and may be related to the different turnover rates of the different mRNAs and proteins (e.g., a higher turnover rate would render TASK3 mRNA less sensitive to siRNA application).

Ser-TASK3-siRNA administration evoked significant changes in pre- and postsynaptic markers predictive of clinical antidepressant activity and reduced immobility in the TST and the latency to feed in the NSFT, used to assess antidepressant-like efficacy in rodents. Interestingly, the NSFT is sensitive to the sustained -but not acute- administration of monoamine reuptake inhibitors and to the acute effects of fast-acting antidepressant treatments, such as ketamine.[28,29] In contrast, Ser-TASK3-siRNA was ineffective in the MBT, which does not assess antidepressant-like activity, supporting the specificity of the observed effects in the TST and NSFT.

The antidepressant-like effects of Ser-TASK3-siRNA are likely mediated by an enhancement of forebrain serotonergic neurotransmission associated to a loss of function of 5-HT_{1A} autoreceptors, as indicated by the lesser ability of the selective 5-HT_{1A} receptor agonist 8-OH-DPAT to reduce 5-HT release in mPFC. This view is also supported by the greater increase of forebrain 5-HT release evoked by the SSRI fluoxetine in Ser-TASK3-siRNA-treated mice, after the attenuation of the 5-HT_{1A} autoreceptor-mediated negative feedback mechanism.[30,31] Similarly, the efficacy of the α2-adrenoceptor agonist clonidine to reduce NE release was lower in Reb-TASK3-siRNA-treated mice, suggesting a reduction of the sensitivity of α2-adrenoceptors. However, this was not accompanied by a greater effect of the selective NET inhibitor to augment extracellular NE in forebrain, as observed with combinations of NET inhibitors and α2-adrenoceptor antagonists.[32,33]

The reasons for the reduced sensitivity of 5-HT_{1A} autoreceptors and α2-adrenoceptors in mice treated with Ser-TASK3-siRNA or Reb-TASK3-siRNA are not fully understood but may be related to the likely increased membrane potential of 5-HT and NE neurons after partial TASK3 inactivation. Indeed, a lower number of constitutively-active TASK3 channels would increase membrane potential,[34] rendering 5-HT and NE neurons less sensitive to the hyperpolarizing actions of 5-HT_{1A} autoreceptors and α2-adrenoceptors. Alternatively, a membrane interaction between G protein-coupled inwardly-rectifying potassium (GIRK)

channels associated to monoamine autoreceptors and TASK3 channels may also be involved.

As observed after the selective local knockdown of 5-HT_{1A} autoreceptors,[10] mice treated with Ser-TASK3-siRNA exhibited a reduced immobility time in the TST. This behavioral effect was associated to an enhancement of 5-HT release only in mice treated with Ser-TASK3-siRNA. The similarity of the effects produced by 5-HT_{1A} and TASK3 knockdown in 5-HT neurons suggest a similar mechanism, reducing self-inhibitory inputs on 5-HT neurons, an effect resulting in an increased serotonergic activity in forebrain leading to increased stress resilience. This view is supported by reduced ability of 8-OH-DPAT to reduce 5-HT release and by the augmentation of fluoxetine effects in Ser-TASK3-siRNA-treated mice, as discussed above. Indeed, an increased expression/function of 5-HT_{1A} autoreceptors is associated with poor efficacy of antidepressant treatments and increased suicidal behavior,[35-38] and mice with a high expression of 5-HT_{1A} autoreceptor show a depressive-like phenotype.[37] It is likely that the reduction of TASK3 expression/function in 5-HT neurons can evoke opposite effects, as observed with 5-HT_{1A} autoreceptors.[8,10,39]

In parallel with the above presynaptic changes, Ser-TASK3-siRNA and Reb-TASK3-siRNA increased neurogenesis, as indicated by the increased number of Ki-67$^+$ and DCX$^+$ newborn cells in the hippocampal formation, as well as the increased expression of plasticity genes such as BDNF, ARC and VEGF. Interestingly these effects, which are produced by prolonged (e.g., 3-4 weeks) treatment with standard antidepressant,[40,41] required only 7-day treatments with Ser-TASK3-siRNA. The shorter time required for Ser-TASK3-siRNA -as compared to SSRI- to induce the above pre- and postsynaptic changes has been previously observed with a sertraline-conjugated siRNA directed against SERT.[9] These temporal differences likely reflect the greater efficacy of RNAi strategies to modulate neuronal function, as compared to standard pharmacological treatments.

The behavioral and neurochemical effects evoked by Reb-TASK3-siRNA were smaller than those evoked by Ser-TASK3-siRNA, and in some instances, they did not reach statistical significance (see Figs. 3 and 4 for comparison). This difference may be explained by at least two different factors. On the one hand, a lesser ability of Reb-TASK3-siRNA to reduce the expression of TASK3 in NE neurons of LC, hence, despite a similar overall reduction of TASK3 mRNA in LC and DR, the reduction of double-labeled cells (TH and TASK3) in LC was lower than that in the DR. On the other hand, 5-HT and NE play differential roles in the treatment of MDD, with 5-HT having a crucial role in resilience to stress, a key factor in the behavioral test used in he present study (TST and NSFT). Indeed, behavioral tests assessing antidepressant-like efficacy.

In summary, the present study shows that the selective reduction of TASK3 expression in 5-HT or NE neurons evokes antidepressant-like effects, which are more marked when targeting raphe 5-HT neurons. One-week treatments with Ser-TASK3-siRNA evoked behavioral and neurobiological changes predictive of clinical antidepressant activity similar to those produced by more prolonged SSRI treatments (e.g. 3-4 weeks). These effects are possibly mediated by an enhancement of the membrane potential of monoamine neurons due to the reduced expression of constitutively active TASK3 channels, which would lead to an increased excitation/inhibition ratio and an enhanced response to excitatory inputs evoked by stress, thus producing an overall increase of monoamine neurotransmission. Further, the extension of neuronal targeting by conjugated siRNA molecules to 5-HT and NE neurons after intranasal administration supports the validity of the present approach as a potential new strategy for a faster and more effective treatment of MDD.

Acknowledgments

We thank María Calvo, Elisenda Coll and Anna Bosch for outstanding technical support in the Confocal microscopy unit (CCiT-UB); and Mireia Galofré and Letizia Campa for their outstanding technical assistance.

Funding

This work was supported by grants SAF2009/08460 (F.A.), SAF2013/48586R (J.M.), SAF2015-68346-P (F.A.) and Retos-Colaboración Subprogram RTC-2014-2812-1 (A.B.), Ministry of Economy and Competitiveness (MINECO) and European Regional Development Fund (ERDF); UE; PI13/01390, Instituto de Salud Carlos III, co-financed by ERDF (A.B.); Basque Government (IT616-13) and the ERDF funds (J.M.); 20003 NARSAD Independent Investigator (A.B.); and Centro de Investigación Biomédica en Red de Salud Mental (CIBERSAM). A.F-C. is a recipient of a fellowship from Spanish Ministry of Education, Culture and Sport.

Conflict of interest

F.A. has received consulting honoraria on antidepressant drugs from Lundbeck and he has been PI of grants from Lundbeck. He is also member of the scientific advisory board of Neurolixis Inc. A.B. and F.A. are authors of the patent WO/2011/131693 for the siRNA and ASO (antisense oligonucleotides) molecules and the targeting approach related to this work. A.M. is board members of nLife Therapeutics S.L. The rest of authors declare no competing financial interest.

References

1. Murray CJ, Vos T, Lozano R, Naghavi M, Flaxman AD Michaud C et al. Disability-adjusted life years (DALYs) for 291 diseases and injuries in 21 regions, 1990-2010: a systematic analysis for the Global Burden of Disease Study 2010. *Lancet* 2012; **380**: 2197-2223

2. Whiteford HA, Degenhardt L, Rehm J, Baxter AJ, Ferrari AJ, Erskine HE et al. Global burden of disease attributable to mental and substance use disorders: findings from the Global Burden of Disease Study 2010. *Lancet* 2013; **382**: 1575-1586

3. Trivedi MH, Rush AJ, Wisniewski SR, Nierenberg AA, Warden D, Ritz L et al. Evaluation of outcomes with citalopram for depression using measurement-based care in STAR*D: implications for clinical practice. *Am J Psychiatry* 2006; **163**: 28-40

4. Trivedi MH, Fava M, Wisniewski SR, Thase ME, Quitkin F, Warden D et al. Medication augmentation after the failure of SSRIs for depression. *N Engl J Med* 2006; **354**: 1243-1252

5. Rush AJ, Trivedi MH, Wisniewski SR, Nierenberg AA, Stewart JW, Warden D et al. Acute and longer-term outcomes in depressed outpatients requiring one or several treatment steps: a STAR*D report. *Am J Psychiatry* 2006; **163**: 1905-1917

6. Artigas F, Bortolozzi A, Celada P (2016) Can we increase speed and efficacy of antidepressant treatments? Part I: General aspects and monoamine-based strategies. *Eur Neuropsychopharmacol* (in press)

7. Artigas F, Celada P, Bortolozzi A. (2016) Can we increase speed and efficacy of antidepressant treatments? Part II: Glutamatergic and RNA interference strategies. *Eur Neuropsychopharmacol* (in press)

8. Bortolozzi A, Castañé A, Semakova J, Santana N, Alvarado G, Cortés R et al. Selective siRNA-mediated suppression of 5-HT1A autoreceptors evokes strong anti-depressant-like effects. *Mol. Psychiatry* 2012; **17**: 612-623

9. Ferrés-Coy A, Galofré M, Pilar-Cuéllar F, Vidal R, Paz V, Ruiz-Bronchal E et al. Therapeutic antidepressant potential of a conjugated siRNA silencing the serotonin transporter after intranasal administration. *Mol. Psychiatry* 2016; **21**: 328-338
10. Ferrés-Coy A, Santana N, Castañé A, Cortés R, Carmona MC, Toth M et al. Acute 5-HT_{1A} autoreceptor knockdown increases antidepressant responses and serotonin release in stressful conditions. *Psychopharmacology (Berl)* 2013; **225**: 61-74
11. Ferrés-Coy A, Pilar-Cuellar F, Vidal R, Paz V, Masana M, Cortés R et al. RNAi-mediated serotonin transporter suppression rapidly increases serotonergic neurotransmission and hippocampal neurogenesis. *Transl Psychiatry* 2013; **15**: 3:e211
12. Rajan S, Wischmeyer E, Xin Liu G, Preisig-Müller R, Daut J, Karschin A et al. TASK-3, a novel tandem pore domain acid-sensitive K+ channel. An extracellular histiding as pH sensor. *J Biol Chem* 2000; **275**: 16650-16657
13. Gotter AL, Santarelli VP, Doran SM, Tannenbaum PL, Kraus RL, Rosahl TW et al. TASK-3 as a potential antidepressant target. *Brain Res* 2011; **1416**: 69-79
14. Borsotto M, Veyssiere J, Moha Ou Maati H, Devader C, Mazella J, Heurteaux C. argeting two-pore domain K(+) channels TREK-1 and TASK-3 for the treatment of depression: a new therapeutic concept. *Br J Pharmacol* 2015; **172**: 771-784
15. Karschin C, Wischmeyer E, Preisig-Müller R, Rajan S, Derst C, Grzeschik KH et al. Expression pattern in brain of TASK-1, TASK-3, and a tandem pore domain K(+) channel subunit, TASK-5, associated with the central auditory nervous system. *Mol Cell Neurosci* 2001; **18**: 632-648
16. Talley EM, Solorzano G, Lei Q, Kim D, Bayliss DA. Cns distribution of members of the two-pore-domain (KCNK) potassium channel family. *J Neurosci* 2001; **21**: 7491-7505
17. Meadows HJ and Randall AD. Functional characterisation of human TASK-3, an acid-sensitive two-pore domain potassium channel. *Neuropharmacology* 2001; **40**: 551-559

18. Franklin KBJ, Paxinos G. *The Mouse Brain in Stereotaxic Coordinates.* Academic Press: New York, USA, 2008
19. Hermanson, G.T., Chapter 6 - Heterobifunctional Crosslinkers, in Bioconjugate Techniques (Third edition). 2013, Academic Press: Boston. p. 299-339
20. Mateo Y, Meana JJ. Determination of the somatodendritic alpha2-adrenoceptor subtype located in rat locus coeruleus that modulates cortical noradrenaline release *in vivo*. *Eur J Pharmacol* 1999; **379**: 53-57
21. Mateo Y, Fernández-Pastor B, Meana JJ. Acute and chronic effects of desipramine and clorgyline on alpha(2)-adrenoceptors regulating noradrenergic transmission in the rat brain: a dual-probe microdialysis study. *Br J Pharmacol* 2001; **133**: 1362-1370
22. Alba-Delagado C, Borges G, Sánchez-Blázquez P, Ortega JE, Horrillo I, Mico JA et al. The function of alpha-2-adrenoceptors in the rat locus coeruleus is preserved in the chronic constriction injury model of neuropathic pain. *Psychopharmacology (Berl)* 2012; **221**: 53-65
23. Ortega JE, Katner J, Davis R, Wade M, Nisenbaum L, Nomikos GG, et al. Modulation of neurotransmitter release in orexin/hypocretin-2 receptor knockout mice: a microdialysis study. *J Neurosci Res* 2012; **90**: 588-596.
24. Samuels BA, Hen R. Novelty-suppressed feeding in the mouse. In Gould TD (ed). *Mood and Anxiety Related Phenotypes in Mice: Characterization Using Behavioral Test, Volume II.* Springer: New York, USA, 2011, pp 107-121
25. Torres GE, Gainetdinov RR, Caron MG. Plasma membrane monoamine transporters: structure, regulation and function. *Nat Rev Neurosci* 2003; **4**: 13-25
26. Gould GG, Pardon MC, Morilak DA, Frazer A. Regulatory effects of reboxetine treatment alone, or following paroxetine treatment, on brain noradrenergic and serotonergic systems. *Neuropsychopharmacology* 2003; **28**: 1633-1641
27. Zhao C, Deng W, Gage FH. Mechanisms and functional implications of adult neurogenesis. *Cell* 2008; **132**: 645-660

28. Wang JW, David DJ, Monckton JE, Battaglia F, Hen R. Chronic fluoxetine stimulates maturation and synaptic plasticity of adult-born hippocampal granule cells. *J Neurosci* 2008; **28**: 1374-1384

29. Brachman RA, McGowan JC, Perusini JN, Lim SC, Pham TH, Faye C et al. Ketamine as a Prophylactic Against Stress-Induced Depressive-like Behavior. *Biol Psychiatry* 2016; **79**: 776-786

30. Artigas F, Romero L, de Montigny C, Blier P. Acceleration of the effect of selected antidepressant drugs in major depression by 5-HT1A antagonists. *Trends Neurosci* 1996; **19**: 378-83

31. Hervás I, Artigas F. Effect of fluoxetine on extracellular 5-hydroxytryptamine in rat brain. Role of 5-HT autoreceptors. *Eur J Pharmacol* 1998; **358**: 9-18

32. Ortega JE, Fernández-Pastor B, Callado LF, Meana JJ. In vivo potentiation of reboxetine and citalopram effect on extracellular noradrenaline in rat brain by α2-adrenoceptor antagonism. *Eur Neuropsychopharmacol* 2010; **20**: 813-822

33. Mateo Y, Pineda J, Meana JJ. Somatodendritic alpha2-adrenoceptors in the locus coeruleus are involved in the in vivo modulation of cortical noradrenaline release by the antidepressant desipramine. *J Neurochem* 1998; **71**: 790-798

34. Washburn CP, Sirois JE, Talley EM, Guyenet PG, Bayliss DA. Serotonergic raphe neurons express TASK channel transcripts and a TASK-like pH- and halothane-sensitive K+ conductance. *J Neurosci* 2002; **22**: 1256-1265

35. Neff CD, Abkevich V, Packer JC, Chen Y, Potter J, Riley R et al. Evidence for HTR1A and LHPP as interacting genetic risk factors in major depression. *Mol Psychiatry* 2009; **14**: 621-630

36. Stockmeier CA, Shapiro LA, Dilley GE, Kolli TN, Friedman L, Rajkowska G. Increase in serotonin-1A autoreceptors in the midbrain of suicide victims with major depression-postmortem evidence for decreased serotonin activity. *J Neurosci* 1998; **18**: 7394-7401

37. Lemonde S, Turecki G, Bakish D, Du L, Hrdina PD, Bown CD et al. Impaired repression at a 5-hydroxytryptamine 1A receptor gene polymorphism associated with major depression and suicide. *J Neurosci* 2003; **23**: 8788-8799

38. Lemonde S, Du L, Bakish D, Hrdina P, Albert PR. Association of the C(-1019)G 5-HT1A functional promoter polymorphism with antidepressant response. *Int J Neuropsychopharmacol* 2004; **7**: 501-506

39. Richardson-Jones JW, Craige CP, Guiard BP, Stephen A, Metzger KL, Kung HF et al. 5-HT1A autoreceptor levels determine vulnerability to stress and response to antidepressants. *Neuron* 2010; **65**: 40-52

40. Dranovsky A and Hen R. Hippocampal neurogenesis: regulation by stress and antidepressants. *Biol Psychiatry* 2006; **59**: 1136-1143

41. David DJ, Samuels BA, Rainer Q, Wang JW, Marsteller D, Mendez I et al. Neurogenesis-dependent and -independent effects of fluoxetine in an animal model of anxiety/depression. *Neuron* 2009; **62**: 479-493

Figure legends

Figure 1 Selective accumulation of sertraline- or reboxetine conjugated nonsense siRNA (Ser-NS-siRNA or Reb-NS-siRNA, respectively) in late endosomal vesicles of TPH_2-positive serotonin or TH-positive norepinephrine neurons after intranasal administration. Mice were intranasally administered with alexa488-PBS (A488-PBS), alexa488-labeled nonsense siRNA (A488-NS-siRNA) or alexa488-labeled Ser- or Reb-NS-siRNA (A488-Ser-NS-siRNA or A488-Reb-NS-siRNA) at 30 $\mu g \cdot day^{-1}$ during 4 days, and were killed 6 h post-administration (n=2 mice/group). **(a-b)** Confocal images showing co-localization (yellow) of A488-Ser-NS-siRNA or A488-Reb-NS-siRNA in dorsal raphe (DR) 5-HT neurons (TPH_2-positive, red) or locus coeruleus (LC) NA neurons (TH-positive, red), respectively, identified with white arrowheads. Cell nuclei were stained with Dapi (blue) **(c-d)** Confocal images showing co-localization (yellow) between Rab7 (late endosome marker, red) with A488-Ser-NS-siRNA or A488-Reb-NS-siRNA (green) in DR or LC neurons, respectively. Vesicles co-localizing are marked with white arrowheads. Cell nuclei were stained with Dapi (blue). Scale bar = 10 μm.

Figure 2 Intranasal sertraline- or reboxetine-conjugated TASK3-siRNA (Ser-TASK3-siRNA or Reb-TASK3-siRNA) treatment reduced TASK3 expression in serotonin neurons of the dorsal raphe (DR) or norepinephrine neurons of the locus coeruleus (LC), respectively. One group of mice received intranasally PBS or Ser-TASK3-siRNA at 75 $\mu g \cdot day^{-1}$ during 7 days. Another group received intranasally PBS or Reb-TASK3-siRNA at 75 $\mu g \cdot day^{-1}$ during 7 days. **(a)** Photomicrographs showing TPH_2^+ neurons expressing TASK3 mRNA (^{33}P-oligonucleotide silver grains) in DR at two AP coordinates: -4.24 to -4.48 mm and -4.48 to -4.72 mm of PBS- and Ser-TASK3-siRNA-treated mice. Scale bar = 10 μm. **(b)** *In situ* hybridization showed that Ser-TASK3-siRNA produce a TASK3 mRNA silencing in the DR (n = 4-6 mice/group). Student's t-test showed an effect of group ($P<0.05$). **(c)** Dipping analysis revealed a significant effect on the percentage of TPH_2^+ neurons expressing TASK3 mRNA

at -4.48 to -4.72 mm coordinates (n = 4-6 mice/group). Two-way ANOVA showed an effect of treatment ($F_{1,14}$ = 14.72, P<0.01). **(d)** Dipping analysis showed a reduction of intracellular TASK3 mRNA density in TPH_2^+ neurons at -4.24 to -4.48 mm coordinates (n = 4-6 mice/group). Two-way ANOVA showed an effect of treatment ($F_{1,14}$ = 17.86, P<0.001). **(e)** Effect of Ser-TASK3-siRNA on TASK3 mRNA in different forebrain areas (n = 6 mice/group). **(f)** Western blot analysis of mPFC, HPC and DR extracts showing TASK3 and actin protein levels. Actin is used as loading control. **(g)** Relative quantification of TASK3 protein expression obtained by normalizing TASK3 by actin protein amount (n = 5-7 mice/group). Student's t-test showed an effect of group (P<0.05) in DR. **(h)** Photomicrographs showing TH^+ neurons expressing TASK3 mRNA (^{33}P-oligonucleotide silver grains) in LC at two AP coordinates: -5.52 to -5.68 mm and -5.68 to -5.80 mm of PBS- and Reb-TASK3-siRNA-treated mice. Scale bar = 10 μm. **(i)** Intranasal Reb-TASK3-siRNA treatment decreased TASK3 mRNA levels in LC (n = 8 mice/group). Student's t-test showed an effect of group (P<0.05). **(j)** Dipping analysis revealed significant reduction on percentage of TH^+ neurons expressing TASK3 mRNA (n = 4-6 mice/group). Two-way ANOVA showed an effect of treatment ($F_{1,17}$ = 17.98, P<0.001). **(k)** Dipping analysis showed a reduction of intracellular TASK3 mRNA density in TH^+ neurons at two AP coordinates studied (n = 4-6 mice/group). Two-way ANOVA showed an effect of treatment ($F_{1,16}$ = 30.44, P<0.0001). **(l)** Effect of Reb-TASK3-siRNA on TASK3 mRNA in different forebrain areas (n = 4-6 mice/group). **(m)** Western blot analysis of mPFC, HPC and LC extracts showing TASK3 and actin protein levels. Actin is used as loading control. **(n)** Relative quantification of TASK3 protein expression obtained by normalizing TASK3 by actin protein amount (n = 6 mice/group). Student's t-test showed an effect of group (P<0.05) in LC. *P<0.05, versus PBS-treated mice; ^P<0.05, ^^P<0.01, ^^^P<0.001 versus PBS-treated mice. Data are mean ± s.e.m.

Figure 3 Sertraline-conjugated TASK3-siRNA (Ser-TASK3-siRNA) induced neurochemical, behavioral and cellular variables predictive of clinical antidepressant activity. Mice received

intranasally PBS or Ser-TASK3-siRNA at 75 μg·day^{-1} during 7 days. **(a)** Ser-TASK3-siRNA treatment reduced the effect of serotonin-1A (5-HT$_{1A}$) receptor 8-OH-DPAT agonist (1 mg·kg^{-1} i.p.) on extracellular serotonin (5-HT) levels in mPFC (n = 9-10 mice/group). Two-way ANOVA showed an effect of treatment ($F_{1,17}$ = 13.4, P<0.01), time ($F_{11,187}$ = 7.692, P<0.0001) and interaction ($F_{11,187}$ = 3.44, P<0.001). **(b)** Fluoxetine (20 mg·kg^{-1} i.p.) increased the extracellular 5-HT concentration significantly more in Ser-TASK3-siRNA than in PBS-treated mice (n = 6 mice/group). Two-way ANOVA showed an effect of treatment ($F_{1,10}$ = 10.90, P<0.01), time ($F_{15,150}$ = 6.965, P<0.0001) and interaction ($F_{15,150}$ = 2.104, P<0.05). **(c)** Ser-TASK3-siRNA treated mice displayed a reduced immobility in the tail suspension test (TST) (n = 11 mice/group). Student's t-test showed an effect of group (P<0.05). **(d)** Effect on novelty suppressed feeding test (NSFT) and survival analysis of NSFT data (n = 19-25 mice/group). Student's t-test showed an effect of group (P<0.01) and log-rank (Mantel-Cox) test showed significant differences between both survival curves (P<0.01). **(e)** PBS and Ser-TASK3-siRNA mice behaved similarly in the marble burying test (MBT) (n= 13-14 mice/group). **(f)** Representative images of Ki-67- and DCX-positive cells in the dentate gyrus (DG) of Ser-TASK3-siRNA or PBS-treated mice. Scale bar = 100 μm. **(g)** Ser-TASK3-siRNA significantly increased Ki-67^{+} and DCX^{+} cells compared to the PBS group (n = 5-7 mice/group). Student's t-test showed an effect of group (P<0.05). **(h)** Representative autoradiograms showing BDNF, ARC and VEGF mRNA expression in the hippocampus of control and TASK3 knockdown mice. Scale bar = 100 μm. **(i)** Bar graphs showing BDNF, ARC and VEGF mRNA expression in different hippocampal subfields including CA1, CA2, CA3 and DG (n = 5-6 mice/group). Two-way ANOVA showed an effect of treatment ($F_{1,40}$ = 55.48, P<0.0001), area ($F_{3,40}$ = 4.019, P<0.05) and interaction ($F_{3,40}$ = 4.022, P<0.05) for BDNF mRNA, an effect of treatment ($F_{1,32}$ = 44.15, P<0.0001) for ARC mRNA and an effect of treatment ($F_{1,36}$ = 30.35, P<0.0001) for VEGF mRNA. *P<0.05, **P<0.01, ****P<0.0001 versus PBS-treated mice. Data are mean ± s.e.m.

Figure 4 Mild antidepressant-like effects produced by reboxetine-conjugated TASK3-siRNA (Reb-TASK3-siRNA). Mice were treated intranasally with a daily dose of PBS or Reb-TASK3-siRNA at 75 $\mu g \cdot day^{-1}$ during an entire week. **(a)** Reb-TASK3-siRNA treatment reduced the effect of $\alpha 2$-adrenoreceptor clonidine agonist (0.3 $mg \cdot kg^{-1}$ i.p.) on extracellular noradrenalin (NA) levels in mPFC (n = 9-10 mice/group). Two-way ANOVA showed an effect of treatment ($F_{1,17}$ = 10.12, P<0.01), time ($F_{11,187}$ = 4.466, P<0.0001) and interaction ($F_{11,187}$ = 2.471, P<0.01). **(b)** Reboxetine (20 $mg \cdot kg^{-1}$ i.p.) increased the extracellular NA similarly in both experimental groups (PBS and Reb-TASK3-siRNA) (n = 8 mice/group). **(c)** Reb-TASK3-siRNA treated mice displayed a reduced immobility in the tail suspension test (TST) versus PBS-treated mice (n = 9-11 mice/group). Student's t-test showed an effect of group (P<0.01). **(d)** Both PBS and Reb-TASK3-siRNA mice behaved similarly in the novelty suppressed feeding test (NSFT) (n = 18 mice/group). **(e)** No anxiety-related effects were observer on the marble burying test (MBT) (n= 19 mice/group). **(f)** Representative images of Ki-67- and DCX-positive cells in the dentate gyrus (DG) of Reb-TASK3-siRNA or PBS-treated mice. Scale bar = 100 μm. **(g)** Reb-TASK3-siRNA did not induce any increase in proliferation ($Ki\text{-}67^+$ cells) or neurogenesis (DCX^+ cells) in DG compared to the PBS group (n = 6 mice/group). **(h)** Representative autoradiograms showing BDNF, ARC and VEGF mRNA expression in the hippocampus of control and TASK3 knockdown mice. Scale bar = 100 μm. **(i)** Bar graphs showing BDNF, ARC and VEGF mRNA expression in different hippocampal subfields including CA1, CA2, CA3 and DG (n = 4-5 mice/group). Two-way ANOVA showed an effect of treatment ($F_{1,28}$ = 15.1, P<0.001) for BDNF mRNA an effect of treatment ($F_{1,28}$ = 27.99, P<0.0001) for ARC mRNA. ^P<0.05, ^^P<0.01 versus PBS-treated mice. Data are mean ± s.e.m.

Figure 5 Sertraline-conjugated TASK3-siRNA (Ser-TASK3-siRNA) treatment in mice facilitated serotonin (5-HT) release in mPFC under a depression-related stress paradigm. Mice received intranasally PBS or Ser-TASK3-siRNA at 75 $\mu g \cdot day^{-1}$ during 7 days. **(a)** During

a stressful situation induced by the tail suspension test (TST), TASK3 knockdown mice allowed a larger increase of extracellular 5-HT in mPFC than PBS-treated mice (n =8-9 mice/group). Two-way ANOVA showed an effect of time ($F_{13,195}$ = 2.928, P<0.001). **(b)** Simultaneously, Ser-TASK3-siRNA-treated mice displayed a reduced immobility in the TST (n =8-9 mice/group). Student's t-test showed an effect of group (P<0.01). *P<0.05, **P<0.01 versus PBS-treated mice. Data are mean ± s.e.m.

33

Figure 1

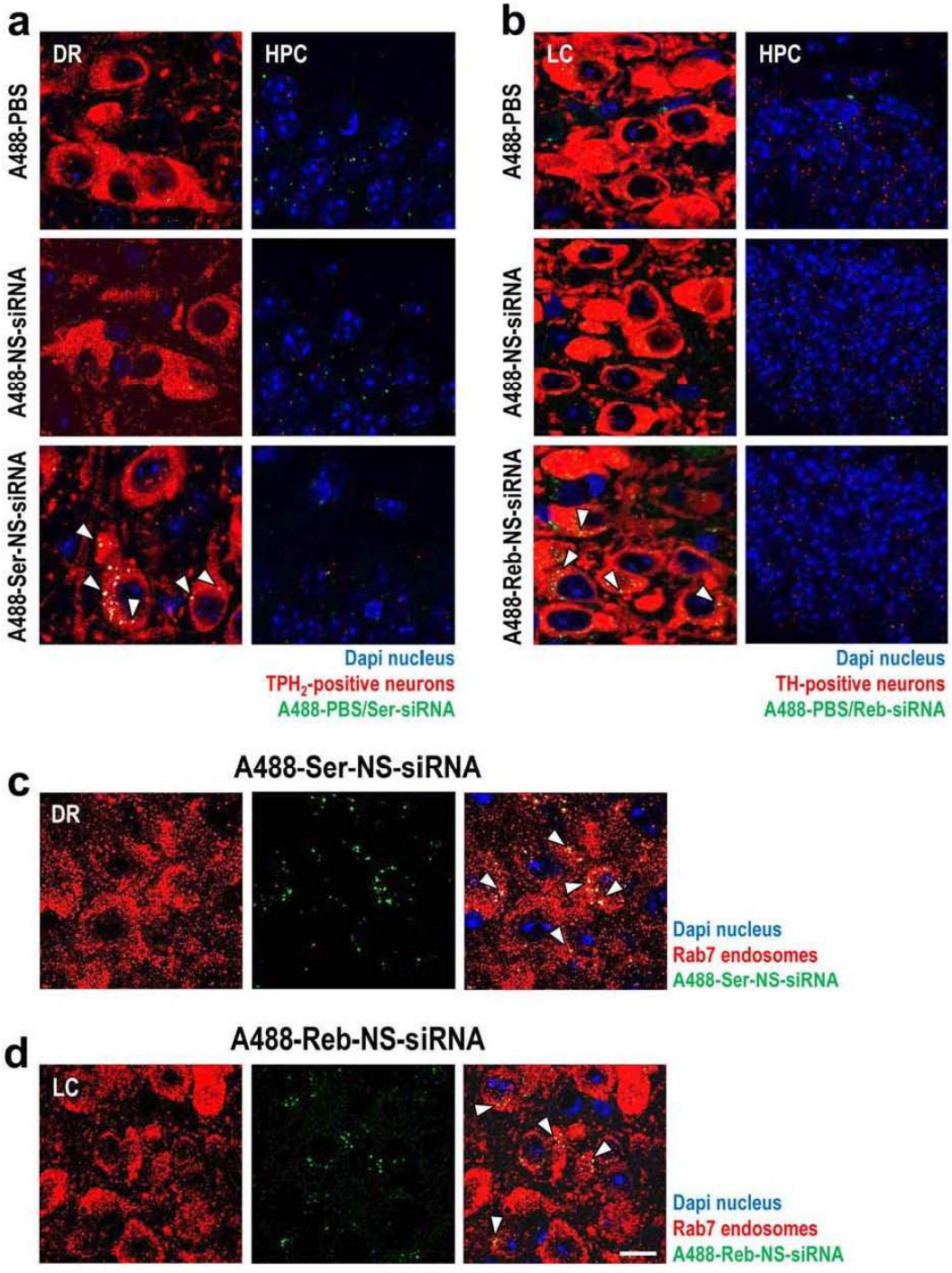
a
DR
HPC
A488-PBS
A488-NS-siRNA
A488-Ser-NS-siRNA
Dapi nucleus
TPH2-positive neurons
A488-PBS/Ser-siRNA
b
LC
HPC
A488-PBS
A488-NS-siRNA
A488-Reb-NS-siRNA
Dapi nucleus
TH-positive neurons
A488-PBS/Reb-siRNA
c
A488-Ser-NS-siRNA
DR
Dapi nucleus
Rab7 endosomes
A488-Ser-NS-siRNA
d
A488-Reb-NS-siRNA
LC
Dapi nucleus
Rab7 endosomes
A488-Reb-NS-siRNA

Figure 2

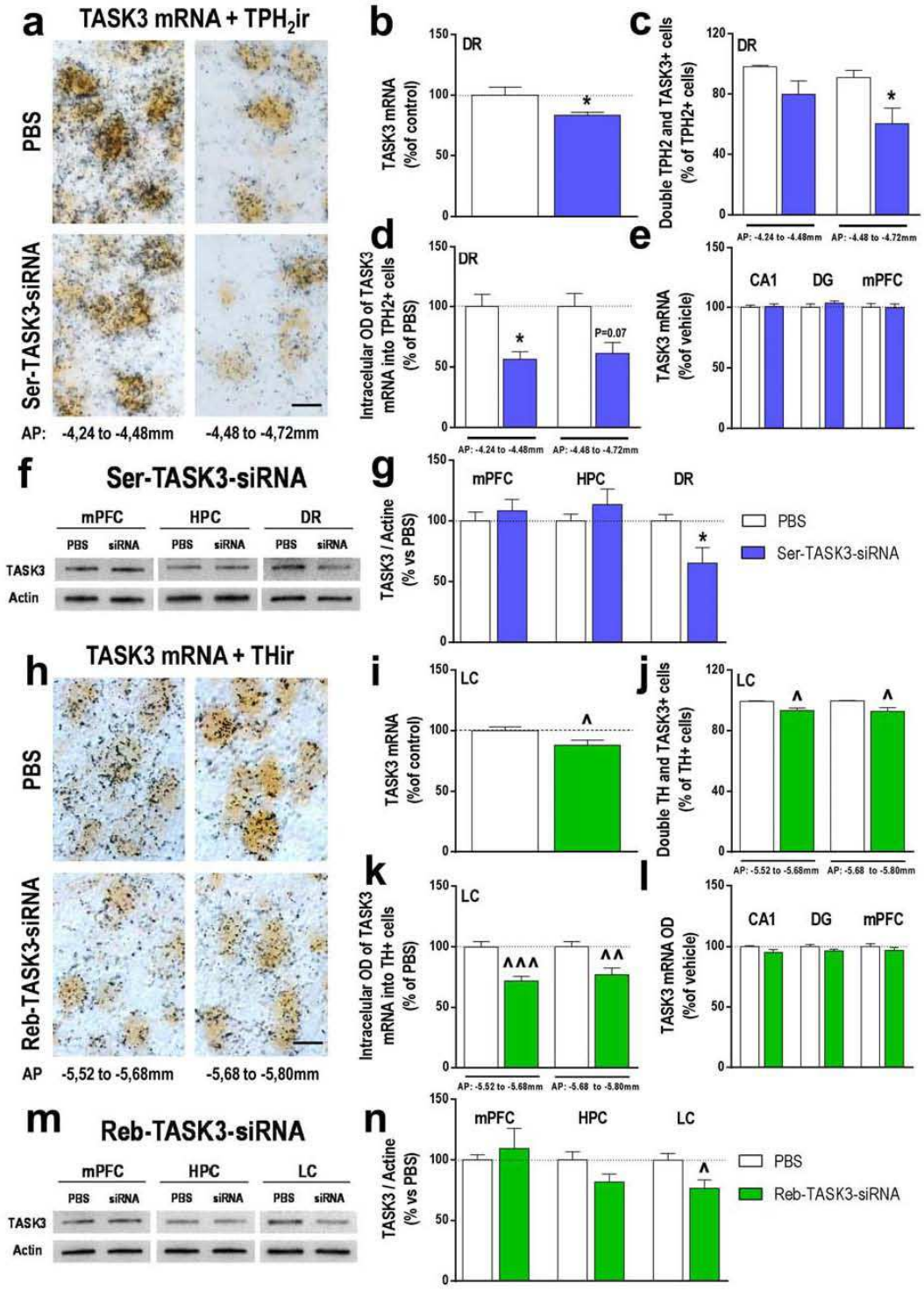
a
TASK3 mRNA + TPH2ir
PBS
Ser-TASK3-siRNA
AP: -4,24 to -4,48mm
-4,48 to -4,72mm
b
DR
TASK3 mRNA (%of control)
c
DR
Double TPH2 and TASK3+ cells (% of TPH2+ cells)
AP: -4.24 to -4.48mm
AP: -4.48 to -4.72mm
d
DR
Intracelular OD of TASK3 mRNA into TPH2+ cells (% of PBS)
P=0.07
e
CA1
DG
mPFC
TASK3 mRNA (%of vehicle)
f
Ser-TASK3-siRNA
mPFC
HPC
DR
PBS
siRNA
TASK3
Actin
g
mPFC
HPC
DR
TASK3 / Actine (% vs PBS)
PBS
Ser-TASK3-siRNA
h
TASK3 mRNA + THir
PBS
Reb-TASK3-siRNA
AP -5,52 to -5,68mm
-5,68 to -5,80mm
i
LC
TASK3 mRNA (%of control)
j
LC
Double TH and TASK3+ cells (% of TH+ cells)
AP: -5.52 to -5.68mm
AP: -5.68 to -5.80mm
k
LC
Intracelular OD of TASK3 mRNA into TH+ cells (% of PBS)
l
CA1
DG
mPFC
TASK3 mRNA OD (%of vehicle)
m
Reb-TASK3-siRNA
mPFC
HPC
LC
PBS
siRNA
TASK3
Actin
n
mPFC
HPC
LC
TASK3 / Actine (% vs PBS)
PBS
Reb-TASK3-siRNA

Figure 3

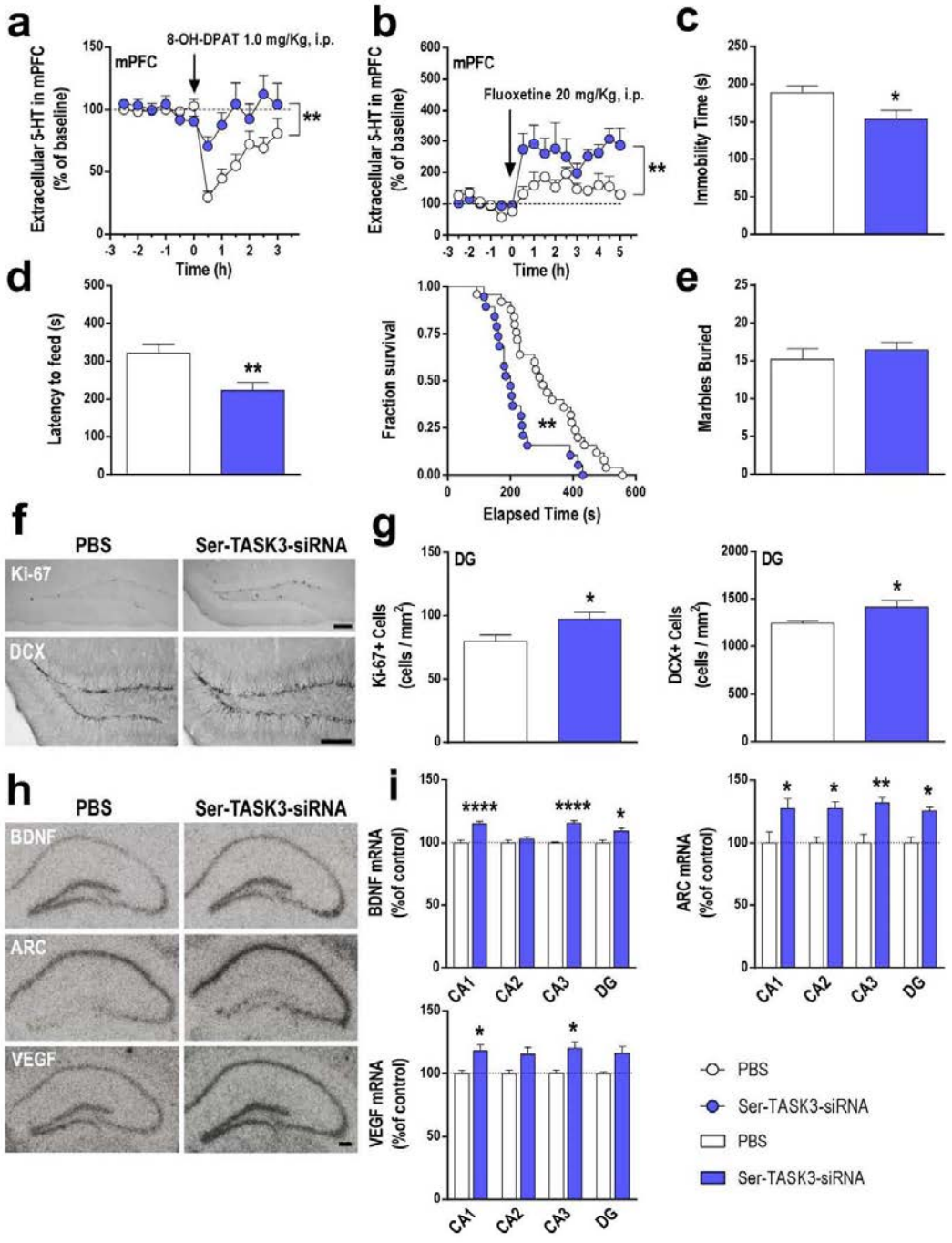
a
8-OH-DPAT 1.0 mg/Kg, i.p.
mPFC
Extracellular 5-HT in mPFC (% of baseline)
Time (h)
**
b
mPFC
Fluoxetine 20 mg/Kg, i.p.
Extracellular 5-HT in mPFC (% of baseline)
Time (h)
**
c
Immobility Time (s)
*
d
Latency to feed (s)
**
Fraction survival
**
Elapsed Time (s)
e
Marbles Buried
f
PBS
Ser-TASK3-siRNA
Ki-67
DCX
g
DG
Ki-67+ Cells (cells / mm2)
DG
DCX+ Cells (cells / mm2)
h
PBS
Ser-TASK3-siRNA
BDNF
ARC
VEGF
i
BDNF mRNA (%of control)
ARC mRNA (%of control)
VEGF mRNA (%of control)
CA1
CA2
CA3
DG
PBS
Ser-TASK3-siRNA
PBS
Ser-TASK3-siRNA

Figure 4

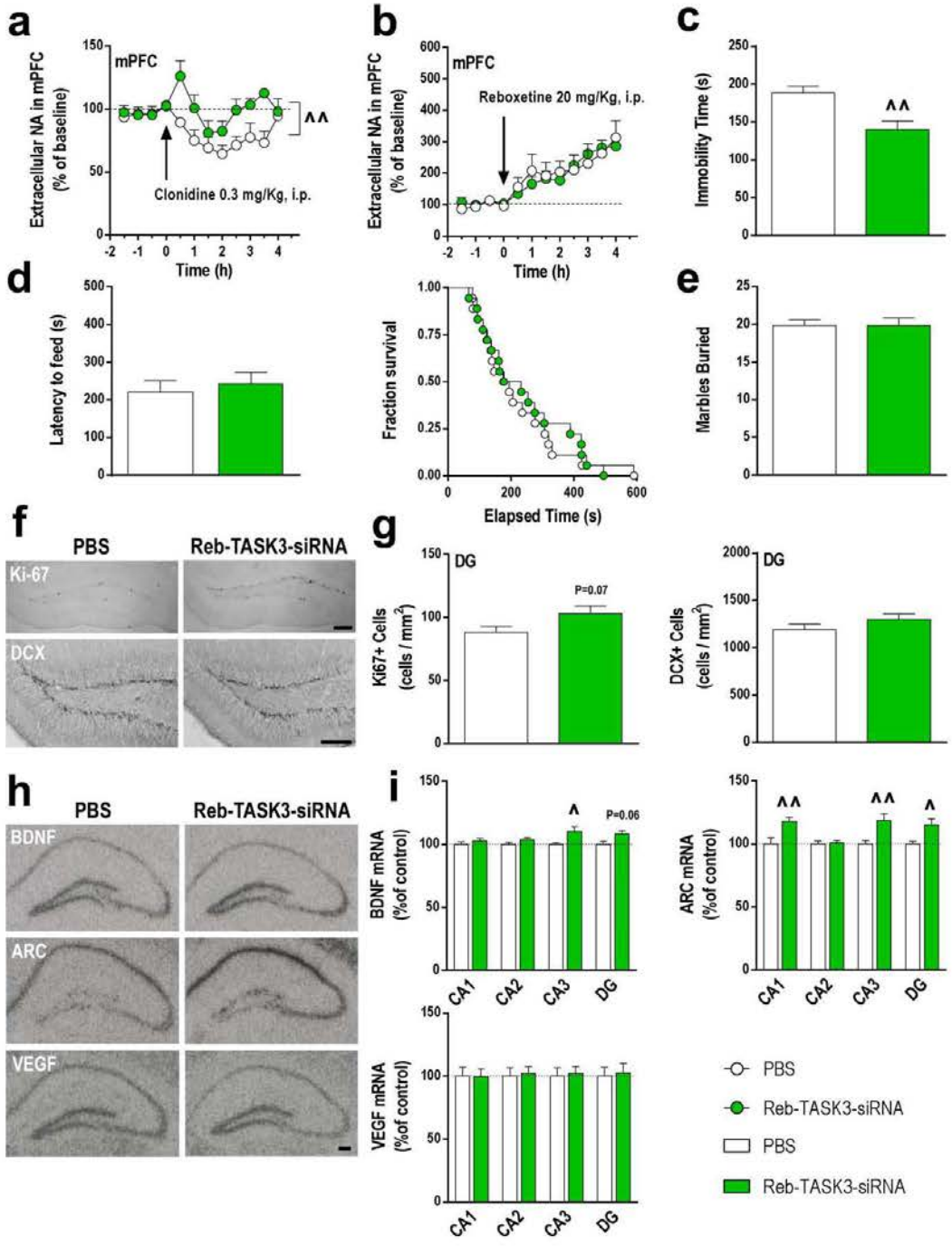
a
mPFC
Extracellular NA in mPFC (% of baseline)
Clonidine 0.3 mg/Kg, i.p.
Time (h)
^^
b
mPFC
Reboxetine 20 mg/Kg, i.p.
Extracellular NA in mPFC (% of baseline)
Time (h)
c
Immobility Time (s)
^^
d
Latency to feed (s)
Fraction survival
Elapsed Time (s)
e
Marbles Buried
f
PBS
Reb-TASK3-siRNA
Ki-67
DCX
g
DG
Ki67+ Cells (cells / mm2)
P=0.07
DG
DCX+ Cells (cells / mm2)
h
PBS
Reb-TASK3-siRNA
BDNF
ARC
VEGF
i
BDNF mRNA (%of control)
^
P=0.06
ARC mRNA (%of control)
^^
^^
^
VEGF mRNA (%of control)
CA1
CA2
CA3
DG
PBS
Reb-TASK3-siRNA
PBS
Reb-TASK3-siRNA

37

Figure 5

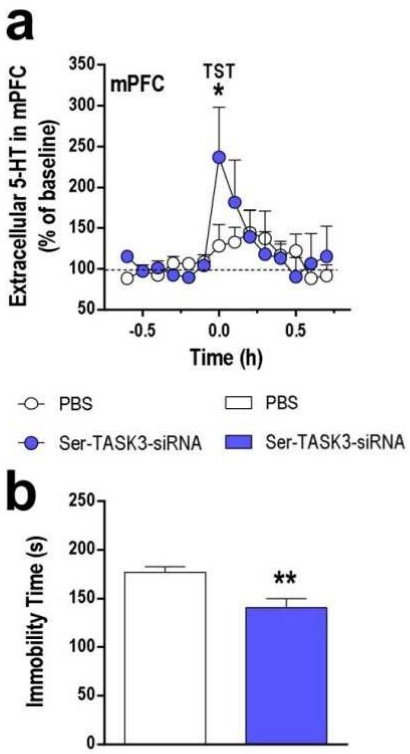
a
mPFC
TST
*
Extracellular 5-HT in mPFC (% of baseline)
350
300
250
200
150
100
50
-0.5
0.0
0.5
Time (h)
PBS
Ser-TASK3-siRNA
PBS
Ser-TASK3-siRNA
b
Immobility Time (s)
250
200
150
100
50
0
**

Supplementary Information for

Selective knockdown of TASK3 potassium channel in monoamine neurons evoke robust antidepressant-like effects

Albert Ferrés-Coy[1,2,3], Neus Fullana[1,2,3], Jorge E Ortega[3,5], Esther Ruiz-Bronchal[1,2,3], Verónica Paz[1,2,3], Andrés Montefeltro[4], Javier J Meana[3,5], Francesc Artigas[1,2,3] and Analia Bortolozzi[1,2,3*]

The PDF file includes:

Materials and Methods

Conjugated siRNA synthesis

The synthesis and purification of sertraline- and reboxetine-siRNA targeting TASK3 potassium channel (Ser-TASK3-siRNA or Reb-TASK3-siRNA, respectively) and sertraline- or reboxetine-conjugated nonsense siRNA (Ser-NS-siRNA or Reb-NS-siRNA, respectively) molecules were performed by nLife Therapeutics S.L. (Granada, Spain) as previously reported.[8,9] In brief, siRNA (sense and antisense strands) synthesis was performed using ultra mild-protected phosphoramidites (Glen Research, Sterling, VA, USA) and H-8 DNA/RNA Automatic synthesizer (K&A Laborgeraete GbR, Schaafheim, Germany). Sense strand was amino-modified by performing a 5'-C6 amino modification and condensation with a succinimide active ester of sertraline (sertraline-NH-CH2C(=O)NH(CH2)5COO-succinimide) making up the peptide linker of the conjugate (sertraline-NH-CH2C(=O)NH(CH2)5COO-sense strand-3'OH). Conjugated single strand oligonucleotides were purified by high performance liquid chromatography using a RP-C18 column (4.6x150 mm, 5 µm) under a linear gradient condition of acetonitrile shifting the concentration from 5% to 35% for 30min in 100mM TEAA (pH 7.0). The molecular weights of the siRNA strands and the conjugate were confirmed by MALDI-TOF mass spectrometry (Ultraflex, Bruker Daltonics). The yield of the conjugates was spectrophotometrically calculated on the basis of absorbance at 260nm wavelength. Complementary strands were annealed in an isotonic RNA-annealing buffer (100mM potassium acetate, 30mM HEPES pH 7.4, 2mM magnesium acetate), pre-incubated by 1min at 90ºC, centrifuged for 15s and incubated 1h at 37ºC. Duplex RNA formation was confirmed using 20% polyacrylamide gel electrophoresis (PAGE, 30mA, 60min) and visualized by silver staining (DNA Silver stain kit, GE Healthcare, Piscataway, NJ). Sequences are shown in Supplementary Table S1.

In situ hybridization

Frozen tissue sections were first brought to room temperature, fixed for 20min at 4ºC in 4% paraformaldehyde in phosphate-buffered saline (1xPBS: 8mM Na_2HPO_4, 1.4mM KH_2PO_4, 136mM NaCl, and 2.6mM KCl), washed for 5min in 3xPBS at room temperature, twice for 5min each in 1xPBS, and incubated for 2min at 21ºC in a solution of predigested pronase (Calbiochem, San Diego, CA) at a final concentration of 24 U/mL in 50mM Tris-HCl, pH 7.5, and 5mM EDTA. The enzymatic activity was stopped by immersion for 30s in 2 mg/ml glycine in 1xPBS. Tissues were finally rinsed in 1xPBS and dehydrated through a graded series of ethanol. For hybridization, the radioactively labeled probes were diluted in a solution containing 50% formamide, 4x standard saline citrate, 1x Denhardt's solution, 10% dextran sulfate, 1% sarkosyl, 20mM phosphate buffer, pH 7.0, 250 $\mu g \cdot ml^{-1}$ yeast tRNA, and 500 $\mu g \cdot ml^{-1}$ salmon sperm DNA. The final concentrations of radioactive probes in the hybridization buffer were in the same range (~1.5 nM). Tissue sections were covered with hybridization solution containing the labeled probes, overlaid with Nescofilm coverslips (Bando Chemical Ind., Kobe, Japan), and incubated overnight at 42ºC in humid boxes. Sections were then washed 4 times (45min each) in a buffer containing 0.6M NaCl and 10mM Tris-HCl (pH 7.5) at 60ºC. Hybridized sections were exposed to Biomax-MR film (Kodak, Sigma-Aldrich, Madrid, Spain) for 1-4 weeks with intensifying screens. For specificity control, adjacent sections were incubated with an excess (50x) of unlabelled probes. The cytoarchitecture of different mouse brain areas were analyzed in an adjacent series of cresyl-violet stained frozen sections.

Immunohistochemistry

Ki-67 (rabbit anti-Ki-67; 1:5000; ab16667, Abcam, Cambridge, UK) and DCX (goat anti-DCX; 1:200; ref.: sc-8066, Santa Cruz Biotechnology, Santa Cruz, CA) staining were carried out in adjacent free-floating hippocampal sections. After endogenous peroxidase inhibition and washes, pre-incubation and incubation were carried out in a 1x PBS/Triton 0.2% solution containing normal serum from secondary antibody host. Additionally, Ki-67 procedure entails an unmasking 30-min-step at 80ºC in 10mM citrate buffer before pre-incubation. Primary

antibodies were incubated overnight at 4ºC, followed by incubation with the corresponding biotinylated goat anti-rabbit (1:200; ref.: BA-1000, Vector Laboratories, Burlingame, CA) or biotinylated donkey anti-goat (1:200; ref.: sc-2042, Santa Cruz Biotechnology), and subsequent incubation in ABC solution (Vector Laboratories) according to the manufacturer's instructions. The color reaction was performed by incubation with diaminobenzidine tetrahydrochloride (DAB) solution. The sections were mounted onto gelatin-coated slides, embedded and investigated on a Nikon Eclipse E1000 microscope (Nikon, Tokyo, Japan) using 20x and 40x objectives. The whole dentate gyrus labeled cells (Ki-67$^+$ or DCX$^+$ neurons) were counted using ImageJ (v1.49g) software in three equidistantly sections between -1.34 and -2.18 mm from bregma for each mouse.

For immunohistochemical identification of reactive astrocytes (rabbit anti-GFAP; 1:1000; ref.: Z0334, DAKO, Barcelona, Spain) or microglia (rabbit anti-Iba-1; 1:1,000; ref.: 019-197741, WAKO, Irvine, CA), we used the same biotin-labeled antibody procedure as before. Briefly, following endogenous peroxidase inhibition and washes, tissues were blocked with normal goat serum, and incubated with the primary antibody overnight at 4ºC. Then, sections were incubated in biotinylated goat anti-rabbit (1:200) for 1h at room temperature. After the subsequent incubation in ABC solution, the color reaction was performed by incubation with DAB. The sections were mounted onto gelatin-coated slides, embedded and investigated on a Nikon Eclipse E1000 microscope (Nikon) using the 40x objective.

TH (rabbit anti-TH; 1:5000; ref.: ab112, Abcam) and TPH_2 (sheep anti-TPH_2; 1:2000; ref.: AB1541, Merck Millipore, Madrid, Spain) staining were performed in dipped TASK3 hybridized slides. Concisely, following endogenous peroxidase inhibition and rinses, pre-incubation and incubation were carried out in a 1x PBS/Triton 0.2% solution containing normal serum from secondary antibody host. Primary antibodies were incubated 2 days at 4ºC, followed by incubation with the corresponding biotinylated goat anti-rabbit (1:500) or biotinylated rabbit anti-sheep (1:500; ref.: BA-6000, Vector Laboratories). Once incubated with ABC solution, the color reaction was conducted with DAB. When embedded, microphotographs of two sections containing either dorsal raphe (DR) at anteroposterior (AP)

coordinates (in mm) of -4.24/-4.48 and -4.48/-4.72 from bregma or locus coeruleus (LC) at AP coordinates (in mm) -5.52/-5.68 and -5.68/-5.80 from bregma were acquired in duplicate for each mouse with the Nikon Eclipse E1000 microscope (Nikon) using the 60x objective. The whole DR- and LC-labeled neurons (TPH_2^+ or TH^+ neurons, respectively) and TASK3 mRNA-containing TPH_2^+ or TH^+ neurons were counted using ImageJ (v1.49g) Software. In addition, intracellular TASK3-mRNA optical density was obtained as the logarithmic ratio between TASK3 dipping-containing TPH_2^+ or TH^+ neurons and the entire photomicrograph non-neuronal area as a background.

Confocal fluorescence microscopy

Brain sections were rinsed with PBS/Triton 0.2%, incubated with normal serum from secondary antibody host and treated with primary antibodies: TH (rabbit anti-TH; 1:1250; ref.: ab112, Abcam), TPH_2 (sheep anti-TPH_2; 1:2500; ref.: AB1541, Merck Millipore), Rab5 (rabbit anti-Rab5; 1:500; ref.: ab18211, Abcam) or Rab7 (mouse anti-Rab7; 1:2000; ref.: R8779-200UL, Sigma-Aldrich). Sections were then incubated overnight at 4ºC, rinsed and treated with their respective secondary Alexa555-conjugated antibody (donkey anti-rabbit, donkey anti-sheep or rabbit anti-mouse; 1:500; ref.: A-31572/A-21436/A-21427, Life Technologies, Carlsbad, CA, USA) for 120min. After subsequent washes, the section were dehydrated and mounted in the anti-fading agent Prolong Gold with DAPI (Life Technologies). DAPI, Alexa488 and Alexa555 images were acquired sequentially using 405, 488 and 561 laser lines, AOBS (Acoustic Optical Beam Splitter) as beam splitter and emission detection ranges 415- 480, 500-550 and 571-625 nm, respectively and, the confocal pinhole set at 1 Airy units. Images were obtained at 400Hz in a 1024 x 1024 pixels format and were composed using ImageJ (1.49g) software.

Behavioral studies

Novelty suppressed feeding. NSF is a conflict test that elicits competing motivations: the drive to eat and the fear of venturing into the center of the brightly lit arena. The NSF test

was carried out during a 10 min period as previously described.[9] The testing apparatus consisted of a plastic box (35x35x20 cm), the floor of which was covered with approximately 2 cm of wooden bedding for each animal. 24h prior to behavioral testing, all food was removed from the home cage. At the time of testing, a single pellet of food was placed on a white paper platform in the center of the box directly illuminated with 1100 luxes. An animal was placed in a corner of the box, and a stopwatch was immediately started. The latency to eat (defined as the mouse sitting on its haunches and biting the pellet with the use of forepaws) was timed. Immediately afterwards, the animal was transferred to its home cage and, the latency to feed and the amount of food consumed by the mouse in the subsequent 5 min was measured. Each mouse was weighed before food deprivation and before testing to assess the percentage of body weight loss.

Tail suspension test. Mice were suspended 30 cm above the bench by adhesive tape placed approximately 1 cm from the tip of the tail. The total duration of immobility during a 6min test was measured.[8-10]

Marble burying test. The MBT task can be used as an indicator of anxiety-like behavior. When exposed to novel bedding/environment mice exhibit digging behavior, which can be quantified using marbles. Concisely, mice were individually placed in a 25 x 25 cm cage containing 25 equidistantly positioned marbles on top of 5 cm of fresh bedding. After 30-min test, each mouse is returned to its home cage and all marbles at least 2/3 buried are counted.[42]

REFERENCES

42. Deacon RM. Digging and marble burying in mice: simple methods for in vivo identification of biological impacts. *Nat Protoc* 2006; **1**: 122-124

43. Chapman CG, Meadows HJ, Godden RJ, Campbell DA, Duckworth M, Kelsell RE et al. Cloning, localization and functional expression of a novel human, cerebellum specific, two pore domain potassium channel. *Brain Res Mol Brain Res* 2000; **82**: 74-83

Supplementary Figures

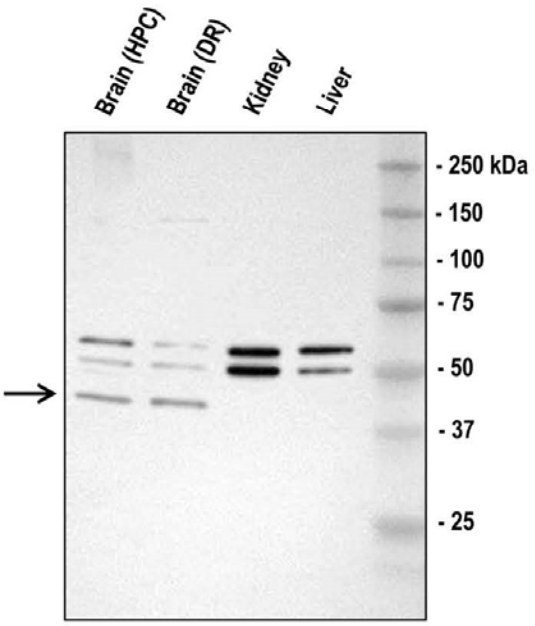

Figure S1 Anti-TASK3 antibody characterization by measuring the differences between western blot bands obtained from TASK3-expressing tissues and TASK3-free tissues, such as liver and kidney.[15,43] Here, two wild-type mice were killed and their liver, kidney and brain dorsal raphe (DR) and hippocampus (HPC) tissues were dissected and pooled. Then, 10 μg of each liver, kidney, DR and HPC protein extract were loaded onto a 4-20 % precast gel and electrophoresed. Once transferred, PVDF membrane was incubated with anti-TASK3 antibody (1:500) overnight. Finally, after horseradish peroxidase-conjugated secondary antibody (1:2500) incubation, proteins were detected by chemiluminiscence. Note that TASK3 band (arrow) was only detected in brain tissues within its predicted 42-47 kDa molecular weight rang.

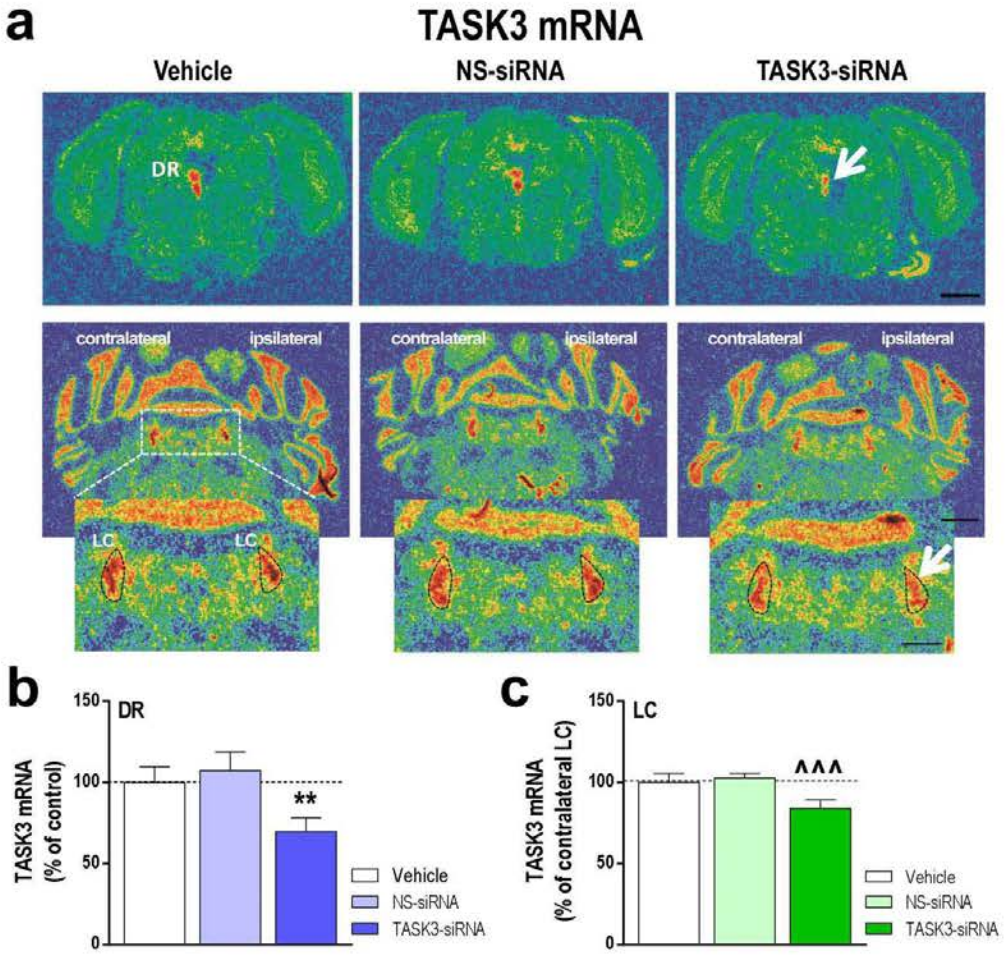

Figure S2 Selective TASK3 mRNA silencing in dorsal raphe (DR) and locus coeruleus (LC) by locally infusion of unmodified TASK3-siRNA. Mice were infused directly into DR or LC with vehicle, nonsense siRNA (NS-siRNA) or TASK3-siRNA at 10 μg·day^{-1} during 2 days. **(a)** Representative autoradiograms showing TASK3 mRNA expression in DR an LC. Scale bars: low = 2 mm and high = 500 μm. **(b)** Intra-DR TASK3-siRNA infusion reduced TASK3 mRNA levels in DR (n = 4-5 mice/group). One-way ANOVA showed an effect of group ($F_{2,11}$ = 19.69, P<0.001). **(c)** Intra-LC TASK3-siRNA infusion reduced TASK3 mRNA levels in LC (n = 4-5 mice/group). One-way ANOVA showed an effect of group ($F_{2,11}$ = 22.7, P<0.001). **P<0.01 versus vehicle-treated mice; ^^^P<0.001 versus vehicle-treated mice. Data are mean ± s.e.m.

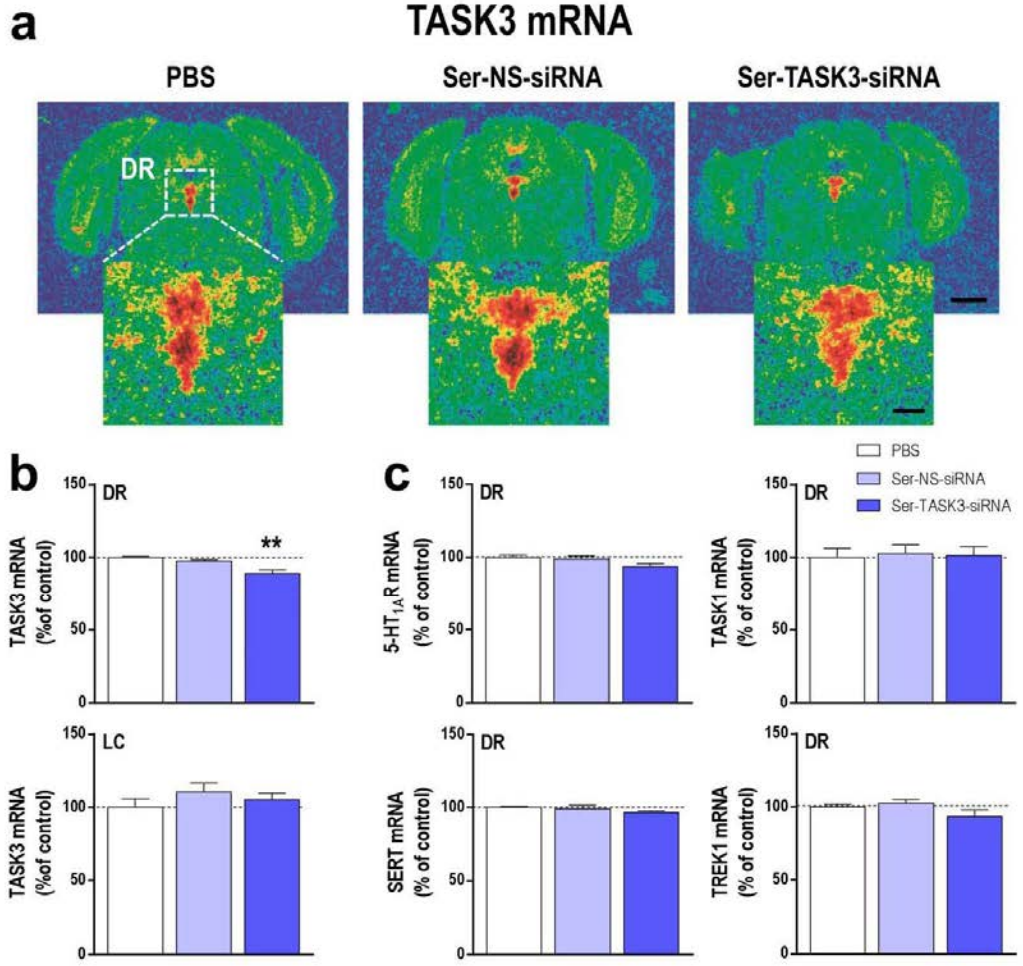

Figure S3 Selective silencing of TASK3 mRNA level in the mouse dorsal raphe (DR) after intranasal administration of sertraline-conjugated TASK3 siRNA (Ser-TASK3-siRNA). Mice received intranasally PBS, sertraline-conjugated nonsense siRNA (Ser-NS-siRNA) or Ser-TASK3-siRNA at 30 $\mu g \cdot day^{-1}$ during 7 days. **(a)** Representative coronal midbrain sections showing TASK3 mRNA density in DR. Scale bars: low = 2 mm and high = 500 μm. **(b)** Effect of Ser-TASK3-siRNA on TASK3 mRNA level in DR and locus coeruleus (LC) (n = 4-5 mice/group). One-way ANOVA showed an effect of group ($F_{2,11}$ = 13.85, P<0.01). **(c)** Quantitative analysis of 5-HT_{1A}R, SERT, TASK1 and TREK1 mRNA densities showed non-

significant effects (n = 4-5 mice/group). **P<0.01 versus PBS-treated mice. Data are mean ± s.e.m.

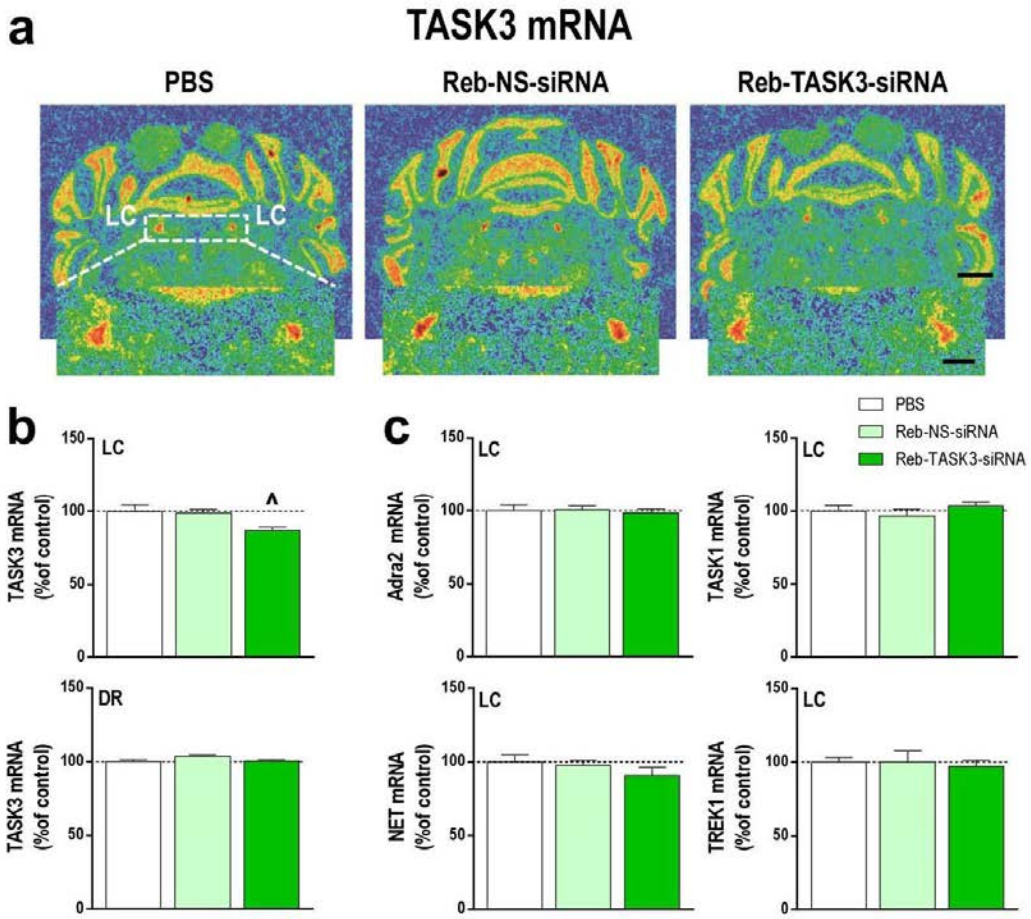

Figure S4 Selective silencing of TASK3 mRNA level in the mouse locus coeruleus (LC) after intranasal administration of reboxetine-conjugated TASK3 siRNA (Reb-TASK3-siRNA). Mice received intranasally PBS, reboxetine-conjugated nonsense siRNA (Reb-NS-siRNA) or Reb-TASK3-siRNA at 75 $\mu g \cdot day^{-1}$ during 7 days. **(a)** Representative coronal midbrain sections showing TASK3 mRNA density in LC. Scale bars: low = 2 mm and high = 500 μm. **(b)** Effect of Reb-TASK3-siRNA on TASK3 mRNA level in LC and dorsal raphe (DR) (n = 4-5 mice/group). One-way ANOVA showed an effect of group ($F_{2,10}$ = 6.151, P<0.05). **(c)** Quantitative analysis of Adra2, NET, TASK1 and TREK1 mRNA densities showed non-

significant effects (n = 4-5 mice/group). ^P<0.05 versus PBS-treated mice. Data are mean ± s.e.m.

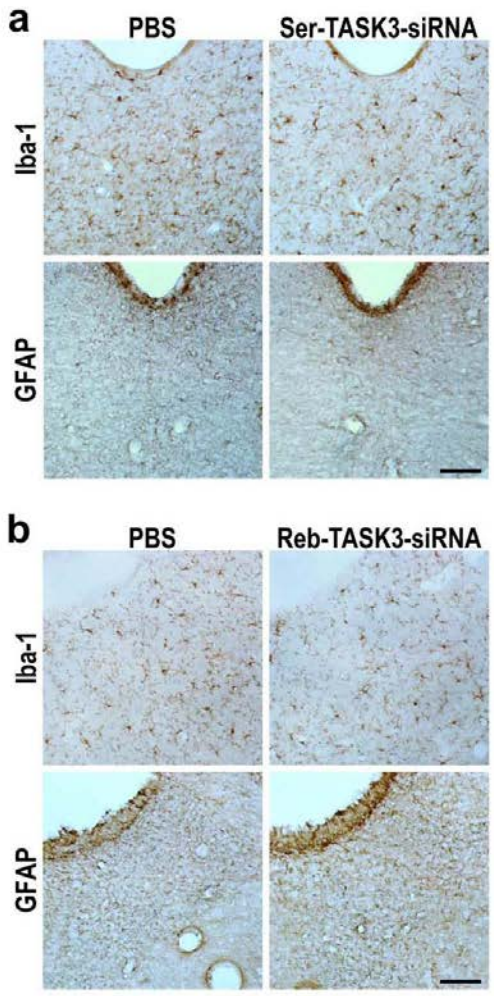

Figure S5 Immunohistochemical assessment of atrogliosis and microglia activation in dorsal raphe (DR) or locus coeruleus (LC) after intranasal administration of sertraline- or reboxetine-conjugated TASK3-siRNA (Ser- Reb-TASK3-siRNA), respectively. One cohort of mice received intranasally PBS or Ser-TASK3-siRNA at 75 $\mu g \cdot day^{-1}$ during 7 days. Another cohort of mice received intranasally PBS or Reb-TASK3-siRNA at 75 $\mu g \cdot day^{-1}$ during 7 days (n = 8 mice/group). **(a-b)** Representative photomicrographs showing adjacent sections throughout the DR and the LC stained with astrocytic GFAP or microglial Iba-1 markers. No differences were found between all experimental groups for any of the markers. Scale bars = 100 μm.

Supplementary Tables

Table S1 Sequences of siRNA molecules used

siRNA	Forward	Reverse
TASK3-siRNA	CCGGGCUACCGUCCACACCTT	GGUGUGGACGGUAGCCCGGTT
NS-siRNA	AGUACUGCUUACGAUACGGTT	CCGUAUCGUAAGCAGUACUTT

Table S2 TPH_2^+ and TH^+ neurons in DR and LC, respectively

	PBS	Ser-TASK3-siRNA	PBS	Reb-TASK3-siRNA
DR TPH_2^+ cells (AP: -4.24 to -4.48 mm)	227.2 ± 25.1	203.0 ± 21.1	-	-
DR TPH_2^+ cells (AP: -4.48 to -4.72 mm)	182.0 ± 11.5	170.4 ± 47.0	-	-
LC TH^+ cells (AP: -5.52 to -5.68 mm)	-	-	62.3 ± 16.1	75.1 ± 22.8
LC TH^+ cells (AP: -5.68 to -5.80 mm)	-	-	21.0 ± 10.6	33.3 ± 17.0

One cohort of mice received intranasally PBS or sertraline- conjugated TASK3-siRNA (Ser-TASK3-siRNA) at 75 $\mu g \cdot day^{-1}$ during 7 days. Another cohort of mice received intranasally PBS or reboxetine-conjugated TASK3-siRNA (Reb-TASK3-siRNA) at 75 $\mu g \cdot day^{-1}$ during 7 days. Two-way ANOVA (factors: AP coordinates and treatment) analysis of dorsal raphe (DR) TPH2+ neurons or locus coeruleus (LC) TH+ neurons showed non-significant differences (n = 4-6 mice/group). Data are mean ± s.e.m.

Table S3 Basal 5-HT and NA dialysate values in the mPFC of mice

Treatment	aCSF (30 min/fraction)	aCSF + Cit 1μM (30 min/fraction)	aCSF + Cit 1μM (6 min/fraction)	maCSF + Des 1μM (30 min/fraction)
PBS	3.67 ± 0.44 (fmol of 5-HT)	15.84 ± 2.29 (fmol of 5-HT)	1.75 ± 0.18 (fmol of 5-HT)	-
Ser-TASK3-siRNA	3.70 ± 1.04 (fmol of 5-HT)	15.54 ± 5.15 (fmol of 5-HT)	2.28 ± 0.27 (fmol of 5-HT)	-
PBS	7.37 ± 0.77 (fmol of NA)	-	-	21.93 ±3.81 (fmol of NA)
Reb-TASK3-siRNA	7.11 ± 0.62 (fmol of NA)	-	-	22.46 ± 3.35 (fmol of NA)

One cohort of mice received intranasally PBS or sertraline- conjugated TASK3-siRNA (Ser-TASK3-siRNA) at 75 $\mu g \cdot day^{-1}$ during 7 days. Another cohort of mice received intranasally PBS or reboxetine-conjugated TASK3-siRNA (Reb-TASK3-siRNA) at 75 $\mu g \cdot day^{-1}$ during 7 days. Student's t-test did not show 5-HT or NA baseline differences between PBS- and siRNA-treated mice in any of the microdialysis conditions used (n = 6-10 mice/group). Data are mean ± s.e.m.

5. Discusión

5.1. Consideraciones generales

En el presente trabajo de Tesis se han utilizado moléculas de siRNAs para regular de modo eficiente y selectivo la expresión de genes implicados en la depresión y su tratamiento. Se ha silenciado selectivamente *in vivo* la expresión del receptor 5-HT_{1A}, el transportador SERT y el canal de potasio TASK3 en las neuronas monoaminérgicas, concretamente serotoninérgicas y noradrenérgicas, de ratón sin alterar la expresión y función de los mismos en otras áreas cerebrales. Aunque esta tecnología está siendo utilizada en varios estudios clínicos para tratar patologías como la retinopatía diabética o la degeneración macular asociada a la edad, entre otros (Vicentini et al., 2013), su aplicabilidad a patologías del cerebro continúa siendo limitada. Esto es debido, entre otros aspectos, a la dificultad de poder acceder al CNS y a la propia complejidad de este órgano constituido por una gran diversidad de tipos celulares responsables de múltiples funciones (Kumar et al., 2007; Roy et al., 2008; Boudreau and Davidson, 2010). Por todo ello, la caracterización *in vivo* de siRNAs contra el receptor 5-HT_{1A}, el transportador SERT y el canal de potasio TASK3 representó un desafío en el desarrollo de la presente Tesis y un nuevo enfoque de la neuropsicofarmacología basada en RNAi. Además, la estrategia de conjugación de los oligonucleótidos con ligandos específicos como sertralina o reboxetina permitió su acumulación en un tipo neuronal concreto utilizando una vía de administración clínica como es la intranasal, proveyendo de carácter translacional a esta tecnología.

La elección de los genes diana se ha realizado en base a la función fisiológica de los mismos y/o a la expresión y función alterada de las variantes alélicas asociadas con una mayor vulnerabilidad a la depresión (Caspi et al., 2003; Lemonde et al., 2003; Rush et al., 2006; Licinio et al., 2009; Gotter et al., 2011). Se ha trabajado con la hipótesis que la modulación post-transcripcional dependiente de siRNAs de los mRNAs de estudio conlleva a una reducción de la expresión de las proteínas diana, incrementando más eficazmente y rápidamente la neurotransmisión serotoninérgica o noradrenérgica frente al bloqueo farmacológico de las mismas.

En primer lugar, se observó que el silenciamiento selectivo del autoreceptor 5-HT_{1A} en el DR inducido por siRNAs aplicados por vía local, intracerebroventricular o

intranasal evoca efectos de tipo antidepresivo en ratones, facilita la neurotransmisión serotoninérgica, incrementa la resiliencia al estrés y potencia el efecto del SSRI fluoxetina. En segundo lugar, se comprobó que la modulación post-transcripcional del SERT mediante siRNAs aplicados localmente en el DR o por vía intranasal tiene un efecto antidepresivo de acción más rápida que el SSRI fluoxetina en ratones "wild-type" o en un modelo de depresión asociado al consumo crónico de corticosterona. En tercer lugar, se mostró que la reducción selectiva de la expresión del canal de potasio TASK3 en neuronas serotoninérgicas o noradrenérgicas inducida por el tratamiento intranasal con siRNAs representa una nueva diana potencial de acción antidepresiva en modelos murinos.

En general, los resultados obtenidos indican que el mecanismo de RNAi constituye una herramienta útil para silenciar *in vivo* y de modo selectivo, eficiente y seguro, la expresión de genes en el CNS. Además, se aporta información relevante acerca de una nueva estrategia de diseño de siRNAs basada en la conjugación química para facilitar su acumulación en neuronas específicas, permitiendo examinar el rol funcional de genes implicados en depresión y/o efecto antidepresivo.

5.2. Especificidad, seguridad y eficacia de los siRNAs empleados

Las secuencias de siRNAs utilizadas (1A-siRNA, SERT-siRNA y TASK3-siRNA, conjugadas o sin conjugar) resultaron seguras, bien toleradas y no mostraron efectos *off-target* de complementariedad incompleta con otros mRNAs, consiguiendo una reducción parcial de la expresión/función de sus respectivas dianas. Además, tanto la administración intracerebral o intranasal de las diferentes secuencias de siRNAs no indujeron toxicidad neuronal, gliosis ni inflamación.

En general, los agentes químicos y también los siRNAs u otras herramientas moleculares pueden producir efectos *off-target* no intencionados (Moss and Taylor, 2003; Sledz et al., 2003). Concretamente para los siRNAs, puede detectarse la represión de la traducción de mRNAs que presenten una secuencia con complementariedad incompleta con el siRNA utilizado (Dykxhoorn and Lieberman,

2006; Jackson et al., 2006). Los resultados de la presente Tesis mostraron que el diseño de los siRNAs fue adecuado para silenciar selectivamente su diana. Así, la reducción de la expresión del autoreceptor 5-HT_{1A}, el SERT o el TASK3 inducida por siRNAs no alteró los niveles de expresión de otros mRNAs evaluados que presentan una alta homología con el mRNA de estudio (por ejemplo: mRNA del receptor 5-HT_{1B} respecto al mRNA del receptor 5-$HT_{1A,}$ mRNA del NET respecto al mRNA del SERT y, mRNAs del TREK1 y TASK1 respecto al mRNA del TASK3).

Además, se ha documentado que los siRNAs, dependiendo o no de la secuencia de bases, pueden activar el sistema inmunitario y las vías de señalización de PKR y TLR, alterando la homeostasis celular (Moss and Taylor, 2003; Sledz et al., 2003; Judge et al., 2005). Los resultados obtenidos aquí mostraron que las secuencias de siRNAs utilizadas y/o las bajas dosis empleadas de los mismos en comparación con otros estudios (Thakker et al., 2004, 2005) son seguras y no activan la inmunidad innata. La infusión intracerebral o administración intranasal de los siRNAs estudiados no indujo la expresión de genes pro-inflamatorios como el factor de necrosis tumoral alfa (TNFα; *tumor necrosis factor alpha*) e interferón gamma (INFγ; *interferon gamma*) a diferencia de la secuencia del siRNA contra la β-galactosidasa (β-Gal-128) utilizada como control positivo de las vías de señalización de TLRs. Además, tampoco se observaron indicios de alteración de la homeostasis celular en ninguno de los tratamientos, como por ejemplo neurodegeneración o alteración de la expresión de genes específicos de neuronas serotoninérgicas (TPH_2, SERT y receptores 5-HT_{1A} y 5-HT_{1B}) o noradrenérgicas (receptor α_2 y NET). Asimismo, no se detectaron diferencias significativas asociadas a la activación de astrocitos o de la microglía después del uso de siRNAs en comparación con los grupos control.

Respecto a la eficacia *in vivo* del silenciamiento de los mRNAs diana, está fue entre el 25% y 50% de los niveles del grupo control. Los resultados coinciden con el descrito en la literatura de siRNAs *in vivo* indicando que la magnitud del silenciamiento depende, entre otros aspectos, del mRNA que se pretende silenciar así como del tipo celular donde es expresado (Shishkina et al., 2004; Thakker et al., 2004, 2005; Salahpor et al., 2007). A efectos estratégicos, esto fue de relevante importancia en el

trabajo 4, dónde se pretendía silenciar el transportar SERT mediante un siRNA conjugado con sertralina que facilita la internalización del oligonucleótido en las neuronas serotoninérgicas a través del propio SERT. Los resultados obtenidos confirmaron que los niveles de la proteína SERT "remanente" fueron suficientes y funcionalmente activos para mediar la acumulación de siRNA. Existe un consenso de obtener reducciones parciales y no totales de la expresión de los mRNA. Esto en parte se debe a que muchas de las patologías neuropsiquiátricas están relacionadas con incrementos o disminuciones de los niveles de proteínas y no con una ausencia total de las mismas en determinadas áreas cerebrales (Dykxhoorn and Lieberman, 2006; Xie et al., 2006; Cryan et al., 2007). Como ejemplo, una diferencia del 30% de los niveles del autoreceptor 5-HT_{1A} fue reportada en pacientes con depresión (Drevets et al., 2007), diferencia que coincide con la reducción de la expresión del autoreceptor 5-HT_{1A} observada utilizando modelos animales transgénicos (Richardson-Jones et al., 2010) y el modelo de siRNAs (trabajo 1 de la presente Tesis).

Pr consiguiente, los datos presentes ponen de manifiesto la eficiencia y carácter bien tolerado de las secuencias de siRNAs utilizadas.

5.3. La conjugación de los siRNAs permite su acumulación *in vivo* en las neuronas monoaminérgicas

La utilización de siRNAs en enfermedades del CNS está siendo retrasada por la dificultad de poder direccionar y acumular los siRNAs hacia áreas cerebrales concretas y/o poblaciones neuronales específicas, así como por la ausencia de un método de administración adecuado (Baker, 2010). En este sentido, la presente Tesis representó un avance considerable en el uso de siRNAs *in vivo* al conjugar químicamente los oligonucleótidos con ligandos selectivos para los transportadores de monoaminas y utilizar una ruta de administración clínica como lo es la vía intranasal.

Otros métodos de conjugación de siRNAs incluyen la unión con péptidos pequeños, con anticuerpos o con ligandos que activan la internalización mediada por proteína G (Soutschek et al., 2004; Song et al., 2005; Kumar et al., 2007; Baker, 2010; Ming et al.,

2010; Juliano et al., 2013, 2015). En nuestro caso, la conjugación con sertralina o reboxetina permitió direccionar selectivamente los siRNAs a las poblaciones neuronales monoaminérgicas de interés. Aunque queda mucho trabajo para poder entender el mecanismo exacto de la acumulación celular selectiva, los resultados obtenidos en los trabajos 1, 4 y 5 sugieren que, los siRNAs son internalizados a través de un mecanismo de endocitosis mediada por transportador e incorporados a la red de transporte endosomal desde donde presumiblemente accederían al citosol (Juliano and Carver, 2015).

Concretamente, el trabajo 1 mostró que el C-1A-siRNA se acumula específicamente en las neuronas serotoninérgicas y es necesario que el transportador SERT sea funcional para la internalización de la molécula. Este punto de vista fue respaldado por: 1) un enriquecimiento selectivo de las moléculas de siRNAs en las la neuronas serotoninérgicas del mesencéfalo, 2) por la reducción de la expresión y función del autoreceptor 5-HT_{1A}, 3) por la ausencia de efectos sobre el receptor 5-HT_{1A} localizado en el HPC, región más cercana al sitio de administración intracerebral en el D3V, y 4) por la falta del efectos del C-1A-siRNA sobre la neurotransmisión serotoninérgica cuando previamente se bloquea el SERT con sertralina.

Posteriormente, en los trabajos 4 y 5, se profundizó acerca del mecanismo de internalización de los siRNAs conjugados. En estos estudios se utilizaron secuencias de siRNAs *nonsense* doblemente conjugadas con alexa488 y sertralina o reboxetina, confirmando la acumulación selectiva de las mismas en neuronas serotoninérgicas o noradrenérgicas, respectivamente, después de la administración intranasal. Si bien no hemos caracterizado el mecanismo de transporte de los siRNAs desde la cavidad nasal hacia las neuronas monoaminérgicas, estudios previos empleando neuropéptidos o moléculas de dextranos con pesos moleculares de 3 y 10 kDa (similar al peso molecular de los siRNAs utilizados que oscilan entre 12 y 14 kDa) indicarían que el pasaje de los mismos hacia el cerebro estaría mediado a través de espacios perivasculares (Thorne et al., 2004; Graff and Pollack, 2005; Hashizume et al., 2008; Lochhead et al., 2015). Del mismo modo, debido a que el bulbo olfatorio recibe proyecciones serotoninérgicas, no puede descartarse un posible transporte

axonal retrógrado de las moléculas de siRNAs hacia la región somatodendrítica de las neuronas serotoninérgicas (Araneda et al., 1999). No obstante, los datos obtenidos en los trabajos 1, 4 y 5 indicarían que la conjugación con el ligando (sertralina o reboxetina), y no la secuencia del siRNA, es la responsable del direccionamiento de las moléculas de oligonucleótidos hacia las neuronas monoaminérgicas.

Además, en el trabajo 4, el análisis de los datos de microscopia confocal indicó que esta acumulación ocurre preferentemente en el DR en comparación al MR. Esto podría deberse a una mayor expresión del SERT en esta área cerebral y a una mayor sensibilidad de las neuronas 5-HT del DR respecto al MR a la acción de los SSRI como previamente se ha reportado (Mamounas et al., 1991; Brown and Molliver, 2000; Hervas et al., 2000).

En conjunto los datos indican que la conjugación de los siRNAs con sertralina o reboxetina permitiría la acumulación selectiva de los mismos en las neuronas serotoninérgicas o noradrenérgicas, respectivamente, después de la administración intracerebroventricular o intranasal. Esto plantea una nueva estrategia terapéutica en neuropsicofarmacología basada en el uso de la tecnología de RNAi.

5.4. La reducción de la expresión del autoreceptor 5-HT_{1A} es suficiente para alterar la vulnerabilidad al estrés y la respuesta a los antidepresivos

Los resultados de la presente Tesis mostraron que la reducción de la expresión del autoreceptor 5-HT_{1A} en ratón inducida por siRNAs evita el mecanismo de autoinhibición de las neuronas serotoninérgicas. Aunque esta situación no modificó la liberación basal de 5-HT, respaldando la idea de que el autoreceptor no es activo en condiciones fisiológicas (Mannoury la Cour et al., 2001; Johnson et al., 2002), si produjo respuestas de tipo antidepresivo en el TST y FST debido, probablemente, a la mayor liberación de 5-HT en condiciones de estrés. Del mismo modo, el menor nivel de expresión/función del autoreceptor 5-HT_{1A} incrementó la respuesta de los fármacos antidepresivos del tipo SSRIs.

Los datos obtenidos de los trabajos 1 y 2 permitieron confirmar la disociación funcional del receptor 5-HT_{1A} según su localización pre- o postsináptica. Se conoce que los agonistas del receptor 5-HT_{1A} tienen propiedades ansiolíticas (Menard and Treit, 1999), y que los ratones *knockout* para este receptor muestran comportamiento de tipo ansioso (Parks et al., 1998; Ramboz et al., 1998). Además, se ha descrito que el rescate del receptor 5-HT_{1A} en hipocampo y corteza, pero no en rafe, durante el desarrollo evita el comportamiento de tipo ansioso observado en los ratones adultos *knockout* para el receptor 5-HT_{1A} (Gross et al., 2002), confirmando el rol preferencial del receptor 5-HT_{1A} postsináptico en las respuestas de ansiedad. En este sentido y en concordancia con estudios previos utilizando ratones transgénicos con una reducción de la expresión del receptor 5-HT_{1A} en los núcleos del rafe (Richardson-Jones et al., 2010), los datos obtenidos en el trabajo 1 y 2 mostraron que la reducción del nivel de expresión del autoreceptor 5-HT_{1A} en el estado adulto es suficiente para afectar al comportamiento de tipo depresivo sin inducir respuestas relacionadas con la ansiedad.

Las diferentes formas de administración del siRNA contra el receptor 5-HT_{1A} (infusión local en el DR, administración intracerebroventricular o intranasal) en ratones produjo: 1) reducción selectiva de los niveles de expresión del autoreceptor 5-HT_{1A}, 2) supresión de la hipotermia y reducción la liberación de 5-HT inducida por el agonista 5-HT_{1A} 8-OH-DPAT, y 3) respuestas de tipo antidepresivo en el FST y TST. Además, el silenciamiento del autoreceptor 5-HT_{1A} aceleró los efectos del SSRI fluoxetina, tal y como se observó en estudios clínicos con el bloqueo farmacológico con pindolol, antagonista del receptor 5-HT_{1A} de acción preferente sobre el autoreceptor (Artigas et al., 1994). Ambos mecanismos, siRNAs y pindolol, confirmaron el rol del autoreceptor en el mecanismo de autoinhibición del sistema serotoninérgico. Sin embargo, mientras la regulación post-transcripcional del nivel del autoreceptor 5-HT_{1A} dependiente de siRNA desencadenó respuestas antidepresivas por sí solo, el bloqueo farmacológico utilizando pindolol no es suficiente para evocar respuestas de tipo antidepresivas, confirmando la eficacia de la modulación post-transcripcional como estrategia terapéutica.

En conjunto, los resultados de los trabajos 1 y 2 argumentan la idea que la reducción del nivel de expresión del autoreceptor 5-HT_{1A} podría convertirse en una nueva estrategia de tratamiento antidepresivo, en especial en aquellos pacientes con sobre-expresión del mismo en los núcleos del rafe. Además, el silenciamiento del 5-HT_{1A} presináptico reduciría el tiempo de aparición de las respuestas clínicas de los SSRIs, retraso en parte asociado con el tiempo requerido para producir la desensibilización del autoreceptor 5-HT_{1A}.

5.5. La reducción de la expresión del SERT mediante RNAi produce efectos antidepresivos muy rápidos

Los datos obtenidos en los trabajos 3 y 4 mostraron que la regulación post-transcripcional de la expresión del SERT en el DR de ratón tiene un gran impacto sobre la neurotransmisión serotoninérgica ya que: 1) facilita la neurotransmisión serotoninérgica, 2) reduce la expresión y función del autoreceptor 5-HT_{1A}, 3) incrementa la proliferación celular y neurogénesis en el DG, y 4) aumenta la expresión de genes asociados a neuroplasticidad en el HPC, todos ellos marcadores predictivos de la acción antidepresiva en ratón. Estos efectos aparecieron más rápidamente después del tratamiento con siRNAs contra SERT que el bloqueo farmacológico con el SSRI fluoxetina.

Concretamente en el trabajo 3, la infusión local durante cuatro días de SERT-siRNA en el DR de ratón redujo la expresión/función del SERT, dejando aumentos cuatro veces superiores de la concentración de 5-HT en el estriado e HPC, en comparación con fluoxetina que requirió 2 semanas de tratamiento. Posiblemente, el aumento de los niveles de 5-HT indujo la rápida desensibilización del autoreceptor 5-HT_{1A}, tal y como se observó después del tratamiento con SERT-siRNA en comparación con el tratamiento con fluoxetina. Estos efectos favorecieron el incremento de la neurogénesis y la neuroplasticidad en el HPC en sólo 4 días de tratamiento con SERT-siRNA, mientras que se necesitaron 15 días de tratamiento con fluoxetina. A nivel comportamental, la modulación post-transcripcional del SERT redujo el tiempo de inmovilidad en el TST. Este efecto fue comparable al obtenido por Thakker y

colaboradores en un estudio anterior, donde encontraron repuestas antidepresivas en el FST utilizando un tratamiento con altas dosis (28 nmol·día^{-1} frente a 0.7 nmol·día^{-1} en la presente Tesis) con la misma secuencia de SERT-siRNA (Thakker et al., 2005).

Del mismo modo, la aplicación intranasal del C-SERT-siRNA en ratones, también desencadenó las respuestas predictivas de la acción antidepresiva descritas anteriormente para SERT-siRNA. Además, se comprobó que el tratamiento con C-SERT-siRNA revierte el modelo murino de depresión asociado al consumo crónico de corticosterona antes que el tratamiento con fluoxetina. Esta rapidez podría ser consecuencia del incremento de la concentración de 5-HT extracelular, observándose con solo 7 días de tratamiento con C-SERT-siRNA valores comparables a los obtenidos tras 28 días de tratamiento con fluoxetina. El rápido incremento de los niveles de 5-HT observados con C-SERT-siRNA posibilita la desensibilización del autoreceptor 5-HT_{1A} antes que el tratamiento con fluoxetina, observándose en solo 7 días los cambios adaptativos necesarios para la acción antidepresiva.

La modulación post-transcripcional del SERT mediante siRNAs, junto con las observaciones descritas en los trabajos 1 y 2 acerca de los efectos de los siRNAs conjugados o sin conjugar contra el receptor 5-HT_{1A}, ponen en relieve la utilidad de las estrategias basadas en el RNAi para facilitar la neurotransmisión serotoninérgica. Además, el uso de una ruta de administración clínica como es la intranasal, aporta un gran valor translacional planteando nuevas perspectivas terapéuticas para el tratamiento de los trastornos del estado de ánimo como la depresión.

5.6. Potencial antidepresivo de la modulación post-transcripcional del TASK3 en neuronas monoaminérgicas

Los datos obtenidos en el trabajo 5 mostraron que la reducción de la expresión del canal de potasio TASK3 en neuronas serotoninérgicas o noradrenérgicas de ratón mediante siRNAs conjugados con sertralina o reboxetina, respectivamente, produce efectos de tipo antidepresivo como: 1) reducción de la función del autoreceptor 5-HT_{1A} o del receptor α_2 de las neuronas serotoninérgicas o noradrenérgicas,

respectivamente, 2) incremento de la proliferación y neurogénesis en el DG, 3) aumento de la expresión de genes asociados a neuroplasticidad en diferentes subregiones del HPC, y 4) respuestas de tipo antidepresivo en el TST y NSFT. Además, como se observó anteriormente con el silenciamiento del autoreceptor 5-HT_{1A}, el tratamiento con Ser-TASK3-siRNA no modificó la liberación basal de 5-HT, soportando la idea que las respuestas de tipo antidepresivo ocurren, probablemente, por la mayor liberación de 5-HT en condiciones de estrés.

Los efectos de tipo antidepresivo del Ser-TASK3-siRNA probablemente están mediados por la facilitación de la neurotransmisión serotoninérgica asociada a la pérdida de la función del autoreceptor 5-HT_{1A}, como sugiere la menor capacidad del agonista 5-HT_{1A} 8-OH-DPAT para reducir la liberación de 5-HT en la mPFC. Esta idea también es compatible con el mayor aumento de la concentración de 5-HT producido por el SSRI fluoxetina en los ratones tratados con Ser-TASK3-siRNA, a los que se habría atenuado el mecanismo de retroalimentación negativo mediado por el autoreceptor 5-HT_{1A} (Artigas et al., 1996; Hervás and Artigas, 1998). Del mismo modo, la eficacia del agonista α_2 clonidina en reducir la liberación de NE fue menor en los ratones tratados con Reb-TASK3-siRNA, sugiriendo una reducción de la sensibilidad del receptor α_2 adrenérgico. La razón de la menor sensibilidad de los autoreceptores 5-HT_{1A} y α_2 adrenérgico en los ratones tratados con Ser-TASK3-siRNA y Reb-TASK3-siRNA, respectivamente, podría estar relacionada, probablemente, al incremento del potencial de membrana de las neuronas serotoninérgicas y noradrenérgicas después de la inactivación parcial del TASK3. De hecho, se ha reportado que la disminución del canal de potasio TASK3, constitutivamente abierto, aumenta el potencial de membrana (Washburn et al., 2002), haciendo a las neuronas serotoninérgicas y noradrenérgicas menos sensibles a las acciones hiperpolarizantes de los autoreceptores 5-HT_{1A} y α_2 adrenérgico.

Los efectos de tipo antidepresivo producidos por Reb-TASK3-siRNA fueron de menor magnitud que los producidos por el Ser-TASK3-siRNA. La menor reducción de células dobles positivas (TH y TASK3) observadas en el LC, en comparación a las dobles positivas (TPH_2 y TASK3) en el DR, apoya que esta diferencia pudiera deberse a la

menor capacidad de Reb-TASK3-siRNA para acumularse selectivamente en las neuronas noradrenérgicas del LC y/o a la menor capacidad del siRNA para reducir la expresión de TASK3 en este tipo celular. Por otro lado, la 5-HT y la NE están implicadas en distintos aspectos del tratamiento antidepresivo, siendo la 5-HT la principal implicada en la resiliencia al estrés, factor clave en los paradigmas comportamentales utilizados (TST y NSFT).

En conjunto, la reducción selectiva de la expresión de TASK3 en neuronas serotoninérgicas o noradrenérgicas produce efectos de tipo antidepresivo destacando su potencial como diana terapéutica. Una semana de tratamiento con Ser-TASK3-siRNA, y en menor medida con Reb-TASK3-siRNA, produce cambios histológicos, neuroquímicos y comportamentales similares a los producidos por un tratamiento de 4 semanas con un fármaco SSRI. Probablemente, estos efectos son debidos al incremento del potencial de membrana de las neuronas monoaminérgicas como resultado de la reducción selectiva del canal TASK3. Además, la selectividad de los siRNAs conjugados para acumularse en neuronas serotoninérgicas o noradrenérgicas después de la administración intranasal, reafirma, junto a los trabajos anteriores, la estrategia del RNAi como una nueva herramienta potencial para un tratamiento más rápido y eficaz de la depresión.

6. Conclusiones

1. Los siRNAs pueden ser utilizados *in vivo* para silenciar de modo selectivo, eficiente y seguro la expresión de genes en neuronas monoaminérgicas implicados en el trastorno depresivo y su tratamiento. Esto plantea una nueva estrategia terapéutica en neuropsicofarmacología basada en el RNAi.

2. La conjugación de siRNAs con sertralina o reboxetina permite su acumulación selectiva en la población neuronal de interés (serotoninérgica o noradrenérgica, respectivamente) a través de una vía de administración clínica como es la administración intranasal. Los siRNAs son internalizados en las neuronas, posiblemente por un mecanismo de endocitosis mediado por transportador, y transportados a compartimentos endosomales profundos.

3. La disminución de la expresión del receptor 5-HT_{1A} en las neuronas serotoninérgicas mediante siRNAs sin modificar o conjugados con sertralina evoca efectos antidepresivos en ratones, probablemente debido a la mayor capacidad de las neuronas serotoninérgicas para liberar 5-HT en condiciones de estrés.

4. La modulación post-transcripcional del SERT en ratones mediante siRNAs sin modificar o conjugados con sertralina, produce un efecto antidepresivo más rápido y potente que el que se obtiene con el bloqueo farmacológico del SERT mediante el SSRI fluoxetina. Además, el *knockdown* del SERT consigue revertir de modo más rápido el comportamiento de tipo depresivo asociado al consumo crónico de corticosterona en comparación al tratamiento con fluoxetina.

5. La reducción de la expresión del canal de potasio TASK3 en neuronas serotoninérgicas mediante la administración intranasal de siRNAs conjugados con sertralina evoca respuestas de tipo antidepresivo en ratón, demostrando el potencial de TASK3 como una nueva diana para el tratamiento de la depresión. Además, el *knockdown* de TASK3 en neuronas noradrenérgicas utilizando siRNAs conjugados con reboxetina, también produce efectos antidepresivos en ratones, aunque de menor magnitud que el observado en neuronas serotoninérgicas.

6. La ruta de administración intranasal de los siRNAs utilizada para silenciar el receptor 5-HT_{1A}, el SERT o el canal de potasio TASK3 proporciona a los estudios gran valor translacional, representando nuevas posibilidades terapéuticas que mejoran las principales limitaciones de los antidepresivos actuales, baja eficacia y acción retardada.

7. Bibliografía

A

Abi-Dargham A, Laruelle M, Aghajanian GK, Charney D, Krystal J (1997). The role of serotonin in the pathophysiology and treatment of schizophrenia. *J Neuropsychiatry Clin Neurosci*, 9(1):1-17

Adell A, Casanovas JM Artigas F (1997). Comparative study in the rat of the actions of different types of stress on the release of 5-HT in raphe nuclei and forebrain areas. *Neuropharmacology*, 36(4-5):735-41

Adell A, Celada P, Abellán MT, Artigas F (2002). Origin and functional role of the extracellular serotonin in the midbrain raphe nuclei. *Brain Res Brain Res Rev*, 39(2-3):154-80

Aghajanian GK and Wang RY (1977). Habenular and other midbrain raphe afferents demonstrated by a modified retrograde tracing technique. *Brain Res*, 18;122(2):229-42

Aghajanian GK and Vandermaelen CP (1982). Intracellular recordings from serotonergic dorsal raphe neurons: pacemaker potentials and the effect of LSD. *Brain Res*, 29;238(2):463-9

Agster KL, Mejias-Aponte CA Clark BD, Waterhouse BD (2013). Evidence for a regional specificity in the density and distribution of noradrenergic varicosities in rat cortex. *J Comp Neurol*, 1;521(10):2195-207

Akiskal HS (2000). Mood disorders: introduction and overview. *In Comprehensive Textbook of Psychiatry, B.J. Sadock and V.A. Sadock, eds. (New York: Lippincott, Williams & Wilkins)*, pp. 1284-1298

Aller MI, Veale Linden AM, Sandu C, Schwaninger M, Evans LJ et al. (2005). Modifying the subunit composition of TASK channels alters the modulation of a leak conductance in cerebellar granule neurons. *J Neurosci*, 7;25(49):11455-67

Alonso R, Griebel G, Pavone G, Stemmelin J, Le Fur G, Soubrié P (2004). Blockade of CRF(1) or V(1b) receptors reverses stress-induced suppression of neurogenesis in a mouse model of depression. *Mol Psychiatry*, 9(3):278-86

Alonso SJ, Arevalo R, Afonso D, Rodríguez M (1991). Effects of maternal stress during pregnancy on forced swimming test behavior of the offspring. *Physiol Behav*, 7;25(49):11455-67

Altieri SC, Garcia-Garcia AL, Leonardo ED, Andrews AM (2013). Rethinking 5-HT1A receptors: emerging modes of inhibitory feedback of relevance to emotion-related behavior. *ACS Chem Neurosci*, 16;4(1):72-83

Alural B, Genc S, Haggarty SJ (2016). Diagnostic and therapeutic potential of microRNAs in neuropsychiatric disorders: Past, present, and future. *Prog Neuropsychopharmacol Biol Psychiatry*, Epub ahead of print

Amargós-Bosch M, Bortolozzi A, Puig MV, Serrats J, Adell A, Celada P et al. (2004). Co-expression and in vivo interaction of serotonin1A and serotonin2A receptors in pyramidal neurons of prefrontal cortex. *Cereb Cortex*, 14(3):281-99

Antoni FA (1986). Hypothalamic control of adrenocorticotropin secretion: advances since the discovery of 41-residue corticotropin-releasing factor. *Endocr Rev*, 7(4):351-78

Anttila SA and Leinonen EV (2001). A review of the pharmacological and clinical profile of mirtazapine. *CNS Drug Rev*, 7(3):249-64

Aoki C, Go CG, Venkatesan C, Kurose H (1994). Perikaryal and synaptic localization of alpha 2A-adrenergic receptor-like immunoreactivity. *Brain Res*, 11;650(2):181-204

Araneda R and Andrade R (1991). 5-Hydroxytryptamine2 and 5-hydroxytryptamine 1A receptors mediate opposing responses on membrane excitability in rat association cortex. *Neuroscience*, 40(2):399-412

Araneda R, Gysling K, Calas A (1999). Raphe serotonergic neurons projecting to the olfactory bulb contain galanin or somatostatin but not neurotensin. *Brain Res Bull*, 49(3):209-14

Arango V, Ernsberger P, Sved AF, Mann JJ (1993). Quantitative autoradiography of alpha 1- and alpha 2-adrenergic receptors in the cerebral cortex of controls and suicide victims. *Brain Res*, 10;630(1-2):271-82

Arborelius L, Owens MJ, Plotsky PM, Nemeroff CB (1999). The role of corticotropin-releasing factor in depression and anxiety disorders. *J Endocrinol*, 160(1):1-12

Ardayfio P and Kim KS. (2006). Anxiogenic-like effect of chronic corticosterone in the light-dark emergence task in mice. *Behav Neurosci*, 120(2):249-56

Artigas F (1993). 5-HT and antidepressants: new views from microdialysis studies. *Trends Pharmacol Sci*, 14(7):262

Artigas F, Perez V, Alvarez E (1994). Pindolol induces a rapid improvement of depressed patients treated with serotonin reuptake inhibitors. *Arch Gen Psychiatry*, 51(3):248-51

Artigas F, Romero L, de Montigny C, Blier P (1996). Acceleration of the effect of selected antidepressant drugs in major depression by 5-HT1A antagonists. *Trends Neurosci,* 19(9):378-83

Artigas F (2013). Serotonin receptors involved in antidepressant effects. *Pharmacol Ther*, 137(1):119-31

Artigas F (2015). Developments in the field of antidepressants, where do we go now? *Eur Neuropsychopharmacol*, 25(5):657-70

Aston-Jones G and Bloom FE (1981). Activity of norepinephrine-containing locus coeruleus neurons in behaving rats anticipates fluctuations in the sleep-waking cycle. *J Neurosci*, 1(8):876-86

Aston-Jones G, Shipley MT, Chouvet G, Ennis M, van Bockstaele E, Pieribone V et al. (1991). Afferent regulation of locus coeruleus neurons: anatomy, physiology and pharmacology. *Prog Brain Res*, 88:47-75

Aston-Jones G, Zhu Y, Card JP (2004). Numerous GABAergic afferents to locus ceruleus in the pericerulear dendritic zone: possible interneuronal pool. *J Neurosci*, 3;24(9):2313-21

B

Baker KG, Halliday GM, Törk I (1990). Cytoarchitecture of the human dorsal raphe nucleus. *J Comp Neurol*, 8;301(2):147-61

Baker M (2010). RNA interference: Homing in on delivery. *Nature*, 22;464(7292):1225-8

Bang H, Kim Y, Kim D (2000). TREK-2, a new member of the mechanosensitive tandem-pore K+ channel family. *J Biol Chem*, 9;275(23):17412-9

Barbee JG, Conrad EJ, Jamhour NJ (2004). The effectiveness of olanzapine, risperidone, quetiapine, and ziprasidone as augmentation agents in treatment-resistant major depressive disorder. *J Clin Psychiatry*, 65(7):975-81

Barnes NM and Sharp T (1999). A review of central 5-HT receptors and their function. *Neuropharmacolgy*, 38(8):1083-152

Bartel DP (2004). MicroRNAs: genomics, biogenesis, mechanism, and function. *Cell*, 23;116(2):281-93

Bartlett DW and Davis ME (2007). Effect of siRNA nuclease stability on the in vitro and in vivo kinetics of siRNA-mediated gene silencing. *Biotechnol Bioeng*, 1;97(4):909-21

Baudry A, Mouillet-Richard S, Schneider B, Launay JM, Kellermann O (2010). miR-16 targets the serotonin transporter: a new facet for adaptive responses to antidepressants. *Science*, 17;329(5998):1537-41

Bayliss DA, Umemiya M, Berger AJ (1995). Inhibition of N- and P-type calcium currents and the after-hyperpolarization in rat motoneurones by serotonin. *J Physiol*, 485(Pt 3):635-47

Bayliss DA, Talley EM, Sirois JE, Lei Q (2001). TASK-1 is a highly modulated pH-sensitive 'leak' K(+) channel expressed in brainstem respiratory neurons. *Respir Physiol*, 129(1-2):159-74

Bayliss DA and Barrett PQ (2008). Emerging roles for two-pore-domain potassium channels and their potential therapeutic impact. *Trends Pharmacol Sci*, 29(11):566-75

Behlke MA (2008). Chemical modification of siRNAs for in vivo use. *Oligonucleotides*, 18(4):305-19

Becker C, Zeau B, Rivat C, Blugeot A, Hamon M, Benoliel JJ (2008). Repeated social defeat-induced depression-like behavioral and biological alterations in rats: involvement of cholecystokinin. *Mol Psychiatry*, 13(12):1079-92

Bekar L, Libionka W, Tian GF, Xu Q, Torres A, Wang X et al. (2008). Adenosine is crucial for deep brain stimulation-mediated attenuation of tremor. *Nat Med*, 14(1):75-80

Benmansour S, Cecchi M, Morilak DA, Gerhardt GA, Javors MA, Gould GG et al. (1999). Effects of chronic antidepressant treatments on serotonin transporter function, density, and mRNA level. *J Neurosci*, 1;19(23):10494-501

Benmansour S, Owens WA, Cecchi M, Morilak DA, Frazer A (2002). Serotonin clearance in vivo is altered to a greater extent by antidepressant-induced downregulation of the serotonin transporter than by acute blockade of this transporter. *J Neurosci*, 1;22(15):6766-72

Benmansour S, Altamirano AV, Jones DJ, Sanchez TA, Gould GG, Pardon MC et al. (2004). Regulation of the norepinephrine transporter by chronic administration of antidepressants. *Biol Psychiatry*, 1;55(3):313-6

Berg AP, Talley EM, Manger JP, Bayliss DA (2004). Motoneurons express heteromeric TWIK-related acid-sensitive K+ (TASK) channels containing TASK-1 (KCNK3) and TASK-3 (KCNK9) subunits. *J Neurosci*, 28;24(30):6693-702

Berman RM, Cappiello A, Anand A, Oren DA, Heninger GR, Charney DS et al. (2000). Antidepressant effects of ketamine in depressed patients. *Biol Psychiatry*, 215;47(4):351-4

Berman RM, Marcus RN, Swanink R, McQuade RD, Carson WH, Corey-Lisle PK et al. (2007). The efficacy and safety of aripiprazole as adjunctive therapy in major depressive disorder: a multicenter, randomized, double-blind, placebo-controlled study. *J Clin Psychiatry*, 68(6):843-53

Berridge CW and Waterhouse BD (2003). The locus coeruleus-noradrenergic system: modulation of behavioral state and state-dependent cognitive processes. *Brain Res Rev*, 42(1):33-84

Berton O and Nestler EJ (2006). New approaches to antidepressant drug discovery: beyond monoamines. *Nat Rev Neurosci*, 7(2):137-51

Berton, McClung CA, Dileone RJ, Krishnan V, Renthal W, Russo SJ (2006). Essential role of BDNF in the mesolimbic dopamine pathway in social defeat stress. *Science*, 10;311(5762):864-8

Bittner S, Budde T, Wiendl H, Meuth SG (2010). From the background to the spotlight: TASK channels in pathological conditions. *Brain Pathol*, 20(6):999-1009

Blakely RD, De Felice LJ, Hartzell HC (1994). Molecular physiology of norepinephrine and serotonin transporters. *J Exp Biol*, 196:263-81

Blazer DG (2000). Mood disorders: epidemiology. *In Comprehensive Textbook of Psychiatry, B.J. Sadock and V.A. Sadock, eds. (New York: Lippincott, Williams & Wilkins)*, pp. 1298-1308

Blier P and de Montigny C (1994). Current advances and trends in the treatment of depression. *Trends Pharmacol Sci*, 15(7):220-6

Blier P and de Bergeron (1995). Effectiveness of pindolol with selected antidepressant drugs in the treatment of major depression. *J Clin Psychopharmacol*, 15(3):217-22

Blier P, Pineyro G, el Mansari M, Bergeron R, de Montigny C (1998). Role of somatodendritic 5-HT autoreceptors in modulating 5-HT neurotransmission. *Ann N Y Acad Sci*, 15;861:204-16

Blier P and de Montigny C (1999). Serotonin and drug-induced therapeutic responses in major depression, obsessive-compulsive and panic disorders. *Neuropsychopharmacolgy*, 21(2 Suppl):91S-98S

Bockenhauer D, Zilberberg N, Goldstein SA (2001). KCNK2: reversible conversion of a hippocampal potassium leak into a voltage-dependent channel. *Nat Neurosci*, 4(5):486-91

Bogdan R, Fitzgibbon H, Woolverton WL, Bethea CL, Iyo AH, Stockmeier CA et al. (2011). 5-HTTLPR genotype and gender, but not chronic fluoxetine administration, are associated with cortical TREK1 protein expression in rhesus macaques. *Neurosci Lett*, 3;503(2):83-6

Boldrini M, Underwood MD, Hen R, Rosoklija GB, Dwork AJ, John Mann J et al. (2009). Antidepressants increase neural progenitor cells in the human hippocampus. *Neuropsychopharmacology*, 34(11):2376-89

Boldrini M, Hen R, Underwood MD, Rosoklija GB, Dwork AJ, Mann JJ et al. (2012). Hippocampal angiogenesis and progenitor cell proliferation are increased with antidepressant use in major depression. *Biol Psychiatry*, 1;72(7):562-71

Borsotto M, Veyssiere J, Moha Ou Maati H, Devader C, Mazella J, Heurteaux C (2015). argeting two-pore domain K(+) channels TREK-1 and TASK-3 for the treatment of depression: a new therapeutic concept. *Br J Pharmacol*, 172(3):771-84

Bortolozzi A and Artigas F (2003). Control of 5-hydroxytryptamine release in the dorsal raphe nucleus by the noradrenergic system in rat brain. Role of alpha-adrenoceptors. *Neuropsychopharmacology*, 28(3):421-34

Bortolozzi A, Castañé A, Semakova J, Santana N, Alvarado G, Cortés R et al. (2012). Selective siRNA-mediated suppression of 5-HT1A autoreceptors evokes strong anti-depressant-like effects. *Mol Psychiatry*, 17(6):612-23

Bortolozzi A, Celada P, Artigas F (2014). Novel therapeutic strategies in major depression: focus on RNAi and ketamine. *Curr Pharm Des*, 20(23):3848-60

Boudreau RL, Rodríguez-Lebrón E, Davidson BL (2011). RNAi medicine for the brain: progresses and challenges. *Hum Mol Genet*, 15;20(R1):R21-7

Boudreau RL and Davidson BL (2010). RNAi therapeutics for CNS disorders. *Brain Res*, 18;1338:112-21

Boudreau RL and Davidson BL (2012). Generation of hairpin-based RNAi vectors for biological and therapeutic application. *Methods Enzymol*, 507:275-96

Braasch DA, Paroo Z, Constantinescu A, Ren G, Oz OK, Mason RP et al. (2004). Biodistribution of phosphodiester and phosphorothioate siRNA. *Bioorg Med Chem Lett*, 8;14(5):1139-43

Brodie BB, Olin JS, Kuntzman RG, Shore PA (1957). Possible interrelationship between release of brain norepinephrine and serotonin by reserpine. *Science*, 28;125(3261):1293-4

Brow P and Molliver ME (2000). Dual serotonin (5-HT) projections to the nucleus accumbens core and shell: relation of the 5-HT transporter to amphetamine-induced neurotoxicity. *J Neurosci*, 1;20(5):1952-63

Brummelkamp TR, Bernards R, Agami R (2002). A system for stable expression of short interfering RNAs in mammalian cells. *Science*, 19;296(5567):550-3

Burch RM, Luini A, Axelrod J (1986). Phospholipase A2 and phospholipase C are activated by distinct GTP-binding proteins in response to alpha 1-adrenergic stimulation in FRTL5 thyroid cells. *Proc Natl Acad Sci U S A*, 83(19):7201-5

Bylund DB, Eikenberg DC, Hieble JP, Langer SZ, Lefkowitz RJ, Minneman KP et al. (1994). International Union of Pharmacology nomenclature of adrenoceptors. *Pharmacol Rev*, 46(2):121-36

C

Cadaveira-Mosquera A, Ribeiro SJ, Reboreda A, Pérez M, Lamas JA (2011). Activation of TREK currents by the neuroprotective agent riluzole in mouse sympathetic neurons. *J Neurosci,* 26;31(4):1375-85

Carlezon WA Jr and Thomas MJ (2009). Biological substrates of reward and aversion: a nucleus accumbens activity hypothesis. *Neuropharmacology*, 56 Suppl 1:122-32

Carvalho AF, Machado JR, Cavalcante JL (2009). Augmentation strategies for treatment-resistant depression. *Curr Opin Psychiatry*, 22(1):7-12

Caspi A, Sugden K, Moffitt TE, Taylor A, Craig IW, Harrington H et al. (2003). Influence of life stress on depression: moderation by a polymorphism in the 5-HTT gene. *Science*, 18;301(5631):386-9

Cedarbaum JM and Aghajanian GK (1978). Afferent projections to the rat locus coeruleus as determined by a retrograde tracing technique*. J Comp Neurol*, 1;178(1):1-16

Celada P, Puig M, Casanovas JM, Guillazo G, Artigas F (2001). Control of dorsal raphe serotonergic neurons by the medial prefrontal cortex: Involvement of serotonin-1A, GABA(A), and glutamate receptors*. J Neurosci*, 15;21(24):9917-29

Celada P, Casanovas JM, Paez X, Artigas F (2002). Control of serotonergic neurons in the dorsal raphe nucleus by the lateral hypothalamus*. Brain Res*, 5;932(1-2):79-90

Celada P, Bortolozzi A, Artigas F (2013). Serotonin 5-HT1A receptors as targets for agents to treat psychiatric disorders: rationale and current status of research*. CNS Drugs*, 27(9):703-16

Chalk AM, Wahlestedt C, Sonnhammer EL (2004). Improved and automated prediction of effective siRNA*. Biochem Biophys Res Commun*, 18;319(1):264-74

Chaouloff F (2013). Social stress models in depression research: what do they tell us? *Cell Tissue Res*, 354(1):179-90

Chemin J, Girard C, Duprat F, Lesage F, Romey G, Lazdunski M (2003). Mechanisms underlying excitatory effects of group I metabotropic glutamate receptors via inhibition of 2P domain K+ channels. *EMBO J*, 15;22(20):5403-11

Chen B, Dowlatshahi D, MacQueen GM, Wang JF, Young LT (2001). Increased hippocampal BDNF immunoreactivity in subjects treated with antidepressant medication. *Biol Psychiatry*, 15;50(4):260-5

Chen H, Zuo D, Zhang J, Zhou M, Ma L (2014). Classification of 2-pore domain potassium channels based on rectification under quasi-physiological ionic conditions. *Channels (Austin)*, 8(6):503-8

Chen X, Talley EM, Patel N, Gomis A, McIntire WE, Dong B et al. (2006). Inhibition of a background potassium channel by Gq protein alpha-subunits. *Proc Natl Acad Sci U S A*, 28;103(9):3422-7

Chourbaji S, Zacher C, Sanchis-Segura C, Dormann C, Vollmayr B, Gass P (2005). Learned helplessness: validity and reliability of depressive-like states in mice. *Brain Res Brain Res Protoc*, 16(1-3):70-8

Citó MC, Silva MI, Santos LK, Fernandes ML, Melo FH, Aguiar JA et al. (2015). Antidepressant-like effect of Hoodia gordonii in a forced swimming test in mice: evidence for involvement of the monoaminergic system. *Braz J Med Biol Res*, 48(1):57-64

Coburn CA, Luo Y, Cui M, Wang J, Soll R, Dong J et al. (2012). Discovery of a pharmacologically active antagonist of the two-pore-domain potassium channel K2P9.1 (TASK-3). *ChemMedChem*, 2;7(1):123-33

Cohen A, Whitfield TW, Kreifeldt M, Koebel P, Kieffer BL, Contet C et al. (2014). Virus-mediated shRNA knockdown of prodynorphin in the rat nucleus accumbens attenuates depression-like behavior and cocaine locomotor sensitization. *PLoS One*, 9;9(5):e97216

Conti B, Maier R, Barr AM, Morale MC, Lu X, Sanna PP et al. (2007). Region-specific transcriptional changes following the three antidepressant treatments electro convulsive therapy, sleep deprivation and fluoxetine. *Mol Psychiatry*, 12(2):167-89

Cook SC and Wellman CL (2004). Chronic stress alters dendritic morphology in rat medial prefrontal cortex. *J Neurobiol*, 60(2):236-48

Coppen A, Shaw DM, Farrell JP (1963). Potentiation of the antidepressive effect of a monoamine-oxidase inhibitor by tryptophan. *Lancet*, 12;1(7272):79-81

Coppen A. (1967). The biochemistry of affective disorders. *Br J Psychiatry*, 113(504):1237-64

Cotter D, Mackay D, Chana G, Beasley C, Landau S, Everall IP (2002). Reduced neuronal size and glial cell density in area 9 of the dorsolateral prefrontal cortex in subjects with major depressive disorder. *Cereb Cortex*, 12(4):386-94

Cryan JF and Lucki I (2000). Antidepressant-like behavioral effects mediated by 5-Hydroxytryptamine(2C) receptors. *J Pharmacol Exp Ther*, 295(3):1120-6

Cryan JF, Mombereau C, Vassout A (2005a). The tail suspension test as a model for assessing antidepressant activity: review of pharmacological and genetic studies in mice. *Neurosci Biobehav Rev*, 29(4-5):571-625

Cryan JF, Valentino RJ, Lucki I (2005b). Assessing substrates underlying the behavioral effects of antidepressants using the modified rat forced swimming test. *Neurosci Biobehav Rev*, 29(4-5):547-69

Cryan JF and Holmes A (2005). The ascent of mouse: advances in modelling human depression and anxiety. *Nat Rev Drug Discov*, 4(9):775-90

Cryan JF and Slattery DA (2007). Animal models of mood disorders: recent developments. *Curr Opin Psychiatry*, 20(1):1-7

Cryan JF, Thakker DR, Hoyer D (2007). Emerging use of non-viral RNA interference in the brain. *Biochem Soc Trans*, 35(Pt 2):411-5

Cunha MP, Pazini FL, Oliveira Á, Bettio LE, Rosa JM, Machado DG et al. (2013). The activation of α1-adrenoceptors is implicated in the antidepressant-like effect of creatine in the tail suspension test. *Prog Neuropsychopharmacol Biol Psychiatry*, 1;44:39-50

Czéh B and Lucassen PJ (2007). What causes the hippocampal volume decrease in depression? Are neurogenesis, glial changes and apoptosis implicated? *Eur Arch Psychiatry Clin Neurosci*, 257(5):250-60

Czirják G and Enyedi P (2002). Formation of functional heterodimers between the TASK-1 and TASK-3 two-pore domain potassium channel subunits. *J Biol Chem*, 15;277(7):5426-32

Czirják G and Enyedi P (2003). Ruthenium red inhibits TASK-3 potassium channel by interconnecting glutamate 70 of the two subunits. *Mol Pharmacol*, 63(3):646-52

D

Dahlstroem A and Fuxe K (1964). Evidence for the existence of monoamine-containing neurons in the central nervous system. I. Demonstration of monoamines in the cell bodies of brain stem neurons. *Acta Physiol Scand Suppl,* Suppl 232:1-55

Dalley JW and Stanford SC (1995). Contrasting effects of the imidazol(in)e alpha 2-adrenoceptor agonists, medetomidine, clonidine and UK 14,304 on extraneuronal levels of noradrenaline in the rat frontal cortex: evaluation using in vivo microdialysis and synaptosomal uptake studies. *Br J Pharmacol,* 114(8):1717-23

David DJ, Samuels BA, Rainer Q, Wang JW, Marsteller D, Mendez I et al. (2009). Neurogenesis-dependent and -independent effects of fluoxetine in an animal model of anxiety/depression. *Neuron*, 28;62(4):479-93

David DJ, Wang J, Samuels BA, Rainer Q, David I, Gardier AM et al. (2010). Implications of the functional integration of adult-born hippocampal neurons in anxiety-depression disorders. *Neuroscientist*, 16(5):578-91

Deacon RM (2006). Digging and marble burying in mice: simple methods for in vivo identification of biological impacts. *Nat Protoc*, 1(1):122-4

de Almeida J and Mengod G (2008). Serotonin 1A receptors in human and monkey prefrontal cortex are mainly expressed in pyramidal neurons and in a GABAergic interneuron subpopulation: implications for schizophrenia and its treatment. *J Neurochem*, 107(2):488-96

de Kloet ER, Joëls M, Holsboer F (2005). Stress and the brain: from adaptation to disease. *Nat Rev Neurosci*, 6(6):463-75

de Montigny C (1977). Neurophysiology and current trends in research on depression. Remarks on the monoaminergic hypothesis of depression. *Union Med Can*, 106(6):805-10

Dennis T, L'Heureux R, Carter C, Scatton B (1987). Presynaptic alpha-2 adrenoceptors play a major role in the effects of idazoxan on cortical noradrenaline release (as measured by in vivo dialysis) in the rat. *J Pharmacol Exp Ther*, 241(2):642-9

Diaz SL, Doly S, Narboux-Nême N, Fernández S, Mazot P, Banas SM et al. (2012). 5-HT(2B) receptors are required for serotonin-selective antidepressant actions. *Mol Psychiatry*, 17(2):154-63

Diazgranados N, Ibrahim L, Brutsche NE, Newberg A, Kronstein P, Khalife S et al. (2010). A randomized add-on trial of an N-methyl-D-aspartate antagonist in treatment-resistant bipolar depression. *Arch Gen Psychiatry*, 67(8):793-802

Dillon DG, Bogdan R, Fagerness J, Holmes AJ, Perlis RH, Pizzagalli DA (2010). Variation in TREK1 gene linked to depression-resistant phenotype is associated with potentiated neural responses to rewards in humans. *Hum Brain Mapp*, 31(2):210-21

Doench JG, Petersen CP, Sharp PA (2003). siRNAs can function as miRNAs. *Genes Dev*, 15;17(4):438-42

Dorr AE and Debonnel G (2006). Effect of vagus nerve stimulation on serotonergic and noradrenergic transmission. *J Pharmacol Exp Ther*, 318(2):890-8

Doyle DA, Morais Cabral J, Pfuetzner RA, Kuo A, Gulbis JM, Cohen SL et al. (1998). The structure of the potassium channel: molecular basis of K+ conduction and selectivity. *Science*, 3;280(5360):69-77

Dranovsky A and Hen R (2006). Hippocampal neurogenesis: regulation by stress and antidepressants. *Biol Psychiatry*, 15;59(12):1136-43

Drevets WC (2001). Neuroimaging and neuropathological studies of depression: implications for the cognitive-emotional features of mood disorders. *Curr Opin Neurobiol*, 11(2):240-9

Drevets WC, Thase ME, Moses-Kolko EL, Price J, Frank E, Kupfer DJ et al. (2007). Serotonin-1A receptor imaging in recurrent depression: replication and literature review. *Nucl Med Biol*, 34(7):865-77

Drevets WC and Furey ML (2010). Replication of scopolamine's antidepressant efficacy in major depressive disorder: a randomized, placebo-controlled clinical trial. *Biol Psychiatry*, 1;67(5):432-8

Dukart J (2014). Electroconvulsive therapy-induced brain plasticity determines therapeutic outcome in mood disorders. *Proc Natl Acad Sci U S A*, 21;111(3):1156-61

Duman RS, Heninger GR, Nestler EJ (1997). A molecular and cellular theory of depression. *Arch Gen Psychiatry*, 54(7):597-606

Duman RS, Malberg J Nakagawa S, D'Sa C (2000). Neuronal plasticity and survival in mood disorders. *Biol Psychiatry*, 15;48(8):732-9

Duman RS, Malberg J, Nakagawa S (2001). Regulation of adult neurogenesis by psychotropic drugs and stress. *J Pharmacol Exp Ther*, 299(2):401-7

Duman RS (2004). Role of neurotrophic factors in the etiology and treatment of mood disorders. *Neuromolecular Med*, 5(1):11-25

Duman RS and Aghajanian GK (2012). Synaptic dysfunction in depression: potential therapeutic targets. *Science*, 5;338(6103):68-72

Duman RS, Li N, Liu RJ, Duric V, Aghajanian G (2012). Signaling pathways underlying the rapid antidepressant actions of ketamine. *Neuropharmacology*, 62(1):35-41

Duman RS (2014). Neurobiology of stress, depression, and rapid acting antidepressants: remodeling synaptic connections. *Depress Anxiety*, 31(4):291-6

Duman RS, Aghajanian GK, Sanacora G, Krystal JH (2016). Synaptic plasticity and depression: new insights from stress and rapid-acting antidepressants. *Nat Med*, 22(3):238-49

Dupart F, Lesage, Fink M, Reyes R, Heurteaux C, Lazdunski M (1997). TASK, a human background K+ channel to sense external pH variations near physiological pH. *EMBO J*, 1;16(17):5464-71

Dwivedi Y, Rao JS, Rizavi HS, Kotowski J, Conley RR, Roberts RC et al. (2003). Abnormal expression and functional characteristics of cyclic adenosine monophosphate response element binding protein in postmortem brain of suicide subjects. *Arch Gen Psychiatry*, 60(3):273-82

Dwivedi Y (2016). Pathogenetic and therapeutic applications of microRNAs in major depressive disorder. *Prog Neuropsychopharmacol Biol Psychiatry*, 4;64:341-8

Dykxhoorn DM and Lieberman J (2006). Knocking down disease with siRNAs. *Cell*, 28;126(2):231-5

E

Eagle A, Mazei-Robison M, Robison AJ (2016). Sucrose Preference Test to Measure Stress-induced Anhedonia. *Bio-protocol*, 6(11): e1822

Elbashir SM, Harborth J, Lendeckel W, Yalcin A, Weber K, Tuschl T (2001). Duplexes of 21-nucleotide RNAs mediate RNA interference in cultured mammalian cells. *Nature*, 24;411(6836):494-8

Enkel T, Spanagel R, Vollmayr B, Schneider M (2010). Stress triggers anhedonia in rats bred for learned helplessness. *Behav Brain Res*, 1;209(1):183-6

Enyeart JJ, Danthi SJ, Liu H, Enyeart JA (2005). Angiotensin II inhibits bTREK-1 K+ channels in adrenocortical cells by separate Ca2+- and ATP hydrolysis-dependent mechanisms. *J Biol Chem*, 2;280(35):30814-28

Enyedi P and Czirják G (2010). Molecular background of leak K+ currents: two-pore domain potassium channels. *Physiol Rev*, 90(2):559-605

F

Fabre V, Boutrel B, Hanoun N, Lanfumey L, Fattaccini CM, Demeneix B et al. (2000). Homeostatic regulation of serotonergic function by the serotonin transporter as revealed by nonviral gene transfer. *J Neurosci*, 1;20(13):5065-75

Fakra E, Hyde LW, Gorka A, Fisher PM, Muñoz KE, Kimak M et al. (2009). Effects of HTR1A C(-1019)G on amygdala reactivity and trait anxiety. *Arch Gen Psychiatry*, 66(1):33-40

Fendt M, Schmid S, Thakker DR, Jacobson LH, Yamamoto R, Mitsukawa K et al. (2008). mGluR7 facilitates extinction of aversive memories and controls amygdala plasticity. *Mol Psychiatry*, 13(10):970-9

Ferrés-Coy A, Santana N, Castañé A, Cortés R, Carmona MC, Toth M et al. (2013a). Acute 5-HT_1A autoreceptor knockdown increases antidepressant responses and serotonin release in stressful conditions. *Psychopharmacology (Berl)*, 225(1):61-74

Ferrés-Coy A, Pilar-Cuellar F, Vidal R, Paz V, Masana M, Cortés R et al. (2013b). RNAi-mediated serotonin transporter suppression rapidly increases serotonergic neurotransmission and hippocampal neurogenesis. *Transl Psychiatry*, 15;3:e211

Ferrés-Coy A, Galofré M, Pilar-Cuéllar F, Vidal R, Paz V, Ruiz-Bronchal E et al. (2016). Therapeutic antidepressant potential of a conjugated siRNA silencing the serotonin transporter after intranasal administration. *Mol Psychiatry*, 21(6):328-38

Fink M, Duprat F, Lesage F, Reyes R, Romey G, Heurteaux C et al. (1996). Cloning, functional expression and brain localization of a novel unconventional outward rectifier K+ channel. *EMBO J*, 16;15(24):6854-62

Fire A, Xu S, Montgomery MK, Kostas SA, Driver SE, Mello CC (1998). Potent and specific genetic interference by double-stranded RNA in Caenorhabditis elegans. *Nature*, 19;391(6669):806-11

Foote SL, Bloom, Aston-Jones G (1983). Nucleus locus ceruleus: new evidence of anatomical and physiological specificity. *Physiol Rev*, 63(3):844-914

Francis D, Diorio J, Liu D, Meaney MJ (1999). Nongenomic transmission across generations of maternal behavior and stress responses in the rat. *Science*, 5;286(5442):1155-8

Frodl T, Schüle C, Schmitt G, Born C, Baghai T, Zill P et al. (2007). Association of the brain-derived neurotrophic factor Val66Met polymorphism with reduced hippocampal volumes in major depression. *Arch Gen Psychiatry*, 64(4):410-6

Fuchs E and Gould E (2000). Mini-review: in vivo neurogenesis in the adult brain: regulation and functional implications. *Eur J Neurosci*, 12(7):2211-4

Fulmer T (2010). Revoking serotonin's auto license. SciBX, 3(5)

Furey ML and Drevets WC (2006). Antidepressant efficacy of the antimuscarinic drug scopolamine: a randomized, placebo-controlled clinical trial. *Arch Gen Psychiatry*, 63(10):1121-9

G

Gaglione M and Messere A (2010). Recent progress in chemically modified siRNAs. *Mini Rev Med Chem*, 10(7):578-95

Gao X and Zhang P (2007). Transgenic RNA interference in mice. *Physiology (Bethesda)*, 22:161-6

Gardier AM, Malagie I, Trillat AC, Jacquot C, Artigas F (1996). Role of 5-HT1A autoreceptors in the mechanism of action of serotoninergic antidepressant drugs: recent findings from in vivo microdialysis studies. *Fundam Clin Pharmacol*, 10(1):16-27

Gaynes BN, Lloyd SW, Lux L, Gartlehner G, Hansen RA, Brode S et al. (2014). Repetitive transcranial magnetic stimulation for treatment-resistant depression: a systematic review and meta-analysis. *J Clin Psychiatry*, 75(5):477-89

Ghasemi M, Raza M, Dehpour AR (2010). NMDA receptor antagonists augment antidepressant-like effects of lithium in the mouse forced swimming test. *J Psychopharmacol*, 24(4):585-94

Gobbi G, Bambico FR, Mangieri R, Bortolato M, Campolongo P, Solinas M et al. (2005). Antidepressant-like activity and modulation of brain monoaminergic transmission by blockade of anandamide hydrolysis. *Proc Natl Acad Sci U S A*, 20;102(51):18620-5

Gold PW and Chrousos GP (1985). Clinical studies with corticotropin releasing factor: implications for the diagnosis and pathophysiology of depression, Cushing's disease, and adrenal insufficiency. *Psychoneuroendocrinology*, 10(4):401-19

Gordon JA and Hen R (2006). TREKing toward new antidepressants. *Nat Neurosci*, 9(9):1081-3

Gotter AL, Santarelli VP, Doran SM, Tannenbaum PL, Kraus RL, Rosahl TW et al. (2011). TASK-3 as a potential antidepressant target. *Brain Res*, 6;1416:69-79

Gould E, McEwen BS, Tanapat P, Galea LA, Fuchs E (1997). Neurogenesis in the dentate gyrus of the adult tree shrew is regulated by psychosocial stress and NMDA receptor activation. *J Neurosci*, 1;17(7):2492-8

Gould E, Tanapat P, McEwen BS, Flügge G, Fuchs E (1998). Proliferation of granule cell precursors in the dentate gyrus of adult monkeys is diminished by stress. *Proc Natl Acad Sci U S A*, 17;95(6):3168-71

Gould GG, Pardon MC, Morilak DA, Frazer A (2003). Regulatory effects of reboxetine treatment alone, or following paroxetine treatment, on brain noradrenergic and serotonergic systems. *Neuropsychopharmacology*, 28(9):1633-41

Gourley SL, Wu FJ, Kiraly DD, Ploski JE, Kedves AT, Duman RS et al. (2008). Regionally specific regulation of ERK MAP kinase in a model of antidepressant-sensitive chronic depression. *Biol Psychiatry*, 15;63(4):353-9

Gourley SL and Taylor JR (2009). Recapitulation and reversal of a persistent depression-like syndrome in rodents. *Curr Protoc Neurosci*, Chapter 9: Unit 9.32

Graff CL and Pollack GM (2005). Nasal drug administration: potential for targeted central nervous system delivery. *J Pharm Sci*, 94(6):1187-95

Gross C, Zhuang X, Stark K, Ramboz S, Oosting R, Kirby L (2002). Serotonin1A receptor acts during development to establish normal anxiety-like behaviour in the adult. *Nature*, 28;416(6879):396-400

Gustavsson A, Svensson M, Jacobi F, Allgulander C, Alonso J, Beghi E et al. (2011). Cost of disorders of the brain in Europe 2010. *Eur Neuropsychopharmacol*, 21(10):718-79

H

Haddjeri N, Blier P, de Montigny C (1998). Long-term antidepressant treatments result in a tonic activation of forebrain 5-HT1A receptors. *J Neurosci*, 1;18(23):10150-6

Haenisch B, Herms S, Mattheisen M, Steffens M, Breuer R, Strohmaier J et al. (2013). Genome-wide association data provide further support for an association between 5-HTTLPR and major depressive disorder. *J Affect Disord*, 25;146(3):438-40

Hajos M, Hajos-Korcsok E, Sharp T (1999). Role of the medial prefrontal cortex in 5-HT1A receptor-induced inhibition of 5-HT neuronal activity in the rat. *Br J Pharmacol*, 126(8):1741-50

Hamani C, Diwan M, Macedo CE, Brandão ML, Shumake J, Gonzalez-Lima F et al. (2010). Antidepressant-like effects of medial prefrontal cortex deep brain stimulation in rats. *Biol Psychiatry*, 15;67(2):117-24

Hamidi M, Drevets WC, Price JL (2004). RNA interference. *Nature*, 11;418(6894):244-51

Hannon GJ (2002). Glial reduction in amygdala in major depressive disorder is due to oligodendrocytes. *Biol Psychiatry*, 15;55(6):563-9

Harrison JK, Pearson WR, Lynch KR (1991). Molecular characterization of alpha 1- and alpha 2-adrenoceptors. *Trends Pharmacol Sci*, 12(2):62-7

Hashizume R, Ozawa T, Gryaznov SM, Bollen AW, Lamborn KR, Frey WH 2nd et al. (2008). New therapeutic approach for brain tumors: Intranasal delivery of telomerase inhibitor GRN163. *Neuro Oncol*, 10(2):112-20

He M, Liu, Y, Wang X, Zhang MQ, Hannon GJ, Huang ZJ (2012). Cell-type-based analysis of microRNA profiles in the mouse brain. *Neuron*, 12;73(1):35-48

Heim C and Nemeroff CB (2001). The role of childhood trauma in the neurobiology of mood and anxiety disorders: preclinical and clinical studies. *Biol Psychiatry*, 15;49(12):1023-39

Herman JP and Cullinan WE (1997). Neurocircuitry of stress: central control of the hypothalamo-pituitary-adrenocortical axis. *Trends Neurosci*, 20(2):78-84

Hervas I and Artigas F (1998). Effect of fluoxetine on extracellular 5-hydroxytryptamine in rat brain. Role of 5-HT autoreceptors. *Eur J Pharmacol*, 25;358(1):9-18

Hervas I, Queiroz CM, Adell A, Artigas F (2000). Role of uptake inhibition and autoreceptor activation in the control of 5-HT release in the frontal cortex and dorsal hippocampus of the rat. *Br J Pharmacol*, 130(1):160-6

Heurteaux C, Lucas G, Guy N, El Yacoubi M, Thümmler S, Peng XD et al. (2006). Deletion of the background potassium channel TREK-1 results in a depression-resistant phenotype. *Nat Neurosci*, 9(9):1134-41

Hines DJ, Schmitt LI, Hines RM, Moss SJ, Haydon PG (2013). Antidepressant effects of sleep deprivation require astrocyte-dependent adenosine mediated signaling. *Transl Psychiatry*, 15;3:e212

Hollon SD, Thase ME, Markowitz JC (2002). Treatment and Prevention of Depression. *Psychol Sci Public Interest*, 3(2):39-77

Holsboer F (2001). Stress, hypercortisolism and corticosteroid receptors in depression: implications for therapy. *J Affect Disord*, 62(1-2):77-91

Holsboer F and Ising M (2008). Central CRH system in depression and anxiety--evidence from clinical studies with CRH1 receptor antagonists. *Eur J Pharmacol*, 7;583(2-3):350-7

Holtmaat A and Svoboda K (2009). Experience-dependent structural synaptic plasticity in the mammalian brain. *Nat Rev Neurosci*, 10(9):647-58

Homayoun H and Moghaddam B (2007). NMDA receptor hypofunction produces opposite effects on prefrontal cortex interneurons and pyramidal neurons. *J Neurosci*, 24;27(43):11496-500

Honoré E (2007). The neuronal background K2P channels: focus on TREK1. *Nat Rev Neurosci*, 8(4):251-61

Hornung V, Guenthner-Biller M, Bourquin C, Ablasser A, Schlee M, Uematsu S et al. (2005). Sequence-specific potent induction of IFN-alpha by short interfering RNA in plasmacytoid dendritic cells through TLR7. *Nat Med*, 11(3):263-70

Hoyer D and Martin G (1997). 5-HT receptor classification and nomenclature: towards a harmonization with the human genome. *Neuropharmacology*, 36(4-5):419-28

Huang YY, Oquendo MA, Friedman JM, Greenhill LL, Brodsky B, Malone KM et al. (2003). Substance abuse disorder and major depression are associated with the human 5-HT1B receptor gene (HTR1B) G861C polymorphism. *Neuropsychopharmacology*, 28(1):163-9

Huot P, Fox SH, Brotchie JM (2011). The serotonergic system in Parkinson's disease. *Prog Neurobiol*, 95(2):163-212

Humphreys DT, Westman BJ, Martin DI, Preiss T (2005). MicroRNAs control translation initiation by inhibiting eukaryotic initiation factor 4E/cap and poly(A) tail function. *Proc Natl Acad Sci U S A*, 22;102(47):16961-6

Hwang EM, Kim E, Yarishkin O, Woo DH, Han KS, Park N et al. (2014). A disulphide-linked heterodimer of TWIK-1 and TREK-1 mediates passive conductance in astrocytes. *Nat Commun*, 5:3227

I

Im HI and Kenny PJ (2012). MicroRNAs in neuronal function and dysfunction. *Trends Neurosci*, 35(5):325-34

Inta D, Lima-Ojeda JM, Lau T, Tang W, Dormann C, Sprengel R et al. (2013). Electroconvulsive therapy induces neurogenesis in frontal rat brain areas. *PLoS One*, 26;8(7):e69869

Ishola IO, Ochieng CO, Olayemi SO, Jimoh MO, Lawal SM (2014). Potential of novel phytoecdysteroids isolated from Vitex doniana in the treatment depression: involvement of monoaminergic systems. *Pharmacol Biochem Behav*, 127:90-100

J

Jackson AL, Burchard J, Schelter J, Chau BN, Cleary M, Lim L et al. (2006). Widespread siRNA "off-target" transcript silencing mediated by seed region sequence complementarity. *RNA*, 12(7):1179-87

Jacobs BL and Azmitia EC (1992). Structure and function of the brain serotonin system. *Physiol Rev*, 72(1):165-229

Jacobs BL, van Praag H, Gage FH (2000). Adult brain neurogenesis and psychiatry: a novel theory of depression. *Mol Psychiatry*, 5(3):262-9

Janicak PG and Dokucu ME (2015). Transcranial magnetic stimulation for the treatment of major depression. *Neuropsychiatr Dis Treat*, 26;11:1549-60

Jiang W, Zhang Y, Xiao L, Van Cleemput J, Ji SP, Bai G et al. (2005). Cannabinoids promote embryonic and adult hippocampus neurogenesis and produce anxiolytic- and antidepressant-like effects. *J Clin Invest*, 115(11):3104-16

Jiménez-Sánchez L, Castañé A, Pérez-Caballero L, Grifoll-Escoda M, López-Gil X, Campa L et al. (2016a). Activation of AMPA Receptors Mediates the Antidepressant Action of Deep Brain Stimulation of the Infralimbic Prefrontal Cortex. *Cereb Cortex*, 26(6):2778-89

Jiménez-Sánchez L, Linge R, Campa L, Valdizán EM, Pazos A, Díaz A, et al (2016b). Behavioral, neurochemical and molecular changes after acute deep brain stimulation of the infralimbic prefrontal cortex. *Neuropharmacology*, 108:91-102

Jindal A, Mahesh R, Bhatt S (2013). Etazolate rescues behavioral deficits in chronic unpredictable mild stress model: modulation of hypothalamic-pituitary-adrenal axis activity and brain-derived neurotrophic factor level. *Neurochem Int*, 63(5):465-75

Jodo E and Aston-Jones G (1997). Activation of locus coeruleus by prefrontal cortex is mediated by excitatory amino acid inputs. *Brain Res*, 12;768(1-2):327-32

Johnson DA, Gartside SE, Ingram CD (2002). 5-HT1A receptor-mediated autoinhibition does not function at physiological firing rates: evidence from in vitro electrophysiological studies in the rat dorsal raphe nucleus. *Neuropharmacology*, 43(6):959-65

Jones BE and Moore RY (1977). Ascending projections of the locus coeruleus in the rat. II. Autoradiographic study. *Brain Res*, 20;127(1):25-53

Judge AD, Sood V, Shaw JR, Fang D, McClintock K, MacLachlan I (2005). Sequence-dependent stimulation of the mammalian innate immune response by synthetic siRNA. *Nat Biotechnol*, 23(4):457-62

Juhasz G, Hullam G, Eszlari N, Gonda X, Antal P, Anderson IM et al. (2014). Brain galanin system genes interact with life stresses in depression-related phenotypes. *Proc Natl Acad Sci U S A*, 22;111(16):E1666-73

Juliano R, Alam MR, Dixit V, Kang H (2008). Mechanisms and strategies for effective delivery of antisense and siRNA oligonucleotides. *Nucleic Acids Res*, 36(12):4158-71

Juliano RL, Carver K, Cao C, Ming X (2013). Receptors, endocytosis, and trafficking: the biological basis of targeted delivery of antisense and siRNA oligonucleotides. *J Drug Target*, 21(1):27-43

Juliano RL and Carver K (2015). Cellular uptake and intracellular trafficking of oligonucleotides. *Adv Drug Deliv Rev*, 29;87:35-45

K

Kalén P, Skagerberg G, Lindvall O (1988). Projections from the ventral tegmental area and mesencephalic raphe to the dorsal raphe nucleus in the rat. Evidence for a minor dopaminergic component. *Exp Brain Res* 73(1):69-77

Kang HJ, Voleti B, Hajszan T, Rajkowska G, Stockmeier CA, Licznerski P et al. (2012). Decreased expression of synapse-related genes and loss of synapses in major depressive disorder. *Nat Med*, 18(9):1413-7

Karege F, Vaudan G, Schwald M, Perroud N, La Harpe R (2005). Neurotrophin levels in postmortem brains of suicide victims and the effects of antemortem diagnosis and psychotropic drugs. *Brain Res Mol Brain Res*, 20;136(1-2):29-37

Karg K, Burmeister M, Shedden K, Sen S (2011). The serotonin transporter promoter variant (5-HTTLPR), stress, and depression meta-analysis revisited: evidence of genetic moderation. *Arch Gen Psychiatry*, 68(5):444-54

Kaufman J, Plotsky PM, Nemeroff CB, Charney DS (2000). Effects of early adverse experiences on brain structure and function: clinical implications. *Biol Psychiatry*, 15;48(8):778-90

Kaufman J and Charney D (2001). Effects of early stress on brain structure and function: implications for understanding the relationship between child maltreatment and depression. *Dev Psychopathol*, 13(3):451-71

Kayser S, Bewernick BH, Grubert C, Hadrysiewicz BL, Axmacher N, Schlaepfer TE (2011). Antidepressant effects, of magnetic seizure therapy and electroconvulsive therapy, in treatment-resistant depression. *J Psychiatr Res*, 45(5):569-76

Kayser S, Bewernick BH, Matusch A, Hurlemann R, Soehle M, Schlaepfer TE (2015). Magnetic seizure therapy in treatment-resistant depression: clinical, neuropsychological and metabolic effects. *Psychol Med*, 45(5):1073-92

Keller MB, McCullough JP, Klein DN, Arnow B, Dunner DL, Gelenberg AJ et al. (2000). A comparison of nefazodone, the cognitive behavioral-analysis system of psychotherapy, and their combination for the treatment of chronic depression. *N Engl J Med*, 18;342(20):1462-70

Kendler KS (1998). Anna-Monika-Prize paper. Major depression and the environment: a psychiatric genetic perspective. *Pharmacopsychiatry*, 31(1):5-9

Kendler KS, Neale MC, Sullivan P, Corey LA, Gardner CO, Prescott CA (1999). A population-based twin study in women of smoking initiation and nicotine dependence. *Psychol Med*, 29(2):299-308

Kennedy SH, Giacobbe P, Rizvi SJ, Placenza FM, Nishikawa Y, Mayberg HS et al. (2011). Deep brain stimulation for treatment-resistant depression: follow-up after 3 to 6 years. *Am J Psychiatry*, 168(5):502-10

Kennard LE, Chumbley JR, Ranatunga KM, Armstrong SJ, Veale EL, Mathie A (2005). Inhibition of the human two-pore domain potassium channel, TREK-1, by fluoxetine and its metabolite norfluoxetine. *Br J Pharmacol*, 144(6):821-9

Kessler RC (1997). The effects of stressful life events on depression. *Annu Rev Psychol*, 48:191-214

Khalid N, Atkins M, Tredget J, Giles M, Champney-Smith K, Kirov G (2008). The effectiveness of electroconvulsive therapy in treatment-resistant depression: a naturalistic study. *J ECT*, 24(2):141-5

Kim Y, Bang H, Kim D (2000). TASK-3, a new member of the tandem pore K(+) channel family. *J Biol Chem*, 31;275(13):9340-7

Kino T and Chrousos GP (2005). Glucocorticoid effects on gene expression; in Steckler T, Kalin NH, Reul JMHM (eds): handbook of stress and the brain. Amsterdam, Elsevier, pp 295-311

Kinoshita A, Shigemoto R, Ohishi H, van der Putten H, Mizuno N (1998). Immunohistochemical localization of metabotropic glutamate receptors, mGluR7a and mGluR7b, in the central nervous system of the adult rat and mouse: a light and electron microscopic study. *J Comp Neurol*, 13;393(3):332-52

Kirouac GJ, Li S, Mabrouk G (2004). GABAergic projection from the ventral tegmental area and substantia nigra to the periaqueductal gray region and the dorsal raphe nucleus. *J Comp Neurol*, 2;469(2):170-84

Kiyashchenko LI, Mileykovskiy BY, Maidment N, Lam HA, Wu MF, John J et al. (2002). Release of hypocretin (orexin) during waking and sleep states. *J Neurosci*, 1;22(13):5282-6

Kosik KS (2006). The neuronal microRNA system. *Nat Rev Neurosci*, 7(12):911-20

Kosinski CM, Risso Bradley S, Conn PJ, Levey AI, Landwehrmeyer GB, Penney JB Jr et al. (1999). Localization of metabotropic glutamate receptor 7 mRNA and mGluR7a protein in the rat basal ganglia. *J Comp Neurol*, 13;415(2):266-84

Kosofsky BE and Molliver ME (1987). The serotoninergic innervation of cerebral cortex: different classes of axon terminals arise from dorsal and median raphe nuclei. *Synapse*, 1(2):153-68

Kovacs M, Rush AJ, Beck AT, Hollon SD (1981). Depressed outpatients treated with cognitive therapy or pharmacotherapy. A one-year follow-up. *Arch Gen Psychiatry*, 38(1):33-9

Krichevsky AM, Sonntaq KC, Isacson O, Kosik KS (2006). Specific microRNAs modulate embryonic stem cell-derived neurogenesis. *Stem Cells*, 24(4):857-64

Krishnan V and Nestler EJ (2008). The molecular neurobiology of depression. *Nature*, 16;455(7215):894-902

Krol J, Loedige I, Filipowicz W (2010). The widespread regulation of microRNA biogenesis, function and decay. *Nat Rev Genet*, 11(9):597-610

Kudryavtseva NN, Bakshtanovskaya IV, Koryakina LA (1991). Social model of depression in mice of C57BL/6J strain. *Pharmacol Biochem Behav*, 38(2):315-20

Kugaya A and Sanacora G (2005). Beyond monoamines: glutamatergic function in mood disorders. *CNS Spectr*, 10(10):808-19

Kumar P, Wu H, McBride JL, Jung KE, Kim MH, Davidson BL et al. (2007). Transvascular delivery of small interfering RNA to the central nervous system. *Nature*, 5;448(7149):39-43

Kuteeva E, Hökfelt T, Ogren SO (2005). Behavioural characterisation of transgenic mice overexpressing galanin under the PDGF-B promoter. *Neuropeptides*, 39(3):299-304

L

Ladd CO, Owens MJ, Nemeroff CB (1996). Persistent changes in corticotropin-releasing factor neuronal systems induced by maternal deprivation. *Endocrinology*, 137(4):1212-8

Lanfumey L and Hamon M (2000). Central 5-HT(1A) receptors: regional distribution and functional characteristics. *Nucl Med Biol*, 27(5):429-35

Lang UE, Hellweg R, Kalus P, Bajbouj M, Lenzen KP, Sander T et al. (2005). Association of a functional BDNF polymorphism and anxiety-related personality traits. *Psychopharmacology (Berl)*, 180(1):95-9

Langer SZ (2015). alfa2-Adrenoceptors in the treatment of major neuropsychiatric disorders. *Trends Pharmacol Sci*, 36(4):196-202

Lapidus KA, Levitch CF, Perez AM, Brallier JW, Parides MK, Soleimani L et al. (2014). A randomized controlled trial of intranasal ketamine in major depressive disorder. *Biol Psychiatry*, 15;76(12):970-6

Lau T, Horschitz S, Berger S, Bartsch D, Schloss P (2008). Antidepressant-induced internalization of the serotonin transporter in serotonergic neurons. *FASEB J*, 22(6):1702-14

Le François B, Czesak M, Steubl D, Albert PR (2008). Transcriptional regulation at a HTR1A polymorphism associated with mental illness. *Neuropharmacology*, 55(6):977-85

Lee A, Rosin DL, Van Bockstaele EJ (1998). alpha2A-adrenergic receptors in the rat nucleus locus coeruleus: subcellular localization in catecholaminergic dendrites, astrocytes, and presynaptic axon terminals. *Brain Res*, 8;795(1-2):157-69

Lee BH, Kim H, Park SH, Kim YK (2007). Decreased plasma BDNF level in depressive patients. *J Affect Disord*, 101(1-3):239-44

Lee HY, Kim YK (2008). Plasma brain-derived neurotrophic factor as a peripheral marker for the action mechanism of antidepressants. *Neuropsychobiology*, 57(4):194-9

Lee Y, Ahn C et al. (2003). The nuclear RNase III Drosha initiates microRNA processing. *Nature*, 25;425(6956):415-9

Lee Y, Kim M, Han J, Choi H, Kim J, Yim J et al. (2004). MicroRNA genes are transcribed by RNA polymerase II. *EMBO J*, 13;23(20):4051-60

Lefkowitz RJ and Caron MG (1988). Adrenergic receptors. Models for the study of receptors coupled to guanine nucleotide regulatory proteins. *J Biol Chem*, 15;263(11):4993-6

Lemonde S, Turecki G, Bakish D, Du L, Hrdina PD, Bown CD et al. (2003). Impaired repression at a 5-hydroxytryptamine 1A receptor gene polymorphism associated with major depression and suicide. *J Neurosci*, 24;23(25):8788-99

Lemonde S, Du L, Bakish D, Hrdina P, Albert PR (2004). Association of the C(-1019)G 5-HT1A functional promoter polymorphism with antidepressant response. *Int J Neuropsychopharmacol*, 7(4):501-6

Lesage F, Guillemare E, Fink M, Duprat F, Lazdunski M, Romey G et al. (1996). TWIK-1, a ubiquitous human weakly inward rectifying K+ channel with a novel structure. *EMBO J*, 1;15(5):1004-11

Lesage F and Lazdunski M (2000). Molecular and functional properties of two-pore-domain potassium channels. *Am J Physiol Renal Physiol*, 279(5):F793-801

Lesage F Terrenoire C, Romey G, Lazdunski M (2000). Human TREK2, a 2P domain mechano-sensitive K+ channel with multiple regulations by polyunsaturated fatty acids, lysophospholipids, and Gs, Gi, and Gq protein-coupled receptors. *J Biol Chem*, 15;275(37):28398-405

Lesch KP, Bengel D, Heils A, Sabol SZ, Greenberg BD, Petri S et al. (1996). Association of anxiety-related traits with a polymorphism in the serotonin transporter gene regulatory region. *Science*, 29;274(5292):1527-31

Lesch KP (2004). Gene-environment interaction and the genetics of depression. *J Psychiatry Neurosci*, 29(3):174-84

Levitt P and Moore RY (1978). Noradrenaline neuron innervation of the neocortex in the rat. *Brain Res*, 13;139(2):219-31

Levitz J, Royal P, Comoglio Y, Wdzjekonski B, Schaub S, Clemens DM et al. (2016). Heterodimerization within the TREK channel subfamily produces a diverse family of highly regulated potassium channels. *Proc Natl Acad Sci U S A*, 12;113(15):4194-9

Levkovitz Y, Harel EV, Roth Y, Braw Y, Most D, Katz LN et al. (2009). Deep transcranial magnetic stimulation over the prefrontal cortex: evaluation of antidepressant and cognitive effects in depressive patients. *Brain Stimul*, 2(4):188-200

Li N, Lee B, Liu RJ, Banasr M, Dwyer JM, Iwata M et al. (2010). mTOR-dependent synapse formation underlies the rapid antidepressant effects of NMDA antagonists. *Science*, 20;329(5994):959-64

Li Y, Luikart BW, Birnbaum S, Chen J, Kwon CH, Kernie SG et al. (2008). TrkB regulates hippocampal neurogenesis and governs sensitivity to antidepressive treatment. *Neuron*, 14;59(3):399-412

Licinio J, Dong C, Wong ML (2009). Novel sequence variations in the brain-derived neurotrophic factor gene and association with major depression and antidepressant treatment response. *Arch Gen Psychiatry*, 66(5):488-97

Lin S and Gregory RI (2015). MicroRNA biogenesis pathways in cancer. *Nat Rev Cancer*, 15(6):321-33

Liotti M and Mayberg HS (2001). The role of functional neuroimaging in the neuropsychology of depression. *J Clin Exp Neuropsychol*, 23(1):121-36

Lipscombe D, Kongsamut S, Tsien RW (1989). Alpha-adrenergic inhibition of sympathetic neurotransmitter release mediated by modulation of N-type calcium-channel gating. *Nature*, 24;340(6235):639-42

Lisanby SH, Luber B, Schlaepfer TE, Sackeim HA (2003). Safety and feasibility of magnetic seizure therapy (MST) in major depression: randomized within-subject comparison with electroconvulsive therapy. *Neuropsychopharmacology*, 28(10):1852-65

Liu RJ, Fuchikami M, Dwyer JM, Lepack AE, Duman RS, Aghajanian GK (2013). GSK-3 inhibition potentiates the synaptogenic and antidepressant-like effects of subthreshold doses of ketamine. *Neuropsychopharmacology*, 38(11):2268-77

Lochhead JJ, Wolak DJ, Pizzo ME, Thorne RG (2015). Rapid transport within cerebral perivascular spaces underlies widespread tracer distribution in the brain after intranasal administration. *J Cereb Brood Flow Metab*, 35(3):371-81

Lopes CM, Rohács T, Czirják G, Balla T, Enyedi P, Logothetis DE (2005). PIP2 hydrolysis underlies agonist-induced inhibition and regulates voltage gating of two-pore domain K+ channels. *J Physiol*, 1;564(Pt 1):117-29

Loughlin SE, Foote SL, Grzanna R (1986). Efferent projections of nucleus locus coeruleus: morphologic subpopulations have different efferent targets. *Neuroscience*, 18(2):307-19

Lucas G, Rymar VV, Du J, Mnie-Filali O, Bisgaard C, Manta S et al. (2007). Serotonin(4) (5-HT(4)) receptor agonists are putative antidepressants with a rapid onset of action. *Neuron*, 6;55(5):712-25

Lyons MJ, Eisen SA, Goldberg J, True W, Lin N, Meyer JM et al. (1998). A registry-based twin study of depression in men. *Arch Gen Psychiatry*, 55(5):468-72

M

Maccari S, Darnaudery M, Morley-Fletcher S, Zuena AR, Cinque C, Van Reeth O (2003). Prenatal stress and long-term consequences: implications of glucocorticoid hormones. *Neurosci Biobehav Rev*, 27(1-2):119-27

Maccari S and Morley-Fletcher S (2007). Effects of prenatal restraint stress on the hypothalamus-pituitary-adrenal axis and related behavioural and neurobiological alterations. *Psychoneuroendocrinology*, 32 Suppl 1:S10-5

Madsen TM, Treschow A, Bengzon J, Bolwig TG, Lindvall O, Tingström A (2000). Increased neurogenesis in a model of electroconvulsive therapy. *Biol Psychiatry*, 15;47(12):1043-9

Maingret F, Lauritzen I, Patel AJ, Heurteaux C, Reyes R, Lesage F et al. (2000). TREK-1 is a heat-activated background K(+) channel. *EMBO J*, 1;19(11):2483-91

Maingret F, Patel AJ, Lazdunski M, Honoré E (2001). The endocannabinoid anandamide is a direct and selective blocker of the background K(+) channel TASK-1. *EMBO J*, 15;20(1-2):47-54

Makeyev EV, Zhang J, Carrasco MA, Maniatis T (2007). The MicroRNA miR-124 promotes neuronal differentiation by triggering brain-specific alternative pre-mRNA splicing. *Mol Cell*, 3;27(3):435-48

Malberg JE and Duman RS (2003). Cell proliferation in adult hippocampus is decreased by inescapable stress: reversal by fluoxetine treatment. *Neuropsychopharmacology*, 28(9):1562-71

Malhi GS, Moore J, McGuffin P (2000). The genetics of major depressive disorder. *Curr Psychiatry Rep*, 2(2):165-9

Malone DA Jr, Dougherty DD, Rezai AR, Carpenter LL, Friehs GM, Eskandar EN et al. (2009). Deep brain stimulation of the ventral capsule/ventral striatum for treatment-resistant depression. *Biol Psychiatry*, 15;65(4):267-75

Mamounas LA, Mullen CA, O'Hearn E, Molliver ME (1991). Dual serotoninergic projections to forebrain in the rat: morphologically distinct 5-HT axon terminals exhibit differential vulnerability to neurotoxic amphetamine derivatives. *J Comp Neurol*, 15;314(3):558-86

Manji HK, Drevets WC, Charney DS (2001). The cellular neurobiology of depression. *Nat Med*, 7(5):541-7

Mannoury la Cour C, Boni C, Hanoun N, Lesch KP, Hamon M, Lanfumey L (2001). Functional consequences of 5-HT transporter gene disruption on 5-HT(1a) receptor-mediated regulation of dorsal raphe and hippocampal cell activity. *J Neurosci*, 15;21(6):2178-85

Marinc C, Preisig-Müller R, Prüss H, Derst C, Veh RW (2011). Immunocytochemical localization of TASK-3 (K(2P)9.1) channels in monoaminergic and cholinergic neurons. *Cell Mol Neurobiol*, 31(2):323-35

Martin KF, Phillips I, Hearson M, Prow MR, Heal DJ (1992). Characterization of 8-OH-DPAT-induced hypothermia in mice as a 5-HT1A autoreceptor response and its evaluation as a model to selectively identify antidepressants. *Br J Pharmacol*, 107(1):15-21

Mateo Y and Meana JJ (1999). etermination of the somatodendritic alpha2-adrenoceptor subtype located in rat locus coeruleus that modulates cortical noradrenaline release in vivo. *Eur J Pharmacol*, 20;379(1):53-7

Mathie A (2007). Neuronal two-pore-domain potassium channels and their regulation by G protein-coupled receptors. *J Physiol*, 15;578(Pt 2):377-85

Mathie A, Al-Moubarak E, Veale EL (2010). Gating of two pore domain potassium channels. *J Physiol*, 1;588(Pt 17):3149-56

Mayberg HS, Lozano AM, Voon V, McNeely HE, Seminowicz D, Hamani C et al. (2005). Deep brain stimulation for treatment-resistant depression. *Neuron*, 3;45(5):651-60

Mazella J, Pétrault O, Lucas G, Deval E, Béraud-Dufour S, Gandin C et al. (2010). Spadin, a sortilin-derived peptide, targeting rodent TREK-1 channels: a new concept in the antidepressant drug design. *PLoS Biol*, 13;8(4):e1000355

McEwen BS (1999). Stress and hippocampal plasticity. *Ann Rev Neurosci*, 22:105-22

McGuffin P, Katz R, Watkins S, Rutherford J (1999). A hospital-based twin register of the heritability of DSM-IV unipolar depression. *Arch Gen Psychiatry*, 53(2):129-36

McGuffin P, Rijsdijk F, Andrew M, Sham P, Katz R, Cardno A (2003). The heritability of bipolar affective disorder and the genetic relationship to unipolar depression. *Arch Gen Psychiatry*, 60(5):497-502

McQuade R and Sharp T (1997). Functional mapping of dorsal and median raphe 5-hydroxytryptamine pathways in forebrain of the rat using microdialysis. *J Neurochem*, 69(2):791-6

McNeely HE, Mayberg HS, Lozano AM, Kennedy SH (2008). Neuropsychological impact of Cg25 deep brain stimulation for treatment-resistant depression: preliminary results over 12 months. *J Nerv Ment Dis*, 196(5):405-10

Meadows HJ and Randall AD (2001). Functional characterisation of human TASK-3, an acid-sensitive two-pore domain potassium channel. *Neuropharmacology*, 40(4):551-9

Meana JJ, Barturen F, García-Sevilla JA (1992). Alpha 2-adrenoceptors in the brain of suicide victims: increased receptor density associated with major depression. *Biol Psychiatry*, 1;31(5):471-90

Menard J and Treit D (1999). Effects of centrally administered anxiolytic compounds in animal models of anxiety. *Neurosci Biobehav Rev*, 23(4):591-613

Millón C, Flores-Burgess A, Narváez M, Borroto-Escuela DO, Santín L, Parrado C et al. (2014). A role for galanin N-terminal fragment (1-15) in anxiety- and depression-related behaviors in rats. *Int J Neuropsychopharmacol*, 31;18(3)

Mineur YS, Belzung C, Crusio WE (2006). Effects of unpredictable chronic mild stress on anxiety and depression-like behavior in mice. *Behav Brain Res*, 25;175(1):43-50

Mineur YS, Obayemi A, Wigestrand MB, Fote GM, Calarco CA, Li AM et al. (2013). Cholinergic signaling in the hippocampus regulates social stress resilience and anxiety- and depression-like behavior. *Proc Natl Acad Sci U S A*, 110(9):3573-8

Mineur YS, Taylor SR, Picciotto MR (2014). Calcineurin downregulation in the amygdala is sufficient to induce anxiety-like and depression-like behaviors in C57BL/6J male mice. *Biol Psychiatry*, 15;75(12):991-8

Ming X, Alam MR, Fisher M, Yan Y, Chen X, Juliano RL (2010). Intracellular delivery of an antisense oligonucleotide via endocytosis of a G protein-coupled receptor. *Nucleic Acids Res*, 38(19):6567-76

Mirkovic K, Palmersheim J, Lesage F, Wickman K (2012). Behavioral characterization of mice lacking Trek channels. *Front Behav Neurosci*, 7;6:60

Moore RY and Bloom FE (1979). Central catecholamine neuron systems: anatomy and physiology of the norepinephrine and epinephrine systems. *Annu Rev Neurosci*, 2:113-68

Mork A, Pehrson A, Brennum LT, Nielsen SM, Zhong H, Lassen AB (2012). Pharmacological effects of Lu AA21004: a novel multimodal compound for the treatment of major depressive disorder. *J Pharmacol Exp Ther*, 340(3):666-75

Moss EG and Taylor JM (2003). Small-interfering RNAs in the radar of the interferon system. *Nat Cell Biol*, 5(9):771-2

Murakami S, Imbe H, Morikawa Y, Kubo C, Senba E (2005). Chronic stress, as well as acute stress, reduces BDNF mRNA expression in the rat hippocampus but less robustly. *Neurosci Res*, 53(2):129-39

Murbartián J, Lei Q, Sando JJ, Bayliss DA (2005). Sequential phosphorylation mediates receptor- and kinase-induced inhibition of TREK-1 background potassium channels. *J Biol Chem*, 26;280(34):30175-84

Murphy BE (1991). Steroids and depression. *J Steroid Biochem Mol Biol*, 38(5):537-59

Murphy DL and Lesch KP (2008). Targeting the murine serotonin transporter: insights into human neurobiology. *Nat Rev Neurosci*, 9(2):85-96

Murphy DL, Fox MA, Timpano KR, Moya PR, Ren-Patterson R, Andrews AM et al. (2008). How the serotonin story is being rewritten by new gene-based discoveries principally related to SLC6A4, the serotonin transporter gene, which functions to influence all cellular serotonin systems. *Neuropharmacology*, 55(6):932-60

Murphy GM Jr, Hollander SB, Rodrigues HE, Kremer C, Schatzberg AF (2004). Effects of the serotonin transporter gene promoter polymorphism on mirtazapine and paroxetine efficacy and adverse events in geriatric major depression. *Arch Gen Psychiatry*, 61(11):1163-9

Murray CJ, Vos T, Lozano R, Naghavi M, Flaxman AD Michaud C et al. (2012). Disability-adjusted life years (DALYs) for 291 diseases and injuries in 21 regions, 1990-2010: a systematic analysis for the Global Burden of Disease Study 2010. *Lancet*, 15;380(9859):2197-223

Murray F, Smith DW, Hutson PH (2008). Chronic low dose corticosterone exposure decreased hippocampal cell proliferation, volume and induced anxiety and depression like behaviours in mice. *Eur J Pharmacol*, 31;583(1):115-27

Murrough JW, Collins KA, Fields J, DeWilde KE, Phillips ML, Mathew SJ et al. (2015). Regulation of neural responses to emotion perception by ketamine in individuals with treatment-resistant major depressive disorder. *Transl Psychiatry*, 17;5:e509

Muscat R and Willner P (1992). Suppression of sucrose drinking by chronic mild unpredictable stress: a methodological analysis. *Neurosci Biobehav Rev*, 16(4):507-17

N

Nahas Z, Marangell LB, Husain MM, Rush AJ, Sackeim HA, Lisanby SH et al. (2005). Two-year outcome of vagus nerve stimulation (VNS) for treatment of major depressive episodes. *J Clin Psychiatry*, 66(9):1097-104

Nakamura K (2013). The role of the dorsal raphé nucleus in reward-seeking behavior. *Front Integr Neurosci*, 27;7:60

Neff CD, Abkevich V, Packer JC, Chen Y, Potter J, Riley R et al. (2009). Evidence for HTR1A and LHPP as interacting genetic risk factors in major depression. *Mol Psychiatry*, 14(6):621-30

Nemeroff CB, Heim CM, Thase ME, Klein DN, Rush AJ, Schatzberg AF et al. (2003). Differential responses to psychotherapy versus pharmacotherapy in patients with chronic forms of major depression and childhood trauma. *Proc Natl Acad Sci U S A*, 25;100(24):14293-6

Nestler EJ (2014). Epigenetic mechanisms of depression. *JAMA Psychiatry*, 71(4):454-6

Nestler EJ, Barrot M, DiLeone RJ, Eisch AJ, Gold SJ, Monteggia LM (2002). Neurobiology of Depression. *Neuron*, 28;34(1):13-25

Nibuya M, Morinobu S, Duman RS (1995). Regulation of BDNF and trkB mRNA in rat brain by chronic electroconvulsive seizure and antidepressant drug treatments. *J Neurosci*, 15(11):7539-47

Nibuya M, Takahashi M, Russell DS, Duman RS (1999). Repeated stress increases catalytic TrkB mRNA in rat hippocampus. *Neurosci Lett*, 28;267(2):81-4

Nobler MS, Luber B, Moeller JR, Katzman GP, Prudic J, Devanand DP et al. (2000). Quantitative EEG during seizures induced by electroconvulsive therapy: relations to treatment modality and clinical features. I. Global analyses. *J ECT*, 16(3):211-28

Nollet M, Le Guisquet AM, Belzung C (2013). Models of depression: unpredictable chronic mild stress in mice. *Curr Protoc Pharmacol*, Chapter 5:Unit 5.65

North RA and Yoshimura M (1984). The actions of noradrenaline on neurones of the rat substantia gelatinosa in vitro. *J Physiol*, 349:43-55

Nowakowski RS, Lewin SB, Miller MW (1989). Bromodeoxyuridine immunohistochemical determination of the lengths of the cell cycle and the DNA-synthetic phase for an anatomically defined population. *J Neurocytol*, 18(3):311-8

O

O'Connor RM, Finger BC, Flor PJ, Cryan JF (2010). Metabotropic glutamate receptor 7: at the interface of cognition and emotion. *Eur J Pharmacol*, 10;639(1-3):123-31

O'Leary OF and Cryan JF (2013). Towards translational rodent models of depression. *Cell Tissue Res*, 354(1):141-53

Ohishi H, Nomura S, Ding YQ, Shigemoto R, Wada E, Kinoshita A et al. (1995). Presynaptic localization of a metabotropic glutamate receptor, mGluR7, in the primary afferent neurons: an immunohistochemical study in the rat. *Neurosci Lett*, 29;202(1-2):85-8

Olpe HR and Steinmann M (1991). Responses of locus coeruleus neurons to neuropeptides. *Prog Brain Res*, 88:241-8

Ongür D, Drevets WC, Price JL (1998). Glial reduction in the subgenual prefrontal cortex in mood disorders. *Proc Natl Acad Sci U S A*, 27;95(22):13290-5

Ota KT and Duman RS (2013). Environmental and pharmacological modulations of cellular plasticity: role in the pathophysiology and treatment of depression. *Neurobiol Dis*, 57:28-37

Outhred T, Das P, Dobson-Stone C, Felmingham KL, Bryant RA, Nathan PJ et al. (2014). The impact of 5-HTTLPR on acute serotonin transporter blockade by escitalopram on emotion processing: preliminary findings from a randomised, crossover fMRI study. *Aust N Z J Psychiatry*, 48(12):1115-25

Overmier JB and Seligman ME (1967). Effects of inescapable shock upon subsequent escape and avoidance responding. *J Comp Physiol Psychol*, 63(1):28-33

Ozcan G, Ozpolat B, Coleman RL, Sood AK, Lopez-Berestein G (2015). Preclinical and clinical development of siRNA-based therapeutics. *Adv Drug Deliv Rev*, 29;87:108-19

Ozpolat B, Sood AK, Lopez-Berestein G (2010). Nanomedicine based approaches for the delivery of siRNA in cancer. *J Intern Med*, 267(1):44-53

P

Paddison PJ, Caudy AA, Hannon GJ (2002). Stable suppression of gene expression by RNAi in mammalian cells. *Proc Natl Acad Sci U S A*, 5;99(3):1443-8

Pandey GN, Ren X, Rizavi HS, Conley RR, Roberts RC, Dwivedi Y (2006). Brain-derived neurotrophic factor and tyrosine kinase B receptor signalling in post-mortem brain of teenage suicide victims. *Int J Neuropsychopharmacol*, 11(8):1047-61

Park JE, Heo I, Tian Y, Simanshu DK, Chang H, Jee D et al. (2011). Dicer recognizes the 5' end of RNA for efficient and accurate processing. *Nature*, 13;475(7355):201-5

Park MR (1987). Monosynaptic inhibitory postsynaptic potentials from lateral habenula recorded in dorsal raphe neurons. *Brain Res Bull*, 19(5):581-6

Parker KJ, Schatzberg AF, Lyons DM (2003). Neuroendocrine aspects of hypercortisolism in major depression. *Horm Behav*, 43(1):60-6

Parks CL, Robinson PS, Sibille E, Shenk T, Toth M (1998). Increased anxiety of mice lacking the serotonin1A receptor. *Proc Natl Acad Sci U S A*, 1;95(18):10734-9

Parsey RV, Olvet DM, Oquendo MA, Huang YY, Ogden RT, Mann JJ (2006). Higher 5-HT1A receptor binding potential during a major depressive episode predicts poor treatment response: preliminary data from a naturalistic study. *Neuropsychopharmacology*, 31(8):1745-9

Patel AJ, Honoré E, Maingret F, Lesage F, Fink M, Duprat F et al. (1998). A mammalian two pore domain mechano-gated S-like K+ channel. *EMBO J*, 3;17(15):4283-90

Paul IA and Skolnick P (2003). Glutamate and depression: clinical and preclinical studies. *Ann N Y Acad Sci,* 1003:250-72

Pazos A and Palacios JM (1985). Quantitative autoradiographic mapping of serotonin receptors in the rat brain. I. Serotonin-1 receptors. *Brain Res*, 4;346(2):205-30

Peña CJ, Bagot RC, Labonté B, Nestler EJ (2014). Epigenetic signaling in psychiatric disorders. *J Mol Biol*, 9;426(20):3389-412

Perez V, Gilaberte I, Faries D, Alvarez E, Artigas F (1997). Randomised, double-blind, placebo-controlled trial of pindolol in combination with fluoxetine antidepressant treatment. *Lancet*, 31;349(9065):1594-7

Perez-Caballero L, Pérez-Egea R, Romero-Grimaldi C, PuigdemontD, Molet J, Caso JR et al. (2014). Early responses to deep brain stimulation in depression are modulated by anti-inflammatory drugs. *Mol Psychiatry*, 19(5):607-14

Perlis RH, Moorjani P, Fagerness J, Purcell S, Trivedi MH, Fava M et al. (2008). Pharmacogenetic analysis of genes implicated in rodent models of antidepressant response: association of TREK1 and treatment resistance in the STAR(*)D study. *Neuropsychopharmacology*, 33(12):2810-9

Peyron C, Petit JM, Rampon C, Jouvet M, Luppi PH (1998a). Forebrain afferents to the rat dorsal raphe nucleus demonstrated by retrograde and anterograde tracing methods. *Neuroscience*, 82(2):443-68

Peyron C, Tighe DK, van den Pol AN, de Lecea L, Heller HC, Sutcliffe JG et al. (1998b). Neurons containing hypocretin (orexin) project to multiple neuronal systems. *J Neurosci*, 1;18(23):9996-10015

Pham K, Nacher J, Hof PR, McEwen BS (2003). Repeated restraint stress suppresses neurogenesis and induces biphasic PSA-NCAM expression in the adult rat dentate gyrus. *Eur J Neurosci*, 17(4):879-86

Pickel VAM and Chan J (1999). Ultrastructural localization of the serotonin transporter in limbic and motor compartments of the nucleus accumbens. *J Neurosci*, 1;19(17):7356-66

Pinder RM and Van Delft AM (1983). The potential therapeutic role of the enantiomers and metabolites of mianserin. *Br J Clin Pharmacol*, 15 Suppl 2:269S-276S

Piñeyro G and Blier P (1999). Autoregulation of serotonin neurons: role in antidepressant drug action. *Pharmacol Rev*, 51(3):533-91

Pittenger C and Duman RS (2008). Stress, depression, and neuroplasticity: a convergence of mechanisms. *Neuropsychopharmacology*, 33(1):88-109

Pollak DD, Rey CE, Monje FJ (2010). Rodent models in depression research: classical strategies and new directions. *Ann Med*, 6;42(4):252-64

Pollak Dorocic I, Fürth D, Xuan Y, Johansson Y, Pozzi L, Silberberg G et al. (2014). A whole-brain atlas of inputs to serotonergic neurons of the dorsal and median raphe nuclei. *Neuron*, 6;83(3):663-78

Polter AM and Li X (2010). 5-HT1A receptor-regulated signal transduction pathways in brain. *Cell Signal*, 22(10):1406-12

Pompeiano M, Palacios JM, Mengod G (1992). Distribution and cellular localization of mRNA coding for 5-HT1A receptor in the rat brain: correlation with receptor binding. *J Neurosci*, 12(2):440-53

Porcelli S Fabbri C, Serretti A (2012). Meta-analysis of serotonin transporter gene promoter polymorphism (5-HTTLPR) association with antidepressant efficacy. *Eur Neuropsychopharmacol*, 22(4):239-58

Porsolt RD, Le Pichon M, Jalfre M (1977). Depression: a new animal model sensitive to antidepressant treatments. *Nature*, 21;266(5604):730-2

Portella MJ, de Diego-Adeliño J, Ballesteros J, Puigdemont D, Oller S, Santos B et al. (2011). Can we really accelerate and enhance the selective serotonin reuptake inhibitor antidepressant effect? A randomized clinical trial and a meta-analysis of pindolol in nonresistant depression. *J Clin Psychiatry*, 72(7):962-9

Pryce CR and Feldon J (2003). Long-term neurobehavioural impact of the postnatal environment in rats: manipulations, effects and mediating mechanisms. *Neurosci Biobehav Rev*, 27(1-2):57-71

Puigdemont D, Perez-Egea R, Portella MJ, Molet J, de Diego-Adeliño J, Gironell A et al. (2012). Deep brain stimulation of the subcallosal cingulate gyrus: further evidence in treatment-resistant major depression. *Int J Neuropsychopharmacol*, 15(1):121-33

Q

Qian Y, Melikian HE, Rye DB, Levey AI, Blakely RD (1995). Identification and characterization of antidepressant-sensitive serotonin transporter proteins using site-specific antibodies. *J Neurosci*, 15(2):1261-74

Qian Y, Galli A, Ramamoorthy S, Risso S, DeFelice LJ, Blakely RD (1997). Protein kinase C activation regulates human serotonin transporters in HEK-293 cells via altered cell surface expression. *J Neurosci,* 1;17(1):45-57

R

Rajkowski J, Majczynski H, Clayton E, Aston-Jones G (2004). Activation of monkey locus coeruleus neurons varies with difficulty and performance in a target detection task. *J Neurophysiol*, 92(1):361-71

Ramamoorthy S and Blakely RD (1999). Phosphorylation and sequestration of serotonin transporters differentially modulated by psychostimulants. *Science*, 30;285(5428):763-6

Ramboz S, Oosting R, Amara DA, Kung HF, Blier P, Mendelsohn M et al. (1998). Serotonin receptor 1A knockout: an animal model of anxiety-related disorder. *Proc Natl Acad Sci U S A*, 24;95(24):14476-81

Rasmusson AM, Shi L, Duman R (2002). Downregulation of BDNF mRNA in the hippocampal dentate gyrus after re-exposure to cues previously associated with footshock. *Neuropsychopharmacology*, 27(2):133-42

Retting GR and Behlke MA (2012). Progress toward in vivo use of siRNAs-II. *Mol Ther*, 20(3):483-512

Reyes BA, Valentino RJ, Xu G, Van Bockstaele EJ (2005). Hypothalamic projections to locus coeruleus neurons in rat brain. *Eur J Neurosci*, 22(1):93-106

Ribeiro L, Busnello JV, Cantor RM, Whelan F, Whittaker P, Deloukas P et al. (2007). The brain-derived neurotrophic factor rs6265 (Val66Met) polymorphism and depression in Mexican-Americans. *Neuroreport*, 6;18(12):1291-3

Richardson-Jones JW, Craige CP, Guiard BP, Stephen A, Metzger KL, Kung HF et al. (2010). 5-HT1A autoreceptor levels determine vulnerability to stress and response to antidepressants. *Neuron*, 14;65(1):40-52

Rietschel M, Mattheisen M, Frank J, Treutlein J, Degenhardt F, Breuer R et al. (2010). Genome-wide association-, replication-, and neuroimaging study implicates HOMER1 in the etiology of major depression. *Biol Psychiatry*, 15;68(6):578-85

Risch SC, Cohen RM, Janowsky DS, Kalin NH, Sitaram N, Gillin JC et al. (1981). Physostigmine induction of depressive symptomatology in normal human subjects. *Psychiatry Res*, 4(1):89-94

Robbins M, Judge A, Ambegia E, Choi C, Yaworski E, Palmer L et al. (2008). Misinterpreting the therapeutic effects of small interfering RNA caused by immune stimulation. *Hum Gene Ther*, 19(10):991-9

Roceri M, Cirulli F, Pessina C, Peretto P, Racagni G, Riva MA (2004). Postnatal repeated maternal deprivation produces age-dependent changes of brain-derived neurotrophic factor expression in selected rat brain regions. *Biol Psychiatry*, 1;55(7):708-14

Rosenberg O, Isserles M, Levkovitz Y, Kotler M, Zangen A, Dannon PN (2011). Effectiveness of a second deep TMS in depression: a brief report. *Prog Neuropsychopharmacol Biol Psychiatry*, 1;35(4):1041-4

Roy I, Stachowiak MK, Bergey EJ (2008). Nonviral gene transfection nanoparticles: function and applications in the brain. *Nanomedicine* 4(2):89-97

Rush AJ and Thase ME (1998). in WPA Series: *Evidence and Experience in Psychiatry*, eds. Maj, M. & Sartorius, N. (Wiley, Chichester, U.K.), 2nd Ed., Vol. 1, pp. 161-206

Rush AJ, Trivedi MH, Wisniewski SR, Stewart JW, Nierenberg AA, Thase ME et al. (2006a). Bupropion-SR, sertraline, or venlafaxine-XR after failure of SSRIs for depression. *N Engl J Med*, 23;354(12):1231-42

Rush AJ, Trivedi MH, Wisniewski SR, Nierenberg AA, Stewart JW, Warden D et al. (2006b). Acute and longer-term outcomes in depressed outpatients requiring one or several treatment steps: a STAR*D report. *Am J Psychiatry*, 163(11):1905-17

Rush RA and Geffen LB (1980). Dopamine beta-hydroxylase in health and disease. *Crit Rev Clin Lab Sci*, 12(3):241-77

Russo SJ, Murrough JW, Han MH, Charney DS, Nestler EJ (2012). Neurobiology of resilience. *Nat Neurosci*, 15(11):1475-84

Russo SJ and Nestler EJ (2013). The brain reward circuitry in mood disorders. *Nat Rev Neurosci*, 14(9):609-25

Rygula R, Abumaria N, Flügge G, Hiemke C, Fuchs E, Rüther E et al. (2006). Citalopram counteracts depressive-like symptoms evoked by chronic social stress in rats. *Behav Pharmacoli*, 17(1):19-29

S

Sachar EJ and Baron M (1979). The biology of affective disorders. *Annu Rev Neurosci*, 2:505-17

Sacher J, Neumann J, Fünfstück T, Soliman A, Villringer A, Schroeter ML (2012). Mapping the depressed brain: a meta-analysis of structural and functional alterations in major depressive disorder. *J Affect Disord*, 140(2):142-8

Sadek AR, Knight GE, Burnstock G (2011). Electroconvulsive therapy: a novel hypothesis for the involvement of purinergic signalling. *Purinergic Signal*, 7(4):447-52

Salahpour A, Medvedev IO, Beaulieu JM, Gainetdinov RR, Caron MG (2007). Local knockdown of genes in the brain using small interfering RNA: a phenotypic comparison with knockout animals. *Biol Psychiatry*, 1;61(1):65-9

Samuels BA and Hen R (2011). Novelty-suppressed feeding in the mouse. In: Gould TD (ed). *Mood and Anxiety Related Phenotypes in Mice: Characterization Using Behavioral Tests, Volume II. (Springer: New York, NY, USA)*, pp. 107-121

Samuvel DJ, Jayanthi LD, Bhat NR, Ramamoorthy S (2005). A role for p38 mitogen-activated protein kinase in the regulation of the serotonin transporter: evidence for distinct cellular mechanisms involved in transporter surface expression. *J Neurosci*, 5;25(1):29-41

Sanacora G, Rothman DL, Mason G, Krystal JH (2003). Clinical studies implementing glutamate neurotransmission in mood disorders. *Ann N Y Acad Sci,* 1003:292-308

Sanacora G, Smith MA, Pathak S, Su HL, Boeijinga PH, McCarthy DJ et al. (2014). Lanicemine: a low-trapping NMDA channel blocker produces sustained antidepressant efficacy with minimal psychotomimetic adverse effects. *Mol Psychiatry*, 19(9):978-85

Sandoz G, Bell SC, Isacoff EY (2011). Optical probing of a dynamic membrane interaction that regulates the TREK1 channel. *Proc Natl Acad Sci U S A*, 8;108(6):2605-10

Santana N, Bortolozzi A, Serrats J, Mengod G, Artigas F (2004). Expression of serotonin1A and serotonin2A receptors in pyramidal and GABAergic neurons of the rat prefrontal cortex. *Cereb Cortex*, 14(10):1100-

Santarelli L, Saxe M, Gross C, Surget A, Battaglia F, Dulawa S et al. (2003). Requirement of hippocampal neurogenesis for the behavioral effects of antidepressants. *Science*, 8;301(5634)805-9

Sapolsky RM (2000). Glucocorticoids and hippocampal atrophy in neuropsychiatric disorders. *Arch Gen Psychiatry*, 57(10)925-35

Sara SJ and Bouret S (2012). Orienting and reorienting: the locus coeruleus mediates cognition through arousal. *Neuron*, 4;76(1):130-41

Sara SJ (2015). Locus Coeruleus in time with the making of memories. *Curr Opin Neurobiol*, 35:87-94

Sari Y (2004). Serotonin1B receptors: from protein to physiological function and behavior. *Neurosci Biobehav Rev*, 28(6):565-82

Savitz J and Drevets WC (2009). Bipolar and major depressive disorder: neuroimaging the developmental-degenerative divide. *Neurosci Biobehav Rev*, 33(5):699-771

Schildkraut JJ (1965). The catecholamine hypothesis of affective disorders. A review of supporting evidence. *Am J Psychiatry*, 122(5):509-22

Schlaepfer TE, Frick C, Zobel A, Maier W, Heuser I, Bajbouj M et al. (2008). Vagus nerve stimulation for depression: efficacy and safety in a European study. *Psychol Med*, 38(5):651-61

Schratt G (2014). Neurobiology: a molecular knife to dice depression. *Nature,* 4;516(7529):45-6

Schratt GM, Tuebing F, Nigh EA, Kane CG, Sabatini ME, Kiebler M (2006). A brain-specific microRNA regulates dendritic spine development. *Nature,* 19;439(7074):283-9

Schumacher J, Jamra RA, Becker T, Ohlraun S, Klopp N, Binder EB (2005). Evidence for a relationship between genetic variants at the brain-derived neurotrophic factor (BDNF) locus and major depression. *Biol Psychiatry,* 15;58(4):307-14

Sequeira A and Turecki G (2006). Genome wide gene expression studies in mood disorders. *OMICS,* 10(4):444-54

Serchov T, Clement HW, Schwarz MK, Iasevoli F, Tosh DK, Idzko M et al. (2015). Increased Signaling via Adenosine A1 Receptors, Sleep Deprivation, Imipramine, and Ketamine Inhibit Depressive-like Behavior via Induction of Homer1a. *Neuron,* 5;87(3):549-62

Serretti A, Artioli P, Lorenzi C, Pirovano A, Tubazio V, Zanardi R (2004). The C(-1019)G polymorphism of the 5-HT1A gene promoter and antidepressant response in mood disorders: preliminary findings. *Int J Neuropsychopharmacol*, 7(4):453-60

Serretti A, Kato M, De Ronchi D, Kinoshita T (2007). Meta-analysis of serotonin transporter gene promoter polymorphism (5-HTTLPR) association with selective serotonin reuptake inhibitor efficacy in depressed patients. *Mol Psychiatry*, 12(3):247-57

Shah A, Carreno FR, Frazer A (2014). Therapeutic modalities for treatment resistant depression: focus on vagal nerve stimulation and ketamine. *Clin Psychopharmacol Neurosci*, 12(2):83-93

Sheline YI, Gado MH, Kraemer HC (2003). Untreated depression and hippocampal volume loss. *Am J Psychiatry*, 160(8):1516-8

Shelton RC, Tollefson GD, Tohen M, Stahl S, Gannon KS, Jacobs TG et al. (2001). A novel augmentation strategy for treating resistant major depression. *Am J Psychiatry*, 158(1):131-4

Shimizu E, Hashimoto K, Okamura N, Koike K, Komatsu N, Kumakiri C et al. (2003). Alterations of serum levels of brain-derived neurotrophic factor (BDNF) in depressed patients with or without antidepressants. *Biol Psychiatry*, 1;54(1):70-5

Shishkina GT, Kalinina TS, Dygalo NN (2004). Attenuation of alpha2A-adrenergic receptor expression in neonatal rat brain by RNA interference or antisense oligonucleotide reduced anxiety in adulthood. *Neuroscience*, 129(3):521-8

Silberg J, Pickles A, Rutter M, Hewitt J, Simonoff E, Maes H et al. (1999). The influence of genetic factors and life stress on depression among adolescent girls. *Arch Gen Psychiatry*, 56(3):225-32

Silva JM, Li MZ, Chang K, Ge W, Golding MC, Rickles RJ et al. (2005). Second-generation shRNA libraries covering the mouse and human genomes. *Nat Genet*, 37(11):1281-8

Skolnick P, Layer RT, Popik P, Nowak G, Paul IA, Trullas R (1996). Adaptation of N-methyl-D-aspartate (NMDA) receptors following antidepressant treatment: implications for the pharmacotherapy of depression. *Pharmacopsychiatry,* 29(1):23-6

Sledz CA, Holko M, de Veer MJ, Silverman RH, Williams BR (2003). Activation of the interferon system by short-interfering RNAs. *Nat Cell Biol,* 5(9):834-9

Smalheiser NR (2014). The RNA-centred view of the synapse: non-coding RNAs and synaptic plasticity. *Philos Trans R Soc Lond B Biol Sci,* 26;369(1652)

Smith K (2011). Trillion-dollar brain drain. *Nature,* 4;478(7367):15

Smith K (2014). Mental health: a world of depression. *Nature,* 13;515(7526):181

Smith MA, Makino S, Kvetnansky R, Post RM (1995). Stress and glucocorticoids affect the expression of brain-derived neurotrophic factor and neurotrophin-3 mRNAs in the hippocampus. *J Neurosci,* 15(3 Pt 1):1768-77

Snove O Jr, Nedland M, Fjeldstad SH, Humberset H, Birkeland OR, Grünfeld T et al. (2004). Designing effective siRNAs with off-target control. *Biochem Biophys Res Commun,* 17;325(3):769-73

Song E, Zhu P, Lee SK, Chowdhury D, Kussman S, Dykxhoorn DM et al. (2005). Antibody mediated in vivo delivery of small interfering RNAs via cell-surface receptors. *Nat Biotechnol,* 23(6);709-17

Song L, Che W, Min-Wei W, Murakami Y, Matsumoto K (2006). Impairment of the spatial learning and memory induced by learned helplessness and chronic mild stress. *Pharmacol Biochem Behav,* 83(2):186-93

Sotelo C, Cholley B, El Mestikawy S, Gozlan H, Hamon M (1990). Direct Immunohistochemical Evidence of the Existence of 5-HT1A Autoreceptors on Serotoninergic Neurons in the Midbrain Raphe Nuclei. *Eur J Neurosci*, 2(12):1144-1154

Soutschek J, Akinc A, Bramlage B, Charisse K, Constien R, Donoghue M et al. (2004). Therapeutic silencing of an endogenous gene by systemic administration of modified siRNAs. *Nature*, 11;432(7014):173-8

Stahl SM (2000). Placebo-controlled comparison of the selective serotonin reuptake inhibitors citalopram and sertraline. *Biol Psychiatry*, 1;48(9):894-901

Starke K (1987). Presynaptic alpha-autoreceptors. *Rev Physiol Biochem Pharmacol*, 107:73-146

Stegmeier F, Hu G, Rickles RJ, Hannon GJ, Elledge SJ (2005). A lentiviral microRNA-based system for single-copy polymerase II-regulated RNA interference in mammalian cells. *Proc Natl Acad Sci U S A*, 13;102(37):13212-7

Steru L, Chermat R, Thierry B, Simon P (1985). The tail suspension test: a new method for screening antidepressants in mice. *Psychopharmacology (Berl)*, 85(3):367-70

Stockmeier CA, Shapiro LA, Dilley GE, Kolli TN, Friedman L, Rajkowska G (1998). Increase in serotonin-1A autoreceptors in the midbrain of suicide victims with major depression-postmortem evidence for decreased serotonin activity. *J Neurosci,* 15;18(18):7394-401

Sun P, Wang F, Wang L, Zhang Y, Yamamoto R, Sugai T et al. (2011). Increase in cortical pyramidal cell excitability accompanies depression-like behavior in mice: a transcranial magnetic stimulation study. *J Neurosci, 9;31*(45):16464-72

Sun H, Kennedy PJ, Nestler EJ (2013). Epigenetics of the depressed brain: role of histone acetylation and methylation. *Neuropsychopharmacology,* 38(1):124-37

Sun L, Luo ZM, Guo XM, Su DF, Liu X (2015). An updated role of microRNA-124 in central nervous system disorders: a review. *Front Cell Neurosci,* 20;9:193

Sweatt JD, Johnson SL, Cragoe EJ, Limbird LE (1985). Inhibitors of Na+/H+ exchange block stimulus-provoked arachidonic acid release in human platelets. Selective effects on platelet activation by epinephrine, ADP, and lower concentrations of thrombin. *J Biol Chem,* 25;260(24):12910-9

T

Taliaz D, Stan N Dar DE, Zangen A (2010). Knockdown of brain-derived neurotrophic factor in specific brain sites precipitates behaviors associated with depression and reduces neurogenesis. *Mol Psychiatry*, 15(1):80-92

Talley EM, Lei Q, Sirois JE, Bayliss DA (2000). TASK-1, a two-pore domain K+ channel, is modulated by multiple neurotransmitters in motoneurons. *Neuron*, 25(2):399-410

Talley EM, Solorzano G, Lei Q, Kim D, Bayliss DA (2001). Cns distribution of members of the two-pore-domain (KCNK) potassium channel family. *J Neurosci*, 1;21(19):7491-505

Talley EM and Bayliss DA (2002). Modulation of TASK-1 (Kcnk3) and TASK-3 (Kcnk9) potassium channels: volatile anesthetics and neurotransmitters share a molecular site of action. *J Biol Chem*, 17;277(20):17733-42

Tatarczynska E, Kłodzińska A, Stachowicz K, Chojnacka-Wójcik E (2004). Effects of a selective 5-HT1B receptor agonist and antagonists in animal models of anxiety and depression. *Behav Pharmacol*, 15(8):523-34

Thakker DR, Natt F, Hüsken D, Maier R, Müller M, van der Putten H et al. (2004). Neurochemical and behavioral consequences of widespread gene knockdown in the adult mouse brain by using nonviral RNA interference. *Proc Natl Acad Sci U S A*, 7;101(49):17270-5

Thakker DR, Natt F, Hüsken D, van der Putten H, Maier R, Hoyer D et al. (2005). siRNA-mediated knockdown of the serotonin transporter in the adult mouse brain. *Mol Psychiatry*, 10(8):782-9

Thase ME, Greenhouse JB, Frank E, Reynolds CF 3rd, Pilkonis PA, Hurley K et al. (1997). Treatment of major depression with psychotherapy or psychotherapy-pharmacotherapy combinations. *Arch Gen Psychiatry,* 54(11):1009-15

Thase ME, Entsuah AR, Rudolph RL (2001). Remission rates during treatment with venlafaxine or selective serotonin reuptake inhibitors. *Br J Psychiatry*, 178:234-41

Thorne RG, Pronk GJ, Padmanabhan V, Frey WH 2nd (2004). Delivery of insulin-like growth factor-I to the rat brain and spinal cord along olfactory and trigeminal pathways following intranasal administration. *Neuroscience*, 127(2):481-96

Toda H, Hamani C, Fawcett AP, Hutchison WD, Lozano AM (2008). The regulation of adult rodent hippocampal neurogenesis by deep brain stimulation. *J Neurosurg*, 108(1):132-8

Tollefson GD and Holman SL (1994). How long to onset of antidepressant action: a meta-analysis of patients treated with fluoxetine or placebo. *Int Clin Psychopharmacol*, 9(4):245-50

Törk I (1990). Anatomy of the serotonergic system. *Ann N Y Acad Sci*, 600:9-34

Torres GE, Gainetdinov RR, Caron MG (2003). Plasma membrane monoamine transporters: structure, regulation and function. *Nat Rev Neurosci*, 4(1):13-25

Trimmer JS (2015). Subcellular localization of K+ channels in mammalian brain neurons: remarkable precision in the midst of extraordinary complexity. *Neuron*, 21;85(2):238-56

Trivedi MH, Rush AJ, Wisniewski SR, Nierenberg AA, Warden D, Ritz L et al. (2006a). Evaluation of outcomes with citalopram for depression using measurement-based care in STAR*D: implications for clinical practice. *Am J Psychiatry*, 163(1):28-40

Trivedi MH, Fava M, Wisniewski SR, Thase ME, Quitkin F, Warden D et al. (2006b). Medication augmentation after the failure of SSRIs for depression. *N Engl J Med*, 23;354(12):1243-52

Trullas R and Skolnick P (1990). Functional antagonists at the NMDA receptor complex exhibit antidepressant actions. *Eur J Pharmacol*, 21;185(1):1-10

Tsai SJ, Hong CJ, Wang YC (1999). Tryptophan hydroxylase gene polymorphism (A218C) and suicidal behaviors. *Neuroreport*, 16;10(18):3773-5

U

Umbriaco D, Anctil M, Descarries L (1990). Serotonin-immunoreactive neurons in the cnidarian Renilla koellikeri. *J Comp Neurol*, 8;291(2):167-78

V

van Praag H, Kempermann G, Gage FH (2000). Neural consequences of environmental enrichment. *Nat Rev Neurosci,* 1(3):191-8

Vandermaelen CP and Aghajanian GK (1983). Electrophysiological and pharmacological characterization of serotonergic dorsal raphe neurons recorded extracellularly and intracellularly in rat brain slices. *Brain Res*, 19;289(1-2):109-19

Varga V, Kocsis B, Sharp T (2003). Electrophysiological evidence for convergence of inputs from the medial prefrontal cortex and lateral habenula on single neurons in the dorsal raphe nucleus. *Eur J Neurosci*, 17(2):280-6

Veale EL, Kennard LE, Sutton GL, MacKenzie G, Sandu C, Mathie A (2007a). G(alpha)q-mediated regulation of TASK3 two-pore domain potassium channels: the role of protein kinase C. *Mol Pharmacol*, 71(6):1666-75

Veale EL, Buswell R, Clarke CE, Mathie A (2007b). Identification of a region in the TASK3 two pore domain potassium channel that is critical for its blockade by methanandamide. *Br J Pharmacol*, 152(5):778-86

Veena J, Srikumar BN, Raju TR, Shankaranarayana Rao BS (2009). Exposure to enriched environment restores the survival and differentiation of new born cells in the hippocampus and ameliorates depressive symptoms in chronically stressed rats. *Neurosci Lett*, 22;455(3):178-82

Vega-Rivera NM, López-Rubalcava C, Estrada-Camarena E (2013). The antidepressant-like effect of ethynyl estradiol is mediated by both serotonergic and noradrenergic systems in the forced swimming test. *Neuroscience*, 10;250:102-11

Vega-Saenz de Miera E, Lau DH, Zhadina M, Pountney D, Coetzee WA, Rudy B (2001). KT3.2 and KT3.3, two novel human two-pore K(+) channels closely related to TASK-1. *J Neurophysiol*, 86(1):130-42

Verhagen M, van der Meij A, van Deurzen PA, Janzing JG, Arias-Vásquez A, Buitelaar JK et al. (2010). Meta-analysis of the BDNF Val66Met polymorphism in major depressive disorder: effects of gender and ethnicity. *Mol Psychiatry*, 15(3):260-71

Vicentini FT, Borgheti-Cardoso LN, Depieri LV, de Macedo Mano D, Abelha TF, Petrilli R et al. (2013). Delivery systems and local administration routes for therapeutic siRNA. *Pharm Res*, 30(4);915-31

Videbech P and Ravnkilde B (2004). Hippocampal volume and depression: a meta-analysis of MRI studies. *Am J Psychiatry*, 161(11):1957-66

Vo N, Klein ME, Varlamova O, Keller DM, Yamamoto T, Goodman RH et al. (2005). A cAMP-response element binding protein-induced microRNA regulates neuronal morphogenesis. *Proc Natl Acad Sci U S A*, 8;102(45):16426-31

Volkov AA, Kruglova NS, Meschaninova MI, Venyaminova AG, Zenkova MA, Vlassov VV et al. (2009). Selective protection of nuclease-sensitive sites in siRNA prolongs silencing effect. *Oligonucleotides*, 19(2):191-202

Vollmayr B and Henn FA (2001). Learned helplessness in the rat: improvements in validity and reliability. *Brain Res Brain Res Protoc*, 8(1):1-7

Vollmayr B, Faust H, Lewicka S, Henn FA (2001). Brain-derived-neurotrophic-factor (BDNF) stress response in rats bred for learned helplessness. *Mol Psychiatry*, 6(4):471-4

Vornlocher HP (2006). Antibody-directed cell-type-specific delivery of siRNA. *Trends Mol Med*, 12(1):1-3

Vreeburg SA, Hoogendijk WJ, van Pelt J, Derijk RH, Verhagen JC, van Dyck R et al. (2009). Major depressive disorder and hypothalamic-pituitary-adrenal axis activity: results from a large cohort study. *Arch Gen Psychiatry*, 66(6):617-26

Vythilingam M, Heim C, Newport J, Miller AH, Anderson E, Bronen R et al. (2002). Childhood trauma associated with smaller hippocampal volume in women with major depression. *Am J Psychiatry*, 159(12):2072-80

W

Wallace DM, Magnuson DJ, Gray TS (2003). Organization of amygdaloid projections to brainstem dopaminergic, noradrenergic, and adrenergic cell groups in the rat. *Brain Res Bull*, 28(3):447-54

Walther DJ, Peter JU, Bashammakh S, Hörtnagl H, Voits M, Fink H et al. (2003). Synthesis of serotonin by a second tryptophan hydroxylase isoform. *Science*, 3;299(5603):76

Wang ZZ, Zhang Y, Liu YQ, Zhao N, Zhang YZ, Yuan L et al. (2013). RNA interference-mediated phosphodiesterase 4D splice variants knock-down in the prefrontal cortex produces antidepressant-like and cognition-enhancing effects. *Br J Pharmacol*, 168(4):1001-14

Warner-Schmidt JL and Duman RS (2006). Hippocampal neurogenesis: opposing effects of stress and antidepressant treatment. *Hippocampus*, 16(3):239-49

Washburn CP, Sirois JE, Talley EM, Guyenet PG, Bayliss DA (2002). Serotonergic raphe neurons express TASK channel transcripts and a TASK-like pH- and halothane-sensitive K+ conductanc. *J Neurosci*, 15;22(4):1256-65

Weiss JM, Goodman PA, Losito BG, Corrigan S, Charry JM, Bailey WH (1981). Behavioral depression produced by an uncontrollable stressor: Relationship to norepinephrine, dopamine, and serotonin levels in various regions of rat brain. *Brain Research Reviews*, 3(2):167-205

Weissman MM, Prusoff BA, Dimascio A, Neu C, Goklaney M, Klerman GL (1979). The efficacy of drugs and psychotherapy in the treatment of acute depressive episodes. *Am J Psychiatry*, 136(4B):555-8

Wellman CL (2001). Dendritic reorganization in pyramidal neurons in medial prefrontal cortex after chronic corticosterone administration. *J Neurobiol,* 15;49(3):245-53

Wesolowska A Nikiforuk A, Stachowicz K, Tatarczyńska E (2006). Effect of the selective 5-HT7 receptor antagonist SB 269970 in animal models of anxiety and depression. *Neuropharmacology, 51*(3):578-86

Wesolowska A and Nikiforuk A (2007). Effects of the brain-penetrant and selective 5-HT6 receptor antagonist SB-399885 in animal models of anxiety and depression. *Neuropharmacology, 52*(5):1274-83

Willner P (1991). Animal models as simulations of depression. *Trends Pharmacol Sci*, 12(4):131-6

Willner P (1997). Validity, reliability and utility of the chronic mild stress model of depression: a 10-year review and evaluation. *Psychopharmacology (Berl)*, 134(4):319-29

Wirz-Justice A and Van den Hoofdakker RH (1999). Sleep deprivation in depression: what do we know, where do we go? *Biol Psychiatry*, 15;46(4):445-53

Wirz-Justice A (2006). Biological rhythm disturbances in mood disorders. *Int Clin Psychopharmacol*, 21 Suppl 1:S11-5

Wittchen HU, Jacobi F, Rehm J, Gustavsson A, Svensson M, Jönsson B et al. (2011). The size and burden of mental disorders and other disorders of the brain in Europe 2010. *Eur Neuropsychopharmacol*, 21(9):655-79

Wohleb ES, Wu M, Gerhard DM, Taylor SR, Picciotto MR, Alreja M et al. (2016). GABA interneurons mediate the rapid antidepressant-like effects of scopolamine. *J Clin Invest*, 1;126(7):2482-94

Wong ML and Licinio J (2004). From monoamines to genomic targets: a paradigm shift for drug discovery in depression. *Nat Rev Drug Discov*, 3(2):136-51

Wong ML, Whelan F, Deloukas P, Whittaker P, Delgado M, Cantor RM et al. (2006). Phosphodiesterase genes are associated with susceptibility to major depression and antidepressant treatment response. P*roc Natl Acad Sci U S A*, 10;103(41):15124-9

Woo DH, Han KS, Shim JW, Yoon BE, Kim E, Bae JY et al. (2012). TREK-1 and Best1 channels mediate fast and slow glutamate release in astrocytes upon GPCR activation. Cell, 28;151(1):25-40

Xi G, Zhang X, Zhang L, Sui Y, Hui J, Liu S et al. (2011). Fluoxetine attenuates the inhibitory effect of glucocorticoid hormones on neurogenesis in vitro via a two-pore domain potassium channel, TREK-1. *Psychopharmacology (Berl)*, 214(3):747-59

Xie FY, Woodle MC, Lu PY (2006). Harnessing in vivo siRNA delivery for drug discovery and therapeutic development. *Drug Discov Today*, 11(1-2):67-73

Y

Yap JJ, Takase LF, Kochman LJ, Fornal CA, Miczek KA, Jacobs BL (2006). Repeated brief social defeat episodes in mice: effects on cell proliferation in the dentate gyrus. *Behav Brain Res*, 25;172(2):344-50

Ye D, Li Y, Zhang X, Guo F, Genq L, Zhang Q et al. (2015). TREK1 channel blockade induces an antidepressant-like response synergizing with 5-HT1A receptor signaling. *Eur Neuropsychopharmacol*, 25(12):2426-36

Yu S, Patchev AV, Wu Y, Lu J, Holsboer F, Zhang JZ et al. (2010). Depletion of the neural precursor cell pool by glucocorticoids. *Ann Neurol*, 67(1):21-30

Yu YW, Tsai SJ, Chen TJ, Lin CH, Hong CJ (2002). Association study of the serotonin transporter promoter polymorphism and symptomatology and antidepressant response in major depressive disorders. *Mol Psychiatry*, 7(10):1115-9

Z

Zarate CA Jr, Singh JB, Carlson PJ, Brutsche NE, Ameli R, Luckenbaugh DA et el. (2006). A randomized trial of an N-methyl-D-aspartate antagonist in treatment-resistant major depression. *Arch Gen Psychiatry*, 63(8):856-64

Zarate CA Jr, Brutsche NE, Ibrahim L, Franco-Chaves J, Diazgranados N, Cravchik A et al. (2012). Replication of ketamine's antidepressant efficacy in bipolar depression: a randomized controlled add-on trial. *Biol Psychiatry*, 1;71(11):939-46

Zarate CA Jr, Mathews D, Ibrahim L, Chaves JF, Marquardt C, Ukoh I et al. (2013). A randomized trial of a low-trapping nonselective N-methyl-D-aspartate channel blocker in major depression. *Biol Psychiatry*, 15;75(4):257-64

Zhao C, Deng W, Gage FH (2008). Mechanisms and functional implications of adult neurogenesis. *Cell*, 22;132(4):645-60

Zhong P, Wang W, Pan B, Liu X, Zhang Z, Long JZ et al. (2014). Monoacylglycerol lipase inhibition blocks chronic stress-induced depressive-like behaviors via activation of mTOR signaling. *Neuropsychopharmacology*, 39(7):1763-76

8. Anexo

Durante el periodo de ejecución de la presente Tesis se ha colaborado en otros estudios, lo que ha posibilitado la participación en los siguientes artículos:

Schneeberger M, Gómez-Valadés AG, Altirriba J, Sebastian D, Ramírez S, Garcia A, Esteban Y, Drougard A, Ferrés-Coy A, Bortolozzi A, Garcia-Roves PM, Jones JG, Manadas B, Zorzano A, Gomis R, Claret M (2015). Reduced alpha-MSH Underlies Hypothalamic ER-Stress-Induced Hepatic Gluconeogenesis. *Cell Rep*, 21;12(3):361-70

Pegueroles C, Ferrés-Coy A, Marti-Solano M, Aquadro CF, Pascual M, Mestres F. (2016). Inversions and adaptation to the plant toxin ouabain shape DNA sequence variation within and between chromosomal inversions of Drosophila subobscura. *Sci Rep*, 31;6:23754